A Comprehensive Analysis of Long Bone Curvature in Neanderthals and Modern Humans Using 3D morphometrics

Isabelle Elisabeth Peter Maria De Groote

A thesis submitted to University
College London in fulfillment of
the requirements for the degree of
Doctor of Philosophy.

2008

ProQuest LLC
789 East Eisenhower Parkway
P.O. Box 1346
Ann Arbor, MI 48106-1346

I, Isabelle De Groote, confirm that the work presented in this thesis is my own. Where information has been derived from other sources, I confirm that this has been indicated in the thesis.

Abstract

Since their discovery Neanderthals were described as having a marked degree of anteroposterior curvature of the femoral shaft. Although initially believed to be pathological, subsequent discoveries of Neanderthal remains made femoral curvature as well as the lateral curvature of the radius to be considered derived Neanderthal features. Femoral curvature has previously been used in racial identification in modern humans but its functional significance is poorly understood. A recent study on Neanderthals and early modern humans found no differences in femoral curvature, but did not consider size-corrected curvature. Therefore, the objectives of this study were to 1) use 3D morphometric landmark and semi-landmark analysis to quantify bone curvature (femur, ulna, radius) in Neanderthals, Upper Palaeolithic and recent modern humans, 2) compare adult bone curvature between these populations, and 3) test hypotheses on the effects of climate, body size, and activity patterns on curvature.

Comparisons between and within populations were made using geometric morphometrics (3D landmarks) and standard multivariate methods. Comparative material involved all available Neanderthal and Upper Palaeolithic modern human femora, ulnae and radii, archaeological (Mesolithic, Neolithic, Medieval) and recent human populations representing a wide geographical and lifestyle range. The study found that there are significant differences in the anatomy of the femur, ulna and radius between Neanderthals and modern humans. Neanderthals have more curved femora and radii than modern humans. Early modern humans are most similar to recent modern humans in their anatomy. Recent modern human analyses indicate that femoral curvature and forearm curvature are responses to disparate influences. Femoral curvature is a good indicator of activity level and habitual loading of the lower limb. Curvature of the forearm is a consequence of cold adaptation and its purpose is to maintain biomechanical function of the forearm despite its foreshortening.

In memory of Charlie.

You knew my strengths,
You knew my weaknesses,
You were my mentor,
You were my friend.

Acknowledgements

First and foremost I thank my supervisors, Dr. Charles Lockwood and Professor Leslie Aiello, who have been as much friends as mentors. I also thank Professor Simon Hillson for his valuable advice.

I am grateful to all the people who provided access to the fossils examined for this thesis: I. Tattersal, G. Sawyer at the American Museum of Natural History New York; R. Kruzynski at the Natural History Museum, London; Y. Rak of the Sackler School of Medicine, Tel Aviv; P. Mennecier at the Musée de l'Homme, Paris; J.-J. Cleyet-Merle at the National Museum of Prehistory, Les Eyzies; V. Merlin-Anglade at the Museum of Périgord, Périguex; M. Teschler-Nicola at the Natural History Museum, Vienna; P. Semal of Royal Belgian Institute of Natural Sciences, Brussels; W. Menghin at the Museum of Prehistory, Berlin; J. Svoboda of the Institute of Archaeology, Dolni Vestonice; M. Dockalova at the Moravian Museum, Brno; P. Velemínský, National Museum Prague; J. Chistov at the Kunstkamera, Saint Petersburg; D. Pezhèmsky, Moscow State University; M. Morgan at the Peabody Museum, Harvard University, Boston; D. Hunt at the National Museum of Natural History, Smithsonian Institute, Washington; P. Bennike at the Medical University, Copenhagen. I would like to thank Philip Mitteroecker and Philip Gunz for the use of their Mathematica functions and Katya Bulygina for her patience in sharing her geometric morphometrics knowledge.

At University College London (UCL) first thanks go to the Anthropology Department Staff for their support throughout my graduate career. I thank all my friends over the years at UCL who provided stimulating conversations, proof readings, much needed distractions and emotional support. I thank all my non-UCL friends and in particular the Buddens, the Hubbards and the Madaras for their support and for letting me be part of their families. Special thanks go to Ruth Brown who is the best "English mum" I could possibly have found.

Finally, I thank my parents, Geertje and Alexander De Groote, for supporting me in the choices I make and for encouraging me to fulfil my potential. I also thank my sister, Sabine, for keeping me with both feet on the ground, and my brother, Bert, for his random chats. I dedicate this thesis to my grandfather, Edouard Van Hove, as without his words of wisdom and funding I would not have been able to embark on this PhD.

This project was supported by the Graduate School, UCL; The Leakey Fund; The Ruggles-Gates Fund for Biological Anthropological Research; The Wenner-Gren Foundation for Anthropological Research; Synthesys; and the UCL Alumni.

Table of contents

List of tables

List of figures

List of appendices

CHAPTER 1. **INTRODUCTION**

1.1. **Purpose of the study**

When in the 19th Century the Feldhofer Neanderthal remains were discovered, researchers noted a marked degree of anterior curvature of the femoral shaft and ascribed it to pathology (Klaatsch, 1901; Boule, 1908; Trinkaus and Shipman, 1993). With the subsequent discoveries of other Neanderthal remains, femoral curvature was considered to be a derived feature of Neanderthals as were the shortened and curved ulna and radius (Klaatsch, 1901; Trinkaus and Shipman, 1993; Churchill, 1998; Golovanova *et al.*, 1999; Czarnetzki, 2000; Weaver, 2003; Yamanaka *et al.*, 2005).

Relatively little work has been done to quantify diaphyseal curvature in Neanderthals, but a recent study analysed patterns of femoral curvature in Neanderthals, recent humans and Late Pleistocene early modern humans (Shackelford and Trinkaus, 2002). Shackelford and Trinkaus (2002) suggested that Neanderthals were indistinguishable from Middle Palaeolithic and early Upper Palaeolithic early modern humans in their degree of absolute anterior curvature. Additionally, most of the individuals in these Palaeolithic populations were found to exhibit a more distal apex of curvature (point of maximum curvature) compared to more recent populations (Shackelford and Trinkaus, 2002). They suggested that this could be correlated with measures of bone hypertrophy or an overall decrease in lower-limb robusticity during the Middle to Upper Palaeolithic. The five regional groups from which their samples originated were significantly different in femoral curvature and Shackelford and Trinkaus (2002) suggested that the overall decrease in femoral curvature in modern humans was due to a decrease in long-distance mobility.

Research from forensic anthropology also suggests that significant differences exist in femoral curvature between modern human populations (Stewart, 1962; Walensky, 1962, 1965; Gilbert, 1975, 1976; Trudell, 1999). Initial studies demonstrated the diagnostic value of femoral curvature in distinguishing between Native American, African-American and Caucasoid American populations (Stewart, 1962; Walensky, 1962, 1965; Gilbert, 1975, 1976; Trudell,

1999). When the research was expanded by increasing the number of populations, no relationship was found between femoral curvature, habitual behavioural patterns and latitudinal position of those populations (Stewart, 1962; Walensky, 1962, 1965; Gilbert, 1975, 1976; Trudell, 1999). Trudell (1999) refined the measurement techniques by taking measurements at three points along the curve and found an 87.12% average accurate race determination for African-Americans and Caucasoids (see Chapter 2 for more details). The more detailed characterisation of curvature possible with 3D morphometrics has the potential to refine the differences between modern human groups.

The Neanderthal radius has also been described as being more laterally curved than that of humans and to fall beyond the higher limits of modern human variation (Fischer, 1906; Botez, 1926 in Patte, 1955; Vandermeersch and Trinkaus, 1995; Carretero *et al.*, 1999; Czarnetzki, 2000). Fischer (1906) described Neanderthals to have a large posterior subtense in the ulna but more recent work has not investigated this.

In the research presented here, I consider the differences and similarities in long bone curvature and position of the apex of curvature of the femur, ulna and radius. This study has three main objectives: 1) to determine the influence of climatic, body size and behavioural correlates on the observed differences in bone curvature in Holocene modern humans, 2) to describe differences in long bone curvature between Neanderthals and modern humans, and 3) to determine how the factors that influence modern human bone curvature can be applied to inform our understanding of Neanderthals and early modern humans.

The first objective involves an analysis of patterns of curvature and anthropometric measurements of modern humans and their relationship to population-specific information such as body size, activity level, time period and climate. This will be done in order to identify the biomechanical and adaptive advantages of different degrees of curvature within modern humans, in order to form predictions for the degree of curvature observed in Neanderthals and early modern humans.

The second objective requires an analysis to test whether there are any significant differences between Neanderthals and modern humans in femoral and lower arm curvature. The long claimed distinction in degree of femoral curvature in Neanderthals was challenged by Shackelford and Trinkaus (2002) who found no difference between Neanderthals and modern

humans. This hypothesis will be tested again here on the curvature of both the femur and the lower arm.

The third objective integrates results for the two main sets of analyses to determine the effect of habitual behaviour, climate and body size on Neanderthal long bone curvature.

1.2. Long bone curvature

Fundamental to the study of skeletal characteristics, such as long bone curvature, is the hypothesis that the traits under investigation are functionally relevant and optimise morphology (Churchill, 2005). The study of postcranial morphology over the past decades has demonstrated that skeletal morphology is under variable environmental and genetic influences. Therefore, some features give more information about the biomechanical environment (Pearson and Lieberman, 2004) while others may yield more information about the evolutionary history of a specific population (Ruff *et al.*, 1991; Pearson, 2000a, 2000b; Lieberman *et al.*, 2001; Pearson and Lieberman, 2004). The observed variation in long bone curvature within and between species needs to be investigated using an approach that considers its possible adaptive benefits.

Long bone curvature is a complex feature to quantify, and its biomechanical environment is difficult to model, as it is subject to different strains during different stages of the gait cycle (Lanyon, 1980; Les *et al.*, 1997; Main and Biewener, 2004). In humans, not all "curved" bones are active during the gait cycle (e.g. radius and ulna) and may be subject to other strains and stresses than when the same skeletal element is involved in locomotion in mammals that are not bipedal. Because of this complexity, it has been difficult to assess the biomechanical role and functional significance of diaphyseal curvature and the functional differences between bones and between species.

Hominoids have a lower degree of curvature than other quadrupedal mammals because their relatively longer limb bones would endure very high bending stress were they as curved as those of other mammals (Biewener, 1983; Swartz, 1990; Bertram and Biewener, 1992; Richmond and Whalen, 2001). The evolutionary significance of long bone curvature in hominins has, to date, not been investigated. Within humans, however, a range of variation in femoral curvature has been reported (Ried, 1924; Genna, 1930; Stewart, 1962; Walensky, 1965; Gilbert, 1975, 1976; Trudell, 1999; Bruns *et al.*, 2002) and, therefore, it is very likely that varying degrees of curvature in humans serve to reduce individual habitual strain levels and to optimise function during habitual behaviour in a specific environment. It is unclear if the habitual strain levels in the lower arm and femur are related and that curvature is therefore a systemic feature.

1.3. Neanderthals and modern humans

Early modern humans differ from recent modern humans in both cranial and postcranial features but Neanderthals differ from recent modern humans much more. Neanderthals have a suite of characteristic cranial traits such as a rounded cranial vault; large browridges, lambdoidal flattening and an occipital bun; a low and long cranium; a juxtamastoid process; suprainiac fossa; a retromolar gap; a chinless mandible; a large nose; and mid-facial prognathism (Boule and Vallois, 1952; Trinkaus, 1983a; Hublin, 1989; Stringer, 1992; Hublin *et al.*, 1998). In contrast to the numerous differences in the cranio-mandibular anatomy of Neanderthals and modern humans, there are only a number of postcranial differences that have been identified as species defining. Most of these postcranial characters have been interpreted as the result of the Neanderthal hyper-polar body shape and muscular hypertrophy (Patte, 1955; Vlcek, 1961b; Rak and Arensburg, 1987; Tompkins and Trinkaus, 1987; Holliday and Trinkaus, 1991; Ruff and Walker, 1993; Ruff *et al.*, 1993; Walker and Leakey, 1993; Ruff *et al.*, 1994; Trinkaus *et al.*, 1994; Vandermeersch and Trinkaus, 1995; Pearson and Grine, 1997; Churchill, 1998; Trinkaus *et al.*, 1998a; Trinkaus *et al.*, 1998b; Trinkaus and Ruff, 1999b; Pearson, 2000b; Holliday and Ruff, 2001; Shackelford and Trinkaus, 2002; Majǿ *et al.*, 2003; Weaver, 2003; Thompson and Nelson, 2005; Shackelford, 2007). Some of these postcranial anatomical specialisations include: a long pubic ramus; an anteriorly placed sacrum; short distal limb segments; a long glenoid fossa and a dorsal sulcus on the scapula; large round apical tufts on the fingers; a thick femoral and tibial shaft; and large knees (Patte, 1955; Vlcek, 1961a; Rak and Arensburg, 1987; Tompkins and Trinkaus, 1987; Holliday and Trinkaus, 1991; Ruff and Walker, 1993; Ruff *et al.*, 1993; Walker and Leakey, 1993; Ruff, 1994b; Trinkaus *et al.*, 1994; Vandermeersch and Trinkaus, 1995; Pearson and Grine, 1997; Churchill, 1998; Trinkaus *et al.*, 1998b; Trinkaus and Ruff, 1999a; Pearson, 2000b; Holliday and Ruff, 2001; Shackelford and Trinkaus, 2002; Majǿ *et al.*, 2003; Weaver, 2003; Thompson and Nelson, 2005; Shackelford, 2007). Other characteristic Neanderthal postcranial features include a long distal phalanx in the thumb; flat carpometacarpal joint of the thumb; low femoral neck-shaft angle; absence of a femoral pilaster/linea aspera; and a curved femur and radius (Aiello and Dean, 1990; Churchill, 1998; Fleagle, 1999; Trinkaus, 2006).

Some of these features may be primitive retentions in Neanderthals (Trinkaus, 1981, 1983a), whereas others may be autapomorphic traits (Howell, 1957; Trinkaus, 2006). The taxonomic value of some of these postcranial features, such as curvature of the femur and radius, has not been established, although it has been suggested that some postcranial features, such as a greater level of robusticity, the absence of a pilaster and low neck-shaft angles, are primitive retentions (Trinkaus, 1983a; Ruff *et al.*, 1993; Pearson, 2000b, 2000a).

Postcranially, compared to Neanderthals, early modern humans are characterised by high stature, high brachial and crural indices (Boule and Vallois, 1952; Trinkaus, 2007) and reduced levels of robusticity which may reflect their African ancestry (Mellars and Stringer, 1989; Aiello, 1993; Stringer, 2000; Stringer, 2002; Trinkaus, 2005). At the same time early modern Europeans exhibit some characteristics which have been considered to be distinctive Neanderthal traits (Boule and Vallois, 1952; Trinkaus, 2007). These characteristics include aspects of the neurocranium, basicranial external morphology, mandibular ramus and symphyseal form, dental morphology and size and aspects of the clavicle, scapula, metacarpals and appendicular proportions (Trinkaus, 2007). To some, the presence of these Neanderthal features and the association of Neanderthals with Upper Palaeolithic style tools (d'Errico *et al.*, 1998; d'Errico, 2003; Ahern *et al.*, 2004; Mellars, 2004; Mellars *et al.*, 2007) supports the idea that when modern humans migrated out of Africa and into Europe there was hybridisation between Neanderthals and early modern humans. The extent to which this hybridisation took place and whether or not it is still apparent in human morphology and genetics is a highly debated topic (Boule and Vallois, 1952; Smith *et al.*, 1989; Frayer *et al.*, 1993, 1994; Wolpoff, 1996; Wolpoff and Caspari, 1997; Wolpoff *et al.*, 2000, Deacon, 1992; Krings *et al.*, 1997; Ovchinnikov *et al.*, 2000; Hawks and Wolpoff, 2001; Caramelli *et al.*, 2003; Carroll, 2003; Hagelberg, 2003; Klein, 2003; Ovchinnikov and Goodwin, 2003; Green *et al.*, 2006; Noonan *et al.*, 2006).

The majority of the literature on modern human origins is focused on cranial, mandibular and dental traits. Postcranial anatomy has received less attention, although there are some excellent descriptions of relevant postcranial material (Boule and Vallois, 1952; Patte, 1955; Heim, 1983; Rak and Arensburg, 1987; Walker and Leakey, 1993; Vandermeersch and Trinkaus, 1995; Holliday, 1997; Pearson, 2000a, 2000b; Shackelford and Trinkaus, 2002; Weaver, 2003; Steudel-Numbers and Tilkens, 2004; Churchill, 2005; Thompson and Nelson, 2005; Shackelford, 2007; Aiello *et al.*, 1999). What is evident is that Neanderthals have a suite of

characteristics which, considered independently, may occur in modern human populations, but which, as a suite, set apart the Neanderthals as a group that is distinct from modern humans.

The focus of most of the earlier work has been on the particularities of Neanderthal features rather than a means of understanding the evolutionary and adaptive processes that led to their distinctiveness or what led to the diversity within modern humans and their distinctiveness from earlier hominins. Using a comparative method to distinguish Neanderthal morphology from that of recent modern humans is useful but only when seen in the context of evolutionary biology and adaptive history. There are three main external influences that need to be considered when interpreting the functional meaning of curvature, which is known to show a wide range of intraspecific variation in modern humans. The first is the effect of body size on curvature, because mammals show positive allometry with curvature. Ruff *et a.l* (1997) proposed that Neanderthals are on average 30% larger than recent humans and that early modern humans are about 10% larger than recent modern humans (Ruff *et al.*, 1997). If curvature is related to body mass, it is predicted that Neanderthals will have higher degrees of curvature than both early and recent modern humans. Within modern humans, populations with the highest body mass are predicted to be more curved than those with lower body mass.

The second influence that needs to be investigated is the effect of habitual behaviour on curvature. Modern humans and Neanderthals most likely did not differ in their subsistence strategies and were probably both hunting and scavenging (Lieberman, 1989; Bar-Yosef, 2004; Pearson *et al.*, 2006). Although there may have been differences in their hunting practices (Marean and Assefa, 1999; Marean and Assefa, 2005; Speth and Tchernov, 1998), their resource acquisition and overall workload involved high activity levels, and this is apparent in the similarities in their post-crania (Lieberman, 1989; Trinkaus *et al.*, 1989) If curvature is a response to activity levels in human populations, it is predicted that Neanderthals, having high activity levels, will display similar levels of degree of curvature to early modern humans and other hunter-gatherers. Within modern humans, it is predicted that individuals and populations with lower activity levels will exhibit lower degrees of curvature.

Thirdly, it is necessary to consider the effect of climate on curvature. Many of the distinctive Neanderthal postcranial features are the consequence of a hyperpolar body form (Hublin, 1989; Ruff, 1991; Weaver, 2003; Weaver and Steudel-Numbers, 2005). If the reported high degree of curvature in Neanderthals is one of those cold-adapted characteristics, recent human populations

from higher latitudes would be predicted to possess higher levels of curvature than those from lower latitudes. Neanderthals, being reported as "hyper-polar" (Weaver, 2003), would be predicted to have a higher degree of curvature than any modern human population. Climatic adaptations in humans are known to become genetic adaptations over time. In Neanderthals and modern humans alike, it is expected that if there were a strong effect of climate on curvature that this would have been established in the population genetically rather than only through individual ontogeny. Through the process of genetic drift and isolation, over time the distribution of the variation in curvature may have become a feature that has taxonomic value.

By identifying the taxonomic value of curvature it may be possible to hypothesize about the relationship between early modern humans and Neanderthals. If Neanderthals are distinct in their long bone curvature from early modern humans, and early modern humans resemble recent modern humans more than they do Neanderthals, (Trinkaus and Shipman, 1993; Churchill, 1998; Golovanova *et al.*, 1999; Weaver, 2003; Yamanaka *et al.*, 2005 but see Shackelford and Trinkaus, 2002). This would support the hypothesis that Neanderthals were excluded from the evolutionary past of modern humans.

1.4. Layout of the thesis

The second chapter provides an overview of human and Neanderthal variation in femur and lower arm anatomy and their biomechanical properties. The chapter continues with a discussion of the possible factors influencing curvature and concludes by outlining the specific hypotheses and associated predictions in order to address the first objective described above.

Chapter 3 describes the materials, methods and statistical approaches used in this research and ends with the order of analysis. Chapter 4 contains the results of the analyses of long bone curvature in recent modern humans. The results of the femur are presented first, followed by the results for the lower arm. The chapter concludes with a discussion of the variation in long bone curvature in modern humans and summarises the predictions for the analyses on Neanderthals and early modern humans. The results for fossil populations are presented in Chapter 5. Finally, Chapter 6 discusses the results and conclusions from this study.

CHAPTER 2. HISTORY OF RESEARCH ON LONG BONE CURVATURE

2.1. Femur

2.1.1. Comparative anatomy of the femur

Hominins like *Homo habilis, Homo erectus, Homo heidelbergensis* and *Homo neanderthalensis* are remarkable in the similarity of their femoral morphology (Kennedy, 1983b, 1983a, 1984). This morphology includes antero-posterior flattening of the shaft reflected in the virtual absence of a pilaster, low neck-shaft angle, medial convexity of the shaft, a very low minimal shaft breadth (waisting) and a medially expanded cortex at the mid-shaft level (compared to anatomically modern humans where the cortex is thickest on the lateral side of the shaft). This results in a more distal crossover of the biomechanical axis with the shaft axis (Kennedy, 1983a; Aiello and Dean, 1990).

Both Trinkaus (1993) and Kennedy (1983a, b) have suggested that the medial convexity of the diaphysis and low neck-shaft angles are a result of higher activity levels (Kennedy, 1983b, 1983a; Trinkaus, 1993 but see Czarnetzki, 2000). They suggest that this high activity level causes the femur to be more medially convex proximally and to develop a larger transverse diameter at mid-shaft (Kennedy, 1983b, 1983a; Trinkaus and Ruff, 1999b). More recently, however, researchers have argued that these features in Neanderthals might be a secondary consequence of a cold-induced body form, related to wider hips and more robust extremities caused by the interaction between genetically determined body proportions and the magnitude of mechanical stress during ontogeny or the direct consequence of variation in relative body size in individuals with cold-adapted bodies (Ruff, 1995; Weaver, 2003).

A cold-adapted body form and wider pelvis may also explain the greater degree of femoral curvature observed in Neanderthals. The wider pelvis may result in different angles of hip joint reaction force relative to the femur and affect the neck-shaft angle and torsion as the head of the

femur would be articulating in a more lateral position than in anatomically modern humans (Ruff, 1995). If the iliac blades are oriented differently, this may lead to a more anterior or posterior orientation of the acetabulae. Alternatively, the wider pelvis may simply cause an increased distance between the acetabulae. Both these cases may lead to higher degree of curvature in order to attain a hominin valgus angle.

2.1.2. Intraspecific variation in femoral curvature.

In addition to the literature on Neanderthal femoral curvature (see Chapter 1: Introduction) several studies have investigated differences in femoral curvature among and between human populations in the light of biomechanical adaptation and forensic science.

Forensic anthropologists studied femoral curvature as it was suggested to be a valuable tool to distinguish race in human remains (Stewart, 1962; Walensky, 1962, 1965; Gilbert, 1975, 1976; Trudell, 1999). Stewart (1962) demonstrated that there was a difference in the expression of anteroposterior curvature of the femur between Caucasians, African-Americans and Native Americans (Dakota). Femoral curvature was measured as subtense by placing the distal condyles on a flat surface (Figure 2-1) and raising the proximal end so that the maximum concavity (deepest point on the anterior surface) on both distal and proximal ends are at the same level (the levelling point). Then the distance was taken from the table to the most anterior side of the femur. The analyses showed that shaft curvature was most pronounced in the Native Americans and least pronounced in African-Americans and that Caucasians occupied an intermediate position.

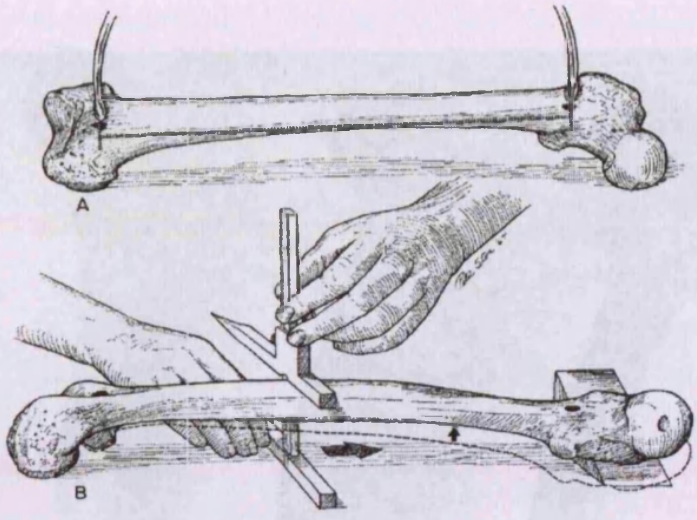

Figure 2-1 Subtense method employed by Walensky (1962).

Native Americans also showed a greater amount of torsion compared to African-Americans and Caucasians, with African-Americans showing the least amount. Individuals with higher degree of torsion also displayed a lower apex of curvature.

The positive correlation between curvature and torsion (Stewart, 1962) was not investigated further in subsequent studies on femoral curvature. Stewart concluded that although femoral curvature does not, as a rule, distinguish between races, a femur with a marked degree of femoral curvature combined with a low degree of torsion distinguished a large proportion of the Native Americans from the Caucasians and African-Americans who have a lower degree of curvature with a high torsion angle (Stewart, 1962).

Walensky (1965) confirmed Stewart's separation of Caucasians, Native Americans and African-Americans when he included the Inuit (Figure 2-2). He concluded that curvature increased with age and population-related functional activity and that differences in postural habits contributed to these racial differences in femoral curvature (Walensky, 1962, 1965).

Figure 2-2 An African-American, Inuit and a Native American femur (from Walensky, 1965) showing increasing amounts of curvature and lowering apices of curvature.

In 1976, Gilbert conducted an investigation into the possible causal factors of femoral curvature in Caucasians, Native Americans and African-Americans (Gilbert, 1976). He expanded Stewart (1962) and Walensky's (1965) sample with seven additional Native American groups representing both pre- and post-colonial samples and looked at their postural habits in relation to their curvature. When only the North American Native Americans were taken into account, together with the African-Americans and Caucasians, Stewart's techniques distinguished Native Americans from African-Americans or Caucasians. However, when he included Native South

American samples, the two groups combined showed only slightly more pronounced femoral curvature than African-Americans. The South American femora were less curved than those of Caucasians and North American Natives. Gilbert (1976) concluded that femoral curvature was not such a useful tool in race assessment and set forth to look into possible causal factors of the trait (Gilbert, 1975).

One of the hypotheses Gilbert (1976) tested was the effect of the equestrian foraging lifestyle of the North Americans of the South Dakota area (Arikara: two sites dating between 1730 – 1830 AD) on femoral curvature, but he noted that the non-equestrian communities had the same degree of curvature as the equestrian ones. The possibility that the Peruvian Natives were less bowed because they were from an earlier sample was refuted because a more recent sample fell within the same range of variation as the ancient sample (Gilbert, 1976).

As mentioned in the previous section, variation due to climate was refuted when Gilbert noted that two groups, living in the same region, showed two different ranges of curvature and that the Inuit, expected to have the most curved femora, were identical to those Natives living in the South. Gilbert (1976) argued that there was little variation in postural habits between the groups and therefore could not support Walensky's hypothesis that femoral curvature depended on postural habits. Instead, he argued that femoral curvature was genetically based but remained plastic and was influenced by gross body weight rather than by temporal, climatic, postural or equestrian influences. He suggested that obese individuals have a more anterior centre of gravity which resulted in greater curvature. He did not follow up on the relation between torsion and femoral curvature (Gilbert, 1976).

Primate long bones are less curved than the long bones of other mammals. Although in most anthropoids bones there is an increase in curvature with body size (Swartz, 1990), experimental work has shown that the ontogenetic development of bone curvature in mammals depends on normal muscle activity and weight-bearing (Lanyon, 1980) and is not influenced by individual variation in body weight. Whether this is the case in humans needs to be determined.

Trudell (1999) revisited race assessment through measurement of anterior femoral curvature and concluded that by increasing the number of measurements taken on the bones, it is possible to discriminate African-Americans and Caucasians (Trudell, 1999). Maximal, bicondylar and oblique length were measured as were the midshaft and subtrochanteric diameters. The curve

was measured along three points as the distance from a flat surface when the femur is positioned in horizontal position and balanced on two blocks with the distal condyles both touching a surface (Figure 2-3) (Trudell, 1999).

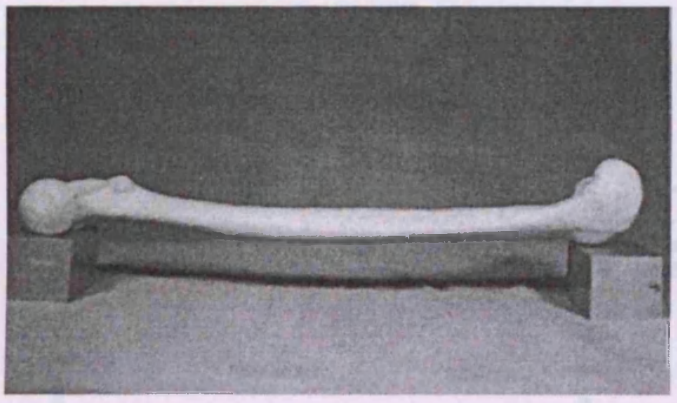

Figure 2-3 Trudell's method of measuring curvature by placing the femur on two blocks (Trudell, 1999).

A discriminant analysis with cross-validation on a series of standard femoral measurements and the three curvature distances of individuals of known sex and age category (below or above 30 years) provided an average accuracy of race determination of 87.12% for both left and right femur. This study was restricted to African-Americans and Caucasians but illustrates the advantage of taking more detailed measurements (Trudell, 1999) and the need to study wider ranges of human populations.

The lack of concordance among the research results presented above demonstrates that there is a need to investigate the variability of femoral curvature among a geographically and behaviourally varied range of populations.

2.1.3. Biomechanics acting on femoral curvature

To push the body upwards, i.e. when walking uphill, muscle forces extend the hip and the knee. Three of the hamstring muscles (semi-tendinosus, semi-membranosus, long head of the biceps femoris) extend the hip but do not create a significant bending moment in the bone and load it in uniaxial compression (Figure 2-4) (Frost, 1967). The fourth hamstring muscle (short head of the

biceps femoris) adds a posterior bending force to the femur. The gluteus maximus and the two gastrocnemii apply bending stress that bend the femur so it is convex posteriorly (Frost, 1967; Cristofolini *et al.*, 1995; Duda *et al.*, 1996; Lengsfeld *et al.*, 1996; Duda *et al.*, 1997; Duda *et al.*, 1998; Trinkaus *et al.*, 1999b; Shackelford and Trinkaus, 2002; Hall, 2004).

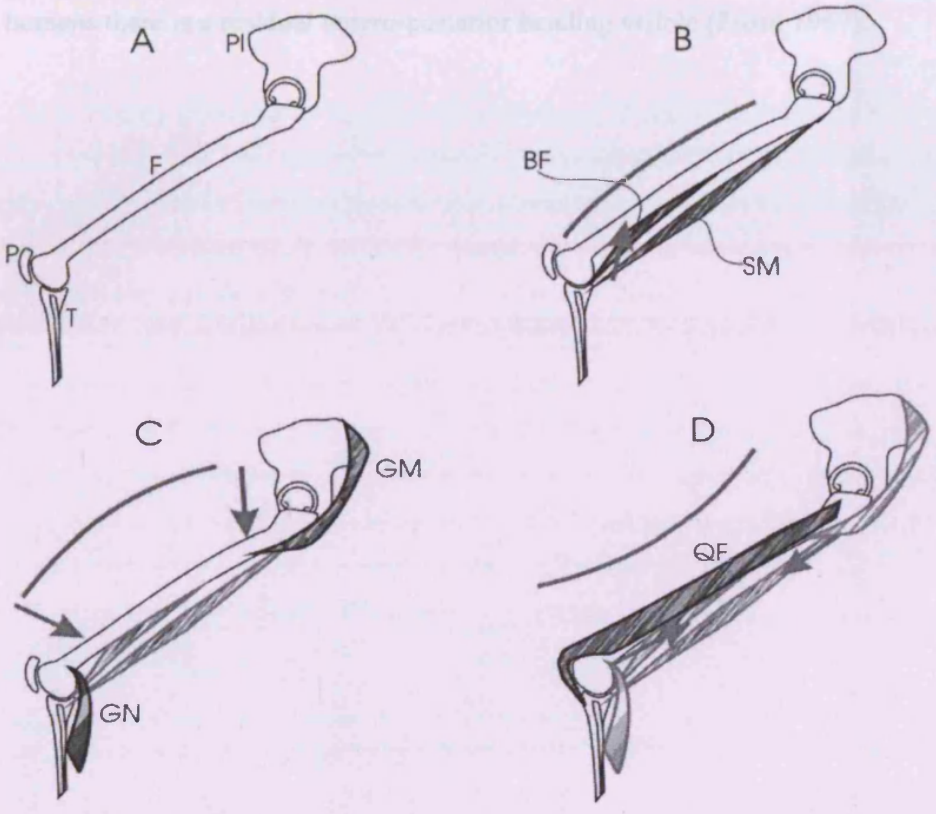

Figure 2-4 Muscles acting on the femur.

Pl: pelvis. F : femur. P :patella. T : tibia. SM : three muscles; semitendinosus, semimembranosus, long head of the biceps femoris. GM: gluteus maximus. GN: gastronemius. QF: quadriceps femoris. A: The femur of a man walking up a step. There is a bending force acting on the femur making it posteriorly convex. B: SM are three of the four hamstring muscles. They extend the hip and do not create bending moments but compression. The short head of the biceps femoris (BF) adds posterior bending. C: The gluteus maximus bends the femur so that is posteriorly convex. The gastrocnemii add to this bending force. D: The quadriceps bends the femur in the opposite way. This dynamic interacting muscle system minimises bending forces in the femur (after Frost, 1967).

The quadriceps muscles exert stress on the femoral shaft in the opposite direction than the gastrocnemius, short head of the biceps femoris and the gluteus muscle so that the shaft is anteriorly convex, creating a balance in the muscle forces acting on the diaphysis. This balance minimises the bending stresses on the femur (Frost, 1967). In most quadrupeds, this balance is close to perfect and femora show little or no anteroposterior curvature in the diaphysis. In humans there is a residual antero-posterior bending visible (Frost, 1967).

2.2. Radius and ulna

2.2.1. Comparative anatomy of lower arm anatomy

From the well pronounced muscle articulations on all upper limb bones, it is suggested that Neanderthals had very powerful forearms (Trinkaus and Churchill, 1988). There are features in the ulna and radius that distinguish Neanderthals from modern humans (Fischer, 1906; Patte, 1955; Trinkaus and Churchill, 1988; Aiello and Dean, 1990; Vandermeersch and Trinkaus, 1995; Pearson and Grine, 1997).

The proximal ulna is different in that the trochlear notch is oriented more anteriorly in Neanderthals than it is in modern humans. Trinkaus and Churchill (1988) propose that this would not have limited the range of movement but was rather an expression of different habitual behaviour such as the increased use of forearms with the elbow flexed. The pronator quadratus crest is very pronounced and also suggests a more muscular forearm, although the interosseous crest is poorly developed and the shaft is relatively narrow (Trinkaus and Churchill, 1988; Aiello and Dean, 1990).

The supinator crest is strongly developed and the shaft shows a greater degree of lateral curvature than that found in modern humans. This may indicate that Neanderthals closely resemble earlier hominins in the morphology and strength of the radius and that the Neanderthal forearm and elbow was especially strong during pronation and supination (Trinkaus and Churchill, 1988).

The position of the radial tuberosity is a measure of lever advantage of the biceps brachii. In the apes, it is positioned more medially. This gives apes a greater mechanical advantage of the biceps brachii in supination. The tendons wrap themselves around the radial shaft and the medial position of the insertion and increases the distance between the proximal and distal insertion of the muscle and results in a larger medial rotation axis of the forearm. If the radial tuberosity is placed more antero-laterally, as it is in modern humans, then power advantage is lost during the

final phases of supination (Trinkaus and Churchill, 1988; Aiello and Dean, 1990; Pearson and Grine, 1997).

The radius curves mainly in a medio-lateral plane while the ulna tends to curve in a dorso-ventral plane. A greater distance between them increases the distance between the insertions of the pronator quadratus and the pronator teres. African apes are less curved than other mammals. Swartz (1990) suggests this is due to long bones of primates being longer than those of other mammals and will therefore produce larger bending stresses during normal locomotion. Higher degrees of radial curvature in anthropoids have been explained to be the result of an increase in size and functional importance of the supinator musculature, but in gibbons was not affected by differential muscle mass (Swartz, 1990). Compared to humans however, apes have a higher degree of lateral curvature. The higher degree of curvature in African apes (Martin and Saller, 1959; Knussman 1967 in Swartz, 1990) and a more lateral insertion of the pronator teres increases the lever advantage (Aiello and Dean, 1990).

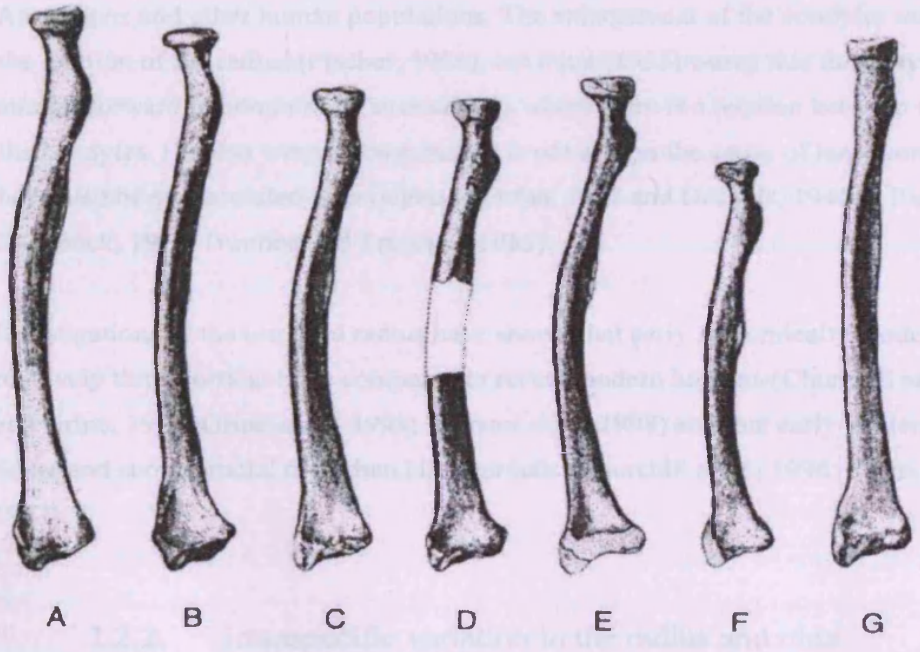

Figure 2-5 Hominoid radii.

Right radii of A=*Gorilla*, B=*Pan*, C=*Pongo*, D= La Chapelle-aux-Saints, E= La Ferrassie I, F= La Ferrassie II, G= recent European (After Czarnetzki, 2000).

The lateral subtense of the radius of the Neanderthals is remarkable and falls on or beyond the higher limits of the modern human variation (Fischer, 1906; Botez, 1926 in Patte, 1955; Vandermeersch and Trinkaus, 1995; Carretero *et al.*, 1999; Czarnetzki, 2000) (Figure 2-5). Although some confusion exists about which technique yields the most accurate measurement of curvature of the lateral side of the radius (See Martin and Saller, 1959 for four different methods to measure curvature), only Fischer (1906) reports a size corrected measure or an index of curvature (subtense/maximum length*100). Quantification of the posterior curvature of the ulna using a subtense technique (Fischer, 1906; Martin, 4a) is not as straightforward as it is for the more evenly shaped bones such as the femur and the radius, but Neanderthals have been described as having a large posterior subtense in the ulna (Fischer, 1906).

The head/length ratio of the radius (head diameter/length*100) is larger in the Neanderthals than it is for any other human population, but there is a large range of variation within modern humans (Patte, 1955). Fischer (1906) and Patte (1955) also report an enlarged distal condyle for the Neanderthals and comment on the presence of this enlargement in Japanese, Africans, Australians and other human populations. The enlargement of the condyles may be caused by the rotation of the radius (Fischer, 1906), but Patte (1955) warns that this may not be as straightforward in hominins as in mammals where there is a relation between rotation and size of the condyles. He also warns biomechanics is not always the cause of large condyles but that they have also been associated with rickets (Marfan, 1912 and Decugis, 1941 in Patte, 1955; Steinbock, 1976; Ivanhoe and Trinkaus, 1983).

Investigations of the ulna and radius have shown that early anatomically modern humans have relatively thick cortical bone compared to recent modern humans (Churchill *et al.*, 1996; Pearson and Grine, 1997; Grine *et al.*, 1998; Pearson *et al.*, 1998) and that early modern humans have a ticker and shorter radial neck than Neanderthals (Churchill *et al.*, 1996; Pearson and Grine, 1997).

2.2.2. Intraspecific variation in the radius and ulna

There are very few studies on variation in longitudinal curvature of the radius and ulna within modern humans. A summary of the morphological variation in modern humans in the ulna and radius is described below.

Within recent human populations, the distal limb segments (tibia and radius) tend to exhibit more relative variability (size independent) than the proximal segments, especially in the lower limb (Holliday and Ruff, 2001). Males and females appear to be slightly different in this pattern. Females vary to an equal degree in both upper and lower distal segments, whereas males show most variability in the lower limb (Holliday and Ruff, 2001). These differences are believed to be allometric since males are larger than females and this allometry can also be found when looking at between-group differences in, for example, cold- and warm-adapted populations (Holliday and Ruff, 2001).

Research on recent human variation of the ulna and radius is limited and most of it dates back to the early 20th Century. In 1906, Fischer made an in-depth study of the variation of the radius and ulna and included both Neanderthal casts and recent modern human populations from different geographic origins. His sample of modern humans consisted of Europeans, Africans, Australians, Polynesians, Melanesians, Birmese, Tierro del Fuegans, Ainu, Japanese, Philippinos and prehistoric Egyptians. Patte (1955) included this study and others in his book on Neanderthals and summarised some of the main differences between modern humans and Neanderthals.

Lapps, Japanese and Medieval Europeans have more robust radii than do Neanderthals. The Africans have the smallest robusticity index but there is a large amount of variation. Also, the Neanderthal ulna is robust for its size (Fischer, 1906; Patte, 1955).

Fischer (1906) reports a mean index for humans in lateral subtense of the radius ranging from 2.5 for the Tierra del Fuegans to 3.2 for the Europeans compared to a mean of 7.4 (S.D.=2.5, n=5, summary data from Carretero *et al.*, 1999) for the Neanderthals. Klaatsch (1901) suggests that radial curvature is a hereditary trait. However, because humans are generally born with straight ulnae and radii, Rouvière (1939, in Patte, 1955) argues that radial lateral curvature is a biomechanical adaptation to the strong development of the flexor muscles of the fingers and thumb.

The mediolateral curvature of the anterior surface of the ulna is difficult to describe because of the sinusoidal shape of the diaphysis. Fischer (1906) used diaphyseal angles for each curve in the anterior ulna and found that Europeans are the least curved, and that Australians and Tierra del

Fuegans possess the highest degree of curvature. Patte (1955) does not repeat this method and does not comment on the curvature of the ulna in Neanderthals.

Fischer (1906) measured the angle the radial tuberosity makes with the perpendicular plane through the styloid process and the ulnar notch. This measurement will give the angle that the radial tuberosity deviates from the axis through the interosseous crest. Modern humans range from 0° to 85° (Fischer, 1906) with the majority ranging between 45° and 60° (Boule and Vallois, 1952). There is a large range of variation within single populations with angles. For example, Europeans range from 22° - 67° (mean=50.2°) and Africans from 39° -85° (mean=63.3). Although a very high angle (from 81° Spy 1 – 88° Neanderthal) was considered a derived Neanderthal feature, in more recent papers, the angle of the radial tuberosity is approximated qualitatively, and it was concluded that although Neanderthals have a very high angle and therefore a more medially oriented radial tuberosity, they do not fall outside of the range of variation of modern humans (Trinkaus and Churchill, 1988; Vandermeersch and Trinkaus, 1995).

Fischer (1906) suggests a correlation between the length of the biceps bracchii muscle tendon and the position of the radial tuberosity. When the arm is part flexed in pronation, with the hand in supination or semisupination, there is a strain on the biceps and therefore the tendon and the tuberosity moves. Habitual use of the arm in that position can cause the individual differences observed in the orientation of the radial tuberosity (Fischer, 1906; Trinkaus and Churchill, 1988; Aiello and Dean, 1990).

When radial neck length is corrected for size by the radial length, the Neanderthals have a relatively long radial neck for radial length and fall with the Africans and Chinese rather than with the Europeans (Vandermeersch and Trinkaus, 1995). A longer radial neck makes the biceps brachii more effective as it has more lever advantage and therefore greater power. There is a large range of variation in radial neck-shaft angle within modern human populations but the Europeans have been suggested to have the largest when compared to other populations (Fischer, 1906).

The joint-axis angle (or neck-shaft) of the ulna is the angle the trochlear notch makes with the shaft axis and is measured by finding the angle between the sagittal axis of the trochlear notch and the shaft axis. In humans, it varies between 0° and 28° and Australians, Phillipinos and

Tierra del Fuegans have slightly higher angles, but there is no trend among populations and no correlation between angle and curvature was observed (Fischer, 1906).

Very few studies have explored the behavioural and environmental factors on lower arm morphology. Robusticity of the upper limb, however, has been investigated in relation to climate and habitual behaviour (Stock, 2002; Stock and Pfeiffer, 2004; Stock, 2006). Although climate has a significant influence on patterns of diaphyseal robusticity, patterns of robusticity of the upper limb correspond best to marine mobility especially in the distal limb elements. This suggests that there may be greater diaphyseal plasticity further away from the trunk and that differences in bone mass in the lower arm are more relevant for functional interpretation of archaeological and fossil samples without being constrained by the energetics of bipedal locomotion (Stock, 2002; Stock and Pfeiffer, 2004; Stock, 2006).

2.2.3. Biomechanics acting on lower arm curvature

The elbow joint acts as a lever and is composed of the humero-ulnar, humero-radial and proximal radio-ulnar joints. All are encapsulated by collateral ligaments. The humero-ulnar joint is composed of the trochlea that articulates with the trochlear fossa of the ulna. This joint serves in flexion and extension. The humero-radial joint is lateral to the humero-ulnar joint. It is formed between the distal part of the humerus and the head of the radius. This joint is not fixed but is restricted in its movement by the humero-ulnar joint. It is used during flexion, extension, supination and pronation. In the proximal radio-ulnar joint, the head of the radius articulates with the radial notch of the ulna. This joint pivots during pronation and supination making the radius roll over the ulna in a medial and then lateral fashion (Frost, 1967; Hall, 2004).

The large number of muscles producing the range of motion of the elbow and forearms complicates a force-analysis for this complex of joints. It is assumed, however, that the strongest flexor muscle of the elbow is the brachialis. Distally, brachialis inserts below the coronoid process. Another elbow flexor, the biceps brachii, inserts in the radial tuberosity and is strongest during supination. The brachio-radialis also aids in flexion and is most effective in the neutral position (between pronation and supination). Its distal insertion is in the base of the styloid process on the lateral aspect of the radius. The strongest extensor muscle is the triceps. The three heads of the triceps insert on the olecranon process of the ulna with a common tendon. The

anconeus muscle attaches to the lateroposterior aspect of the ulna and is only a minor extensor of the elbow (Frost, 1967; Hall, 2004).

The pronator teres muscle, the supinator and the pronator quadratus are involved in pronation and supination. These are inserted in the proximal and distal radio-ulnar joints. The interosseous space between ulna and radius determines the degree of pronation and supination an individual can achieve (Yasutomi *et al.*, 2002). Yasutomi (2002) used three dimensional models to reconstruct different sizes of interosseous space and found that when the axis of rotation in pronation and supination passed through the interosseous region the rotation was more than 40% radially, ulnarly, anteriorly and posteriorly. However, when the axis of rotation was deviated from this region, there was significant loss of supination and pronation (14% radially, 7% ulnarly, 5% anteriorly and 4% posteriorly) and restriction by the elastic interconnecting membrane (Yasutomi *et al.*, 2002).

The pronator quadratus is the major pronator muscle and is assisted by the pronator teres. The pronator quadrutus attachments are on the lower anterior ulna and the lower anterior radius. The pronator teres inserts laterally in the middle of the shaft of the radius and has a minor role in flexion. The supinator muscle is the major supinator and is assisted by the biceps when the elbow is flexed to 90° or less. The supinator muscle inserts on the lateral proximal part of the ulna and the lateral proximal part of the radius (Hall, 2004).

The elbow is not a weight-bearing bone but sustains large loads throughout its activity cycle. Most of the compressive loading is at the elbow and greater forces are generated when the hands are rotated in pronation. Larger forces are also generated during certain activities. As the attachment of the triceps muscle on the ulna is closer to the elbow than are the brachialis and the biceps, the moment arm is smaller and because of this lever advantage, the flexor muscles have to generate less force than the extensors to create the same amount of joint torque (Frost, 1967; Hall, 2004).

2.3. Possible causes for variation in long bone curvature

2.3.1. Neanderthals and rickets

Some scholars have suggested that Neanderthal curvature in the ulna and radius is the result of rickets (Ivanhoe, 1970; Ivanhoe and Trinkaus, 1983; Czarnetzki, 2000) or osteomalacia (Czarnetzki, 2000). Rickets is a medical condition whereby the osteoid (the organic material in bone) fails to calcify in a growing animal or human. Individuals with rickets have a deficient vitamin D metabolism. Other dietary deficiencies in the calcium or phosphorus metabolism may produce rickets. This results in skeletal deformity and short stature.

Figure 2-6 X-ray image of an infant with severe rickets.
Note the medio-lateral curve as opposed to the the antero-posterior curve observed in Neanderthals. From www.dwb.unl.edu (last accessed 19/06/2008)

Natural vitamin D is formed in the skin under the stimulus of ultraviolet light and is present in fish liver oil (Stuart-Macadam and Iscan, 1989; Wood *et al.*, 1992). Because there is no widespread evidence of Neanderthals eating fish (with the exception of shell fish consumption at Gibraltar) (Hockett and Haws, 2005) and their inhabitation of the Northern regions of Europe, Ivanhoe suggests Neanderthals experienced an insufficient amount of vitamin D in their diet and as a consequence of rickets show skeletal deformities such as abnormal long bone curvature (Ivanhoe, 1970; Ivanhoe and Trinkaus, 1983; Czarnetzki, 2000). However, the curvature observed in Neanderthals is an accentuation of normal anteroposterior curvature of the diaphysis (Steinbock, 1976) and never assumes the irregular mediolateral curvature associated with rickets (Figure 2-6) (Ivanhoe and Trinkaus, 1983). Neither does rickets explain the observed variation in anterior curvature between modern human populations.

2.3.2. Biomechanics and bone remodelling

Wolff's Law states that bones grow and remodel throughout an individual's life in order to adapt to their mechanical environment. The bone senses, transduces, and responds to loads by molecular and physiological mechanisms (Pearson and Lieberman, 2004; Ruff *et al.*, 2006).

Long bones of other terrestrial mammals also display some longitudinal long-bone curvature and the magnitude of this may vary across bones, species and even between individuals (Lanyon and Baggott, 1976; Lanyon, 1980; Biewener, 1983; Lanyon, 1987; Swartz, 1990). Several mammals have been used in experimental studies to investigate the functional meaning and development of longitudinal curvature and how this may affect strain and stress distributions in the shaft (Frost, 1967; Lanyon and Bourn, 1979; Lanyon, 1980; Biewener, 1983; Lanyon, 1987; Bertram and Biewener, 1988; Pead and Lanyon, 1990; Swartz, 1990; Les *et al.*, 1997; Main and Biewener, 2004; Yamanaka *et al.*, 2005). Several studies (Lanyon, 1980; Biewener, 1983; Bertram and Biewener, 1988; Bertram and Biewener, 1992; Biewener and Bertram, 1994; Main and Biewener, 2004) have established that if there is an absence of loading from muscle activity and weight-bearing during ontogeny, long bones fail to develop their appropriate bone mass or longitudinal curvature, despite achieving their normal length. Lanyon (1980) concluded that there are certain aspects of bones that are genetically determined but that other features require a normal mechanical environment to develop.

Lieberman and Pearson (2001) performed an experimental study testing the hypothesis whether cortical bone growth (modelling) and repair (Haversian remodelling) are responses to exercise-induced mechanical loading and whether the remodelling varied with loading and the position in the skeleton. Exercised juvenile sheep had higher periosteal modelling than Haversion remodelling rates than non-exercised controls (Lieberman and Pearson, 2001). Mid-shaft periosteal growth was higher proximally and mid-shaft Haversian remodelling was higher distally. Growing animals thus modulate modelling versus remodelling ,respectively ,to loading at different skeletal locations. This is to optimize cross-sectional strength relative to the kinetic energy cost of accelerating added mass (Lieberman and Pearson, 2001). Ruff *et al.* (2006) suggest that rates of remodelling and rates of bone turnover vary greatly at different skeletal sites and that there is no simple relation between the orientation of loads, such as strains and stresses, and the cross-sectional geometry of long bones (Lieberman and Pearson, 2001; Ruff *et al.*, 2006).

If, however, curvature only develops under a normal developmental activity regime, it can be assumed that it has a functional advantage to either the bone itself or to the anatomical structures around it. The relationship between forces and modelling and remodelling of long bones is complex. If one considers the long bone as a long and slender beam, it is assumed that the optimal function of this bone to resist applied stresses and minimise strain is through axial compression (Frost, 1967; Bertram and Biewener, 1988; Hall, 2004). This loading configuration distributes most material in the plane of deformation, and cortical bone is stronger under compression than under tension (Frost, 1967; Lanyon and Baggott, 1976; Lanyon, 1980; Bertram and Biewener, 1988; Pead and Lanyon, 1990; Hall, 2004). Applying axial loading to a bone that is longitudinally curved, results in a bending moment that is proportional to the displacement of the diaphysis perpendicular to the longitudinal interarticular axis (Frost, 1967; Swartz, 1990; Hall, 2004). Because of this bending, tensile and compressive stresses are unevenly distributed through the bone and even small external loads can create large strains within the bone (Lanyon, 1980). Reducing curvature while axially loading long bones should result in the lowest strain levels.

However, the long bones of mammals are not loaded purely axially and long bones can experience significant bending moments due to curvature and muscle and joint reaction forces that are not perfectly aligned with the axis of the bone (Bertram and Biewener, 1988). Also, in

the human femur, the positions of the articulation and muscle attachments, such as the medial displacement of the femoral head (Trinkaus, 1993; Anderson and Trinkaus, 1998), and the contraction of the adductor and gluteal abductor muscles, cause the femur to be subjected to some degree of mediolateral bending (Ruff, 1995). In one legged stance, most of that bending stress may be reduced through associated tension in the iliotibial tract and musculature (Lengsfeld *et al.*, 1996; Taylor *et al.*, 1996; Les *et al.*, 1997; Simões *et al.*, 2000). Ruff (2000) suggests that anteroposterior bending could be the cause of anteroposterior expansion of the femoral midshaft in response to high activity and mobility levels (Ruff, 2000b).

Taylor and colleagues (1996) investigated loading through the femur in one-legged stance in humans by measuring the dominant mode of loading in the femur in a finite element analysis. In a finite element analysis the material properties and loading of the skeletal elements or joints are modelled and analysed to better understand the biomechanics and orthopedics (Richmond *et al.*, 2005). The results showed that the human femur is loaded primarily through compression rather than through torsion or bending (Taylor *et al.*, 1996). They also found that the anterior and posterior stresses on the femur are negligible and that this is probably due to the reduction of overall bending stresses in the femur due to the application of muscle forces. If a bone is loaded in bending, this would increase the biological and locomotor cost of bone production because the bone would need to resist these stresses and consequently be thicker (Taylor *et al.*, 1996; Skerry, 2008).

When the femur is loaded through bending stress, one would expect deflection of the femoral head and an uneven load transfer through the distal condyles but evidence shows uniform pressure distribution in both condyles (Taylor *et al.*, 1996). The major limitation of this study was that it was done during one phase of gait and therefore is not necessarily applicable to the whole gait cycle. It may be that the loading stresses differ throughout the cycle but anatomical features of the femur suggest this is not so.

Duda *et al.* (1996) found that differences in muscle attachments result in different biomechanical properties of individuals. Not only is bone remodelled when applying different stresses, but so are the soft tissues such as muscles and tendons. Duda *et al.* also recognise that when one neglects the major muscles, compression, bending and torsion may be overestimated and not play as significant a role as first assumed and return the diaphyseal bending stresses to ones of axial compression (Duda *et al.*, 1997; Duda *et al.*, 1998).

Modelling the system of interacting muscles and bone in stance is important for understanding the functional significance of curvature but does not explain differences in femoral curvature between individuals as it remains difficult to measure the *in vivo* levels and distributions of diaphyseal strains in individuals (Pedersen *et al.*, 1997). Also the complex ways in which muscles or parts of muscles contract and of joint reaction forces during gait with varying burden-carrying levels in a natural setting, make it impossible to fully understand the resulting strains in the femur, especially as there is evidence for variation in the human femoral muscles that would certainly affect the muscle forces applied to the femur (Duda *et al.*, 1996). Nonetheless, it remains possible that curvature serves to lower bending stresses relative to straight bones by reducing bending moments placed on the diaphysis and in that way returning the bone to an environment of axial compression (Frost, 1967; Hall, 2004).

Most experimental work though, has demonstrated that curvature increases bending strains and that the direction of the curve does not necessarily correspond with the tension surface of a bone when it is loaded (Lanyon and Baggott, 1976; Lanyon and Bourn, 1979; Lanyon *et al.*, 1979; Lanyon, 1980; Biewener, 1983; Lanyon and Rubin, 1986; Lanyon, 1987; Swartz, 1990; Simões *et al.*, 2000). For a weight-bearing bone, longitudinal curvature may be crucial because it reduces the ability to withstand high levels of loading and be a compromise between bone strength and predicting bending strains and material failure (Lanyon, 1980, 1987; Bertram and Biewener, 1988). Bertram and Biewener (1988) argue that axial compressive loading is unstable as a catastrophic shift from compressive stress to bending stress in a straight column is equally likely to bend in a random direction. A curved bone, however, is more likely to bend in the direction of its longitudinal curvature regardless of the orientation of the bending moment applied to the bone and is therefore predictable. Alexander (1981) demonstrated that structures that are likely to be subjected to unpredictable loads would need to build in a safety factor for maintaining the biological structure, even if that safety factor would be more metabolically costly to maintain and transport (Alexander, 1981). The final anatomy of the bone will thus be a compromise between the demands of load carrying (curvature negatively affects strength) and predictability (Bertram and Biewener, 1988).

Lanyon and Bourn (1979) also suggest that femoral bending may facilitate larger muscle packing and/or place the muscle vector more parallel to the diaphyseal axis. Curvature allows for the positioning of large muscle bellies while allowing the slender muscle attachments to be close

to the joints. Having muscles adjacent to the bone exerts pressure on the periosteum, increases bone resorption, and may cause curvature. This hypothesis is supported by the concavity of the radius and tibia of many mammals with respect to the flexor musculature, allowing for greater volume (Lanyon *et al.*, 1979; Lanyon, 1980).

The presence of intermediate strains from curvature-induced bending stress may also be advantageous for bone to maintain a minimum bone mass. Reduction of loading results in a decrease in bone mass (Lanyon and Baggott, 1976; Lanyon and Bourn, 1979; Lanyon *et al.*, 1979; Lanyon, 1980; Ruff *et al.*, 1991; van Der Meulen *et al.*, 1993; Carter *et al.*, 1996; Lieberman *et al.*, 2001; Lieberman and Pearson, 2001; Pearson and Lieberman, 2004; Ruff *et al.*, 2006). Therefore, if the bone was loaded in purely axial compression, there may not be enough strain for the bone to benefit physiologically. Strain levels can be increased by augmenting the degree of bone curvature or by reducing bone cross-sectional area and/or second moment of area until an optimum between physiological benefit and risk of failure has been achieved (Lanyon, 1980).

To summarise, there are four main biomechanical hypotheses explaining longitudinal curvature of the long bones: 1) curvature lowers bending stress by translating bending stress to axial compression (Frost, 1967; Hall, 2004), 2) curvature facilitates muscle expansion and packing (Lanyon *et al.*, 1979; Lanyon, 1980), 3) curvature is a compromise between bone strength and predictability of bending strains and material failure (Lanyon, 1980, 1987; Bertram and Biewener, 1988), or 4) generates strains necessary for optimal strength (Lanyon, 1980).

2.3.3. Body size

It is understood that loading of the long bone diaphysis is proportional to body mass (Ruff, 2000b). Robusticity, which is a response to loading, has an allometric relationship with body size (van Der Meulen *et al.*, 1993; Ruff, 2000a; Stock, 2002; Stock and Pfeiffer, 2004). Anthropoids show and overall positive allometry in their curvature (Swartz, 1990) so larger anthropoids have a higher degree of curvature. This allometric relationship is similar to that of a broader group of mammals (Swartz, 1990 but see Biewener, 1983; Bertram and Biewener, 1992) but primates are much less curved than mammals at any given size in order to allow for relatively longer limbs but retaining low levels of bending stress (Swartz, 1990).

2.3.4. Activity levels

Variation in robusticity levels is often suggested to be an adaptation to activity levels and habitual behaviour, and a substantial amount of research has focused on the changes in skeletal robusticity throughout human evolution and the evidence for overall gracilisation (Ruff *et al.*, 1993; Ruff *et al.*, 1994; Trinkaus *et al.*, 1994; Trinkaus *et al.*, 1999a; Pearson, 2000a, 2000b; Ruff and Trinkaus, 2000; Shackelford and Trinkaus, 2002; Shackelford, 2007). Several recent studies have also been conducted to understand patterns of skeletal robusticity in modern humans (Larsen, 1995; Ruff and Trinkaus, 2000; Stock and Pfeiffer, 2004; Stock, 2006; Carlson *et al.*, 2007). Understanding patterns in robusticity may aid in understanding long bone curvature if both are remodelling responses to similar strains and stresses.

The relationship between skeletal robusticity and habitual behaviour, and more specifically terrestrial mobility, has been investigated primarily using mid-shaft femoral cross-sectional geometry. This research is based on the prediction that repetitive anteroposterior loading on the lower limb during subsistence strategy-related terrestrial mobility will result in thickening of the cross-sectional geometry in the anteroposterior plane (Ruff, 1987, 1994a; Larsen *et al.*, 1995; Holt, 2003; Stock and Pfeiffer, 2004), and this is supported by the strength circularity indices (I_x/ I_y) at the femoral midshaft and its strong correspondence with terrestrial robusticity (Stock, 2006). If there is a correlation between robusticity and curvature, the anteroposterior bending that is observed may be a response to the increased curvature of the diaphyseal shaft.

Holt (2003) demonstrates there is a relationship between femoral anteroposterior bending strength, lower limb robusticity and declining terrestrial mobility from the Upper Palaeolithic through Mesolithic in Europe. Changes in postcranial robusticity with a shift away from hunting and gathering and the adoption of agriculture also suggest that increased sedentism is visible in the external (Ruff *et al.*, 1984; Larsen, 1995 but see Bridges, 1989a; Bridges *et al.*, 2000) and internal dimensions of long bones (Ruff, 1987; Brock and Ruff, 1988). This is supported by the higher prevalence and severity of osteoarthritis in hunter-gatherers compared to agriculturalists (Ortner, 1968; Larsen, 1983; Bridges, 1989b; Larsen, 1995). Although this pattern of decreasing robusticity is present in human populations, generally, males appear to be more pronounced in their reduction than females. This may reflect the changes in types of activity that were greater in males than they were in females (Ruff, 1987). This comparison of cross-sectional geometry and the anterior-posterior bending stress (I_x) and medial-lateral bending stress (I_y) is accompanied by a reduction in sexual dimorphism with the transition from hunting to gathering to agriculture (Ruff, 1994a). Sexual dimorphism in hunter-gatherers is the result of the role of males to travel long distances and hunting compared to the more sedentary role of females in gathering and childcare (Ruff, 1987).

Recently, robusticity has been investigated throughout the skeleton and there is a growing body of evidence that aquatic foraging and the habitual use of watercraft for subsistence has an influence on upper limb robusticity (Stock and Pfeiffer, 2001; Weiss, 2003; Stock and Pfeiffer, 2004; Stock, 2006; Shackelford, 2007). There is a trend for distal elements to show a stronger relationship between hypertrophy and behaviour but robusticity at femoral midshaft (measured as strength circularity index – shape index) shows the greatest correspondence to terrestrial mobility.

Recently, it has become increasingly clear that the relationships between postcranial robusticity, mobility and activity patterns are not as straightforward as initially believed and that levels of robusticity may vary at different sites of the bone (Stock, 2006). In the limbs, correlation between robusticity and terrestrial or marine mobility increases from proximal to distal. Therefore, stronger relationships would be expected between bone modelling and remodelling in response to strain in the distal elements compared to proximal elements (Stock and Pfeiffer, 2001; Stock, 2006).

Diaphyseal robusticity in the upper limb bones have often been used as evidence for differences in habitual behaviour throughout human evolution (Trinkaus *et al.*, 1994; Vandermeersch and Trinkaus, 1995; Pearson *et al.*, 1998; Trinkaus *et al.*, 1999a; Pearson, 2000a, 2000b; Ruff and Trinkaus, 2000) and Stock (2006) suggests that there is greater variability in the robusticity of the distal limb segments that is associated with habitual behaviour, especially in the mid-shaft of the ulna.

If long bone curvature is a response to activity levels and habitual loading, it is predicted to be highest in populations with high activity levels (Ruff *et al.*, 1984; Larsen, 1995; Ruff, 1999) and to vary between males and females (particularly in hunter-gatherers) (Brock and Ruff, 1988; Ruff, 1994a; Larsen, 1995). Also, with increasing sedentism through time, a decreasing degree of curvature would be predicted.

The complexity of the relationship between loading and robusticity is subject to additional factors, the main ones being the susceptibility of bone to strain during ontogeny (Ruff *et al.*, 1994; Lieberman *et al.*, 2001; Pearson and Lieberman, 2004) and the effect of climate (Pearson, 2000b; Weaver, 2003).

2.3.5. Climate

Climate affects body size and proportions and it has been suggested that greater robusticity in individuals from colder climates may be an indirect effect of a larger body size (Trinkaus and Ruff, 1999b; Trinkaus and Ruff, 1999a; Stock, 2006). Other studies have found a direct effect of climate on cross-sectional geometry (Stock, 2006) and external robusticity (Ruff, 1995; Pearson, 2000b; Weaver, 2003; Stock, 2006).

Bergmann and Allen's rules apply to body size and proportions in mammals and their relation to thermo-regulation. There is a positive relationship between body size (weight) (Bergmann, 1847) and a negative relationship between limb length relative to body mass with increasing distance from the equator (Allen, 1877). Considerable studies on a range of human populations have confirmed these principles also apply to humans. Body breadth is correlated most strongly with temperature, and differences in limb proportions and body size are established through

genetic adaptation and not through individual ontogeny (Y'Edynak, 1976; Eveleth and Tanner, 1990; Ruff *et al.*, 1994; Pearson, 2000b; Van Andel, 2003; Weaver, 2003; Ruff *et al.*, 2005). There have been recent changes in the compliance of modern humans to these ecological principles due to dietary improvements of many hunter-gatherers and the adoption of a more urban trading subsistence strategy (Katzmarzyk and Leonard, 1998). Therefore, care must be taken when analysing differences within modern humans and especially when drawing conclusions for palaeoanthropological studies (Stock, 2002).

In an evolutionary context, body size and limb proportions have been used to interpret environmental adaptation and migration, especially when explanations are sought for the differences in Neanderthal and early modern human body build. Weaver (2003) argued that the relationship between robust femora and cold climate in Neanderthals can be explained as a secondary consequence of the wide cold-adapted Neanderthal bodies and that the shape of the Neanderthal femur can be explained as a secondary consequence of the cold-adapted bodies vs. the warm adapted bodies of modern humans (Weaver, 2003).. Because the breadth of the pelvis is much wider in Neanderthals, the femur responds to this with larger articulations, thicker and more rounded shafts, a lower neck-shaft angle and a broader proximal shaft than in modern humans (Ruff and Walker, 1993; Ruff *et al.*, 1993; Weaver, 2002, 2003).

From the publications on race assessment discussed above, a clear relationship has not been demonstrated between femoral curvature and climate (Bookstein *et al.*, 2003) but it is worth considering this again in light of the current research, through investigating the possible relationship between overall skeletal morphology and long bone curvature. Long term climatic adaptation may have an important effect on the size and shape of long bone diaphysis (Pearson, 2000b).

2.4. Hypotheses and predictions

The background provided by the two preceding Chapters (1 and 2) on bone curvature in Neanderthals and modern humans suggests three main hypotheses to explain variation in long bone curvature in recent modern humans. These hypotheses and the associated predictions will be the basis for the analysis and are listed below.

Hypothesis 1: A high degree of curvature is related to body size.

Body size affects the mechanical loadings of weight-bearing skeletal elements and cross-sectional diaphyseal properties. Biewener (1983) suggested curvature is a mechanism by which large animals reduce bone stresses because body mass increases more rapidly than the cross-sectional area of bones. Although this relationship is clear for weight-bearing bones such as the femur, Swartz (1990) demonstrated that curvature of the radius in anthropoids was also allometrically related to body size, and could not find a relationship between curvature and differences (tension or compression) in loading regime between brachiators and non-brachiators.

Associated predictions:
- Body size is positively correlated with degree of femoral and radial curvature.
- Males have higher degrees of curvature than females, because males are, on average, larger.

Hypothesis 2: Curvature is a response to increased activity levels

Several predictions follow from the expected relationship of habitual behaviour of long bone curvature. Males have higher activity levels than females, especially in hunter-gatherer societies where division of labour is most pronounced, and this may result in sexual dimorphism in curvature (Larsen, 1995). Activity levels in adults decrease with age (Caspersen *et al.*, 2000; Norman *et al.*, 2002), so curvature may also decrease with increasing age.

Habitual use of the forearm in a part-flexed position during pronation, with the hand in supination or semi-supination, results in a more medially placed radial tuberosity, increased strain in the forearm and may result in a relatively longer radial neck (Trinkaus, 1988). This increased strain is expected to result in more curvature.

Associated predictions:

- Males, having higher activity levels than females, also have higher degrees of curvature.
- There will be a positive correlation between curvature and robusticity.
- Populations with higher levels of aquatic mobility will have the most laterally curved radii and most posteriorly curved ulnae.
- With increasing individual age and decreasing activity levels, there will be a decrease in curvature.
- With increasing sedentism through time in Europe, there will be a decrease in curvature.
- Position of the radial tuberosity and radial neck length will be correlated with curvature.
- A higher degree of femoral curvature will be associated with a more distal apex of curvature

Hypothesis 3: Curvature is a consequence of adaptation to cold climate.

Individuals in high latitudes have relatively shorter distal limbs and relatively larger articulations than those living in warm climates (Ruff, 1994b). The shape of the femur has been suggested to be a consequence of long term climatic adaptations in the pelvis. The wide pelvis in cold-adapted populations results in relatively larger articulations, greater shaft robusticity and low neck-shaft angles, as well as longer relative neck length and increased torsion (Weaver, 2003). Little is known about how cold adaptation affects the lower arm.

Associated predictions:

- There will be a positive correlation between curvature and latitude (used as a quantitative measure for average temperature).
- There will be a positive correlation between curvature and robusticity of the epiphyses and shaft.
- There will be a positive correlation between femoral curvature, relative neck-length and torsion and neck-shaft angle.

CHAPTER 3. MATERIALS AND METHODS

3.1. Materials

The materials included in this study can be divided into two groups: 1) Neanderthals and early anatomically modern humans, and 2) the comparative recent modern human sample. The recent modern human sample is a geographically and behaviourally diverse sample that was chosen to investigate the influence of climatic, body size/body proportions and activity levels on curvature.

3.1.1. Neanderthal and early anatomically modern human fossils

Neanderthals and early anatomically modern human remains are relatively abundant compared to other hominin fossils but the sample is smaller than would be ideal for a comprehensive comparative analysis. All available femora, ulnae and radii were studied, and where the original was missing or damaged, casts were used. The sample is comprised of complete or nearly complete bones.

3.1.1.1. Neanderthals

The sample of Neanderthals represents Middle Palaeolithic Western European (so-called "classic" Neanderthals) and western Asian Neanderthal sites (Table 3-1) dating from 65Ka-35Ka BP. A short description and some key references for each site is included below with the most recent first.

Table 3-1 Summary of the Neanderthal sample, by region.

NEANDERTHAL

		complete specimens		
Adult		Femur	Ulna	Radius
Europe				
Spy 1 [a]				X
Spy 2 [a]		X		
La Ferrassie 1 [b]			X	X
La Ferrassie 2 [b]		X	X	X
La Quina H5 [b]			X	X
La Chapelle aux Saints [b]		X	X	X
Le Régourdou [c]			X	X
Levant				
Kebara [d]			X	X
	N	3	7	8

Adult cast		Femur	Ulna	Radius
Europe				
Le Moustier [e]		X	X	X
Neanderthal [f]		X	X *	X
western Asia				
Shanidar 1 [g]			X	X
Shanidar 5 [g]			X	
Shanidar 6 [g]				X
	N	2	4	4

[a] Royal Belgian Intitute for Natural Sciences, Brussels [b] Musee de l'Homme, Paris [c] Musee du Perigord, Périgeux, [d] Tel Aviv University [e] Museum für Vor- und Frühgeschichte in Berlin [f] Rheinisches Museum in Bonn [g] Smithsonian Institute Washington, * pathological

Spy

Two partial skeletons and some juvenile fragments were discovered in Spy, 15 km west of Namur, Belgium, in 1886 by M. Lohest and M. De Puydt (Fraipont and Lohest, 1887). The fossils were associated with Mousterian tools (Bordes, 1959), but because of the early date of the excavation and poor excavation techniques, dating is problematic. The fossils are tentatively dated to 40-35 Ka BP based on associated faunal remains (Cordy, 1988).

Spy 1 is believed to be an adult male of approximately 35 years old. The calotte, a partial maxilla and partial postcranial remains are preserved. Spy 2, also a partial male skeleton, consists of a calotte and some isolated teeth and postcranial remains. There is some confusion about the postcranial elements and their association with either Spy 1 or Spy 2. Only Spy 1 has a completely preserved radius and was included in the analyses. The other specimens are too fragmentary to be included. Both specimens are undoubtedly Neanderthals (Fraipont and Lohest, 1887; Boule and Vallois, 1952).

The Spy remains reside in the Royal Belgian Institute of Natural Sciences in Brussels, by courtesy of the family of Professor Max Lohest (1857-1926).

La Ferrassie

The site of La Ferrassie, France, was discovered in 1909 by D. Peyrony and L. Capitan and yielded the remains of two adults (La Ferrassie 1 and 2) and possibly 6 or 7 juveniles (La Ferrassie 4a, 4b, 5: neonates or fetuses; La Ferrassie 3 and 7, possibly same individual: +/- 10 years old; La Ferrassie 6: +/- 3 years old; La Ferassie 8: +/- 2 years old) (Heim, 1968). The remains were found in a rock shelter 3.5 km from Bugue, France, and were associated with Mousterian tools and a cold-climate fauna. The site dates to approximately 40 Ka BP (Heim, 1968; Puech, 1981) and the skeletal material could have possibly been intentially buried (Peyrony, 1934 in Schwartz and Tattersall, 2002).

La Ferrassie 1 is a partial skeleton of an adult male (+/- 45 years old) and La Ferrassie 2 is an adult female (25-30 years old) (Heim, 1968). La Ferassie 1 is the best preserved but the femora were too incomplete to be included in the sample. The ulna and radius from both the left and the right side were included. For La Ferrassie 2 the femora, and radius and ulna from the right side are included in the sample.

Le Moustier

The site of Le Moustier comes from the village of Le Moustier, France, which is located about 10 km from Les Eyzies de Tayac. The hominin remains were discovered by O. Hauser in 1908 who later sold them to the Museum für Vor- und Frühgeschichte in Berlin. The rock shelter contained artefacts of the Mousterian tradition and is dated to 40.3 +/-2.6 Ka BP using TL dating on burnt flint (Bordes, 1959; Valladas *et al.*, 1986) and ESR dating on associated mammal bones (Mellars and Grun, 1991).

Cut-marks and bone modifications indicate that Le Moustier 1 was killed intentionally by peri-mortal impacts, the head was decapitated, the mandible forcibly disarticulated and the corpse (obviously completely dismembered) defleshed. (Ullrich, 2005 p. 304). The adolescent skull is certain to belong to a Neanderthal. It has a low forehead, double arched browridge, a low vault, lambdoidal flattening, a suprainiac depression and an occipital bun.

During WWII most of Le Moustier 1 was destroyed and only the skull and some of the postcranial elements remain (Day, 1986; Schwartz and Tattersall, 2002). Due to a wartime fire the original fossils are heavily distorted. Reliable measurements can only be taken on casts made from the originals (Thompson and Nelson, 2000). Only a plaster cast of the reconstruction of the left femur, right ulna and right radius are complete enough to be included in the sample. Thomson and Nelson (2005) remarked on the exaggerated length of the cast of the radius and the reconstruction of both extremities. They describe the radial shaft as strongly laterally curved and having a medially oriented radial tuberosity. The original radius was missing most of the epiphyses but they have been reconstructed on the cast. The ulna is mostly preserved. The trochlear notch faces anteriorly. There is no clear radial notch on the cast. The femur is partly reconstructed. The lesser trochanter, greater trochanter, 1/3 of the femoral head and most of the distal epiphyses are reconstructed.

Neanderthal (also Feldhofer)

The Feldhofer Neanderthal is the type specimens for *Homo neanderthalensis* and was found in 1856 by workmen from a quarry in the Neanderthal Valley, about 11 km east of Düsseldorf, Germany. Neither artifacts nor mammalian bones were recovered from the site, although re-excavation of the old mining deposits since 1998 (Schmitz *et al.*, 2002; Schmitz, 2006) revealed stone tools and faunal remains along with more Neanderthal remains (Day, 1986; Schmitz *et al.*, 2002). There are now three individuals represented from the site. On the basis of mtDNA analysis of the original Feldhofer remains Krings and colleagues (1997) demonstrated that the Neanderthal genome was different from that of modern humans. Further mtDNA analyses of the more recently discovered Feldhofer remains yield sequences similar to those of other Neanderthals and are different from those of modern humans (Schmitz, 2006). Carbon-14 dating of the newly discovered remains indicates an age of approximately 40 Ka BP.

The Feldhofer 1 skull has a clear Neanderthal anatomy, and suture fusion suggests an age of approximately 50 years at death (Day, 1986; Schwartz and Tattersall, 2002). The postcranium includes two femora, two ulnae and the right radius. Although there is evidence of slight deformation on the femora and the radius, the left ulna is too pathological to be included in the study. The long bones are thick and show pronounced muscular attachments. The humeri are straight but the radius is curved and has a large radial tuberosity. The fracture related pathology on the left elbow would have limited the movement of the joint. The femur is cylindrical and shows signs of a third trochanter (Heim, 1981, 1982, 1983).

La Quina H5

The site of La Quina, 25 km south of Angoulème, France, was found in 1872, but it was not until 1908 that Henri-Martin discovered the first hominid remains (Martin, 1921). A total of 27 individuals are preserved; however, only one individual, H5, is included here (left ulna and radius). H5 is a partial adult skeleton that was found associated with Mousterian of the La Quina tradition (Debénath *et al.*, 1998). Although the hominin remains come from different layers, H5

comes from the earlier levels belonging to OIS 4 and dating to approximately 65 Ka BP (Mellars, 1996). A more recent date of 40-42 Ka BP based on chronometric data has also been reported (Zilhao, 2006).

Shanidar

In 1951 R. Solecki discovered the site of Shanidar in the Zagros Mountains in Iraq, approximately 400 km north of Baghdad. The remains of at least nine partial skeletons were found in a large cave (Solecki, 1957, 1961, 1975). Although modern human burials were discovered in the upper layers of the site, the Shanidar Neanderthals were found in a single layer associated with Mousterian tools, hearths and local fauna (Solecki, 1957, 1961). The Mousterian Neanderthal layer was ^{14}C dated to approximately 50.6 Ka BP (Bar-Yosef, 1989).

Six adults, one young adult and two infants were found at the site and were described by Stewart (Stewart, 1962, 1963, 1977) and Trinkaus (Trinkaus, 1978, 1982a, 1982c, 1982b, 1983b). The skulls show a long low cranial vault, a large supraorbital torus, mid-facial prognathism, a transverse occipital torus and a rounded vault in occipital view. The mandible lacks a chin and the anterior teeth are heavily worn. Because of these features, their classification as Neanderthals has never been questioned (Solecki and Solecki, 1974; Solecki, 1975; Stewart, 1977; Trinkaus, 1978; Trinkaus and Zimmerman, 1979; Stringer and Trinkaus, 1980; Trinkaus, 1982a, 1982c, 1982b; Trinkaus and Zimmerman, 1982; Ivanhoe and Trinkaus, 1983; Trinkaus, 1983a).

The post-crania from the site show a high degree of robusticity and display signs of powerful musculature. The sample used here includes the left ulna and radius of Shanidar 1, the right ulna of Shanidar 5, and the left radius of Shanidar 6. Because of the current relocation of the material from the Baghdad Museum, casts of this material were measured at the Smithsonian Institution.

La Chapelle-aux-Saints

This partial Neanderthal skeleton was discovered in 1908 by A. and J. Bouyssonie and L. Bardon near the village of La Chapelle-aux-Saints, 40 km from Brive, France. It was found buried in a cave (Bardon *et al.*, 1908 in Schwartz and Tattersall, 2002) and associated with an

advanced Mousterian industry and mammals representative of a temperate climate (Boule, 1908). The layer from which the specimen came has an absolute date of 47-56 Ka BP using ESR dating on mammal teeth (Grün and Stringer, 1991).

The skeleton is fairly complete and belonged to an aged adult male. The specimen has typical Neanderthal features such as an occipital bun, supra-iniac fossa, small mastoid processes and mid-facial projection (Boule, 1908; Trinkaus, 1985). The right side of the postcranial skeleton is well preserved, and the right femur, ulna and radius are included in the sample. There are signs of degenerative joint disease in the skeleton consistent with its inferred old age (Trinkaus, 1985). In general, the long bones are short and thick with strong muscle markings and short distal limb segments compared to its proximal limb segments. The humeri are straight but the femur and radius are bowed (Trinkaus, 1985).

Kebara

The Mugharet el-Kebara is approximately 13 km south of Wadi el-Mughara on the western slope of Mount Carmel in Israel. The excavation of the site began in 1927. During the early stages of the excavation the fragmentary remains of an infant were discovered (Kebara 1). In 1983, an adult Neanderthal burial was recovered (Kebara 2 – commonly referred to as simply Kebara) (Goldberg and Bar-Yosef, 1998).

Although the skull and most of the lower limbs are missing the skeleton is well preserved. The skeleton is estimated to be that of a 25-35 year old male individual. The pelvis indicates that Neanderthal pelves are fundamentally different from modern human ones, even when compared to modern humans from the same time period. They have a long superior pubic ramus which probably stems from a more externally rotated innominate bone and may be attributed to differences in locomotion and posture related biomechanics (Rak and Arensburg, 1987; Rak, 1990). The layer from which the adult burial originates dates to approximately 60-48 Ka BP (Goldberg and Bar-Yosef, 1998). The occupation layer also contained Mousterian tool technology (Bar-Yosef *et al.*, 1986).

The radius and ulna from both sides are included in the sample. The partially preserved femur lacks its distal epiphyses and is too fragmentary to be used.

Le Régourdou

In 1957, R. Constant discovered a collapsed limestone cave 2 km north of Montignac, France, containing Mousterian tools, and the remains of two individuals: one partial skeleton of a young adult (Régourdou 1) and some pedal elements (Régourdou 2) (Piveteau, 1959). The site was re-excavated by Bonifay from 1957 onwards and based on the sedimentology, fauna and Middle Palaeolithic technology he assigned the specimen to OIS 4 (roughly 65Ka BP) (Bonifay and Vandermeersch, 1962; Bonifay, 1964).

The individual is probably a young adult in its mid-twenties. It is not possible to determine its sex as the cranium and the pelvis are poorly preserved. The right ulna and radius are complete enough to include in the sample. The cranial morphology shows a clear Neanderthal affinity as does the morphology of the postcranial skeleton (Piveteau, 1959; Vandermeersch and Trinkaus, 1995).

3.1.1.2. Early modern humans

The sample represents early anatomically modern humans from Europe and western Asia (Table 3-2). A short description and some key references for each site is included below in chronological order from most recent to oldest.

Table 3-2 Summary of Early Modern Human sample, by region.

		complete specimens		
Adult		Femur	Ulna	Radius
Europe				
Abri Pataud [a]			X	X
Chancelade [b]		X	X	
Combe Capelle [b]		X	X	X
Western Asia				
Sungir [c]		X	X	X
Pavlov [d]				X
Dolni Vestonice 13 [d]		X	X	X
Dolni Vestonice 14 [d]		X	X	
Dolni Vestonice 15 [d]		X*	X*	X*
Dolni Vestonice 16 [d]		X	X	X
Levant				
Ein Gev [e]		X	X	
Ein Gev Nahal [e]				X
Ohalo II [e]		X	X	X
Qafzeh 9 [e]		X	X	X
Skhul IV [f]			X	X
	N	9	10	10
Adult cast		Femur	Ulna	Radius
Europe				
St. Germain [g]		X	X	X
Western Asia				
Kostienki 14 [h]		X	X	X
	N	2	2	2

[a] Musee de l'Homme, [b] Musee du Perigeux, [c] Laboratory for reconstruction, Moscow [d] Dolni Vestonice, [e] Tel Aviv University, [f] Harvard Peabody Museum, Boston, USA, [g] Musée National du Prehistoire, [h] Kunstcamera St Petersburg

*pathological

Ein Gev

The site of Ein Gev is 1 km east of the Sea of Galilee in northern Israel. The site was excavated originally by Stekelis and Bar Yosef in 1965. The archaeology at the site is Epipalaeolithic Kebaran, and ^{14}C dating on charred bone indicates an age of 15700 BP +/-415 (; Davis, 1974).

The human remains at the site come from a burial and probably belonged to an adult female (30-40 years old) (Stekelis and Bar-Yosef, 1965). The bones were quite fragmentary at the time of discovery, but most parts could be restored. Despite the restoration it was only possible to include the ulna in the analyses (Arensburg and Bar-Yosef, 1973).

Chancelade

In 1888 M. Hardy discovered a Magdalenian skeleton at the site of Raymunden in the village Chancelade, near Périgeux, France (Sollas, 1927; Billy, 1969). The deposits are believed to be a burial and the skeleton is reported to have been covered with ochre. The almost complete skeleton is that of a 40-46 year old man who was approximately 1.6m tall. The cranium was once mistakenly believed to be that of an Eskimo and the Eskimo-like features were interpreted in light of the cold environment during the "Magdalenian Age" (Testut, 1925 in Keith, 1925; Sollas, 1927). The skull is clearly that of a modern human and is associated with an archaeological deposit of Magdalenian III or IV, dating most probably between 17-12 Ka BP (Ruff and Walker, 1993; Trinkaus *et al.*, 1999a). The associated fauna are indicative of cold conditions but an absolute date for the site has not yet been established.

The postcranial remains were described by Billy (1969). Subsequent publications by other authors have demonstrated some of the highest values for robusticity found in any early modern human (e.g. Ruff and Walker, 1993; Trinkaus *et al.*, 1999a). The left femur was poorly reconstructed and extremely fragile but the right femur is included in the sample as well as the right ulna, although there was some reconstruction of the femoral head and distal condyles but none of the landmarks were affected.

Saint-Germain-la-Rivière

The site of Saint-Germain-la-Rivière, France, is an early Magdalenien rock shelter and dated to between 17-14 Ka BP using ^{14}C dating (Costamagno, 2002; Drucker and Henry-Gambier, 2005). It was excavated on and off between 1929 and 1996. A complete adult human skeleton of was discovered in 1934 (Blanchard, 1935; Vaufrey, 1935). The skeleton was discovered in a burial structure made out of rocks and was adorned with marine shells and teeth of red deer and reindeer. The skeleton is believed to be that of a young adult female (Vaufrey, 1935; Henry-Gambier *et al.*, 2002). Carbon and nitrogen isotope ratios in the bone collagen of the young woman indicate that the main source of protein was large herbivores. She did not consume significant amount of fish and her subsistence pattern reflects a less opportunistic diet that generally attributed to humans from the early Magdalenian (Drucker and Henry-Gambier, 2005).

The original fossils were not available for study, so a cast was measured. The left ulna, right radius and right femur were included in the sample. The patella of the right femur is fused to condyles but did not affect the landmark collection.

Ein Gev Nahal

Nahal Ein Gev is an Upper Palaeolithic burial of an almost complete skeleton in the north of Israel. The associated archaeology is Levantine Aurignacian, which places the individual in the Upper Palaeolithic rather than Epi-Palaeolithic. Direct dating of the remains has not been successful but sites with similar deposits, such as Ohalo II, have been dated to 19Ka BP (Arensburg, 1977).

The skeleton is believed to be that of a 30-35 year old female. She had gracile cranial features and short stature (approx. 157 cm). The skull is different from other Upper Palaeolithic crania in its size and shape. Morphologically, it is most similar to Cro-Magnon II and Predmostí IV, which has been suggested to be an indication of common ancestry (Arensburg, 1977; Belfer-Cohen *et al.*, 2004). The remains are badly damaged and most of the long bone epiphyses were crushed. Because of this extensive damage, only the right radius was sufficiently reconstructed to be included in the sample.

Abri Pataud 6

The rock shelter of Abri Pataud was found in the town of Les Eyzies de Tayac in 1958 by H. Movius (Movius, 1966, 1975). Thirteen individuals were recovered, however, most of these are incomplete. The best preserved specimens are a female cranium, Pataud 1, and an adult skeleton, Pataud 6. The most recent estimated date for the site is between 20-30 Ka BP (Movius, 1966, 1975; Mellars *et al.*, 1987; Pettitt *et al.*, 2003). The human remains most probably come from the upper levels of the site and, if this is correct, would date to approximately 22 Ka BP (Mellars *et al.*, 1987; Pettitt *et al.*, 2003).

The remains were associated with a Proto-Magdelenian industry (Movius, 1966). In the current study only the left ulna and radius of Pataud 6 were used.

Ohalo II

Ohalo is an Upper Palaeolithic site in the Levant near the Sea of Galilee that dates to 23,500-22,500 BP base on radiocarbon dating (Nadel and Hershkovitz, 1991). Excavations revealed brush huts, hearths and a human grave. Ohallo II H2 is a relatively complete adult male skeleton estimated to have been between 35 and 40 years at death. The left radius and ulna were damaged and only the right side is included in the sample (Hershkovitz *et al.*, 1995).

Sungir (also Sounghir)

The Sungir site has been excavated since 1957 and is located approximately 200 km northeast of Moscow. It has yielded both a single and a double burial. The single burial is that of an adult male (Sungir 1). The double burial is that of an adolescent male and female (Sungir 2 and Sungir 3, respectively). All three burials burials were in extended, supine position. Sungir 2 and 3 were lying head to head and were covered in red ochre.

The burials have been directly dated using radiocarbon dating. Sungir 1 is 22.5-23.4 Ka old, whereas the Sungir 2 and 3 double burial is 23.5-24.5 Ka old and thus slightly older than Sungir 1 (Pettitt and Bader, 2000; Ovchinnikov and Goodwin, 2003 but see Kuzmin *et al.*, 2004). The

Sungir 3 girl has a pathology that is remarkably similar to the observed chondrodysplasia calcificans punctata of Dolni Vestonice 15 (personal observation , Trinkaus *et al.*, 2001). The pathology presents itself with severe skeletal deformaties of the long bones. The right femur, ulna and radius of Sungir 1, the adult male, is included in the sample.

Pavlov I

The site of Pavlov, containing two skeletons (Pavlov I and Pavlov II), is located close to Dolni Vestonice and approximately 35 km South of Brno, Czech Republic. The site was found and excavated in 1952 by B. Klima. The tool industry at the site is known as Eastern Gravettian (Vlcek, 1961a, 1961b, 1991; Svoboda, 1994; Adovasio *et al.*, 1996).

The Palov I skeleton is an adult, most likely male, and includes a partial cranium, maxilla, mandible, isolated teeth and a partial skeleton. The burial dates to 27 -25 Ka BP based on radiocarbon dating (Klima, 1987). The remains are believed to be those of an early modern human. Because it is a fairly robust skeleton and cranial features, such as overall robusticity and a swollen sub-lambdoidal area reminiscent of an occipital bun, the Pavlov skeleton has been suggested to be a link between archaic Europeans (Neanderthals) and modern humans (Smith *et al.*, 1982; Wolpoff, 1996). Only the right radius of Pavlov I was sufficiently well preserved to be included in the sample.

Dolni Vestonice (also Dolni Věstonice)

Dolni Vestonice is a complex of sites in and around the village of Dolni Vestonice, 35 km South of Brno in the Czech Replublic. The sites were discovered by Absolon in 1925 and later excavated by Klima from 1949-1987. There are 16 individuals represented at the cluster of settlements and they probably all date to approximately 26.5 Ka BP (Svoboda and Vlcek, 1991; Formicola *et al.*, 2001).

There are two areas at the site: one containing most of the occupational information and one with the human remains. The associated industry is Gravettian, which is accompanied by engraved bone tools and clay figurines. Most of the human remains are burials. The "triple burial" of

individuals XIII, XIV and XV is that of three young, possibly genetically related, adults who were buried together with grave goods. The central skeleton, which is probably a female, has pathologies causing severe bone deformation of the femora and forearm (chondrodysplasia calcificans punctata, Trinkaus *et al.*, 2001). The other individuals are males (Klima, 1987; Bahn, 1988; Alt *et al.*, 1997; Trinkaus *et al.*, 2000; Formicola *et al.*, 2001). Although the human remains are considered to be modern humans and are relatively gracile, some authors have suggested that they retain primitive and Neanderthal-like features and are indicative of continuity in the region (Smith *et al.*, 1982)

All three individuals from the triple burial are relatively well preserved and have at least one well preserved femur, ulna and radius. Because of its severe pathology, Dolni Vestonice XV was excluded from the analyses. The left femur, ulna and radius of Dolni Vestonice XVI, both femora, ulnae and radii of Dolni Vestonice XIII, and both femora and ulnae and the left radius of Dolni Vestonice XIV were included in the sample. The separate femoral head of Dolni Vestonice XIV was held in place during data collection.

Combe Capelle

The rock shelter of Combe Capelle, 20 km Southeast of Bergerac, France, was discovered in 1909. It has yielded a partial hominin skeleton dated to approximately 28-25 Ka years (Valladas *et al.*, 2003). The skeleton was associated with Gravettian tools and its morphological affinities are clearly modern (Lenoir and Dibble, 1995).

The skeleton was lost during the same fire that destroyed the Le Moustier adolescent Neanderthal remains, but in 2002 the skull was rediscovered in the museum. Regretfully, the postcranial skeleton is still missing (Hoffmann and Wegner, 2002). However, there are well preserved original plaster casts of the left and right femora and ulnae that were included in these analyses. There are minor areas of the original bone that are damaged, such as some abrasion of the distal femoral condyles and the lack of the styloid process, but this should not seriously affect the results. The right radius was also complete enough to be included.

Kostenki 14 (also Markina Gora)

The site of Kostenki (Markina Gora) is in the Voronezh region in Russia. The site is part of a complex of sites that provides an important stratigraphic sequence for the region between the Carpathian and Ural Mountains (Sinitsyn and Hoffecker, 2006). It has yielded a number of skeletal remains: a 5-6 year old child (Kostenki 15), an elderly man (Kostenki 2), a 9-10 year old child (Kostenki 12) and a well preserved skeleton of a young adult male (Kostenki 14). Kostenki 14 was discovered in a grave and covered with yellow and red ochre (Jelinek *et al.*, 1969).

The skeleton came from the lowermost cultural layers at Markina Gora and is radiocarbon dated to at least 36-37 Ka BP (Sinitsyn, 2003). It is a young male that was probably around 160 cm tall. The supraorbital torus is modern-human-like. Jelinek (1969) also describes Kostenki 14 as being similar to the remains from Grimaldi and Cro-Magnon.

Although the remains are not currently available for research because a monograph is in preparation, the curator at the Kunstkamera in Saint-Petersburg, Russia, allowed the inclusion of the casts in the analyses. The right femur and ulna and the left radius are sufficiently preserved to be analysed.

Qafzeh (also Jebel Qafzeh)

The site of Qafzeh in Israel was discovered in 1933 by R. Neuville (Vandermeersch, 1981). The site is 2.5 km south of Nazareth and is located on Mount Carmel. Up to 12 individuals have been discovered in the cave. The tool industry is Levalloiso-Mousterian with some backed knives and burins of Upper Palaeolithic character (Vandermeersch, 1981). There is a thermoluminescence date of 100 Ka BP +/- 10 Ka (Grün and Stringer, 1991).

The human remains belong to eight adults (Qafzeh 1,2,3,5,6,7,8,9), three infants (Qafzeh 4, 4a, 10) and one ten-year old child (Qafzeh 11). A detailed description of the human remains can be found in Vandermeersch (1981). In general, the postcranial features are modern and do not show distinct Neanderthal or other archaic features (Vandermeersch, 1981). Trinkaus suggests, however, that both Qafzeh and Skhul (see below) have a mosaic of features and argues that

morphological and archaeological evidence can best be explained by continuity between archaic and modern humans (Trinkaus, 1981).

The postcranial remains of Qafzeh 9, an adult male, were complete enough for the right femur and ulna, and left radius to be included in the analyses.

Skhul (also es-Skhul)

At least 10 individuals were found at the site of Mugharet es-Skhul (usually referred to in the literature as "Skhul") on Mount Carmel, in southeastern Israel. The site was discovered in 1929 during an excavation directed by D. A. E. Garrod (Garrod and Bate, 1937). Most of the bones were associated and showed little disturbance, indicating that they were probably buried intentionally (Garrod and Bate, 1937)

The remains are associated with the Levalloiso-Mousterian and the fauna is similar to that at the adjacent site of Tabun. Mean ESR age estimates place the site between 81 and 101 Ka BP (Grün and Stringer, 1991) and TL dating dates the site to an average of 119 Ka BP (Valladas *et al.*, 1998).

At the site, seven adults and three juvenile individuals are represented. Most of these are partial skeletons and are considered to be anatomically modern. The skeletons are long and slender compared to Neanderthals. There are some primitive features present, though, such as the stout foot and finger bones and well-developed thumbs (Vandermeersch, 1981; Trinkaus, 1993; Niewoehner, 2001). One theory attributes the apparent persistence of these to inbreeding between early moderns moving into the region from Africa, and Neanderthals coming in from Europe (Kramer *et al.*, 2001). Alternative views see the Skhul and Qafzeh people as members of an early modern population that evolved in the Levant (Vandermeersch, 1981; Rightmire, 1998).

The radius and ulna of Skhul IV are included in the sample.

3.1.2. Modern populations

The modern human comparative sample was chosen specifically to test hypotheses of factors that explain long bone curvature (see Chapter 2 for details). The sample consists of adult femora, ulnae and radii. All the individuals in this sample are skeletally adult based on closure of the epiphyses and pathological individuals were excluded. For 93 individuals the age at death was known. Sex of the individuals was recorded from the museum catalogues or, if pelvis and cranium were available, sex was determined by observation. Individuals where sex determination was impossible and where the museum had no information were labelled as unknown.

The relatively small number of individuals per population is due to the availability of postcranial material in museum collections. In order to capture the range of variation in modern humans throughout the world, some small samples were included as part of groups created for further analyses (See section 3.2 in this Chapter). Where possible the femur, ulna and radius from the same side of the skeleton were included in the sample. When this was not possible bones from opposite sides of the skeleton were included. Table 3-3 below reflects the total number of individuals represented in the sample rather than the number of bones. Sample numbers of particular bones are specified in the results chapters.

Table 3-3 Summary of recent modern human sample, alphabetically.

Population	N	Collection	Location
African-American	12	African-Americans Terry Collection	Smithsonian, Washington
Alaskan Aleut	15	Aleutian Islands Collection	Peabody, Harvard
Andaman Islands	17	College of Surgeons Collection	NHM, London
Arizona Native	20	Canyon del Muertos	NHM, New York
Australian Aboriginals	13	College of Surgeons Collection	NHM, London
Belgian Medieval	29	Spy and Gutschoven	RBINS, Brussels
Belgian Neolithic	72	Furfooz, Maurenne, Hastière, Dinant	RBINS, Brussels
British Neolithic	2	Coldrum	NHM, London
Chinese	9	Chinese Cemetary, Karluk Quad Alaska	Smithsonian, Washington
Colorado Native	4	Montezuma County, Colorado	Peabody, Harvard
Czech Medieval	39	Moravian Empire Collection	NHM, Prague
Danish Medieval	15	Sankt Bendtskirke, Ringsted	University, Copenhagen
Danish Neolithic	49	Korshoj Adby, Guldhoj, Borreby	University Copenhagen
Egyptian	5	Egyptian Dynasty	NHM, Paris
English Medieval	21	Scarborough	NHM, London
English Urban	21	Spitalfields 18th-19thC	NHM, London
French Medieval	16	Villebourg, St. Gabriel	NHM, Paris
French Neolithic	24	Valée du Petit Morin	NHM, Paris
Greenland Inuit	31	Tuqutut, Ilutalik, Uunartoq, Ilorsuit	University, Copenhagen
Khoi or KhoiKhoi	10	Oxford Collection	NHM, London
Kazach	7	Southern Volga Region	St. Petersburg
Lapland	17	Russian Saami	Moscow State Univ.
Natufian	16	Mallaha	University, Tel Aviv
New Mexico	9	Aztec Ruins	NHM, New York
Ohio Native	18	Madissonville, Ohio	Peabody, Harvard
Peruvian	13	Ancon (Lima)	NHM, Paris
Point Hope Alaska	15	Alaskan Inuit	NHM, New York
Pygmy	4	Lituri Central Africa	RBINS, Brussels
Russian Eskimo	15	Siberian Peninsula, Ekveni	Moscow State University
Russian Mesolithic	22	Vasilievski	St.-Petersburg
Siberia	16	Sibstey, Salehard Siberia	Moscow State University
South Dakota Native	13	Campbell County, Ohae Reservoir	Smithsonian, Washington
Tasmanian	2	Tasmania	NHM, London, Brussels
Tierra del Fuego	2	Tierra del Fuego, Argentina	NHM, Vienna
TOTAL	593	individuals	

NHM = Natural History Museum; RBINS= Royal Belgian Institute of Natural Sciences

African-American

The African-American sample is from the Terry collection. It was collected by Robert J. Terry (1871-1966) from a local St. Louis hospital and institutional morgues. The material in the collection consists primarily of urban living individuals whose bodies became property of the state when they were not claimed, or whose relatives signed over the bodies to the state. The Terry collection consists of 1728 individuals of known age, sex, ethnic origin, cause of death and pathological conditions and twelve individuals were randomly sampled.

Alaskan Aleut and Point Hope Alaskan

The Alaskan Aleut and the Point Hope Alaskan are archaeological samples. The Alaskan Aleut are members of the Inupiak, a subdivision of the Inuit. They traditionally lived in groups of 20-200 in the northern arctic region and relied mainly on large sea mammal hunting for subsistence. They hunted these animals with stone, bone, ivory and wooden tools such as harpoons, arrows and knives. Their diet is almost entirely carnivorous, as there is very little plant material available in the area. Some populations have been found to eat sea weeds and grasses or the stomach contents of the animals hunted (Burch and Burch Jr., 2006).

Andaman Islands

The Andaman Islands are located in the Indian Territorial part of the Bay of Bengal. The Andamanese are hunter-gatherers, who rely on eating indigenous mammals, plants and fish acquired with stone, bone, wooden tools and nets (Radcliffe-Brown, 1948).

Arizona Native Americans

The Native Amerindians from Arizona come from a site called Canyon del Muertos, Tempe. The Los Muertos site was occupied by the Hohokom cultures and dates to approximately 500AD – 1500AD (Haury, 1945). Analysis of the palaeo-environment of central Arizona suggests that as

early as 750 AD the climate was arid and the irrigation canals dating back to 1150AD indicate that horticulture farming may have been practiced at the site (Haury, 1945).

Australian Aboriginals

The Australian Aboriginal remains are curated at the Natural History Museum in London. The individuals come from a variety of places in Australia and are pre- and post-contact. Although the individuals may have had different cultural backgrounds, most tribes were terrestrial foragers and will be treated in the analyses as such. They used spears and throwing sticks to acquire their foods and lived in semi-nomadic villages (Jupp, 2001).

Belgian Medieval

The Belgian Medieval sample is curated at the Royal Belgian Institute of Natural Sciences in Brussels. The sample comes from two very small rural villages in Belgium: Spy Bastin (13^{th} C AD) and Gutschoven (Carolingian Empire 751-986 AD). They were all farmers or craftsmen (personal communication, Semal).

Belgian Neolithic

The Belgian Neolithic sample is curated at the Royal Belgian Institute of Natural Sciences in Brussels. The Belgian Neolithic sample comprises individuals from the Middle and Late Neolithic period (+/- 5000 BP to +/- 2900 BP cal. in the Seine-Oise-Marne district). The specimens come from four different sites with Dinant being the oldest (4230-4040 BP) and Furfooz being the youngest (3300-2930 BP) (Cauwe *et al.*, 2001). Although the sample comes from graves in rock shelters or in the open air and from settlements organised around flint mines, it is believed that all the individuals had similar agricultural lifestyles (Toussaint *et al.*, 2001).

British Neolithic

The British Neolithic sample was extremely fragmentary. The sample was collected from a mass grave in Coldrum, Kent, and its fragmentary nature is due to the removal and reburial of the remains during ceremonies. The sample skeletal morphology suggests that during this period in England there was a shift to agriculture from mixed foraging but precise information on this population is not available (Clinch, 1904; Wysocki and Whittle, 2000). The sample dates back to approximately 3900-4000 BC (Whittle *et al.*, 2007).

Chinese

This 20th century Chinese sample was curated at the Smithsonian Institution, Washington D. C.. The remains were collected from the Kurlak Cemetery in Alaska and consists only of males. This Chinese cemetery was used to bury the remains of the Chinese labourers that worked at a local fish cannery. These Chinese are assumed to be short-term immigrants there as there is no sign of females or children in the cemetery. Most of the settlers came from Cantonese Southern China (Hdrlicka, 1944).

Colorado Native

This sample was curated at the Peabody Museum, Harvard University, Boston. The Native Amerindians from Colorado come from a site approximately 15km from Cortez in Montezuma County, south-western Colorado. Although ethnic affiliation was not certain, most of the county was inhabited by the Anasazi and the site dates back to Basketmaker III (600-700AD). They were mainly terestrial hunter-gatherers (Crum, 1996). Due to poor preservation few individuals from this population could be included in the sample.

Czech Medieval

The sample of Czech Medieval is curated at the Natural History Museum in Prague. The individuals come from the time of the Great Moravian Empire (9th C AD – end 10th C. AD)

(Dekan, 1981) and are believed to come from a farming population that lived on the lands surrounding one of the burghs (personal communication, P. Veliminsk, curator).

Danish Medieval

This sample comes from a cemetery in Denmark (Sankt Bendts Kirke in Ringsted) and is curated at the Medical University of Copenhagen. The material was excavated in 2000 and dates back to 1080 AD – early 1100s AD. At the time, farming was the main source of subsistence, although it was frequently supplemented by the consumption of fish. The material has not been published (but see Panum Baastrup, 2002).

Danish Neolithic

The Danish Neolithic (approximately 3000 BC) sample is a collection from different sites throughout Denmark. The remains included in this project are from Korshoj Adby, Uggerslev, Guldhoj and Borreby Island. The individuals lived in small settlements. Although fish was most important during the Mesolithic, there is evidence for a dietary shift, and the Neolithic diet consisted mainly of terrestrial food which was hunted, farmed and bred (cattle) (Pia Bennike, personal communication; Bröste *et al.*, 1956; Tauber, 1981; Richards *et al.*, 2003).

Egyptian

The Egyptian sample date to the Old Kingdom and are curated at the Musée de l'Homme in Paris. The catalogue indicated that the individuals were low status mummies from the Old Kingdom (3000 BC). The Old Kingdom Egyptians were intensive agriculturalists growing crops along the Nile Valley using irrigation systems (Kamil, 1996).

English Medieval

The Medieval British sample comes from Scarborough Castle Hill. It is a Medieval lay cemetery sample dating to the middle to late Medieval period (11^{th}-16^{th} Centuries AD). The lay individuals buried at the site practiced farming and some fishing (Little, 1943; Mays, 1997).

English Urban

This is a sample of late 18^{th} –early 19^{th} century Huguenots from the crypt of Spitalfields church in London, England (Molleson and Cox, 1993). The individuals included in this sample are all named adults with known ages at death. Individuals of both sexes and from different ages were randomly selected. The population was an urban population of craftsmen and merchants.

French Medieval

The sample comes from two sites, Villebourg in Central France and St. Gabriel in the South of France and is dated to both the Merovingian (511-751) and Carolingian period (751-986 AD). Both samples are assumed to have been farmers although little is known about them (personal communication, P. Mennecier, curator). The sample has not been sexed or aged.

French Neolithic

The French Neolithic material comes from multiple burial sites in the Valée du Petit Morin, northern France. The area has a long agricultural history and these individuals are believed to have practiced intensive agriculture. The sample was collected during the 19^{th} Century and relocated after the Second World War from the Musée des Antiquités in St. Germain des Prés, France. The collection is substantial, but none of the postcranial bones are individually catalogued nor is there any information available other than the time-period (personal communication Mennecier, Bails). Therefore, each bone is considered as a separate individual.

Greenland Inuit

The Greenland Inuit sample comes from several coastal sites in Greenland: Tuqutut, Ilutalik, Uunartoq and Ilorsuit. Populations from these sites are all prehistoric and had traditional Inuit lifestyles, relying mainly on fish and sea mammals for their subsistence (Bennike, 2006 personal communication). The postcranial remains are not stored individually, and little or no information is known on age or sex. Each bone is considered a separate individual unless taphonomy and size made it possible to identify certain sets of bones to belong to a single individual.

Hottentot (also Khoi or Khoikhoi)

This sample is curated at the Natural History Museum in London. The Khoi or Khoikhoi have been historically referred to as 'Hottentots'. They are a historical division of the Khoi-San group from southwestern Africa. The Khoi were pastoralists and practiced animal husbandry of sheep, goats and cattle. This made it possible for them to live in larger groups than surrounding hunter-gatherer populations. They grazed their animals on the large open plains until they were forced into more arid land by the expansion of the Bantu into Southern Africa (Boonzaier *et al.*, 1996).

Kazach

The Kazach sample comes from a prehistoric site in the Southern Volga river region in present-day Kazachstan. Little is known about the collection other than that the individuals most probably led a traditional lifestyle of nomadic pastoralism (personal communication, J. Chistov).

Lapland Saami (Also Sami or Lapps)

This sample is from the Kola Peninsula and is believed to be pre-historic (personal communication, 2007, D. Pezhémsky). The Sami, also referred to as Lapps, are indigenous people of the North of Europe, and live in an area covering the north of Sweden, Norway, Finland an the Kola Peninsula in Russia. They were traditionally nomadic and relied on a range of subsistences: fishing, trapping, sheep and reindeer herding, etc.

(http://virtual.finland.fi/netcomm/news/showarticle.asp?intNWSAID=26473 last accessed 18/01/2008). They are a genetically distinct group and were probably the first to inhabit this northern area shortly after the glacial ice retreated (Ingman and Gyllensten, 2007).

Natufian

The postcranial specimens from the sites of Hayonim and Ein Mallaha are extremely fragmentary so only a small sample could be collected.

The Natufian is a Mesolithic culture that existed in the Levant between 14.5-11.5 Ka BP. They are thought to have built permanent settlements before the onset of agriculture. This is evident at sites such as Hayonim and Ein Mallaha, where living stuctures form villages were alongside burial structures. The Natufian were terrestrial hunter-gatherers and harvested wild cereals and grasses and tended to live close to permanent water sources. This harvesting of wild cereals is thought to reflect the onset of agriculture Munro (2004). The Natufian used stone tools that were predominantly microlith but also made sickle blades, grinding stones and bone tools such as harpoons and fish-hooks (Bar-Yosef, 1998; Munro, 2004).

New Mexico Native American

The sample of pre-contact Native Americans from New Mexico is a collection of an unidentified population, but the remains were mistakingly associated with the Aztec Ruins (an Anasazi village misnamed "Aztec" see http://www.nps.gov/azru/) and have not yet been studied (Lister and Lister, 1990). The association to the Anasazi and the knowledge that Pueblo also lived in the region make it difficult to establish which cultural group these individuals came from. In any case, there are similarities in lifestyles between these groups: most peoples of this region lived in permanent or semi-permanent settlements and were agriculturalists (G. Sawyer, 2005, personal communication; Lister and Lister, 1990).

Ohio Native Americans

The sample from Ohio comes from a village and cemetery near Madisonville and was described in a book by Hooten and Willoughby (1920). The anatomical analysis suggested a close morphological similarity to the Iroquois but Hooten (1920) concluded that more research on nearby groups would be necessary in order to assign population affinity. This population most probably practiced horticulture (Willoughby and Hooten, 1920).

Peruvian

This is a collection of ten Peruvian prehistoric mummies from the coastal Ancon region in the Lima province in central Peru. The coastal Peruvian populations are believed to have practiced an intensive agricultural lifestyle (Moseley, 2001). There are two individuals from Chorrillos, which is south of Lima and also a coastal area where a similar agricultural lifestyle was practiced (Moseley, 2001).

Pygmy

Four twentieth-century Pygmy individuals (probably Aka) from Central African Republic are included in the sample. The term Pygmy as used here is a derogatory term that refers to a short statured group of populations from central Africa, but no better name is available to describe these different tribes of forest living groups. The Pygmy have hunter-gatherer lifestyles and mainly live in the African rainforest. The modern Aka, compared to some other Pygmy groups, spend most of their time in the forest and build semi-permanent camps where most of the family resides. Foraging makes up most of the subsistence of this group, although some meat is acquired through collective net hunting (Bahuchet, 1990; Hewlett, 1996).

Russian Eskimo

The sample of Siberian Peninsula Eskimo is from a site in Ekveni. It is believed that the individuals lived a traditional life on the northern ice caps and along the coast of the Siberian

Peninsula, relying mainly on fish and sea mammals for their subsistence (D. Pezhemsky, curator, 2007 personal communication).

Russian Mesolithic

This Russian Mesolithic sample is curated is from a site in Vasilievsky. Vasilievsky is an island in the Baltic Sea and is a district of Saint Petersburg, Russia. An excavation yielded a Mesolithic sample of which 15 specimens were digitised. The individuals were unsexed and not sorted per individual. The indigenous people of the area were hunter-gatherers and may have been seasonally nomadic (personal communication, J. Chistov). The close proximity to the sea might have made it possible for the inhabitants to settle in the region year-round and include a significant amount of fish in their diet.

Siberia

The Siberian sample is curated at two museums: the Royal Institute for Natural Sciences, Brussels and the Museum of Anthropology at the State University of Moscow. The Belgium sample comprises two individuals, which were excavated in Sibestey and were found in close proximity of each other. The Russian sample comes from Evenki in Northern Transbaikalia, Siberia, and are dated to 1000BC-1000AD. Modern inhabitants of Evenki still practice a traditional lifestyle, and there is no reason to believe that this lifestyle was not also characteristic of the archaeological peoples. Abe (2005) describes small semi-permanent, family group settlements subsisting on small scale year round mammal hunting. They preferred large game such as mutton and reindeer but hunted other animals opportunistically for the rest of the year (Abe, 2005).

South Dakota Native Americans

The South Dakota Native American sample was found on the Oahe Reservation and is from after 1750 AD. They are most likely Arikara, although the sample is not assigned to a specific population. The post-contact Arikara had some sedentary settlements and were mainly

equestrian hunter-gatherers. They were not practicing agriculture or horticulture at these sites (Owsley and Jantz, 1994).

Tasmanian

Two Tasmanians are included in the sample. One specimen is curated at the Royal Institute for Natural Sciences in Brussels, the other, until recently, was curated at the Natural History Museum in London. The Tasmanians are the extinct aboriginal population of Tasmania, an island 275 km south of Australia, and were a physically distinct population from the Australian Aborigines because of the separation of Tasmania from greater Australia between 12000 and 6000 BP (Wunderly, 1938; Henrich, 2004).

They had no clothing or control of fire and the archaeological record shows that they stopped eating deep sea fish around 4000 years ago but still ate crayfish and shellfish. They were mainly hunter-gatherers who hunted birds, kangaroo, wallaby and opossum (Wunderly, 1938; Henrich, 2004).

Tierra del Fuego

Tierra del Fuego is an archipelago south of the southernmost tip of mainland Argentina. The southernmost point of the Islands is Cape Horn. A right femur, ulna and radius of a single individual that was described as having syphilis in the left side of the body was included along with an isolated femur belonging to a different individual. It is unclear to which of the Feugian groups this material belongs. However, the relatively small stature of the individual with the femur, ulna and radius would seem to preclude an Ona affinity while the stature of the isolated femur is consistent with Ona affinity.

The Fuegians are not a homogenous group but rather three distinct groups, living on different islands with different languages, different appearances and different cultures. The first group are the Aliculufs (also Halakwulup or Alacaluf), the second the Yahgans (also Yagan or Yaganes). These two groups are the most closely related in appearance. They are stocky and short statured, wore very little or no clothes, despite the cold weather conditions, lived in canoes and fed off

mussels, snails, crabs, and fish. The third group is distinctly different. They are the Ona and are very tall and have been described as "giant Indians". They used no canoes and were hunter-gatherers (Gusinde, 1939; Bollen, 2000). The Fuegians were described as being morphologically close to Neanderthals (Gusinge, 1939; Martin, 1959; Genna, 1930).

3.2. Methods

This project employs a comparative approach to assess the patterns of morphological variation in hominins in relation to aspects of body size, environmental and behavioural variability. The primary features under consideration here are curvature and apex of curvature of the femur, ulna and radius. However, the collection and analysis of univariate measurements and other shape variables were collected and analysed for two purposes: 1) to aid in the interpretation of curvature as part of the rest of the morphology, and 2) to investigate the overall morphology of each of these bones for the individuals and groups.

The functional significance of long bone curvature in humans is not well understood, and a variety of hypotheses have been suggested to explain curvature in modern humans and Neanderthals (Chapter 2). Each of the hypotheses under consideration will be considered independently. Data for each individual is combined with environmental, geographic and behavioural information for the population.

3.2.1. Population data and categories

3.2.1.1. Time period

The European sample is divided into four categories based on time period of the sample, and is regardless of activity pattern. These categories are: Mesolithic, Neolithic, Medieval and 18^{th}-19^{th} century.

3.2.1.2. Environmental data

A number of environmental variables were collected for each of the modern human population samples: latitude, temperature, rainfall, and altitude.

Latitude: Mean latitude of the site at which the remains were discovered. Latitude is a good

proxy for climate as it shows a strong relationship with both mean annual and effective temperature (Rose and Vinicius, 2008). Absolute latitude is used for investigating the relationship between climate and skeletal variables.

Temperature: Average annual temperature at the place of origin is used to create a distance (difference) matrix (data from Hijmans *et al.*, 2005) in order to determine if average annual temperature and curvature are correlated.

Rainfall: A matrix similar to that for annual temperature was created for average annual rainfall (data from Hijmans *et al.*, 2005) in order to determine if there is a correlation between average annual rainfall and curvature.

Altitude: Average altitude at the place of origin of the population. A dissimilarity matrix for this variable is used to test for a relationship between differences in elevation and curvature of the femur because high altitude areas are typically hilly or mountainous with complex topography. Possible caveats are high altitude plains where little elevation differences are found (data from Hijmans *et al.*, 2005. See also http://www.worldclim.org/).

3.2.1.3. Activity levels and subsistence strategy

Although there is a variety of ways to quantify the activity levels involved in subsistence activity or habitual behaviour (see Stock, 2002), osteological museum collections are often limited to making broad cultural generalizations about habitual behaviour. Therefore, the confidence that can be had in numerical estimates of number of moves a year, distance used over the course of the year and length of the average movement is very low. Bearing this in mind, the populations were first classified into three broad categories related to habitual activity levels.

The "low activity" group are those who lived in urban areas and traded for their food in an urban setting: mobility levels and activity levels are low. The "moderate activity" group are individuals who lived in permanent settlements and relied on intensive agriculture for subsistence: mobility levels are low but activity levels are generally high. The "high activity" group are foragers (hunter-gatherers) but also horticulturalists and pastoralists: mobility levels and activity levels are high in all of these populations. Pastoralist communities, such as the Saami, have been

included into the group of hunter-gatherers in some previous studies because their herding lifestyle involves long seasonal migrations and thus entails a higher level of mobility than the more sedentary agricultural populations (Pearson, 2000b).

Within these three broad activity categories, the "high activity" group was divided into five more narrow subsistence categories: pedestrian, equestrian and aquatic foragers, horticulturalists and pastoralists. These categories are used to test for differences in curvature associated with specific habitual subsistence behaviours. It is important to consider these generalisations, and bear in mind that they may not apply to every individual in the population.

3.2.2. Individual data

In addition to the categorical data for populations, individual data and univariate measurements were collected for each specimen. Table 3-4 is a list of data collected for each individual.

Table 3-4 Summary of individual data collected during this project.

Category	Description
Place of origin	Place where the remains were found or collected
Population	Population name
Age	Absolute age for those known or mean of the estimated age range
Age category	Young adult: epiphyseal sutures visible
	Adult: no visible epiphyseal sutures or age-related pathologies
	Old adult: mild signs of old age such as osteoporosity, arthritis present (severe cases excluded)
Sex	male or female or unknown
Side	left or right

3.2.3. Univariate measurements

Standard univariate measurements used in osteometric research were collected using the landmarks (see Appendix 1-Appendix 7). Most of these were described in Martin and Saller (1959). The distances or angles were calculated from the 3D coordinates (see below 3.3.4.) using geometric methods or vector algebra. Some of these measurements may not directly feature in the analyses because they were used to calculate indices and ratios.

3.2.4. Bone shape

In order to capture shape of the long bones, geometrical morphometrics is employed here (Bookstein, 1991; Adams *et al.*, 2004). The relevant analytical approaches have been developed by a number of authors and are summarised in O'Higgins (2000) and Gunz *et al.* (2005).

Geometric morphometrics offer considerable advantages over linear measurements because results can be visualised as configurations of landmarks in the original space of the specimens rather than only as secondary plots and diagrams. This study also includes the use of semi-landmarks, allowing for the incorporation of outline and surface information. Semi-landmarks make it possible to include point and outline information in a single analysis and to consider the curves separately or as part of the whole bone morphology.

The data for each individual are configurations of homologous landmarks and semi-landmarks. Each configuration is partitioned into its size and its shape. Size is represented in the analysis by centroid size, which is the square root of the sum of squared Euclidean distances from each landmark to the mean of the landmark coordinates. Shape is represented by the difference in coordinates of corresponding landmarks between specimens. These shape coordinates are the curves along the surface of the diaphysis and the epiphyses. Differences between the configurations can then be used in multivariate analysis incorporating other environmental and behavioural variables or correlated with centroid size to explore the relationship between shape and size (Bookstein, 1991; Runestad *et al.*, 1993;

Bookstein, 1996; O'Higgins and Jones, 1998; O'Higgins, 2000; Delson *et al.*, 2001; Lockwood *et al.*, 2002; Adams *et al.*, 2004; Gunz *et al.*, 2004; Marcus *et al.*, 2004; Gunz *et al.*, 2005).

3.2.4.1. Equipment and software

For the collection of the landmarks and semi-landmarks a Microscribe 3DX digitiser (Immersion Corporation), a laptop computer, Microsoft Excel and Microscribe Utility Software v.4.0 (MUS v. 4.0) were used. The digitiser includes a fine-tipped or ball-tipped stylus attached to a set of mechanical arms. The tips cannot be used during the same session as they have different lengths. The digitiser measures with an accuracy of 0.23mm (intra-observer error is discussed below) and is not sensitive to temperature, humidity, atmospheric pressure, or magnetic field.

Landmarks are discrete points that were recorded individually each time the tip of the stylus is activated . The initial semi-landmarks were recorded by placing the tip of the stylus on the start point and recording data continuously (every 5 mm for adult) along the length of the desired curve using the auto-plot function in the Microscribe Utility Software v.4.0.

Mathematica 5.1 for Windows (Wolfram Research) is a mathematical software program used for pre-treatment of the semi-landmarks. The methods used to do this are described below (3.2.4.3). After treatment of the semi-landmarks the landmark configurations were imported into Morphologika 2 (O'Higgins and Jones, 1998).

3.2.4.2. Data acquisition and specimen set-up

All bones were initially placed on an osteometric board where the 25%, 50% and 80% levels were taken and marked with small round stickers. The bone was then placed in the upright position in a support with clamps. Both clamps were covered with rubber material to ensure grip and minimal damage to the bone. The distal articulation was placed on the lowest clamp, ensuring the edges of the articular surface could still be accessed with the digitizer. For the ulna and radius an elastic band was used to keep the bone from moving throughout the digitising process. The proximal end was positioned so that it rested between the fingers of the upper

clamp. This secured the bone without obstructing any measurements. The upper clamp was then closed ensuring that the bone was not damaged but well secure (Figure 3-1). For the femur some extra points were marked before mounting it into the clamps. These were the most superior point on the head of the femur and the most inferior point on the distal condyles.

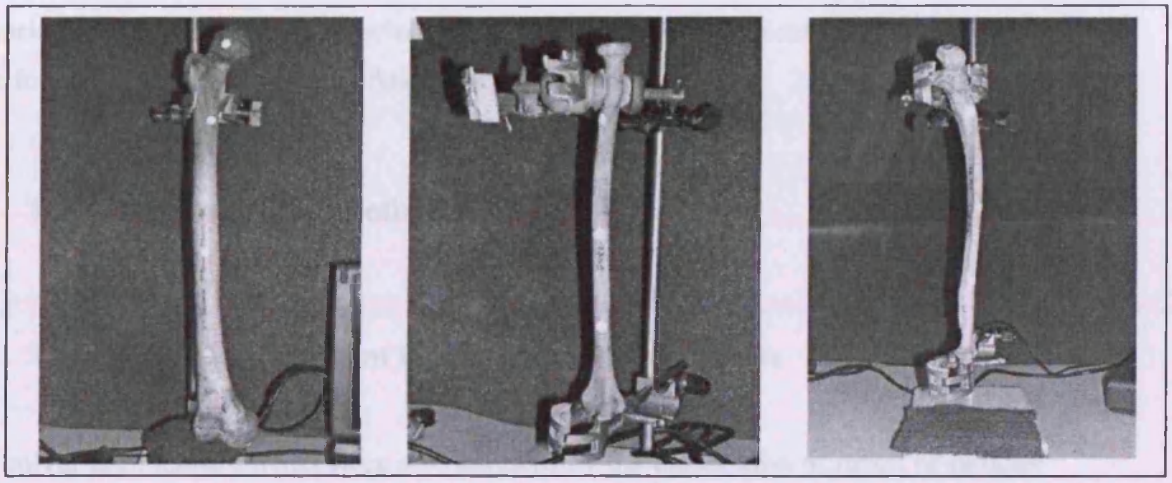

Figure 3-1 Specimen set up for the femur, radius and ulna using clamps and a test tube stand.

3.2.4.3. Landmarks and semi-landmarks

Landmark points should be homologous across specimens. Geometric homology in morphometrics is not the same as biological homology (similarity due to common descent). In its present use homology refers to corresponding discrete geometric structures in different individuals, species or throughout developmental stages. Landmarks and semi-landmarks are the representations of such structures (Gunz *et al.*, 2005).

Landmarks have been categorised by Bookstein (Bookstein, 1991). Type I landmarks are precise juxtapositions of tissues such as triple points of suture intersections. Type II landmarks are associated with, for example, the maximum of a curvature on local structures with a biomechanical implication. Type III landmarks are extremal points or mathematically constructed points like the endpoints of length, breadth, and proportional levels on a bone (e.g. 80%, 50%, 25%) (Bookstein, 1991). Many structures, like the long bone diaphysis, lack precise landmark positions. Points on curves, for example, cannot be said to correspond with the same

points across the sample, except in so far the curve itself is the same. Semi-landmarks allow for surfaces and curves in between type I, II or III landmarks to be included in the analysis by representing parts of biological structures that correspond across specimens.

Thirty-seven landmarks and four curves comprised of semi-landmarks were collected on the femur; twenty-nine landmarks and two curves were collected on the radius; and thirty-six landmarks and one curve was collected on the ulna. A list of landmarks and landmark diagrams can be found in the Appendix 1 to Appendix 6.

3.2.5. Analytical methods

3.2.5.1. Size adjustment for the linear measurements

Some univariate measurements were size adjusted by the calculation of ratios or indices (Appendix 1 to Appendix 6) multiplied by 100 to facilitate comparisons. Using indices eliminates the effect of scale on the measurement, although allometric effects are not estimated.

3.2.5.2. Procrustes methods

Superimposition methods were used to register landmarks and eliminate variation due to overall size. General Procrustes analysis (GPA; also referred to as GLS: Generalised Least Squares) superimposes landmarks using least-squared estimates for rotation and translation. First, the centroid (square root of sum of squared Euclidean distances from each landmark to the mean of the landmark coordinates) of each landmark configuration was fitted to the origin (1st specimen), and configurations were scaled to a common unit size (Adams et al., 2004; Bookstein, 1991).

The landmark configurations were then rotated and translated to obtain an optimal or closest fit between all points of the configuration and the origin (Adams et al., 2004; Bookstein, 1991; Bookstein, 1996; O'Higgins, 2000). This process was subsequently repeated for all other configurations in order to compute the mean shape. The squared root of the sum of the square

coordinate differences after superimposition is a measure of the differences in shape between landmark configurations and is called the procrustes distance (Bookstein, 1996).

3.2.5.3. Treatment of semi-landmarks

Before General Procrustes Analysis semi-landmarks must be registered so that they are homologous for comparison between individuals (following Gunz *et al.*, 2005). First, a cubic spline is fitted through the recorded landmarks, and this cubic spine is resampled every 1mm. Then a desired number of equidistant points are selected along each of the curves. To test if the number of semi-landmarks impacts repeatability, 10 or 20 semi-landmarks on the femur were chosen. A small number of semi-landmarks (compared to the infinitely large number of points on the curve) eases computational demand and is sufficient to describe femoral curvature. An alternative to equidistant points is to slide the desired number of landmarks along the tangents to the curve, but this is unnecessary for simple curves (Gunz *et al.*, 2005; Bookstein, 1996).

After this registration procedure the configurations were exported into Morphologika 2 (O'Higgins and Jones, 1998) for further analysis, together with the other landmarks recorded during data collection.

3.2.5.4. Principal component analysis

Principal component analysis (PCA) employs two or more observations for each individual, which are then combined to produce uncorrelated indices that explain different dimensions in the data with fewer variables than the original observations. These indices (called Principal Components) are ordered so that the first explains the largest amount of variation and the second explains the second largest amount of variation, and so on. In geometric morphometrics Principal Components Analysis is based on relative warps. Relative warps are linear combinations of partial warps and their scores (Dytham, 1999).

The whole range of "warps" in geometric morphometrics are derived from thin-plate spine analysis (Slice, 2005). This is the projection of the points after GPA on a space that is tangent to Kendall's shape space. The shape space is a generalized curved space with more than three dimensions that can be compared to the surface of the earth and the set of possible shapes for any given landmark configurations with the same number of landmarks and dimensions

(Monteiro *et al.*, 2000). Here, the distances between the points between two sets of landmarks (referred to as the distances between pairs of points) approximate the Procrustes distances. The first landmark configuration is usually the reference, the group mean, and the second configuration is the target. The differences between single pairs of points are calculated as the displacements of right angles out of the plane of the reference. Those equations are recombined to express the totality of differences between the two (Adams et al., 2004; Bookstein, 1991; Mitteroecker et al., 2005; Slice, 2005).

The graphical representation of landmark configurations makes it easy to visualise shape differences (Lockwood et al., 2002; Slice, 2005). These differences are computed during PCA and represent the total shape variability into un-correlated variance-maximising variables (also called principal components). The percentage variance explained by each of the principal components is used to determine which components to examine (based on a scree plot of eigenvalues). These scores (PC scores) can then be used as data in multivariate analyses and combined with other variables (Adams et al., 2004; Bookstein, 1991; Mitteroecker et al., 2005; Slice, 2005).

There is another benefit to the use of the 3D morphometric techniques and this is the possibility to use only partial landmark configurations in the PCA. Therefore, in order to analyse different anatomical features separately, subsets of landmarks and semi-landmarks can be selected and Principal Component Scores can be used to represent a certain trait, rather than the total bone shape. Visualisations using vector plots of the shape changes along the Principal Components can then be used to interpret the changes in morphology (Slice, 2005). Subsets of data used in the analysis here are described in the results chapters (Chapter 4 and 5).

3.2.5.5. Intra-observer error

To test the repeatability of the 3D landmarks themselves, data were recorded on three human skeletons at University College London. Each specimen was measured three times in one week.The Procrustes distances from GPA superimpositions of the landmark and semi-landmark configurations were used as a measure of observer error (Lockwood et al., 2002). This value increases with increasing shape difference between two specimens. Also, when repeat measurements from the same individual are superimposed using GPA, it is possible to identify

the landmarks with the greatest error. Floating landmarks such as the middle of a surface or the individual curves were expected to vary most.

Error results for the geometric morphometric analysis varied depending on how many semi-landmarks were chosen. Using 20 semi-landmarks, error differences between the three repeats (mean difference 0.017, n=9 comparisons) were nearly as great as variation between different specimens (mean difference 0.018, n=27 comparisons). Using the 10 semi-landmarks, the mean difference between specimens was 0.034 for 27 comparisons, and the mean difference between repeats was 0.015 for nine comparisons. Using 10 semi-landmarks along with fixed landmarks, the difference between specimens (mean difference 0.045, n=27 comparisons) was greater than variation between repeats (mean difference 0.017, n=9 comparisons). These positive results for a introduced number of semi-landmarks imply that the curve itself was sufficiently described by ten semi-landmarks, and additional landmarks reflected error such as slight horizontal movement of the hand when recording a curve down the smooth and featureless anterior surface of the femur. For this reason, ten semi-landmarks were used in all analyses.

3.2.5.6. Discriminant function analyses

Using SPSS v.15 discriminant functions were calculated using the principal component scores for groups of individuals. This technique maximizes differences between known groups and makes predictions about individuals for which the group is not known (Dytham, 1999). In the analyses, groups were Neanderthals, early modern humans and recent modern humans. Only principal components that were found to explain a substantial amount of variation (see Chapter 5) are considered for inclusion (Dytham, 1999; Weaver, 2002).

3.2.5.7. Analysis of Variance (ANOVA)

ANOVA was used to determine the effect of factors influencing curvature. Post-hoc tests were performed to identify differences between the samples. The samples were grouped in categories (see section 3.2.1). Both a Hochberg's GT2 (for very different sample sizes, Field, 2000, p. 341) and a Games-Howell procedure (for small and uneven sample sizes where homogeneity of variance is not assumed for all samples, Field, 2000 p. 341) were used in SPSS v.15.

3.2.5.8. Mantel test

Mantel tests were used to investigate relationships between morphological and environmental distances between pairs of populations using Passage v1 (Rosenberg, 2001). A distance matrix is a way of describing the difference (dissimilarity) between pairs of populations. A Mantel test tests the null hypothesis that distances in the first matrix are independent of distances in the second matrix. The statistic used for the measure of the correlation between the two matrices is the Pearson correlation coefficient. In order to test the null hypothesis, a randomization procedure is used which compares the original value of the correlation coefficient to that found by randomly reallocating the order of the elements in one of the matrices (Manly, 1997).

For each Mantel test morphological distance matrices of PC scores for curvature, apex of curvature and the whole bone are correlated to the distance matrices of the environmental factors: temperature, rainfall, altitude. Although a number of authors have used Mahalanobis distances (Ackermann, 2002; Harvati, 2003a; Harvati, 2003b; González-José *et al.*, 2004; Harvati and Weaver, 2006) this project uses Procrustes distances only as they are not affected by uneven sample sizes and do not assume similar covariance structures for all groups (Smith *et al.*, 2007).

3.2.5.9. Other univariate analyses

Depending on the hypothesis being tested, a variety of univariate statistical analyses were used, including Student's *t*-test and Pearson's correlation analyses. For correlations with ontogenic age, a non-parametric Kendall's Tau b was used as not all ages were represented and the age of some individuals was determined from skeletal markers.

For the ulna and radius the effect of asymmetry was investigated using Student's *t*-test. The sample was collected using the best preserved side of the skeleton. In samples where preservation is good, this resulted in a 50/50 split. In some cases, however, one of the sides was unavailable for research. The effect of side was tested using a Pearson's Chi-Square test on the recent modern human sample. Despite the results being affected by small sample sizes or

samples with only one side represented ($N<5$), in about 50% of cases the test is highly significant ($p<0.001$) indicating that the sampling of left and right was not independent. For this reason, all analyses on the radius and ulna that were performed on the pooled sample were conducted also for the right side only. If the significance values were affected, those results will also be reported.

3.3. Order of analysis for Chapter 4

The purpose of the results in Chapter 4 is to test the series of hypotheses and predictions set out in Chapter 2. The results will be presented first for the femur and then for the lower arm. The order and protocol of the analyses in both sections is described here.

Although multiple tests are conducted that test for statistical significance, the Bonferroni correction was not applied. This is part of a general concern that overuse of the Bonferroni method may result in overly conservative results (see Moran, 2003; Nakagawa, 2004). Also, in this work most of the tests are performed to address specific predictions and hypotheses, and the chance of spurious significance is reduced. For the more exploratory parts of the analysis, caution is applied when results do not fit any a priori expectation, but at the same time these results are highlighted given the general lack of detailed previous work on these skeletal elements.

3.3.1. Shape data

Initially, Procrustes coordinates for all individuals were analysed using Principal Components Analysis to partition the total shape variability into un-correlated variance-maximising variables. The percentage variance explained by each of the principal components was used to determine which components to examine, based on where eigenvalues level off on a scree plot. Graphical representations of landmark configurations are used to visualise shape differences and to match each principal component to components of curvature or other aspect of shape variation.

3.3.2. Correlations between shaft shape and univariate measurements.

In order to identify the covariates with curvature and understand curvature as part of the rest of the anatomy, Pearson's correlations were performed to look for covariates between 1) the univariate measurements, 2) the univariate measurements and curvature and 3) the univariate measurements and other aspects of bone shape. These analyses were performed on the whole

recent human sample and on the high-activity category because expression of skeletal differences is more pronounced in the latter group. Some predictions were made (see Chapter 2: Hypotheses and predictions) about the relationship of curvature to these univariate measurements, but most of these correlations were exploratory.

The following Pearson's correlations were performed:

- Femoral shape with neck-shaft angle, torsion angle, femur length, neck length, shaft shape ratios (at subtrochanteric, midshaft and subpilastric level), robusticity (distal condyles, midshaft and head).
- Radius shape with robusticity (head, midshaft and distal articulation), radius length, neck-shaft angle, position of the radial tubercle, dorsal and lateral subtense, neck length, head shape and midshaft shape.
- Ulna shape with maximum length, olecranon size, midshaft shape, radial notch size, trochlear notch orientation, olecranon orientation, coronoid-olecranon ratio, length of the pronator crest, position of the brachialis insertion and robusticity.

3.3.3. Body size

Research on the use of skeletals element in body size estimation has argued for the use of lower limb bone dimensions to predict body size for modern humans and fossil hominins (see review in Ruff, 2000a; Auerbach and Ruff, 2004; Ruff *et al.*, 2005). As articular dimensions are relatively insensitive to variations in the mechanical environment compared to diaphyseal breadth (which can over- or underestimate body size in populations with different activity levels), the femoral head diameter has often been used (Ruff, 1991; McHenry, 1992; Grine *et al.*, 1995) as has bi-iliac breadth (McHenry, 1992; Ruff *et al.*, 1994). Because it was unknown whether specimens would have the pelvis preserved and less estimation is involved for femoral head diameter than for bi-iliac breadth, femoral head-diameter is used as an indicator for body size in this study.

Absolute femoral head diameter was used here to investigate the relationship of body size with curvature. It is known that robusticity scales with body size (van Der Meulen *et al.*, 1993; Ruff, 2000a; Stock, 2002; Stock and Pfeiffer, 2004), and this pattern was first confirmed for this sample. Subsequently, the correlation between curvature and body size will be investigated using

population means for principal components related to curvature. For the lower arm, this part of the analysis is possible only when femoral head diameter of the individual was known.

3.3.4. Sex

In order to assess sexual dimorphism in curvature, all individuals of known sex were compared using a Student's *t*-test for robusticity and curvature, as well as for the other bone shape PCs and the univariate femur measurements. If there is a significant relationship between body size and curvature, it is expected that sexual dimorphism in curvature is at least partly related to differences in body size between males and females. Sex differences may also be related to different bone modelling and remodelling rates in males and females or differences in activity levels due to sexual division of labour. Similar predictions have been made for robusticity, and the present sample will therefore be analysed for external robusticity (at midshaft, distal and proximal condyles) in order to determine whether the sample follows patterns established previously for humans. Because sexual division of labour is more pronounced as general activity levels increase, the tests are repeated for the "high activity" category (foragers, horticulturalists and pastoralists), "moderate activity" (intensive agriculturalists) and "low activity" (urban trader) category samples separately.

3.3.5. Age

In order to investigate whether curvature decreases with decreasing activity levels through adulthood, a Spearman's rank correlation was performed on individuals of known age or estimated age. Spearman's rank correlations were also used to investigate the effect of increasing age on other aspects of shaft and epiphyseal shape and other univariate measurements to see if they aid the interpretation of trends observed in curvature. Because age is not known or estimated for the majority of the sample, age categories (See section 3.2.2 for details) were used to test the predicted relationship for the sample as a whole.

3.3.6. Activity patterns

The purpose of these analyses is to investigate if curvature is higher in populations with high activity levels. The samples were divided into three main categories based as described in section 3.2.1.3. For each of these analyses, the high activity category was divided into five subsistence categories to investigate if there are differences between specific foraging strategies in curvature of the lower arm and the femur. Other shaft shape variables and univariate measurements were also analysed in order to test the effect of activity levels on the other aspects of morphology.

3.3.7. Climate and latitude

Although no direct benefit of having a higher degree of curvature in colder climates has been suggested, curvature may be a consequence of a cold-adapted body shape. In this analysis, climate and specifically temperature is quantified using the latitudinal position of the population (Ruff, 1994b; Rose and Vinicius, 2008). After Pearson's correlations are performed between latitude and curvature, the other shaft shape variables and univariate measurements are also investigated to determine the suite of morphological features which vary in response to climatic conditions. The analyses will be repeated for the high activity category because these populations may be more exposed to temperature extremes than are populations in the moderate and low activity categories.

3.3.8. Evolution over time

In order to test for changes in curvature with increasing sedentism, the European sample is divided into four categories: Mesolithic, Neolithic, Medieval and 18^{th}-19^{th} Century. Differences in curvature are analysed by means of an ANOVA for principal components representing curvature and apex of curvature.

3.3.9. Mantel test

A Mantel test is used to test for correlations between environmental factors (temperature, rainfall, and altitude) and curvature (degree of curvature and apex of curvature) and whole bone shape. Five thousand permutations were performed for each of the tests.

3.3.10. Systemic influences

To investigate whether curvature is systemic, the sample for which all three bones are represented was used. A Pearson's correlation analysis was performed on the population means for the degree of curvature related PCs for all three bones.

CHAPTER 4. INTRASPECIFIC DIFFERENCES IN LONG BONE CURVATURE IN MODERN HUMANS

4.1. Objective

Chapter 2 illustrated the effects of bone remodelling in response to use. Distinctive anatomical features of the long bones are modified during development in ways that optimise strength and adaptability in response to different activity levels. Here, the behavioural and environmental effects on long bone morphology among modern humans are explored with the aim of providing a context to understand the fossil populations.

In the results described below the abbreviations of the principal components (PCs) names are made up of three parts. The first designates the landmark set included in the study (i.e. "acurve "stands for anterior curve). The second designates the sample included (i.e. "AMH" stands for all recent modern humans). The third is the PC number (i.e. "PC2" stands for the second PC).

4.2. The femur

4.2.1. Femur shape principal components explained

The following analyses are based on the entire sample of modern humans and the analyses were carried out using the methodology described in Chapter 3. The magnitude and pattern of variation for the femoral anterior, posterior, medial and lateral curves are visualised using Morphologika®. Variation in the femoral proximal and distal epiphyses are analysed in a similar fashion. The curves are semi-landmarks on the diaphyseal surface only, whereas the epiphysis analysis uses fixed landmarks (for details see Chapter 3: Materials and Methods). In figures, viewing angles were chosen to best illustrate similarities and differences. For the curves, this is in lateral view, unless otherwise stated. Arrows indicate areas of change.

4.2.1.1. Anterior surface (acurve)

The first four PCs of the anterior curve analysis explain 61.9%, 8.49%, 7.06% and 6.33%, respectively, of the variation (total 73.9%). Subsequent PCs explain minimal amounts of the variation and are not considered further. The distribution of populations in Figure 4-1 shows the wide range of variation for PC1 compared to PC2.

PC1 clearly reflects differences in degree of anteroposterior curvature or subtense (Figure 4-1 and Figure 4-2a). PC2 reflects the position of the apex of curvature (Figure 4-1 and Figure 4-2b). PC3 is the medial or lateral deviation of the distal end of the curve in anterior view (Figure 4-2 c). PC4 is the degree to which the curve is mediolaterally sinusoidal from anterior view (Figure 4-2d).

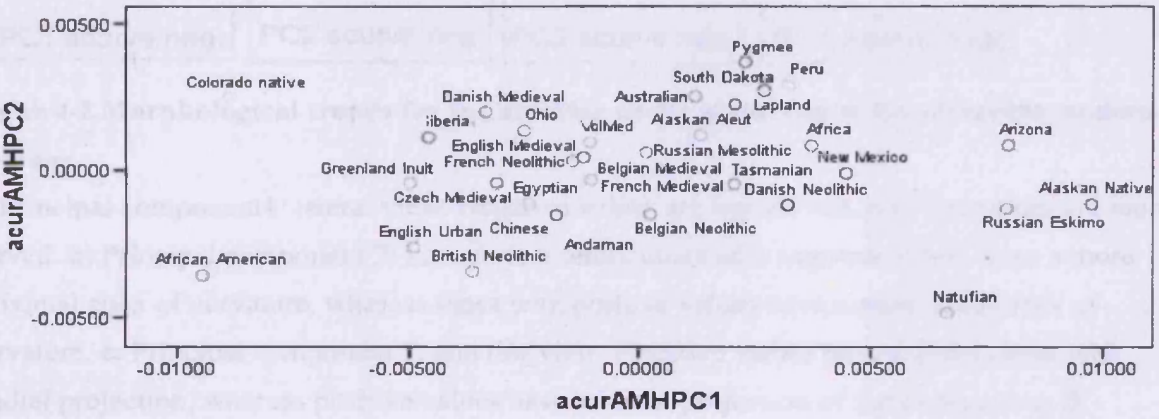

Figure 4-1 The first and second PCs for the anterior curve of the femur. All recent modern human samples.

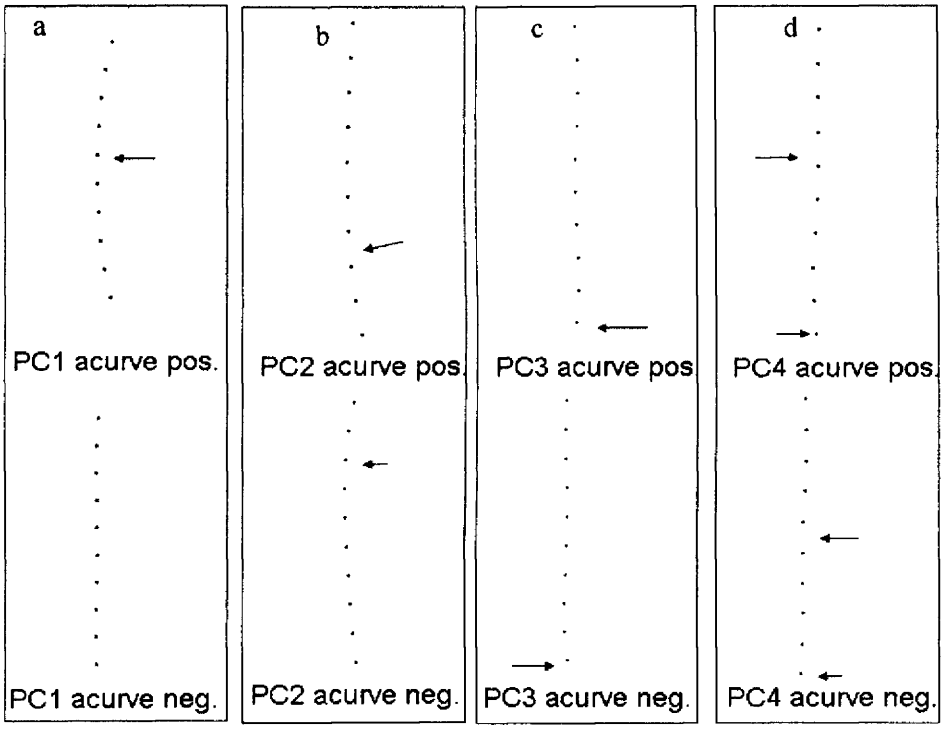

Figure 4-2 Morphological trends for the anterior curve of the femur for all recent modern humans.

a: Principal component1: lateral view. Negative values are less curved, positive values are more curved. **b**: Principal component 2: lateral view. Individuals with negative values have a more proximal apex of curvature, whereas those with positive values have a more distal apex of curvature. **c**: Principal component 3: anterior view. Negative values have a distal curve with medial projection, whereas positive values have a lateral projection of the distal curve. **d**: Principal component 4: anterior view. Negative values are the straightest, whereas positive values indicate a sinusoidal shape. Positive and negative visualisations correspond to the most extreme positive and negative scores for each PC.

4.2.1.2. Posterior surface (pcurve)

The first four PCs of the posterior curve analysis explain 28.7%, 14.5%, 10.5% and 6.38%, respectively, of the variation (total 60.08%). Subsequent PCs explain minimal amounts of the variation and are not considered further.

The posterior PCs are very similar to the anterior curve. PC1 reflects variation in the degree of anterior curvature (Figure 4-3 and Figure 4-4 a). PC2 is the posterior projection of the proximal end of the curve (Figure 4-4 b). PC3 is related to the apex of curvature (Figure 4-3 and Figure 4-4c). PC4 is the direction of the posterior projection of the distal end of the curve (Figure 4-4d). Population distribution for the degree and apex of curvature is shown in Figure 4-3.

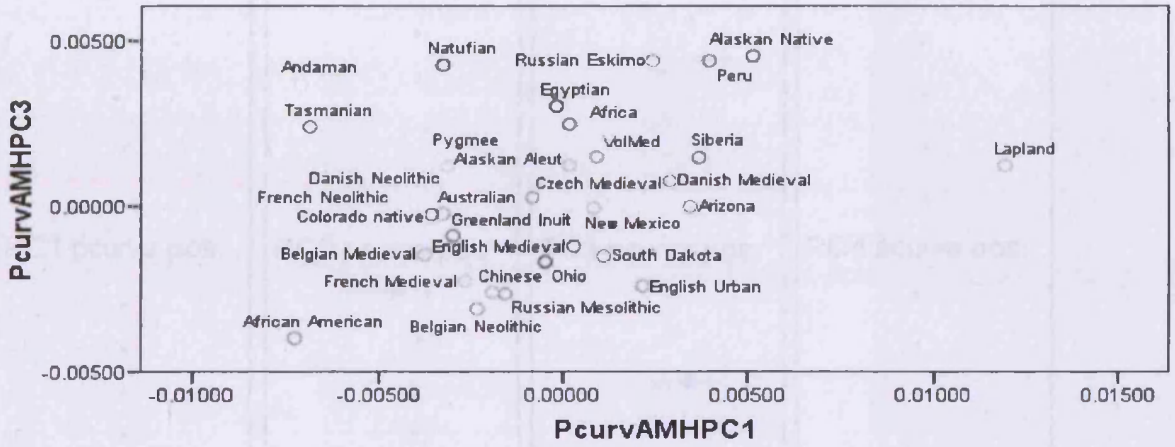

Figure 4-3 The first and third PCs for the posterior curve of the femur. All recent modern human samples. PCs are explained in Figure 4-4.

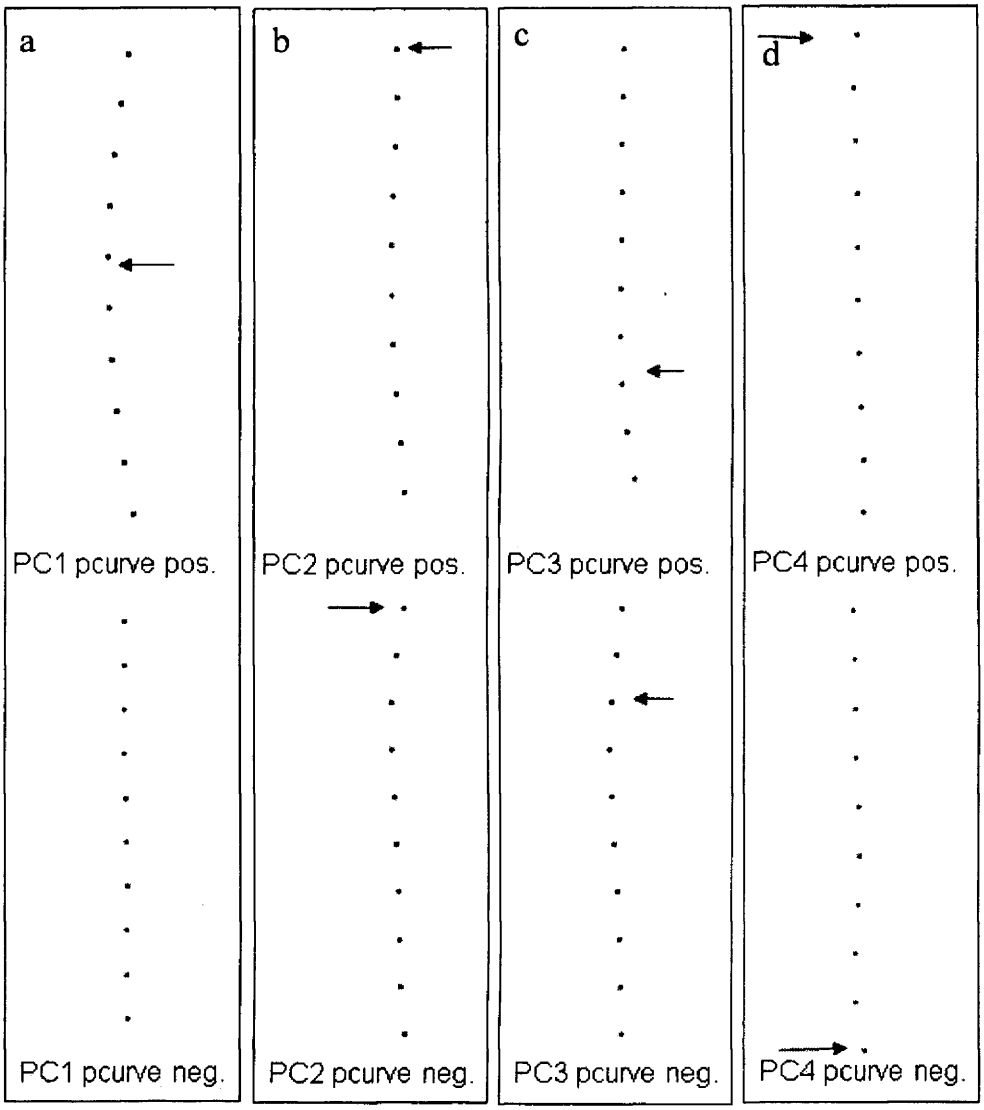

Figure 4-4 Morphological trends for the posterior curve of the femur for all recent modern humans. **a**: Principal component 1: lateral view. Negative values have a low and positive values have a high degree of curvature. **b**: Principal component 2: lateral view. Positive values have a less posteriorly projected proximal posterior surface and negative values are more posteriorly projected. **c**: Principal component 3: lateral view. Negative values have a higher apex of curvature and positive values have a lower apex of curvature. **d**: Principal component 4: anterior view. Positive values have a less posteriorly projected distal posterior surface and negative values are more posteriorly projected distally. Positive and negative visualisations correspond to the most extreme positive and negative scores for each PC.

4.2.1.3. Medial surface (mcurve)

The first three PCs of the medial curve analysis explain 49.1%, 17.2%, and 5.52% „respectively, of the variation (total 71.82%). Subsequent PCs explain minimal amounts of the variation and are not considered further. Distribution of populations is shown in Figure 4-5.

Patterns in the first two PCs are similar to those of the anterior curve. PC1 reflects differences in degree of anteroposterior curvature (Figure 4-5 and Figure 4-6a). PC2 is related to the apex of curvature (Figure 4-5 and Figure 4-6b). PC3 is the posterior projection of the distal end of the curve and the evenness of the curve (Figure 4-6c).

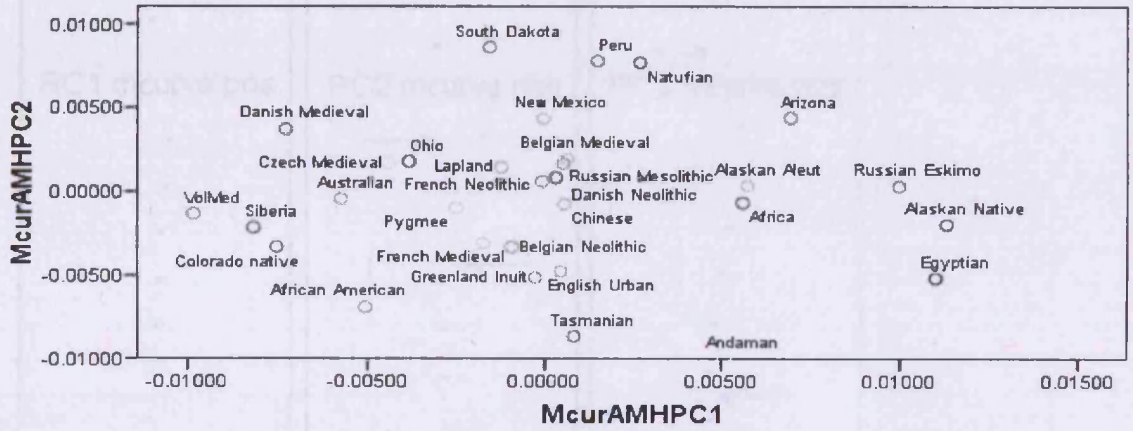

Figure 4-5 The first and second PCs for the medial curve of the femur. All recent modern human samples. PCs are explained in Figure 4-6Figure 4-4.

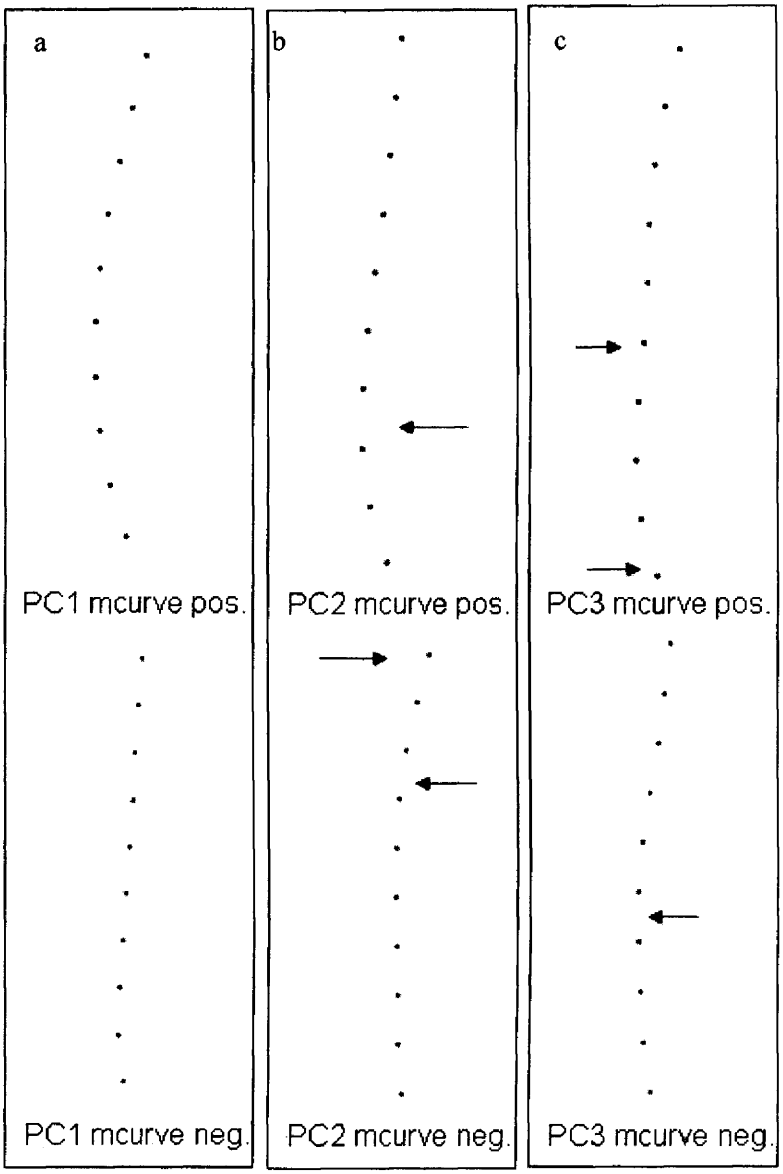

Figure 4-6 Morphological trends for the medial curve of the femur for all recent modern humans. All in lateral view

a: Principal component 1. Positive values have a higher degree of curvature compared to negative values. **b**: Principal component 2. Positive values have a lower apex of curvature, whereas negative values have a more proximal apex of curvature. **c**: Principal component 3. Positive values are more flattened off with increased posterior projection of the distal curve, whereas negative values reflect a shaft surface approaching an arc of a circle with a lower degree of posterior projection distally. Positive and negative visualisations correspond to the most extreme positive and negative scores for each PC.

4.2.1.4. Lateral surface (lcurve)

The first four PCs of the lateral curve analysis explain 43.8%, 15.2%, 9.08% and 4.82% ,respectively, of the variation (total 72.93%). Subsequent PCs explain minimal amounts of the variation and are not considered further. Distribution of the populations are shown in Figure 4-7.

As in the other curves anterior curvature is the most important factor (PC1) (Figure 4-7 and Figure 4-8a). (Figure 4-7 and Figure 4-8a). The other principal components for the lateral curve are the most difficult to interpret. PC2 is related to the "straightening" of the lateral surface of the femur at the level of the lesser trochanter (Figure 4-8b). PC3 is related to the apex of curvature and the anterior or posterior orientation of the proximal curve (Figure 4-7 and Figure 4-8c). PC4 is the sinusoidal shape of the lateral surface in anterior view (Figure 4-8d).

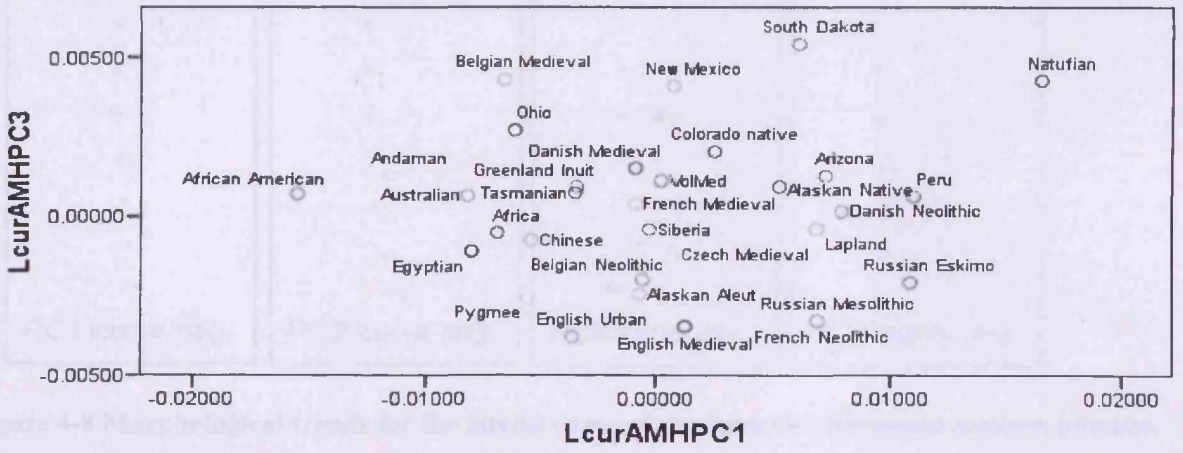

Figure 4-7 The first and second PCs for the lateral curve of the femur. All recent modern human samples. PCs are explained in Figure 4-8.

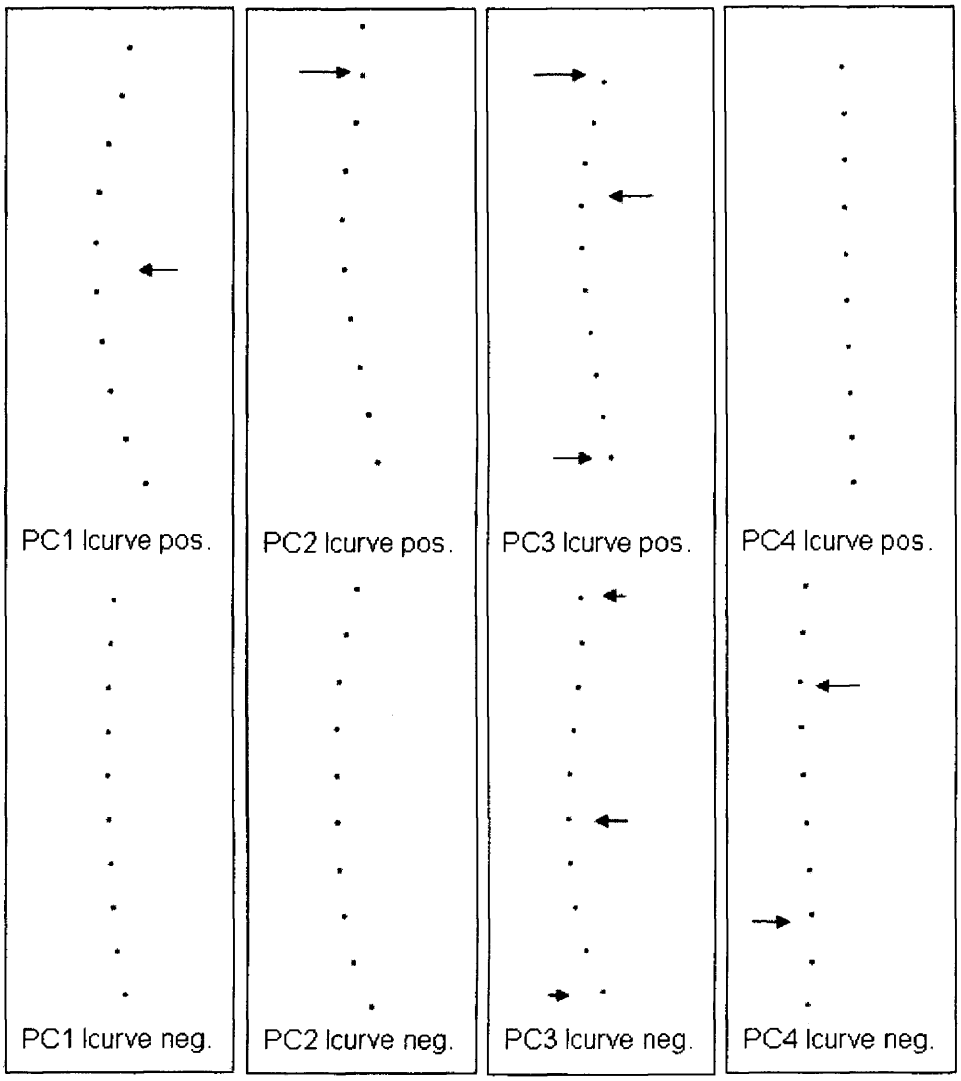

Figure 4-8 Morphological trends for the lateral curve of the femur for all recent modern humans. **a**: Principal component 1: lateral view. Positive values have a higher degree of curvature and negative values have lower degrees of curvature. **b**: Principal component 2: lateral view. Negative values have a curve that approximates an arc on a circle, whereas positive values which have a flattening at the proximal end of the curve **c**: Principal component 3: lateral view. Negative values have a lower apex of curvature and more anterior orientation of the proximal curve compared to positive values which have a higher apex of curvature and a posteriorly oriented proximal curve. **d**: Principal component 4: anterior view. Positive values are the straightest, whereas negative values have an S-curve. Positive and negative visualisations correspond to the most extreme positive (right) and negative (left) PC scores on the scale.

4.2.1.5. Proximal and distal epiphyses (Epi)

The first five PCs of the epiphyses analysis explain 14%, 9.45%, 7.40%, 4.80% and 4.80%, respectively, of the variation (total 39.64%). Subsequent PCs explain minimal amounts of the variation and are not considered further.

PC1 reflects differences in width of the distal epiphyses and neck-shaft angle (Figure 4-9a). PC2 is related to the overall width of the femur and its epiphyses (Figure 4-9b). PC3 is related to the width of the distal epiphyses and degree of torsion (Figure 4-9c). PC4 is not easily interpreted. The changes along the principal component are very subtle, and this PC will therefore not be considered further in the subsequent analyses. PC5 is related to the length of the femoral neck (Figure 4-9d).

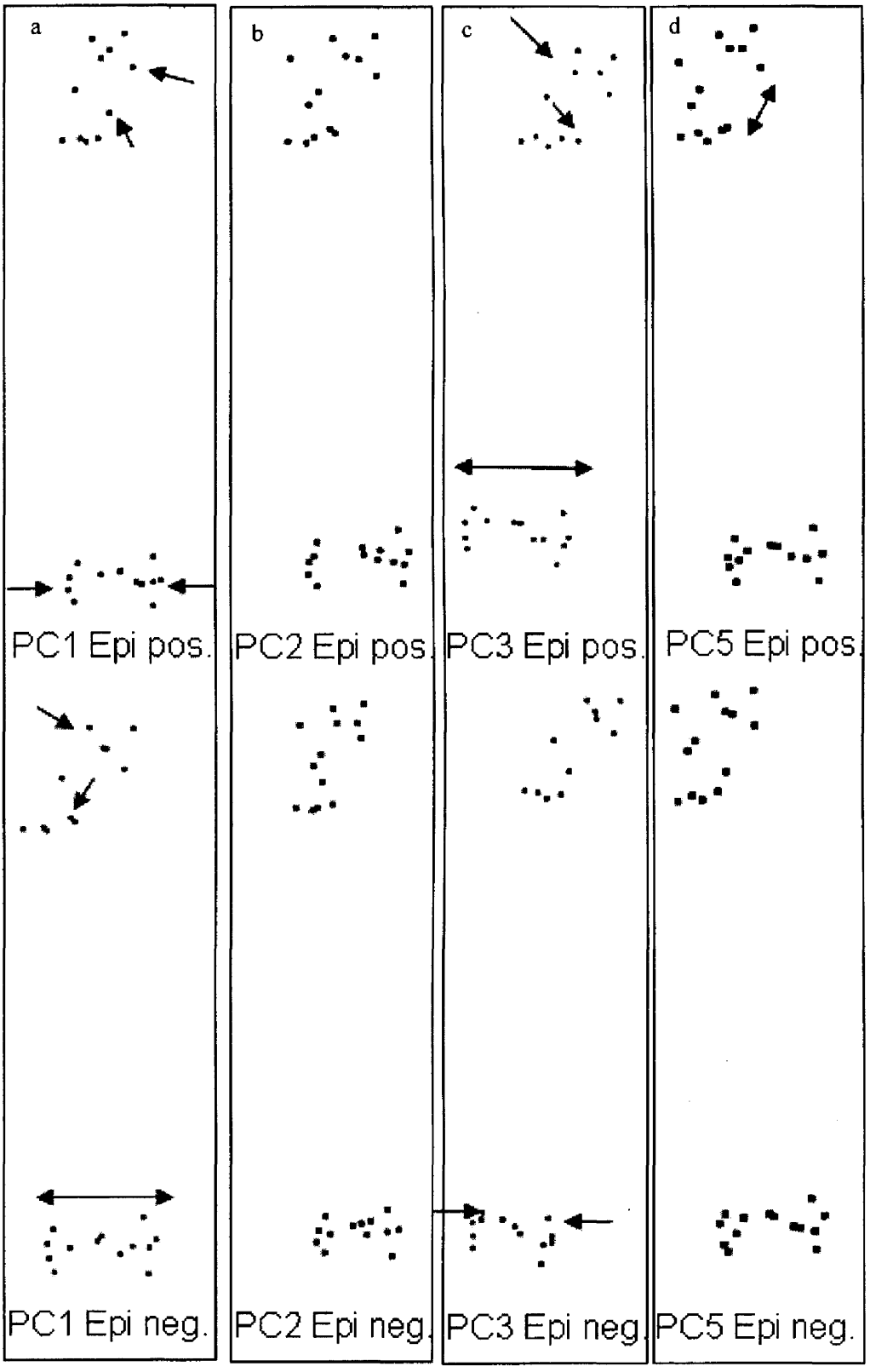
a
b
c
d
PC1 Epi pos.
PC2 Epi pos.
PC3 Epi pos.
PC5 Epi pos.
PC1 Epi neg.
PC2 Epi neg.
PC3 Epi neg.
PC5 Epi neg.

Figure 4-9 Morphological trends for the epiphyses of the femur for all recent modern humans. All anterior view.

a: Principal component 1. Individuals with negative values have wider distal epiphyses, wider shafts and a smaller neck-shaft angle compared to those with positive values. **b**: Principal component 2. Individuals with negative values have narrower epiphyses, heads, neck and proximal shaft compared to those with positive values. **c**: Principal component 3. Individuals with negative values have narrower distal epiphyses, and more torsion compared to those with positive values. **d**: Principal component 5. Individuals with negative values have a shorter neck compared to those with positive values. Positive and negative visualisations correspond to the most extreme positive and negative scores for each PC.

4.2.1.6. Summary

Degree of anterior curvature is the most important PC for all four curves (acurveAMHPC1, pcurveAMHPC1, mcurveAMHPC1, lcurveAMHPC1). This is reflected in the significant correlations between the scores for the curvature PCs (Table 4-1). Because the curves are similar in this respect, only the anterior and posterior curve will be analysed for degree of anterior curvature. There is no correlation between the PCs of the epiphyses and the four curvature PCs.

Apex of curvature (or the position along the shaft where the maximum subtense is located) is the major factor in acurveAMHPC2, pcurveAMHPC3, mcurveAMHPC2, lcurveAMHPC3. Most of these principal components are significantly correlated, although correlations are lower than for PCs related to the degree of curvature (Table 4-12). AcurveAMHPC2 and pcurveAMHPC3 will be used in further analyses to represent the position of the apex of curvature.

The other principal components for each of the four curves explain minor variation in curve shape and will be included in the analyses to explore other aspects of shaft shape in relation to curvature.

Table 4-1 Pearson's correlation matrix: femoral curvature PCs (n= 428).

		acurAMHPC1	PcurvAMHPC1	McurAMHPC1
PcurvAMHPC1	r	0.454**		
	P	<0.001		
McurAMHPC1	r	0.656**	0.241**	
	P	<0.001	<0.001	
LcurAMHPC1	r	0.572**	0.382**	0.358**
	P	<0.001	<0.001	<0.001

** Correlation is significant at the 0.01 level (2-tailed).

* Correlation is significant at the 0.05 level (2-tailed).

Table 4-2 Pearson's correlation matrix femoral apex of curvature PCs (N=428)

		acurAMHPC2	PcurvAMHPC3	McurAMHPC2
PcurvAMHPC3	r	0.238**		
	P	<0.001		
McurAMHPC2	r	0.370**	0.127**	
	P	<0.001	0.008	
LcurAMHPC3	r	0.022	0.018	0.153*
	P	0.647	0.708	0.002

** Correlation is significant at the 0.01 level (2-tailed).

* Correlation is significant at the 0.05 level (2-tailed).

4.2.2. Correlations between PCs and univariate measurements

The purpose of these analyses is to establish covariates between the shape PCs and univariate measurements in order to place curvature in the context of the rest of the anatomy of the femur.

All modern humans

The curvature PCs vary in their correlations with the univariate measurements (Table 4-3). Overall, curvature of the posterior surface is positively correlated with robusticity (head, condyles and midshaft). A rounder midshaft shape (midshaftratio) is correlated with a low degree of anterior curvature. A rounder proximal shaft (subtrochratio) is correlated with a low degree of posterior curvature.

The different apex of curvature PCs vary in their correlations (Table 4-4). Neck-shaft angle and torsion angle are negatively correlated with the position of the apex of curvature (acurveAMHPC2). Robusticity of the condyles is correlated with a lower apex of curvature (EpiAMHPC1). Shaft shape at the subpilastric ratio is negatively correlated with apex of curvature (acurvAMHP2 and pcurvAMHPC3).

Increasing epiphyseal robusticity is correlated (headrob and condylediamratio) with a more posteriorly projected proximal posterior surface (pcurvAMHPC2) (Table 4-5). Torsion angle is positively correlated with a more flattened off medial surface with increased distal projection of the distal curve (McurveAMHPC3). Longer femora have less flattening off proximally of the lateral surface (this flattening reflects the shorter femoral shaft by including the slope towards the lesser trochanter) (Table 4-6).

Table 4-3 Pearson's correlation matrix for femoral curvature PCs and univariate measurements for all modern human populations (N=36).

		acurAMHPC1	PcurvAMHPC1
FemLength	r	-0.104	-0.087
	P	0.548	0.615
Neck-shaft angle	r	-0.028	-0.046
	P	0.871	0.788
torsionangle	r	-0.012	0.178
	P	0.943	0.300
subtrochratio	r	0.189	0.375**
	P	0.270	0.024
midshaftratio	r	0.450**	0.133
	P	0.006	0.439
subpilratio	r	0.188	0.201
	P	0.273	0.239
condylediamratio	r	0.162	0.454**
	P	0.345	0.005
robustindex	r	-0.240	0.207
	P	0.159	0.226
headrob	r	0.187	0.460**
	P	0.274	0.005
necklengthratio	r	0.128	0.501**
	P	0.458	0.002

* Correlation is significant at the 0.05 level (2-tailed).
** Correlation is significant at the 0.01 level (2-tailed).

Table 4-4 Pearson's correlation matrix for apex of curvature PCs and univariate measurements for all modern human populations (N=36).

		acurAMHPC2	PcurvAMHPC3
FemLength	r	-0.304	-0.327
	P	0.071	0.052
Neck-shaft angle	r	-0.437**	0.035
	P	0.008	0.838
torsionangle	r	-0.423*	-0.129
	P	0.010	0.452
subtrochratio	r	-0.047	0.058
	P	0.787	0.737
midshaftratio	r	-0.307	0.001
	P	0.068	0.994
subpilratio	r	-0.417*	-0.346*
	P	0.012	0.039
condylediamratio	r	-0.114	0.389*
	P	0.508	0.019
robustindex	r	-0.067	-0.231
	P	0.696	0.176
headrob	r	-0.038	0.285
	P	0.828	0.093
necklengthratio	r	-0.068	0.116
	P	0.695	0.501

* Correlation is significant at the 0.05 level (2-tailed).
** Correlation is significant at the 0.01 level (2-tailed).

Table 4-5 Pearson's correlation matrix for other shaft shape PCs and univariate measurements for all modern human populations (N=36).

		acurAMHPC3	acurAMHPC4	PcurvAMHPC2	PcurvAMHPC4	McurAMHPC3	LcurAMHPC2	LcurAMHPC4
FemLength	r	-0.086	-0.039	0.038	0.183	-0.119	-0.464*	-0.130
	P	0.618	0.820	0.826	0.286	0.489	0.004	0.450
Neck-shaft angle	r	0.086	0.204	-0.030	-0.087	0.333	-0.256	0.158
	P	0.617	0.232	0.860	0.613	0.047	0.133	0.357
torsionangle	r	-0.023	0.264	0.078	0.046	0.364*	-0.192	0.195
	P	0.893	0.120	0.653	0.790	0.029	0.261	0.254
subtrochratio	r	-0.338*	0.209	-0.225	0.043	-0.044	0.031	-0.337*
	P	0.044	0.220	0.187	0.801	0.799	0.857	0.044
midshaftratio	r	-0.045	-0.003	-0.172	0.161	0.284	-0.193	-0.262
	P	0.793	0.986	0.315	0.350	0.093	0.258	0.123
subpilratio	r	-0.131	0.107	-0.083	0.219	0.180	-0.399	-0.244
	P	0.445	0.534	0.632	0.199	0.292	0.016	0.151
condylediamratio	r	-0.009	-0.028	-0.396*	0.145	0.200	0.075	-0.140
	P	0.956	0.873	0.017	0.398	0.243	0.665	0.415
robustindex	r	0.166	-0.184	-0.187	0.254	-0.252	0.031	-0.159
	P	0.332	0.283	0.275	0.135	0.138	0.858	0.356
headrob	r	-0.182	-0.036	-0.416*	-0.100	0.285	0.101	-0.125
	P	0.287	0.837	0.012	0.562	0.092	0.558	0.468
necklengthratio	r	0.000	0.047	-0.141	0.097	0.094	0.154	0.036
	P	1.000	0.786	0.411	0.575	0.585	0.368	0.835

* Correlation is significant at the 0.05 level (2-tailed).

** Correlation is significant at the 0.01 level (2-tailed).

Table 4-6 Pearson's correlation matrix for femoral epiphyses shape PCs and univariate measurements for all human populations (N=36).

		EpiAMHPC1	EpiAMHPC2	EpiAMHPC3	EpiAMHPC5
FemLength	r	-0.305	0.080	-0.110	0.208
	P	0.071	0.644	0.525	0.223
Neck-shaft angle	r	0.265	0.072	-0.200	0.040
	P	0.119	0.676	0.242	0.818
torsionangle	r	0.020	-0.129	-0.119	0.204
	P	0.908	0.454	0.490	0.232
subtrochratio	r	-0.103	-0.290	-0.195	0.096
	P	0.549	0.086	0.256	0.576
midshaftratio	r	0.060	0.029	-0.339*	0.177
	P	0.728	0.868	0.043	0.302
subpilratio	r	-0.115	0.131	-0.137	0.150
	P	0.503	0.447	0.425	0.381
condylediamratio	r	-0.274	-0.383*	-0.294	0.366*
	P	0.106	0.021	0.082	0.028
robustindex	r	-0.479**	-0.040	-0.150	-0.014
	P	0.003	0.816	0.382	0.936
headrob	r	-0.284	-0.439*	-0.176	0.396
	P	0.093	0.007	0.303	0.017
necklengthratio	r	-0.244	-0.199	0.159	0.085
	P	0.151	0.245	0.354	0.622

* Correlation is significant at the 0.05 level (2-tailed).

** Correlation is significant at the 0.01 level (2-tailed).

Populations with high activity levels only

The populations with high activity levels (N=21) are included in the same analyses and all the modern humans above. Overall, degree of curvature is positively correlated with midshaft and subpilastric shaft shape (for anterior curvature) and robusticity (for posterior curvature) (Table 4-7). The length of the neck is related to the posterior curvature. Anterior curvature is related to a rounder shaft shape at midshaft. The different apex of curvature PCs also vary in their correlations with the univariate measurements (Table 4-8). As epiphyseal robusticity increases (headrob and condylediamratio), apex of the posterior curve moves distally.

Increasing epiphyseal robusticity is correlated (headrob and condylediamratio) with a more posteriorly projecting proximal posterior surface (pcurvAMHPC2) (Table 4-9). The length of the femur is positively correlated with a more even lateral curve that does not straighten out at the level of the lesser trochanter (lcurveAMHPC2). Midshaft robusticity is negatively correlated with shaft and epiphyseal width and neck-shaft angle (EpiAMHPC1) and with robusticity of the proximal and distal epiphyses (EpiAMHPC2) (Table 4-10).

Table 4-7 Pearson's correlation matrix for femoral curvature and univariate measurements for populations with high activity levels (N=21).

		acurAMHPC1	PcurvAMHPC1
FemLength	r	0.150	0.027
	P	0.515	0.907
Neck-shaft angle	r	-0.109	-0.300
	P	0.639	0.186
torsionangle	r	-0.142	-0.104
	P	0.539	0.654
subtrochratio	r	0.322	0.398
	P	0.154	0.074
midshaftratio	r	0.724**	0.235
	P	<0.001	0.306
subpilratio	r	0.540*	0.176
	P	0.011	0.446
condylediamratio	r	0.260	0.445*
	P	0.256	0.043
robustindex	r	0.276	0.640**
	P	0.225	0.002
headrob	r	0.042	0.489*
	P	0.858	0.024
necklengthratio	r	-0.076	0.478*
	P	0.745	0.028

* Correlation is significant at the 0.05 level (2-tailed).
** Correlation is significant at the 0.01 level (2-tailed).

Table 4-8 Pearson's correlation matrix for femoral apex of curvature and univariate measurements for populations with high activity levels (N=21).

		acurAMHPC2	PcurvAMHPC3
FemLength	r	-0.290	-0.258
	P	0.202	0.259
Neck-shaft angle	r	-0.479	0.029
	P	0.028	0.900
torsionangle	r	-0.292	-0.028
	P	0.200	0.904
subtrochratio	r	0.190	0.223
	P	0.409	0.331
midshaftratio	r	-0.299	0.042
	P	0.188	0.857
subpilratio	r	-0.311	-0.177
	P	0.170	0.444
condylediamratio	r	-0.159	0.568**
	P	0.492	0.007
robustindex	r	0.020	-0.015
	P	0.932	0.947
headrob	r	0.008	0.476*
	P	0.972	0.029
necklengthratio	r	-0.138	0.148
	P	0.551	0.521

*=Correlation is significant at the 0.05 level (2-tailed).
**=Correlation is significant at the 0.01 level (2-tailed).

Table 4-9 Pearson's correlation matrix for other femoral shaft shape PCs and univariate measurements for populations with high activity levels (N=21).

		acurAMHPC3	acurAMHPC4	PcurvAMHPC2	PcurvAMHPC4	McurAMHPC3	LcurAMHPC2	LcurAMHPC4
FemLength	r	-0.241	0.151	0.126	0.109	0.115	-0.515*	-0.152
	P	0.293	0.515	0.586	0.639	0.620	0.017	0.511
Neck-shaft angle	r	0.175	-0.358	-0.117	-0.174	0.349	-0.357	0.021
	P	0.448	0.111	0.614	0.450	0.121	0.112	0.926
torsionangle	r	0.054	-0.424	-0.025	-0.116	0.305	-0.192	0.137
	P	0.815	0.055	0.915	0.617	0.179	0.404	0.554
subtrochratio	r	-0.405	-0.012	-0.305	-0.010	-0.279	0.159	-0.382
	P	0.069	0.957	0.179	0.965	0.221	0.491	0.087
midshaftratio	r	-0.085	-0.088	-0.177	0.180	0.283	-0.303	-0.324
	P	0.714	0.704	0.442	0.436	0.214	0.181	0.152
subpilratio	r	-0.113	0.086	-0.100	0.145	0.097	-0.383	-0.325
	P	0.625	0.711	0.665	0.531	0.676	0.086	0.151
condylediamratio	r	-0.061	-0.368	-0.484*	0.118	0.296	0.134	-0.309
	P	0.791	0.101	0.026	0.611	0.193	0.562	0.172
robustindex	r	0.043	-0.199	-0.267	0.163	-0.042	0.242	-0.049
	P	0.854	0.387	0.242	0.480	0.857	0.291	0.833
headrob	r	-0.169	-0.442*	-0.534*	-0.151	0.364	0.218	-0.210
	P	0.464	0.045	0.013	0.514	0.105	0.342	0.361
necklengthratio	r	0.079	-0.148	-0.185	0.107	0.084	0.263	-0.064
	P	0.732	0.523	0.422	0.645	0.719	0.249	0.782

* Correlation is significant at the 0.05 level (2-tailed).

** Correlation is significant at the 0.01 level (2-tailed).

Table 4-10 Pearson's correlation matrix for femoral epiphyses shape PCs and univariate measurements for populations with high activity levels (N=21).

		EpiAMHPC1	EpiAMHPC2	EpiAMHPC3	EpiAMHPC5
FemLength	r	-0.221	-0.015	-0.147	0.323
	P	0.335	0.949	0.525	0.153
Neck-shaft angle	r	0.489*	0.070	-0.331	-0.298
	P	0.024	0.762	0.143	0.190
torsionangle	r	0.171	-0.210	-0.188	-0.171
	P	0.457	0.361	0.415	0.458
subtrochratio	r	-0.064	-0.409	-0.180	-0.207
	P	0.781	0.066	0.436	0.367
midshaftratio	r	0.133	-0.003	-0.270	0.004
	P	0.566	0.990	0.236	0.985
subpilratio	r	0.123	0.083	-0.207	-0.228
	P	0.596	0.721	0.369	0.321
condylediamratio	r	-0.241	-0.475*	-0.285	0.387
	P	0.292	0.030	0.210	0.083
robustindex	r	-0.589**	-0.154	-0.197	0.003
	P	0.005	0.505	0.392	0.990
headrob	r	-0.400	-0.566**	-0.232	0.391
	P	0.072	0.007	0.312	0.080
necklengthratio	r	-0.405	-0.239	0.247	-0.034
	P	0.069	0.298	0.281	0.883

* Correlation is significant at the 0.05 level (2-tailed).

** Correlation is significant at the 0.01 level (2-tailed).

Summary

Overall, the anterior and posterior degrees of curvature are correlated with different variables. Individuals with higher levels of posterior curvature have higher levels of robusticity. Individuals with a high degree of anterior curvature have a rounder shaft at midshaft. Increased robusticity of the distal and proximal epiphyses is also correlated with a more distal apex of curvature of the posterior curve. A more proximal posterior apex of curvature is found with high neck-shaft and torsion angles.

4.2.3. Factors influencing curvature in modern humans

The following analyses focus on the relationship between anterior femoral curvature and the behavioural, environmental and biological variables that might be expected to influence curvature. These correlation analyses test the hypotheses and predictions presented in Chapter 2.

4.2.3.1. Body Size

The purpose of these analyses is to investigate the correlation between body size and curvature. Body size is known to be correlated with diaphyseal variables, such as cross-sectional geometry and robusticity (Ruff, 2000a; Stock, 2002; Shackelford, 2007) and may also have an effect on curvature. The relationship between body size and robusticity (subtrochanteric, midshaft and subpilastric) and curvature is analysed for the whole sample.

Using anteroposterior head diameter as an estimate for body size (Ruff, 1991; McHenry, 1992; Grine *et al.*, 1995) for the modern human sample (36 populations) the relationship between body size and robusticity and body size and femoral curvature and apex of curvature are investigated. There is a significant correlation between body size and the three different measures of robusticity (Table 4-11). There is no correlation between curvature and the position of the apex of curvature and body size (Table 4-12).

Table 4-11 Pearson's correlations for body size (head diameter) and robusticity of the femur (N=36).

HeadAPdiameter		
PcurvAMHPC1	r	0.215
	P	0.208
PcurvAMHPC3	r	-0.207
	P	0.225
acurAMHPC1	r	-0.010
	P	0.952
acurAMHPC2	r	-0.259
	P	0.128

* = Correlation is significant at the 0.05 level (2-tailed).
** = Correlation is significant at the 0.01 level (2-tailed).

Table 4-12 Pearson's correlations for body size (head diameter) and robusticity of the femur (N=36).

headAPdiameter		
condylediamratio	r	0.525
	P	0.001
robustindex	r	0.541
	P	0.001
headrob	r	0.524
	P	0.001

* Correlation is significant at the 0.05 level (2-tailed).
** Correlation is significant at the 0.01 level (2-tailed).

Summary

There is no allometric relationship between body size and curvature or apex of curvature.

4.2.3.2. Sex

The purpose of these analyses is to investigate the effect of sex on curvature and apex of curvature as well as other aspects of bone morphology. Differences between males and females can either be the consequence of higher body size in males than in females (Student's *t*-test; t=6.507; P<0.001), different bone modelling and remodelling rates in males and females, or due to different loading regimes and activity levels because of sexual division of labour.

Curvature

Although robusticity (midshaft and distal epiphyses) is also related to AP femoral head diameter (body size) (Table 4-13) and males have a larger AP femoral head diameter (body size) than females (Student's *t*-test; t=6.507; P<0.001), the analysis above did not find a correlation with

body size and curvature. For the whole sample of known sex (N=102 males and 89 females), curvature is males is not greater than in females (Table 4-14).

Table 4-13 Student's *t*-test results for robusticity in modern human males and females.

	Sex	N	Mean	S.D.	T	P
condylediamratio	male	102	17.35	1.35	2.618	0.010*
	female	89	16.84	1.33		
robustindex	male	102	12.59	0.99	3.231	0.002*
	female	89	12.09	1.13		
headrob	male	102	18.59	1.75	1.877	0.062
	female	89	18.14	1.59		

* P = significant at the 0.05 level.

Table 4-14 Student's *t*-test results for femoral curvature in modern human males and females.

	Sex	N	Mean	S.D.	T	P
acurAMHPC1	male	102	-0.00129	0.009428	1.237	0.217
	female	89	-0.00298	0.009359		
PcurvAMHPC1	male	102	-0.00104	0.008312	-1.093	0.276
	female	89	0.00029	0.008623		

* P = significant at the 0.05 level.

For the samples in this study the prediction that the effect of sex on robusticity and curvature is more evident in groups with high activity levels than in populations with moderate or low activity levels is only partly met. The prediction is met for two out of three measures of robusticity for those with high activity levels (N=41 males and 44 females) and as for the whole sample, males have higher midshaft and distal epiphysis robusticity (condylediamratio) than females (Table 4-15). For the high activity group the degree of curvature is higher in males for the anterior surface but not for the posterior (Table 4-18). For the moderate activity group (N=34 males and 28 females), there is a significant difference in midshaft robusticity (Table 4-16) but no difference in curvature (Table 4-19, Table 4-20). For the low activity group, there are no differences between males and females in robusticity (Table 4-17) or curvature (Table 4-20). In the analysis of the entire human sample the differences between males and females with high activity levels are masked by the similarity between males and females with moderate and low activity levels.

Table 4-15 Student's *t*-test results for robusticity in modern humans with high activity levels.

	Sex	N	Mean	S.D.	T	P
condylediamratio	male	42	17.34	1.19	2.542	0.010*
	female	44	16.61	1.43		
robustindex	male	42	12.59	1.09	2.089	0.038*
	female	44	12.05	1.32		
headrob	male	42	18.49	1.85	0.588	0.558
	female	44	18.27	1.71		

* P = significant at the 0.05 level.

Table 4-16 Student's *t*-test results for robusticity in modern humans with moderate activity levels.

	Sex	N	Mean	S.D.	T	P
condylediamratio	male	34	17.77	1.38	1.261	0.212
	female	28	17.36	1.11		
robustindex	male	34	12.85	0.78	3.865	<0.001*
	female	28	12.07	0.81		
headrob	male	34	19.06	1.53	1.792	0.078
	female	28	18.37	1.46		

* P = significant at the 0.05 level.

Table 4-17 Student's *t*-test results for robusticity in modern humans with low activity levels.

	Sex	N	Mean	S.D.	T	P
condylediamratio	male	26	16.82	1.39	0.444	0.659
	female	18	16.64	1.22		
robustindex	male	26	12.24	1.00	-0.098	0.922
	female	18	12.27	1.05		
headrob	male	26	18.15	1.78	1.115	0.271
	female	18	17.58	1.45		

* P = significant at the 0.05 level.

Table 4-18 Student's *t*-test results for curvature in modern humans with high activity levels.

	Sex	N	Mean	S.D.	T	P
acurAMHPC1	male	42	0.00237	0.00899	2.143	0.035*
	female	44	-0.00198	0.00979		
PcurvAMHPC1	male	42	-0.00043	0.00864	-0.686	0.494
	female	44	0.00087	0.00892		

* P = significant at the 0.05 level.

Table 4-19 Student's *t*-test results for curvature in modern humans with moderate activity levels.

	Sex	N	Mean	S.D.	T	P
acurAMHPC1	male	34	-0.00241	0.00874	0.119	0.906
	female	28	-0.00267	0.00872		
PcurvAMHPC1	male	34	-0.00071	0.00793	-0.413	0.681
	female	28	0.00012	0.00779		

* P = significant at the 0.05 level.

Table 4-20 Student's *t*-test results for curvature in modern humans with low activity levels.

	Sex	N	Mean	S.D.	T	P
acurAMHPC1	male	26	-0.00575	0.00897	0.002	0.998
	female	18	-0.00575	0.00891		
PcurvAMHPC1	male	26	-0.00246	0.00841	-0.725	0.472
	female	18	-0.00050	0.00936		

* P = significant at the 0.05 level.

Apex of curvature

For all individuals (N=102 males and 89 females), females have a lower apex of curvature than males (acurveAMHPC2; p=0.034) (Table 4-21). This difference is not present in groups with high activity levels (N=42 males and 44 females) (Table 4-22) or low activity levels (N=26 males and 18 females) (Table 4-24). Only for groups with moderate activity levels (N=34 males and 28 females) (Figure 4-16 and Table 4-25) is there a significant difference between males and females.

Table 4-21 Student's *t*-test results for apex of curvature in modern human males and females.

	Sex	N	Mean	S.D.	T	P
acurAMHPC2	male	102	-0.00053	0.00403	-2.137	0.034*
	female	89	0.00074	0.00417		
PcurvAMHPC3	male	102	-0.00056	0.00532	-0.125	0.900
	female	89	-0.00047	0.00523		

* P = significant at the 0.05 level.

Table 4-22 Student's *t*-test results for apex of curvature in modern humans with high activity levels.

	Sex	N	Mean	S.D.	T	P
acurAMHPC2	male	42	0.00053	0.00426	-1.463	0.147
	female	44	0.00178	0.00361		
PcurvAMHPC3	male	42	-0.00026	0.00508	-1.296	0.199
	female	44	0.00109	0.00457		

* P = significant at the 0.05 level.

Table 4-23 Student's *t*-test results for apex of curvature in modern humans with moderate activity levels.

	Sex	N	Mean	S.D.	T	P
acurAMHPC2	male	34	0.00055	0.00307	-2.733	0.008*
	female	28	0.00198	0.00422		
PcurvAMHPC3	male	34	-0.00019	0.00630	-.299	0.766
	female	28	0.00264	0.00560		

* P = significant at the 0.05 level.

Table 4-24 Student's *t*-test results for apex of curvature in modern humans with low activity levels.

	Sex	N	Mean	S.D.	T	P
acurAMHPC2	male	26	-0.00223	0.00430	-0.996	0.325
	female	18	-0.00338	0.00280		
PcurvAMHPC3	male	26	-0.00204	0.00407	-1.725	0.092
	female	18	-0.00426	0.00440		

* P = significant at the 0.05 level.

Other shaft shapes

Males have significantly straighter proximal posterior diaphyses whereas those of females slope posteriorly (pcurveAMHPC2, Student's *t*-test, p=0.031) (Table 4-25).

Table 4-25 Student's *t*-test results for other aspects of shaft shape in modern human males and females.

	Sex	N	Mean	S.D.	T	P
acurAMHPC3	male	102	-0.00004	0.00310	-0.076	0.939
	female	89	0.00000	0.00391		
acurAMHPC4	male	102	-0.00008	0.00383	-0.659	0.511
	female	89	0.00027	0.00338		
PcurvAMHPC2	male	102	0.00157	0.00597	2.178	0.031*
	female	89	-0.00029	0.00574		
PcurvAMHPC4	male	102	0.00030	0.00396	1.913	0.572
	female	89	-0.00082	0.00407		
McurAMHPC3	male	102	-0.00045	0.00430	-1.357	0.176
	female	89	0.00033	0.00345		
LcurAMHPC2	male	102	-0.00019	0.00659	-0.243	0.808
	female	89	0.00006	0.00711		
LcurAMHPC4	male	102	-0.00020	0.00354	0.842	0.401
	female	89	-0.00070	0.00469		

* P = significant at the 0.05 level

Epiphysis morphology

Males and females are similar in their epiphyseal morphology. None of the PCs show distinct differences between males and females for the whole sample (Table 4-26). There is only one significant sex difference for the subsample with low activity levels for EpiAMHPC3 (Table 4-27; Table 4-28; Table 4-29). This suggests that males have wider distal condyles and more torsion than females with low activity levels.

Table 4-26 Student's *t*-test results for epiphysis shape in modern human males and females.

	Sex	N	Mean	S.D.	t	P
EpiAMHPC1	male	101	-0.00185	0.01291	-0.553	0.581
	female	89	-0.00078	0.01367		
EpiAMHPC2	male	101	0.00069	0.01054	0.361	0.719
	female	89	0.00014	0.01059		
EpiAMHPC3	male	101	-0.00120	0.00971	0.623	0.534
	female	89	-0.00212	0.01060		
EpiAMHPC5	male	101	0.00038	0.00711	1.929	0.055
	female	89	-0.00157	0.00673		

* P = significant at the 0.05 level.

Table 4-27 Student's *t*-test results for epiphysis shape in modern humans with high activity levels.

	Sex	N	Mean	S.D.	T	P
EpiAMHPC1	male	41	0.00262	0.01458	0.805	0.423
	female	44	-0.00012	0.01657		
EpiAMHPC2	male	41	-0.00172	0.01109	-0.586	0.559
	female	44	-0.00036	0.01030		
EpiAMHPC3	male	41	-0.00387	0.00988	-0.337	0.737
	female	44	-0.00311	0.01100		
EpiAMHPC5	male	41	-0.00175	0.00692	1.115	0.268
	female	44	-0.00335	0.00633		

* P = significant at the 0.05 level.

Table 4-28 Student's *t*-test results for epiphysis shape in modern humans with moderate activity levels.

	Sex	N	Mean	S.D.	t	P
EpiAMHPC1	male	34	-0.00550	0.01137	-1.477	0.145
	female	28	-0.00131	0.01085		
EpiAMHPC2	male	34	0.00249	0.01022	0.609	0.545
	female	28	0.00078	0.01193		
EpiAMHPC3	male	34	-0.00025	0.00990	-0.860	0.393
	female	28	0.00196	0.01027		
EpiAMHPC5	male	34	0.00049	0.00710	0.512	0.610
	female	28	-0.00044	0.00721		

* P = significant at the 0.05 level.

Table 4-29 Student's *t*-test results for epiphysis shape in modern humans with low activity levels.

	Sex	N	Mean	S.D.	t	P
EpiAMHPC1	male	26	-0.00410	0.00999	-0.738	0.465
	female	18	-0.00191	0.00920		
EpiAMHPC2	male	26	0.00213	0.00969	0.460	0.648
	female	18	0.00078	0.00937		
EpiAMHPC3	male	26	0.00178	0.00833	2.875	0.006*
	female	18	-0.00557	0.00834		
EpiAMHPC5	male	26	0.00357	0.00638	1.328	0.191
	female	18	0.00107	0.00577		

* P=significant at 0.05 level.

Univariate measurements

Males have significantly longer femora in the combined modern human sample (Table 4-30) and in each of the three activity subsamples (Table 4-31; Table 4-32; Table 4-33). Males with high activity levels also have a rounder distal shaft (subpilratio) than females.

Table 4-30 Student's *t*-test results for univariate measurements in modern human males and females.

	Sex	N	Mean	S.D.	t	P
Femur length	male	102	444.96	31.57	8.514	<0.001*
	female	89	408.28	27.40		
Neck-shaft angle	male	102	127.40	6.19	-0.396	0.693
	female	89	127.76	6.69		
Torsion angle	male	102	16.55	6.82	0.189	0.851
	female	89	16.37	6.52		
subtrochratio	male	102	76.40	9.36	0.695	0.488
	female	89	75.44	9.66		
midshaftratio	male	102	114.79	17.91	0.561	0.575
	female	89	113.24	20.15		
subpilratio	male	102	91.41	15.72	2.128	0.035*
	female	89	86.50	16.08		

* P = significant at the 0.05 level.

Table 4-31 Student's *t*-test results for univariate measurements in modern humans with high activity levels.

	Sex	N	Mean	S.D.	t	P
Femur length	male	42	437.07	37.05	4.943	<0.001*
	female	44	400.27	31.89		
Neck-shaft angle	male	42	127.98	6.48	-1.453	0.150
	female	44	130.00	6.37		
Torsion angle	male	42	16.66	6.77	-0.754	0.453
	female	44	17.76	6.77		
subtrochratio	male	42	75.38	10.57	-0.454	0.651
	female	44	76.37	9.59		
midshaftratio	male	42	112.59	16.30	0.892	0.374
	female	44	109.19	18.88		
subpilratio	male	42	89.71	13.76	3.454	0.001*
	female	44	80.00	12.31		

* P = significant at the 0.05 level.

Table 4-32 Student's *t*-test results for univariate measurements in modern humans with moderate activity levels.

	Sex	N	Mean	S.D.	t	P
Femur length	male	34	453.43	24.07	7.206	0.000*
	female	28	409.41	23.77		
Neck-shaft angle	male	34	125.56	5.38	0.333	0.741
	female	28	125.07	5.98		
Torsion angle	male	34	15.09	5.54	0.520	0.605
	female	28	14.37	5.23		
subtrochratio	male	34	74.33	8.74	1.402	0.166
	female	28	71.02	9.87		
midshaftratio	male	34	112.43	19.34	-0.482	0.631
	female	28	114.75	18.11		
subpilratio	male	34	84.76	14.09	-1.256	0.214
	female	28	89.17	13.32		

* P = significant at the 0.05 level.

Table 4-33 Student's *t*-test results for univariate measurements in modern humans with low activity levels.

	Sex	N	Mean	S.D.	t	P
Femur length	male	26	446.63	28.38	3.239	0.002*
	female	18	422.66	15.98		
Neck-shaft angle	male	26	128.85	6.35	1.246	0.220
	female	18	126.36	6.73		
Torsion angle	male	26	18.29	8.12	1.097	0.279
	female	18	15.68	7.19		
subtrochratio	male	26	80.74	6.55	0.188	0.851
	female	18	80.37	6.10		
midshaftratio	male	26	121.41	17.49	0.090	0.929
	female	18	120.85	23.94		
subpilratio	male	26	102.83	14.99	0.927	0.359
	female	18	97.89	20.45		

* P = significant at the 0.05 level.

Summary

For the whole sample males have longer and more robust femora than females. Males also have relatively wider knees and straighter proximal anterior shafts. Males do not have higher levels of curvature when the whole recent modern human sample is considered. Therefore, curvature is not due to differences in bone modelling and remodelling between males and females.

The prediction that males would have a higher degree of curvature and higher robusticity due to having higher activity levels is supported for groups with high activity levels in which division of labour is more pronounced.

4.2.3.3. Age

The purpose of these analyses is to investigate the changes in femoral curvature throughout adulthood. If curvature is a plastic feature that responds to habitual loading, it is predicted that as activity levels decrease with increasing age (for this skeletally adult sample up to 87 years old), so will degree of curvature. Of the whole sample, only 88 individuals had known ages or age range estimates (represented populations: African-American, Aleut, Andamanese, Australians, English Medieval and 18^{th} – 19^{th} Century, Ohio Native, Natufian, Danish Medieval and Czech Medieval. These populations represent all three activity groups).

There is no relationship between age after adulthood and curvature nor is there a relationship with apex of curvature or the other PCs (Table 4-34). When the univariate measurements are compared to age there are three significant trends visible: age is negatively correlated with torsion and neck-shaft angle and positively correlated with robusticity of the distal condyles (condylediamratio). Older individuals have wider knees relative to shaft length, lower femoral torsion and lower neck-shaft angles (Table 4-35).

Table 4-34 Kendall's Tau b correlations for PCs and age (N=88).

Curvature			*Other shaft shape PCs*		
acurAMHPC1	r	-0.050	acurAMHPC3	r	0.097
	P	0.641		P	0.370
PcurvAMHPC1	r	-0.008	acurAMHPC4	r	0.163
	P	0.943		P	0.130
			PcurvAMHPC2	r	-0.109
				P	0.314
			PcurvAMHPC4	r	0.135
				P	0.208
Apex of curvature			McurAMHPC3	r	-0.063
acurAMHPC2	r	-0.144		P	0.558
	P	0.181	McurAMHPC4	r	0.171
PcurvAMHPC3	r	0.089		P	0.112
	P	0.411	LcurAMHPC2	r	-0.072
				P	0.506
			LcurAMHPC4	r	-0.159
				P	0.138

*=Correlation is significant at the α=0.05

Table 4-35 Kendall's Tau b correlations for univariate measurements and age (N=88).

r	Femur length	-0.002	r	subpilratio	-0.108
P		0.984	P		0.317
r	Neck-shaft angle	-0.368	r	condylediamratio	0.247
P		<0.001*	P		0.020*
r	Torsion angle	-0.354	r	necklengthratio	0.068
P		0.001*	P		0.531
r	subtrochratio	0.145	r	robustindex	0.145
P		0.177	P		0.177
r	midshaftratio	-0.003	r	headrob	0.032
P		0.980	P		0.769

*=Correlation is significant at the α=0.05

When age categories (see Chapter 3 for more information) were used instead of absolute age of the individual, the ANOVA showed no significant difference between the groups (Table 4-36).

Table 4-36 ANOVA results for adult age categories on curvature PCs (N=4)

	F	Sig.
acurAMHPC1	0.985	0.374
PcurvAMHPC1	0.557	0.573

*=significant at α=0.05

Summary

The prediction is not met. There is no trend towards lower degrees of curvature with increasing age. Neck-shaft angle and torsion angle decrease with increasing age and the relative size of the distal condyles increases.

4.2.3.4. Activity levels

The purpose of the following analyses is to determine if there are differences in degree and apex of curvature between samples with different activity levels, using the activity groups and subsistence categories described in Chapter 3 and summarised in Appendix 8.

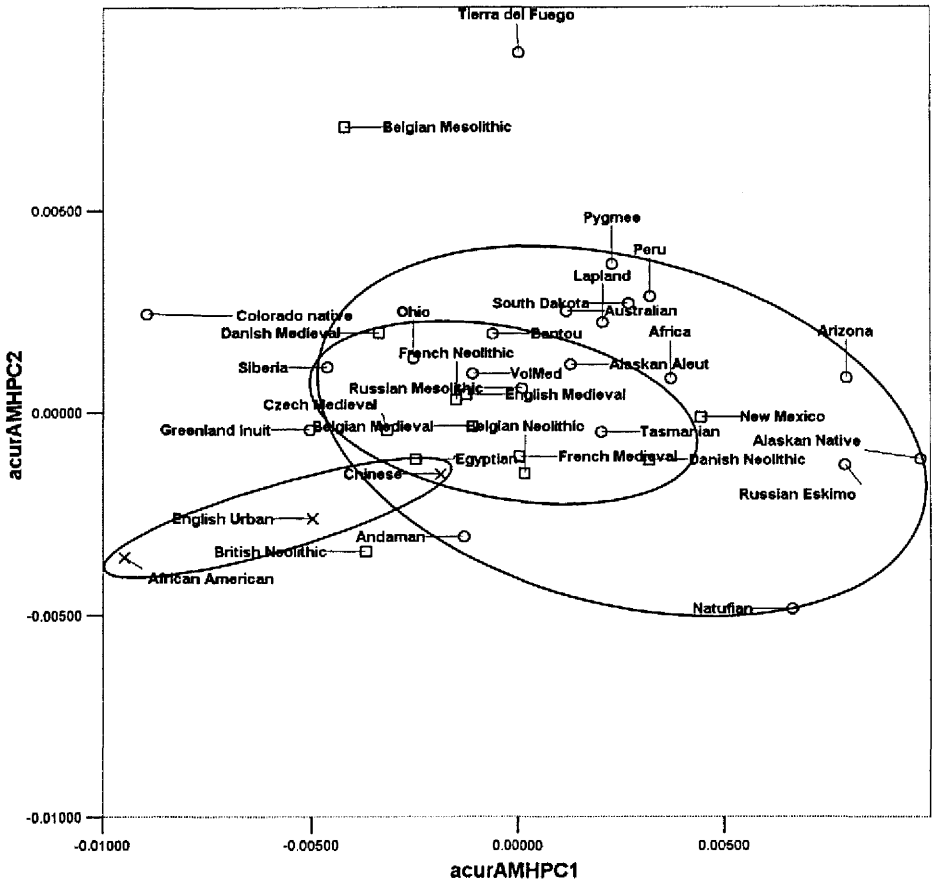

Figure 4-10 Distribution of the activity level categories in the space of PC1 (degree of curvature) and PC2 (apex of curvature) of the anterior curve for all modern humans.

Circles: high activity; squares: moderate activity; crosses: low activity.

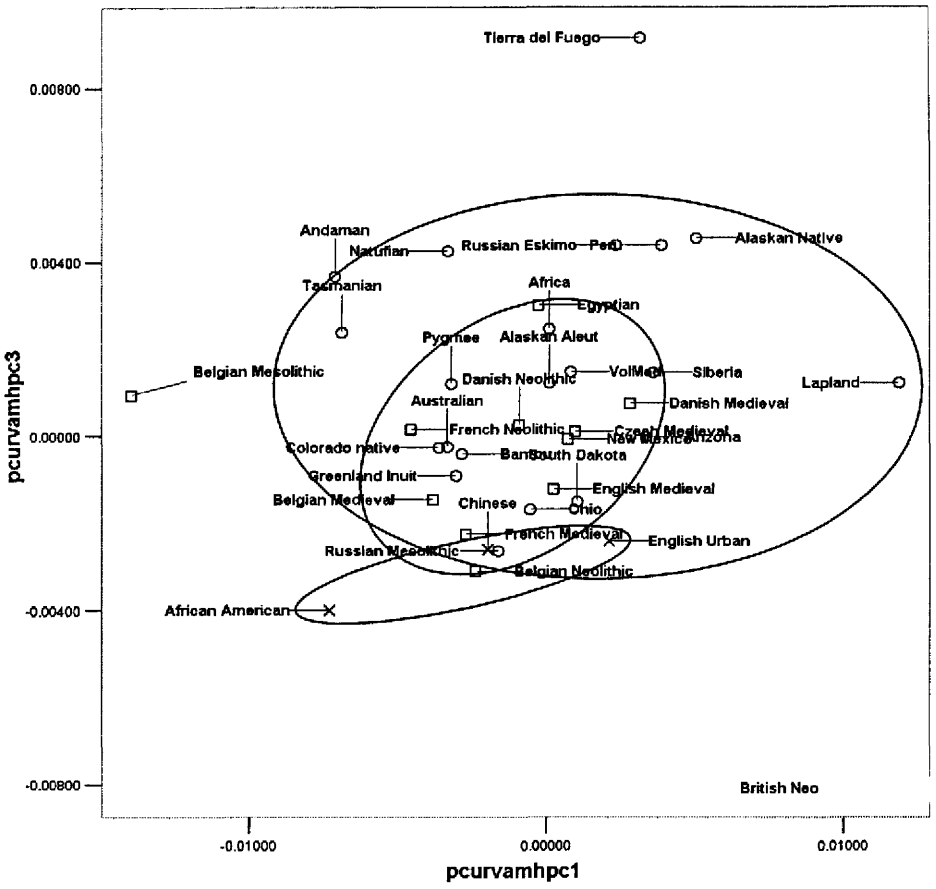

Figure 4-11 Distribution of the activity level categories in the space of PC1 (degree of curvature) and PC2 (apex of curvature) of the posterior curve for all modern humans.

Circles: high activity; squares: moderate activity; crosses: low activity.

Curvature

The activity groups are significantly different in anterior but not in posterior curvature (Table 4-37). For the two curvature related PCs, those with high activity levels are the most curved and those with low activity levels are the least curved (Figure 4-12) (Appendix 12). However, the principal source of variation is the difference between low activity populations and all others.

Table 4-37 ANOVA results for activity levels and femoral curvature PCs.

d.f.=2	F	Sig.
acurAMHPC1	8.900	0.000*
PcurvAMHPC1	1.698	0.184

*=significant at α=0.05

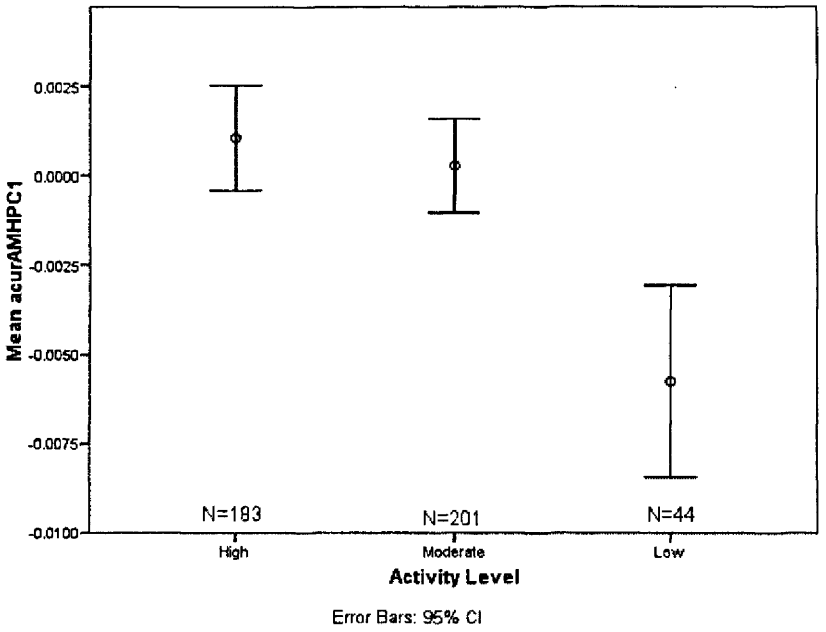

Figure 4-12 Anterior femoral curvature for modern humans, by activity level. Mean and 95% confidence interval (whiskers).

For the subsistence categories, there are significant differences in the degree of posterior curvature (PcurAMHPC1) (Table 4-38). The pastoralists have a higher degree of posterior curvature than all other categories (Figure 4-13) (Appendix 13).

Table 4-38 ANOVA results for high activity subsistence categories and femoral curvature PCs.

d.f.=5	F	Sig.
acurAMHPC1	0.528	0.715
PcurvAMHPC1	5.246	0.001*

*=significant at α=0.05

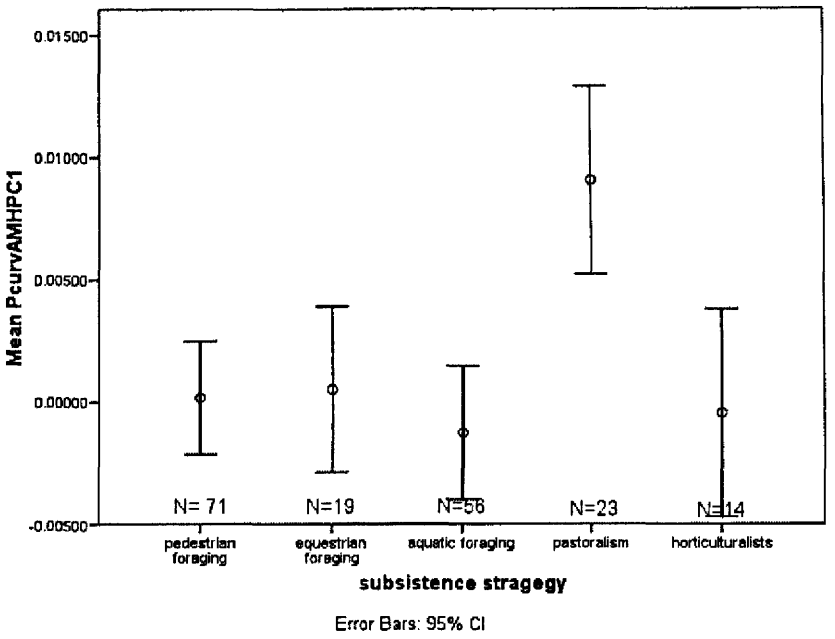

Figure 4-13 Posterior femoral curvature for modern humans, by subsistence strategy. Mean and 95% confidence interval (whiskers).

Apex of curvature

The activity groups are significantly different for apex of curvature in both PCs (Table 4-39). Post-hoc procedures show that high and low activity categories are different from each other. Low activity groups have the most proximal apex of curvature, high acitivity groups the most distal and moderate activity groups are intermediate (Figure 4-14 and Figure 4-15) (Appendix 14).

Table 4-39 ANOVA results for activity levels and the apex of femoral curvature PCs.

d.f.=2	F	Sig.
acurAMHPC2	13.407	<0.001*
PcurvAMHPC3	11.744	<0.001*

*=significant at α=0.05

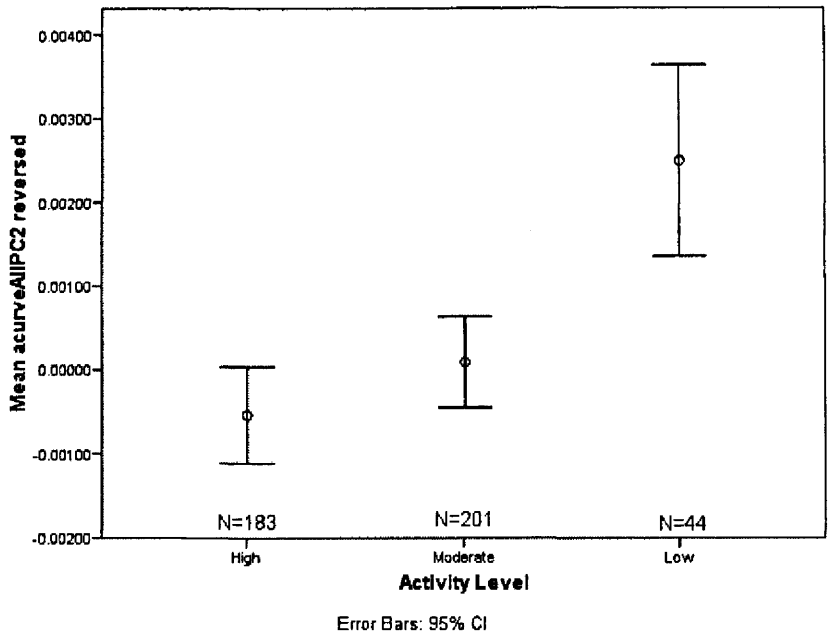

Figure 4-14 Anterior femoral apex of curvature for modern humans, by activity level. Scale is reversed so that higher values indicate a more proximal apex of curvature. Mean and 95% confidence interval (whiskers).

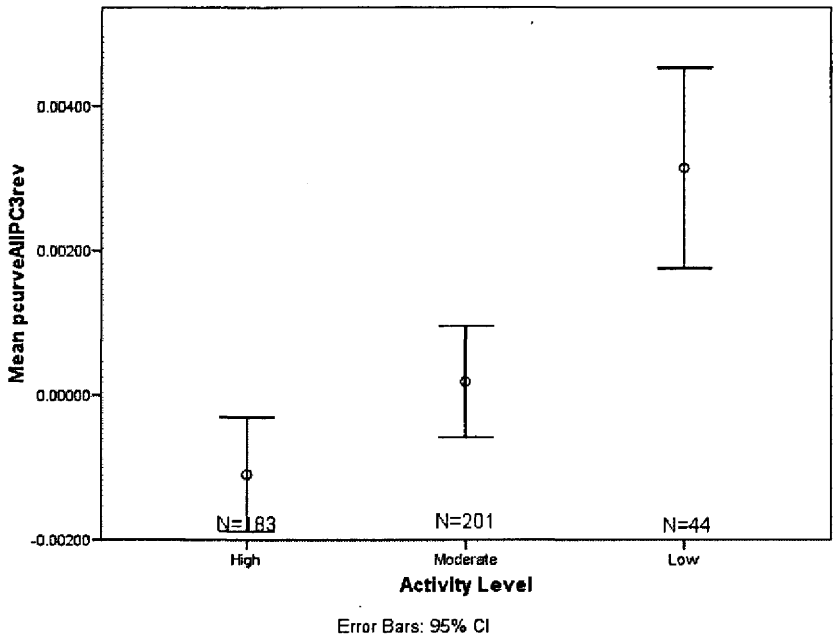

Figure 4-15 Posterior femoral apex of curvature for modern humans, by activity level. Scale is reversed so that higher values indicate a more proximal apex of curvature. Mean and 95% confidence interval (whiskers).

The anterior apex of curvature is significantly different for the high activity subsistence groups (Table 4-40). Post-hoc procedures show that the equestrian foragers have the most distal apex of curvature. The aquatic foragers have the most proximal apex of curvature and are significantly different from the equestrian foragers and (Appendix 15) (Figure 4-16).

Table 4-40 ANOVA results for subsistence categories and the apex of femoral curvature PCs.

d.f.=5	F	Sig.
acurAMHPC2	5.008	0.001*
PcurvAMHPC3	1.631	0.169

*=significant at α=0.05

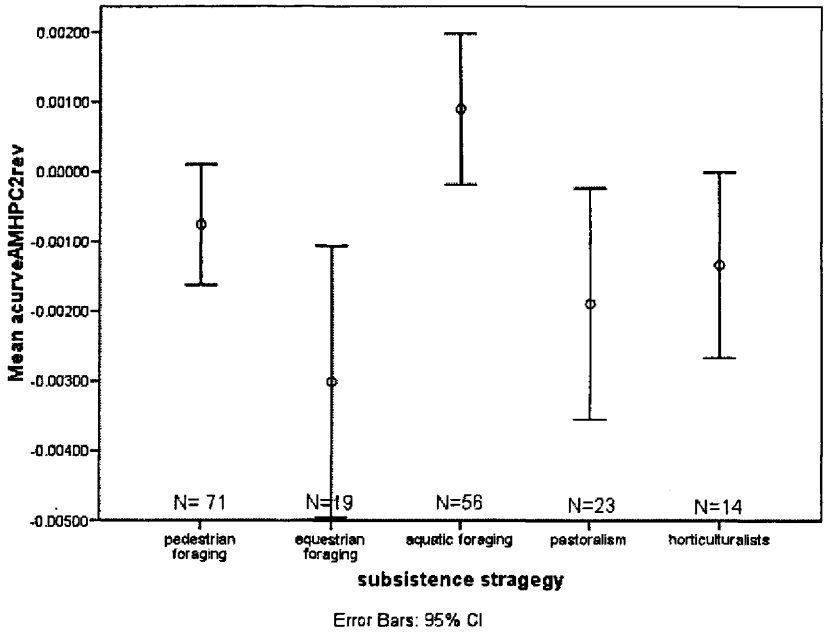

Figure 4-16 Anterior femoral apex of curvature for modern humans, by subsistence strategy. Scale is reversed so that higher values indicate a more proximal apex of curvature. Mean and 95% confidence interval (whiskers).

Other elements of shaft shape

Four of the other shaft shape PCs (pcurveAMHPC4, mcurveAMHPC3, lcurveAMHPC2 and LcurveAMHPC4) are affected by activity level (Table 4-41) (Figure 4-2, Figure 4-4, Figure 4-6, Figure 4-8). Post-hoc procedures show that the distal end of the diaphysis in the moderate activity groups is straighter, whereas in high activity groups it is more posteriorly projected distally (Appendix 15). This could be an indication of more posterior expansion of the distal condyles (pcurveAMHPC4) (Figure 4-17). The moderate activity groups also have a more even curve that approximates and arc of a circle with less posterior projection of the distal medial surface compared to the high activity level groups who have a more flattened off medial curve with increased posterior projection distally (mcurveAMHPC3) (Figure 4-18). The high and moderate activity groups have a "straightening" of the femur at the level of the lesser trochanter, whereas those with low activity levels have a lateral surface that approximates the surface of a circle (lcurveAMHPC2) (Figure 4-19). The low activity populations are also significantly different ($P<0.001$) in having a lateral surface that, in anterior view, is sinusoidally shaped, whereas high and moderate activity groups have a more even lateral surface (lcurveAMHPC4) (Figure 4-20).

Table 4-41 ANOVA results for activity levels and the other femoral shaft shape PCs.

d.f.=2	F	Sig.
acurAMHPC3	1.217	0.297
acurAMHPC4	0.598	0.550
PcurvAMHPC2	1.036	0.356
PcurvAMHPC4	8.651	<0.001*
McurAMHPC3	9.654	<0.001*
LcurAMHPC2	7.661	0.001*
LcurAMHPC4	9.852	<0.001*

*=significant at α=0.05

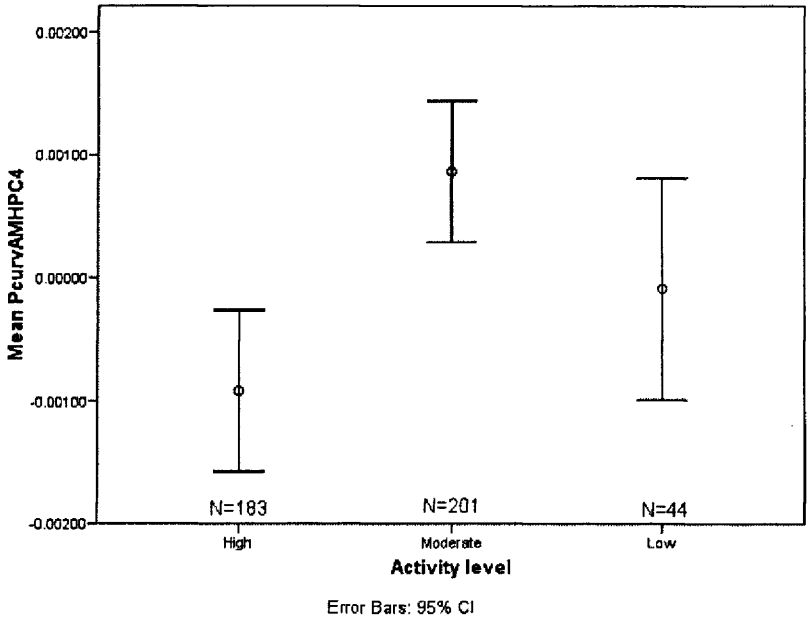

Figure 4-17 PcurvAMHPC4 for modern humans, by activity level. Mean and 95% confidence interval (whiskers).

Negative values have a posterior expansion of the distal epiphyses reflecting more posteriorly projecting condyles.

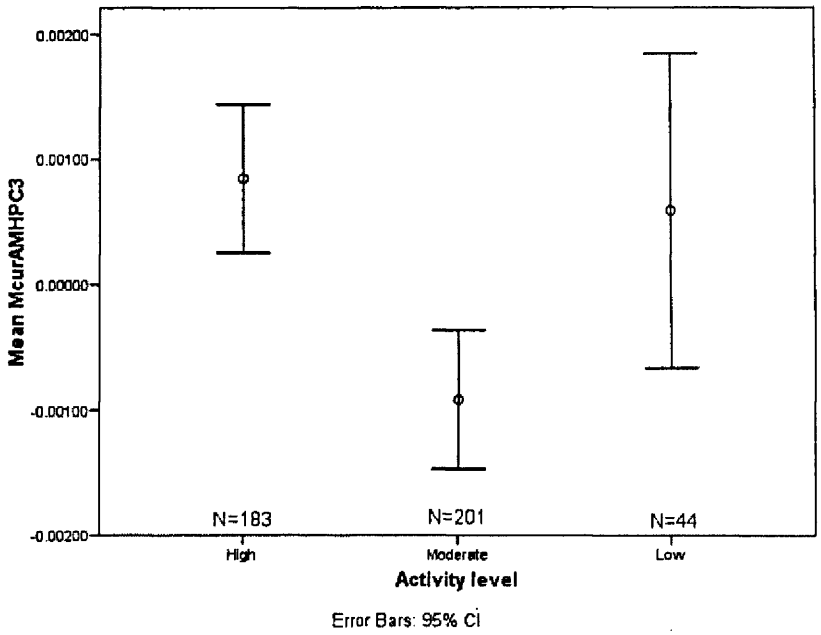

Figure 4-18 McurvAMHPC3 for modern humans, by activity level. Mean and 95% confidence interval (whiskers).

High values have a more flattened off medial curve with increased posterior projection distally.

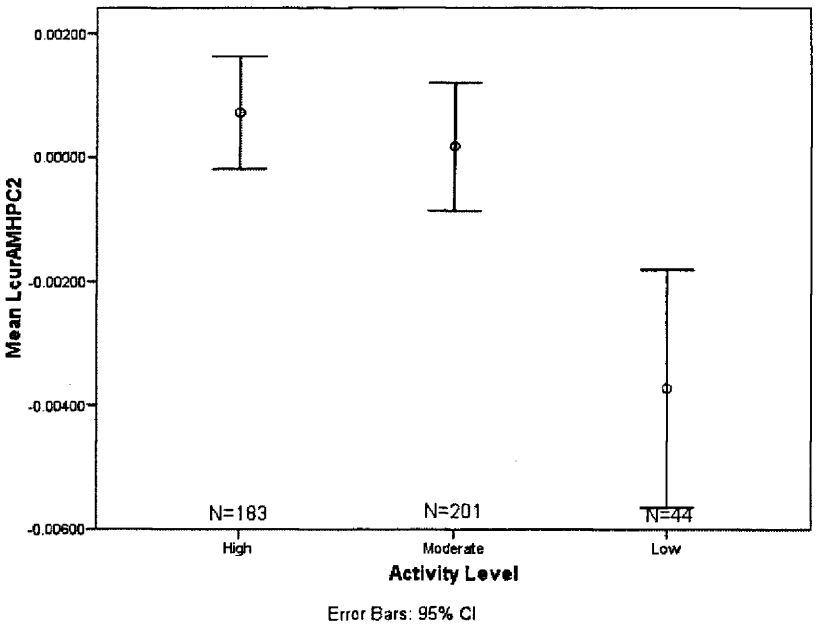

Figure 4-19 LcurvAMHPC2 for modern humans, by activity level. Mean and 95% confidence interval (whiskers).

Low values have a lateral surface that approximates an arc of a circle.

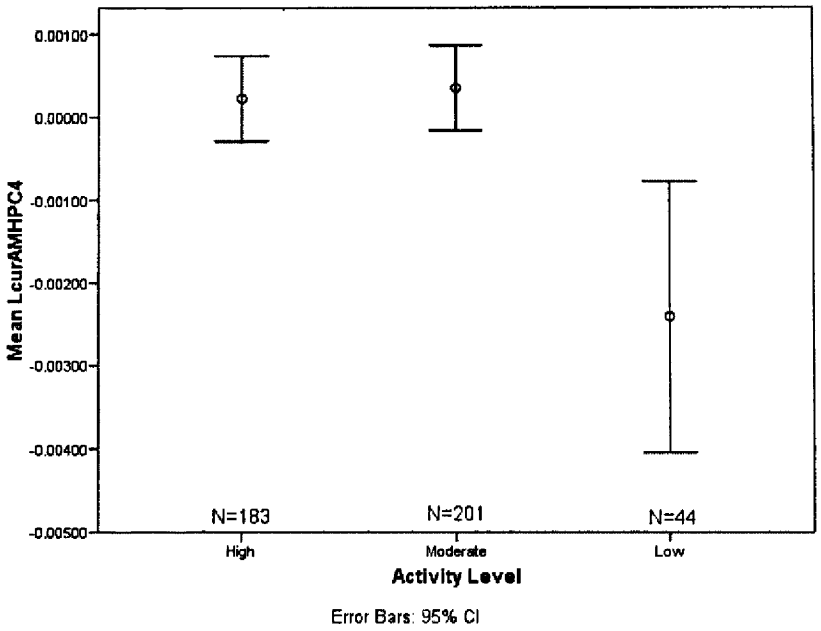

Figure 4-20 LcurvAMHPC4 for modern humans, by activity level. Mean and 95% confidence interval (whiskers).

Lower values have a lateral surface that in anterior view is sinusoidally shaped.

The same analysis for the other shaft shape PCs was repeated for the high activity subsistence groups (Table 4-42). There are significant differences between the groups for pcurveAMHPC2 and post-hoc comparisons indicate that equestrian foragers have a significantly proximally straighter posterior diaphyseal surface compared to aquatic foragers and pastoralists (Figure 4-21 and Appendix 17).

Table 4-42 ANOVA results for subsistence categories and the other femoral shaft shape PCs.

d.f.=5	F	Sig.
acurAMHPC3	0.462	0.763
acurAMHPC4	0.755	0.556
PcurvAMHPC2	3.219	0.014*
PcurvAMHPC4	0.645	0.631
McurAMHPC3	2.132	0.079
LcurAMHPC2	1.295	0.274
LcurAMHPC4	1.701	0.152

*=significant at α=0.05

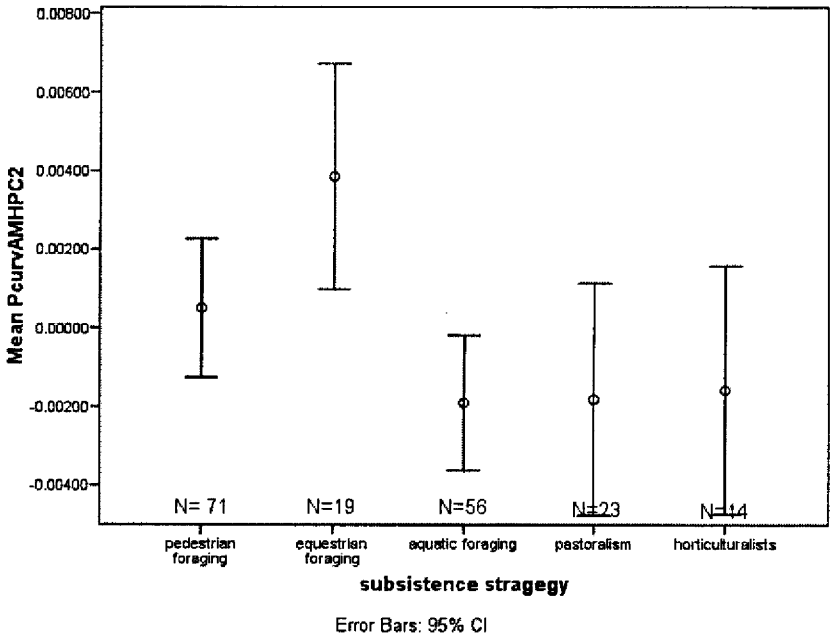

Figure 4-21 PcurvAMHPC2 for modern humans, by subsistence strategy. Mean and 95% confidence interval (whiskers).

High values have a proximally straighter posterior diaphyseal surface.

Univariate measurements

The activity groups are significantly different in femur length, neck-shaft angle, torsion, shaft shape at the sub-trochanteric and sub-pilastric level, neck length ratio and robusticity of the shaft and head (Table 4-43, Figure 4-22 - Figure 4-29).

High activity groups have significantly more robust and shorter femora with a higher neck-shaft angle and a shorter neck than low activity groups (Appendix 18) (Figure 4-23 -Figure 4-29). Moderate activity groups also have a longer femur than high activity groups (Figure 4-22). The low activity groups have rounder shafts at the sub-trochanteric and sub-pilastric level and are anteroposteriorly wide at the midshaft level compared to high and moderate activity groups (Figure 4-24 - Figure 4-26).

Table 4-43 ANOVA results for activity level and the univariate measurements of the femur.

d.f.=2	F	Sig.
Femur length	8.712800964	<0.001*
Neck-shaft angle	8.140769238	<0.001*
Torsion angle	1.75641636	0.174
subtrochratio	8.481384719	<0.001*
midshaftratio	3.590933717	0.028*
Subpilratio	17.37404345	<0.001*
condylediamratio	1.959586004	0.142
necklengthratio	11.89107459	<0.001*
robustindex	6.519969349	0.002*
Headrob	6.39445168	0.002*

*=significant at α=0.05

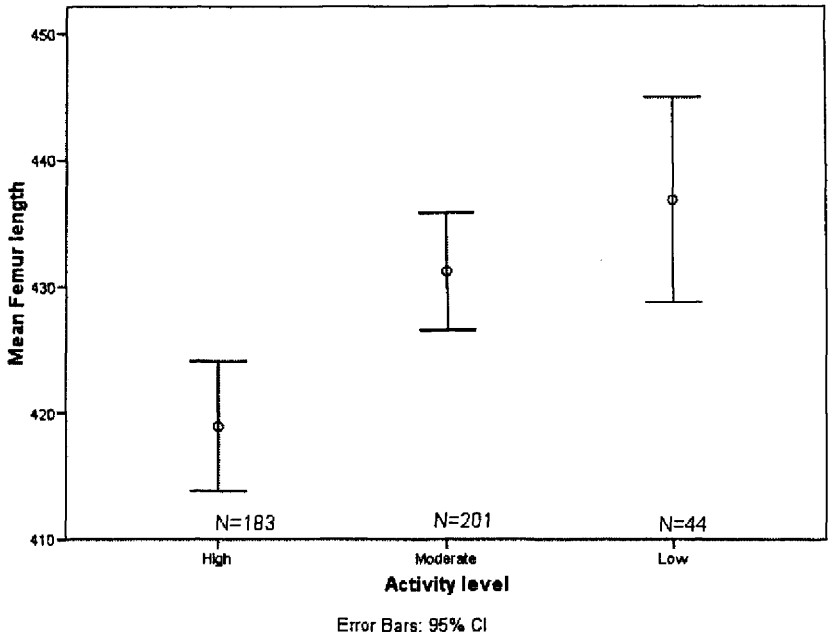

Figure 4-22 Femur length for modern humans, by activity level. Mean and 95% confidence interval (whiskers).

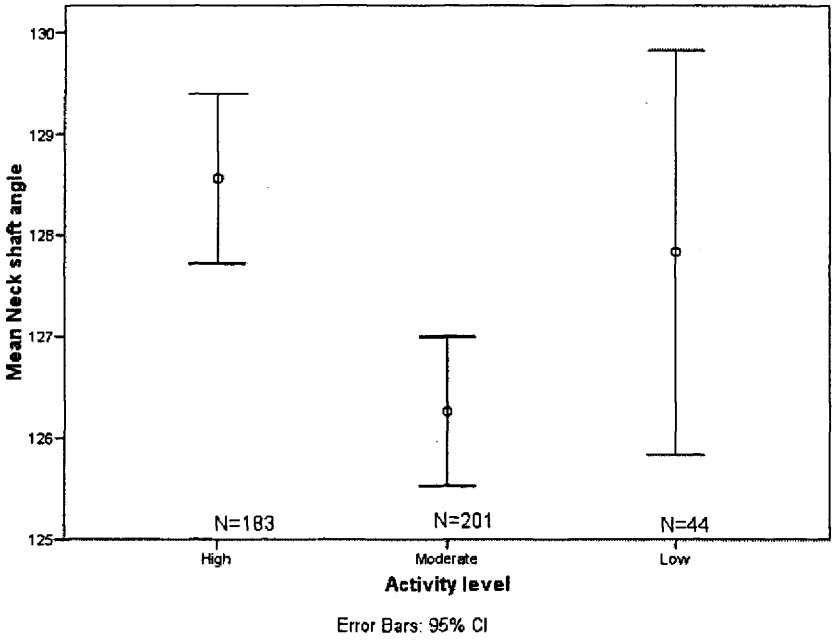

Figure 4-23 Neck-shaft angle for modern humans, by activity level. Mean and 95% confidence interval (whiskers).

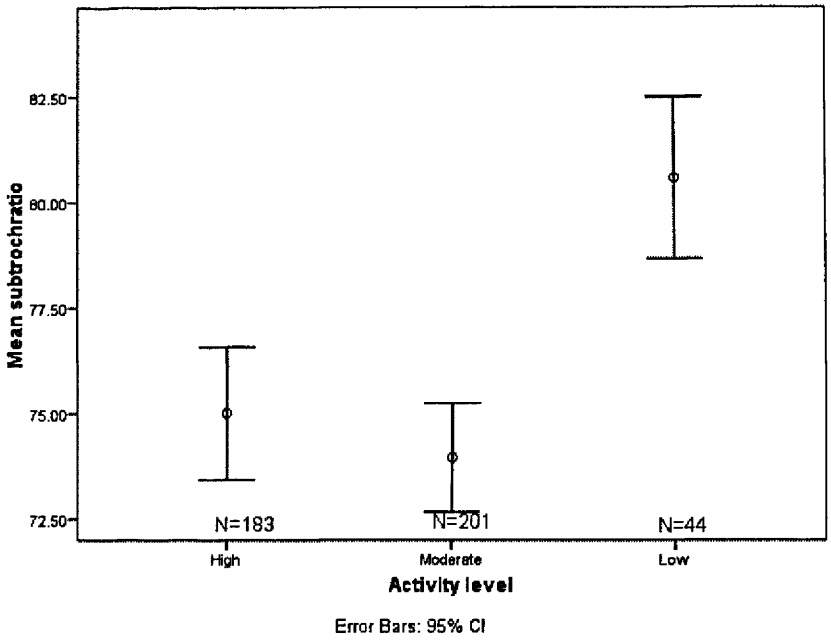

Figure 4-24 Subtrochanteric shape ratio for modern humans, by activity level. Mean and 95% confidence interval (whiskers).

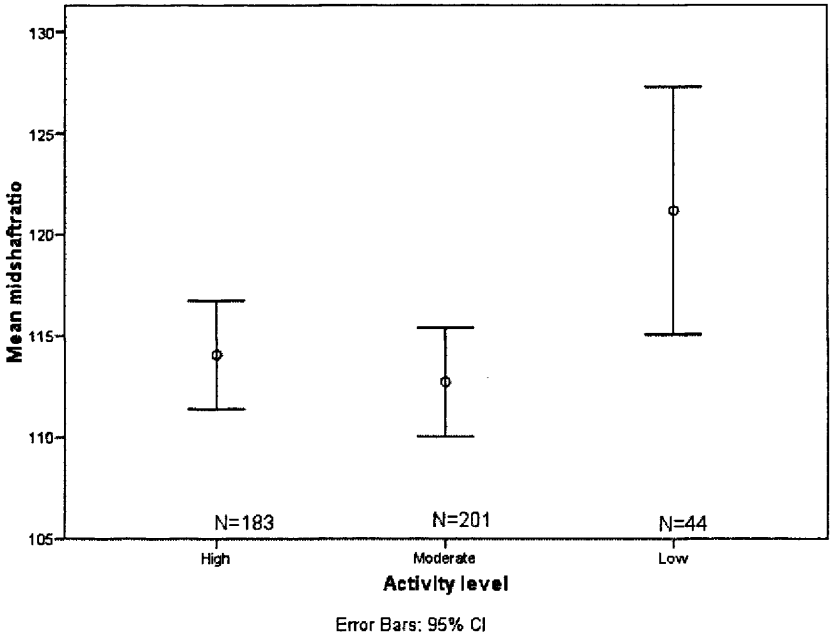

Figure 4-25 Midshaft shape ratio for modern humans, by activity level. Mean and 95% confidence interval (whiskers).

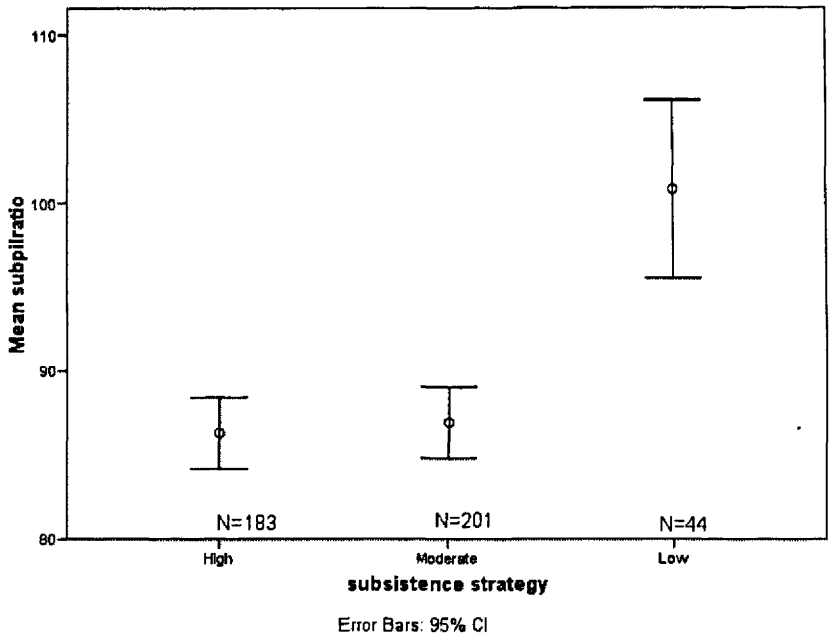

Figure 4-26 Subpilastric shape ratio for modern humans, by activity level. Mean and 95% confidence interval (whiskers).

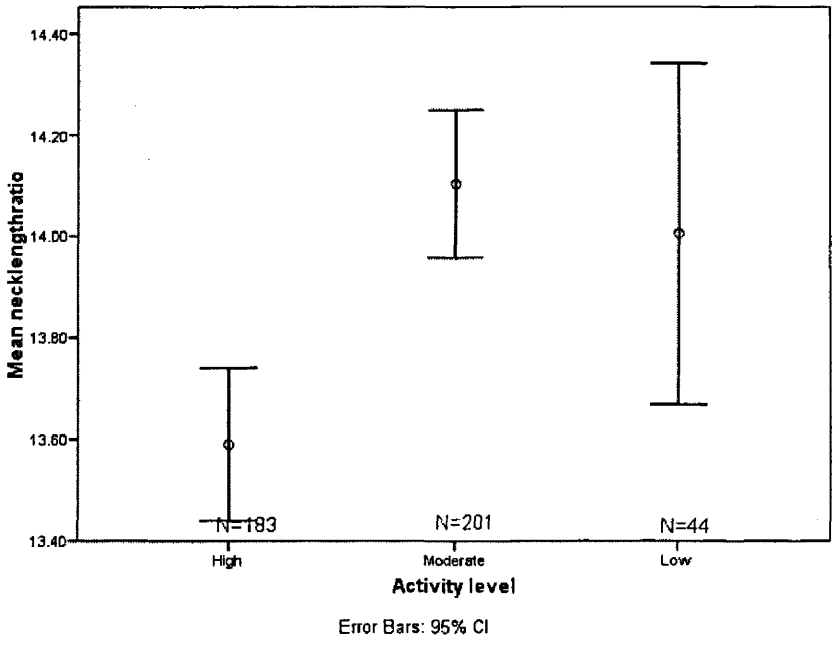

Figure 4-27 Neck-length ratio for modern humans, by activity level. Mean and 95% confidence interval (whiskers).

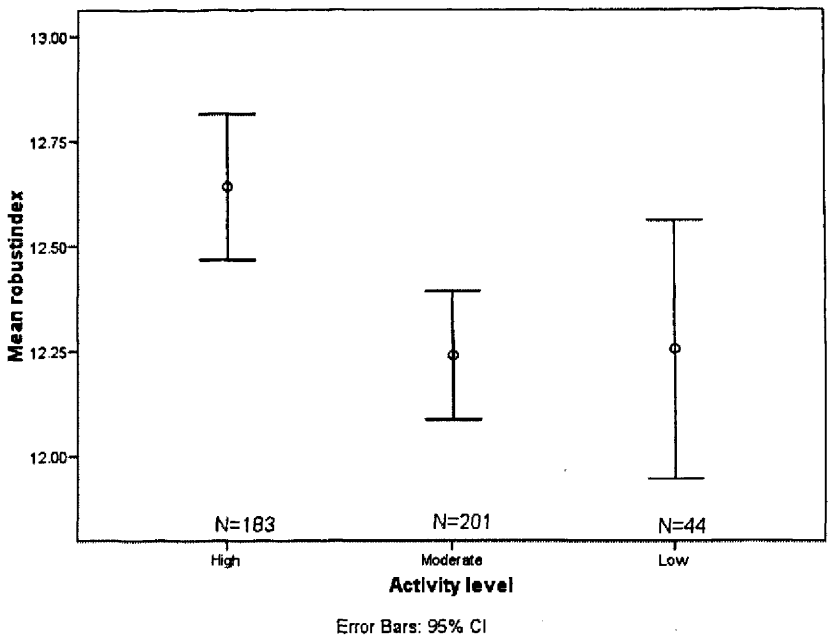

Figure 4-28 Robusticity index for modern humans, by activity level. Mean and 95% confidence interval (whiskers).

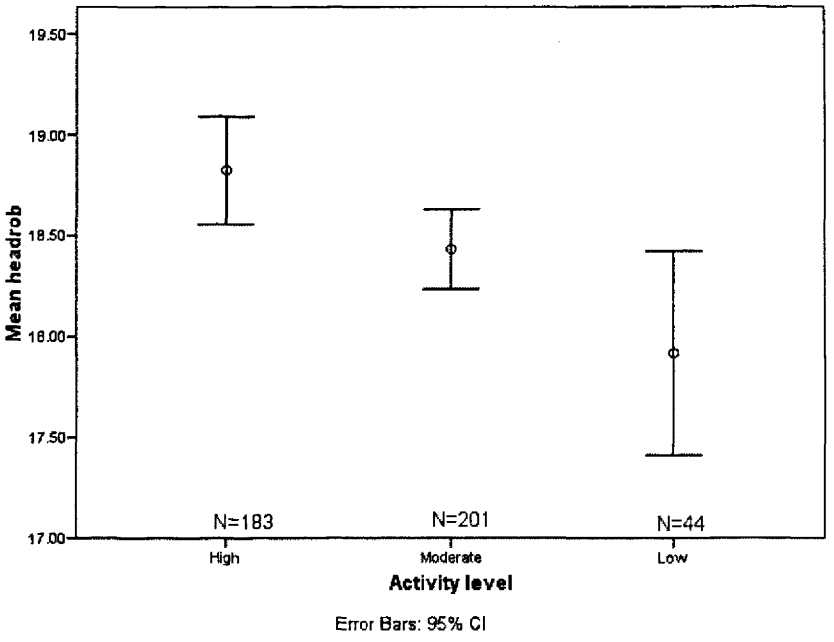

Figure 4-29 Femoral head robusticity for modern humans, by activity level. Mean and 95% confidence interval (whiskers).

The subsistence categories with high activity levels are also different for some of the univariate measurements (Table 4-44). Most univariate measurements have significant between group differences, with the exception of sub-trochanteric and sub-pilastric shaft shape.

The post-hoc procedures (Appendix 19) show that the aquatic foragers have shorter femora than all other groups (not statistically significant for horticulturalists) (Figure 4-30). Equestrian foragers and pastoralists have lower neck-shaft angles (Figure 4-31). Equestrian foragers have the lowest amount of femoral torsion and the smallest femoral head size (Figure 4-32, Figure 4-33). There is a trend from anteroposteriorly wide to round shafts through the different subsistence strategies, but not all groups are significantly different from each other. This trend may reflect changes in the anatomy with the adoption of subsistence strategies with lower activity intensity (Figure 4-33). Pastoralists have the highest robusticity indices at midshaft (Figure 4-34).

Table 4-44 ANOVA results for subsistence categories and the femoral univariate measurements.

d.f.=5	F	Sig.
Femur length	6.784	<0.001*
Neck-shaft angle	6.068	<0.001*
Torsion angle	4.853	0.001*
subtrochratio	1.617	0.172
midshaftratio	3.282	0.013*
Subpilratio	1.530	0.196
condylediamratio	5.644	<0.001*
necklengthratio	10.559	<0.001*
Robustindex	7.917	<0.001*
Headrob	2.792	0.028*

*=significant at α=0.05

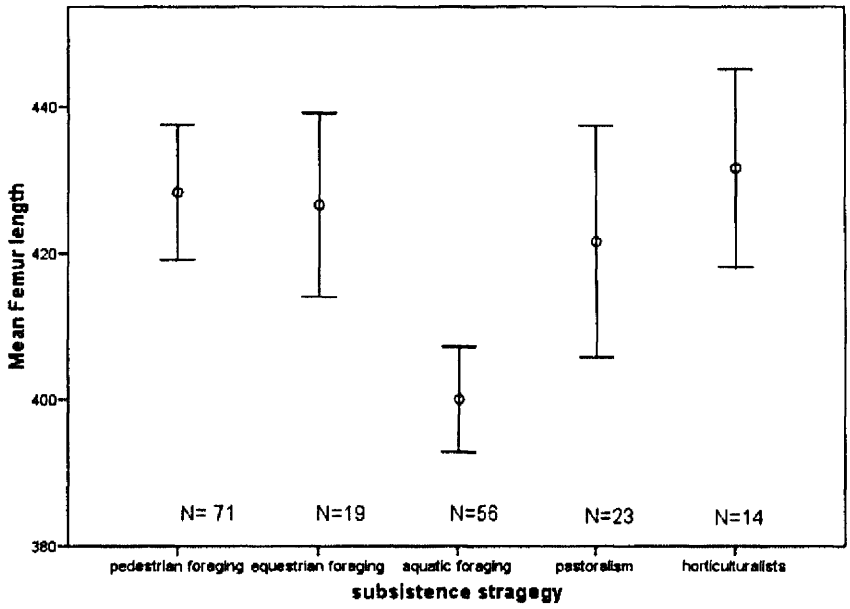

Figure 4-30 Femur length for modern humans, by subsistence strategy. Mean and 95% confidence interval (whiskers).

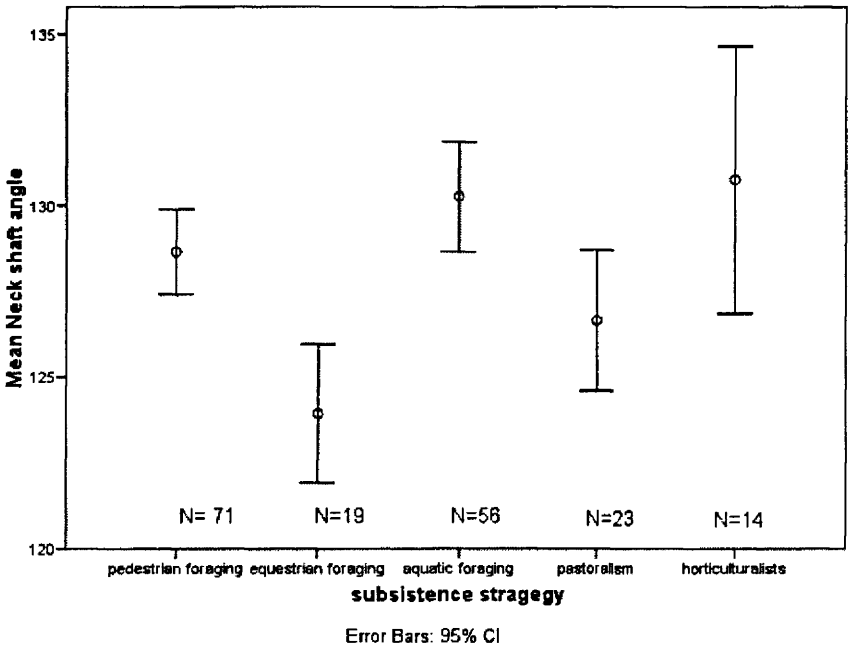

Figure 4-31 Neck-shaft angle for modern humans, by subsistence strategy. Mean and 95% confidence interval (whiskers).

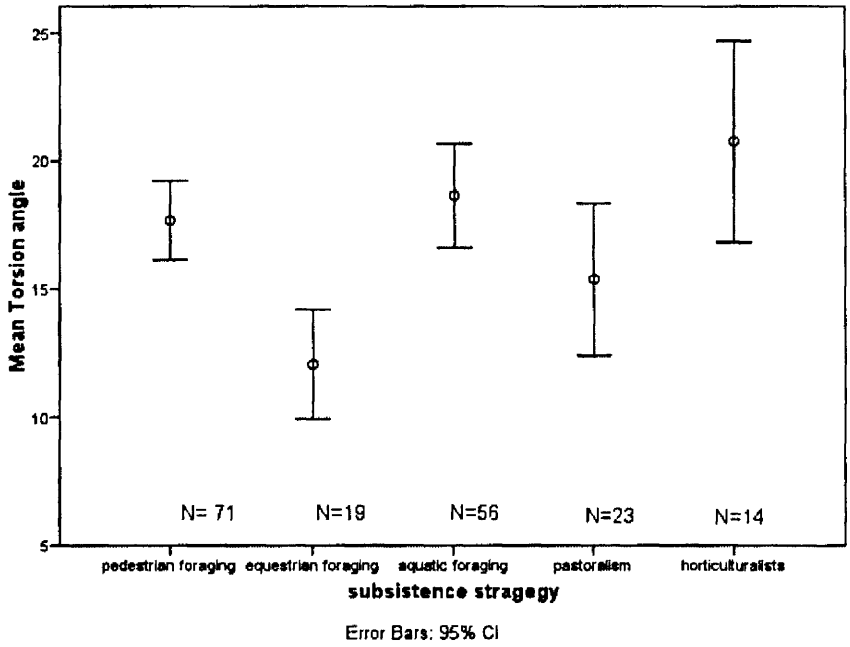

Figure 4-32 Torsion angle for modern humans, by subsistence strategy. Mean and 95% confidence interval (whiskers).

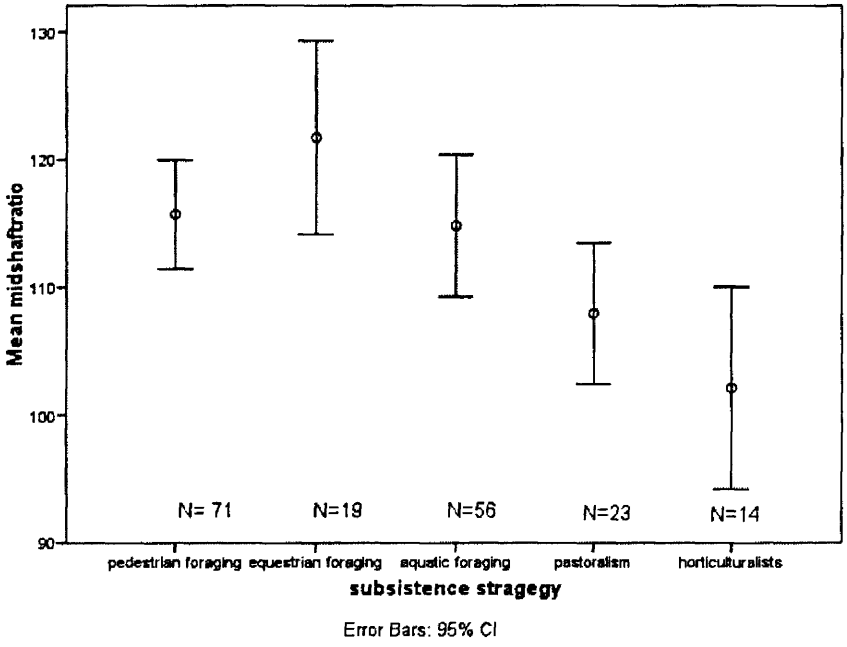

Figure 4-33 Midshaft shape for modern humans, by subsistence strategy. Mean and 95% confidence interval (whiskers).

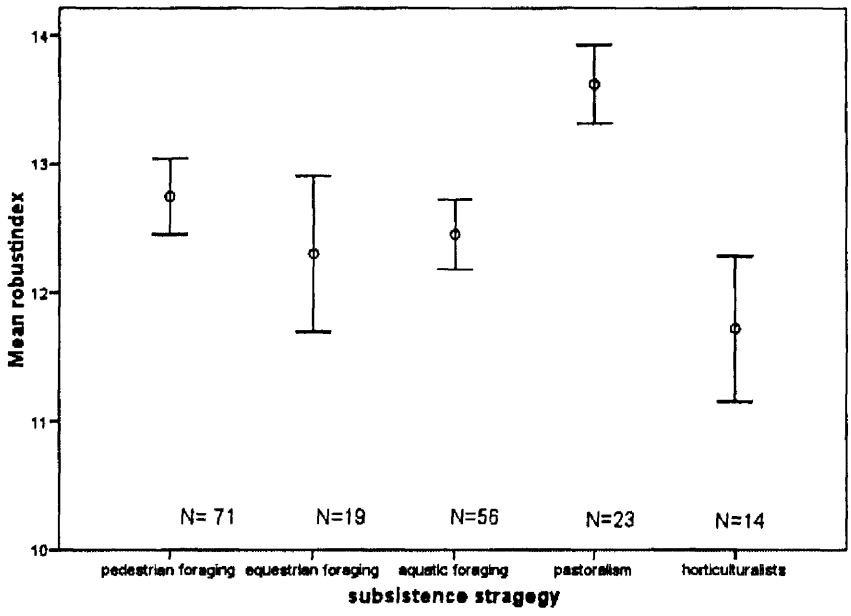

Figure 4-34 Robusticity index for modern humans, by subsistence strategy. Mean and 95% confidence interval (whiskers).

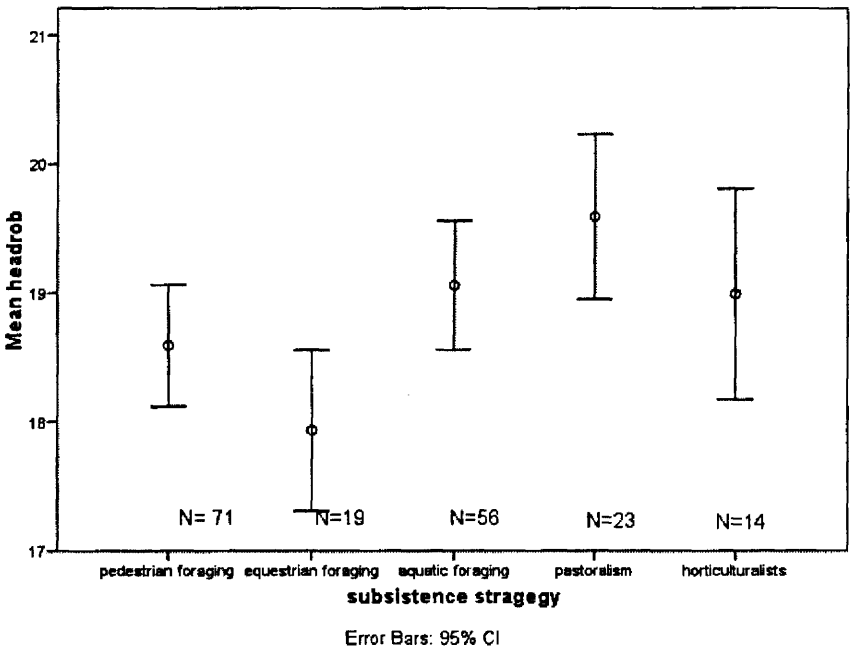

Figure 4-35 Femoral head robusticity for modern humans, by subsistence strategy. Mean and 95% confidence interval (whiskers).

Epiphysis shape

The activity level groups are significantly different for 2 out of 5 epiphysis shape PCs (EpiAMHPC2 and EpiAMHPC5) (Table 4-45; Figure 4-36 and Figure 4-37). Groups with high activity levels have wider epiphyses compared to groups with moderate or low activity levels, and both high and moderate activity groups have a shorter neck than groups with low activity levels (Appendix 20).

For the subsistence groups, 3 out of 4 PCs were significantly different: EpiAMHPC1, EpiAMHPC3 and EpiAMHPC5 (Table 4-46). Pastoralists have wider epiphyses than horticulturalists, pedestrian and aquatic foragers. The equestrian foragers are intermediate (EpiAMHPC2) (Figure 4-38). Pedestrian foragers have less torsion and have wider distal epiphyses than equestrian foragers and pastoralists but are not different from the aquatic foragers and horticulturalists (EpiAMHPC3) (Figure 4-39). Aquatic foragers have a longer neck than pedestrian and equestrian foragers. The other categories are not different from each other (EpiAMHPC5) (Figure 4-40) (Appendix 21).

Table 4-45 ANOVA results for activity level categories and the femoral epiphyses shape PCs.

d.f.=2	F	Sig.
EpiAMHPC1	2.045	0.131
EpiAMHPC2	5.218	0.006*
EpiAMHPC3	1.472	0.231
EpiAMHPC5	3.425	0.033*

*=significant at α=0.05

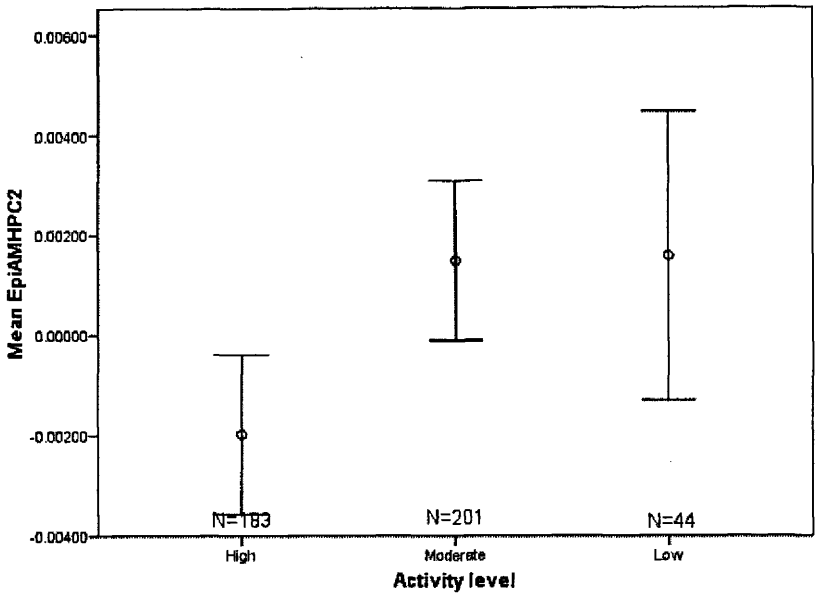

Figure 4-36 EpiAMHPC2 (epiphysis width) for modern humans, by activity level. Mean and 95% confidence interval (whiskers).

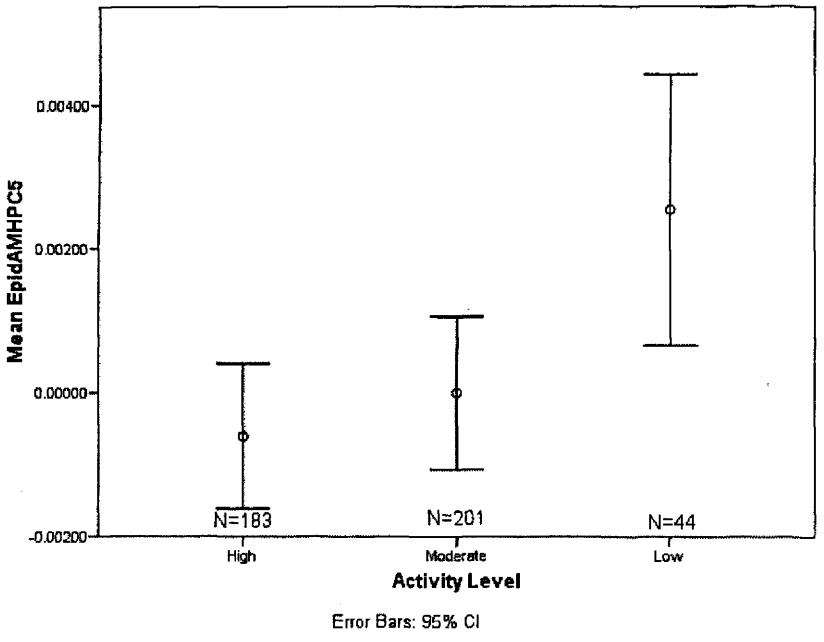

Figure 4-37 EpiAMHPC5 (neck length) for modern humans, by activity level. Mean and 95% confidence interval (whiskers).

Table 4-46 ANOVA results for subsistence categories and the femoral epiphyses shape PCs.

d.f.=5	F	Sig.
EpiAMHPC1	5.386	<0.001*
EpiAMHPC2	1.144	0.337
EpiAMHPC3	10.683	<0.001*
EpiAMHPC5	6.502	<0.001*

*=significant at α=0.05

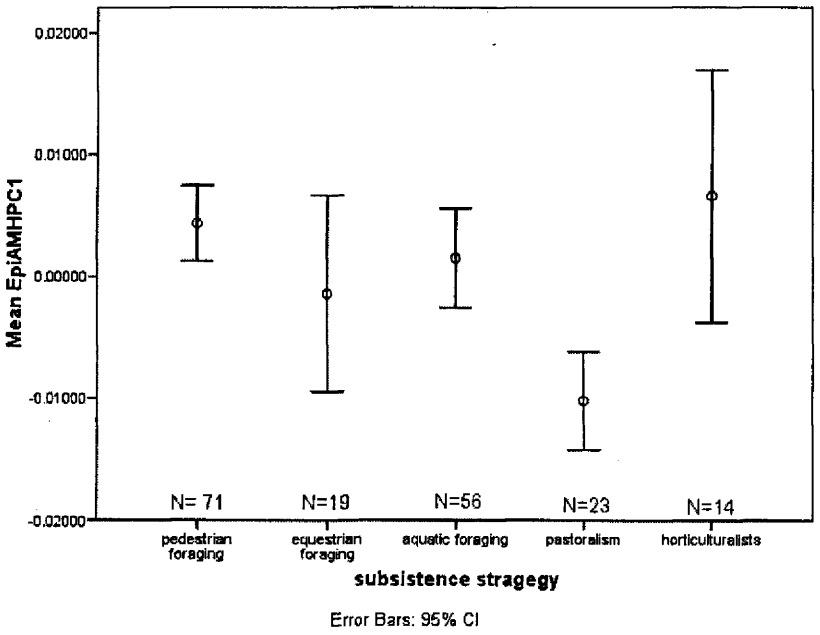

Figure 4-38 EpiAMHPC1 (epiphysis width) for modern humans, by subsistence strategy. Mean and 95% confidence interval (whiskers).

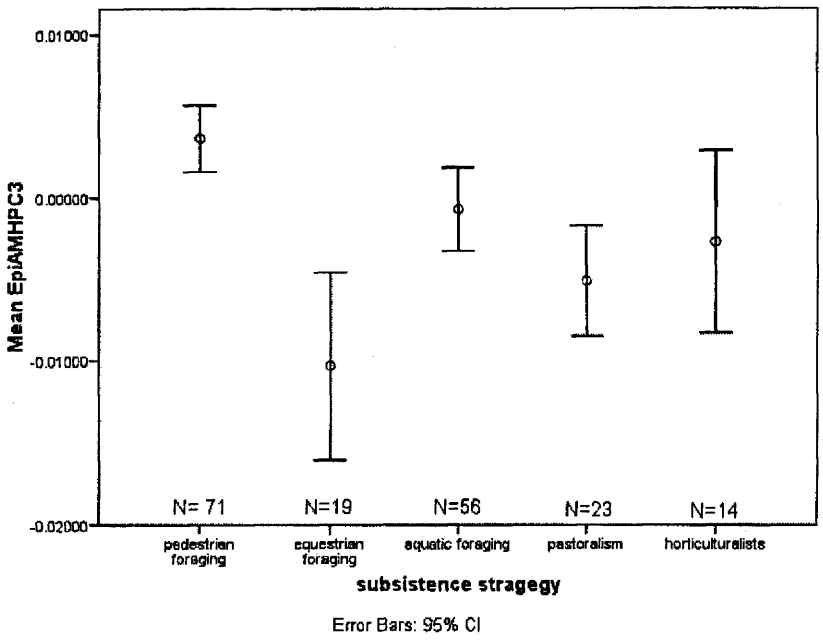

Figure 4-39 EpiAMHPC3 (torsion and distal epiphysis width) for modern humans, by subsistence strategy. Mean and 95% confidence interval (whiskers).

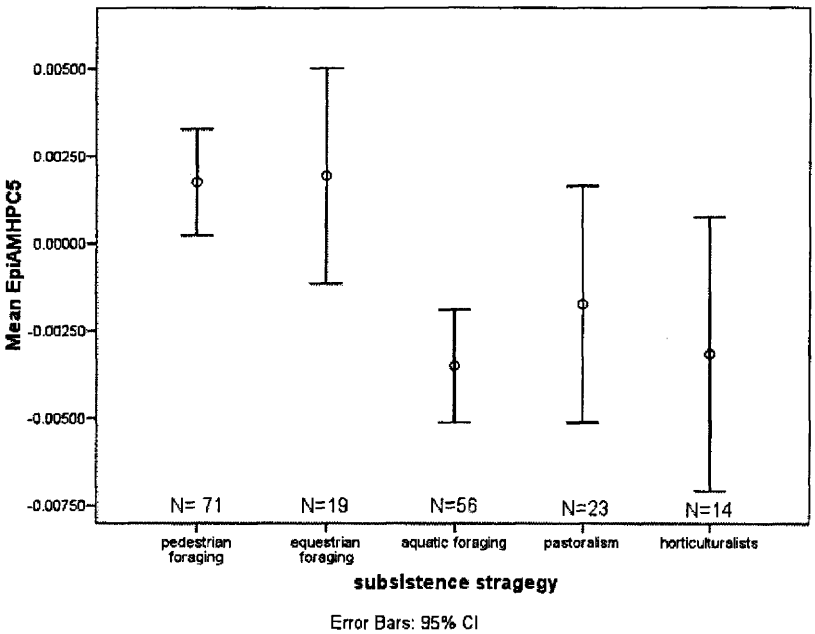

Figure 4-40 EpiAMHPC5 (neck length) for modern humans, by subsistence strategy. Mean and 95% confidence interval (whiskers).

Summary

As predicted, the high activity group has a higher degree of curvature and a lower apex of curvature than the low activity group. The moderate activity group is intermediate and significantly more curved that the low activity group. Within the high activity groups the pastoralists were the most curved. This may reflect their higher levels of terrestrial mobility compared to the other high activity categories. Aquatic foragers have the highest apex of curvature. This could be a reflection of their preference for the use of watercraft for subsistence-related activity and reflect the resulting reduced amount of terrestrial mobility. Increased curvature for the high activity groups coincides with increased robusticity, a more mediolaterally wide shaft and a shorter femoral neck.

4.2.3.5. Evolution over time in Europe

The purpose of the following analyses is to determine if, with time, patterns of curvature have been affected by the adoption of increasingly sedentary lifestyles in Europe (Appendix 8).

Curvature

The prediction is that European populations from the Mesolithic through to the 18^{th}-19^{th} century would show decreasing degrees of curvature (Figure 4-41 and Figure 4-42). There is no significant difference between time periods in Europe (Table 4-47). The degree of anterior curvature does decrease (Figure 4-43), but the posterior curve shows a different pattern (Figure 4-44 and Figure 4-45).

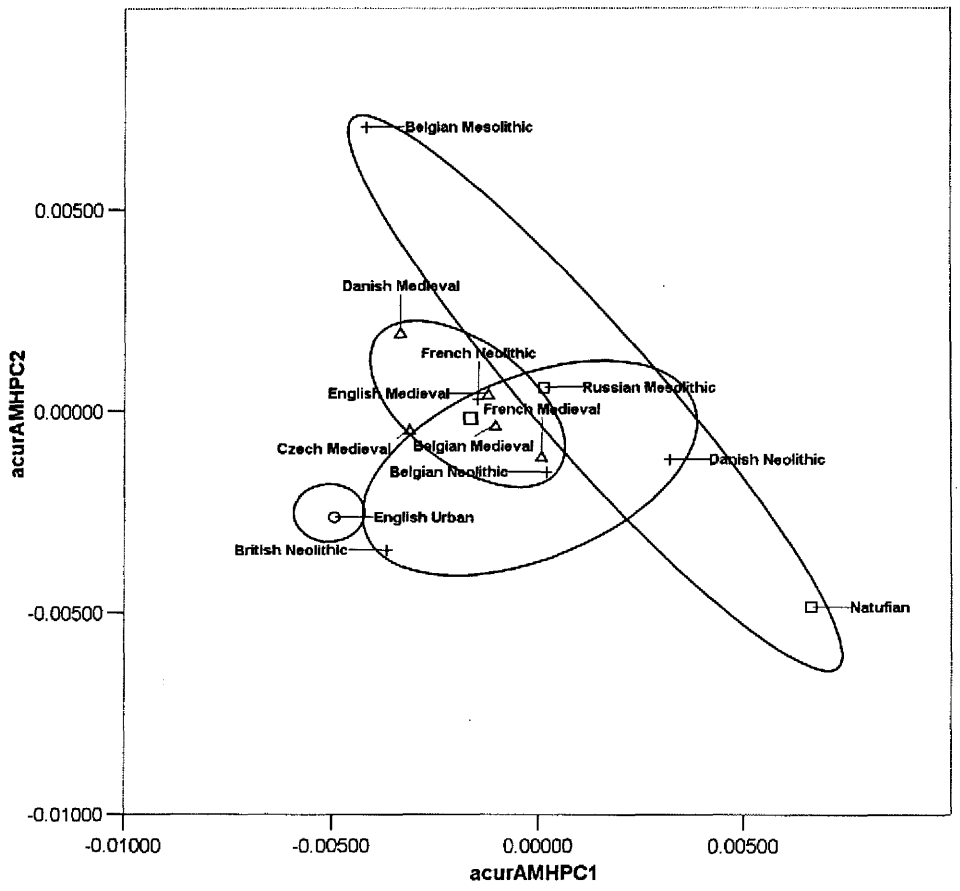

Figure 4-41 Distribution of time periods in the space of PC1 (degree of curvature) and PC2 (apex of curvature) of the anterior curve for all modern humans.

Circles: 18^{th}-19^{th} C, triangles: Medieval, squares: Mesolithic, crosses: Neolithic.

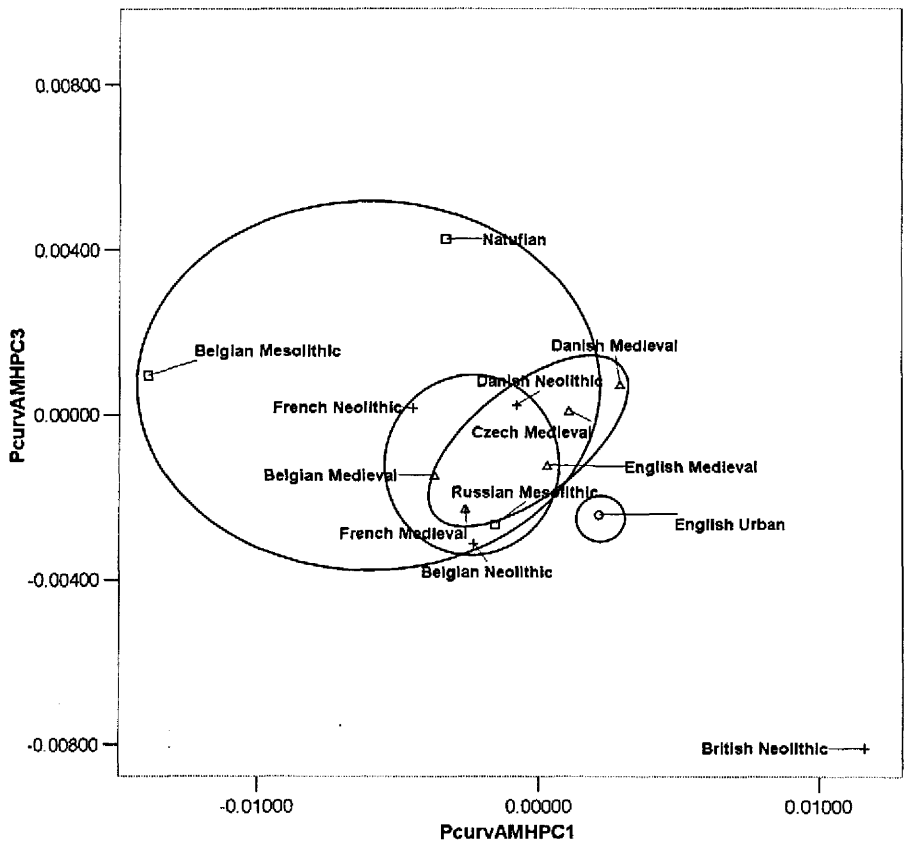

Figure 4-42 Distribution of the time periods in the space of PC1 (degree of curvature) and PC3 (apex of curvature) of the posterior curve for all modern humans.

Circles: 18^{th}-19^{th} C; triangle: Medieval; squares: Mesolithic; crosses: Neolithic.

Table 4-47 ANOVA results for time period and the femoral curvature PCs.

d.f.=3	F	Sig.
acurAMHPC1	1.993	0.117
PcurvAMHPC1	1.551	0.203

*=significant at α=0.05

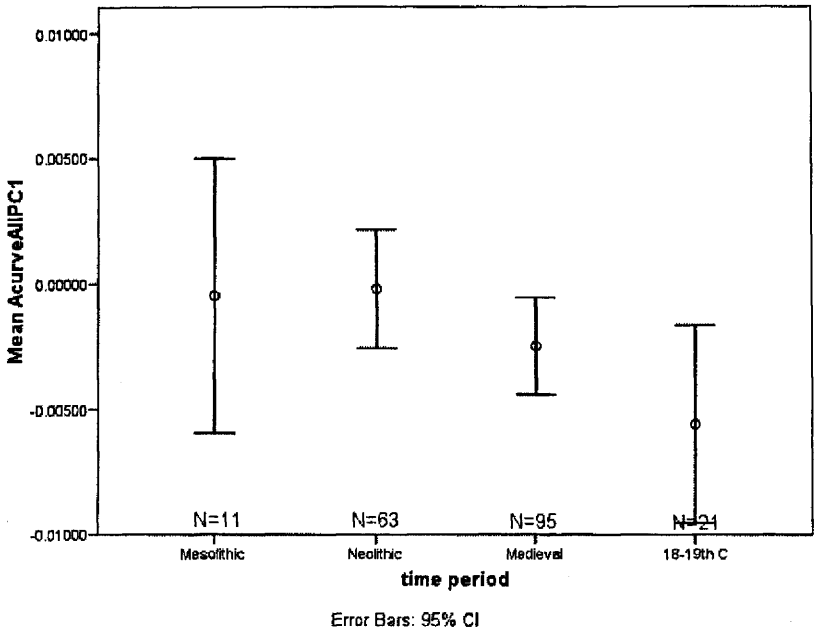

Figure 4-43 Anterior femoral curvature for modern Europeans, by time period. Mean and 95% confidence interval (whiskers).

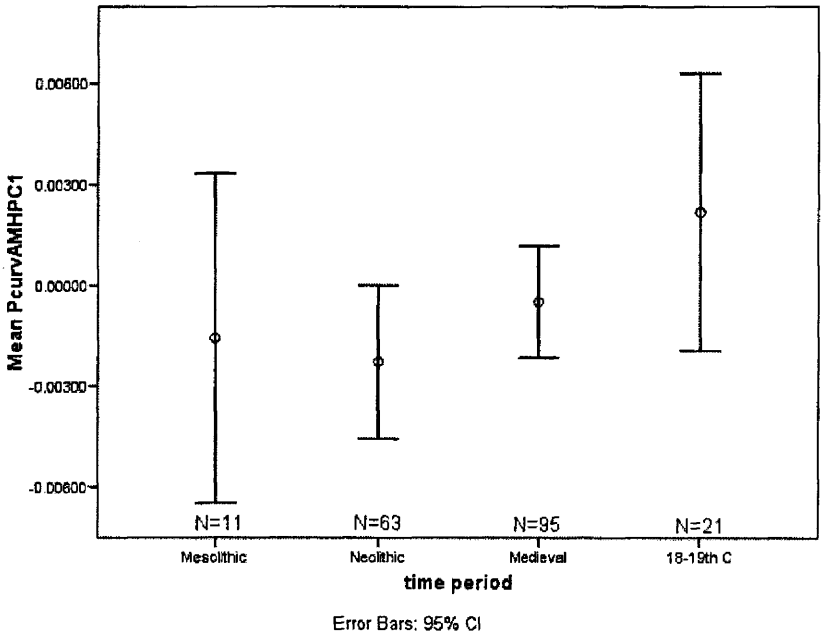

Figure 4-44 Posterior femoral curvature for modern Europeans, by time period. Mean and 95% confidence interval (whiskers).

Apex of curvature

Time period has a significant effect on the anterior apex of curvature (Table 4-48). Post-hoc comparisons show that 18th-19th century samples have a higher apex of curvature compared to Medieval samples but are not significantly different from the other populations (Appendix 22) (Figure 4-45).

Table 4-48 ANOVA results for time period and the femoral curvature PCs

d.f.=3	F	Sig.
acurAMHPC2	3.557	0.015*
PcurvAMHPC3	0.796	0.498

*=significant at α=0.05

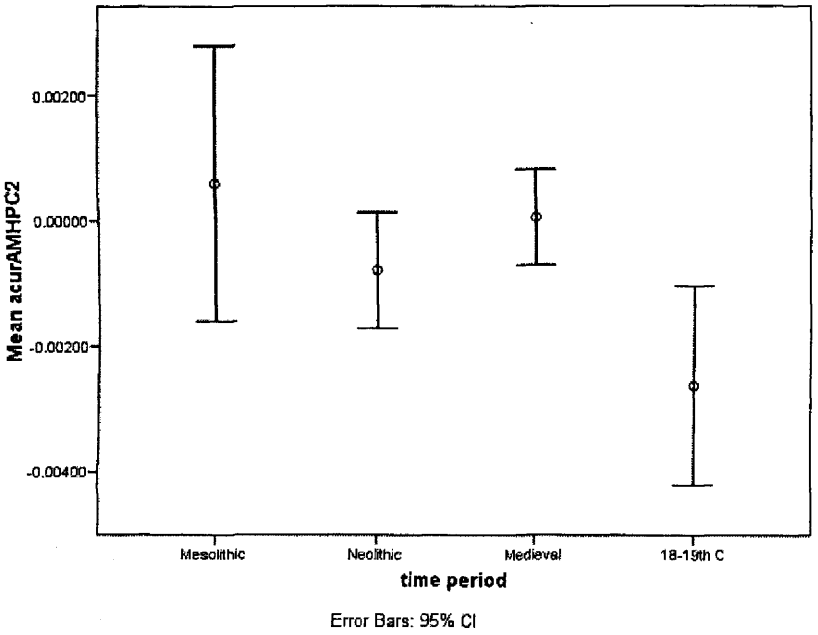

Figure 4-45 Anterior apex of femoral curvature for modern Europeans, by time period. Mean and 95% confidence interval (whiskers).

Summary

The prediction is not supported because no significant differences between the time periods were found. The plots, however, show that with increasing sedentism there is a decreasing trend in degree of anterior curvature. The posterior curve follows an opposite pattern, however. This may be because time period does not accurately reflect a decrease in activity levels and loading.

4.2.3.6. Climate and latitude

As discussed in Chapter 3 latitude is used here as a general proxy for climate (Appendix 8). There is no correlation between latitude and curvature, or apex of curvature (Table 4-51). Individuals in higher latitudes have wider proximal and distal epiphyses (EpiAMHPC1) (Table 4-49).

The relationship between the univariate measurements and latitude are also investigated and follow previously established patterns (Table 4-50). Individuals living in higher latitudes have higher levels of robusticity and a relatively longer femoral neck. There was a positive correlation between femur length and latitude. This relationship was surprising but when the data were investigated, the correlation appeared skewed by small-bodied populations living in low latitudes (Figure 4-46) and by the lack of tall equatorial groups in the sample. When the Andamanese, Pygmy and Peruvian are excluded the correlation is negative, but not significant ($r=-0.353$; $P=0.051$; $N=31$).

Table 4-49 Pearson's correlations for curvature, apex of curvature, diaphyseal shape and epiphyses shape PCs and latitude (climate) on the femur (N=35).

Absolute latitude ° (N=35)								
Curvature			*Other shaft shape*			*Epiyphyses*		
PcurvAMHPC1	r	0.302	acurAMHPC3	r	-0.082	EpiAMHPC1	r	-0.437**
	P	0.078		P	0.639		P	0.009
acurAMHPC1	r	-0.079	acurAMHPC4	r	-0.110	EpiAMHPC2	r	-0.228
	P	0.654		P	0.528		P	0.187
			PcurvAMHPC2	r	-0.129	EpiAMHPC3	r	0.254
				P	0.459		P	0.141
			PcurvAMHPC4	r	0.131	EpiAMHPC4	r	-0.213
Apex of curvature				P	0.452		P	0.218
acurAMHPC2	r	-0.023	McurAMHPC3	r	0.119	EpiAMHPC5	r	0.180
	P	0.897		P	0.498		P	0.301
PcurvAMHPC3	r	-0.105	LcurAMHPC2	r	0.119			
	P	0.550		P	0.496			
			LcurAMHPC4	r	-0.194			
				P	0.263			

* Correlation is significant at the 0.05 level (2-tailed).

** Correlation is significant at the 0.01 level (2-tailed).

Table 4-50 Pearson's correlations for femoral univariate measurements and latitude (climate) on the femur (N=35).

Absolute latitude °					
Univariate measurements					
FemLength	r	0.354*	subpilratio	r	-0.077
	P	0.037		P	0.659
Neck-shaft angle	r	-0.428*	condylediamratio	r	0.430*
	P	0.010		P	0.010
torsionangle	r	-0.179	necklengthratio	r	0.547**
	P	0.304		P	0.001
subtrochratio	r	-0.096	robustindex	r	0.524**
	P	0.585		P	0.001
midshaftratio	r	0.047	headrob	r	0.535**
	P	0.789		P	0.001

* Correlation is significant at the 0.05 level (2-tailed).
** Correlation is significant at the 0.01 level (2-tailed).

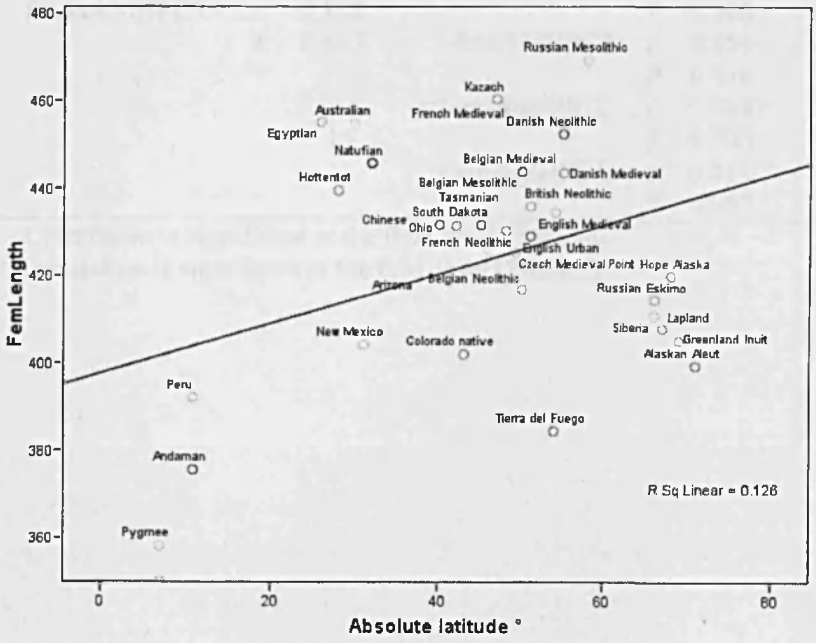

Figure 4-46 Femur length and absolute latitude for the recent modern human sample including the small bodied equatorial samples: Pygmy, Peruvian and Andamanese samples.

Femur shape PCs for groups with high activity levels only

Because the high activity groups have more anteriorly curved femora than the moderate and low activity levels and the high activity groups are possibly more exposed to climatic conditions without permanent housing and insulation, the correlations were repeated for the high activity

groups. The correlation between epiphysis width and neck-shaft angle stands (EpiAMHPC1). There is still no correlation between degree and apex of curvature and latitude. A positive correlation exists with LcurAMHPC2, indicating that individuals living in higher latitudes have femora that are straighter at the level of the lesser trochanter (Table 4-51).

Table 4-51 Pearson's correlations for curvature, apex of curvature, diaphyseal shape and epiphyses shape PCs and latitude (climate) on the femur in high activity groups (N=17).

Absolute latitude °								
Curvature			*Other shaft shape*			*Epicondyles*		
acurAMHPC1	r	-0.079	acurAMHPC3	r	0.334	EpiAMHPC1	r	-0.487*
	P	0.764		P	0.190		P	0.047
PcurvAMHPC1	r	0.461	acurAMHPC4	r	-0.254	EpiAMHPC2	r	-0.275
	P	0.063		P	0.325		P	0.285
Apex of curvature			PcurvAMHPC2	r	-0.341	EpiAMHPC3	r	0.338
acurAMHPC2	r	0.035		P	0.180		P	0.185
	P	0.895	PcurvAMHPC4	r	0.079	EpiAMHPC4	r	0.101
PcurvAMHPC3	r	0.112		P	0.763		P	0.701
	P	0.667	McurAMHPC3	r	0.259	EpiAMHPC5	r	-0.207
				P	0.316		P	0.425
			LcurAMHPC2	r	0.539*			
				P	0.025			
			LcurAMHPC4	r	0.011			
				P	0.967			

* Correlation is significant at the 0.05 level (2-tailed).
** Correlation is significant at the 0.01 level (2-tailed).

4.2.3.7. Mantel test

The Mantel tests take a different approach from the latitude analysis, in this case comparing environmental differences to shape differences. Results are summarised in Table 4-52. There is a significant correlation between anterior femoral curvature (acurvePC1 distances) and altitude differences. No correlation exists between curvature (acurvePC1 distances), apex of curvature (acurvePC2 distances) or the whole femur shape (includes all PCs used in the analyses above) and average rainfall and average temperature differences.

Table 4-52 Results of the Mantel tests performed for environmental distance matrices - femur

	Ant. curvature		apex of curvature		all femur PCs	
	r	P	r	P	r	P
altitude	0.354	0.001*	-0.037	0.614	-0.041	0.618
rainfall	-0.090	0.784	0.054	0.339	0.099	0.239
temperature	0.129	0.080	-0.066	0.736	0.145	0.097

r = Pearson correlation coefficient. All probabilities based on 5000 permutations.

4.2.4. Summary

Curvature

There is no correlation between body size and femoral curvature so the prediction that curvature would be related to body size was not met. Shaft shape and measures of external robusticity are covariates of anteroposterior femoral curvature. Individuals with a higher degree of curvature have higher robusticity levels and are more anteroposteriorly wide. This supports the prediction that degree of curvature and robusticity are related.

Anterior curvature does not relate to climate but is a good indicator of activity levels. Groups with high activity levels are the most curved and, among them, especially those with high levels of terrestrial mobility (pastoralists). Groups with low activity levels are the least curved. Aquatic foragers are less curved than the other high activity groups. This is in support of the prediction made in Chapter 2. Altitude differences are correlated with anterior curvature differences which

may support the importance of the effect of terrestrial mobility over subsistence related activity. There is no difference between all males and females, and there is no correlation between body size and degree of curvature. Therefore, the observed differences in degree curvature between males and females in high activity groups reflects sexual division of labour, rather than sex differences in body size or bone modelling and remodelling rates.

Apex of curvature

Apex of curvature is also not related to body size or climate. There is some indication that higher levels of external robusticity and a more anteroposteriorly wide shaft are related to a more distal apex of curvature. Apex of curvature is a good indicator of activity levels. Groups with high activity levels have a more distal apex. Group with low activity levels have the most proximal apex of curvature. Among the high activity level subsistence strategies, aquatic foragers have the most proximal apex of curvature and the equestrian foragers the most distal.

Rest of the morphology

No predictions were made about other aspects of shaft shape and the univariate measurements; however, there were some interesting results. The low activity group had a lateral surface that approximated an arc of a circle more and a lateral surface that, from an anterior view, was more sinusoidal than moderate and high activity groups who show a straightening of the proximal lateral surface. The equestrian foragers stood apart from the other subsistence categories in having a proximally straighter posterior diaphyseal surface compared to aquatic foragers and pastoralists. There is no relationship between climate and femoral shaft shape but individuals from colder areas do have greater epiphyseal robusticity.

The high activity groups had more robust femora (at midshaft and epiphyseal) with a higher neck-shaft angle and relatively longer femoral neck length. Low activity groups had more anteroposteriorly wide femoral shafts compared to high and moderate activity groups who were not different from each other. Among the high activity groups the equestrian foragers and pastoralists had the lowest neck-shaft angles and in the pastoralists this was combined with high levels of midshaft robusticity.

4.3. The lower arm

As for the femur, the analyses on the lower arm are based on the entire sample of modern humans and the PCs for the radius and ulna will be presented first with their respective visualisations. Subsequently, the results are presented in the same order as the femur.

4.3.1. Radius principal components explained

4.3.1.1. Medial surface (mcurve)

The first three PCs of the medial curve explain 40.4%, 19.7% and 8.75%,,respectively, of the variation (total 68.9%). Subsequent PCs explain minimal amounts of the variation and are not considered further. Figure 4-47 shows the distributions for the populations for PC1 and PC2.

PC1 reflects the differences in lateral curvature of the interosseous crest (Figure 4-47 and Figure 4-48a). PC2 is related to the medial expansion of the proximal interosseous crest and the mediolateral direction of the distal end of the medial surface (Figure 4-47 and Figure 4-48b). PC3 is the sinusoidal shape of the medial surface in the anteroposterior plane (Figure 4-48c).

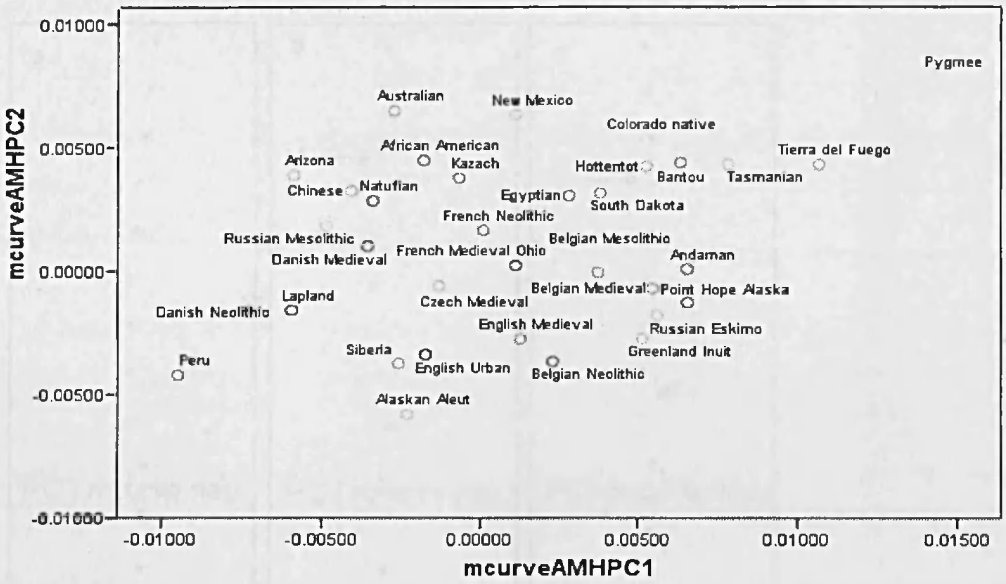

Figure 4-47 The first and second PCs for the medial curve of the radius. All recent modern human samples. PCs are explained in Figure 4-48.

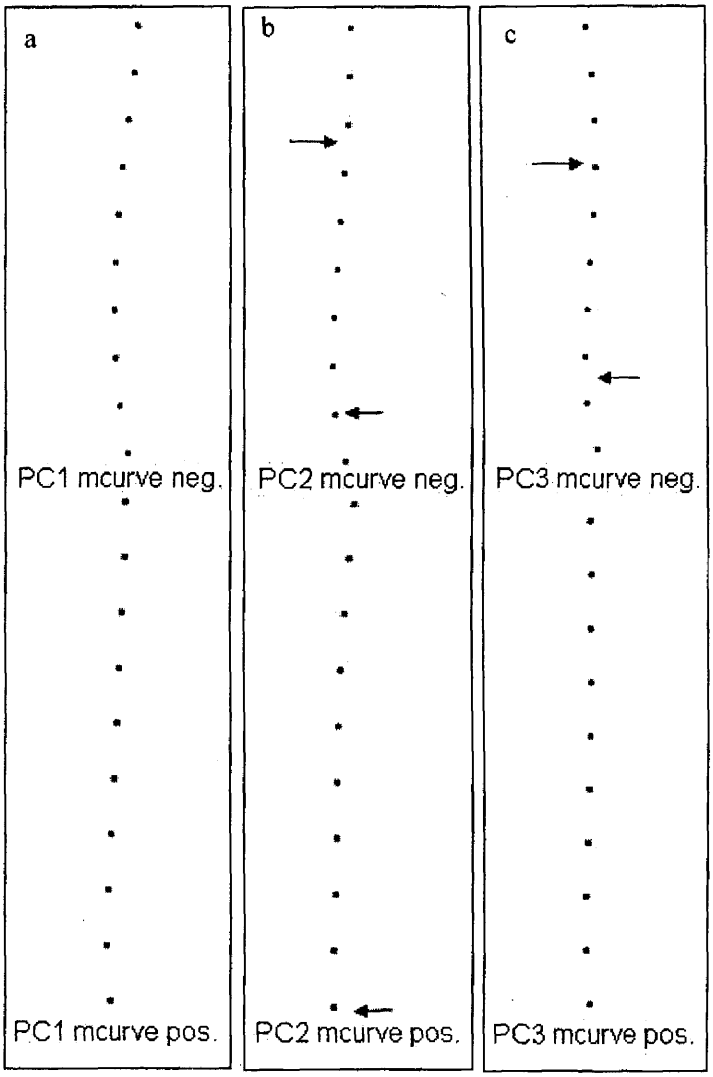

Figure 4-48 Morphological trends for the medial curve of the radius for all recent modern humans. **a**: Principal component 1: anterior view. Negative values are more curved. **b**: Principal component 2: anterior view. Negative values show an increased medial extension of the proximal interosseous crest and a medial direction of the distal curve (more medially expanded ulnar notch), whereas positive values show no medial expansion of the interosseous crest and an ulnar notch that is not medially projected. **c**: Principal component 3: medial view. Negative values have a more sinusoidal shape than positive values which are straighter. Positive and negative visualisations correspond to the most extreme positive and negative scores for each PC.

4.3.1.2. Lateral surface (lcurve)

The first three PCs of the lateral curve explain 40.4%, 19.7% and 8.75%, respectively, of the variation (total 68.9%). Subsequent PCs explain minimal amounts of the variation and are not considered further.

As for the medial curve, PC1 of the lateral surface reflects differences in lateral curvature (Figure 4-49 and Figure 4-50a). The lateral curve is not affected by the development of the interosseous crest and can give a better indication of an apex of curvature for the radius. PC2 is influenced by the position of the apex of curvature and the direction of the distal end of the lateral surface (Figure 4-49 and Figure 4-50b). PC3 relates to the sinusoidal shape of the lateral curve in the anteroposterior plane (Figure 4-50c).

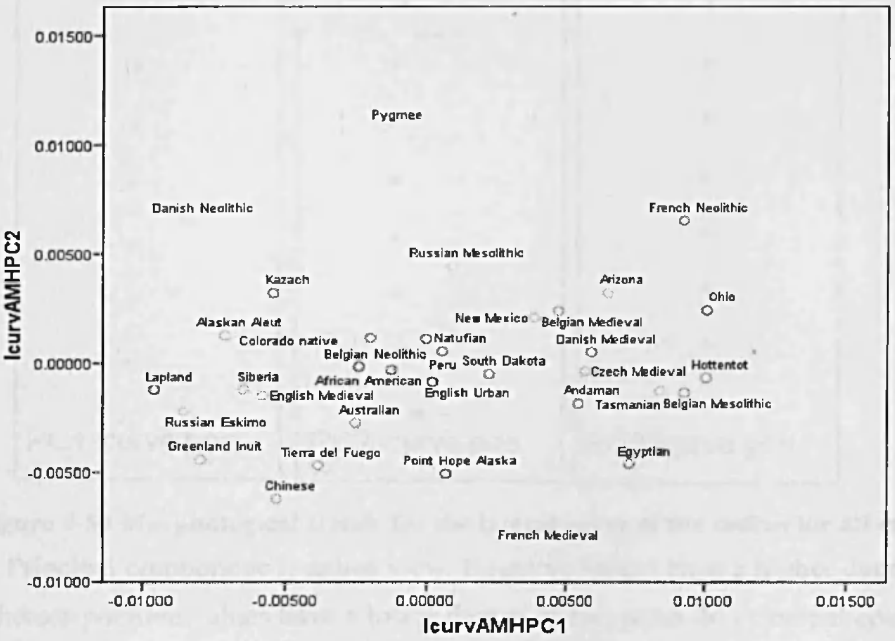

Figure 4-49 The first and second PCs for the lateral curve of the radius. All recent modern human samples. PCs are explained in Figure 4-50.

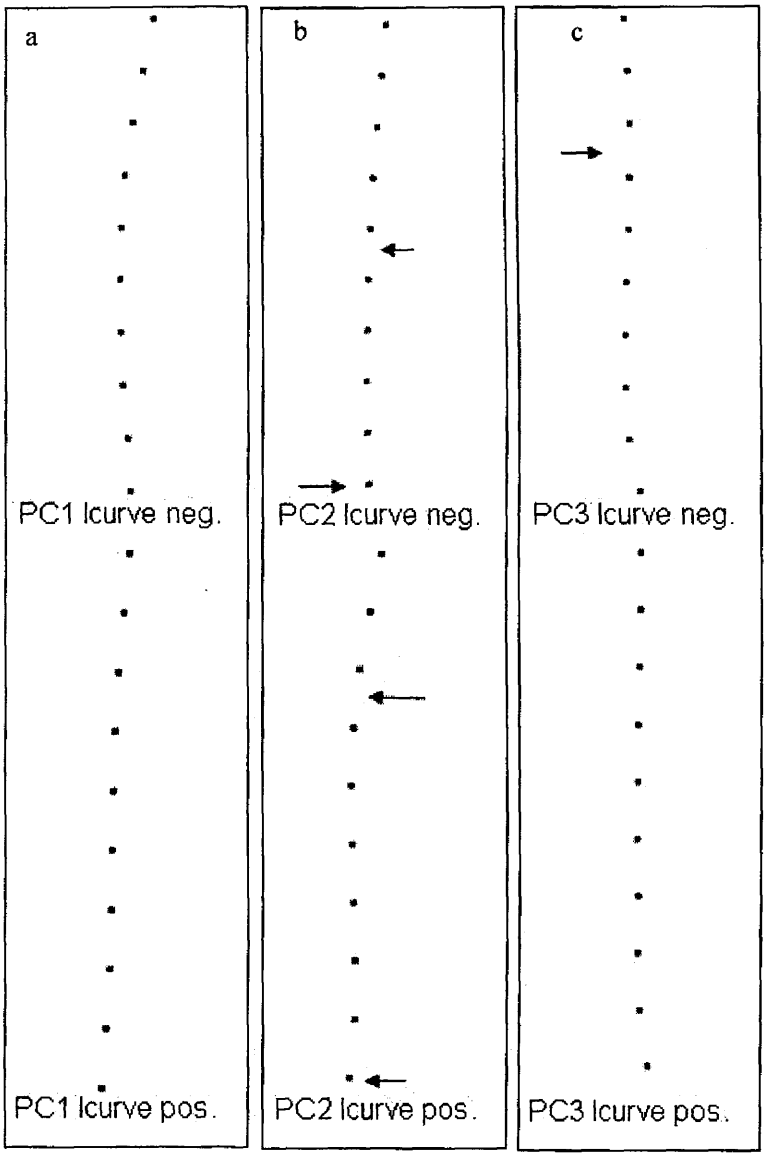

Figure 4-50 Morphological trends for the lateral curve of the radius for all recent modern humans. **a**: Principal component 1: antior view. Negative values have a higher degree of curvature whereas positive values have a lower degree of curvature. **b**: Principal component 2: anterior view: Positive values have a more proximal apex of curvature and a more laterally projecting styloid process, whereas negative values have their apex of curvature at midshaft and lack the lateral projection of the styloid process.**c**: Principal component 3: lateral view. Negative values are more sinusoidal compared to positive values. Positive and negative visualisations correspond to the most extreme positive and negative scores for each PC.

4.3.1.3. Epiphyses (Epi)

The first 2 PCs of the epiphysis analysis explain 34.8% and 8.89%,,respectively, of the variation (total 43.7%). Subsequent PCs explain minimal amounts of the variation and are not considered further.

PC1 reflects the direction of the head and the distal articular surface in relation to the shaft (Figure 4-51a). PC2 relates to the length of the radial neck between the radial tuberosity and 80% level of the shaft and the orientation of the tip of the styloid process (Figure 4-51b).

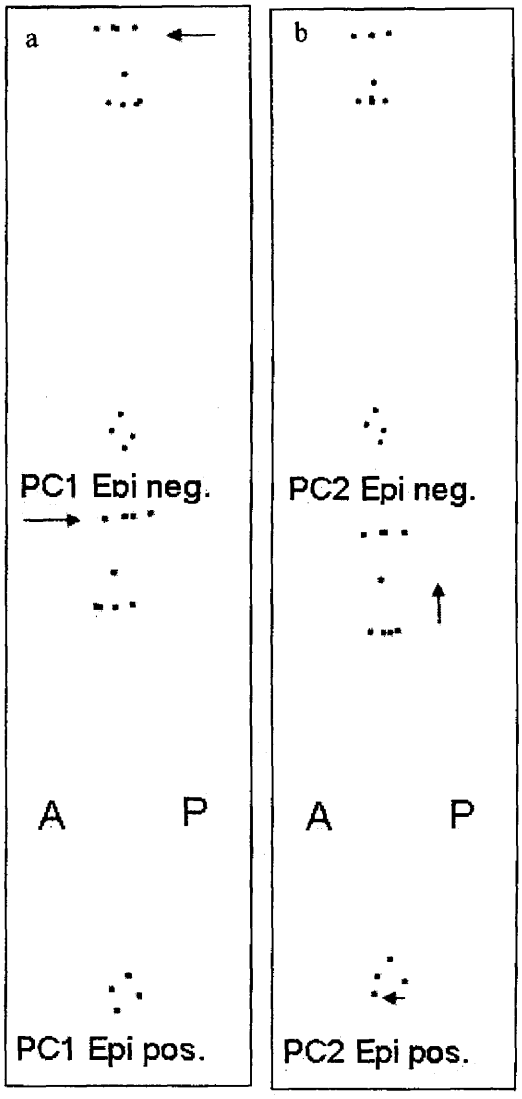

Figure 4-51 Morphological trends for the epiphyses of the radius for all recent modern humans. All medial view.

a: Principal component 1. Individuals with negative values have a more anteriorly oriented head, whereas those with positive values are more posteriorly oriented. **b**: Principal component 2. Negative values indicate a shorter distance between the radial tuberosity and the 80% level of the shaft and a more medially located styloid process, and positive values have a longer neck and more anteriorly located styloid process. Positive and negative visualisations correspond to the most extreme positive and negative scores for each PC.

4.3.1.4. Summary

Lateral curvature is the most important PC for both the medial and the lateral shaft surfaces (mcurveAMHPC1 and lcurveAMHPC1). This is reflected in the significant correlation between the scores for the curvature PCs (r=0.271) (Table 4-53). There is no correlation between the PCs of the epiphyses and the two curvature PCs (Table 4-54).

Table 4-53 Pearson's correlation matrix: radial curvature PCs (n= 360)

		mcurAMHPC1	lcurAMHPC1	mcurAMHPC2	mcurAMHPC3
lcurvAMHPC1	r	0.271			
	P	<0.001**			
mcurveAMHPC2	r		0.162		
	P		0.002**		
mcurveAMHPC3	r		-0.023		
	P		0.658		
lcurvAMHPC2	r	-0.367		0.046	0.080
	P	<0.001**		0.380	0.129
lcurvAMHPC3	r	0.275		0.131	
	P	<0.001**		0.013*	

** Correlation is significant at the 0.01 level (2-tailed).
* Correlation is significant at the 0.05 level (2-tailed).

Table 4-54 Pearson's correlation matrix: radial curvature and epiphyses PCs (n= 349).

		EpiAMHPC1	EpiAMHPC2
mcurveAMHPC1	r	-0.059	-0.084
	P	0.270	0.118
lcurvAMHPC1	r	-0.004	0.026
	P	0.943	0.627
mcurveAMHPC2	r	-0.261	-0.026
	P	0.000**	0.626
mcurveAMHPC3	r	0.304	0.027
	P	0.000**	0.617
lcurvAMHPC2	r	0.011	-0.090
	P	0.841	0.092
lcurvAMHPC3	r	-0.176	-0.049
	P	0.001**	0.360

** Correlation is significant at the 0.01 level (2-tailed).
* Correlation is significant at the 0.05 level (2-tailed).

Correlations between the other shaft shape PCs indicate that individuals who have a higher degree of medial curvature (mcurveAMHPC1) have an apex of curvature at midshaft (mcurveAMHPC2), less medial expansion of the proximal interosseous crest and the mediolateral direction of the distal end of the medial surface (lcurveAMHPC2) and a less

sinusoidal shaft (lcurveAMHPC3). A higher degree of lateral curvature (lcurveAMHPC1) and increased sinusoidal shape (lcurveAMHPC3) is correlated with an increased development of the proximal interosseous crest and increased medial projection of the radial notch (mcurveAMHPC2).

Correlations between the epiphysis PCs show that a more posteriorly projected head results in a more developed proximal interosseous crest, a more developed radial notch (mcurveAMHPC2) and a more sinusoidal shape (lcurveAMHPC3 but see lcurveAMHPC2). Correlation coefficients are significant but low (see 4.3.4.1. Left and Right differences).

4.3.2. Ulna principal components explained

4.3.2.1. Posterior surface (pcurve)

The first four PCs of the posterior curve analysis explain 34.2%, 22.6%, 13.3% and 6.43%, respectively, of the variation (total 76.53%). Subsequent PCs explain minimal amounts of the variation and are not considered further. The distribution of the populations along PC1 and 2 is shown in Figure 4-52.

PC1 reflects differences in mediolateral curvature (Figure 4-52 and Figure 4-53a). PC2 is the sinusoidal shape of the shaft in the mediolateral plane (Figure 4-52 and Figure 4-53b). PC3 relates to the sinusoidal shape of the shaft in the anteroposterior plane (Figure 4-53c) and best reflects the posterior subtense described in the literature (Fischer, 1904). PC4 is the direction of the proximal shaft (Figure 4-53d).

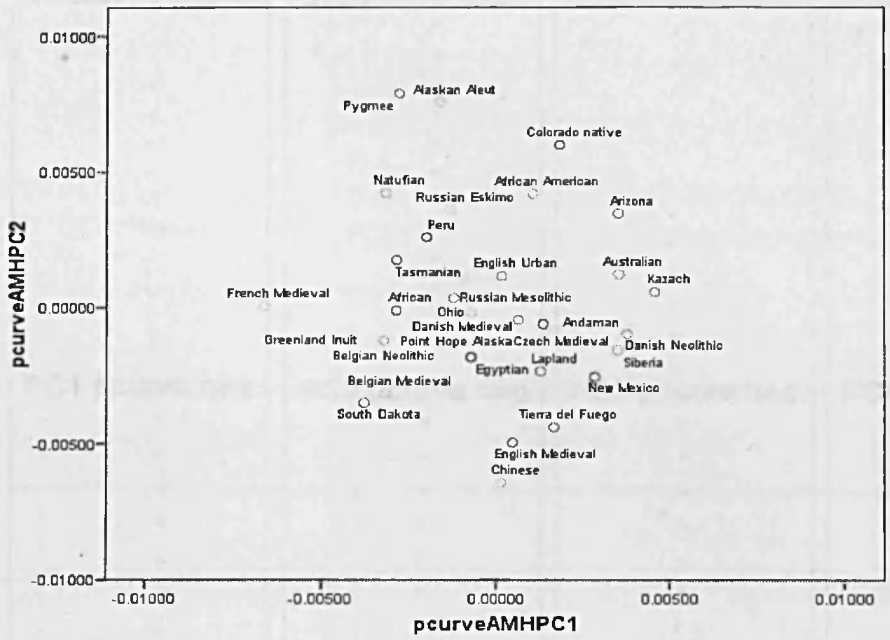

Figure 4-52 The first and second PCs for the posterior curve of the ulna. All recent modern human samples. PCs are explained in Figure 4-53.

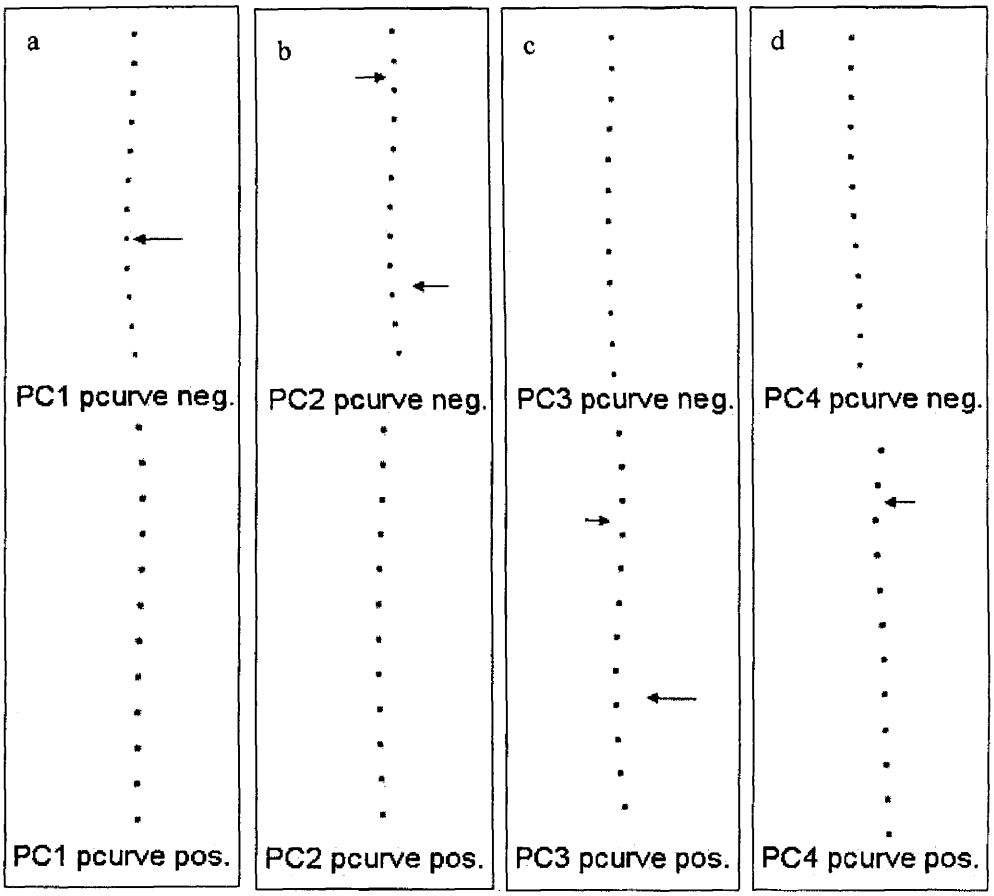

Figure 4-53 Morphological trends for the posterior curvature of the ulna for all recent modern humans.

a: Principal component 1: anterior view. Negative values have a higher degree of mediolateral curvature, whereas positive values have a lower degree of curvature. **b**: Principal component 2: anterior view. Positive values have a straight shaft while negative values are sinusoidal in the mediolateral plane. **c**: Principal component 3: medial view Positive values are more sinusoidal in the anteroposterior plane compared to negative values. **d**: Principal component 4: medial view. Positive values show a bent proximal shaft indicating a more anteriorly projected ulnar head, whereas negative values are relatively straight. Positive and negative visualisations correspond to the most extreme positive and negative scores for each PC.

4.3.2.2. Proximal ulna (prox)

The first four PCs of the proximal ulna analysis explain 22.0%, 18.4%, 7.84% and 4.33%, respectively, of the variation (total 52.6%). Subsequent PCs explain minimal amounts of the variation and are not considered further.

PC1 reflects differences in the orientation of the proximal ulna in relation to the shaft (Figure 4-54 and Figure 4-55a). PC2 relates to the distance between the 80% level of the shaft and the coronoid process (Figure 4-55b). PC3 shows the orientation of the trochlear notch (Figure 4-55c). PC4 is related to the size and dimensions of the trochlear notch (Figure 4-55d). Population distribution for the orientation of the proximal ulna and the distance between the 80% level of the shaft and the coronoid process is shown in Figure 4-54.

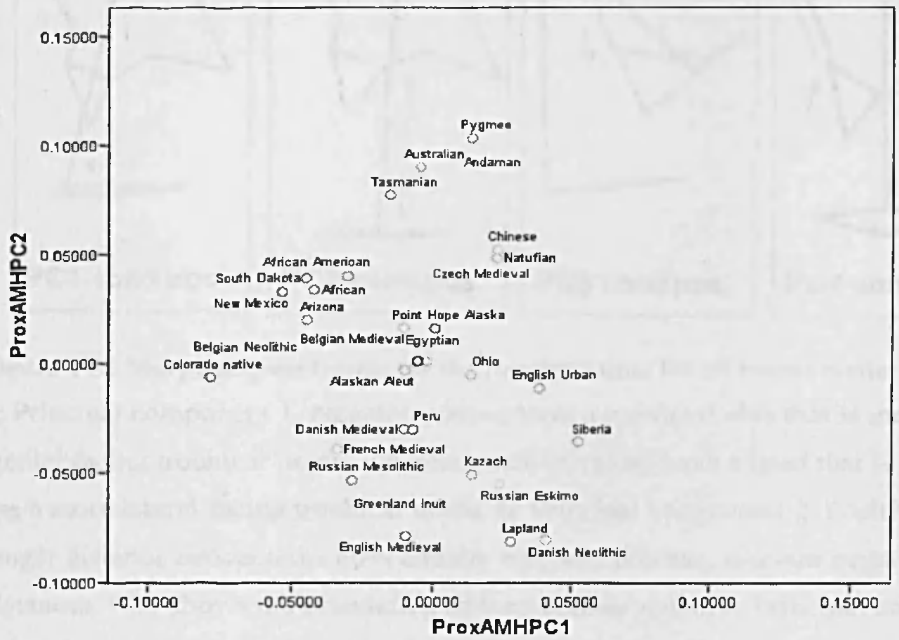

Figure 4-54 The first and second PCs for the proximal ulna. All recent modern human samples. PCs are explained in figure Figure 4-55.

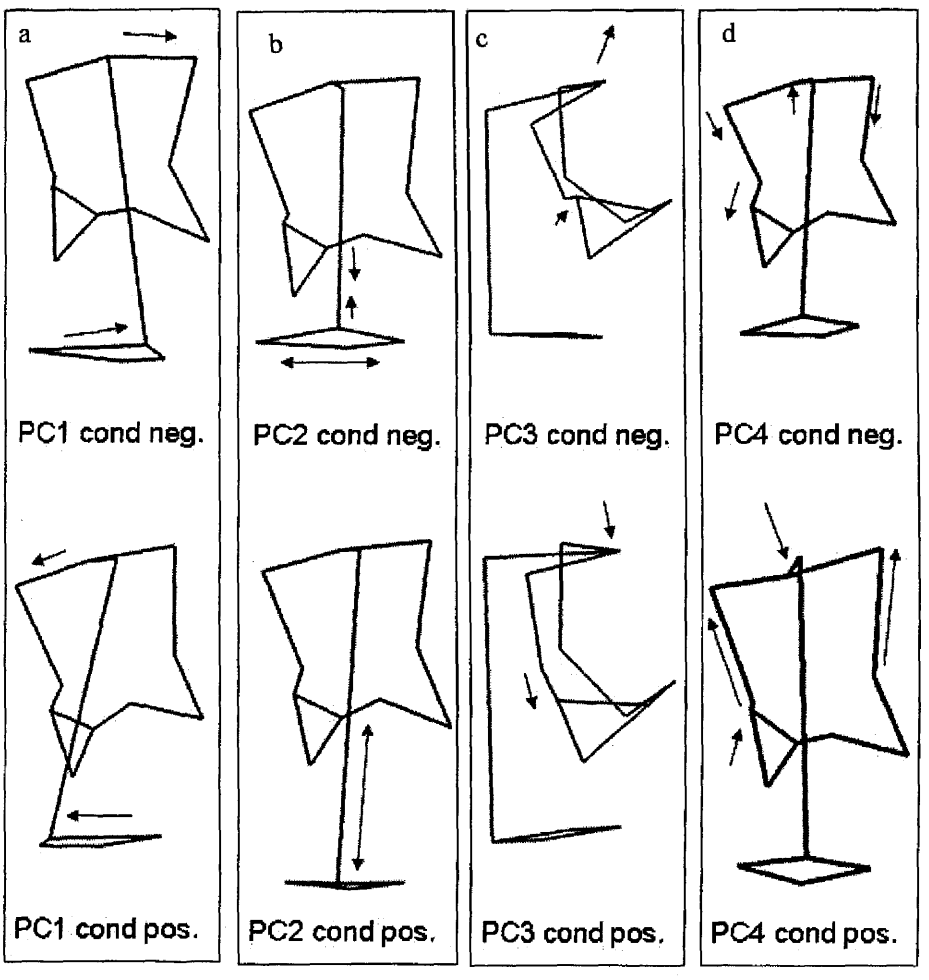

Figure 4-55 Morphological trends for the proximal ulna for all recent modern humans.

a: Principal component 1. Negative values have a proximal ulna that is medially projected with a medial facing trochlear notch, whereas positive values have a head that is laterally projected and has a more lateral facing trochlear notch. **b**: Principal component 2. Positive values have a longer distance between the 80% and the coronoid process, whereas negative values have short distances. PC3 shows the orientation of the trochlear notch. **c**: Principal component 3. Negative values have a more proximo-anterior facing trochlear notch and positive values have a more anterior facing trochlear notch. **d**: Principal component. Positive values have a deeper trochlear notch with a higher radial notch and a lower olecranon process compared to the negative values. Positive and negative visualisations correspond to the most extreme positive and negative scores for each PC.

4.3.2.3. Summary

Because the analysis of the ulna has the main goal of identifying the correlates with radial curvature, and the bone is one that is not frequently studied, the analyses below are exploratory and will consider all the PCs described above. The correlations between the posterior curve and the proximal ulna PCs shows there is a negative correlation between the distance between the 80% level of the shaft and the coronoid process (proxAMHPC2) and the sinusoidal shape in the anteroposterior plane. Individuals with a greater distance between the 80% level of the shaft and the coronoid process have a more sinusoidal shaft shape in the anteroposterior plane (Table 4-55).

Table 4-55 Pearson's correlation matrix: posterior surface and proximal ulna PCs (n= 347).

		proxAMHPC1	proxAMHPC2	proxAMHPC3	proxAMHPC4
pcurveAMHPC1	r	0.121*	-0.057	-0.025	-0.012
	P	0.024	0.286	0.646	0.828
pcurveAMHPC2	r	0.090	0.006	0.098	-0.083
	P	0.093	0.906	0.068	0.124
pcurveAMHPC3	r	0.023	-0.243**	-0.048	-0.074
	P	0.669	<0.001	0.374	0.167
pcurveAMHPC4	r	-0.085	-0.078	0.098	-0.075
	P	0.113	0.147	0.067	0.162

* = Correlation is significant at the 0.05 level (2-tailed).
** = Correlation is significant at the 0.01 level (2-tailed).

4.3.3. Correlations between PCs and univariate measurements

All modern humans

Curvature of the medial curve of the radius is positively correlated with robusticity of the head and distal articulation. McurveAMHPC2 and lcurveAMHPC3 are negatively correlated with robusticity of the distal articulation and show that individuals with relatively larger distal articulations have a medial projection on the proximal interosseous crest and a more pronounced ulnar notch (mcurveAMHPC2) and are more sinusoidal (lcurveAMHPC3) compared to those with smaller distal articulations. There is also a positive correlation between midshaft and head

robusticity and a more sinusoidal radius (N=35) (Table 4-56).

Lateral curvature of the radial shaft is not correlated with any of the univariate measurements. Individuals with a relatively longer radial neck and an anteroposterioly narrow head have a higher apex of curvature and a more laterally projecting styloid process (lcurveAMHPC2). There is a relationship between increased robusticity of the distal articulation, a relatively longer radial neck and a more anteriorly located styloid process (EpiAMHPC2) (Table 4-56).

Anteroposterior sinusoidal shape of the ulnar shaft (pcurveAMH3) is related to the olecranon orientation, relative size of the proximal ulna and relative position of the brachial tuberosity. The mediolateral orientation of the proximal ulna (proxAMHPC1) is positively correlated with the coronoid-olecranon size ratio, the size of the brachial tuberosity, length of the pronator crest and midshaft robusticity. Individuals with a shorter distance between the tip of the coronoid process and the 80% level of the shaft (proxAMHPC2) have a smaller proximal ulna size, a smaller radial notch surface area, a higher coronoid-olecranon size ratio, a larger brachial tuberosity and increased robusticity at the 25% level of the shaft and greater distal articulation robusticity. Individuals with a more proximoanteriorly facing rather than an anteriorly facing trochlear notch (proxAMHPC3) have a relatively smaller olecranon, a more proximoanteriorly facing trochlear notch, greater angle of the proximal ulna and increased distal articulation robusticity. The depth of the trochlear notch and the position of the radial notch (proxAMHPC4) are positively correlated with the midshaft shape ratio, the position of the radial notch and robusticity at the 25% of the shaft (Table 4-57; Table 4-58).

Table 4-56 Pearson's correlation matrix for radius shape PCs and univariate measurements for all modern human populations (N=35).

		mcurveAMHP C1	lcurvAMHP C1	mcurveAMHP C2	mcurveAMHP C3	lcurvAMHP C2	lcurvAMHP C3	EpiAMHP C1	EpiAMHP C2
Midshaftrobusticit									
y	r	-0.257	-0.072	0.112	0.021	0.206	-0.380	0.249	-0.117
	P	0.136	0.679	0.523	0.903	0.236	0.024*	0.149	0.503
Headrobusticity	r	-0.506	-0.045	-0.263	-0.341	-0.266	-0.502	0.124	0.205
	P	0.002**	0.799	0.127	0.045*	0.122	0.002**	0.477	0.238
distArtShaftSizeR	r	-0.539	-0.138	-0.421	-0.289	-0.046	-0.518	0.045	0.345
atio	P	0.001**	0.428	0.012*	0.092	0.793	0.001**	0.799	0.043*
Max_ Length	r	-0.220	0.310	0.331	-0.328	0.077	0.005	-0.271	-0.076
	P	0.205	0.070	0.052	0.054	0.662	0.975	0.115	0.665
neck-shaft angle °	r	0.334	0.077	-0.168	-0.033	0.140	0.266	0.229	-0.217
	P	0.050*	0.662	0.334	0.852	0.424	0.122	0.186	0.211
PosRadTubML	r	0.095	-0.095	-0.142	-0.032	0.023	-0.065	0.246	-0.215
	P	0.588	0.586	0.415	0.854	0.896	0.710	0.154	0.215
DorsalST	r	-0.316	0.120	-0.283	0.048	0.209	-0.538	0.146	-0.123
	P	0.064	0.492	0.099	0.784	0.228	0.001**	0.404	0.480
LateralST	r	0.346	-0.121	-0.016	0.049	-0.038	0.017	0.418	0.069
	P	0.042*	0.489	0.925	0.781	0.828	0.923	0.012*	0.692
NeckLengthRatio	r	-0.012	-0.047	0.098	0.327	0.476	-0.186	0.140	-0.194
	P	0.945	0.787	0.576	0.055	0.004**	0.284	0.424	0.264
HeadShapeRatio	r	-0.121	0.107	-0.122	-0.132	-0.480	-0.075	0.209	0.174
	P	0.490	0.542	0.483	0.450	0.004**	0.669	0.228	0.317
midshaftShapeRat	r	0.338	0.071	0.208	-0.088	0.054	0.588	-0.185	-0.280
io	P	0.047*	0.685	0.231	0.614	0.758	<0.001	0.286	0.103

* = Correlation is significant at the 0.05 level (2-tailed).

** = Correlation is significant at the 0.01 level (2-tailed).

Table 4-57 Pearson's correlation matrix for ulna shape PCs and univariate measurements for all modern human populations (N=35).

		Max_ Length	Olec-shaftratio	MidShaftShape	Radial Notch Surface ratio	TrochNotchOri	Olec-orient angle
pcurveAMHPC1	r	0.004	0.055	0.267	0.162	0.213	0.270
	P	0.981	0.766	0.139	0.375	0.241	0.135
pcurveAMHPC2	r	-0.197	-0.260	0.121	-0.152	-0.241	-0.339
	P	0.279	0.150	0.511	0.405	0.184	0.058
pcurveAMHPC3	r	-0.297	0.413*	-0.140	0.090	0.058	0.442*
	P	0.098	0.019	0.443	0.624	0.751	0.011
pcurveAMHPC4	r	0.239	-0.009	0.250	0.233	-0.389	-0.176
	P	0.188	0.963	0.167	0.200	0.028	0.336
ProxAMHPC1	r	-0.291	0.081	0.100	-0.012	-0.021	0.190
	P	0.106	0.660	0.587	0.946	0.911	0.298
ProxAMHPC2	r	-0.102	-0.493**	0.279	-0.627**	-0.265	-0.732**
	P	0.579	0.004	0.122	<0.001	0.143	<0.001
ProxAMHPC3	r	0.011	-0.422*	0.105	-0.138	-0.570**	-0.434*
	P	0.951	0.016	0.568	0.452	0.001	0.013
ProxAMHPC4	r	0.235	-0.147	0.536**	0.206	-0.343	-0.365*
	P	0.195	0.422	0.002	0.258	0.055	0.040

* = Correlation is significant at the 0.05 level (2-tailed).

** = Correlation is significant at the 0.01 level (2-tailed).

Table 4-58 Pearson's correlation matrix for ulna shape PCs and univariate measurements for all modern human populations (N=35).

		CorOleRatio	BrachRatio	pron.cr. length	Robust 50%	Robust 25%	Robust dist art
pcurveAMHPC1	r	0.320	-0.115	0.202	0.226	0.317	0.293
	P	0.074	0.531	0.267	0.214	0.077	0.104
pcurveAMHPC2	r	-0.317	-0.142	0.064	-0.086	-0.247	-0.261
	P	0.077	0.439	0.729	0.638	0.173	0.150
pcurveAMHPC3	r	0.110	0.382*	0.194	0.250	0.138	0.295
	P	0.548	0.031	0.287	0.167	0.452	0.102
pcurveAMHPC4	r	0.020	0.143	-0.315	-0.028	0.178	0.116
	P	0.913	0.435	0.079	0.881	0.331	0.526
ProxAMHPC1	r	0.519**	0.390	0.579**	0.608**	0.139	0.208
	P	0.002	0.027	0.001	<0.001	0.447	0.253
ProxAMHPC2	r	-0.448**	-0.544**	-0.150	-0.329	-0.499**	-0.648**
	P	0.010	0.001	0.414	0.066	0.004	<0.001
ProxAMHPC3	r	0.032	-0.106	0.006	0.282	-0.013	-0.409*
	P	0.861	0.563	0.974	0.118	0.945	0.020
ProxAMHPC4	r	0.186	0.418*	-0.253	0.117	0.444**	0.222
	P	0.307	0.017	0.163	0.523	0.011	0.223

* = Correlation is significant at the 0.05 level (2-tailed).

** = Correlation is significant at the 0.01 level (2-tailed).

Populations with high activity levels only

For high activity groups, lateral curvature of the radius is not correlated with robusticity. Medial curvature is correlated with the robusticity of the articulations, but not with robusticity at midshaft. Robusticity of the distal articulation is negatively correlated with mcurveAMHPC2 and lcurveAMHPC3 and shows that individuals with relatively larger distal articulations have an increased medial extension of the proximal interosseous crest, a medial direction of the distal curve (more medially expanded ulnar notch) and are more sinusoidal compared to those with smaller distal articulations (Table 4-59).

The correlation between the shape PCs of the ulna and the univariate measurements are the same as for the whole sample. Only, there is no relationship between the depth of the trochlear notch (ProxAMHPC4) and the position of the radial notch and robusticity at the 25% of the shaft (Table 4-66; Table 4-67)

Table 4-59 Pearson's correlation matrix for radius PCs and univariate measurements for populations with high activity levels (N=20).

		mcurveAMHPC1	lcurvAMHPC1	mcurveAMHPC2	mcurveAMHPC3	lcurvAMHPC2	lcurvAMHPC3	EpiAMHPC1	EpiAMHPC2
Midshaftrobusticity	r	-0.311	-0.198	0.121	0.235	0.388	-0.421	0.305	-0.086
	P	0.182	0.402	0.613	0.318	0.091	0.064	0.191	0.718
Headrobusticity	r	-0.536	-0.076	-0.239	-0.266	-0.216	-0.335	0.082	0.321
	P	0.015*	0.749	0.310	0.258	0.361	0.149	0.731	0.167
distArtShaftSizeRatio	r	-0.705	-0.227	-0.507	-0.144	0.027	-0.469	0.115	0.426
	P	0.001**	0.336	0.022*	0.545	0.909	0.037*	0.630	0.061
Max_ Length	r	-0.319	0.332	0.335	-0.264	0.211	0.202	-0.296	0.017
	P	0.171	0.153	0.149	0.261	0.372	0.393	0.205	0.944
neck-shaft angle °	r	0.302	0.199	-0.147	-0.094	-0.177	0.234	0.088	-0.123
	P	0.195	0.399	0.536	0.694	0.456	0.321	0.712	0.606
PosRadTubML	r	-0.045	-0.274	-0.064	0.082	0.035	-0.093	0.137	0.021
	P	0.852	0.242	0.790	0.732	0.882	0.696	0.565	0.931
DorsalST	r	-0.204	-0.140	-0.280	0.366	0.402	-0.536	0.301	-0.023
	P	0.387	0.555	0.232	0.113	0.079	0.015*	0.197	0.922
LateralST	r	0.263	-0.241	0.022	0.133	0.105	0.058	0.693	-0.074
	P	0.262	0.307	0.927	0.576	0.659	0.808	0.001**	0.756
NeckLengthRatio	r	0.251	-0.157	0.069	0.520	0.630	-0.244	0.239	-0.418
	P	0.286	0.509	0.771	0.019*	0.003**	0.300	0.310	0.066
HeadShapeRatio	r	-0.038	0.188	-0.022	-0.222	-0.468	0.075	0.172	0.412
	P	0.873	0.426	0.928	0.347	0.037*	0.754	0.467	0.071
midshaftShapeRatio	r	0.219	0.141	0.312	-0.238	-0.004	0.712	-0.282	-0.211
	P	0.354	0.554	0.180	0.313	0.986	<0.001**	0.229	0.372

* = Correlation is significant at the 0.05 level (2-tailed).

** = Correlation is significant at the 0.01 level (2-tailed).

Table 4-60 Pearson's correlation matrix for ulna PCs and univariate measurements for populations with high activity levels (N=19)

		Max_ Length	Olec-shaftratio	MidShaftShape	Rad.Notch Surf.	TrochNotchOri	Olec-orient angle
pcurveAMHPC1	r	0.021	0.091	0.035	0.268	0.085	0.217
	P	0.932	0.710	0.886	0.266	0.730	0.372
pcurveAMHPC2	r	-0.173	-0.184	0.057	-0.148	-0.182	-0.317
	P	0.479	0.450	0.817	0.547	0.455	0.186
pcurveAMHPC3	r	-0.275	0.516*	-0.022	0.077	0.240	0.487*
	P	0.255	0.024	0.928	0.754	0.323	0.035
pcurveAMHPC4	r	0.145	-0.068	0.295	0.181	-0.380	-0.075
	P	0.553	0.781	0.220	0.459	0.109	0.759
ProxAMHPC1	r	-0.283	0.112	0.122	-0.033	-0.078	0.110
	P	0.241	0.648	0.619	0.894	0.750	0.653
ProxAMHPC2	r	-0.080	-0.470*	0.340	-0.593**	-0.413	-0.834**
	P	0.744	0.042	0.155	0.008	0.079	<0.001
ProxAMHPC3	r	0.013	-0.555*	0.061	-0.267	-0.661**	-0.533*
	P	0.957	0.014	0.804	0.269	0.002	0.019
ProxAMHPC4	r	0.243	-0.336	0.493*	0.104	-0.388	-0.403
	P	0.315	0.160	0.032	0.672	0.100	0.087

* = Correlation is significant at the 0.05 level (2-tailed).

** = Correlation is significant at the 0.01 level (2-tailed).

Table 4-61: Pearson's correlation matrix for ulna PCs and univariate measurements for populations with high activity levels (N=19).

		CorOleRatio	BrachRatio	pron.cr. length	Robusticity at 50%	Robusticity at 25%	Robust dist artic
pcurveAMHPC1	r	0.323	-0.187	0.317	0.415	0.369	0.257
	P	0.177	0.443	0.186	0.077	0.120	0.288
pcurveAMHPC2	r	-0.281	-0.253	0.038	-0.174	-0.497*	-0.391
	P	0.244	0.296	0.879	0.476	0.031	0.097
pcurveAMHPC3	r	0.342	0.592**	0.235	0.222	0.154	0.419
	P	0.151	0.008	0.332	0.362	0.528	0.074
pcurveAMHPC4	r	-0.046	0.046	-0.291	-0.102	0.093	0.049
	P	0.853	0.852	0.227	0.677	0.704	0.841
ProxAMHPC1	r	0.600**	0.502*	0.737**	0.690**	0.189	0.242
	P	0.007	0.028	<0.001	0.001	0.438	0.317
ProxAMHPC2	r	-0.565*	-0.616**	-0.145	-0.342	-0.547*	-0.744**
	P	0.012	0.005	0.553	0.151	0.015	<0.001
ProxAMHPC3	r	-0.137	-0.255	-0.105	0.239	-0.103	-0.590**
	P	0.575	0.292	0.669	0.324	0.673	0.008
ProxAMHPC4	r	0.097	0.293	-0.207	0.087	0.278	0.010
	P	0.691	0.224	0.396	0.724	0.249	0.968

* = Correlation is significant at the 0.05 level (2-tailed).

** = Correlation is significant at the 0.01 level (2-tailed).

4.3.4. Factors influencing curvature in modern humans

The following analyses will focus on the relationship between radial curvature and ulna shaft shape and the behavioural, environmental and biological variables that might be expected to influence morphology. These analyses address the same hypotheses and predictions tested for the femur.

4.3.4.1. Bilateral asymmetry of the lower arm

Left and right side are not different in degree of radial curvature (Table 4-71) (N=143 left and 218 right radii). Left radii have a more developed proximal interosseous crest and radial notch (mcurveAMHPC2) and a straighter shaft, whereas the right radius is more sinusoidal and lacks the proximal development on the interosseous crest (mcurveAMHPC3) (Table 4-71). Left radii have a more posteriorly oriented radial head (EpiAMHPC1) than right radii. The high *t*-value for EpiAMHPC1 indicates that the shape differences along the PC axis translate into the differences between right and left (Table 4-62).

The ulna shows marked asymmetry. Right ulnae have more medial curvature (pcurveAMHPC1) and are more sinusoidal in the mediolateral plane than left ulnae (pcurveAMHPC2) (Table 4-63). Right ulnae have a proximal ulna that is medially projected with a medial facing trochlear notch (proxAMHPC1), have a more proximo-anterior trochlear notch (proxAMHPC3), and a deeper trochlear notch with a higher radial notch and a lower olecranon process (proxAMHPC4) (Table 4-63).

Table 4-62 Student's *t*-test results for bilateral asymmetry in radius shape in modern humans.

	Side	N	Mean	S.D.	t	P
McurveAMHPC1	left	143	-0.00098	0.01019	-1.388	0.166
	right	218	0.00064	0.01120		
lcurvAMHPC1	left	142	0.00007	0.01215	0.100	0.920
	right	218	-0.00005	0.01100		
McurveAMHPC2	left	143	-0.00211	0.00702	-5.110	<0.001**
	right	218	0.00138	0.00588		
McurveAMHPC3	left	143	0.00274	0.00583	8.495	<0.001**
	right	218	-0.00179	0.00429		
lcurvAMHPC2	left	142	0.00038	0.00808	0.753	0.452
	right	218	-0.00027	0.00795		
lcurvAMHPC3	left	142	-0.00057	0.00571	-1.653	0.099
	right	218	0.00038	0.00504		
EpiAMHPC1	left	137	0.02254	0.01440	25.945	<0.001**
	right	212	-0.01457	0.01210		
EpiAMHPC2	left	137	0.00054	0.01164	0.722	0.471
	right	212	-0.00035	0.01108		

* Significant at α=0.05

Table 4-63 Student's *t*-test results for bilateral asymmetry in ulna shape in modern humans.

	Side	N	Mean	S.D.	t	P
PcurveAMHPC1	right	227	-0.00064	0.00900	-2.156	0.032*
	left	118	0.00148	0.00800		
PcurveAMHPC2	right	227	-0.00053	0.00736	-2.109	0.036*
	left	118	0.00117	0.00650		
PcurveAMHPC3	right	227	-0.00006	0.00539	-0.226	0.822
	left	118	0.00008	0.00565		
PcurveAMHPC4	right	227	0.00013	0.00386	0.815	0.416
	left	118	-0.00022	0.00370		
proxAMHPC1	right	227	-0.03983	0.05087	-18.678	<0.001*
	left	118	0.07760	0.06324		
proxAMHPC2	right	227	0.00152	0.07100	0.497	0.620
	left	118	-0.00254	0.07397		
proxAMHPC3	right	227	-0.00404	0.04851	-2.325	0.021*
	left	118	0.00826	0.04262		
proxAMHPC4	right	227	0.00715	0.03195	5.450	<0.001*
	left	118	-0.01354	0.03616		

*=significant at α=0.05

Univariate measurements

Left radii have lower neck-shaft angles, a more medially located radial tuberosity, and a higher dorsal and lateral subtense (Table 4-64).

Right ulnae have larger proximal ulnae (Olec-shaftratio) that are oriented more in line with the shaft axis both mediolaterally (head orientation angle) and anteroposteriorly (troch-notch orientation) (Table 4-65). Right ulnae also have more equal coronoid and olecranon heights

(CorOleRatio), a shorter pronator crest and lower robusticity at midshaft and at the 25% level of the shaft.

Table 4-64 Student's *t*-test results for univariate measurements of the radius in modern humans.

		N	Mean	S.D.	t	P
Max_ Length	left	143	232.49	19.68	-1.926	0.055
	right	218	236.57	19.72		
neck-shaft angle °	left	143	40.84	15.69	5.632	0.000*
	right	218	32.72	11.64		
PosRadTubML	left	143	17.71	7.93	4.837	0.000*
	right	218	14.05	6.37		
DorsalST	left	143	7.14	2.16	4.227	0.000*
	right	218	6.24	1.86		
LateralST	left	143	7.81	2.93	5.941	0.000*
	right	218	6.14	2.37		
NeckLengthRatio	left	143	11.20	1.33	1.789	0.074
	right	217	10.92	1.56		
OlecShapeRatio	left	143	106.42	8.98	1.845	0.066
	right	217	104.70	8.46		
Midshaft Shape Ratio	left	143	84.51	16.40	-0.376	0.707
	right	217	85.10	13.21		

* Significant at α=0.05

Table 4-65 Student's *t*-test results for univariate measurements of the ulna in modern humans.

	Side	N	Mean	S.D.	t	P
Max_ Length	right	227	251.82	20.45	1.843	0.066
	left	119	247.56	20.32		
Olec-shaft ratio	right	227	9.21	0.97	2.922	0.004*
	left	119	8.88	1.01		
MidShaft Shape	right	227	109.52	35.16	-0.245	0.806
	left	119	110.40	24.38		
Radial Notch Surf. ratio	right	227	29.77	7.86	0.397	0.692
	left	119	29.43	6.72		
TrochNotchOri	right	227	19.76	6.15	-3.181	0.002*
	left	119	22.06	6.79		
Olec-orient angle	right	227	23.42	4.64	-3.491	0.001*
	left	119	25.39	5.64		
CorOleRatio	right	227	105.62	1.69	-15.168	0.000*
	left	119	108.93	2.32		
BrachRatio	right	227	23.01	1.91	0.402	0.688
	left	119	22.93	1.63		
Rel. pron. cr. size	right	227	14.15	3.77	-3.592	<0.001*
	left	119	15.63	3.33		
Robusticity at 50%	right	227	9.94	1.39	-8.091	<0.001*
	left	119	11.18	1.29		
Robusticity at 25%	right	227	10.25	1.41	-2.071	0.039*
	left	119	10.58	1.45		
Robust dist artic	right	227	15.59	1.83	-0.001	1.000
	left	119	15.59	1.94		

*=significant at α=0.05

Results below are reported for the pooled sample only, unless the significance values are affected. In the analyses investigating sex differences all variables affected by bilateral asymmetry are performed for the right side only.

4.3.4.2. Body size

Anteroposterior diameter of the femoral head is used as an measure of body size (for those specimens for which the femur is also preserved) (Ruff, 1991; McHenry, 1992; Grine *et al.*, 1995). Based on this size surrogate there is no correlation between curvature of the radius and the shape of the ulna shaft and body size. (Table 4-66; Table 4-67).

Table 4-66 Pearson's correlations for body size (head diameter) and radial curvature (N=27).

HeadAPdiam		
mcurveAMHPC1	r	0.165
	P	0.409
lcurvAMHPC1	r	-0.020
	P	0.921

* = Correlation is significant at the 0.05 level (2-tailed).
** = Correlation is significant at the 0.01 level (2-tailed).

Table 4-67 Pearson's correlations for body size (head diameter) and ulna shaft shape (N=27).

HeadAPdiam		
UlnpcurveAMHPC1	r	0.163
	P	0.418
UlnpcurveAMHPC2	r	-0.154
	P	0.442

* = Correlation is significant at the 0.05 level (2-tailed).
** = Correlation is significant at the 0.01 level (2-tailed).

4.3.4.3. Sex

As for the femur the purpose of these analyses is to investigate sexual dimorphism in the lower arm.

Curvature

For the whole sample of radii of known sex (N=90 males and 82 females), the prediction that

males have higher robusticity (Table 4-68) because they have higher activity levels than females was met but males and females were not different in degree of radial curvature (Table 4-69).

Table 4-68 Student's *t*-test results for robusticity in modern human males and females.

	Sex	N	Mean	S.D.	t	P
Midshaftrobusticity	male	90	20.55	2.05	6.329	0.000*
	female	82	18.64	1.89		
Headrobusticity	male	90	30.67	2.73	7.636	0.000*
	female	82	27.48	2.73		
distArtShaftSizeRatio	male	90	37.25	3.12	8.530	0.000*
	female	83	33.37	2.84		

* Significant at α=0.05

Table 4-69 Student's *t*-test results for radius curvature PCs in modern human males and females.

	Sex	N	Mean	S.D.	t	P
mcurveAMHPC1	male	90	.00034	.01030	0.261	0.794
	female	83	-.00008	.01054		
lcurvAMHPC1	male	90	-.00034	.01170	-1.624	0.106
	female	83	.00251	.01140		

* Significant at α=0.05

It was demonstrated in the analyses of the femur that there is evidence that division of labour is most pronounced in groups with high activity levels. Therefore, the expectation is that the effect of sex on robusticity and curvature is more evident in those groups than for the whole sample (Table 4-70; Table 4-71). The prediction is met for robusticity (N=39 males and 38 females) and as is the case for the whole sample, males and females are significantly different for shaft and epiphyseal robusticity. Degree of curvature is not different between males and females with high activity levels.

Table 4-70 Student's *t*-test results for radius robusticity in modern human males and females with high activity levels.

	Sex	N	Mean	S.D.	t	P
Midshaftrobusticity	male	39	20.46	2.36	2.970	0.004*
	female	38	19.01	1.89		
Headrobusticity	male	39	29.39	2.80	4.727	<0.001*
	female	38	26.34	2.87		
distArtShaftSizeRatio	male	39	36.23	3.54	3.817	<0.001*
	female	38	33.30	3.19		

* Significant at α=0.05

Table 4-71 Student's *t*-test results for radius curvature PCs in modern human males and females with high activity levels.

	Sex	N	Mean	S.D.	t	P
mcurveAMHPC1	male	39	.00199	.01118	1.284	0.203
	female	38	-.00094	.00864		
lcurvAMHPC1	male	39	-.00013	.01314	-0.376	0.708
	female	38	.00101	.01335		

* Significant at α=0.05

Other shaft shape PCs

The other shaft shape PCs are bilaterally asymmetric so only the right side is analysed. For all individuals (N=61 males and 50 females) females have a more pronounced proximal interosseous crest and ulnar notch (mcurveAMHPC2) and have a more sinusoidal anteroposterior shaft shape (mcurveAMHPC3) (Table 4-72). The difference in anteroposterior shaft shape (mcurveAMHPC3) is also present in the groups with high activity levels, but not the difference in the interosseous crest and the ulnar notch (Table 4-73).

Table 4-72 Student's *t*-test results for radius shaft shape PCs in modern human males and females – right only.

	Sex	N	Mean	S.D.	t	P
mcurveAMHPC2	male	61	0.00277	0.00485	2.986	0.003*
	female	50	-0.00037	0.00626		
mcurveAMHPC3	male	61	-0.00097	0.00365	3.074	0.003*
	female	50	-0.00309	0.00357		
lcurvAMHPC2	male	61	0.00049	0.00774	0.332	0.741
	female	50	0.00000	0.00755		
lcurvAMHPC3	male	61	-0.00108	0.00526	-1.900	0.060
	female	50	0.00088	0.00557		

* Significant at α=0.05

Table 4-73 Student's *t*-test results for radius shaft shape PCs in modern human males and females with high activity levels – right only.

	Sex	N	Mean	S.D.	t	P
mcurveAMHPC2	male	26	0.00301	0.00440	0.685	0.497
	female	22	0.00197	0.00607		
mcurveAMHPC3	male	26	-0.00051	0.00325	2.413	0.020*
	female	22	-0.00276	0.00320		
lcurvAMHPC2	male	26	0.00195	0.00868	0.328	0.744
	female	22	0.00117	0.00744		
lcurvAMHPC3	male	26	0.00138	0.00467	-0.893	0.376
	female	22	0.00263	0.00506		

* Significant at α=0.05

The first and second PC for the ulna show bilateral asymmetry. Therefore the analyses are performed on the right side only. There is no sexual dimorphism in the right ulna (65 males and 49 females) for any of the shaft shape PCs (Table 4-74). In the right ulnae of the high activity group (30 males and 22 females), males have a straighter shaft in the mediolateral plane compared to females (pcurveAMHPC2) (Table 4-75).

Table 4-74 Student's *t*-test results for ulna shaft shape PCs in modern human males and females – right only.

	Sex	N	Mean	S.D.	t	P
pcurveAMHPC1	male	65	-0.00071	0.00849	-0.404	0.687
	female	49	-0.00009	0.00781		
pcurveAMHPC2	male	65	-0.00028	0.00704	0.634	0.527
	female	49	-0.00119	0.00821		
pcurveAMHPC3	male	65	-0.00070	0.00549	0.806	0.422
	female	49	-0.00150	0.00483		
pcurveAMHPC4	male	65	0.00060	0.00416	1.017	0.311
	female	49	-0.00017	0.00374		

*=significant at α=0.05

Table 4-75 Student's *t*-test results for ulna shaft shape PCs in modern human males and females with high activity levels – right only.

	Sex	N	Mean	S.D.	t	P
pcurveAMHPC1	male	30	-0.00280	0.00891	-1.691	0.097
	female	22	0.00104	0.00680		
pcurveAMHPC2	male	30	0.00185	0.00678	2.626	0.011*
	female	22	-0.00311	0.00667		
pcurveAMHPC3	male	30	-0.00114	0.00577	-0.163	0.871
	female	22	-0.00091	0.00398		
pcurveAMHPC4	male	30	0.00084	0.00413	1.771	0.083
	female	22	-0.00115	0.00376		

*=significant at α=0.05

Epiphysis shape

EpiAMHPC1 shows significant side differences so only the right side is analysed. Males and females are similar in their radial epiphysis morphology for the whole sample (Table 4-76) and for high activity groups alone (Table 4-77).

Table 4-76 Student's *t*-test results for radius epiphyses PCs in modern human males and females – right only.

	Sex	N	Mean	S.D.	t	P
EpiAMHPC1	male	61	-0.01280	0.01340	0.007	0.994
	female	46	-0.01282	0.01286		
EpiAMHPC2	male	61	-0.00064	0.00961	-0.994	0.322
	female	46	0.00148	0.01243		

* Significant at α=0.05

Table 4-77: Student's *t*-test results for radius epiphyses PCs in modern human males and females with high activity levels – right only.

	Sex	N	Mean	S.D.	t	P
EpiAMHPC1	male	26	-0.01415	0.01310	0.847	0.402
	female	20	-0.01715	0.01015		
EpiAMHPC2	male	26	-0.00130	0.00807	-0.995	0.325
	female	20	0.00141	0.01043		

* Significant at α=0.05

There is bilateral asymmetry in the PCs for the proximal ulna. Therefore, these analyses are performed on the right ulna only. Males have a longer distance between the 80% level of the shaft and the tip of the coronoid process than females (65 males and 49 females) (proxAMHPC2) (Table 4-78). For right ulnae of the high activity groups (30 males and 22 females) there is no difference in proximal ulna shape (Table 4-79).

Table 4-78 Student's *t*-test results for the proximal ulna PCs in modern human males and females – right only.

	Sex	N	Mean	S.D.	t	P
proxAMHPC1	male	65	-0.03654	0.04761	-0.684	0.495
	female	49	-0.02985	0.05661		
proxAMHPC2	male	65	0.00007	0.07346	-2.226	0.028*
	female	49	0.03047	0.07042		
proxAMHPC3	male	65	-0.00449	0.05483	-1.806	0.074
	female	49	0.01340	0.04886		
proxAMHPC4	male	65	0.00790	0.02668	-1.663	0.099
	female	49	0.01769	0.03616		

*=significant at α=0.05

Table 4-79 Student's *t*-test results for the proximal ulna PCs in modern human males and females with high activity levels – right only.

	Sex	N	Mean	S.D.	t	P
proxAMHPC1	male	30	-0.05290	0.04030	-0.047	0.962
	female	22	-0.05228	0.05352		
proxAMHPC2	male	30	0.01240	0.07383	-0.700	0.487
	female	22	0.02739	0.07958		
proxAMHPC3	male	30	0.00746	0.05689	0.537	0.594
	female	22	-0.00047	0.04609		
proxAMHPC4	male	30	0.00099	0.02458	-0.343	0.733
	female	22	0.00395	0.03755		

*=significant at α=0.05

Univariate measurements

Males have significantly longer radii (Max_Length, $p<0.001$ for both all AMH and high activity groups only) (Table 4-80). When all individuals are considered females have a relatively shorter radial neck (NeckLengthRatio), but this sexual dimorphism disappears when only groups with high activity levels are considered (Table 4-81).

Table 4-80: Student's *t*-test results for the univariate measurements of the radius in modern human males and females. Underlined variables show bilateral asymmetry and were analysed for the right side only.

	Sex	N	Mean	S.D.	t	P
Max_ Length	male	90	248.43	16.5	9.572	<0.001*
	female	83	225.3	15.18		
neck-shaft angle °	male	61	33.51	12.11	0.947	0.346
	female	50	31.12	14.48		
PosRadTubML	male	61	14.65	7.64	1.397	0.165
	female	50	12.82	5.78		
DorsalST	male	61	6.68	1.94	1.671	0.098
	female	50	6.08	1.86		
LateralST	male	61	6.09	2.5	0.369	0.713
	female	50	5.93	1.9		
NeckLengthRatio	male	90	11.23	1.6	2.41	0.017*
	female	82	10.69	1.3		
HeadShapeRatio	male	90	107.19	7.83	0.867	0.387
	female	82	106.09	8.85		
midshaftShapeRation	male	90	84	13.05	-0.258	0.797
	female	82	84.57	16.18		

* Significant at α=0.05

Table 4-81 Student's *t*-test results for the univariate measurements of the radius in modern human males and females with high activity levels. Underlined variables show bilateral asymmetry and were analysed for the right side only.

	Sex	N	Mean	S.D.	t	P
Max_ Length	male	39	247.75	16.52	5.057	<0.001*
	female	38	227.18	19.12		
neck-shaft angle °	male	26	31.64	7.74	-0.938	0.353
	female	22	34.63	13.94		
PosRadTubML	male	26	13.97	6.35	0.683	0.498
	female	22	12.75	5.97		
DorsalST	male	26	6.4	2.17	1.437	0.157
	female	22	5.53	1.95		
LateralST	male	26	5.89	2.79	0.483	0.631
	female	22	5.54	2.1		
NeckLengthRatio	male	39	10.63	1.39	0.201	0.841
	female	38	10.57	1.28		
HeadShapeRatio	male	39	107.02	8.85	1.132	0.261
	female	38	104.56	10.17		
midshaftShapeRation	male	39	87.02	14.87	0.272	0.787
	female	38	85.93	19.89		

* Significant at α=0.05

Males have longer ulnae than females (Max_Length, $p<0.001$ for both all AMH and high activity groups only) (Table 4-82). When all individuals are considered, males are rounder at the ulnar midshaft and are more robust at the midshaft and at the 25% level of the shaft than females. These differences disappear when only high activity groups are analysed (Table 4-83).

Table 4-82 Student's *t*-test results for the univariate measurements of the ulna in modern human males and females. Underlined variables show bilateral asymmetry and were analysed for the right side only.

	Sex	N	Mean	S.D.	t	P
Max_ Length	male	101	262.48	18.79	9.364	<0.001*
	female	79	238.23	15.02		
Olecshaftration	male	66	9.37	1.03	2.886	0.005*
	female	49	8.85	0.89		
MidShaftShape	male	101	106.28	22.80	-3.430	0.001*
	female	79	123.07	41.91		
Radial Notch Surface ratio	male	101	31.56	8.25	3.582	<0.001
	female	79	27.43	6.85		
TrochNotchOri	male	66	20.49	6.92	1.476	0.143
	female	49	18.67	6.01		
Olec-orient angle	male	101	23.88	4.99	1.033	0.303
	female	79	23.06	5.68		
CorOleRation	male	66	106.04	1.45	2.807	0.006*
	female	49	105.22	1.66		
brachRatio	male	101	22.84	1.92	0.626	0.532
	female	79	23.03	2.09		
Rel. pron. cr. size	male	66	14.12	4.08	0.888	0.376
	female	49	14.80	4.04		
Robusticity at 50%	male	101	10.81	1.34	3.543	0.001*
	female	79	10.06	1.50		
Robusticity at 25%	male	66	10.73	1.53	3.052	0.003*
	female	49	9.89	1.33		
Robust dist artic	male	101	15.70	1.92	0.802	0.424
	female	79	15.47	1.83		

*=significant at α=0.05

Table 4-83 Student's *t*-test results for the univariate measurements of the ulna in modern human males and females with high activity levels. Underlined variables show bilateral asymmetry and were analysed for the right side only.

	Sex	N	Mean	S.D.	t	P
Max_ Length	male	47	262.15	18.75	5.918	<0.001*
	female	37	238.4	17.61		
Olec-shaftratio	male	30	8.99	0.94	1.595	0.117
	female	22	8.59	0.87		
MidShaftShape	male	47	103.11	24.65	-0.984	0.328
	female	37	109.2	32.11		
Radial Notch Surface ratio	male	47	28.07	7.84	1.202	0.233
	female	37	26.09	7.09		
TrochNotchOri	male	30	19.78	6.49	1.091	0.281
	female	22	17.76	6.71		
Olec-orient angle	male	47	23.22	4.81	-1.617	0.11
	female	37	25.18	6.27		
CorOleRation	male	30	105.58	1.4	1.676	0.1
	female	22	104.92	1.41		
brachRatio	male	47	22.05	1.85	0.232	0.748
	female	37	21.91	2.12		
Size pron.cr. rel. length	male	30	14.74	3.86	0.747	0.458
	female	22	13.92	3.94		
Robusticity at 50%	male	47	10.9	1.4	1.635	0.106
	female	37	10.39	1.45		
Robusticity at 25%	male	30	10.75	1.51	1.516	0.136
	female	22	10.17	1.12		
Robust dist artic	male	47	15.01	1.84	0.021	0.983
	female	37	15	1.89		

*=significant at α=0.05

Summary

There is no sexual dimorphism in curvature of the shaft of the radius or the ulna. Females have shorter and less robust radii than do males. Females also have a more anteroposterior sinusoidal radial shaft shape. Females have a smaller ulna that is more sinusoidal than that of males.

4.3.4.4. Age

Of the whole sample, there were 93 radii from individuals of known age and 97 ulnae.

There is no relationship between age and curvature and epiphyseal shape of the radius (Table 4-84), for the pooled and right-only sample. A negative correlation with mcurveAMHPC2 and lcurveAMHPC3 indicate that younger individuals have an increased medial extension of the

proximal interosseous crest and a medial direction of the distal curve (more medially expanded ulnar notch) and have a more sinusoidal shape compared to older individuals.

Table 4-84 Kendall's Tau b correlations for radius PCs and age (N=93).

		Specimen age
Curvature		
McurAllPC1	r	0.085
	P	0.238
LcurAllPC1	r	-0.029
	P	0.690
Shaft shape		
McurAllPC2	r	0.232**
	P	0.001
McurAllPC3	r	-0.077
	P	0.283
LcurAllPC2	r	-0.026
	P	0.717
LcurAllPC3	r	0.266**
	P	<0.001
Epiphyses shape		
EpiAllPC1	r	0.121
	P	0.095
EpiAllPC2	r	0.269**
	P	<0.001

* = Correlation is significant at the 0.05 level (2-tailed).
** = Correlation is significant at the 0.01 level (2-tailed).

There is no relationship between age and the shape of the shaft or the proximal ulna (Table 4-85). There is a weak correlation (r=0.182, P=0.041) between proxAMHPC1 and age for the right ulnae. Older individuals have a more medially projected proximal ulna with a more medial facing trochlear notch.

Table 4-85 Kendall's Tau b correlations for ulna PCs (N=97).

shaft shape			*Proximal ulna*		
pcurveAMHPC1	r	0.094	proxAMHPC1	r	0.080
	P	0.181		P	0.257
pcurveAMHPC2	r	-0.003	proxAMHPC2	r	-0.094
	P	0.965		P	0.181
pcurveAMHPC3	r	0.012	proxAMHPC3	r	-0.020
	P	0.869		P	0.781
pcurveAMHPC4	r	0.001	proxAMHPC4	r	0.105
	P	0.993		P	0.135

* = Correlation is significant at the 0.05 level (2-tailed).
** = Correlation is significant at the 0.01 level (2-tailed).

Univariate measurements

Age is positively correlated with head-shaft size ratio (Table 4-86). Older individuals have larger heads relative to shaft length compared to younger individuals. For the ulna the position of the brachial tuberosity may shift more distally but this correlation is absent in the right only sample (r=0.163; P=0.068). There is a weak positive correlation between distal articulation robusticity and age (Table 4-87).

Table 4-86 Kendall's Tau b correlations for the univariate measurements on the radius and age (N=97).

		Specimen age
Max_ Length	r	-0.009
	P	0.902
neck-shaft angle °	r	0.075
	P	0.296
PosRadTubML	r	0.193**
	P	0.007
DorsalST	r	0.055
	P	0.446
LateralST	r	-0.013
	P	0.860
NeckLengthRatio	r	-0.092
	P	0.201
HeadShapeRatio	r	0.190**
	P	0.009
midshaftShapeRatio	r	-0.087
	P	0.226
HeadShaftSizeRatio	r	0.175*
	P	0.016
Robusticity		
Midshaftrobusticity	r	-0.016
	P	0.829
Headrobusticity	r	0.174*
	P	0.016
distArtShaftSizeRatio	r	0.113
	P	0.114

* = Correlation is significant at the 0.05 level (2-tailed).
** = Correlation is significant at the 0.01 level (2-tailed).

Table 4-87 Kendall's Tau b correlations for univariate measurements on the ulna (N=97).

			Proximal ulna			*robusticity*		
Max_ Length	r	-0.001	Olec-orient angle	r	0.130	Robusticity at 50%	r	-0.023
	P	0.985		P	0.065		P	0.745
Olec-shaftratio	r	0.171*	CorOleRatio	r	0.042	Robusticity at 25%	r	0.054
	P	0.015		P	0.553		P	0.446
MidShaftShape	r	-0.010	brachRatio	r	0.231**	Robust dist artic	r	0.189**
	P	0.886		P	0.001		P	0.007
Rad. Notch Surf. ratio	r	0.047	Rel. pron.cr. size	r	0.036			
	P	0.500		P	0.608			
TrochNotchOri	r	0.076						
	P	0.280						

* = Correlation is significant at the 0.05 level (2-tailed).

** = Correlation is significant at the 0.01 level (2-tailed).

When age categories were used in order test for the effect of age on radial curvature the ANOVA showed no significant effect (Table 4-88). For the ulna, adults have the shortest distance between the 80% level of the shaft and the tip of the coronoid process (proxAMHPC2.) (Table 4-89, Figure 4-56).

Table 4-88 ANOVA results for age categories and radius curvature PCs.

d.f.=2	F	Sig.
mcurveAMHPC1	0.191886894	0.825
lcurvAMHPC1	0.516318658	0.597

*=significant at α=0.05

Table 4-89 ANOVA results for age categories and ulna shape PCs.

d.f.=2	F	Sig.
pcurveAMHPC1	0.575	0.563
pcurveAMHPC2	1.490	0.227
pcurveAMHPC3	0.637	0.530
pcurveAMHPC4	0.194	0.824
proxAMHPC1	0.403	0.669
proxAMHPC2	3.505	0.031*
proxAMHPC3	0.425	0.654
proxAMHPC4	2.412	0.091

*=significant at α=0.05

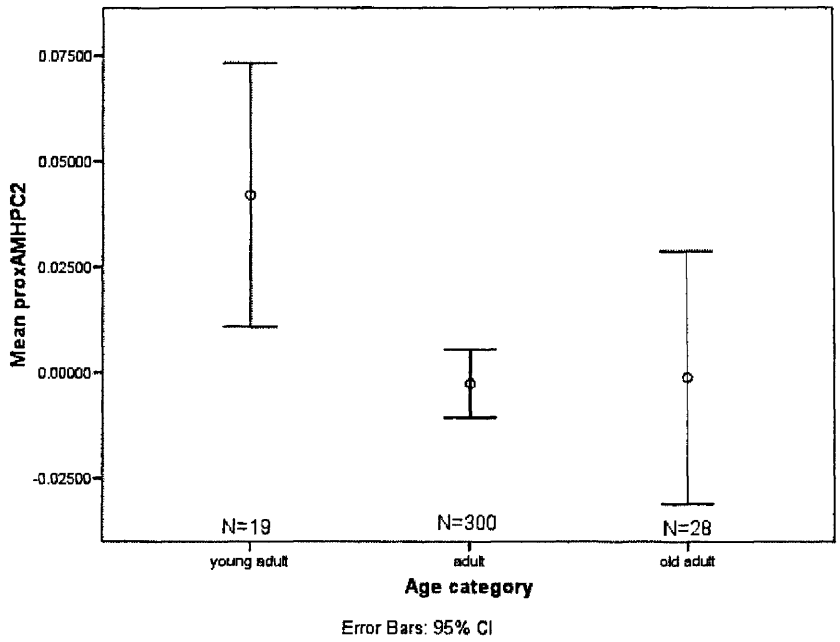

Figure 4-56 ProxAMHPC2 for modern humans, by age strategy. Mean and 95% confidence interval (whiskers).

High values have a greater distance between the tip of the coronoid process and the 80% level of the shaft.

Summary

There is no relationship between age and curvature, nor are there curvature differences when the age categories are used. Younger individuals have an increased medial extension of the proximal interosseous crest and a medial direction of the distal curve (more medially expanded ulnar notch) and have a more sinusoidal shape compared to older individuals. Older individuals have larger heads relative to shaft length compared to younger individuals.

4.3.4.5. Activity levels

The following analyses use the same categories used in the analyses of the femur. The distribution of the populations (Appendix 8) for the first PCs of the radius and ulna are presented in Figure 4-57 to Figure 4-59).

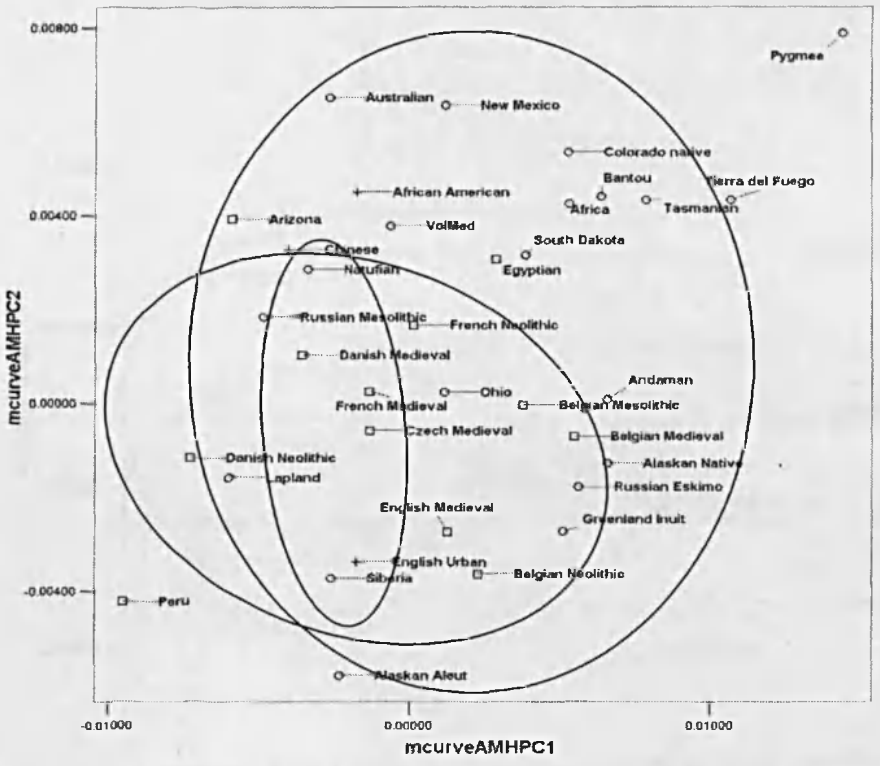

Figure 4-57 Distribution of the activity level categories in the space of PC1 (degree of curvature) and PC2 (medial expansion of the interosseous crest) of the medial curve of the radius for all modern humans. Circles: high activity, squares: moderate activity, crosses: low activity.

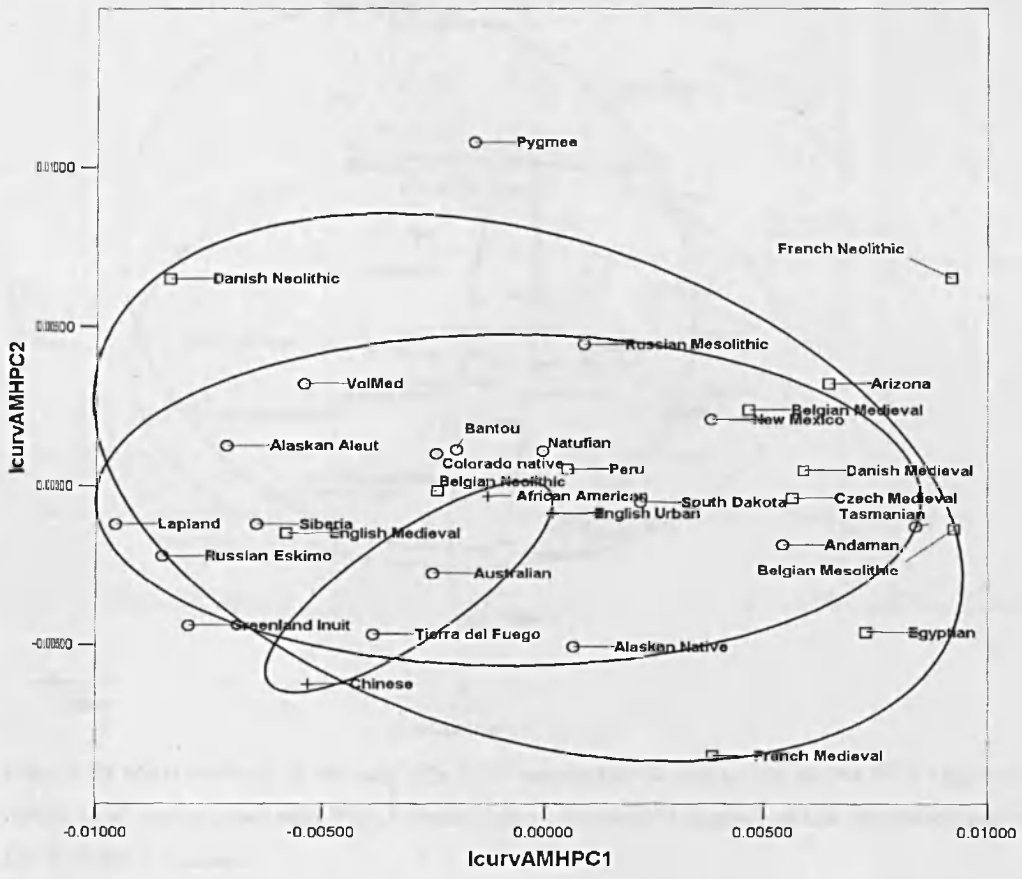

Figure 4-58 Distribution of the activity level categories in the space of PC1 (degree of curvature) and PC2 (apex of curvature) of the lateral curve of the radius for all modern humans.

Circles: high activity, squares: moderate activity, crosses: low activity.

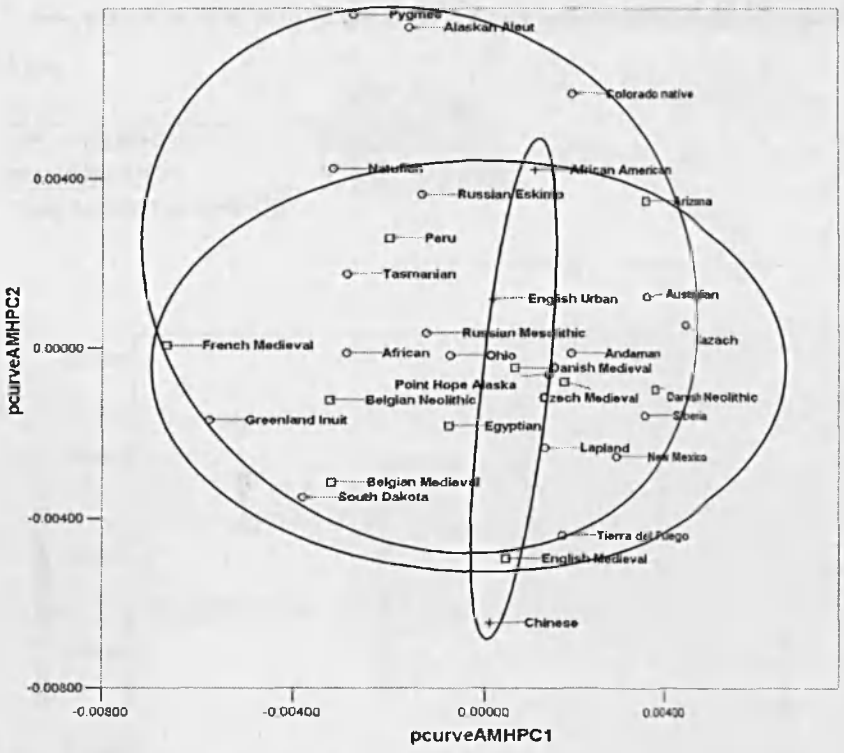

Figure 4-59 Distribution of the activity level categories in the space of the PC1 (degree of mediolateral curvature) and PC2 (mediolateral sinusoidal shape) of the posterior curve of the ulna for all modern humans.

Circles: high activity, squares: moderate activity, crosses: low activity.

Curvature

There are no differences in the curvature of the radius across activity levels(Table 4-90). There are differences between high activity subsistence strategies for both curvature PCs, however (Table 4-91). The horticulturalists are the least curved and significantly different in lateral curvature from equestrian foragers and pastoralists (lcurveAMHPC1) (Appendix 23,Figure 4-60). The post-hoc comparisons show no significant pairwise differences for mcurveAMHPC1.

Table 4-90 ANOVA results for activity levels and radius curvature PCs.

d.f.=2	F	Sig.
mcurveAMHPC1	2.936920496	0.054
lcurvAMHPC1	2.417027448	0.091

*=significant at α=0.05

Table 4-91 ANOVA results for high activity subsistence subsistence strategies and radius curvature PCs.

d.f.=4	F	Sig.
mcurveAMHPC1	2.612	0.037*
lcurvAMHPC1	4.566	0.002*

*=significant at α=0.05

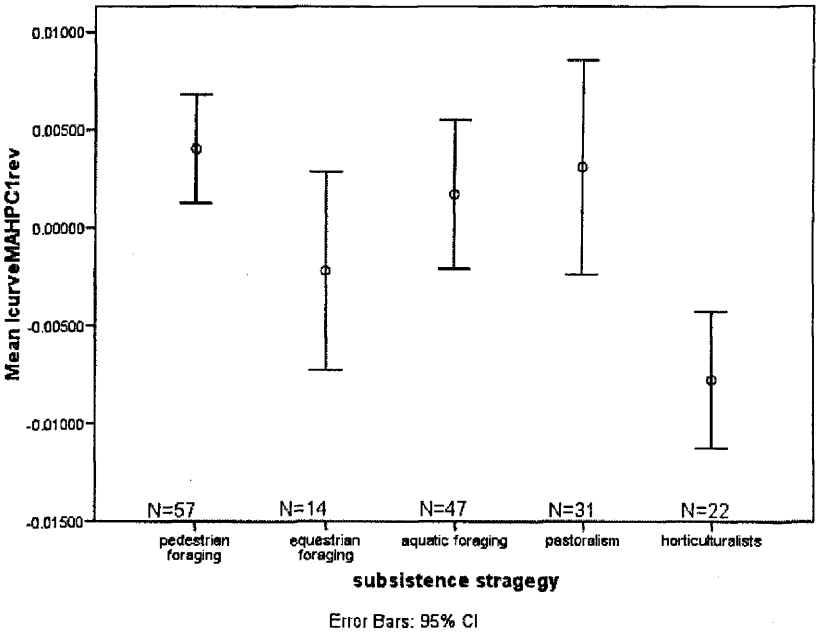

Figure 4-60 Lateral curvature of the radius for modern humans, by subsistence strategy.
The scale of lcurveAMHPC1 is reversed so that the higher values indicate a higher degree of curvature. Mean and 95% confidence interval (whiskers).

Other shaft shape PCs

The different activity level groups are significantly different in radial shaft shape in one out of four PCs (lcurveAMHPC3) (Table 4-92). Post-hoc tests of the lcurveAMHPC3 show that high activity groups have the straightest shaft compared to the more sinusoidal shaft in moderate and low activity groups (Appendix 24 and Figure 4-61).

Table 4-92 ANOVA results for activity levels and radius shaft shape PCs.

d.f.=2	F	Sig.
mcurveAMHPC2	1.181	0.308
mcurveAMHPC3	1.402	0.247
lcurvAMHPC2	2.217	0.110
lcurvAMHPC3	13.799	0.000*

*=significant at α=0.05

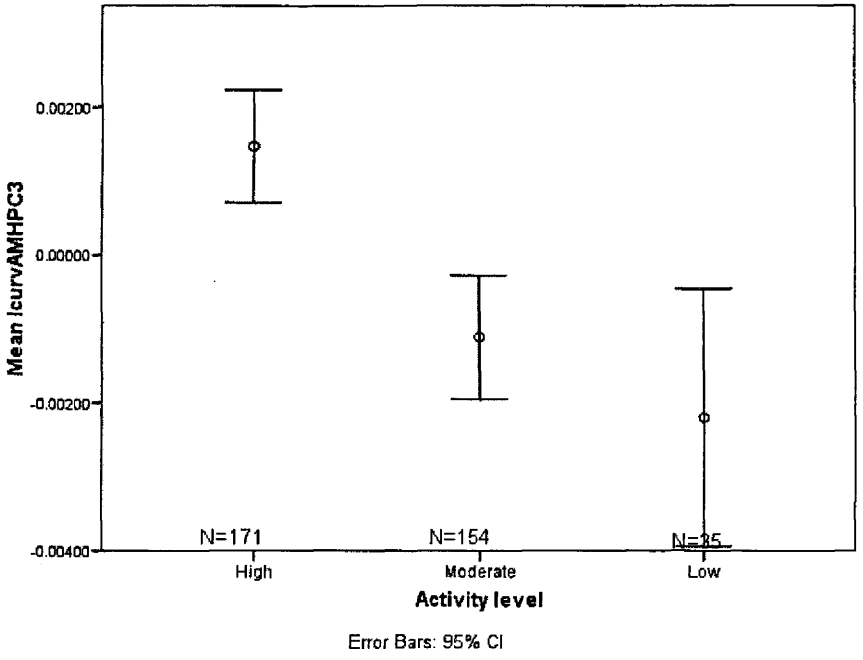

Figure 4-61 LcurvAMHPC3 (high values have the least sinusoidal shaft) of the radius for modern humans, by high activity subsistence strategy. Mean and 95% confidence interval (whiskers).

For two out of four other radial shaft shape PCs the high activity subsistence categories are significantly different (Table 4-93). Compared to pedestrian foragers, aquatic foragers have an increased medial extension of the proximal interosseous crest and a medial direction of the distal curve (more medially expanded ulnar notch) (mcurveAMHPC2) (Figure 4-62). Pastoralists have the most sinusoidal shaft compared to other subsistence categories (lcurveAMHPC3) (Appendix 25) (Figure 4-63).

For the ulna, there are no significant differences in shaft shape between the different activity groups or subsistence patterns (Table 4-94; Table 4-95).

Table 4-93 ANOVA results for subsistence strategies with high activity levels and radius shaft shape PCs.

d.f.=4	F	Sig.
mcurveAMHPC2	2.458	0.048*
mcurveAMHPC3	1.555	0.189
lcurvAMHPC2	1.795	0.132
lcurvAMHPC3	3.499	0.009*

*=significant at α=0.05

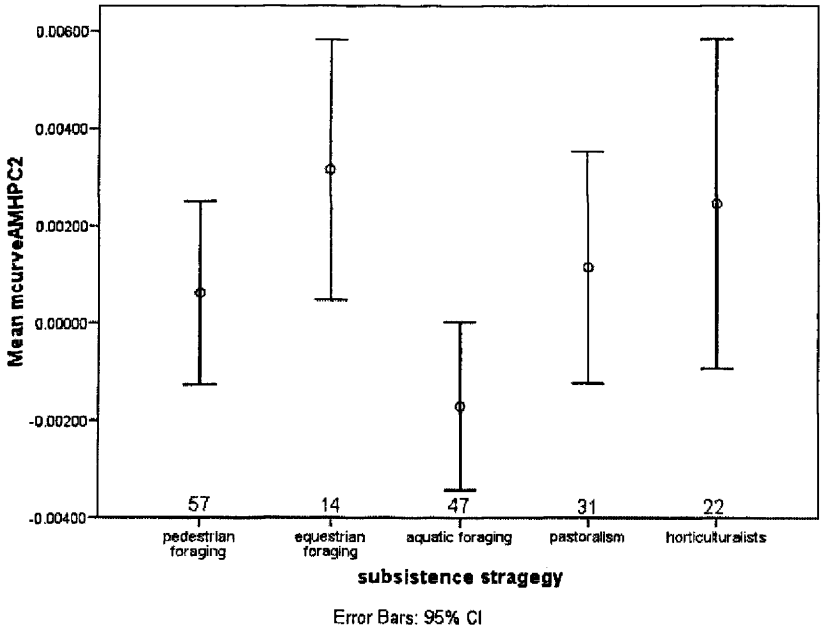

Figure 4-62 McurvePC2 of the radius for modern humans, by high activity subsistence strategy. Mean and 95% confidence interval (whiskers).

Low values have increased medial extension of the proximal interosseous crest.

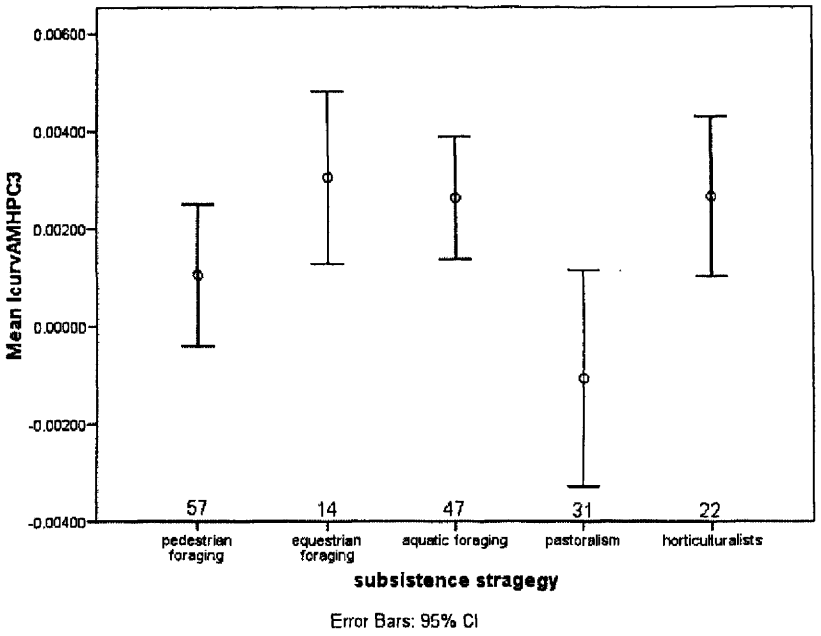

Figure 4-63 LcurvePC3 (low values are more sinusoidal) of the radius for modern humans, by high activity subsistence strategy. Mean and 95% confidence interval (whiskers).

Table 4-94 ANOVA results for activity levels and ulna shaft shape PCs.

d.f.=2	F	Sig.
pcurveAMHPC1	0.048	0.953
pcurveAMHPC2	1.339	0.264
pcurveAMHPC3	2.793	0.063
pcurveAMHPC4	0.602	0.548

*=significant at α=0.05

Table 4-95 ANOVA results for subsistence strategies with high activity levels and ulna shaft shape PCs.

d.f.=4	F	Sig.
pcurveAMHPC1	1.035	0.391
pcurveAMHPC2	1.398	0.237
pcurveAMHPC3	0.606	0.659
pcurveAMHPC4	1.153	0.334

*=significant at α=0.05

Epiphysis shape

Although there is a significant difference between the activity levels for radial epiphysis shape, the post-hoc procedures did not find differences between the three activity levels (Table 4-96 and Appendix 26).

For the high activity subsistence groups there is a significant difference between pastoralists and aquatic and equestrian foragers for EpiAMHPC2 (Table 4-97). Pastoralists have a more posteriorly oriented head than horticulturalists and aquatic and equestrian foragers (Figure 4-64 and Appendix 27).

Table 4-96 ANOVA results for activity levels and radius epiphyses PCs.

d.f.=2	F	Sig.
EpiAMHPC1	3.163	0.044*
EpiAMHPC2	0.213	0.809

*=significant at α=0.05

Table 4-97 ANOVA results for subsistence groups with high activity levels and radius epiphyses PCs.

d.f.=4	F	Sig.
EpiAMHPC1	6.008	<0.001*
EpiAMHPC2	1.024	0.397

*=significant at α=0.05

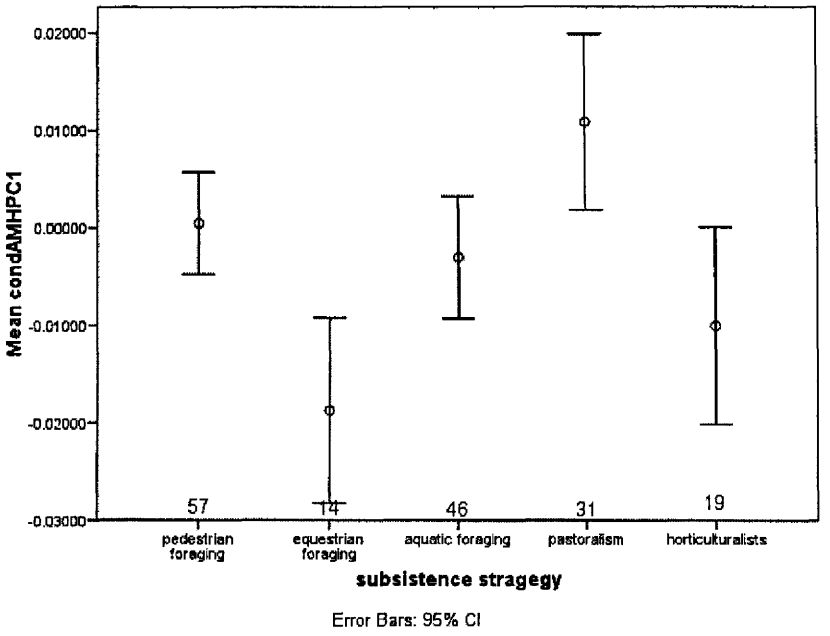

Figure 4-64 EpiAMHPC2 for modern humans, by subsistence strategy. The scale of lcurveAMHPC1 is reversed to ease interpretations (have a more posteriorly oriented head). Mean and 95% confidence interval (whiskers).

High values have a more posteriorly oriented head.

The activity levels are significantly different for proxAMHPC4 (Table 4-98). Populations with low activity levels have a deeper trochlear notch with a higher radial notch and a lower olecranon process compared to the high and moderate activity groups (Appendix 27, Figure 4-65).

Table 4-98 ANOVA results for activity levels and the proximal ulna PCs.

d.f.=2	F	Sig.
proxAMHPC1	0.981	0.376
proxAMHPC2	0.716	0.490
proxAMHPC3	1.370	0.256
proxAMHPC4	8.148	<0.001*

*=significant at α=0.05

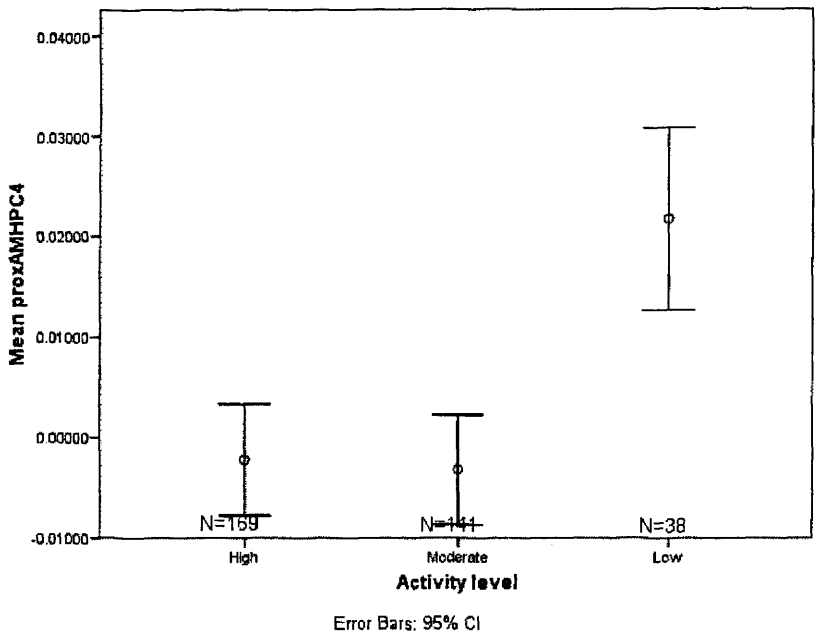

Figure 4-65 ProxAMHPC4 for modern humans, by activity level. Mean and 95% confidence interval (whiskers).

High values have a deeper trochlear notch with a higher radial notch and a lower olecranon process.

The high activity subsistence groups are different for proxAMHPC2 and proxAMHPC4 (Table 4-99). Equestrian and aquatic foragers have a greater distance between the 80% shaft level and the tip of the coronoid process compared to pastoralists who have the shortest distance. Also, aquatic foragers have a shallower trochlear notch with a lower radial notch and a higher olecranon process compared to pastoralists and pedestrian and equestrian foragers (Figure 4-66 and Figure 4-67) (Appendix 29).

Table 4-99 ANOVA results for subsistence strategy and the proximal ulna PCs.

d.f.=4	F	Sig.
proxAMHPC1	1.025	0.396
proxAMHPC2	3.600	0.008*
proxAMHPC3	2.263	0.065
proxAMHPC4	5.188	0.001*

*=significant at α=0.05

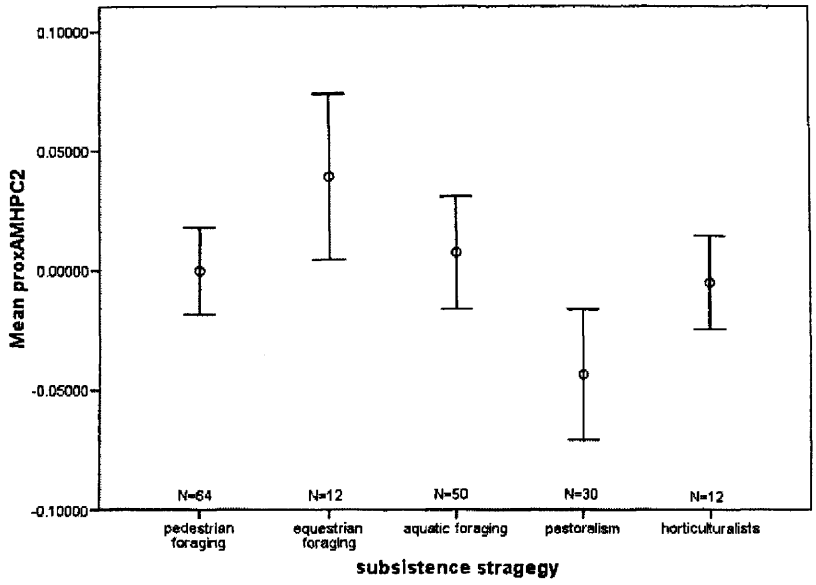

Figure 4-66 ProxAMHPC2 for modern humans, by subsistence strategy. Mean and 95% confidence interval (whiskers).

High values greater distance between the tip of the coronoid process and the 80% level of the shaft.

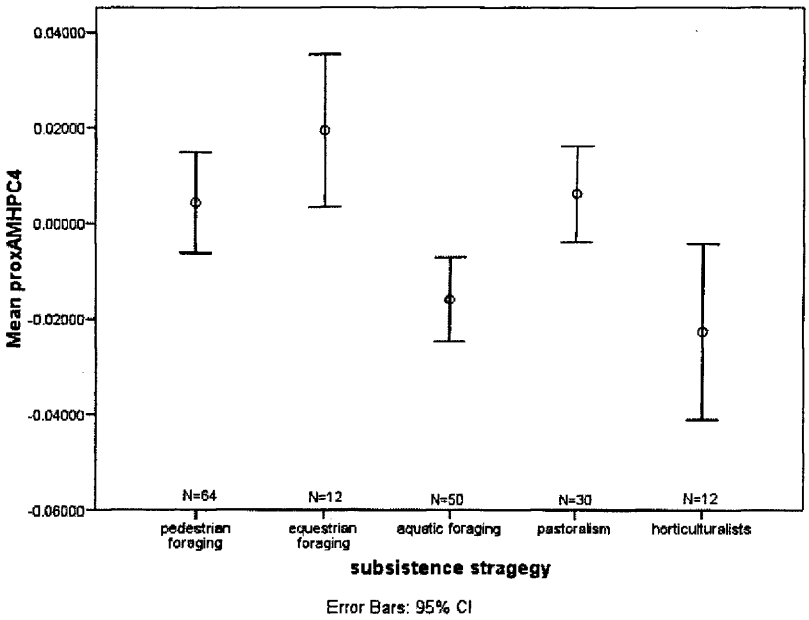

Figure 4-67 ProxAMHPC4 for modern humans, by subsistence strategy. Mean and 95% confidence interval (whiskers).

High values have a deeper trochlear notch with a higher radial notch and a lower olecranon process.

Univariate measurements

The activity groups are different for radial head robusticity (Table 4-100; Appendix 30; Figure 4-68). The high activity subsistence strategies are significantly different in robusticity at all three levels of the radial shaft (head, midshaft and distal articulation) (Table 4-101). Pastoralists are the most robust overall, whereas horticulturalists and aquatic foragers have the least robust radii (Appendix 31 and Figure 4-69 - Figure 4-71).

Table 4-100 ANOVA results for activity level and radius robusticity.

d.f.=2	F	Sig.
Midshaftrobusticity	2.461	0.087
Headrobusticity	10.563	<0.001*
distArtShaftSizeRatio	1.979	0.140

*=significant at α=0.05

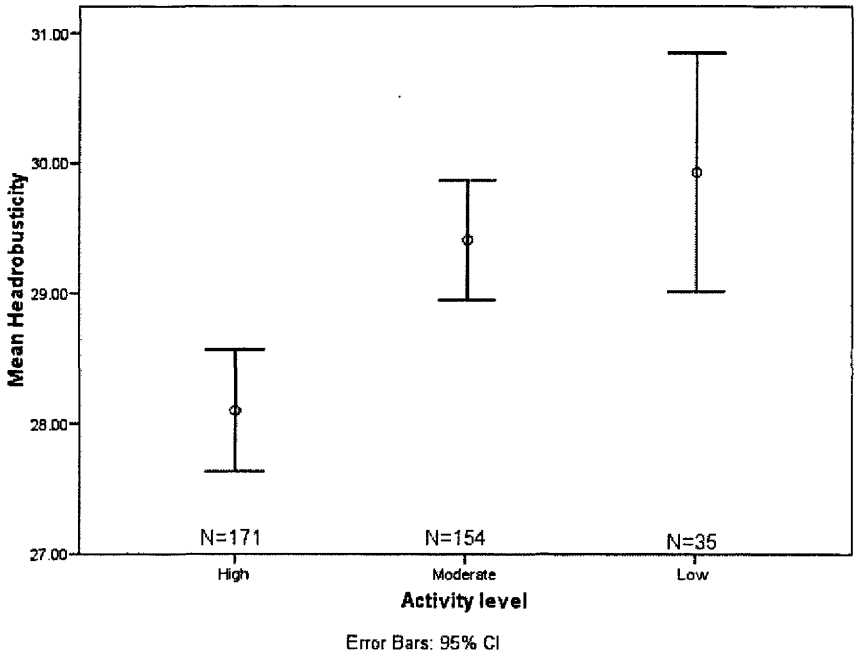

Figure 4-68 Head robusticity for modern humans, by activity level. Mean and 95% confidence interval (whiskers).

Table 4-101 ANOVA results for subsistence strategy and radius robusticity.

d.f.=4	F	Sig.
Midshaftrobusticity	3.869	0.005*
Headrobusticity	5.260	0.001*
distArtShaftSizeRatio	5.186	0.001*

*=significant at α=0.05

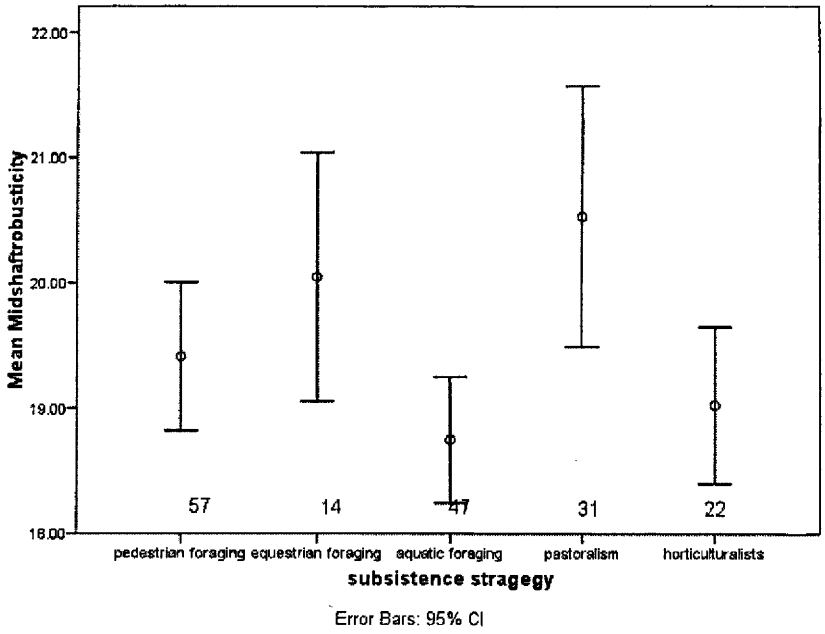

Figure 4-69 Midshaft robusticity for modern humans, by subsistence strategy. Mean and 95% confidence interval (whiskers).

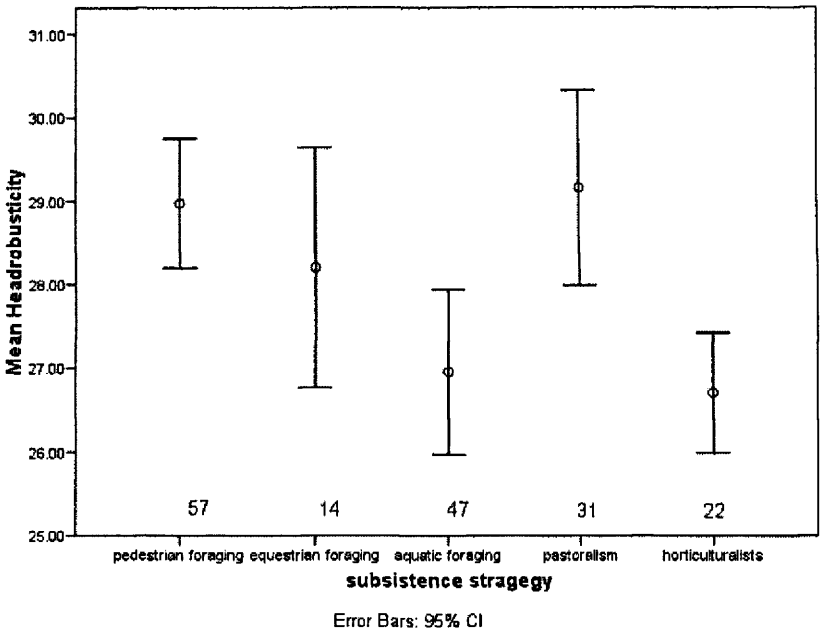

Figure 4-70 Head robusticity for modern humans, by subsistence strategy. Mean and 95% confidence interval (whiskers).

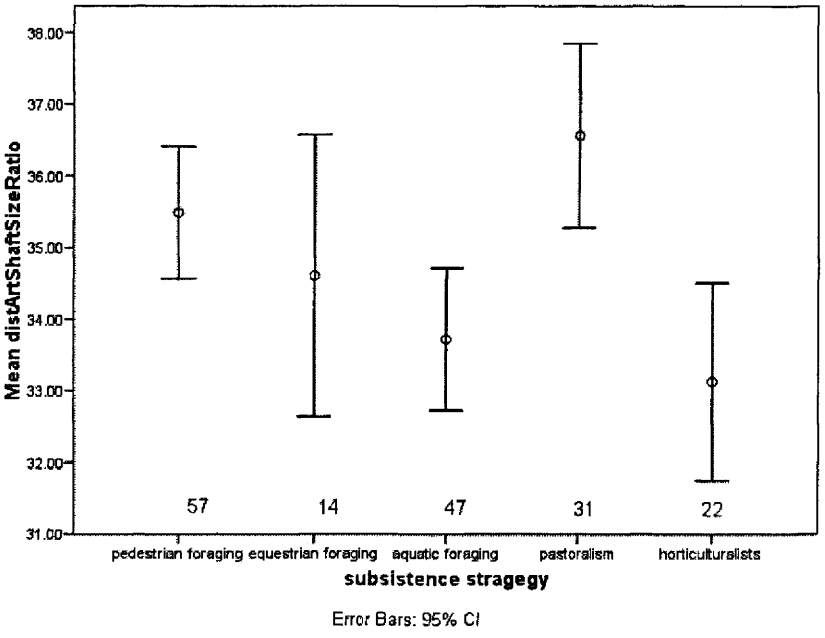

Figure 4-71 Relative distal articulation size for modern humans, by subsistence strategy. Mean and 95% confidence interval (whiskers).

There is a significant difference for the activity groups for a series of univariate measurments of the radius. Low activity groups have a smaller neck-shaft angle and a more medially placed radial tuberosity (Table 4-102; Figure 4-72 and Figure 4-73). High activity groups have a shorter neck than both moderate and low activity groups and less dorsal subtense than moderate activity groups (Appendix 31 and Figure 4-74 and Figure 4-75). The differences for two univariate measurements affected by bilateral asymmetry disappear when only the right side is considered (Neck-shaft angle and position and radial tuberosity) (Appendix 33; Table 4-103).

Table 4-102 ANOVA results for activity level and univariate measurements on the radius.

d.f.=2	F	Sig.
Max_ Length	1.652	0.193
neck-shaft angle °	7.426	0.001*
PosRadTubML	4.402	0.013*
DorsalST	3.493	0.031*
LateralST	1.271	0.282
NeckLengthRatio	14.594	<0.001*
HeadShapeRatio	1.064	0.346
midshaftShapeRation	1.320	0.268

*=significant at α=0.05

Table 4-103 ANOVA results for activity level and univariate measurements on the radius – right only.

d.f.=2	F	Sig.
Max_ Length	0.088	0.916
neck-shaft angle °	1.224	0.296
PosRadTubML	1.240	0.291
DorsalST	5.140	0.007*
LateralST	1.836	0.162
NeckLengthRatio	10.080	<0.001*
HeadShapeRatio	1.198	0.304
midshaftShapeRatio	1.390	0.251

*=significant at α=0.05

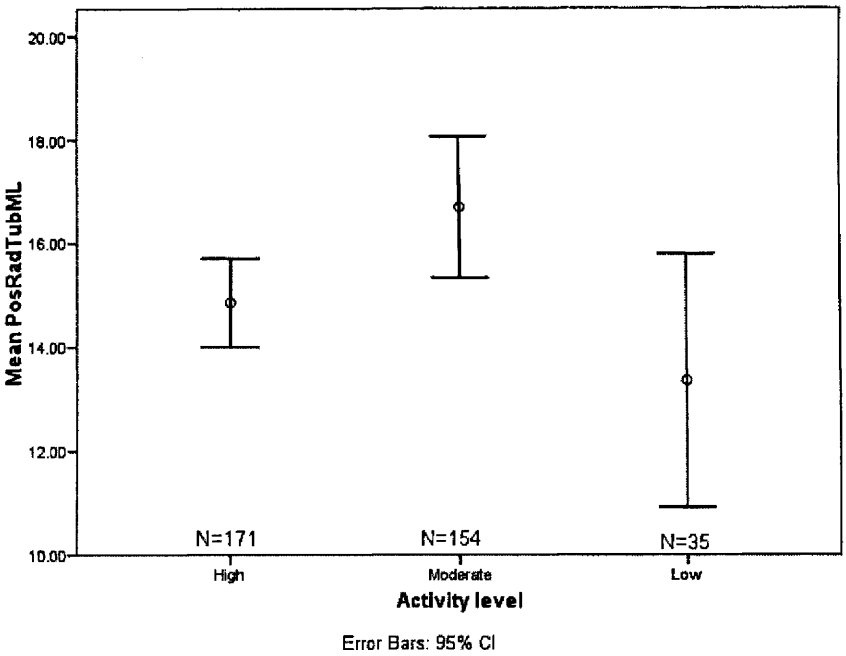

Figure 4-72 Position of the radial tuberosity for modern humans, by activity level. Lower values are more medially placed. Mean and 95% confidence interval (whiskers).

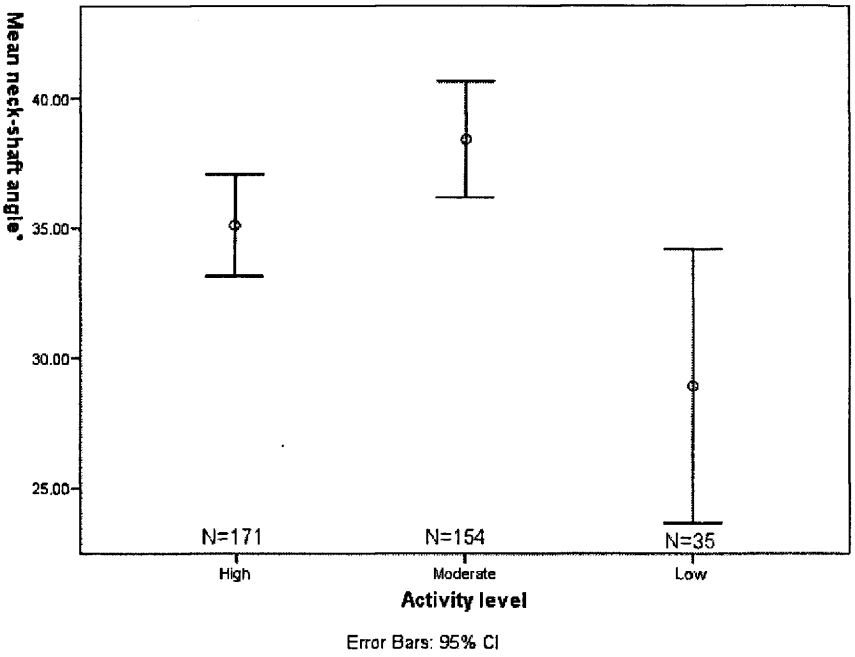

Figure 4-73 Neck-shaft angle for modern humans, by activity level. Mean and 95% confidence interval (whiskers).

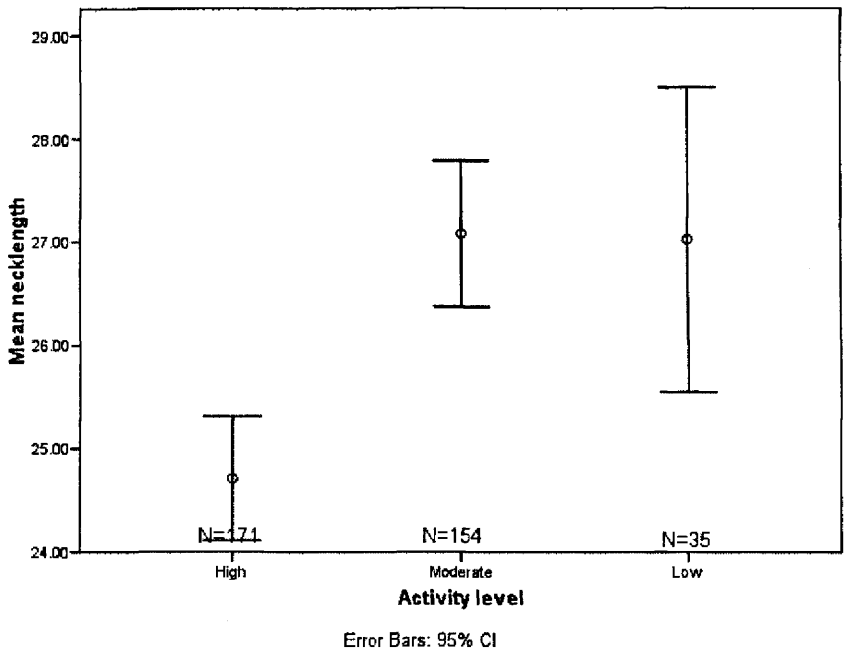

Figure 4-74 Relative radial neck length for modern humans, by activity level. Mean and 95% confidence interval (whiskers).

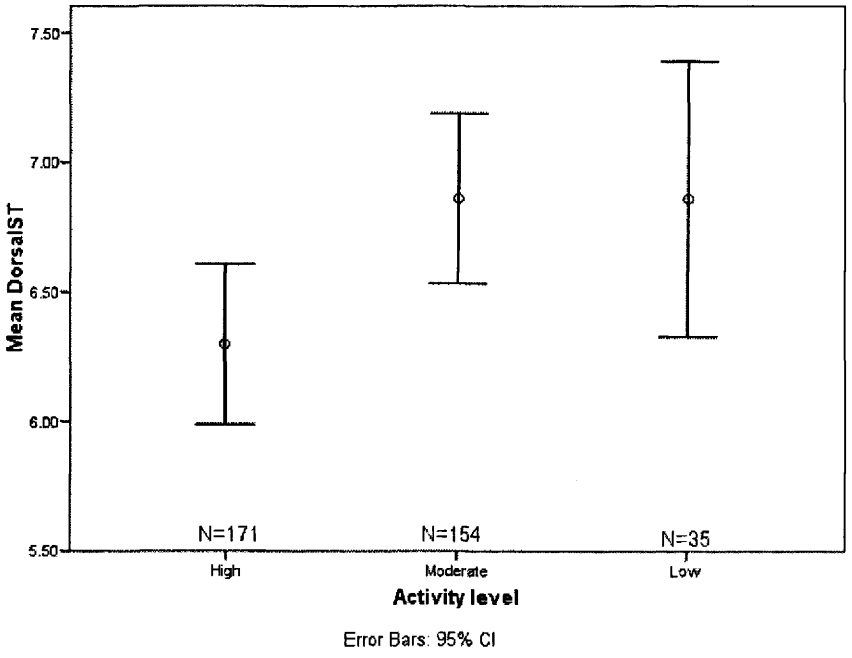

Figure 4-75 Dorsal subtense for modern humans, by activity level. Mean and 95% confidence interval (whiskers).

Within the high activity groups (Table 4-104; Figure 4-76 - Figure 4-81) the aquatic foragers have significantly shorter radii with a high neck-shaft angle (Figure 4-76). Equestrian foragers have the lowest neck-shaft angle (Figure 4-77). Pastoralists have the lowest midshaft shape ratio, indicating a more developed interosseous crest on the radius compared to pedestrian foragers, horticulturalists and aquatic foragers who have higher midshaft shape ratios (Appendix 34; Figure 4-81).

Table 4-104 ANOVA results for subsistence strategy and univariate measurements on the radius.

d.f.=4	F	Sig.
Max_ Length	8.039	<0.001*
neck-shaft angle °	12.630	<0.001*
PosRadTubML	2.626	0.036*
DorsalST	2.647	0.035*
LateralST	2.246	0.066
NeckLengthRatio	4.062	0.004*
HeadShapeRatio	0.429	0.787
midshaftShapeRatio	6.885	<0.001*

*=significant at α=0.05

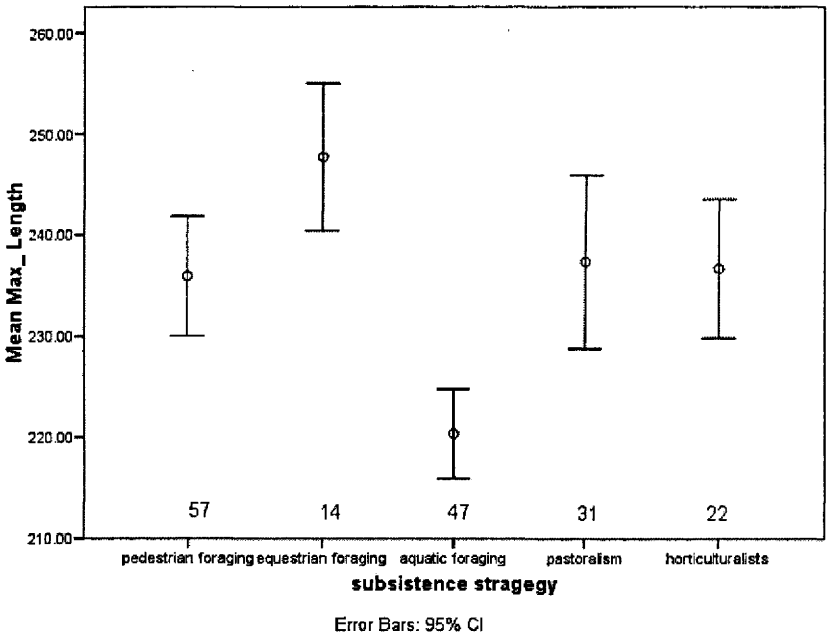

Figure 4-76 Maximum length for modern humans, by subsistence strategy. Mean and 95% confidence interval (whiskers).

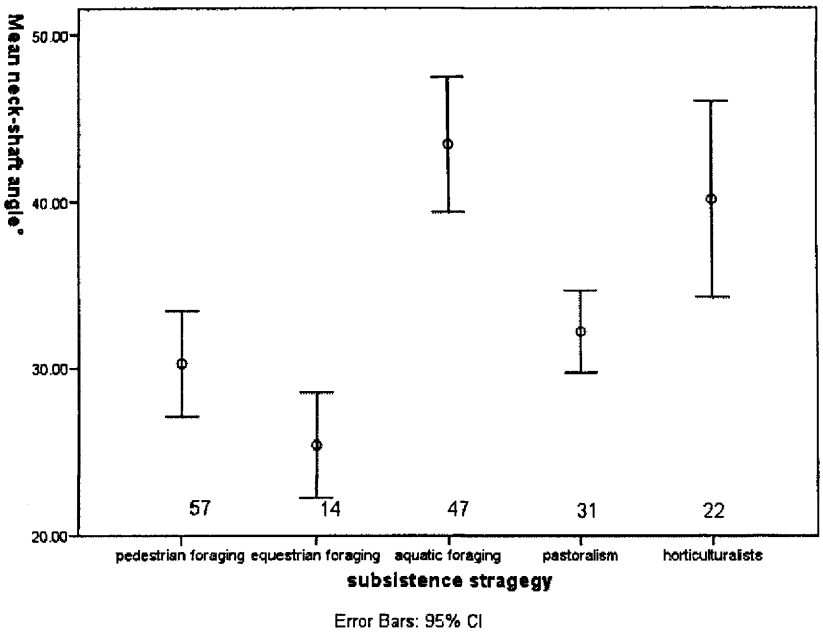

Figure 4-77 Neck-shaft angle for modern humans, by subsistence strategy. Mean and 95% confidence interval (whiskers).

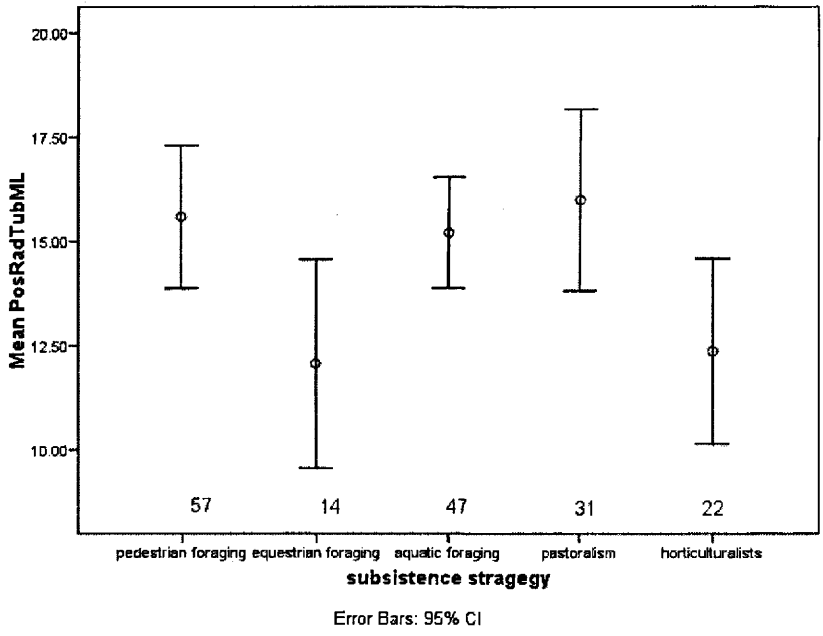

Figure 4-78 Position of the radial tuberosity for modern humans, by subsistence strategy. Lower values are more medially placed. Mean and 95% confidence interval (whiskers).

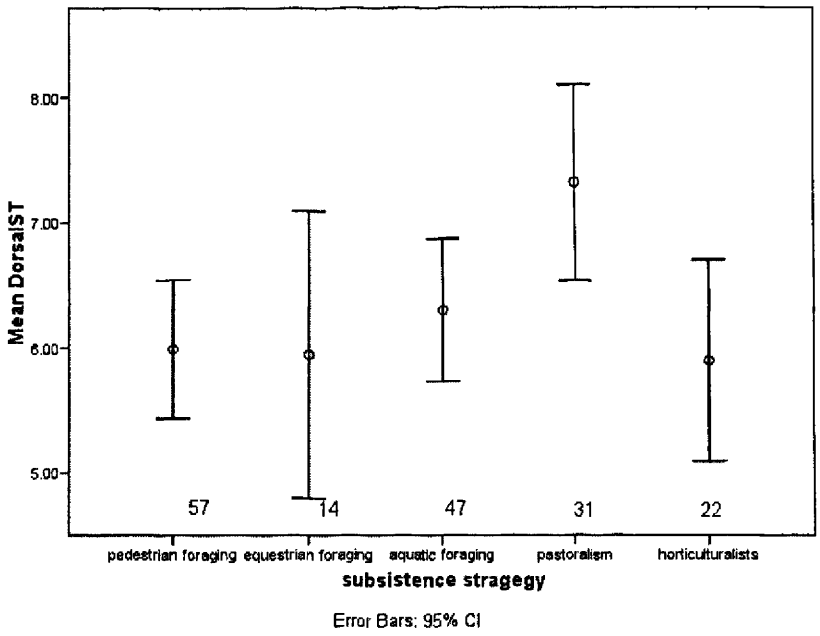

Figure 4-79 Dorsal subtense for modern humans, by subsistence strategy. Mean and 95% confidence interval (whiskers).

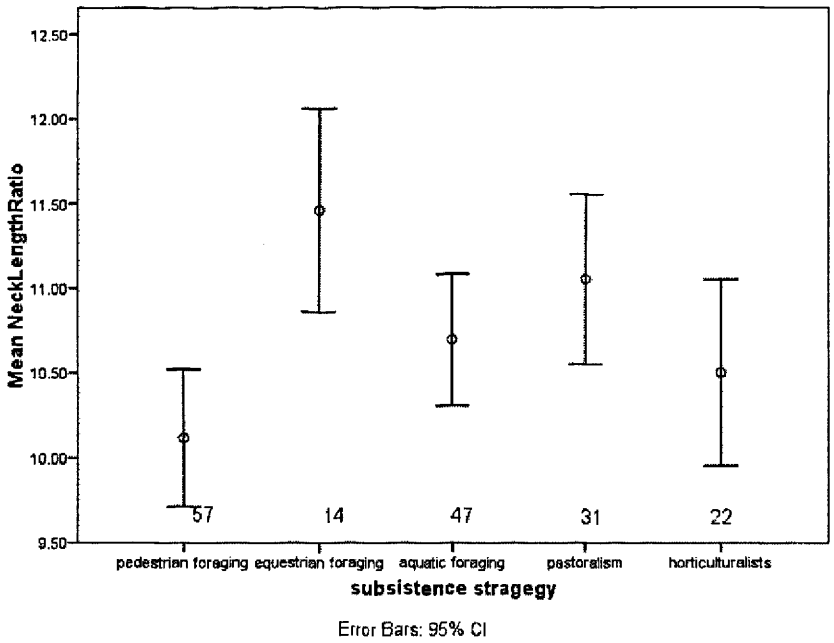

Figure 4-80 Neck length ratio for modern humans, by subsistence strategy. Mean and 95% confidence interval (whiskers).

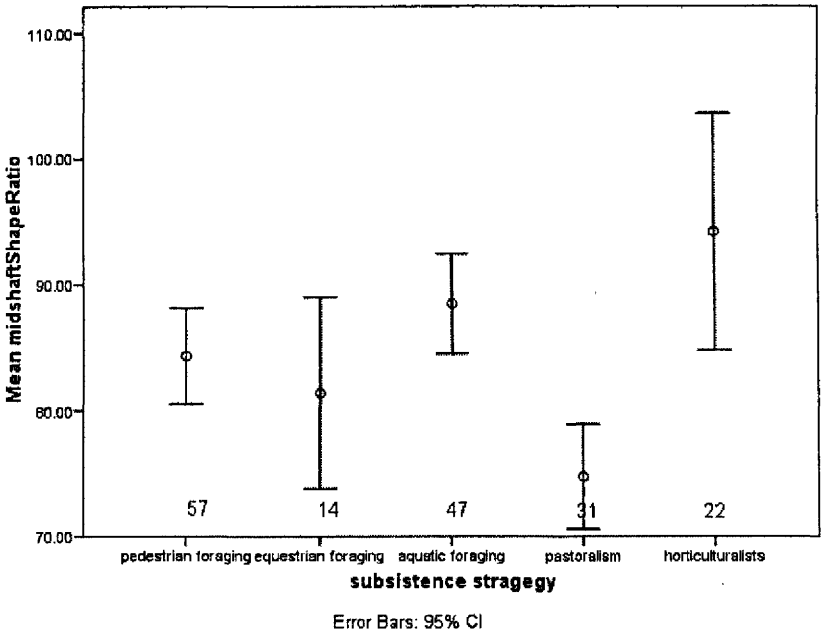

Figure 4-81 Midshaft shape ratio for modern humans, by subsistence strategy. Mean and 95% confidence interval (whiskers).

The activity groups are significantly different for most univariate measurements of the ulna (Table 4-105). High activity groups have shorter ulnae, smaller radial notches, a smaller coronoid-olecranon size ratio and are more robust than moderate activity groups (Appendix 35 and Figure 4-82 - Figure 4-90). Low activity groups are more robust at the 25% level of the shaft, have a lower brachial tuberosity and a higher midshaft shape ratio than do high and moderate activity groups (Figure 4-88 and Figure 4-83).

Table 4-105 ANOVA results for activity levels and univariate measurements on the ulna.

d.f.=2	F	Sig.
Max_ Length	3.052	0.049*
Olec-shaftratio	2.884	0.057
MidShaftShape	5.442	0.005*
Rad. Notch Surf. ratio	6.115	0.002*
TrochNotchOri	5.749	0.004*
Olec-orient angle	3.219	0.041*
CorOleRatio	4.763	0.009*
brachRatio	7.265	0.001*
Size pron.cr. rel. length	1.490	0.227
Robusticity at 50%	6.382	0.002*
Robusticity at 25%	5.571	0.004*
Robust dist artic	1.624	0.199

*=significant at α=0.05

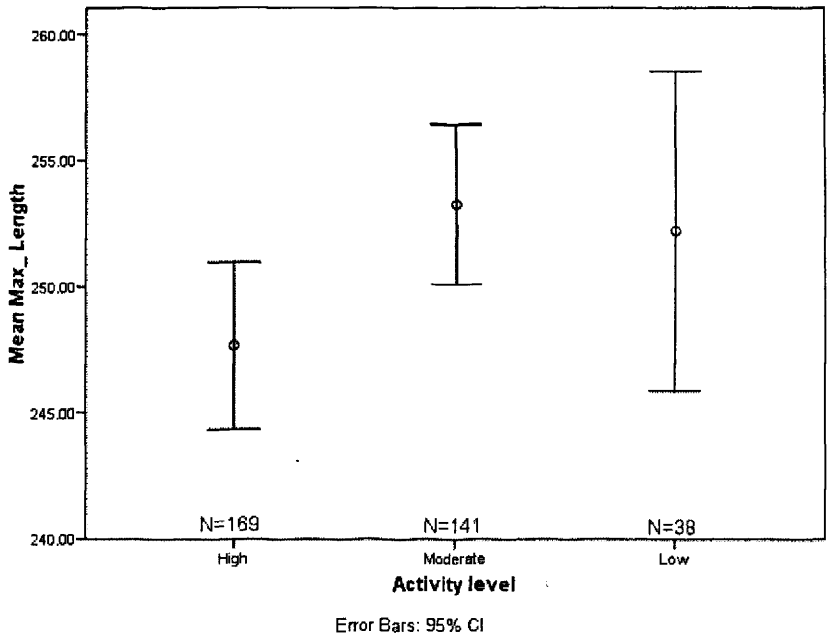

Figure 4-82 Maximum length for modern humans, by activity level.

Mean and 95% confidence interval (whiskers).

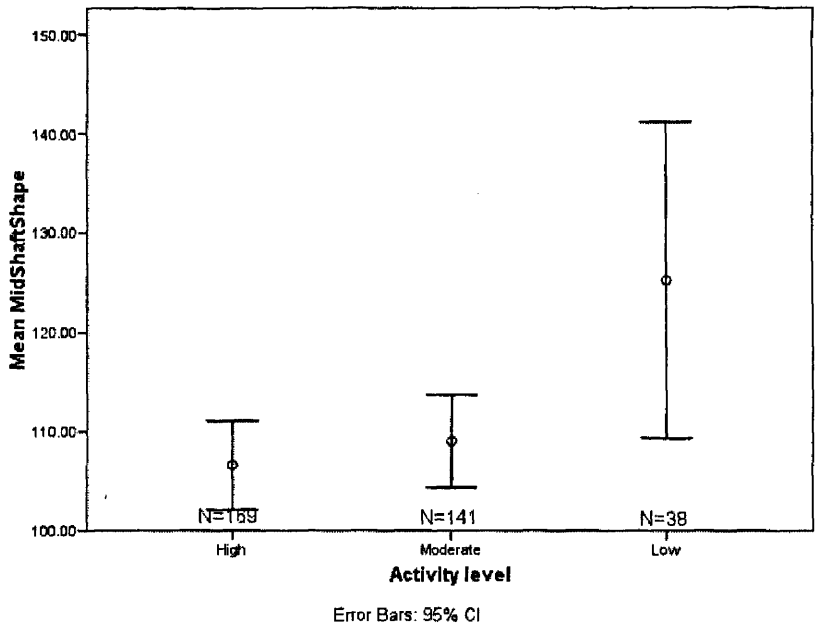

Figure 4-83 Midshaft shape for modern humans, by activity level.

Mean and 95% confidence interval (whiskers).

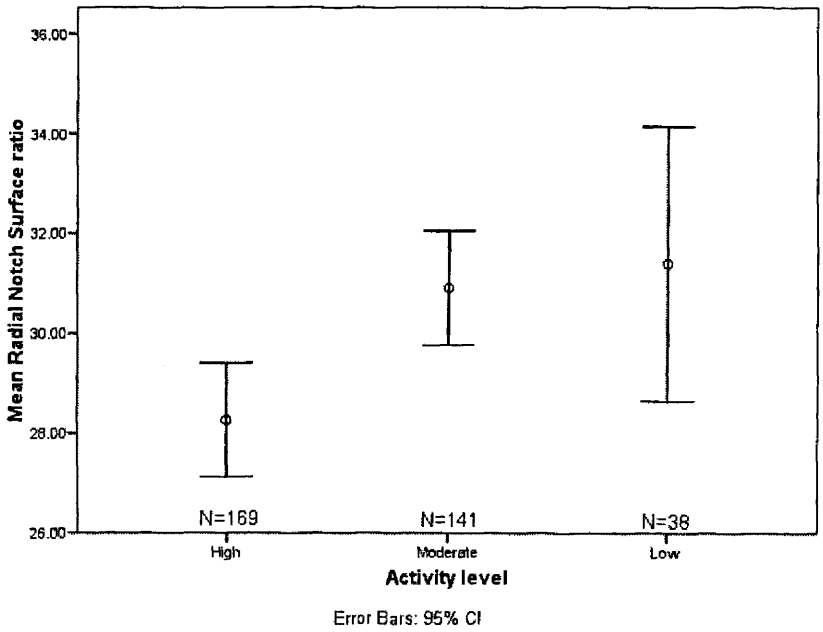

Figure 4-84 Radial notch surface area for modern humans, by activity level.

Mean and 95% confidence interval (whiskers).

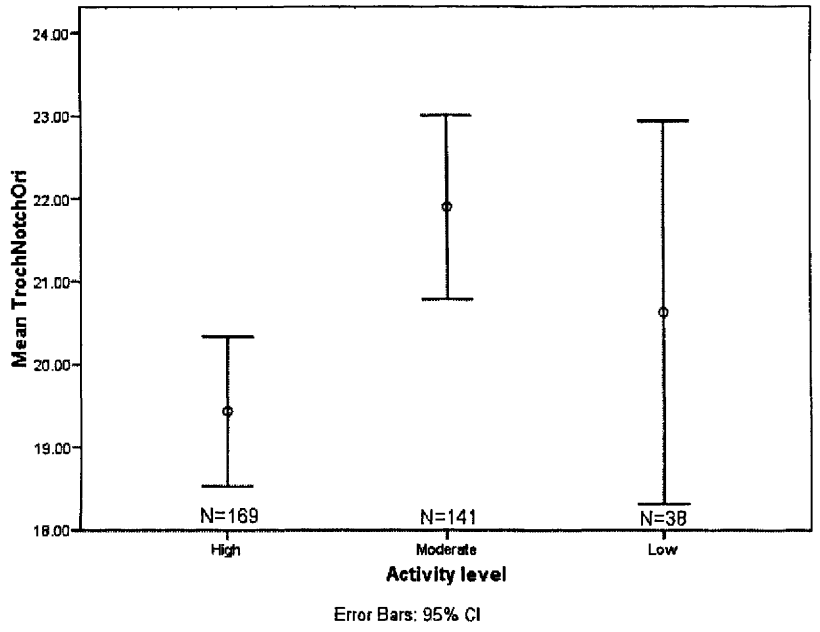

Figure 4-85 Trochlear notch orientation for modern humans, by activity level.
Mean and 95% confidence interval (whiskers).

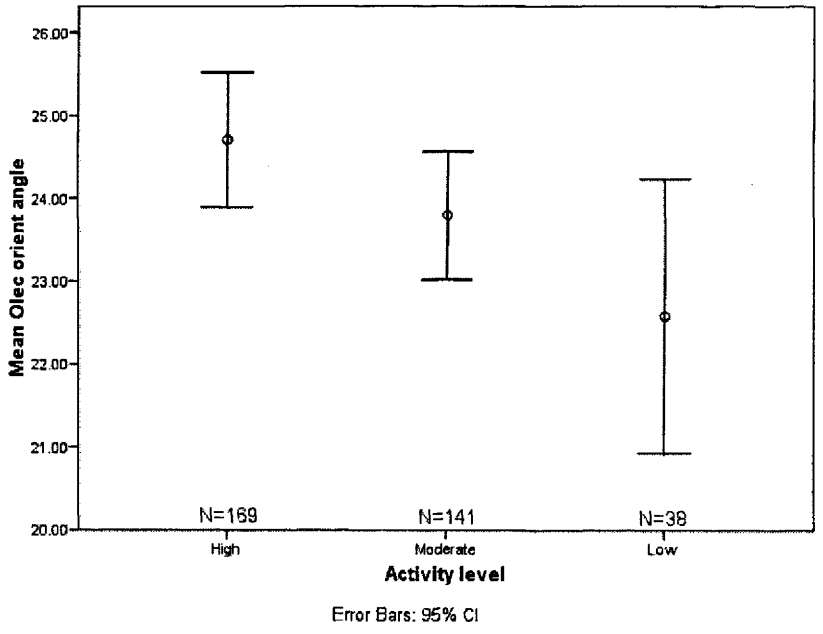

Figure 4-86 Olecranon orientation angle for modern humans, by activity level.
Mean and 95% confidence interval (whiskers).

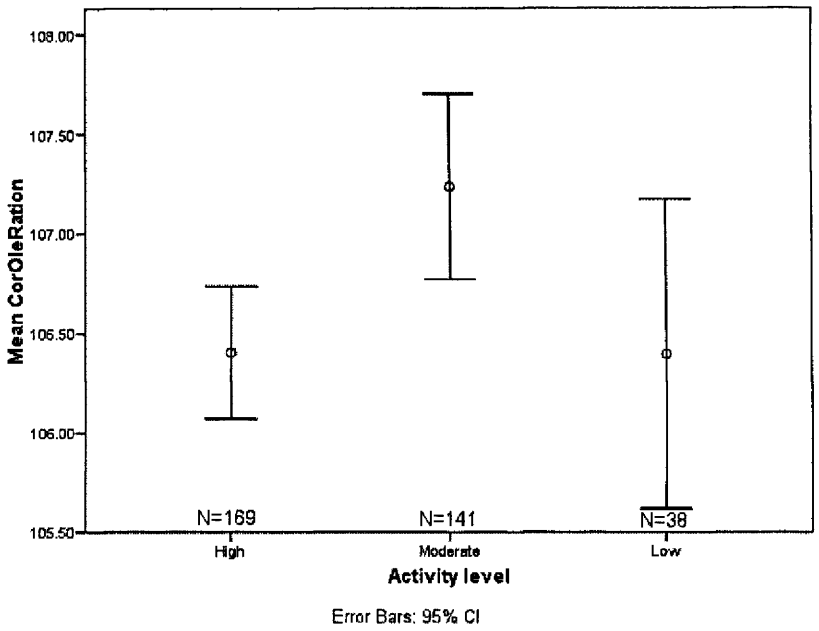

Figure 4-87 Coronoid-olecranon ratio for modern humans, by activity level.
Mean and 95% confidence interval (whiskers).

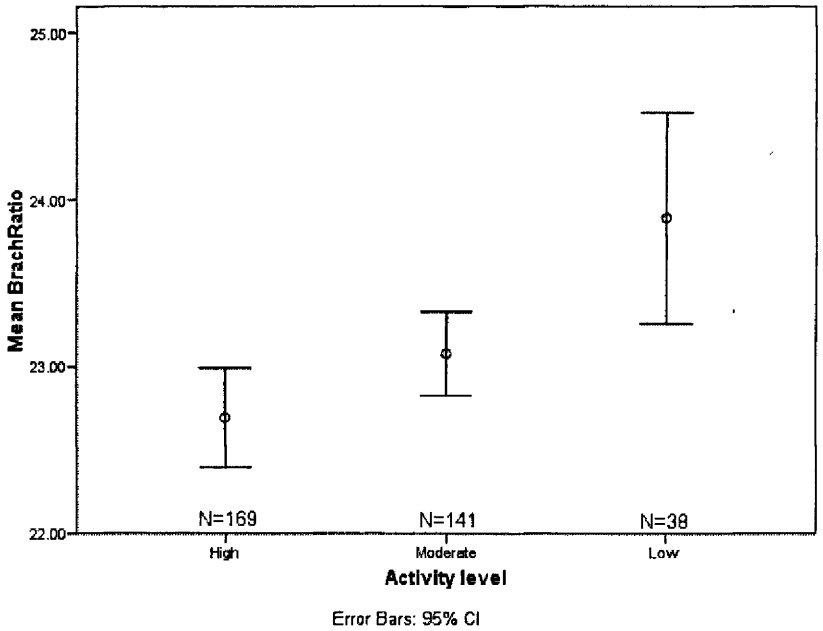

Figure 4-88 Brachial muscle attachment ratio for modern humans, by activity level. Higher values have a relatively lower insertion. Mean and 95% confidence interval (whiskers).

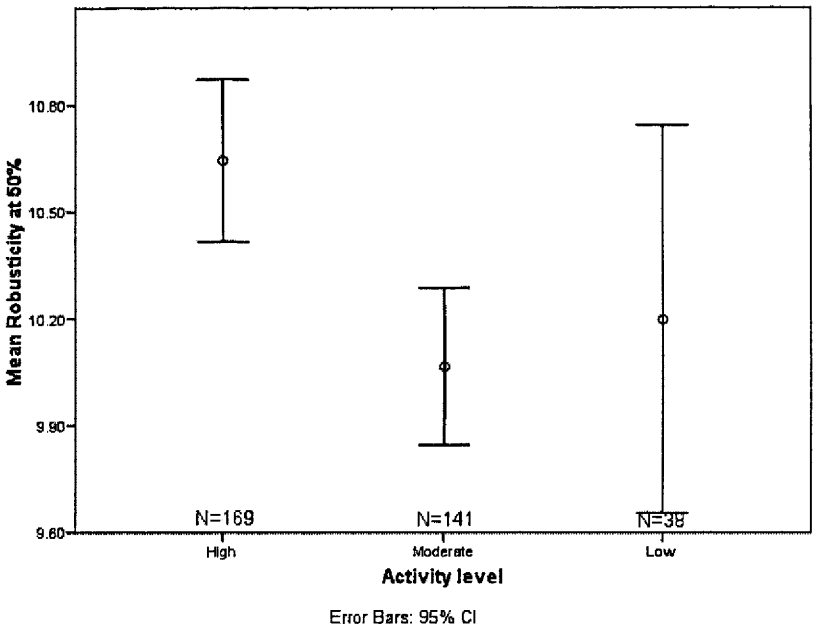

Figure 4-89 Robusticity at 50% shaft level for modern humans, by activity level. Mean and 95% confidence interval (whiskers).

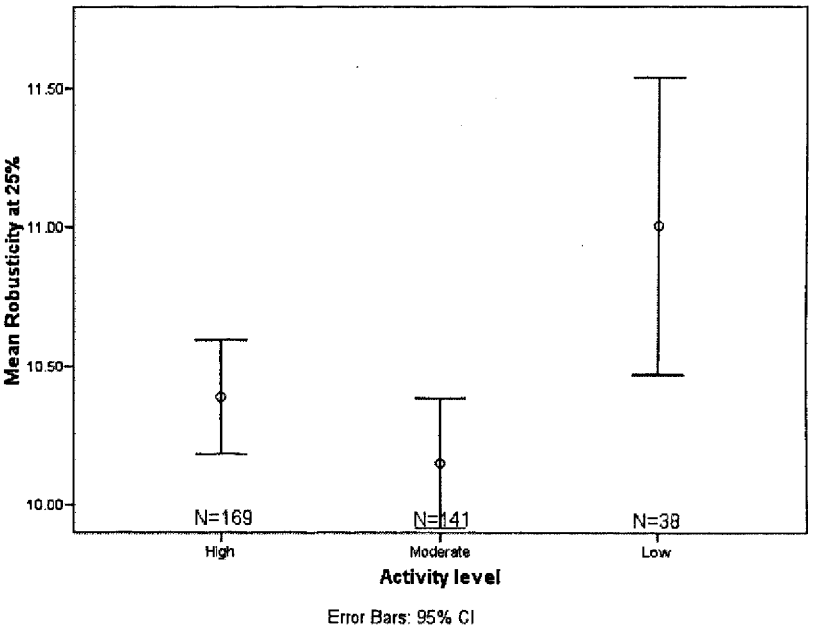

Figure 4-90 Robusticity at 25% shaft level for modern humans, by activity level. Mean and 95% confidence interval (whiskers).

There are significant differences between the high activity subsistence categories for all univariate measurements of the ulna (except midshaft shape) (Table 4-106 and Appendix 36). Aquatic foragers have the shortest ulnae and have the relatively largest proximal ulnae (Figure 4-91). The pastoralists have the largest radial notch surface. The aquatic foragers and the horticulturalists have the smallest radial notch surface and are different from the pedestrian foragers and pastoralists (Figure 4-94). Pastoralists have the largest olecranon angle compared to pedestrian and equestrian foragers (Figure 4-96). The coronoid-olecranon ratio is largest in pastoralists and smallest in equestrian foragers. Aquatic and pedestrian foragers and horticulturalists are intermediate (Figure 4-97). Pastoralists have the lowest brachilis insertion, the horticulturalists the highest (Figure 4-92). The horticulturalists also have the longest pronator crest, whereas equestrian foragers have the shortest (Figure 4-98). The equestrian foragers have the lowest midshaft robusticity, pastoralists the highest (Figure 4-99). At the 25% level of the shaft, pastoralists are still the most robust, but the least robust are the horticulturalists (Figure 4-100).

Table 4-106 ANOVA results for subsistence patterns and univariate measurements on the ulna.

d.f.=4	F	Sig.
Max_ Length	8.622	<0.001*
Olec-shaftratio	4.050	0.004*
MidShaftShape	1.589	0.180
Radial Notch Surface ratio	8.722	<0.001*
TrochNotchOri	2.604	0.038*
Olec-orient angle	3.290	0.013*
CorOleRation	9.836	<0.001*
BrachRatio	2.534	0.042*
Size pronator crest rel. lenth	2.838	0.026*
Robusticity at 50%	11.390	<0.001*
Robusticity at 25%	15.183	<0.001*
Robust dist artic	3.471	0.009*

*=significant at α=0.05

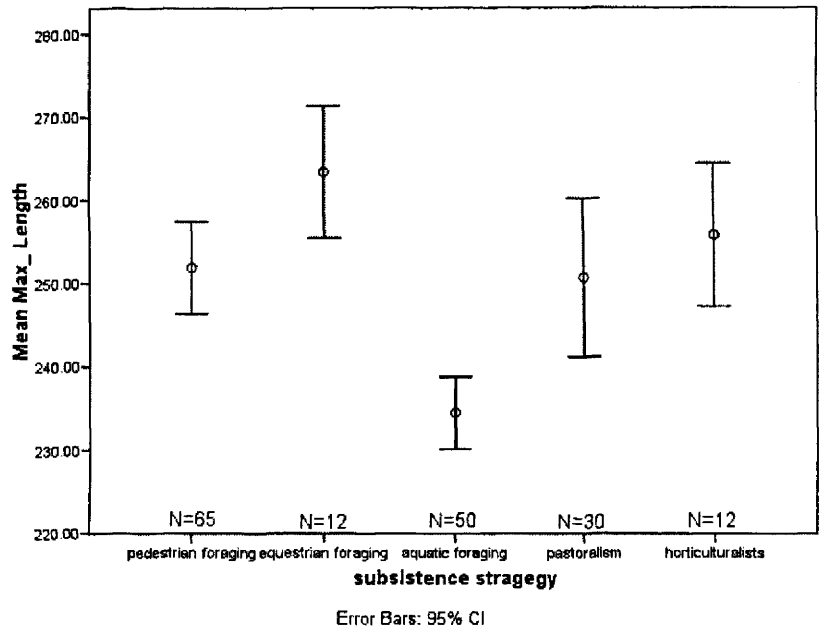

Figure 4-91 Ulna maximum length for modern humans, by subsistence strategy. Mean and 95% confidence interval (whiskers).

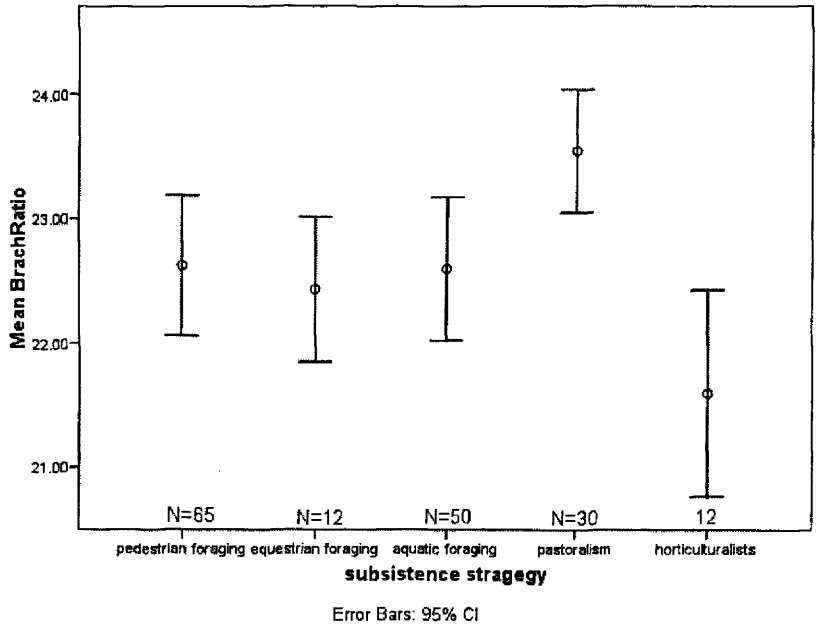

Figure 4-92 Position of the brachial tuberosity for modern humans, by subsistence strategy. Mean and 95% confidence interval (whiskers).

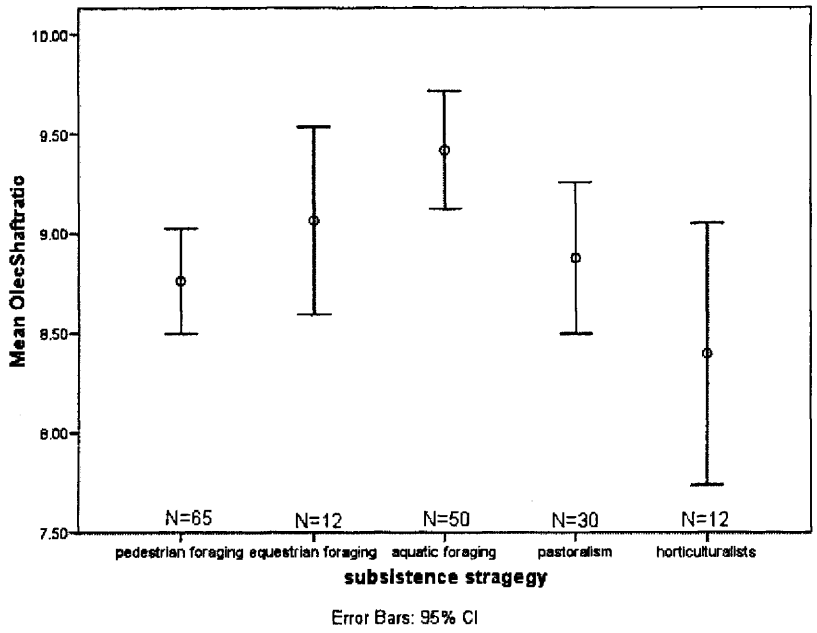

Figure 4-93 Olecranon-shaft size ratio for modern humans, by subsistence strategy. Mean and 95% confidence interval (whiskers).

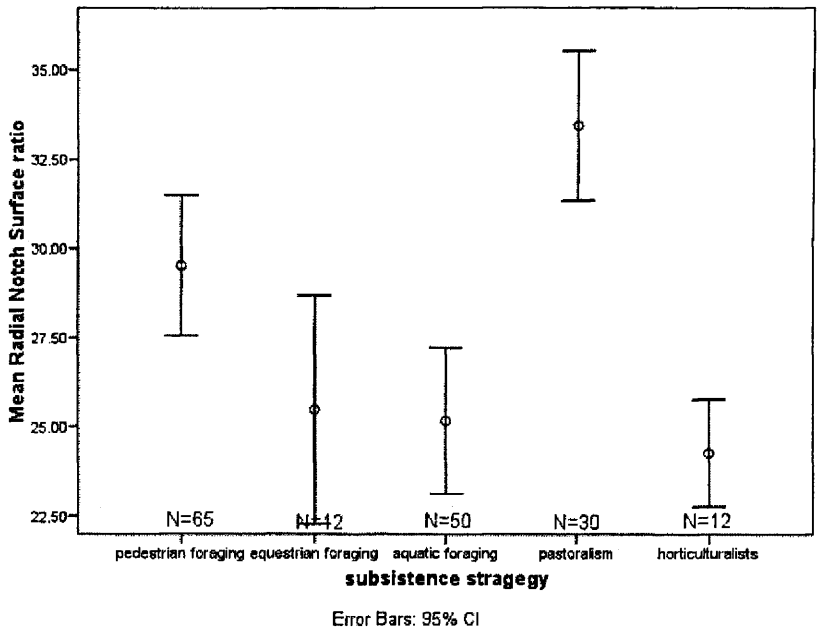

Figure 4-94 Radial notch surface ratio for modern humans, by subsistence strategy. Mean and 95% confidence interval (whiskers).

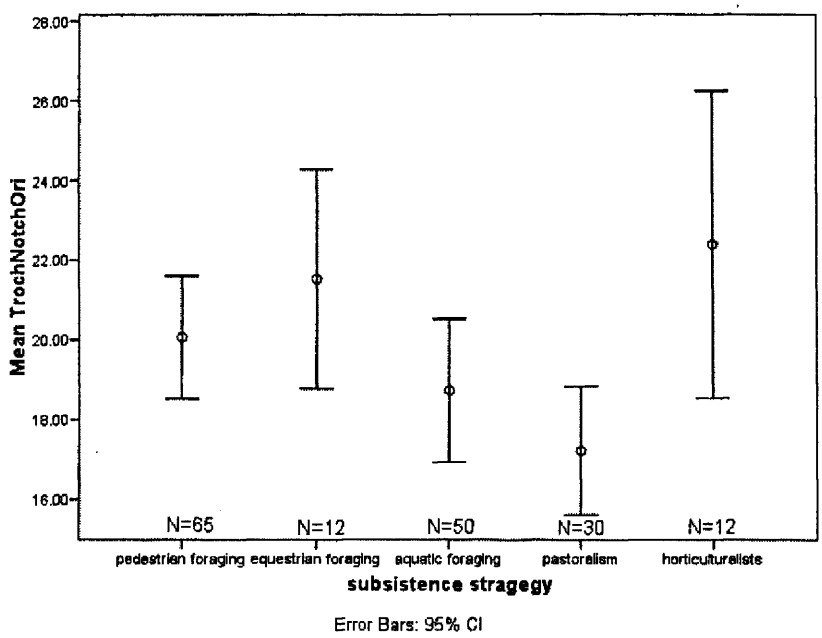

Figure 4-95 Trochlear notch orientation for modern humans, by subsistence strategy. Mean and 95% confidence interval (whiskers).

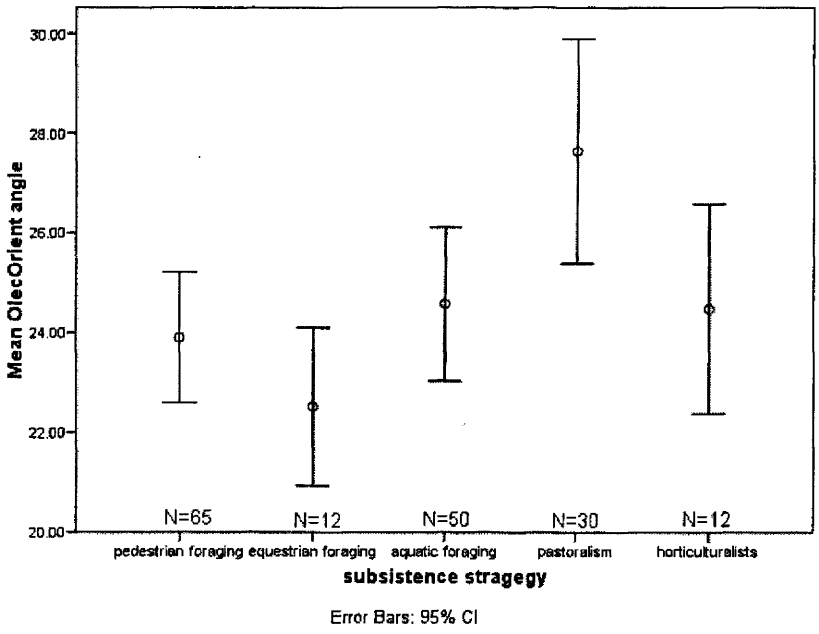

Figure 4-96 Olecranon orientation angle for modern humans, by subsistence strategy.
Mean and 95% confidence interval (whiskers).

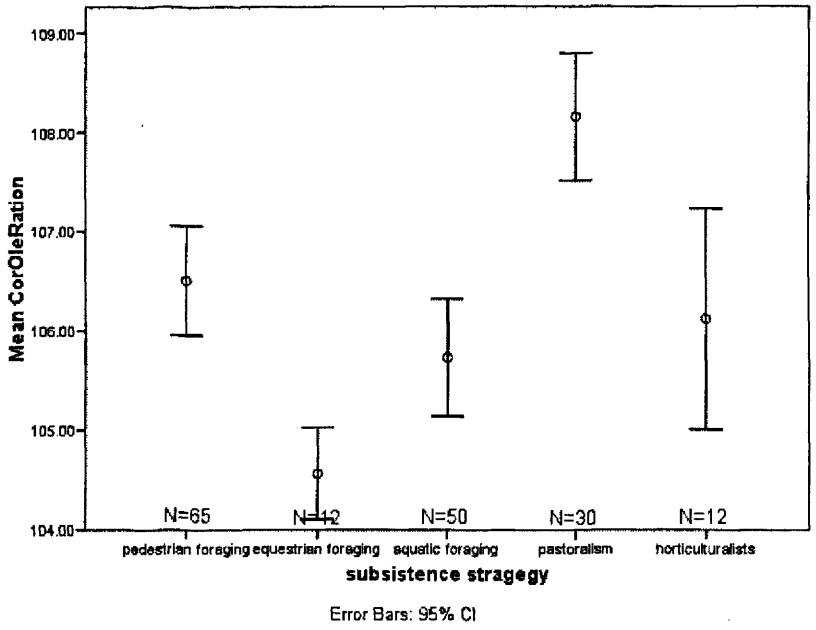

Figure 4-97 Coronoid-olecranon ratio for modern humans, by subsistence pattern.
Mean and 95% confidence interval (whiskers).

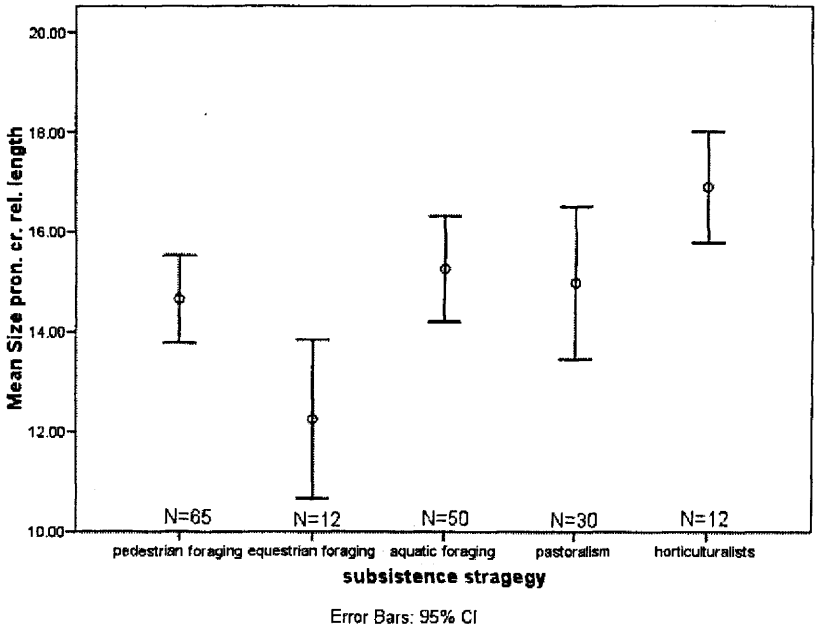

Figure 4-98 Relative size of the pronator crest for modern humans, by subsistence pattern.
Mean and 95% confidence interval (whiskers).

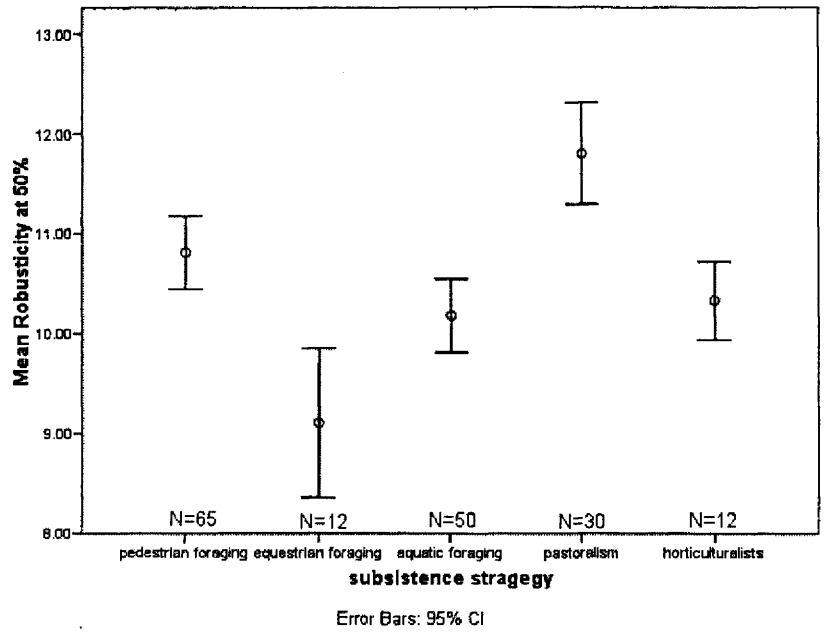

Figure 4-99 Robusticity at 50% shaft level for modern humans, by subsistence pattern. Mean and 95% confidence interval (whiskers).

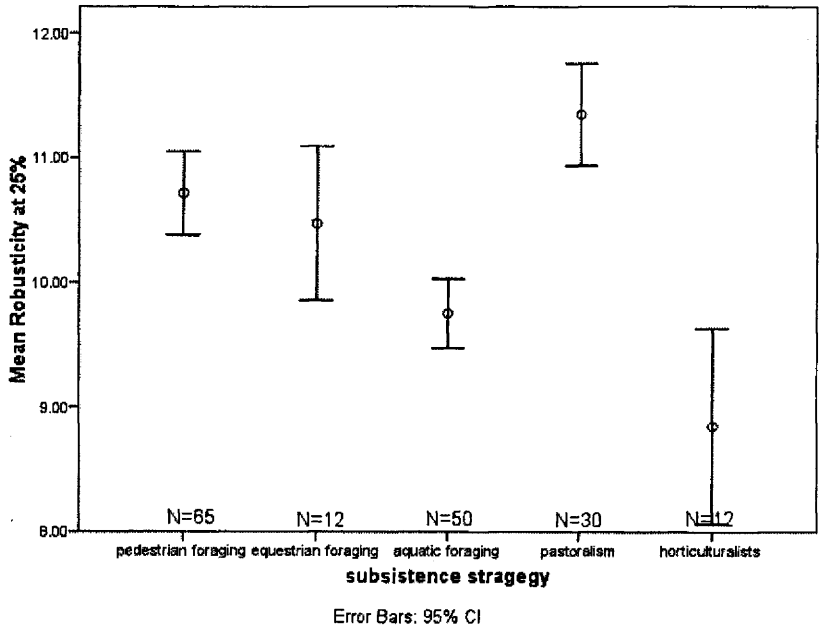

Figure 4-100 Robusticity at 25% shaft level for modern humans, by subsistence pattern. Mean and 95% confidence interval (whiskers).

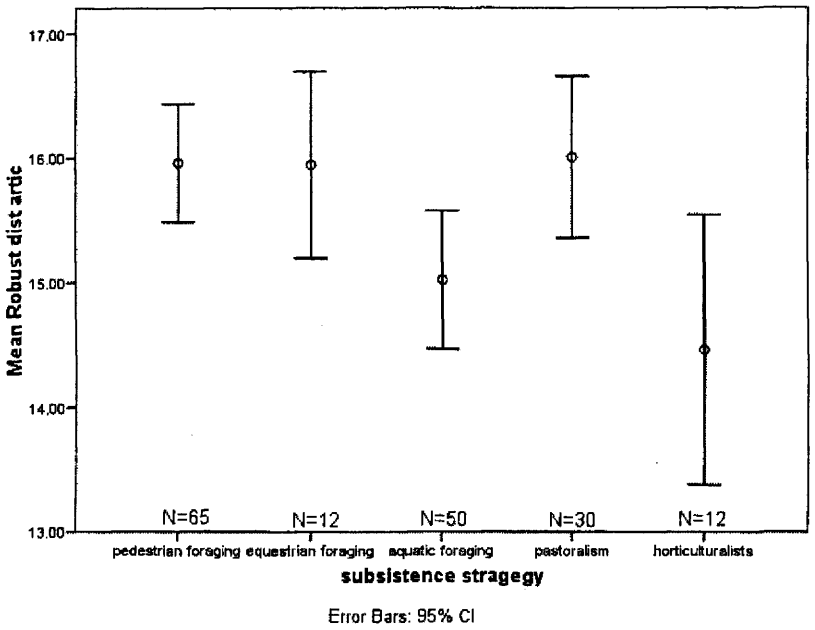

Figure 4-101 Robusticity of the distal articulation for modern humans, by subsistence pattern. Mean and 95% confidence interval (whiskers).

4.3.4.6. Evolution over time in Europe

Curvature

For the radius, only the lateral surface curvature (lcurveAMHPC1) is significantly affected through time. However; it doesn not show a steady decrease.The Medieval populations are the least laterally curved (Figure 4-102) (Table 4-107) (Appendix 37; Appendix 8).

Table 4-107 ANOVA results for time-period and curvature of the radius.

d.f.=3	F	Sig.
mcurveAMHPC1	0.836	0.476
lcurvAMHPC1	6.092	0.001*

*=significant at α=0.05

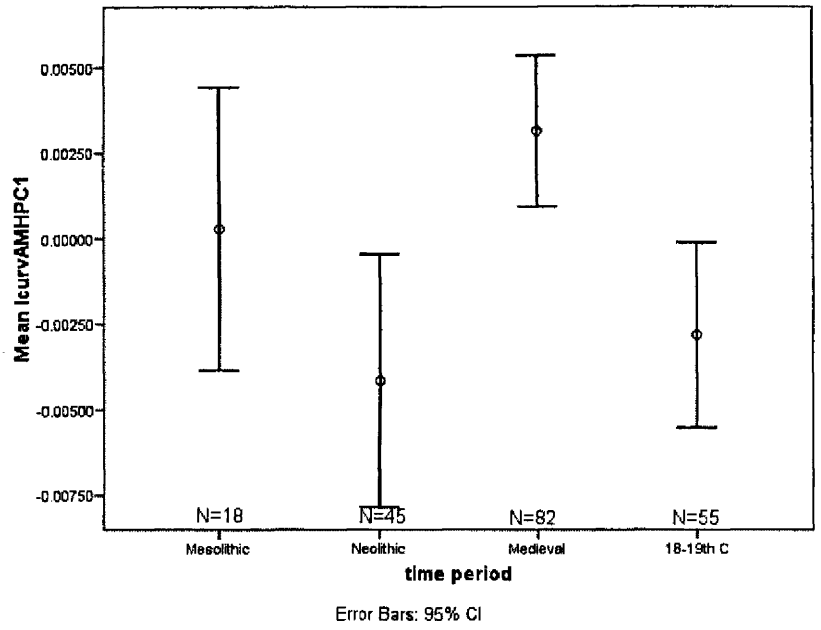

Figure 4-102 Lateral curvature of the radius for modern Europeans, by time period.
Mean and 95% confidence interval (whiskers).

Ulna shape

The time periods are significantly different for two of the ulna PCs (Table 4-108; Appendix 38), but none of the significant variables shows a steady change through time. The Neolithic individuals have more anteroposteriorly sinusoidal shafts than the Medieval sample (pcurveAMHPC3) (Figure 4-103) and the 18th and 19th Century sample has a deeper trochlear notch (proxAMHPC4) (Figure 4-104).

Table 4-108 ANOVA results for time-period and ulna shape.

d.f.=3	F	Sig.
pcurveAMHPC1	0.127	0.944
pcurveAMHPC2	1.696	0.171
pcurveAMHPC3	3.326	0.022*
pcurveAMHPC4	0.356	0.785
proxAMHPC1	2.512	0.061
proxAMHPC2	1.188	0.317
proxAMHPC3	1.109	0.348
proxAMHPC4	4.881	0.003*

*=significant at α=0.05

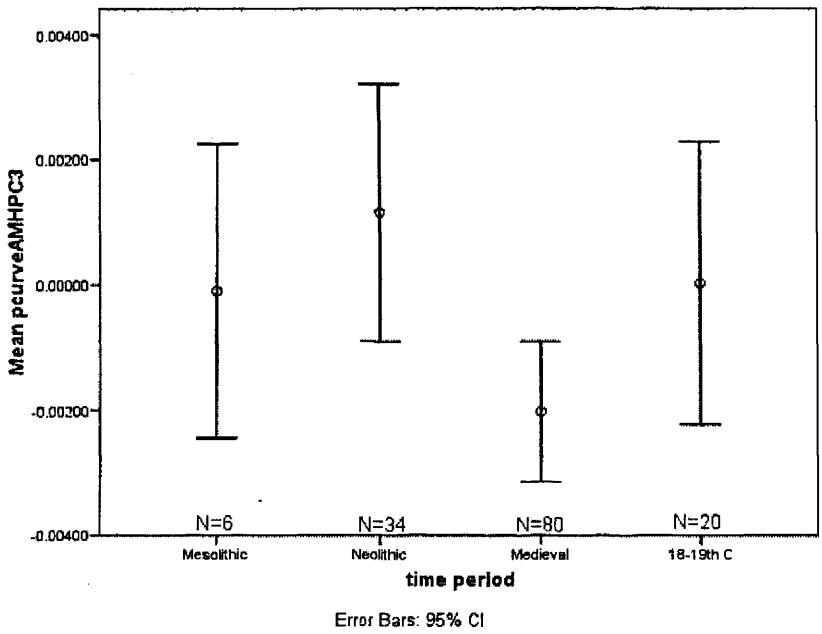

Figure 4-103 PcurveAMHPC3 (high values have a more anteroposteriorly sinusoisal shaft) of the radius for modern Europeans, by time period.

Higher values have more anteroposteriorly sinusoisal shafts. Mean and 95% confidence interval (whiskers).

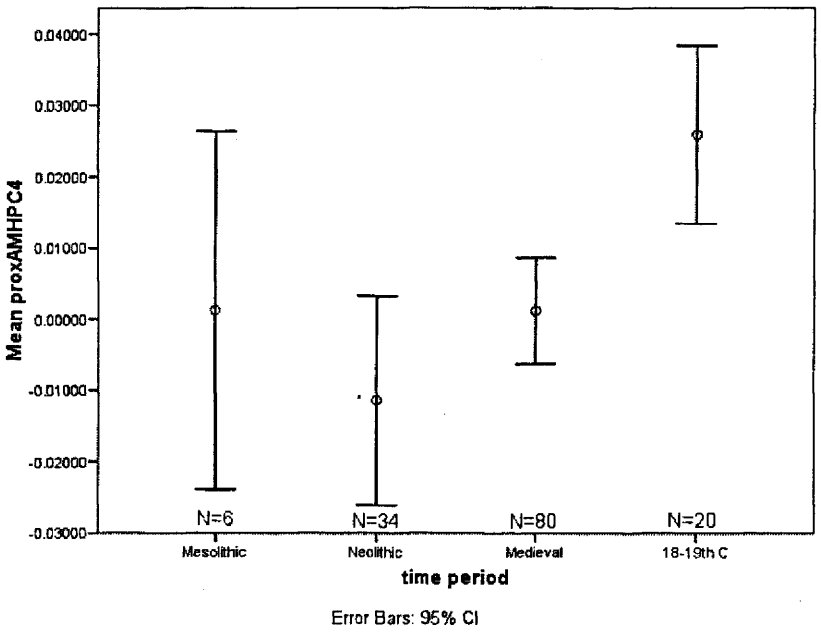

Figure 4-104 ProxAMHPC4 (high values have a deeper trochlear notch) of the radius for modern Europeans, by time period.

Higher values have a deeper trochlear notch. Mean and 95% confidence interval (whiskers).

Summary

Although there are some differences among samples from different time periods there are no general trends for aspects of radius and ulna shape through time in Europe.

4.3.4.7. Climate and latitude

As for the femur analysis, latitude is used here as a general proxy for climate (Appendix 8). Individuals from higher latitudes have a higher degree of lateral radial curvature than those from lower latitudes (LcurveAMHPC1) (Table 4-109; Figure 4-105). There are no correlations between the radial epiphysis shape PCs and latitude (Table 4-109). The other shaft shape PCs show that individuals from higher latitudes have an increased medial extension of the proximal interosseous crest with amore medial expanded ulnar notch (mcurveAMHPC2) (Figure 4-106) and a more sinusoidal shape than those living in low latitudes (mcurveAMHPC3) (Table 4-109 and Figure 4-107).

Table 4-109 Pearson's correlations for curvature, apex of curvature, diaphyseal shape and epiphyses shape PCs and latitude (climate) on the radius (N=34).

Latitude °					
Curvature			*Other diaphyseal shape*		
mcurveAMHPC1	r	-0.177	mcurveAMHPC2	r	-0.550
	P	0.316		P	0.001**
lcurvAMHPC1	r	-0.371	mcurveAMHPC3	r	-0.362
	P	0.031*		P	0.035*
Epiphyses shape			lcurvAMHPC2	r	-0.227
EpiAMHPC1	r	0.229		P	0.197
	P	0.193	lcurvAMHPC3	r	-0.247
EpiAMHPC2	r	0.227		P	0.159
	P	0.196			

* Correlation is significant at the 0.05 level (2-tailed).

** Correlation is significant at the 0.01 level (2-tailed).

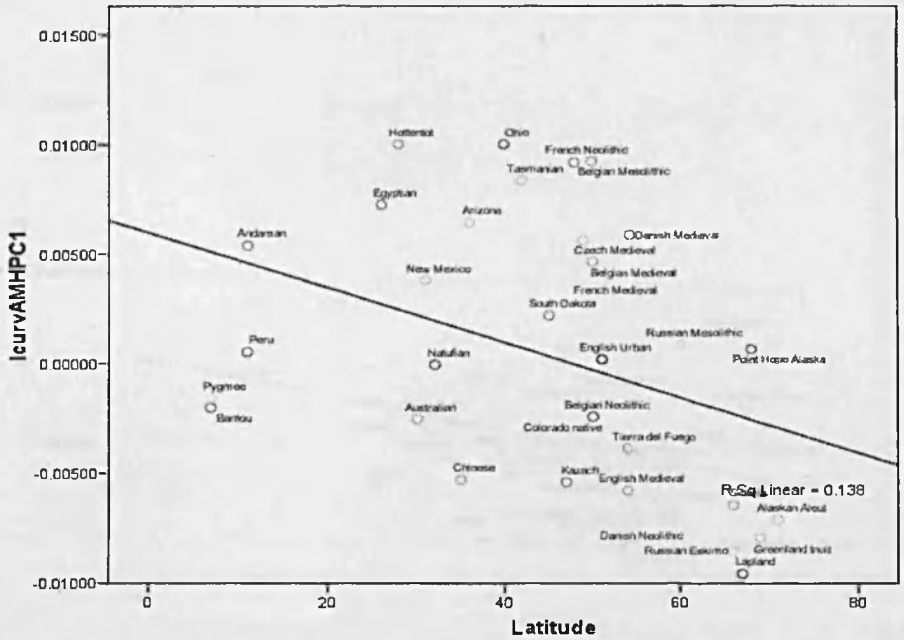

Figure 4-105 Lateral curvature of the radius (lcurveAMHPC1) and latitude for recent modern humans.

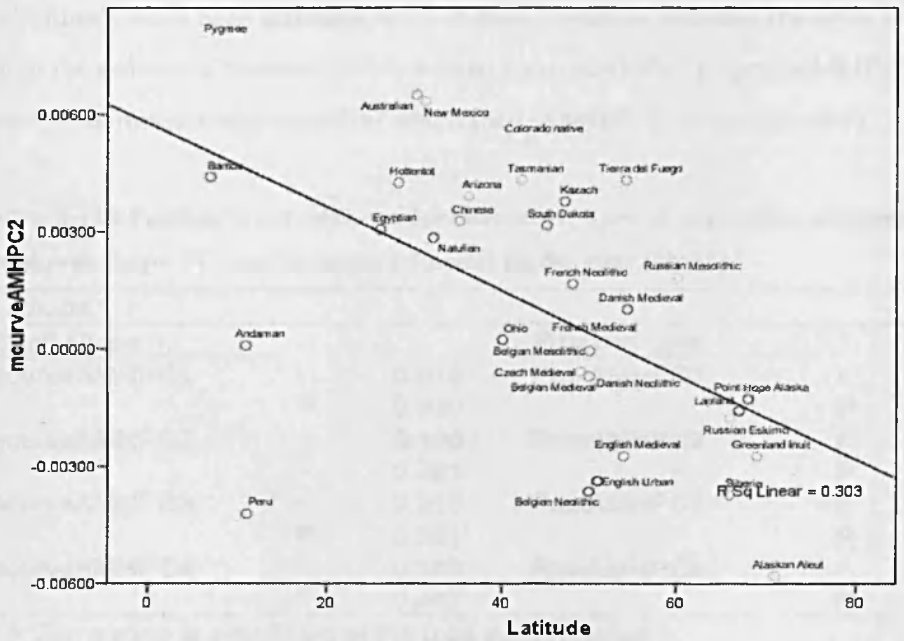

Figure 4-106 Medial expansion of the interosseous crest (mcurveAMHPC2) and latitude for recent modern humans.

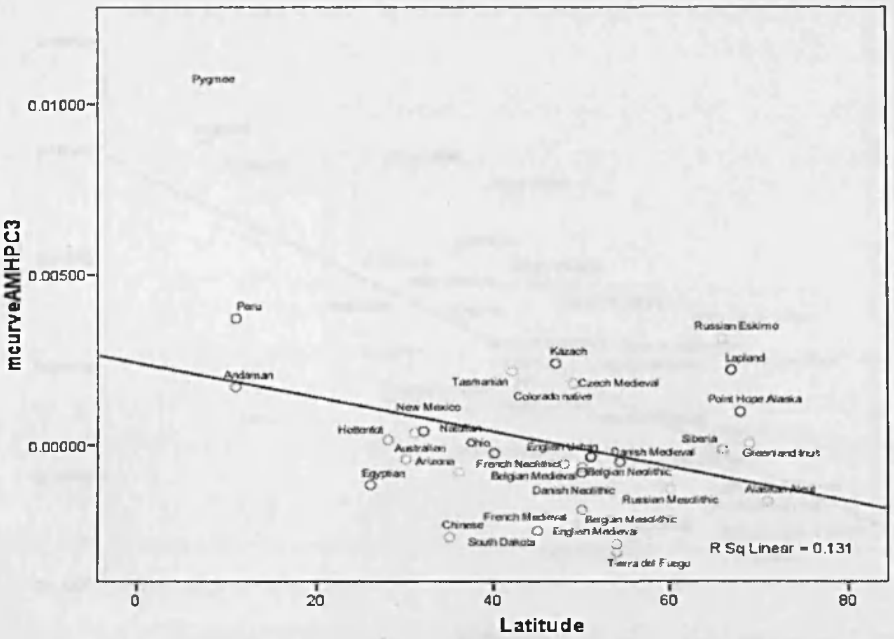

Figure 4-107 Sinusoidal shape of the radius (mcurveAMHPC3) and latitude for recent modern humans.

Individuals from high latitudes have shorter distances between the 80% level of the shaft and the tip of the coronoid process (Table 4-110) (proxAMHPC2). (proxAMHPC2) (Figure 4-108) and a more proximo-anterior trochlear notch (proxAMHPC3) (Figure 4-109).

Table 4-110 Pearson's correlations for curvature, apex of curvature, diaphyseal shape and epiphyses shape PCs and latitude (climate) on the ulna (N=32).

Latitude °					
Shaft shape			*Proximal ulna*		
pcurveAMHPC1	r	0.019	ProxAMHPC1	r	0.174
	P	0.920		P	0.350
pcurveAMHPC2	r	-0.196	ProxAMHPC2	r	-0.644**
	P	0.291		P	<0.001
pcurveAMHPC3	r	0.318	ProxAMHPC3	r	-0.365*
	P	0.081		P	0.043
pcurveAMHPC4	r	0.142	ProxAMHPC4	r	-0.099
	P	0.447		P	0.595

* = Correlation is significant at the 0.05 level (2-tailed).
** = Correlation is significant at the 0.01 level (2-tailed).

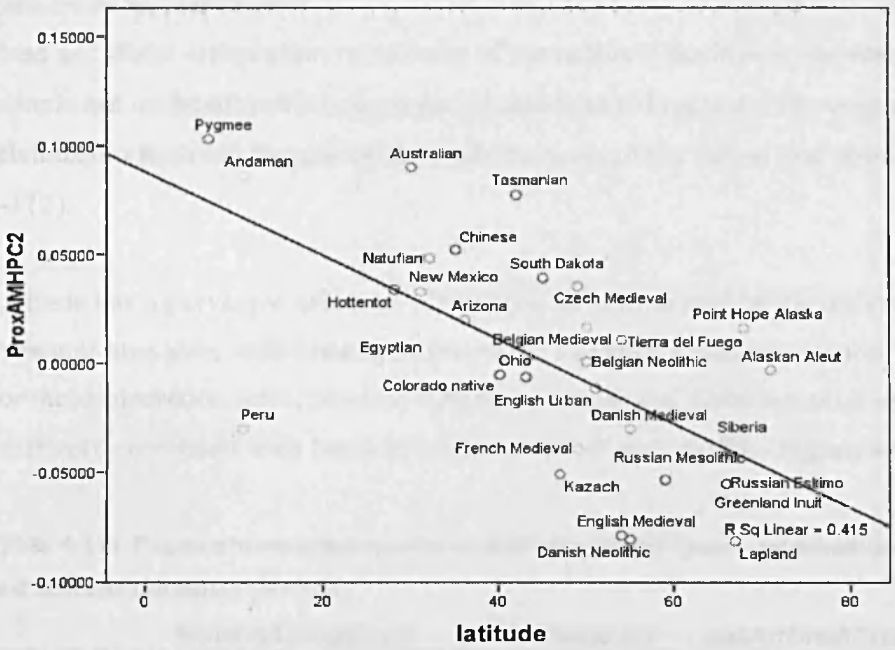

Figure 4-108 Distance between the 80% shaft level and the tip of the coronoid process (proxAMHPC2) and absolute latitude for recent modern humans.

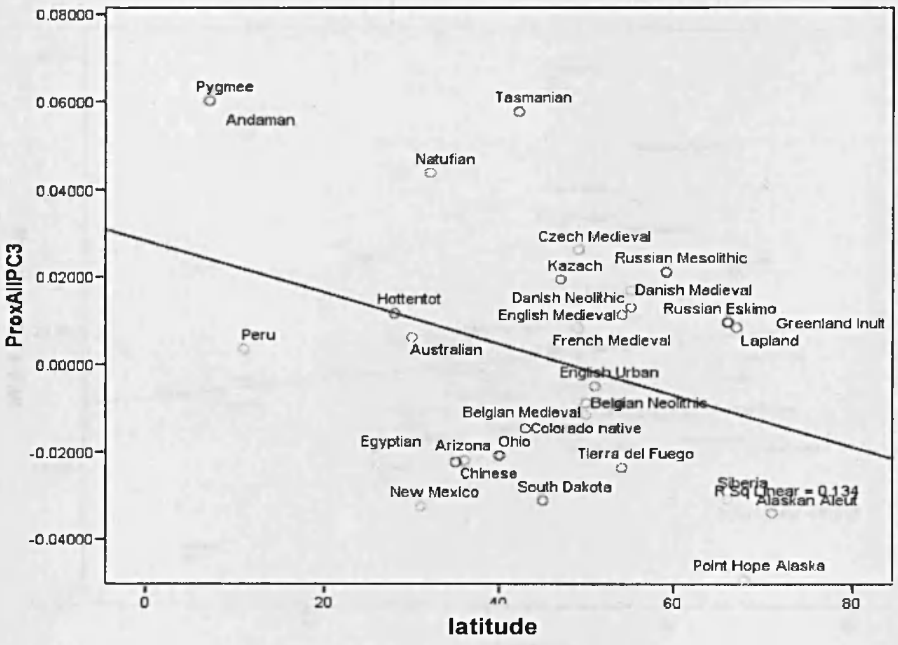

Figure 4-109 Orientation of the trochlear notch (proxAMHPC3) and absolute latitude for recent modern humans.

Univariate measurements

Head and distal articulation robusticity of the radius is positively correlated with absolute latitude but midshaft robusticity is not (Table 4-111; Figure 4-110 - Figure 4-112). There is no relationship between the univariate measurements of the radius and absolute latitude (Table 4-112).

Latitude has a pervasive effect on ulna shape as represented by the univariate measurements. Proximal ulna size, radial notch surface area, trochlear notch orientation, olecranon orientation, coronoid-olecranon ratio, brachial tuberosity length and distal articulation robusticity are positively correlated with latitude (Table 4-113, Figure 4-113 - Figure 4-118).

Table 4-111 Pearson's correlations for radius robusticity (head, midshaft and distal articulation) and latitude (climate) (N=34).

		Midshaftrobusticity	Headrobusticity	distArtShaftSizeRatio
Latitude	r	0.178	0.457	0.493
	P	0.314	0.007**	0.003**

* = Correlation is significant at the 0.05 level (2-tailed).
** = Correlation is significant at the 0.01 level (2-tailed).

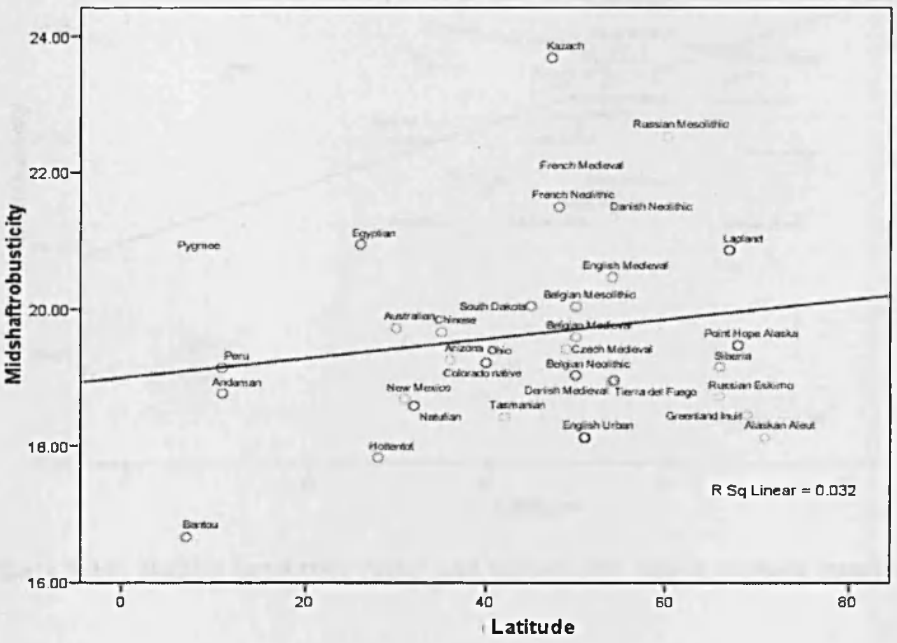

Figure 4-110 Radius midshaft robusticity and latitude for recent modern humans.

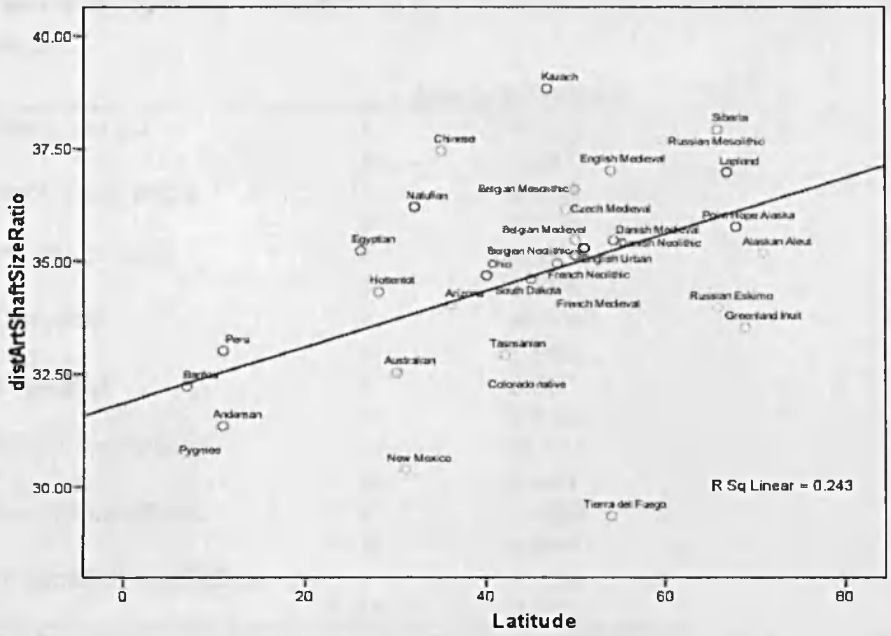

Figure 4-111 Radius distal articulation robusticity and latitude for recent modern humans.

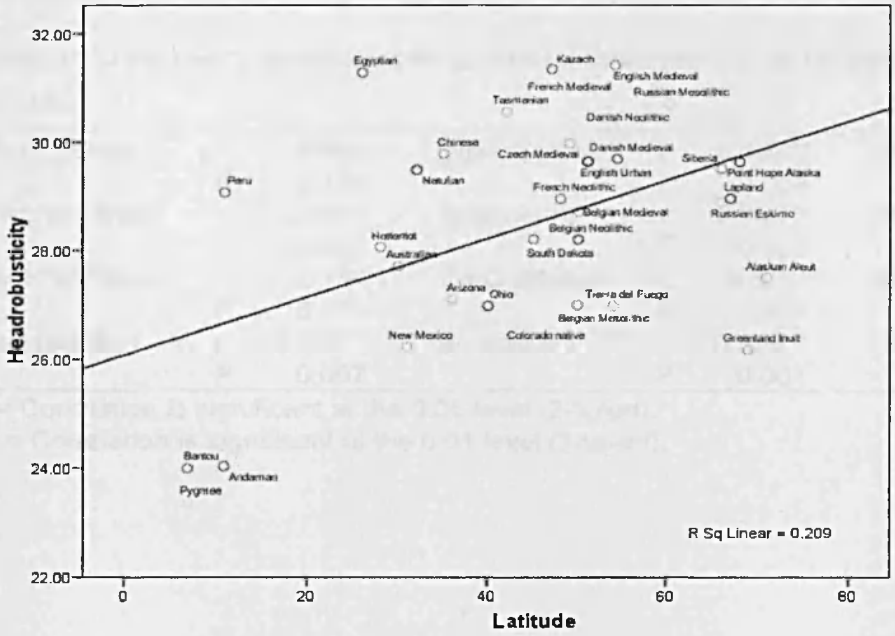

Figure 4-112 Radius head robusticity and latitude for recent modern humans.

Table 4-112 Pearson's correlations for univariate measurements on the radius and latitude (climate) (N=34).

		Absolute Latitude
Max_ Length	r	-0.188
	P	0.287
neck-shaft angle °	r	0.092
	P	0.605
PosRadTubML	r	-0.094
	P	0.598
DorsalST	r	-0.009
	P	0.958
LateralST	r	0.081
	P	0.648
NeckLengthRatio	r	-0.137
	P	0.441
HeadShapeRatio	r	-0.029
	P	0.869
midshaftShapeRation	r	-0.198
	P	0.263

* = Correlation is significant at the 0.05 level (2-tailed).
** = Correlation is significant at the 0.01 level (2-tailed).

Table 4-113 Pearson's correlations for univariate measurements on the ulna and latitude (climate) (N=31).

Max_ Length	r	0.063	TrochNotchOri	r	0.487**	pron.cr. size	r	0.313
	P	0.736		P	0.005		P	0.087
Olec-shaftratio	r	0.590**	Olec-orient	r	0.609**	Robust 50%	r	0.100
	P	<0.001		P	<0.001		P	0.591
MidShaftShape	r	-0.154	CorOleRation	r	0.376*	Robust 25%	r	0.295
	P	0.409		P	0.037		P	0.107
Rad Not Surf	r	0.476**	BrachRatio	r	0.568**	Robust dist art	r	0.625*
	P	0.007		P	0.001		P	<0.001

* = Correlation is significant at the 0.05 level (2-tailed).
** = Correlation is significant at the 0.01 level (2-tailed).

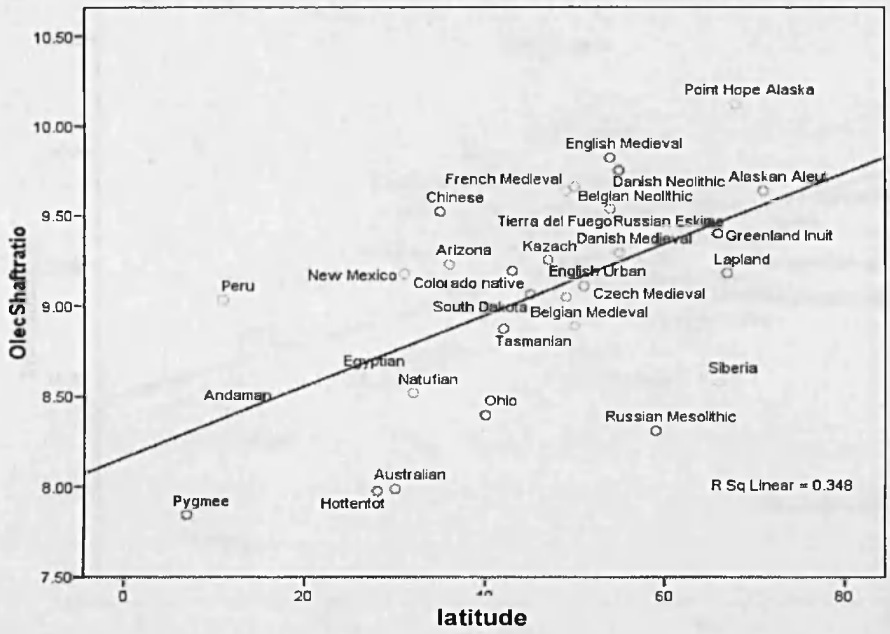

Figure 4-113 Scatterplot for olecranon shaft ratio and latitude for recent modern humans.

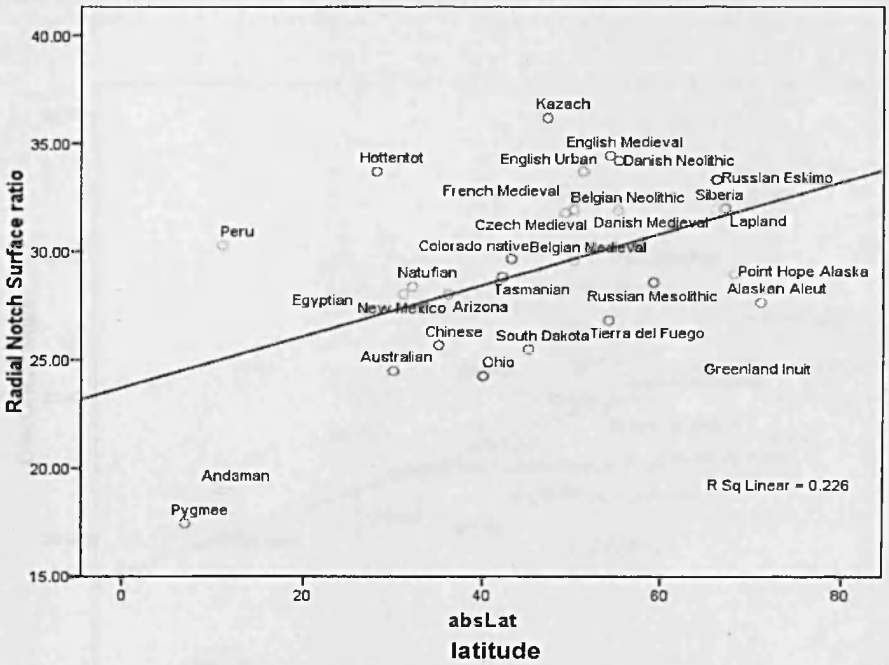

Figure 4-114 Radial notch surface area and latitude for recent modern humans.

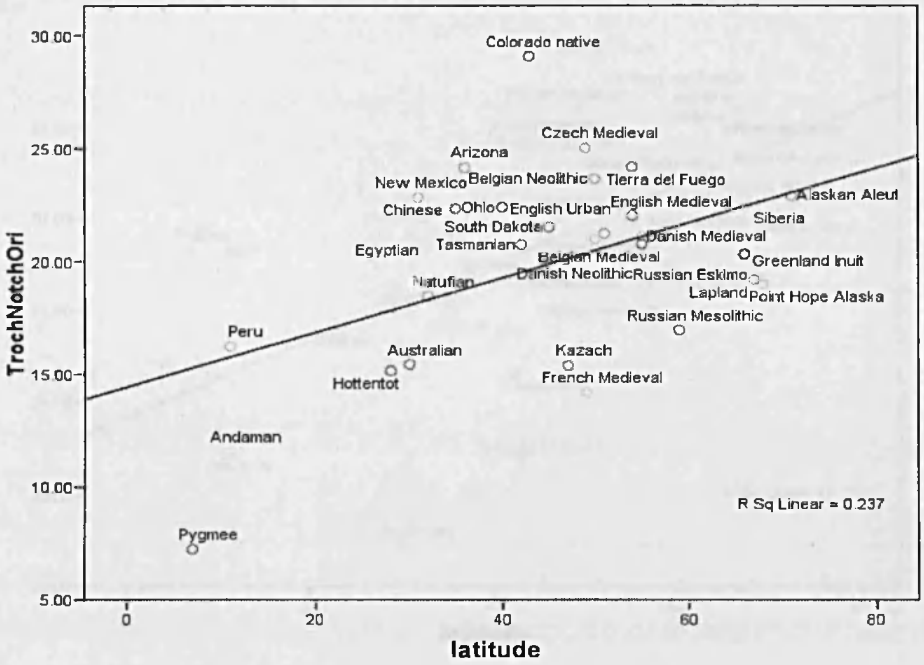

Figure 4-115 Orientation of the trochlear notch and latitude for recent modern humans.

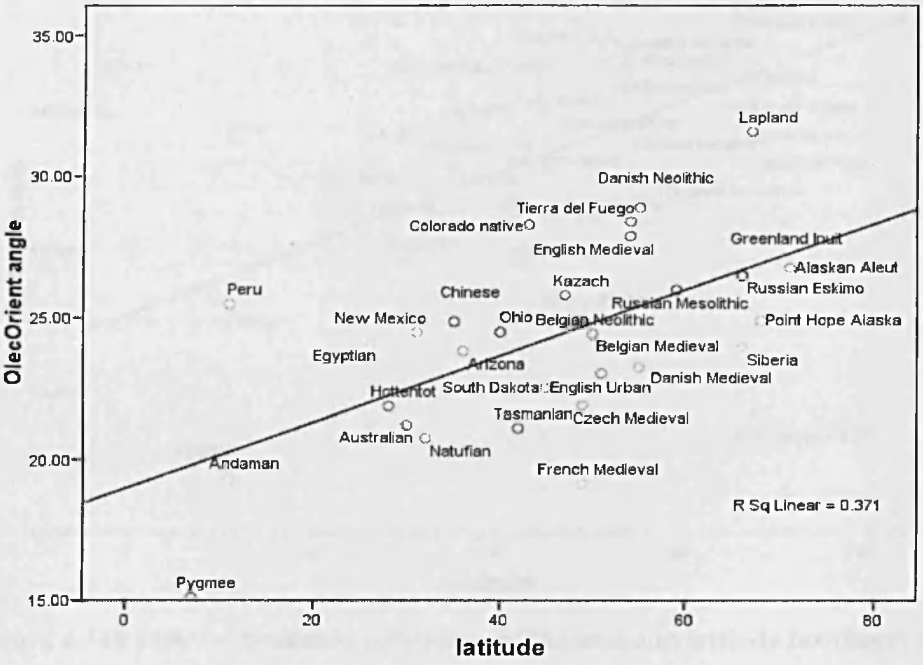

Figure 4-116 Olecranon orientation angle and latitude for recent modern humans.

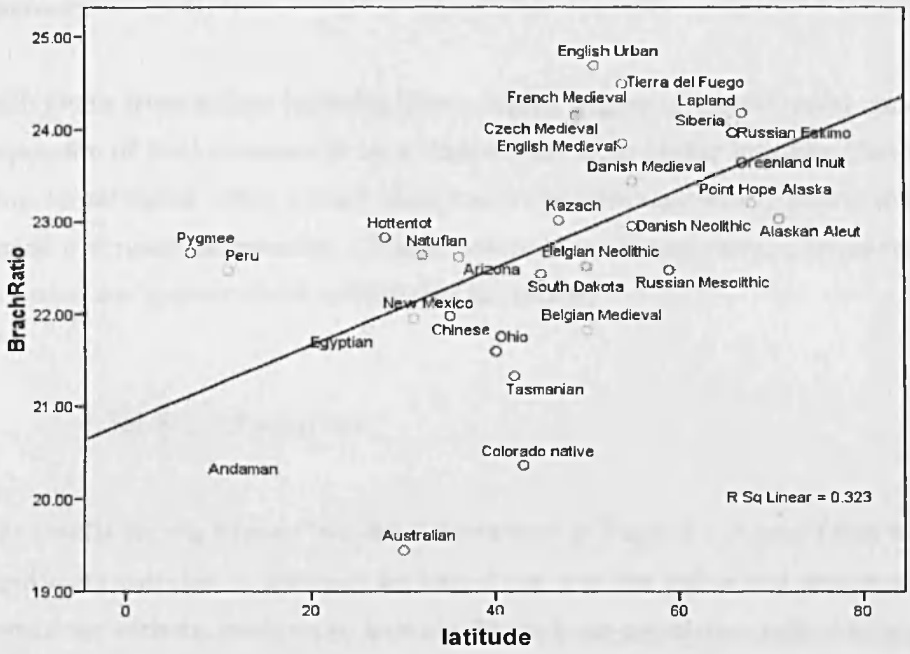

Figure 4-117 Position of the brachial muscle insertion and latitude for recent modern humans.

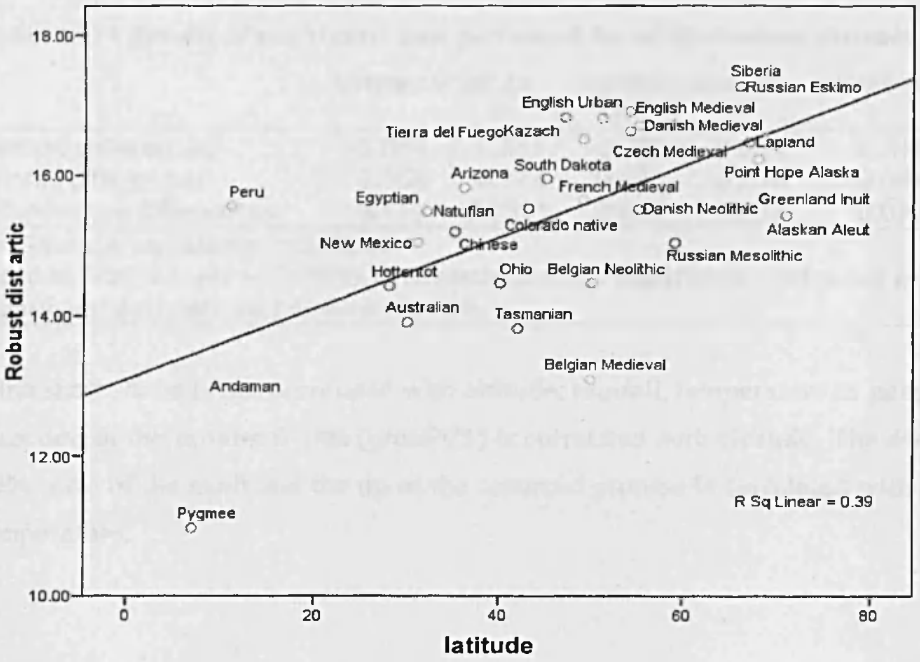

Figure 4-118 Distal articulation robusticity of the ulna and latitude for recent modern humans.

Summary

Individuals from higher latitudes have a higher degree of lateral radial curvature and medial expansion of the interosseous crest. Individuals from higher latitudes also have a larger proximal ulna, larger radial notch surface area, a more proximo-anteriorly facing trochlear notch, a more lateral olecranon orientation, a higher coronoid-olecranon ratio, a lower relative brachial insertion and greater distal articulation robusticity.

4.3.4.8. Mantel test

The results for the Mantel test are summarised in Table 4-114 and Table 4-115. There is a significant correlation between the lateral curve of the radius and temperature which is consistent with the analysis of latitude. There is no correlation with curvature or the whole radius shape, altitude and average rainfall.

Table 4-114 Results of the Mantel tests performed for environmental distance matrices – radius.

	lateral curvature		medial curvature		whole radius shape	
	r	P	R	P	r	P
altitude differences	-0.068	0.817	-0.027	0.604	0.216	0.034*
rainfall differences	0.058	0.774	0.085	0.205	0.054	0.327
temperature differences	0.119	0.032*	0.052	0.268	0.077	0.214

r = Pearson correlation coefficient
Randomisation tests with 5000 permutations show significance values of $p<0.05$ for all significant correlations between matrices.

Ulna shaft shape is not correlated with altitude, rainfall, temperature or geographic distance. The direction of the proximal ulna (proxPC1) is correlated with altitude. The distance between the 80% level of the shaft and the tip of the coronoid process is correlated with rainfall and temperature.

Table 4-115 Results of the Mantel tests performed for environmental distance matrices - ulna

	pcurve1		pcurve2		proximal ulna 1		proximal ulna 2		whole bone	
	r	P	R	P	r	P	r	P	r	P
altitude differences	0.074	0.222	0.155	0.105	0.327	0.010*	-0.07	0.761	0.123	0.137
rainfall differences	-0.101	0.841	0.087	0.251	-0.133	0.818	0.221	0.016*	0.161	0.085
temperature differences	-0.076	0.825	0.159	0.057	-0.12	0.857	0.163	0.024*	0.113	0.103

r = Pearson correlation coefficient

Randomisation tests with 5000 permutations show significance values of $p<0.05$ for all significant correlations between matrices.

4.3.5. Summary

Overall, there is no asymmetry between the between left and right radial curvature (medial or lateral). For the ulna there is some asymmetry in the medial curvature and the mediolateral sinusoidal shape of the shaft.

The predictions that curvature of the radius and ulna would be related to body size and activity levels were not met. There is no sexual dimorphism in radial curvature or in ulnar shaft shape but males are more robust. There are no general trends through time in Europe or with individual age. Curvature does not vary significantly between groups with different activity levels. Within high activity groups, horticulturalists show the lowest degree of lateral curvature, and the equestrian foragers and pastoralists show the highest degree. Pastoralists are the most robust in both ulna and radius. There is a positive correlation between latitude and lateral radius curvature. The Mantel test also showed correlations between colder temperature and more pronounced curvature. Specimens with more robust radii have less medial curvature.

A minority of the analyses presented here was exploratory rather than performed to address specific predictions. The significant results from these analyses were used to aid the interpretation of long bone curvature. However, there were a few significant results which did not fit any a priori expectation and for which the significance was close to 0.05. Therefore, it is likely that these occurred because multiple tests were conducted on the same data, and the Bonferroni correction was not applied (see section 3.3). These results include the straighter proximal posterior femoral diaphyses of males, whereas those of females slope posteriorly (pcurveAMHPC2, Student's *t*-test, p=0.031), and the more medial projection of the proximal ulna and more medially facing trochlear notch of older individuals (proxAMHPC1 Kendall tau b; r=0.182, P=0.041). There are a couple of cases where the significance value is low, but the results did not follow the predicted trend and cannot be functionally explained. These results are a more anteroposterior sinusoidal ulnar shaft in Neolithic populations (pcurveAMHPC3: ANOVA; F=3.326, P=0.022) and a deeper trochlear notch in the 18^{th}-19^{th} century sample (proxAMHPC4: ANOVA; F=4.881, P=0.003).

4.4. Systemic effects of curvature

The correlations between curvature of the different bones are weak (Table 4-116) (N=27 populations). Posterior femoral curvature and medial radial curvature are correlated. The anteroposterior sinusoidal shape of the ulna (posterior subtense) is correlated with lateral radial curvature and anterior femoral curvature.

Table 4-116 Pearson's correlations for curvature and apex of curvature PCs between the femur, radius and ulna (N=218).

		FemacurAMHPC1	FemPcurvAMHPC1	RadmcurveAMHPC1	RadlcurvAMHPC1
Radmcurve AMHPC1	r	0.051	-0.108		
	P	0.456	0.110		
RadlcurvAMHPC1	r	-0.029	-0.136*		
	P	0.669	0.044		
UlnpcurveAMHPC1	r	-0.037	0.051	-0.032	-0.067
	P	0.591	0.452	0.642	0.327
UlnpcurveAMHPC2	r	0.022	-0.106	-0.088	-0.052
	P	0.750	0.118	0.196	0.447
UlnpcurveAMHPC3	r	0.151*	-0.005	-0.015	-0.158*
	P	0.026	0.941	0.830	0.019
UlnpcurveAMHPC4	r	0.042	-0.012	-0.037	-0.109
	P	0.540	0.862	0.590	0.110

* = Correlation is significant at the 0.05 level (2-tailed).

** = Correlation is significant at the 0.01 level (2-tailed).

4.5. Discussion

Three different hypotheses were proposed to explain the variation in long bone curvature between modern human populations in Chapter 2. The results of the foregoing analyses will be discussed in relation to the predictions of these hypotheses.

Hypothesis 1: A high degree of curvature is related to body size.

Long bone curvature in mammals is allometrically scaled with body size (Biewener, 1983; Swartz, 1990). Biewener (1983) suggested that increased curvature is a mechanism by which animals reduce bone stresses because curvature responds more rapidly to body size increase than does bone cross-sectional area. Loading of the femoral diaphysis in humans is proportional to body size (Ruff, 2000b) and morphological features, such as robusticity, are also allometrically related to body size. On this basis, a relationship between curvature and body size is predicted in the load-bearing femur. The relationship is expected to be somewhat different in the arm as the ulna and radius are not weight-bearing bones and, therefore, are not axially loaded.

Femur

For this sample, the results demonstrate that there is a relationship between external robusticity and body size (estimated using femoral head diameter as a proxy) for both the femur and radius. However, none of the curvature PCs of the femur are correlated with body size, except in the populations with high activity levels where division of labour is most pronounced.

Lower arm

External robusticity is related to body size (estimated using femoral head diameter). There is no correlation between the curvature of the radius and the ulna and body size. There is a difference between males and females in forearm robusticity but not in curvature of the radius. Females with high activity levels have a more mediolateral sinusoidal shape compared to males, but this difference is not present for the whole sample.

Although there is a difference in femoral curvature between males and females in populations with high activity levels, the lack of sexual dimorphism in long bone curvature for the whole

sample suggests that the differences are not due to the fact that males have larger bodies or because they have different hormone levels.

Hypothesis 2: Curvature is a response to increased activity levels.

Femur

Femoral curvature has two aspects. The first is the degree of curvature and the second is the position of the apex of curvature. These are not statistically covariates but they behave similarly in their relationships with habitual behaviour and environmental factors. In general, as degree of curvature increases, the apex of curvature moves inferiorly. This confirms the hypothesis suggested by Shackelford and Trinkaus (2002) that a high degree of curvature is associated with a more inferior apex of curvature.

Individuals from populations with high activity levels have more curved femora and have a lower apex of curvature than those from populations with moderate and low activity levels. This relationship with activity is also reflected in a correlation of femoral curvature with skeletal measures of activity such as external robusticity. It was predicted that if curvature and robusticity were related that there would be a decrease in femoral curvature occurring with agriculture and then with urbanism (Ruff *et al.*, 1993; Trinkaus and Ruff, 1999b; Ruff and Trinkaus, 2000; Holt, 2003). This is confirmed in the temporal trend for femoral curvature in the European sample and supports the hypothesis suggested by Shackelford and Trinkaus (2002) that low levels of curvature are related to a decrease in long-distance mobility. There is also no trend in curvature with increasing age and decreasing activity intensity, however.

For the sample of high activity level populations, males have more curved femora than do females. This difference disappears when the whole sample is considered and reflects a postulated reduction in division of labour from the onset of the adoption of agriculture where both sexes participate in agricultural activities (Ruff, 1999). Ruff (1999) suggests the importance of terrain relief on anteroposterior hypertrophy of the femoral shaft. During downhill walking the impact of the force is dissipated at incremental angles rather than at a straight angle through the bone resulting in less impact on the joints. The estimation of terrain relief for each of the modern human samples was beyond the scope of this study, but a matrix correlation between anterior femoral curvature and altitude of the mean location of population (which could

potentially serve as a proxy for relief), show that there is potential to develop this idea further. In order to do this, it would be necessary to include samples in these analyses for which terrain relief and home range data is available and for which other factors such as climate, and activity levels remain constant.

These results support the hypothesis that femoral curvature is a bone response to stresses and strains present during habitual behaviour. Populations with an aquatic subsistence strategy have less biomechanical stress on the lower limb (Stock and Pfeiffer, 2001; Stock, 2002; Stock, 2006) compared to the other subcategories within high activity groups, and this is shown in that the lowest degree of curvature and highest apex of curvature in aquatic foragering populations. The pastoralists have the highest terrestrial mobility and also the highest degree of curvature.

The results presented here demonstrate the potential of femoral curvature as a predictor of activity intensity. Femoral curvature may be a better predictor than cross-sectional robusticity (Ruff, 1987; Pearson, 2000b; Ruff and Trinkaus, 2000; Stock, 2002; Stock and Pfeiffer, 2004; Stock, 2006) which is affected also by both activity levels and climate (Pearson, 2000b; Stock, 2006).

There were four biomechanical hypothese for long bone curvature: 1) curvature lowers bending stress by translating bending stress to axial compression (Frost, 1967; Hall, 2004), 2) curvature facilitates muscle expansion and packing (Lanyon *et al.*, 1979; Lanyon, 1980), 3) curvature is a compromise between bone strength and predictability of bending strains and material failure (Lanyon, 1980, 1987; Bertram and Biewener, 1988), or 4) generates strains necessary for optimal strength (Lanyon, 1980). Out of the four biomechanical hypotheses for long bone curvature that were suggested in Chapter 2, it is unlikely that the stress reduction hypothesis (Frost, 1967) accounts for the differences in femoral curvature between these human populations as it has been widely demonstrated that most of the stress in the long bones is bending stress and that increased curvature is correlated with increases in bending stress (Lanyon and Baggott, 1976; Lanyon and Bourn, 1979; Lanyon *et al.*, 1979; Lanyon, 1980; Biewener, 1983; Lanyon and Rubin, 1986; Lanyon, 1987; Bertram and Biewener, 1988; Swartz, 1990; Biewener and Bertram, 1994; Main and Biewener, 2004).

The second hypothesis suggests that curvature facilitates muscle packing (Lanyon, 1980). By increasing curvature the tendons are able to attach close to the joints while the curvature of the

shaft accommodates the large bellies of the muscles in the midshaft region (Lanyon, 1980). During ontogeny the development of the muscles on the concave side of the shaft increases the periosteal pressure on the shaft which results in increased concavity and curvature. This hypothesis is supported by the radius and tibia of many mammals (Lanyon, 1980), but Swartz (1990) found no correlation between musculature and curvature in anthropoids. However, this study does provide support for the hypothesis in that increased curvature is found in humans from groups with high activity levels who are likely to be more muscular than those from groups with lower activity levels

The third hypothesis suggests that a high degree of curvature increases bending moments which ultimately may increase bone strength. Maintaining a moderate amount of strain is necessary for maintenance of bone mass (Lanyon, 1980; Biewener, 1983; Biewener and Bertram, 1994; Pearson and Lieberman, 2004; Ruff *et al.*, 2006). Therefore, increased curvature may provide a physiological benefit without affecting second moments of area or cross-sectional area (Lanyon, 1980). This is supported in the results from this study in that high degrees of femoral curvature tend to be correlated with increased levels of robusticity.

The fourth hypothesis suggests that curvature gives predictability to the direction of bone failure (Lanyon, 1980, 1987; Bertram and Biewener, 1988). Because the bone is loaded through bending stress rather than axially when it is curved, it is predicted that if a large amount of stress is applied, the bone is most likely to suffer from failure (fracture) in the direction of the curvature. Therefore, rather than maintaining low amounts of strain by having a straight and axially loaded shaft, curvature serves as safety factor of a biological structure requiring increased strength in a single location, rather than across the bone (Alexander, 1981). This is supported by the results presented here in that individuals with a higher degree of curvature have a more anteroposteriorly wide shaft. Results from studies of cross-sectional robusticity suggest that the cortical bone at midshaft is thickened in the anteroposterior plane (Ruff, 1999), and therefore in the direction of the curve, rather than in the mediolateral plane. In order to fully understand this interaction, however, it is necessary to combine the curvature data with measures of cross-sectional geometry.

The shape analysis also found that the human femoral shaft shows variation in the sinusoidal shape of the lateral side of the shaft. Populations with lower activity levels had significantly more sinusoidal femoral shafts compared to the moderate and high activity group. These

differences could be due to a decrease in bone remodelling rates and lack of physiologically beneficial strains in the shaft. Lower levels of habitual loading can potentially cause the bone to be less dense and, therefore, more susceptible to the pressure of muscles, or cause the bone to take on a sinusoidal shape because there is no need for maintaining structural integrity. The lack of a correlation with other morphological and behavioural factors makes the sinusoidal aspect of femoral curvature difficult to interpret.

In summary, the hypotheses discussed above suggest that femoral curvature is a result of increased activity levels and can be biomechanically explained by facilitating greater muscle mass, generating physiologically beneficial strains and may increase the predictability of material failure.

Lower arm

The radius has two curves which were used in the analyses. The medial curve describes the development of the interosseous crest, whereas the lateral curved describes the overall degree of curvature of the bone. There was no difference between populations representing the different activity levels for either the medial or the lateral curve. However, there were some differences between the subsistence groups. The horticulturalists were the least curved. Horticulturalists use their upper limbs for subsistenc-related activity, though, so this result cannot be explained by intensity of subsistence-related activity.

It was predicted that the aquatic foragers would have the highest degrees of overall curvature. They had a high degree of lateral curvature but a low degree of medial curvature reflecting the strong development of the interosseous crest. The aquatic foragers also had a proximal medial development on the interosseous crest and a medially expanded ulnar notch. These may reflect the increased use of the forearm during the use of watercraft and stronger development of the interosseous membrane. Although none of the shaft shape PCs of the ulna showed differences between the activity levels or subsistence groups, the aquatic foragers have the longest ulnar neck (greatest distance between the tip of the coronoid and the 80% level of the shaft). While it was predicted that there would be a correlation between the position of the radial tuberosity and the neck-length of the radius and radial curvature these predictions were not supported by the results. There was no difference between males and females and radial curvature and ulna shaft shape.

Although some of the results support the hypothesis that curvature is a bone response to stresses and strains during habitual behaviour, the results are inconclusive and may be explained by the differences in climate instead (see more below).

Hypothesis 3: Curvature is a consequence of adaptation to cold climate.

Based on Bergmann and Allen's rule related to body size and body proportions, it is known that individuals from colder climates have shortened distal limbs and that these differences are established through genetic adaptations rather than individual ontogeny (Y'Edynak, 1976; Eveleth and Tanner, 1990; Ruff *et al.*, 1994; Pearson, 2000b; Van Andel, 2003; Weaver, 2003; Ruff *et al.*, 2005). Foreshortening of the limbs may have an effect on curvature.

Femur

As was shown in the past (Pearson, 2000b; Stock, 2006), there was a significant correlation between latitude and robusticity. Neither femoral curvature nor apex of curvature shows any significant patterns with latitude, despite the correlation of latitude with other morphological features, such as femoral length and epiphysis size. This would suggest that other morphological elements that are under strong climatic influence, such as the pelvis width, neck-shaft angle (correlated with torsion angle) and body size (from femoral length) (Ruff, 1995; Weaver, 2003) would not be correlated with curvature. With the exception of pelvis width, all these variables were explored, and none were correlated with either degree of curvature or position of the apex of curvature. Therefore, femoral curvature is not a consequence of adaptation to cold climate.

Lower arm

Lateral curvature of the radius is related to climate. This is also reflected in the higher degree of lateral curvature for the aquatic foragers who have the lowest mean annual temperature (Inuit, Russian Eskimo, Greenland Inuit – but less Andamanese). The low degree of curvature for the horticulturalists can be explained by the relative warm climate in which these groups live (New Mexico and Ohio). The development of the proximal interosseous crest of the radius is also highly correlated with climate but is likely a sign of the habitual aquatic subsistence-related behaviour (such as the use of watercraft). The aquatic foragers show a higher radial neck-shaft

angle which may be related to the use of the forearm during the use of watercraft or fishing. Aquatic foragers do not stand out in the other univariate measurements of the radius or ulna.

Robusticity of the distal articulation of both the ulna and the radius is highly correlated with climate reflecting the relatively short forearm bones. The radius in populations from higher latitudes is more sinusoidal but shows no particular patterns in the rest of its morphology with climate other than curvature. For the ulna there are some interesting patterns. Individuals from higher latitudes have larger proximal ulnas, larger neck-shaft angles (joint-axis angle), a more inferior insertion of the brachial tuberosity, a smaller distance between 80% of the shaft and the tip of the olecranon, a more proximoanterior trochlear notch, a more anteroposteriorly sinusoidal shape, a less mediolateral sinusoidal shape and a larger radial notch surface area. The anteroposterior sinusoidal shape of the ulna is correlated with lateral curvature of the radius and reflects the posterior subtense discussed in Fischer (1909).

An increase in lateral radial curvature, a more sinusoidal radial shaft and the increased anteroposterior sinusoidal shape of the ulna is likely a consequence of the shortening of the lower limbs. In the light of the biomechanical hypotheses discussed above for the femur, curvature of the ulna and radius cannot be explained by factors caused by axial loading of the shaft. Curvature of the forearm is most likely a way of facilitating muscle packing in response to the reduction in relative long bone length in cold-adapted populations. Maintaining the tendon insertions of muscles close to the joints and preventing shortening of the muscles inserting on the shaft (and therefore prevent loss of contraction function of the *pronator teres*) aids horizontal muscle packing by allowing space for the muscle bellies (Lanyon, 1980). It also maximises the degree of pronation and supination by maintaining the size and axis of rotation (Yasutomi *et al.*, 2002). The next step in testing this hypothesis is to combine data from this study with data on muscle development.

The other biomechanical hypotheses explaining curvature of the forearm do not have any direct support from the data in this study. Despite the size of the radial articular surfaces being correlated with radial curvature, there is no correlation with midshaft robusticity. The correlations between ulnar shaft shape and robusticity are not consistent across the bone. Therefore, these results are inconclusive in their support for the "material failure predictability" hypothesis (Bertram and Biewener, 1988). In order to test the hypothesis of physiological benefit to the bone, it is necessary to combine the curvature data of the forearm sample in this study

with measures of cross-sectional geometry. Very little is known about cross-sectional geometry of the ulna and radius and midshaft shape of the radius and external shape ratios in these modern human samples were not correlated with lateral or medial curvature.

Predicting curvature in Neanderthals and early modern humans.

The results of the variation in curvature of the femur, ulna and radius within modern humans indicate that there are patterns of longitudinal long bone curvature but that these are different for the upper and lower limb. Several of the conclusions from the analyses of recent humans are especially relevant and can provide a framework for looking at the meaning of long bone curvature in Palaeolithic samples. Long bone curvature follows different trends than robusticity and is not necessarily a response to the same types of loading (Ruff *et al.*, 1993; Ruff *et al.*, 1994; Trinkaus *et al.*, 1994; Trinkaus *et al.*, 1999a; Pearson, 2000b; Ruff and Trinkaus, 2000; Shackelford and Trinkaus, 2002; Stock, 2002; Stock and Pfeiffer, 2004; Stock, 2006; Carlson *et al.*, 2007; Shackelford, 2007).

The highest levels of curvature for the femur were identified in samples with high activity levels. Therefore, it is hypothesised that both early modern humans and Neanderthals will possess high degrees of femoral curvature and a more distal apex of curvature. The curvature of the radius and ulna is strongly influenced by climate. Individuals from colder climates tend to have more curved ulnae and radii. Neanderthals, as a group, were subject to cold climatic conditions for a more extended period of time than any modern human population, so it is hypothesised that they have "hyperpolar" adaptations to the climate in which they lived (Boule and Vallois, 1952; Trinkaus, 1981; Churchill, 1998; Pearson, 2000a, 2000b; Aiello and Wheeler, 2003; Weaver, 2003; Krause *et al.*, 2007; Shackelford, 2007). Hence, the Neanderthals radius is predicted to have a higher degree of lateral curvature and a more sinusoidal shape, and the ulna is predicted to be more anteroposteriorly sinusoidal than any other modern human sample. The early modern humans are predicted to have less radial and ulnar curvature than Neanderthals as they were not exposed to the cold European climate for the same extended time. Depending on the time the early modern humans spent in the cold European climate, it can be hypothesised that they, too, may have a high degree of curvature. However, as modern humans were likely to have originated in tropical Africa (Mellars and Stringer, 1989; Smith *et al.*, 1989; Bar-Yosef, 1992; Deacon, 1992; Stringer, 1992; Ingman *et al.*, 2000; Pearson, 2000a; Stringer, 2002; White *et al.*, 2003; Mellars, 2004) they may display very low levels of curvature.

These hypotheses will be tested in Chapter 5.

CHAPTER 5. LONG BONE CURVATURE IN NEANDERTHALS, EARLY AND RECENT MODERN HUMANS.

5.1. Objective

The purpose of the interspecific analyses is to determine where fossil specimens fall relative to patterns of variation in long bone curvature in recent modern humans. The Neanderthal and early modern human fossil specimens are included in the General Procrustes Analyses and in the Principal Component analyses. The inclusion of the fossils in the Principal Component analysis slightly changes the distribution of the shape changes along the principal components and will be discussed below.

In order to examine variation in long bone morphology, the principal component scores are used in Analyses of Variance (ANOVAs) and post-hoc tests using pairwise comparisons. As in Chapter 4, the Hochberg GT2 and Games-Howell procedures were used (discussed in more detail in Chapter 3: Materials and Methods) and the results will be discussed for significant F-scores. For these analyses, fossil hominins are either grouped as Neanderthals or early modern humans. To determine the relationship between the different aspects of morphology and group differences, discriminant functions are calculated using the principal component scores as independent variables.

In the results described below the abbreviations of the principal components (PCs) names are made up of three parts. The first designates the landmark set included in the study (i.e. "acurve" stands for anterior curve). The second designates the sample included (i.e. "ALL" stands for all fossils and all recent modern humans). The third is the PC number (i.e. "PC2" stands for second PC), e.g. "AcurveAllPC1".

5.2. Femur

5.2.1. Femur principal components explained

As was the case for the investigation of intraspecific variation within modern humans, the changes for each of the curves and the proximal and distal epiphyses (epiphyses) along each principal component are visualised using Morphologika®. Although the PCs are very similar to those obtained when only the modern humans are considered, there are differences between the PC scores and shape changes along the PCs. Therefore, the PCs will be explained again below. The figures presented correspond to the most extreme positive and negative individuals on the scale for each PC. The curves are semi-landmarks only, whereas the epiphyses are landmarks. Viewing angles were chosen to illustrate similarities and differences most clearly. For the curves, this is in lateral view, unless otherwise stated in the Figure captions. The Neanderthal sample consists of eight specimens, the early modern humans sample consists of 13 specimens, and 428 individuals are included in the recent modern human sample.

5.2.1.1. Anterior surface (acurve)

The first three principal components explain 63.7%, 9.62%, and 7.30% of the variance, ,respectively ,(total 80.06%). Subsequent PCs explain minimal amounts of the variation and are not considered further.

AcurveAllPC1 reflects variation in degree of anterior curvature or subtense (Figure 5-1a). The second principal component (acurveAllPC2) is related to the position of the apex of curvature (Figure 5-1b). The third principal component is the shape of the shaft in anterior view (Figure 5-1c). Negative values are more sinusoidal, whereas positive values are straight.

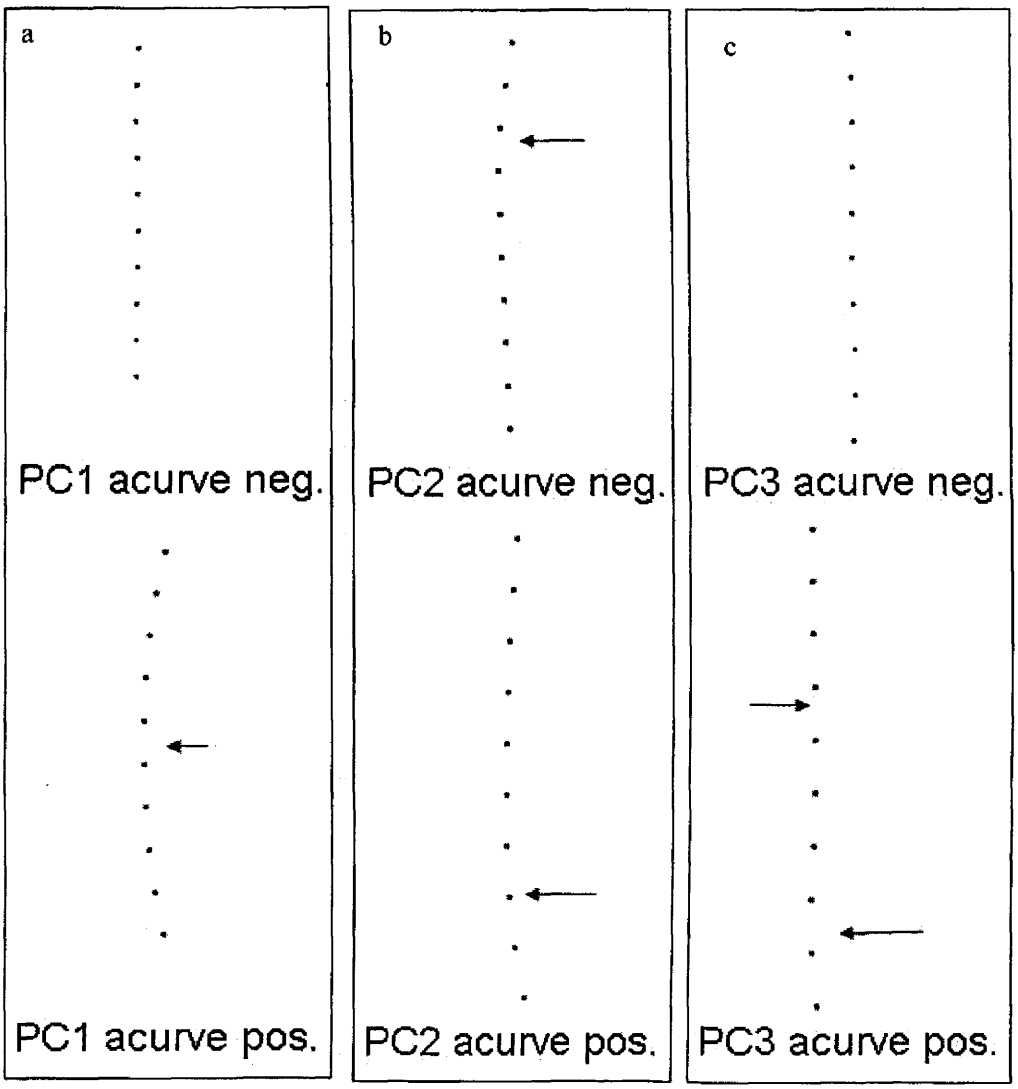

Figure 5-1 Morphological trends for the anterior curve of the femur for Neanderthals, early and recent modern humans.

a: Principal component 1: lateral view. Negative values are less curved, positive values are more curved. **b**: Principal component 2: lateral view. Individuals with negative values have a more proximal apex of curvature, whereas those with positive values have a more distal apex of curvature. **c**: Principal component 3: anterior view. Negative values are the straightest, whereas positive values indicate a mediolaterally sinusoidal shape. Positive and negative visualisations correspond to the most extreme positive and negative scores for each PC.

5.2.1.2. Posterior surface (pcurve)

The first four principal components of the posterior curve analysis explain 34.9%, 14.8%, 11.4% and 7.47%,,respectively, of the variation (total 68.5%). Subsequent PCs explain minimal amounts of the variation and are not considered further.

The posterior curve is very similar to the anterior curve. PcurveAllPC1 reflects differences in degree of curvature or subtense (Figure 5-2a) (note that pcurveAllPC1 is loaded in an opposite direction from the other curvature PCs). The second principal component (pcurveAllPC2) is the shape of the shape of the curve in posterior view (Figure 5-2b). The third principal component (pcurveAllPC3) is related to the apex of the posterior curve (Figure 5-2c). The fourth principal component (pcurveAMHPC4) is the direction of the distal end of the curve (Figure 5-2d).

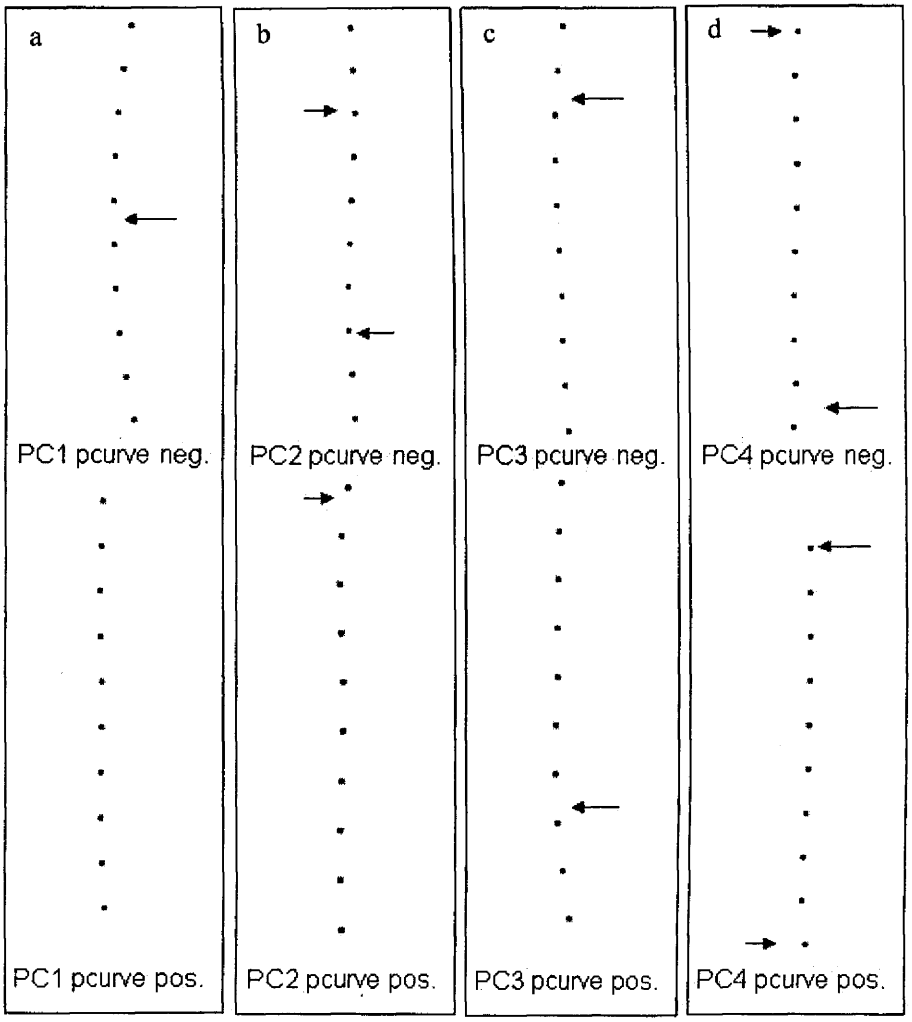

Figure 5-2 Morphological trends for the posterior curve of the femur for Neanderthals, early and recent modern humans.

a: Principal component 1: lateral view. Negative values are more curved, positive values are less curved. **b**: Principal component 2: anterior view. Negative values are the straightest, whereas positive values are mediolaterally sinusoidal. **c**: Principal component 3: lateral view Negative values have a higher apex of curvature compare to positive values. **d**: Principal component 4: lateral view. Positive individuals have a more posteriorly projected distal curve. Positive and negative visualisations correspond to the most extreme positive and negative scores for each PC.

5.2.1.3. Medial surface (mcurve)

The first three principal components of the medial curve analysis explain 49.9%, 16.6%, and 15.39% ,respectively ,of the variation (total 83.1%). Subsequent PCs explain minimal amounts of the variation and are not considered further.

As was the case in the analysis on modern humans the component mcurveAllPC1 reflects differences in degree of anterior curvature (Figure 5-3a). The second principal component (mcurveAllPC2) is related to the position of the apex of curvature (Figure 5-3b). The third principal component (mcurveAllPC3) is the posterior extension of the distal end of the curve and the evenness of the curve (Figure 5-3c).

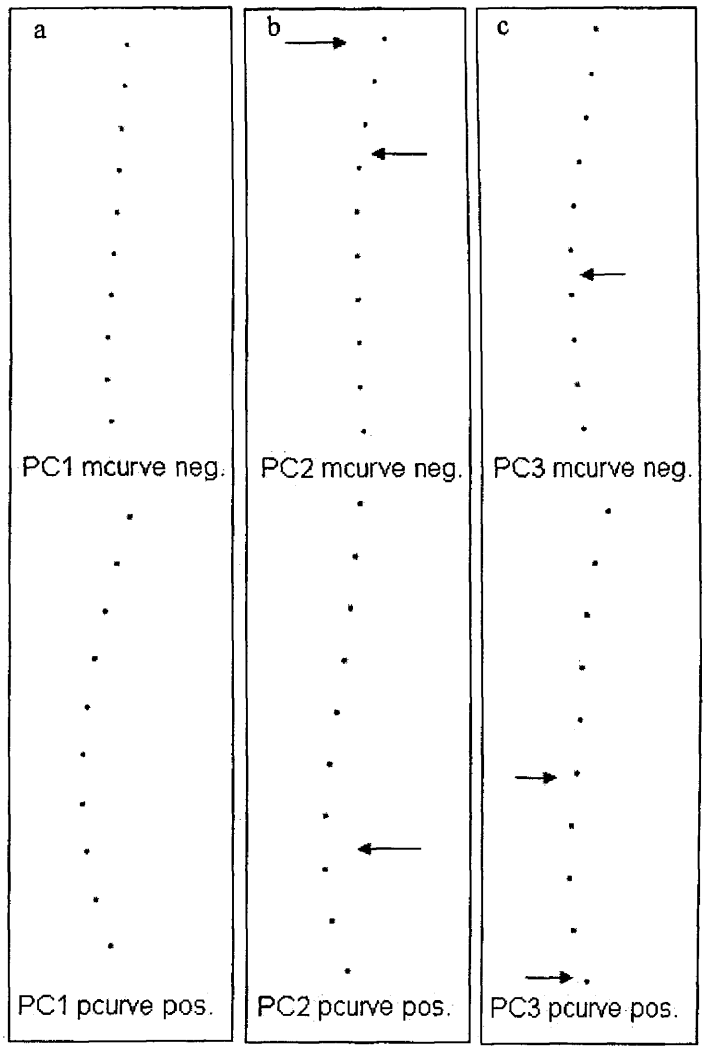

Figure 5-3 Morphological trends for the medial curve of the femur for Neanderthals, early and recent modern humans. All lateral view.

a: Principal component 1. Negative values are less curved, positive values are more curved. **b**: Principal component 2. Negative values have a higher apex of curvature compare to positive values. **c**: Principal component 3. Positive values are more flattened off with increased posterior projection of the distal curve, whereas negative values have a curve that approximates an arc of a circle. Positive and negative visualisations correspond to the most extreme positive and negative scores for each PC.

5.2.1.4. Lateral surface (lcurve)

The first four principal components of the lateral curve analysis explain 51.3%, 15.5%, 9.54% and 5.44%,,respectively, of the variation (total 81.78%). Subsequent PCs explain minimal amounts of the variation and are not considered further.

The component lcurveAllPC1 reflects differences in anterior curvature or subtense (Figure 5-4a). The second principal component (lcurveAllPC2) is related to the position of the apex of curvature and the direction of the proximal part of the surface (Figure 5-4b). The third principal (lcurveAllPC3) component is related to the "straightening" of the femur at the level of the lesser trochanter (Figure 5-4c). The fourth principal component (lcurveAllPC4) is the shape of the lateral surface in anterior view (Figure 5-4d).

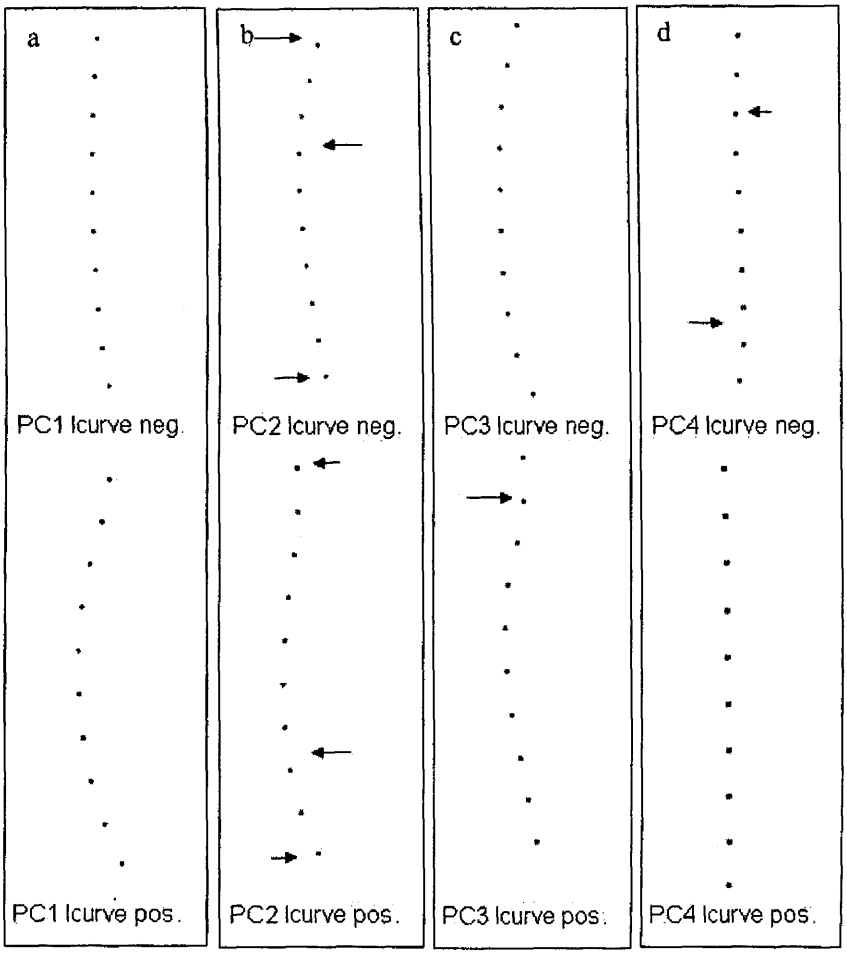

Figure 5-4 Morphological trends for the lateral curve of the femur for Neanderthals, early and recent modern humans.

a: Principal component 1: lateral view. Negative values are less curved, positive values are more curved. **b**: Principal component 2: lateral view. Negative values have a more distal apex of curvature and little posterior direction of the proximal curve, whereas those with positive values have a more proximal apex of curvature and a more posteriorly projecting proximal curve. **c**: Principal component 3: lateral view. Positive values show a flattening off at the level of the lesser trochanter and negative values are evenly curved. **d**: Principal component 4: anterior view. Positive values are the straightest, whereas negative values have a mediolaterally sinusoidal shape. Positive and negative visualisations correspond to the most extreme positive and negative scores for each PC.

5.2.1.5. Proximal and distal epiphyses (Epi)

The first five principal components of the epiphysis analysis explain 14.5%, 9.62%, 7.47%, 5.30% and 4.34%,,respectively, of the variation (total 43.9%). Subsequent PCs explain minimal amounts of the variation and are not considered further.

The component epiAllPC1 reflects differences in the width of the distal epiphyses and the neck-shaft angle (Figure 5-5a). The second principal component (epiAllPC2) is related to the overall width of the femur and the position of the lesser trochanter (Figure 5-5b). The third principal component (epiAllPC3) is related to the width of the distal epiphyses and degree of torsion (Figure 5-5c). The fourth principal component (epiAllPC4) is hard to interpret and it is unclear what it relates to. The changes along the principal component axis are very subtle and this PC will not be included in any of the the subsequent analyses. The fifth principal component (epiAllPC5) relates to the length of the neck and the depth of the distal epiphyses (Figure 5-5d).

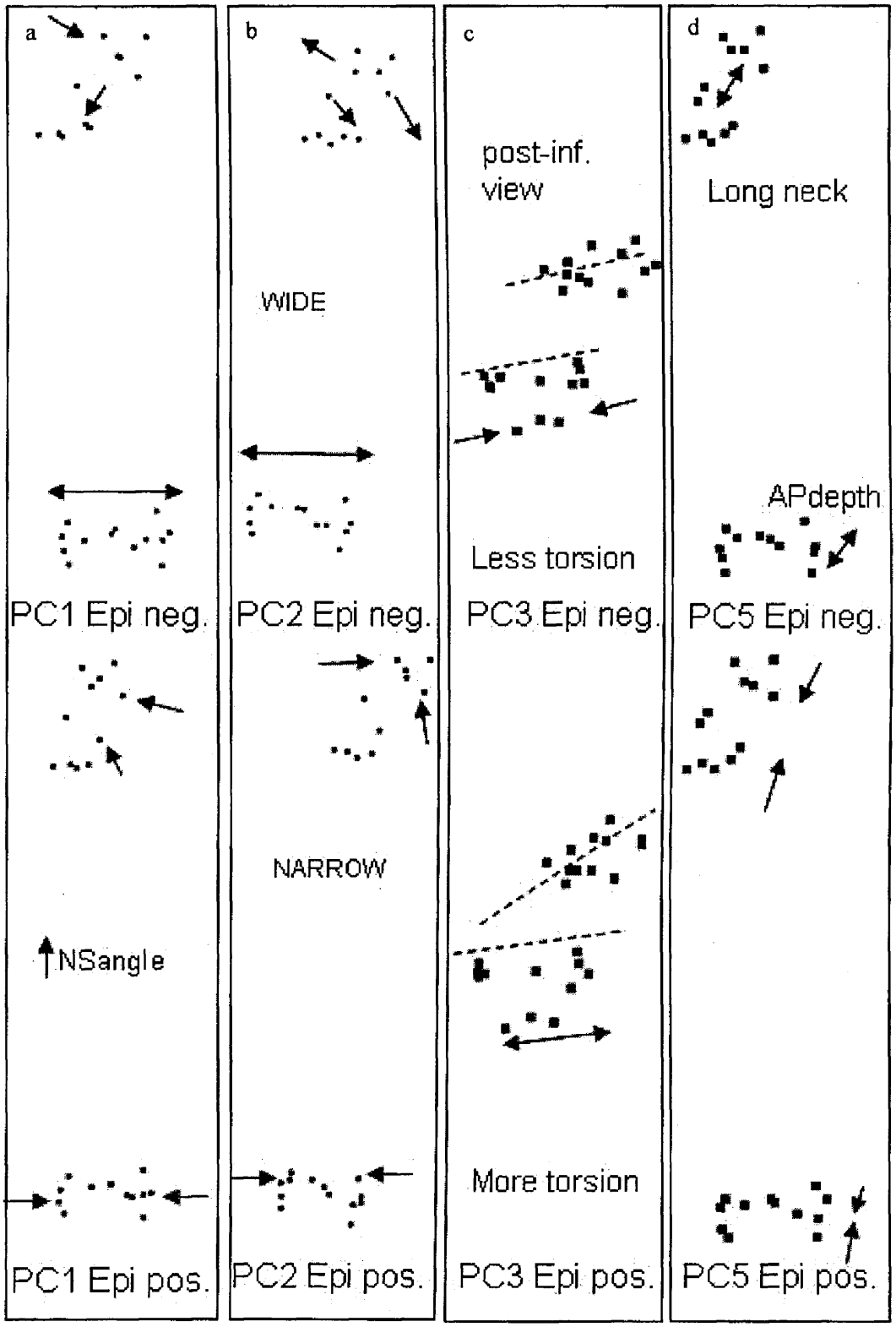
a
b
c
d
post-inf.
view
Long neck
WIDE
APdepth
Less torsion
PC1 Epi neg.
PC2 Epi neg.
PC3 Epi neg.
PC5 Epi neg.
NARROW
NSangle
More torsion
PC1 Epi pos.
PC2 Epi pos.
PC3 Epi pos.
PC5 Epi pos.

Figure 5-5 Morphological trends for the epiphyses of the femur for Neanderthals, early and recent modern humans.

a: Principal component 1: anterior view. Individuals with negative values have wider distal epiphyses and a lower neck-shaft angle. **b**: Principal component 2: anterior view. Negative values have wider distal epiphyses and heads and a lower lesser trochanter, whereas positive values are narrow and have a relatively higher lesser trochanter. **c**: Principal component 3: superior view. Individuals with negative values have wider distal epiphyses and less torsion than those with positive values. **d**: Principal component 5. Individuals with negative values have a long neck and deep knees compared to individuals with positive values. Positive and negative visualisations correspond to the most extreme positive and negative scores for each PC.

5.2.1.6. Summary

As in the analysis of recent modern human populations, anterior curvature is the most important principal component in all four curves (acurveAllPC1, pcurveAllPC1, mcurveAllPC1, lcurveAllPC1). This is reflected in the significant correlations between all these curves (note that pcurveAllPC1 is loaded in the opposite direction from the other curvature PCs and is therefore negatively correlated with them) (Table 5-1). For this reason, only acurveAllPC1 and pcurveAllPC1 will be analysed and discussed.

The position of the apex of curvature is the major factor in acurveAllPC2, pcurveAllPC3, mcurveAllPC2 and lcurveAllPC2, so only acurveAllPC2 and pcurveAllPC3 will be discussed. These are also all correlated, but none of the r-values are high (Table 5-2). The other principal components for the curves explain minor changes in surface shape and will be included in subsequent analyses.

Table 5-1 Pearson's correlation matrix: femoral curvature PCs (n= 449). Neanderthals, early and recent modern humans.

		AcurveAllPC1	pcurveAllPC1	McurveAllPC1
pcurveAllPC1	r	-0.529**		
	P	<0.001		
McurveAllPC1	r	0.645**	-0.271**	
	P	<0.001	<0.001	
LcurveAllPC1	r	0.601**	-0.434**	0.368**
	P	<0.001	<0.001	<0.001

* = Correlation is significant at the 0.05 level (2-tailed).
** = Correlation is significant at the 0.01 level (2-tailed).

Table 5-2 Pearson's correlation matrix: femoral apex of curvature PCs (n= 449). Neanderthals, early and recent modern humans.

		AcurveAllPC2	pcurveAllPC3	McurveAllPC2
pcurveAllPC3	r	0.172**		
	P	<0.001		
McurveAllPC2	r	0.361**	0.152**	
	P	<0.001	<0.001	
LcurveAllPC2	r	0.389**	0.177**	0.213**
	P	<0.001	<0.001	<0.001

* = Correlation is significant at the 0.05 level (2-tailed).
** = Correlation is significant at the 0.01 level (2-tailed).

5.2.2. Differences in femoral morphology between Neanderthals, early and recent modern humans.

5.2.2.1. Curvature

The groups are significantly different for both curvature PCs: acurveAllPC1, pcurveAllPC1 (Table 5-3). Neanderthals have the highest degree of anterior and posterior curvature, followed by early modern humans. Recent modern humans are the straightest (Figure 5-6 and Figure 5-7). Statistically, Neanderthals are different for both principal components from recent modern humans. Early modern humans are different from Neanderthals for acurvAllPC1 only (Appendix 39). Box plots are used in order to display curvature and apex of curvature for the separate fossils.

Table 5-3 ANOVA results for palaeogroup[1] and femoral curvature PCs.

d.f.=2	F	Sig.
AcurveAllPC1	22.839	<0.001*
pcurveAllPC1	31.810	<0.001*

*=significant at α=0.05

[1] Palaeogroup refers to the three categories commonly used in palaeoanthropological research that are included in these analyses: Neanderthals, early anatomically modern humans, recent modern humans.

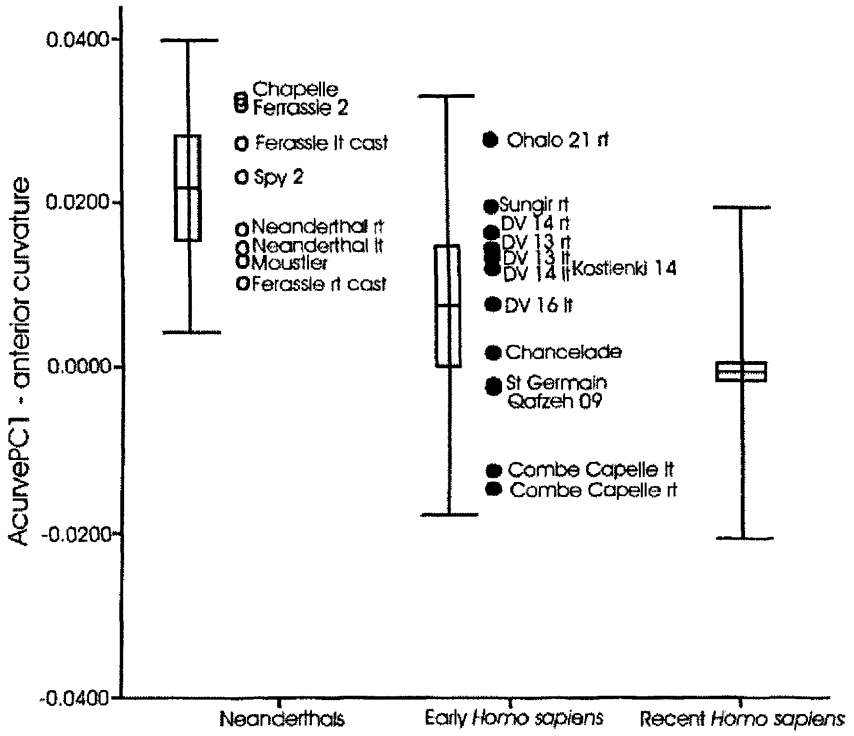

Figure 5-6 The anterior curve of the femur for Neanderthals, early and recent modern humans. (Line=mean, Box= 2 S.E., whiskers: 2 S.D.). The higher values for Neanderthalss indicate that they are more curved than the modern humans.

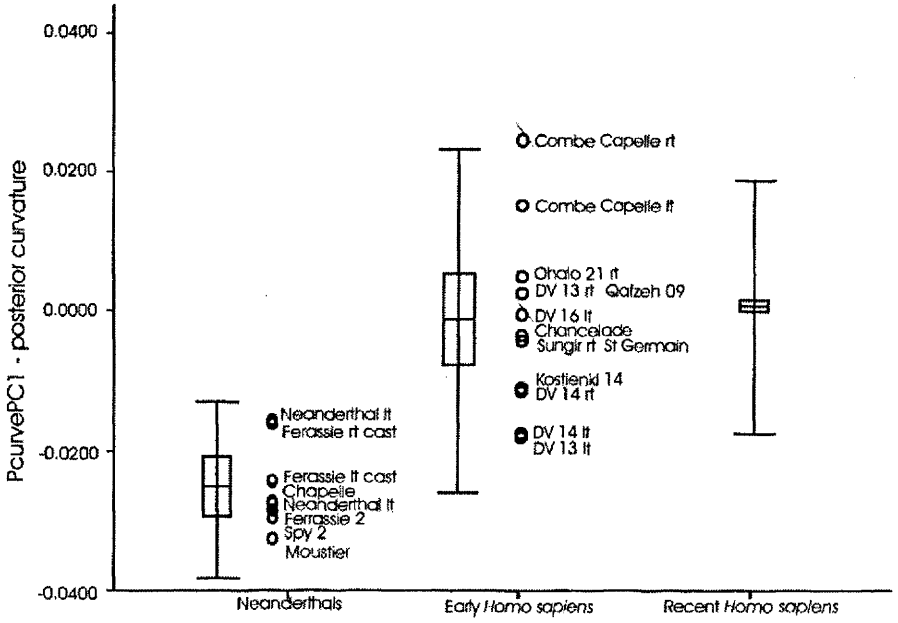

Figure 5-7 The posterior curve of the femur for Neanderthals, early and recent modern humans. (Line=mean, Box= 2 S.E., whiskers: 2 S.D.). The lower values for Neanderthal indicates that they are more curved than the modern humans.

5.2.2.2. Apex of curvature

The groups are significantly different for the position of the apex of curvature in one PC (Table 5-4). On the anterior surface, Neanderthals have the lowest apex of curvature and are significantly different from early and recent modern humans (Figure 5-8 and Appendix 40).

Table 5-4 ANOVA results for palaeogroup and femoral apex of curvature PCs.

d.f.=2	F	Sig.
AcurveAllPC2	9.376	0.000*
pcurveAllPC3	0.365	0.694

*=significant at α=0.05

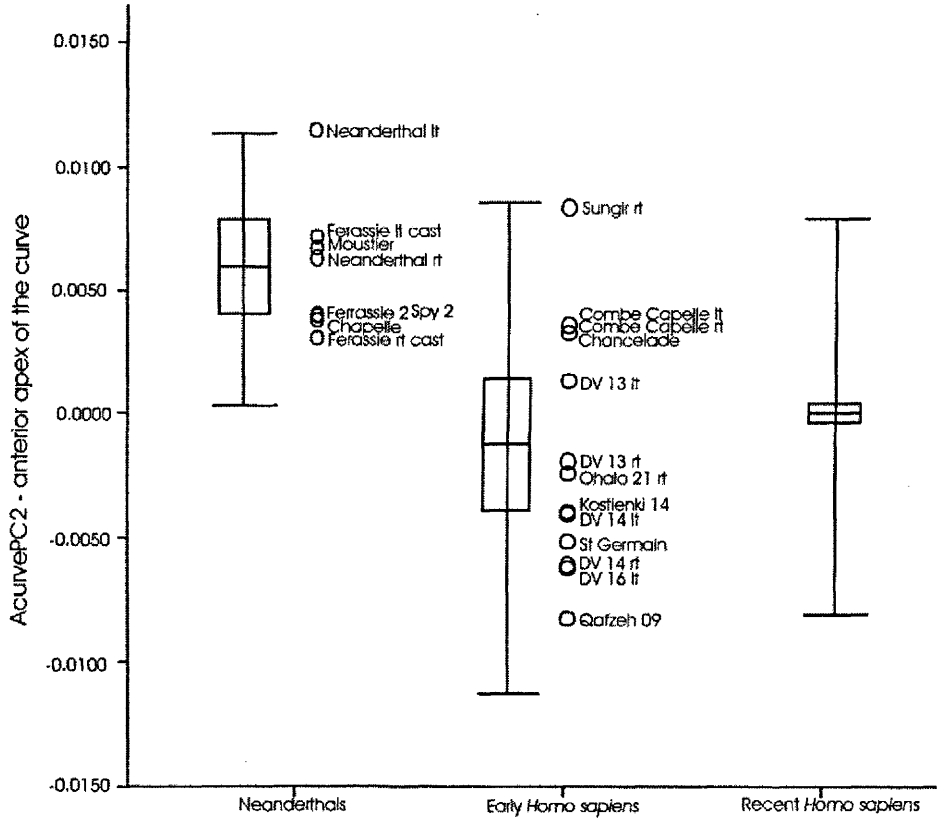

Figure 5-8 The anterior apex of curvature of the femur for Neanderthals, early and recent modern humans. (Line=mean, Box= 2 S.E., whiskers: 2 S.D.). The higher value for Neanderthals indicates a lower apex of curvature.

5.2.2.3. Other shaft shape

The groups are significantly different for only one of the other shaft shape PCs (Table 5-5). The post-hoc tests shows that Neanderthals may have a lateral curve that straightens at the level of the lesser trochanter (lcurveAllPC3)(Appendix 41).

Table 5-5 ANOVA results for palaeogroup and other femoral shaft shape PCs.

d.f.=2	F	Sig.
AcurveAllPC3	0.263	0.769
pcurveAllPC2	1.510	0.222
pcurveAllPC4	1.736	0.177
McurveAllPC3	1.925	0.147
LcurveAllPC3	3.010	0.050*
LcurveAllPC4	2.345	0.097

*=significant at α=0.05

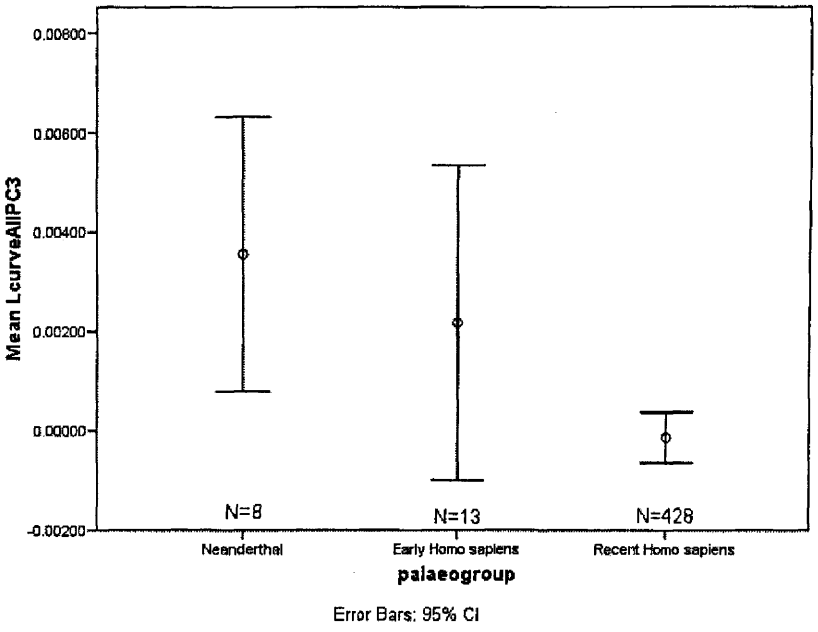

Figure 5-9 LcurAllPC3 for Neanderthals, early and recent modern humans.
The lower values for Neanderthals indicate wider distal epiphyses and a lower neck-shaft angle. Mean and 95% confidence interval (whiskers).

5.2.2.4. Epiphysis shape

Neanderthals have more robust epiphyses, a lower neck-shaft angle and a lower lesser trochanter than early and recent modern humans (EpiAllPC1 and EpiAllPC2) (Table 5-6 and Figure 5-10 and Figure 5-11; Appendix 42). Neanderthals also have less torsion (EpiAllPC3) (Figure 5-12) and a long neck and deep distal condyles (EpiAllPC5) (Figure 5-13).

Table 5-6 ANOVA results for palaeogroup and other femoral shaft shape PCs.

d.f.=2	F	Sig.
EpiAllPC1	14.000	<0.001*
EpiAllPC2	5.954	0.003*
EpiAllPC3	3.179	0.043*
EpiAllPC5	4.825	0.008*

*=significant at α=0.05

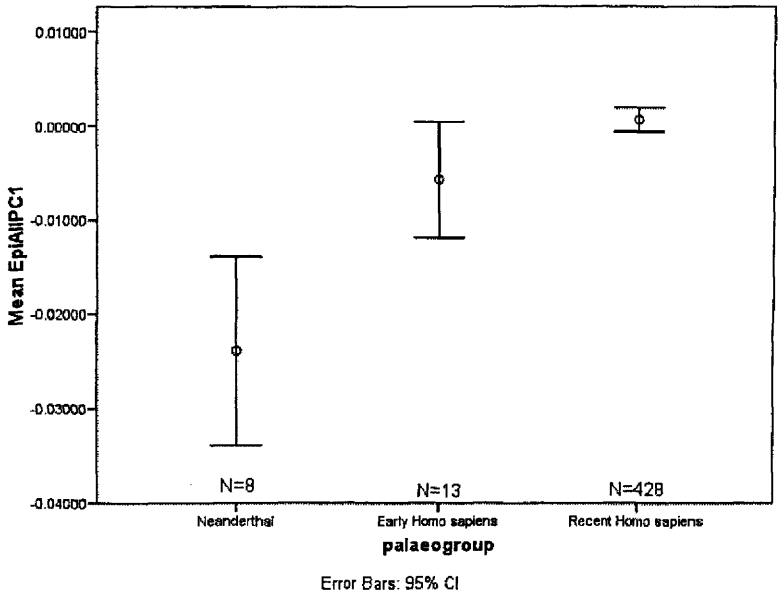

Figure 5-10 EpiAllPC1 for Neanderthals, early and recent modern humans.
The lower values for Neanderthals indicate wider distal epiphyses and a lower neck-shaft angle. Mean and 95% confidence interval (whiskers).

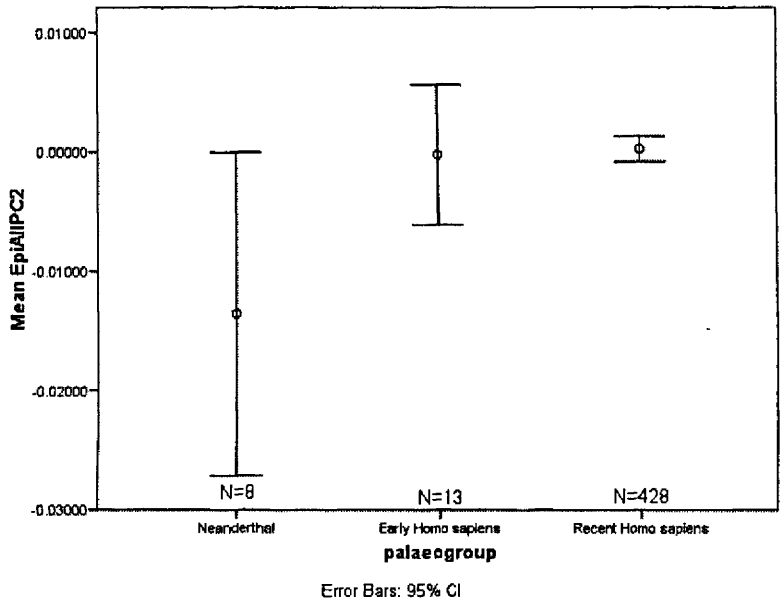

Figure 5-11 EpiAllPC2 for Neanderthals, early and recent modern humans.

The lower values for the Neanderthals indicate wider distal epiphyses and heads and a lower lesser trochanter. Mean and 95% confidence interval (whiskers).

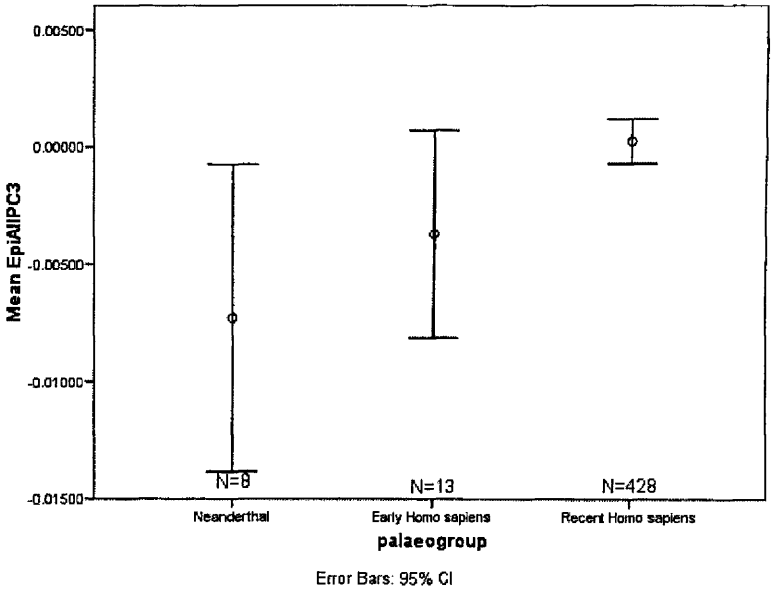

Figure 5-12 EpiAllPC3 for Neanderthals, early and recent modern humans.

The lower values for Neanderthals indicate wider distal epiphyses and less torsion than modern human groups with positive values. Mean and 95% confidence interval (whiskers).

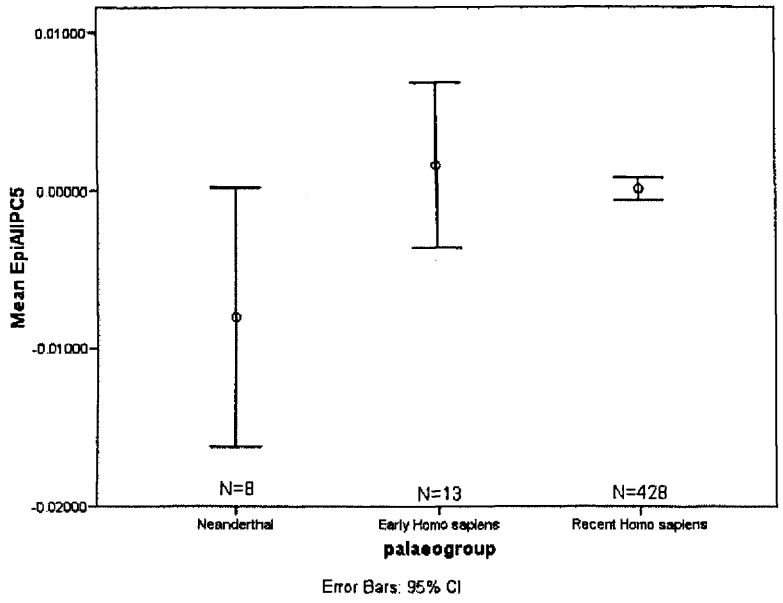

Figure 5-13 EpiAllPC5 for Neanderthals, early and recent modern humans.
The lower values for Neanderthals indicate a long neck and anteroposteriorly deep distal epiphyses. Mean and 95% confidence interval (whiskers).

5.2.2.5. Univariate measurements

The groups are significantly different for all univariate measurements (Figure 5.7). The highest F-scores are for head-robusticity, neck-length, neck-shaft angle and robusticity index (Table 5-8). Post-hoc tests (Appendix 43) indicate that Neanderthals have the largest femoral head, longest neck and largest distal epiphyses compared to early and recent modern humans, although their midshaft robusticity and neck-shaft angle is comparable to that of early modern humans (Figure 5-23; Figure 5-21 and Figure 5-15). Early modern human femora are longer and have lower torsion angles, are more robust, and have higher midshaft and subpilastric ratios than do recent modern humans (Figure 5-14; Figure 5-16; Figure 5-22; Figure 5-18; Figure 5-19). Early modern human femora have a high midshaft shape ratio, which probably reflects the strong expression of the linea aspera. Neanderthal femora have an almost round shaft at the midshaft level and lack a clear linea aspera (Figure 5-18).

Table 5-7 Descriptives for Neanderthals, early and recent modern humans and the univariate measurements of the femur.

		N	Mean	S.D.
Femur length	Neanderthal	8	430.25	32.06
	Early *Homo sapiens*	13	456.14	34.17
	Recent *Homo sapiens*	428	426.52	34.18
Neck-shaft angle	Neanderthal	8	118.68	5.21
	Early *Homo sapiens*	13	124.27	7.63
	Recent *Homo sapiens*	428	127.41	5.71
Torsion angle	Neanderthal	8	10.43	14.87
	Early *Homo sapiens*	13	11.17	9.02
	Recent *Homo sapiens*	428	16.73	6.91
subtrochratio	Neanderthal	8	84.87	10.42
	Early *Homo sapiens*	13	80.46	16.23
	Recent *Homo sapiens*	428	75.09	9.85
midshaftratio	Neanderthal	8	103.02	14.49
	Early *Homo sapiens*	13	128.38	20.95
	Recent *Homo sapiens*	428	114.16	19.11
subpilratio	Neanderthal	8	87.63	9.83
	Early *Homo sapiens*	13	102.06	18.80
	Recent *Homo sapiens*	428	88.08	15.73
condylediamratio	Neanderthal	8	18.87	1.39
	Early *Homo sapiens*	13	17.12	1.18
	Recent *Homo sapiens*	428	17.11	1.33
necklengthratio	Neanderthal	8	15.85	2.62
	Early *Homo sapiens*	13	13.98	1.09
	Recent *Homo sapiens*	428	13.87	1.07
robustindex	Neanderthal	8	13.66	1.01
	Early *Homo sapiens*	13	13.44	0.93
	Recent *Homo sapiens*	428	12.41	1.15
headrob	Neanderthal	8	22.35	1.00
	Early *Homo sapiens*	13	18.72	1.37
	Recent *Homo sapiens*	428	18.54	1.65

Table 5-8 ANOVA results for palaeogroup and femoral univariate measurements.

d.f.=2	F	Sig.
Femur length	4.775	0.009*
Neck-shaft angle	10.688	<0.001*
Torsion angle	6.679	0.001*
subtrochratio	5.363	0.005*
midshaftratio	4.933	0.008*
subpilratio	4.984	0.007*
condylediamratio	6.882	0.001*
necklengthratio	12.322	<0.001*
robustindex	9.604	<0.001*
headrob	21.204	<0.001*

*=significant at α=0.05

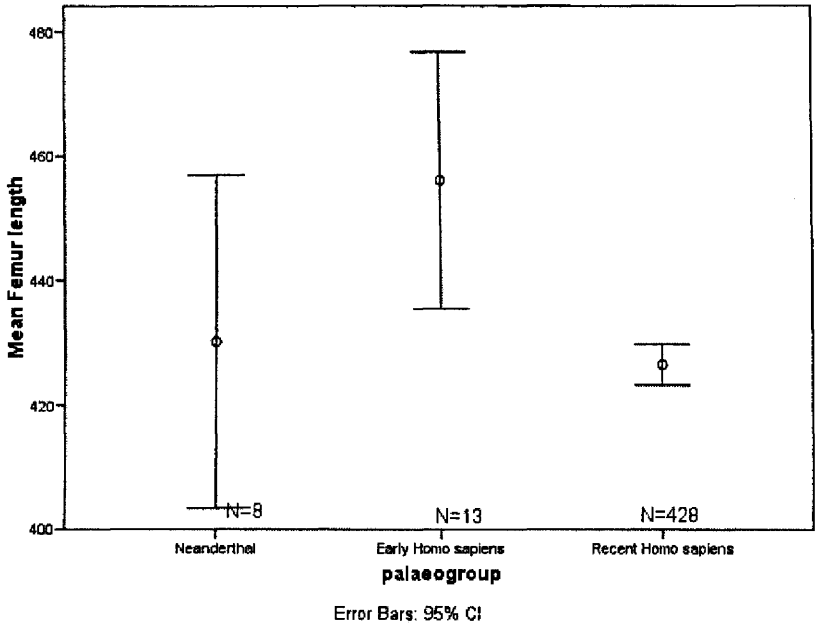

Figure 5-14 Femur length for Neanderthals, early and recent modern humans. Mean and 95% confidence interval (whiskers).

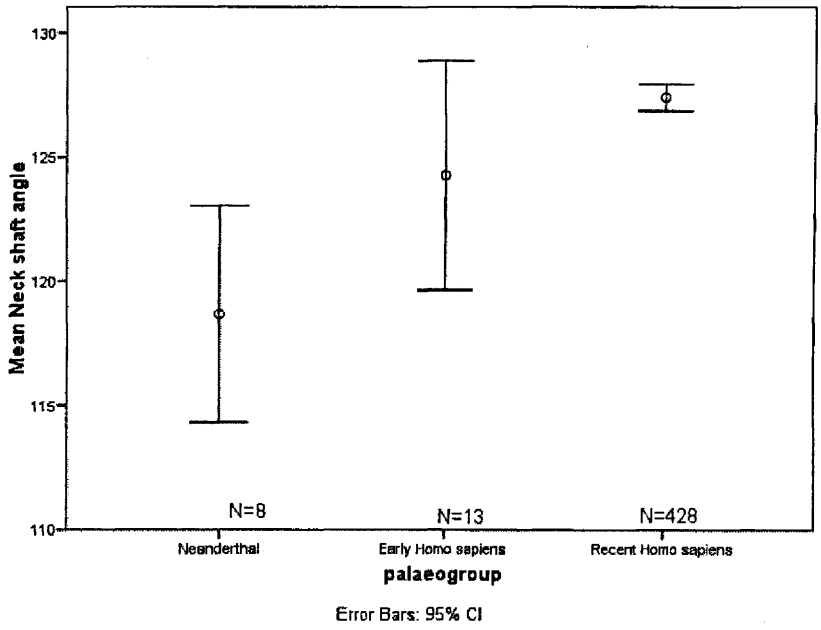

Figure 5-15 Neck-shaft angle for Neanderthals, early and recent modern humans. Mean and 95% confidence interval (whiskers).

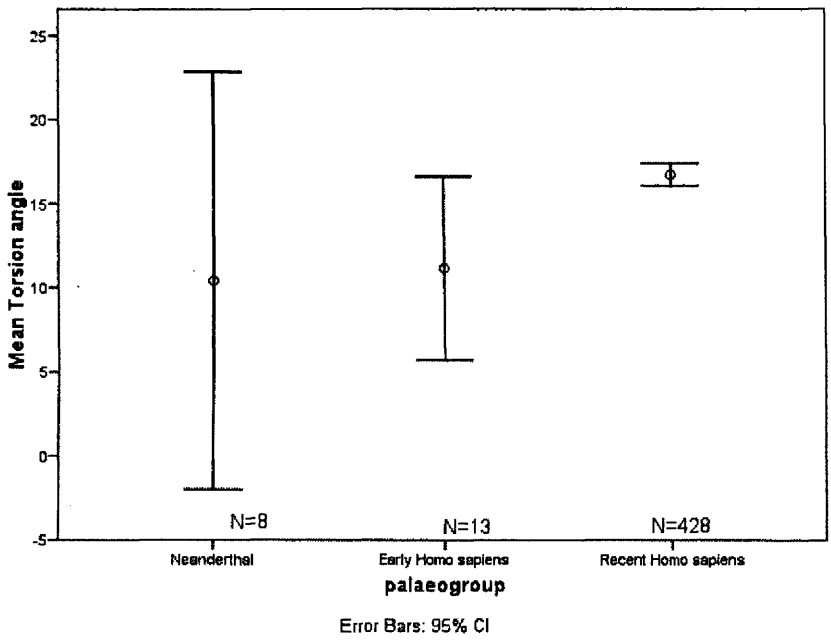

Figure 5-16 Torsion angle for Neanderthals, early and recent modern humans. Mean and 95% confidence interval (whiskers).

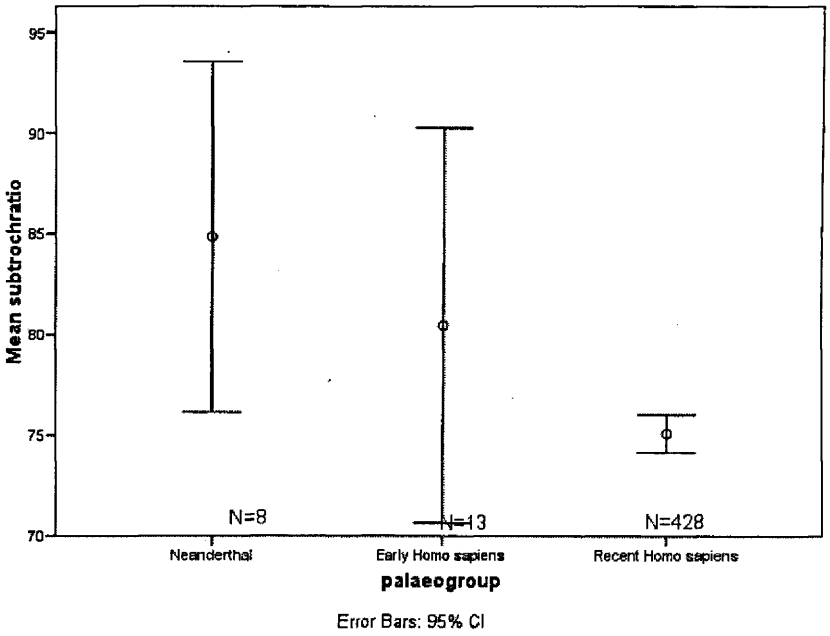

Figure 5-17 Subtrochanteric ratio for Neanderthals, early and recent modern humans. Mean and 95% confidence interval (whiskers).

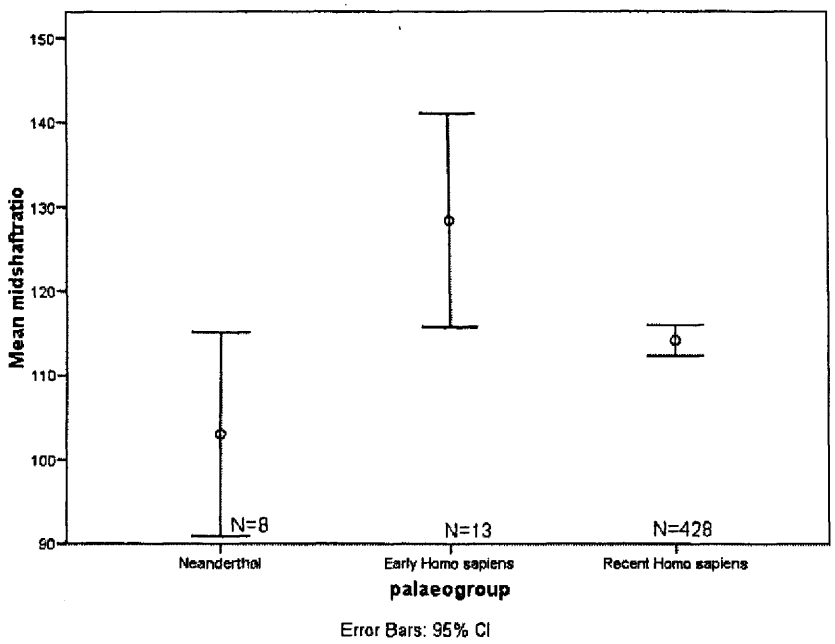

Figure 5-18 Midshaft ratio for Neanderthals, early and recent modern humans. Mean and 95% confidence interval (whiskers).

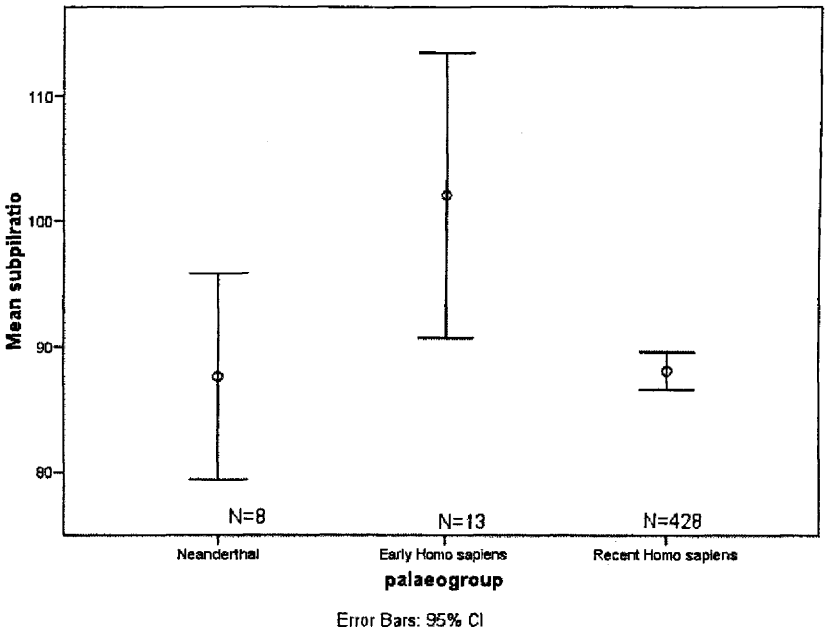

Figure 5-19 Subpilastric ratio for Neanderthals, early and recent modern humans. Mean and 95% confidence interval (whiskers).

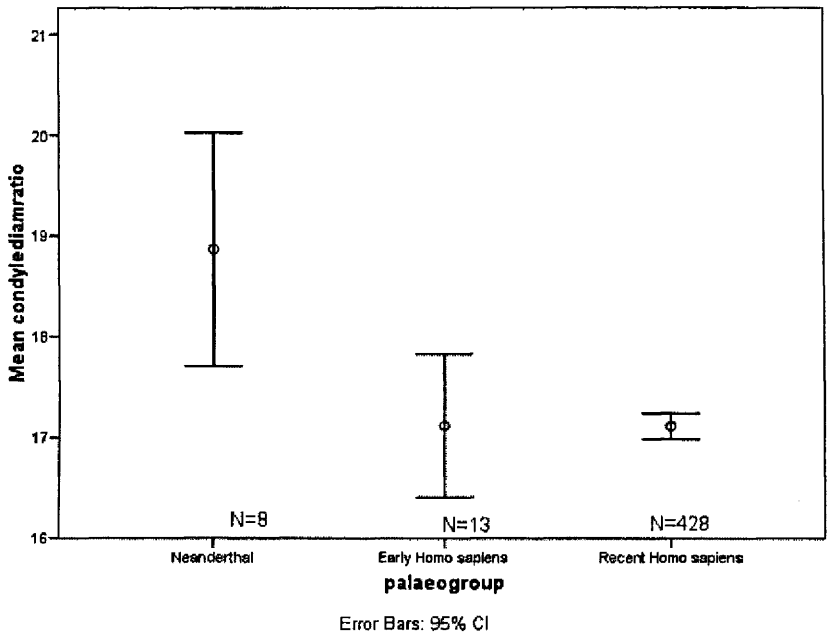

Figure 5-20 Condyle robusticity for Neanderthals, early and recent modern humans. Mean and 95% confidence interval (whiskers).

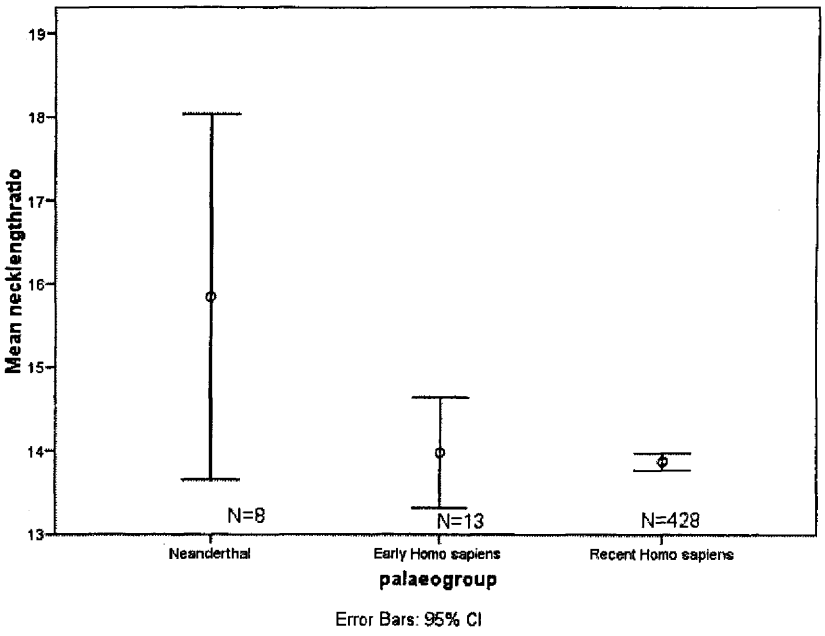

Figure 5-21 Neck length ratio for Neanderthals, early and recent modern humans. Mean and 95% confidence interval (whiskers).

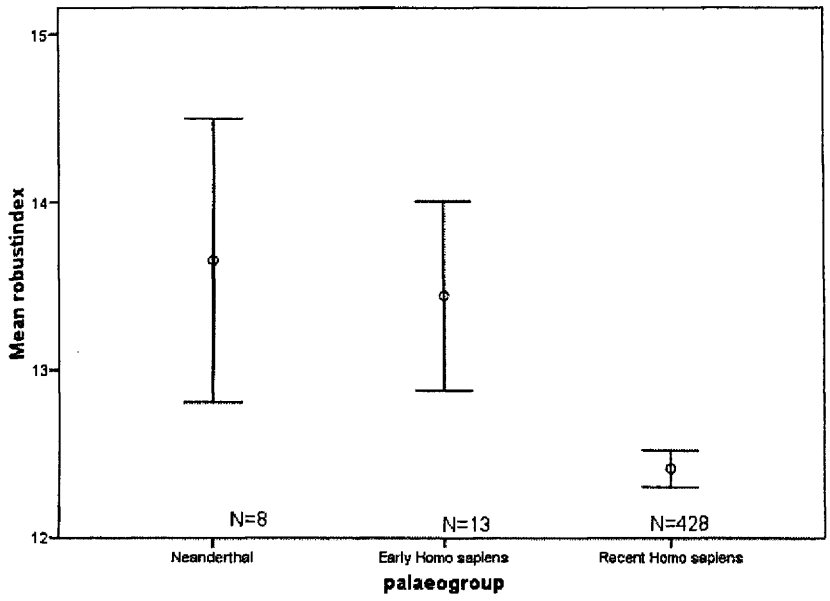

Figure 5-22 Robusticity index for Neanderthals, early and recent modern humans. Mean and 95% confidence interval (whiskers).

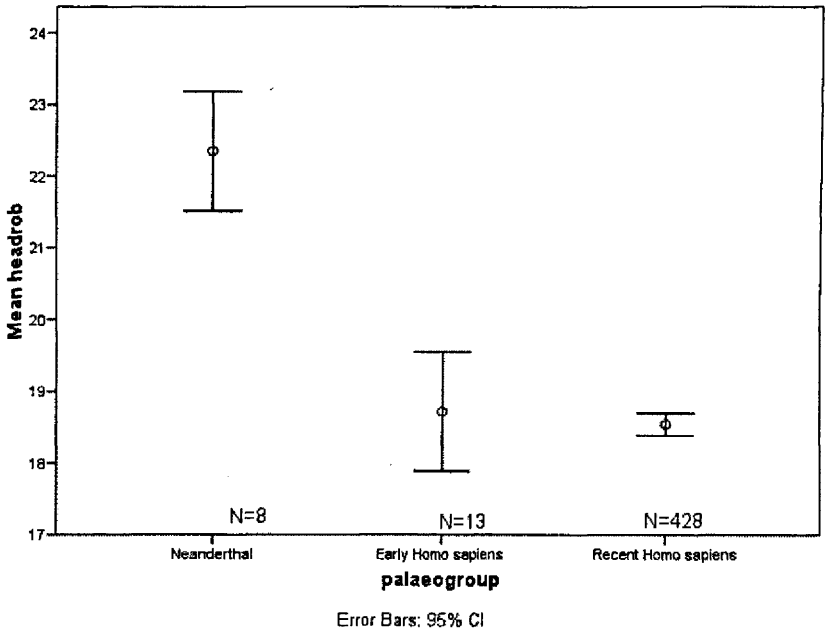

Figure 5-23 Head robusticity for Neanderthals, early and recent modern humans. Mean and 95% confidence interval (whiskers).

5.2.2.6. Discriminant function analysis

A DFA with cross-validation using all PCs (included in the above analyses) and univariate measurements used in the analyses above was used to separate Neanderthals, early and recent modern humans. Function 1 separates best between Neanderthals and modern humans in general, whereas function 2 separates early modern humans from recent modern humans (Figure 5-24). The variables in Table 5-9 appear in the order of their discriminating power. Function 1 reflects (ordered according to decreasing correlation between the variable and the function) degree of curvature, robusticity of the head, width of the distal and proximal femur, neck-length ratio, low neck-shaft angle, robusticity. Function 2 reflects the midshaft and subpilastric shaft shape, femur length, and other aspects of shaft shape (Table 5-9).

For these three populations (Neanderthals, early and recent modern humans) with very uneven sample sizes, the expected proportion of correct random classification based on sample size is ~90%. The DFA with cross-validation was able to correctly classify Neanderthals and recent modern humans relatively succesfully with 87.5% (7 out of 8 Neanderthals) and 99.5% (425 out of 427 modern humans) classified correctly. Early modern humans were almost all classified as recent modern humans (92.3% - 12 out of 13), although none were classified as Neanderthals. Overall, for the three groups together, this gives 96.7% of correct classification.

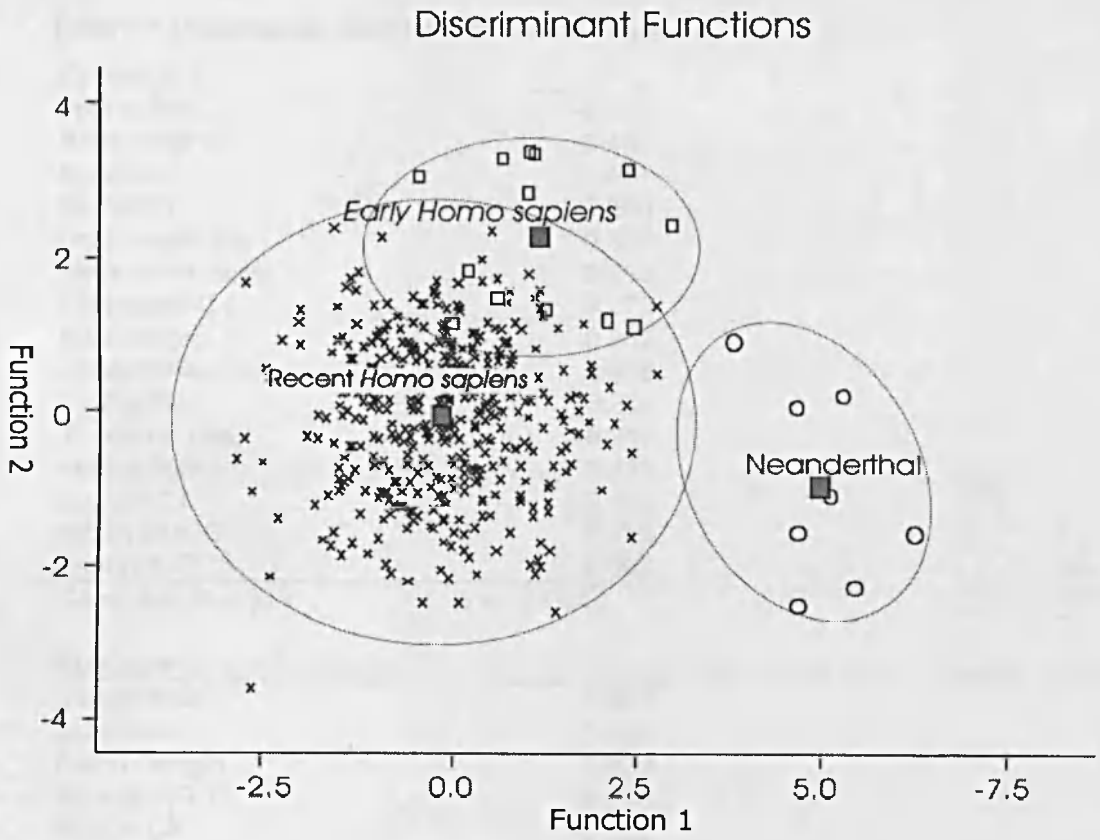

Figure 5-24 Discriminant Function 1 and 2 for Neanderthals, early and recent modern humans.

Table 5-9 Discriminant function coefficients - femur.

Function 1	
pcurveAllPC1	-0.528
AcurveAllPC1	0.457
headrob	0.427
EpiAllPC1	-0.360
necklengthratio	0.326
Neck-shaft angle	-0.313
LcurveAllPC1	0.273
robustindex	0.262
condylediamratio	0.239
EpiAllPC2	-0.225
Torsion angle	-0.215
subtrochratio	0.213
EpiAllPC3	-0.165
McurveAllPC1	0.115
AcurveAllPC3	0.043
Canonical R= .571	Λ = <0.001

Function 2	
midshaftratio	0.351
subpilratio	0.350
Femur length	0.328
AcurveAllPC2	-0.278
EpiAllPC4	-0.252
LcurveAllPC2	-0.244
LcurveAllPC4	0.238
pcurveAllPC4	0.214
McurveAllPC3	-0.196
EpiAllPC5	0.188
pcurveAllPC2	0.173
AcurveAllPC4	0.132
McurveAllPC2	-0.127
pcurveAllPC3	-0.077
Canonical R= .380	Λ = <0.001

5.2.3. Summary

Neanderthals have femora with a higher degree of anterior curvature than do early modern humans and recent modern humans. They also have the most distal apex of curvature. They have wider and deeper distal epiphyses, larger femoral heads, lower neck-shaft angles (only compared to early modern humans) and are the most robust (significantly different from recent modern humans only). Discriminant function classification very successfully distinguished Neanderthals from the recent modern human groups, but the overlap between early and recent modern humans resulted in frequent misclassification of early modern humans into the much larger and more variable recent modern human group.

5.3. The lower arm

The results presented here will first discuss the principal components and visualisations, using the same approach that was used for the section on the femur. The radius sample consists of 15 Neanderthals, 15 early modern humans and 361 recent modern humans. The ulna sample consists of 13 Neanderthals, 21 early modern humans and 344 recent modern humans.

5.3.1. Radius shape principal components explained

5.3.1.1. Medial surface (mcurve)

The first three PCs of the medial curve explain 46.1%, 13.2% and 8.94%, respectively, of the variation (total 68.2%). Subsequent PCs explain minimal amounts of the variation and are not considered further.

PC1 reflects the variation in lateral curvature of the radius (Figure 5-25a). PC2 is related to the medial expansion of the proximal interosseous crest and the direction of the distal end of the medial surface (Figure 5-25b). PC3 is the sinusoidal shape of the shaft in the anteroposterior plane (Figure 5-25c).

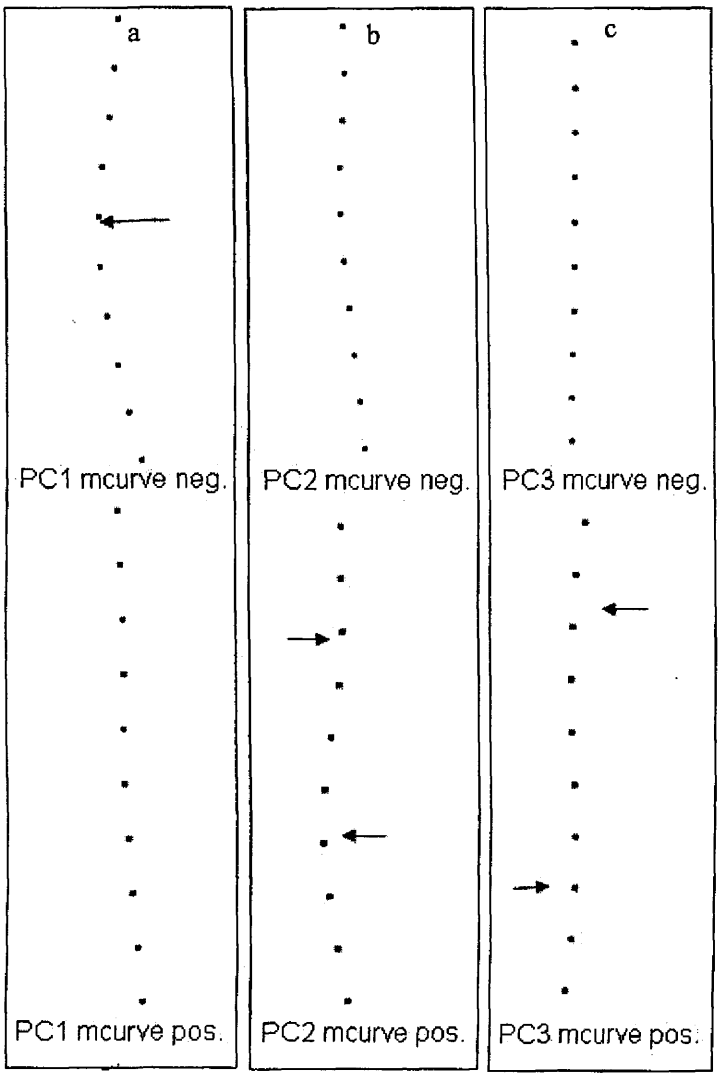

Figure 5-25 Morphological trends for the medial curve of the radius for Neanderthals, early and recent modern humans.

a: Principal component 1: anterior view. Negative values have a higher degree of curvature than positive values. **b**: Principal component 2: anterior view. Positive values show an increased medial extension of the proximal interosseous crest and a medial direction of the distal curve (more medially expanded ulnar notch), whereas negative values show no medial expansion of the proximal interosseous crest and an ulnar notch that is not medially projected. **c**: Principal component 3: lateral view. Positive values have a more sinusoidal shape, whereas negative values have no sinusoidal shape. Positive and negative visualisations correspond to the most extreme positive and negative scores for each PC.

5.3.1.2. Lateral curve (lcurve)

The first three PCs of the lateral curve explain 40.6%, 20.9% and 9.43% ,respectively ,of the variation (total 70.9%). Subsequent PCs explain minimal amounts of the variation and are not considered further.

Similar to the analyses on modern humans PC1 reflects differences in lateral curvature (Figure 5-26a). PC2 is influenced by the apex of curvature and the direction of the distal end of the lateral surface (Figure 5-26b). PC3 relates to the sinusoidal shape of the lateral curve in the anteroposterior plane (Figure 5-26c).

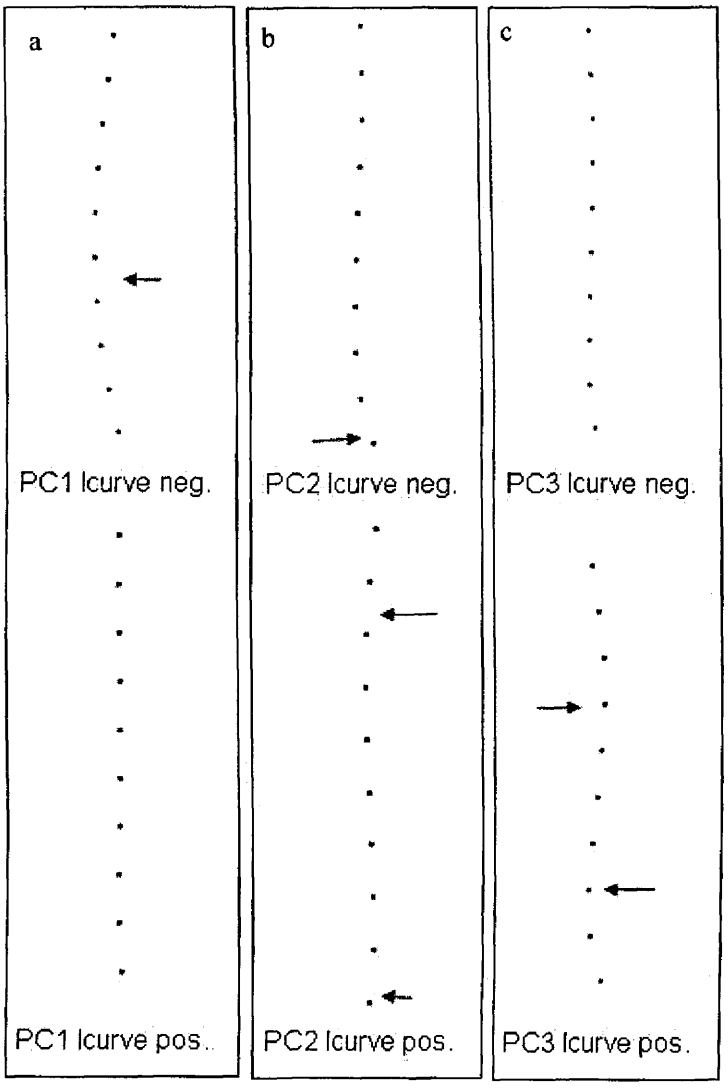

Figure 5-26 Morphological trends for the lateral curve of the radius for Neanderthals, early and recent modern humans.

a: Principal component 1: anterior view. Negative values have a higher degree of curvature whereas positive values have a lower degree of lateral curvature. **b**: Principal component 2: anterior view. Positive values have a more proximal apex of curvature and a more laterally projecting styloid process, whereas negative values have their apex of curvature at midshaft and lack the lateral projection of the styloid process. **c**: Principal component 3: lateral view. Positive values are more sinusoidal. Negative values are not sinusoidal. Positive and negative visualisations correspond to the most extreme positive and negative scores for each PC.

5.3.1.3. Epiphyses (Epi)

The first two PC's of the epiphysis analysis explain 33.3% and 8.53%,,respectively, of the variation (total 41.8%). Subsequent PCs explain minimal amounts of the variation and are not considered further. When scatterplots of the PCs were observed, PC6 (4.71% of variation) showed Neanderthals to have primarily positive values and is therefore included in the following analyses.

PC1 reflects the direction of the head and the distal articular surface in relation to the shaft (Figure 5-27a). PC2 relates to the length of the radius between the radial tuberosity and 80% level of the shaft and the orientation of the tip of the styloid process (Figure 5-27b). PC6 is related to the position of the radial turberosity (Figure 5-27c).

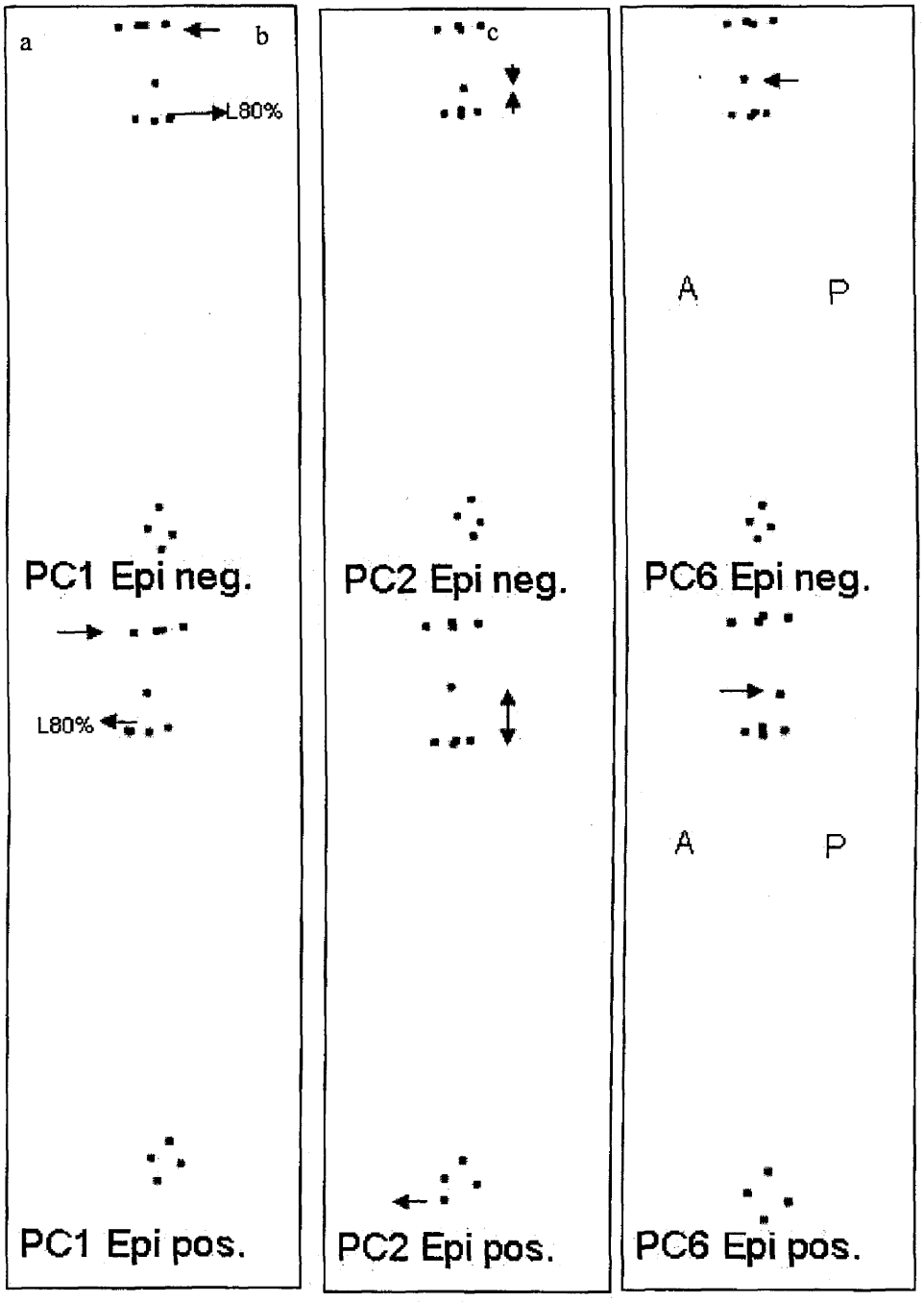

Figure 5-27 Morphological trends for the epiphyses of the radius for Neanderthals, early and recent modern humans. All medial view.

a: Principal component 1. Individuals with negative values have a more anteriorly oriented head, whereas those with positive values are more posteriorly oriented. **b**: Principal component 2.

Negative values indicate a shorter distance between the radial tubercle and the 80% level of the shaft and a more posteriorly located styloid process and positive values have a longer distance and a more anteriorly located styloid process. **c**: Principal component 6. Individuals with negative values have a more anteriorly located radial tuberosity compared to those with positive values who have a more posteriorly located tuberosity. Positive and negative visualisations correspond to the most extreme positive and negative scores for each PC.

5.3.1.4. Summary

Degree of mediolateral curvature is the most important PC for both medial and lateral surface (mcurveAllPC1 and lcurveAllPC1). This is reflected in the significant correlation (r=0.369) between the two curvature PCs. There is no significant correlation between the PCs of the epiphyses and the two curvature PCs (Table 5-10 and Table 5-11).

Correlations between the other shaft shape PCs indicate that individuals who have a lower degree of medial curvature (mcurveAllPC1) have an apex of curvature at midshaft and a weakly developed styloid process (lcurveAllPC2), and a less sinusoidal shaft (lcurveAllPC3) (Table 5-12). A higher degree of lateral curvature is related to an increased development of the proximal interosseous crest and increased medial projection of the radial notch (mcurvePC2). There is no correlation between the epiphysis and the other shaft shape PCs (Table 5-13).

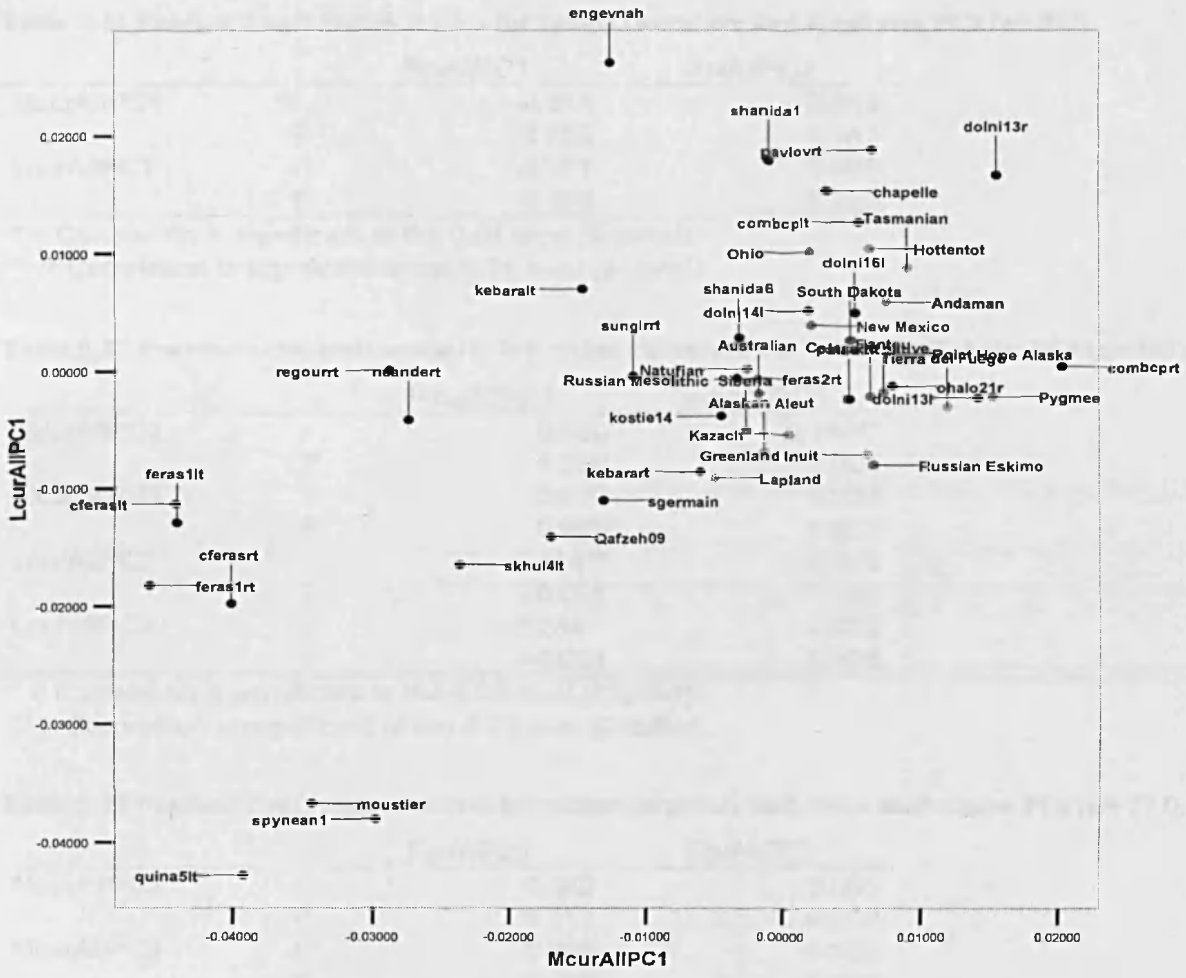

Figure 5-28 The first PCs for the medial and lateral curve of the radius.

Both PCs reflect the degree of mediolateral curvature (negative values are more curved). All Neanderthals, early modern humans and recent modern human samples.

Table 5-10 Pearson's correlation matrix for radius curvature PCs (n= 391).

		McurAllPC1
LcurAllPC1	r	0.369
	P	<0.001**

* = Correlation is significant at the 0.05 level (2-tailed).

** = Correlation is significant at the 0.01 level (2-tailed).

Table 5-11 Pearson's correlation matrix for radius curvature and epiphyses PCs (n= 377).

		EpiAllPC1	ApiAllPC2
McurAllPC1	r	-0.013	-0.049
	P	0.799	0.347
LcurAllPC1	r	-0.071	0.062
	P	0.169	0.228

* = Correlation is significant at the 0.05 level (2-tailed).
** = Correlation is significant at the 0.01 level (2-tailed).

Table 5-12 Pearson's correlation matrix for radius curvature and other shaft shape PCs (n= 391).

		McurAllPC1	LcurAllPC1
McurAllPC2	r	0.000	-0.144**
	P	1.000	0.004
McurAllPC3	r	0.000	0.002
	P	0.999	0.972
LcurAllPC2	r	-0.414**	0.000
	P	<0.001	0.999
LcurAllPC3	r	-0.284**	0.000
	P	<0.001	0.998

* = Correlation is significant at the 0.05 level (2-tailed).
** = Correlation is significant at the 0.01 level (2-tailed).

Table 5-13 Pearson's correlation matrix for radius epiphyses and other shaft shape PCs (n= 377).

		EpiAllPC1	EpiAllPC2
McurAllPC2	r	0.082	0.005
	P	0.111	0.919
McurAllPC3	r	0.045	-0.098
	P	0.381	0.058
LcurAllPC2	r	-0.066	-0.040
	P	0.200	0.435
LcurAllPC3	r	0.061	0.101
	P	0.237	0.051

* = Correlation is significant at the 0.05 level (2-tailed).
** = Correlation is significant at the 0.01 level (2-tailed).

5.3.2. The ulna principal components explained

5.3.2.1. Posterior curve (pcurve)

The first four PCs of the posterior curve analysis explain 33.7%, 23.3%, 13.4% and 6.31%,,respectively, of the variation (total 76.71%). Subsequent PCs explain minimal amounts of the variation and are not considered further.

PC1 reflects differences in mediolateral curvature (Figure 5-29a). PC2 is the sinusoidal shape of the shaft in the mediolateral plane (Figure 5-29b). PC3 relates to the sinusoidal shape of the lateral curve in the anteroposterior plane (Figure 5-29c). PC4 is the deflection of the proximal shaft (Figure 5-29d).

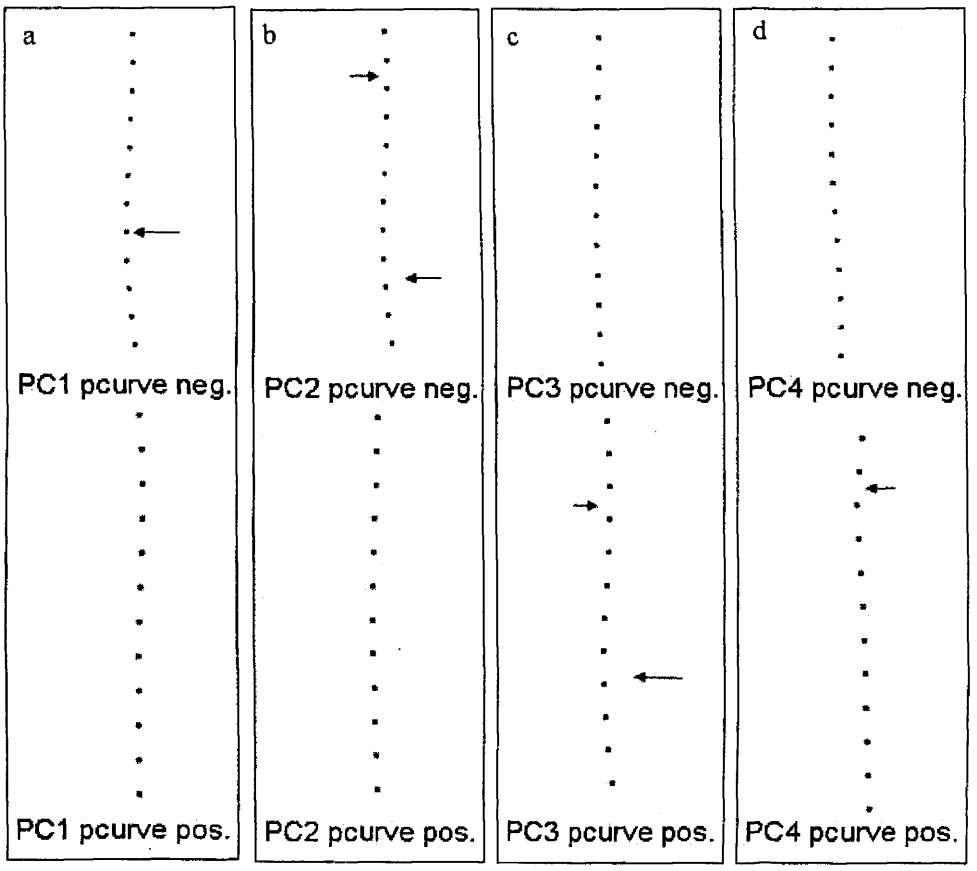

Figure 5-29 Morphological trends for the posterior curve of the ulna for Neanderthals, early and recent modern humans.

a: Principal component 1: anterior view. Negative values have a higher degree of mediolateral curvature, whereas positive values have a lower degree of curvature. **b**: Principal component 2: anterior view. Positive values have less of a sinusoidal shape in the mediolateral plane than negative values. **c**: Principal component 3: medial view. Positive values are more sinusoidal compared to negative values. **d**: Principal component 4: medial view. Positive values show a bent proximal shaft indicating a more anteriorly projected head, whereas negative values are relatively straight. Positive and negative visualisations correspond to the most extreme positive and negative scores for each PC.

5.3.2.2. Proximal ulna (prox)

The first three PCs of the lateral curve analysis explain 20.4%, 16.6% and 7.89%,,respectively,,of the variation (total 44.9%). Subsequent PCs explain minimal amounts of the variation and are not considered further.

PC1 reflects differences in the orientation of the proximal ulna in relation of the shaft (Figure 5-30a). PC2 relates to the distance between the 80% level of the shaft and the coronoid process (Figure 5-30b). PC3 shows the orientation of the trochlear notch (Figure 5-30c).

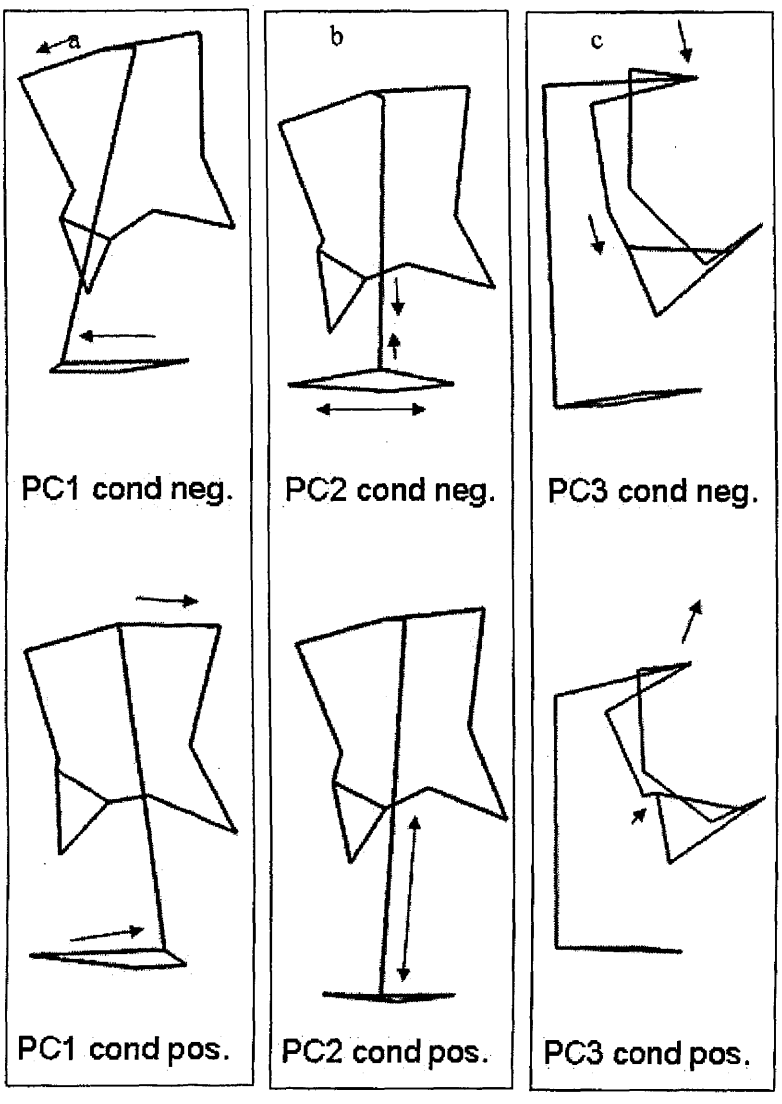

Figure 5-30 Morphological trends for the proximal ulna for Neanderthals, early and recent modern humans.

a: Principal component 1: anterior view. Positive values have a proximal ulna that is medially projected with a medial facing trochlear notch, whereas negative values have a proximal ulna that is laterally projected and has a more lateral facing trochlear notch. **b**: Principal component 2: anterior view. Positive values have a longer distance between the 80% and the coronoid process, whereas negative values have short distances. **c**: Principal component 3: lateral view. Positive values have a more proximo-anterior facing trochlear notch and negative values have a more anterior facing trochlear notch. Positive and negative visualisations correspond to the most extreme positive and negative scores for each PC.

5.3.2.3. Summary

There is no significant correlation between the shaft PCs nor are the proximal ulna PCs significantly related (Table 5-14). The correlations between the posterior curve and the proximal ulna PCs showed that individuals with a greater distance between the 80% level of the shaft and the coronoid process (proxALLPC2) have a more sinusoidal shaft shape in the anteroposterior plane (pcurveALLPC3). Also, individuals with a more proximo-anterior trochlear notch (proxAllPC3) have a less mediolaterally sinusoidal shaft shape (pcurveALLPC2).

Table 5-14 Pearson's correlation matrix: ulna PCs (n= 344).

		pcurAllPC1	pcurAllPC2	pcurAllPC3	pcurAllPC4	ProxAllPC1	ProxAllPC2
pcurAllPC2	r	0.000					
	P	1.000					
pcurAllPC3	r	0.000	0.000				
	P	0.996	0.999				
pcurAllPC4	r	0.000	0.000	0.000			
	P	0.999	0.998	0.998			
ProxAllPC1	r	-0.108*	-0.074	-0.007	0.064		
	P	0.036	0.155	0.886	0.213		
ProxAllPC2	r	-0.081	-0.070	-0.222**	-0.040	0.002	
	P	0.117	0.173	<0.0001	0.435	0.976	
ProxAllPC3	r	-0.016	-0.194**	0.083	0.006	0.002	-0.001
	P	0.764	<0.001	0.107	0.915	0.970	0.992

* = Correlation is significant at the 0.05 level (2-tailed).
** = Correlation is significant at the 0.01 level (2-tailed).

5.3.3. Differences in lower arm morphology between Neanderthals, early and recent modern humans.

5.3.3.1. Curvature

The groups are significantly different for both curvature PCs: mcurveAllPC1 and lcurveAllPC1 (Table 5-15). Neanderthals have a higher degree of lateral and medial curvature than early and recent modern humans (Figure 5-31 and Figure 5-32). The early and recent modern human samples are not different from each other (Appendix 44).

Table 5-15 ANOVA results for palaeogroup and radius curvature PCs.

d.f.=2	F	Sig.
McurAllPC1	35.297	<0.001*
LcurAllPC1	5.804	0.003*

*=significant at α=0.05

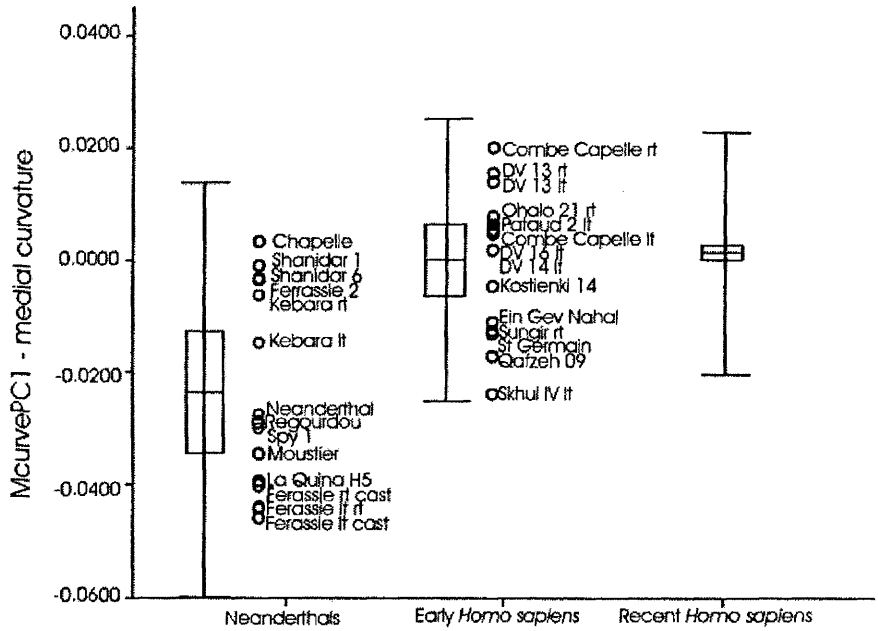

Figure 5-31 The medial curve of the radius for Neanderthals, early and recent modern humans. (Line=mean, Box= 2 S.E., whiskers: 2 S.D.). The lower values for Neanderthal radii indicate that they are more curved than those of modern humans.

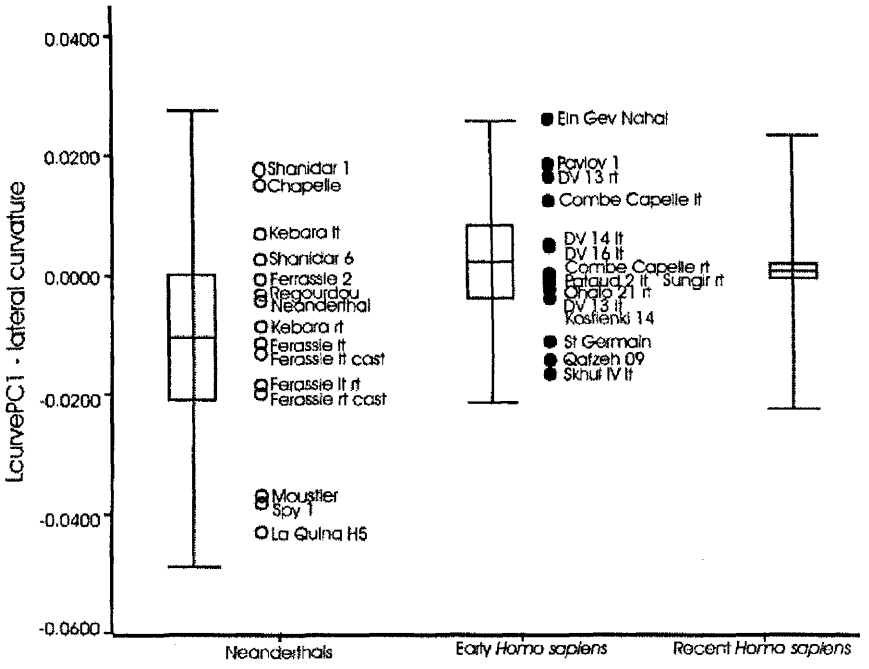

Figure 5-32 The lateral curve of the radius for Neanderthals, early and recent modern humans t. (Line=mean, Box= 2 S.E., whiskers: 2 S.D.). The lower values for Neanderthal radii indicate that they are more curved than those of modern humans.

5.3.3.2. Other shaft shape

For the radius, the groups are significantly different for the lateral shaft shape PCs only (Table 5-16). Neanderthals have an apex of curvature at midshaft and lack a lateral projection of the styloid process compared to those of modern humans, who have a more proximal apex and a more projecting styloid process (lcurveAllPC2) (Figure 5-33). Neanderthals also have a more sinusoidal radius in the anteroposterior plane compared to that of modern humans (lcurveAllPC3) (Figure 5-34) (early modern humans only significantly different using Hochberg's GT2 (Appendix 44).

Table 5-16 ANOVA results for palaeogroup and other radius shaft shape PCs.

d.f.=2	F	Sig.
McurAllPC2	0.359	0.698
McurAllPC3	0.296	0.744
LcurAllPC2	12.742	<0.001*
LcurAllPC3	11.243	<0.001*

*=significant at α=0.05

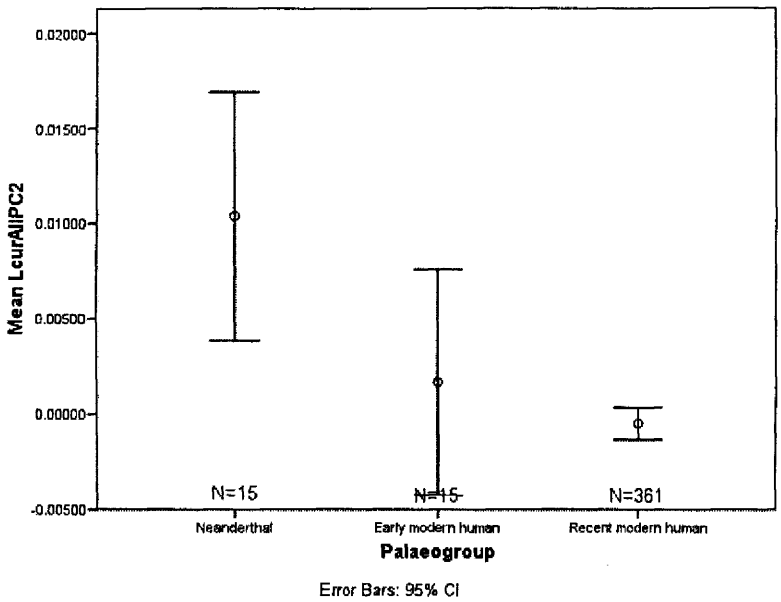

Figure 5-33 LcurAllPC2 for Neanderthals, early and recent modern humans.

The higher values for the Neanderthals indicate an apex of curvature at midshaft and a lack of lateral projection of the styloid process. Mean and 95% confidence interval (whiskers).

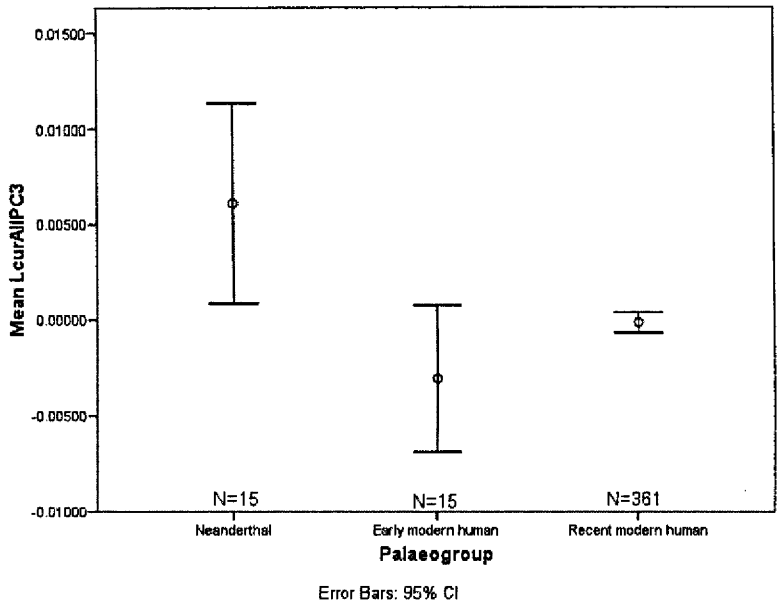

Figure 5-34 LcurAllPC3 for Neanderthals, early and recent modern humans.
The higher values for the Neanderthals indicate a more sinusoidal radius in the anteroposterior plane. Mean and 95% confidence interval (whiskers).

For the ulna, the groups are significantly different for two of the shaft shape PCs (Table 5-17). Neanderthals have less mediolateral curvature of the ulnar shaft compared to early and recent modern humans (pcurveAllPC1) (Figure 5-35). Neanderthals also have a less mediolateral sinusoidal ulnar shaft shape compared to recent modern humans (Figure 5-36) (Appendix 46).

Table 5-17 ANOVA results for palaeogroup and ulna shaft shape PCs.

d.f.=2	F	Sig.
pcurveAllPC1	3.302	0.038*
pcurveAllPC2	8.540	<0.001*
pcurveAllPC3	0.100	0.904
pcurveAllPC4	0.888	0.412

*=significant at α=0.05

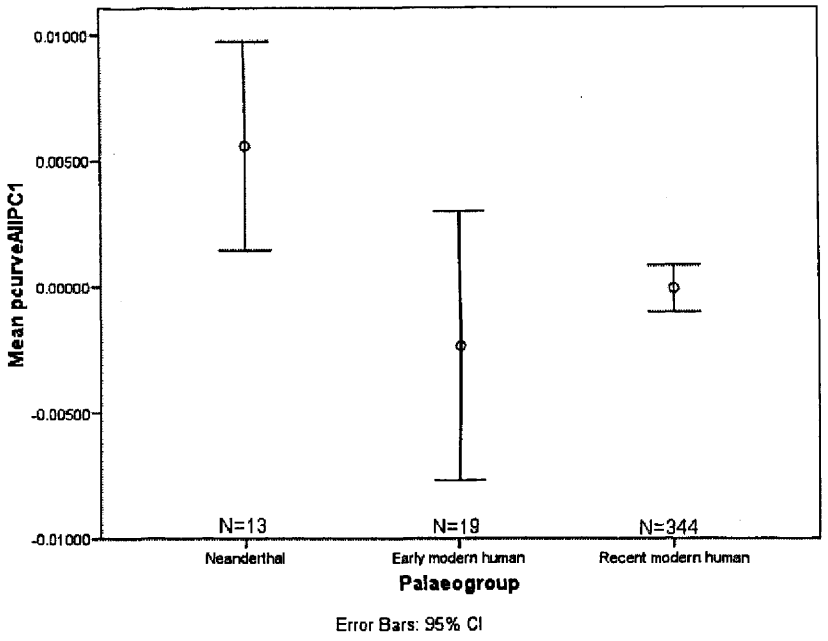

Figure 5-35 PcurAllPC1 for Neanderthals, early and recent modern humans.

The higher values for the Neanderthals indicate less mediolateral curvature of the ulnar shaft. Mean and 95% confidence interval (whiskers).

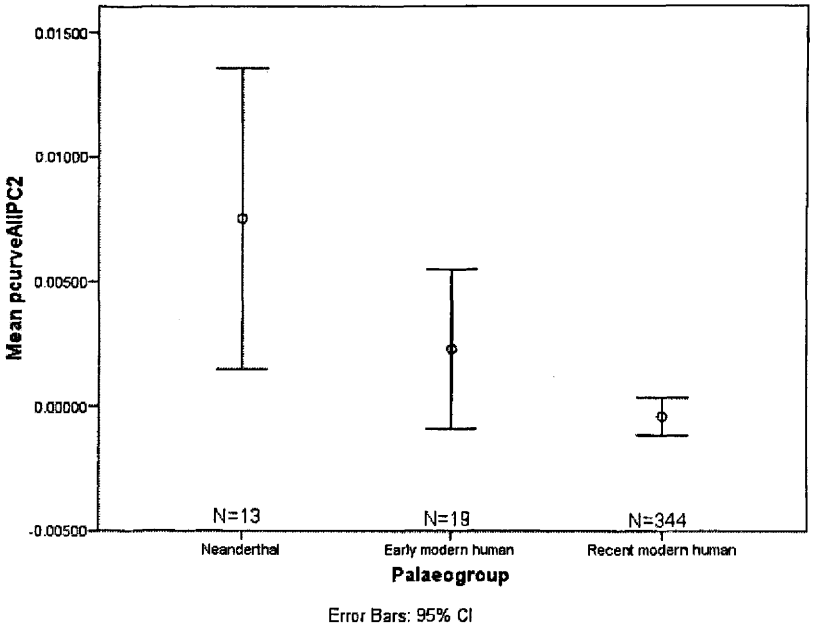

Figure 5-36 PcurAllPC2 for Neanderthals, early and recent modern humans.

The higher values for the Neanderthals indicate a less mediolateral sinusoidal ulnar shaft shape. Mean and 95% confidence interval (whiskers).

5.3.3.3. Epiphyses shape

The groups are similar in their radial epiphyseal shape (Table 5-18). For the ulna, the groups are significantly different for two proximal shape PCs (Table 5-19). Neanderthals have a shorter distance between the 80% level of the shaft and the coronoid process compared to early modern humans (ProxAllPC2) (Figure 5-37). There is a trend from Neanderthals to recent modern humans in having a more proximo-anterior rather than an anterior facing trochlear notch and all groups are significantly different from each other (ProxAllPC3) (Appendix 47) (Figure 5-38).

Table 5-18 ANOVA results for palaeogroup and radius epiphysis shape PCs.

d.f.=2	F	Sig.
EpiAllPC1	0.089	0.915
EpiAllPC2	0.195	0.823
EpiAllPC6	0.416	0.660

*=significant at α=0.05

Table 5-19 ANOVA results for palaeogroup and proximal ulna PCs.

d.f.=2	F	Sig.
ProxAllPC1	1.045	0.353
ProxAllPC2	3.761	0.024*
ProxAllPC3	32.235	<0.001*

*=significant at α=0.05

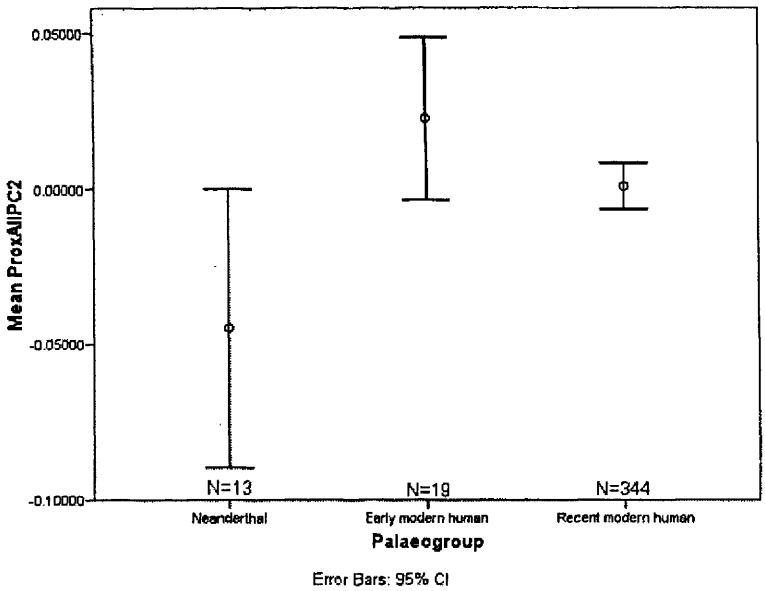

Figure 5-37 ProxAllPC2 for Neanderthals, early and recent modern humans.
The lower values for the Neanderthals indicate a shorter distance between the 80% level of the shaft and the coronoid process. Mean and 95% confidence interval (whiskers).

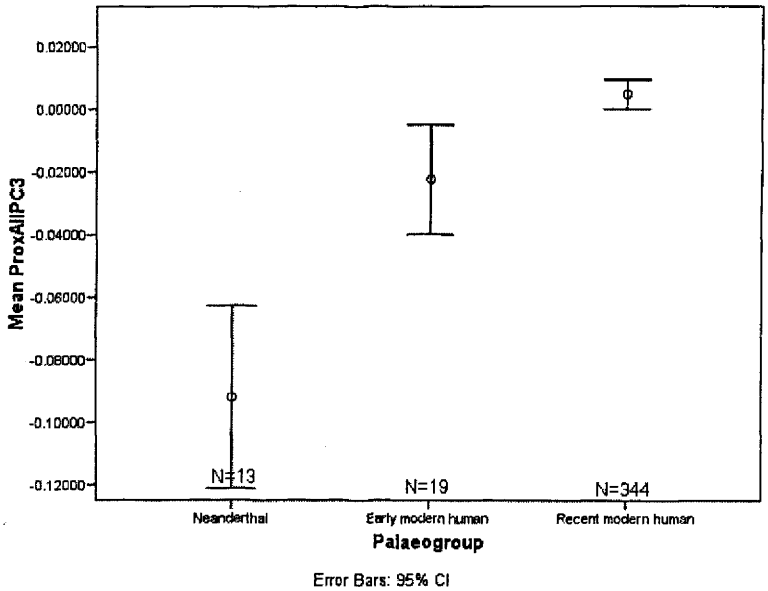

Figure 5-38 ProxAllPC3 for Neanderthals, early and recent modern humans.
The lower values for the Neanderthals indicate a more proximo-anterior rather than an anterior facing trochlear notch. Mean and 95% confidence interval (whiskers).

5.3.3.4. Univariate measurements

The groups are significantly different for most univariate measurements of both the radius and the ulna (Table 5-20 and Table 5-21). Recent modern humans have shorter radii than early modern humans (Figure 5-39). Neanderthals have a more mediolaterally located radial tuberosity than early and recent modern humans (Figure 5-40). Neanderthals have a higher degree of dorsal and lateral subtense, a longer radial neck and a more anteroposteriorly wide radial head than early and recent modern humans (Figure 5-41; Figure 5-42; Figure 5-43). The early modern humans are similar to the recent modern humans for those features. The midshaft shape ratio shows no difference between the samples, but a downward trend in the means suggests a trend toward more anteroposterior flattening and mediolateral widening which can be interpreted as the increased development of the interosseous crest with time (Figure 5-44) (Appendix 48).

Table 5-20 Descriptives of palaeogroup and the univariate measurements of the radius.

		N	Mean	S.D.
Max_ Length	Neanderthal	15	234.11	23.33
	Early modern human	15	254.09	20.14
	Recent modern human	361	234.95	19.78
neck-shaft angle °	Neanderthal	15	36.31	14.26
	Early modern human	15	30.17	12.80
	Recent modern human	361	35.94	13.95
PosRadTubML	Neanderthal	15	22.86	11.95
	Early modern human	15	15.51	4.13
	Recent modern human	361	15.50	7.24
DorsalST	Neanderthal	15	10.78	3.54
	Early modern human	15	7.01	2.04
	Recent modern human	361	6.59	2.03
LateralST	Neanderthal	15	15.19	22.40
	Early modern human	15	9.49	3.32
	Recent modern human	361	6.80	2.73
NeckLengthRatio	Neanderthal	15	12.31	2.21
	Early modern human	15	10.97	1.30
	Recent modern human	36	11.03	1.48
HeadShapeRatio	Neanderthal	15	120.07	21.10
	Early modern human	15	103.68	8.86
	Recent modern human	361	105.38	8.70
midshaftShapeRation	Neanderthal	15	93.99	32.44
	Early modern human	15	92.49	25.03
	Recent modern human	361	84.85	14.57

Table 5-21 ANOVA results for palaeogroup and univariate measurements of the radius.

d.f.=2	F	Sig.
Max_ Length	6.689	0.001*
neck-shaft angle °	1.247	0.289
PosRadTubML	7.176	0.001*
DorsalST	28.571	<0.001*
LateralST	21.517	<0.001*
NeckLengthRatio	5.215	0.006*
HeadShapeRatio	17.861	<0.001*
midshaftShapeRatio	3.813	0.023*

*=significant at α=0.05

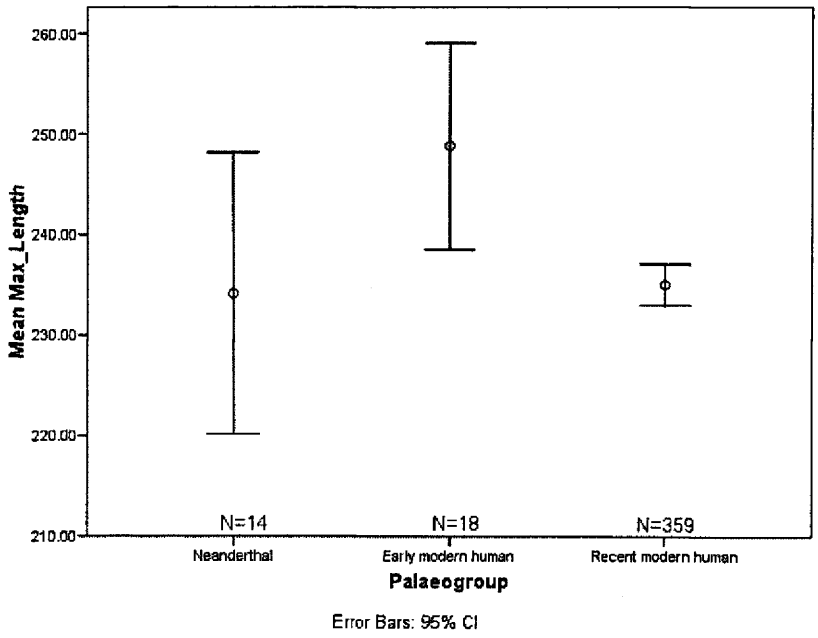

Figure 5-39 Maximum radius length for Neanderthals, early and recent modern humans. Mean and 95% confidence interval (whiskers).

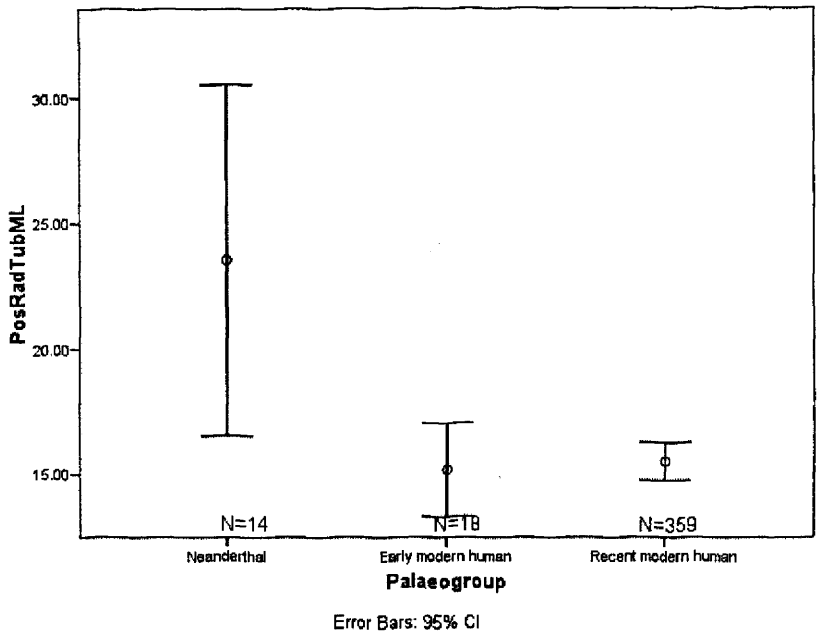

Figure 5-40 Position of the radial tuberosity for Neanderthals, early and recent modern humans. Mean and 95% confidence interval (whiskers).

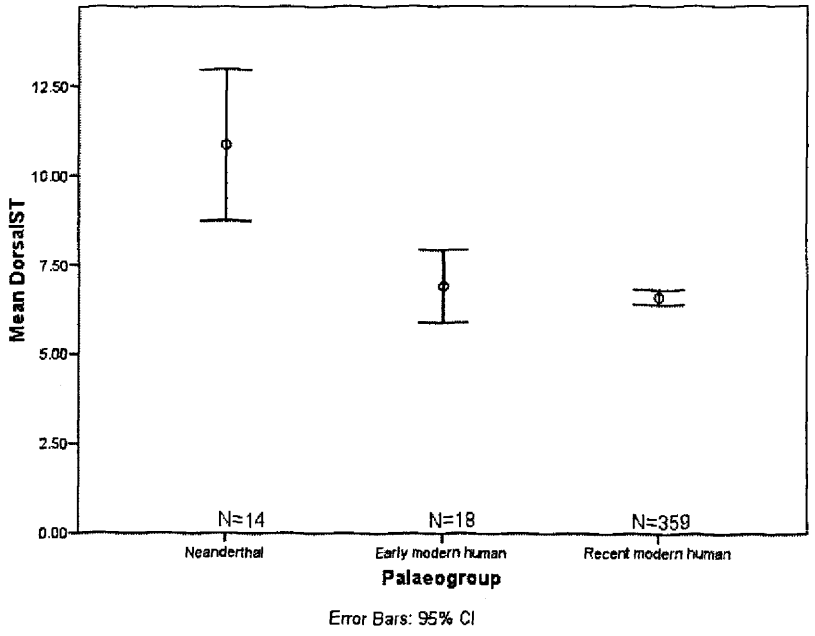

Figure 5-41 Dorsal subtense for Neanderthals, early and recent modern humans. Mean and 95% confidence interval (whiskers).

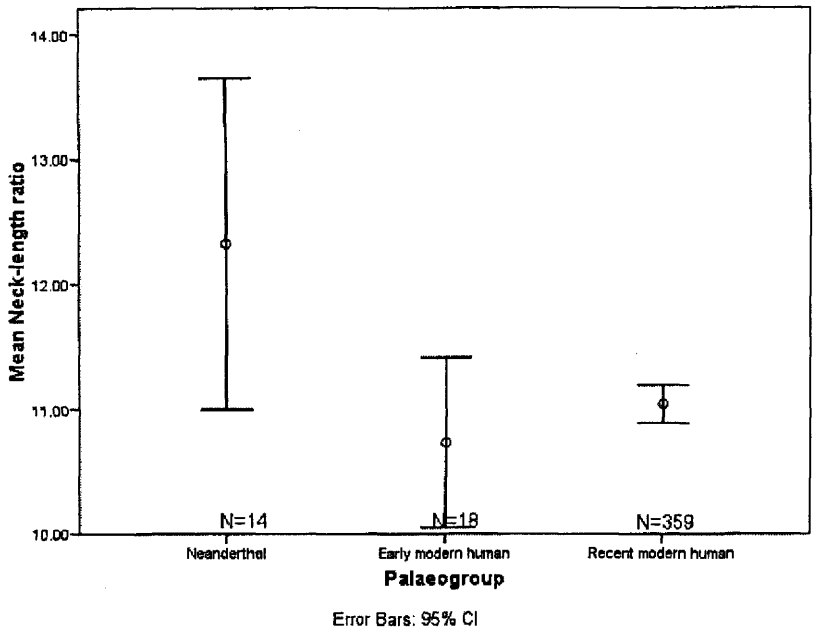

Figure 5-42 Relative radius neck length for Neanderthals, early and recent modern humans. Mean and 95% confidence interval (whiskers).

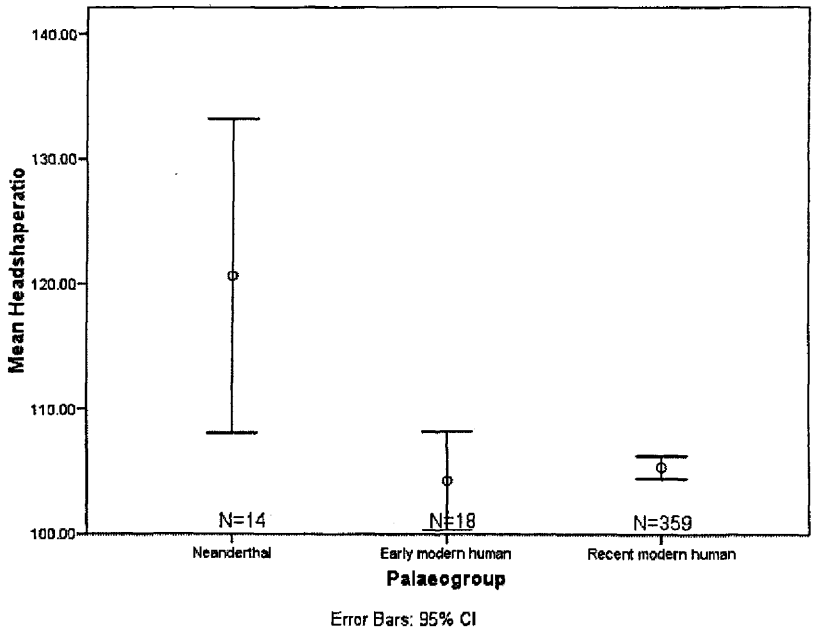

Figure 5-43 Head shape ratio for Neanderthals, early and recent modern humans. Mean and 95% confidence interval (whiskers).

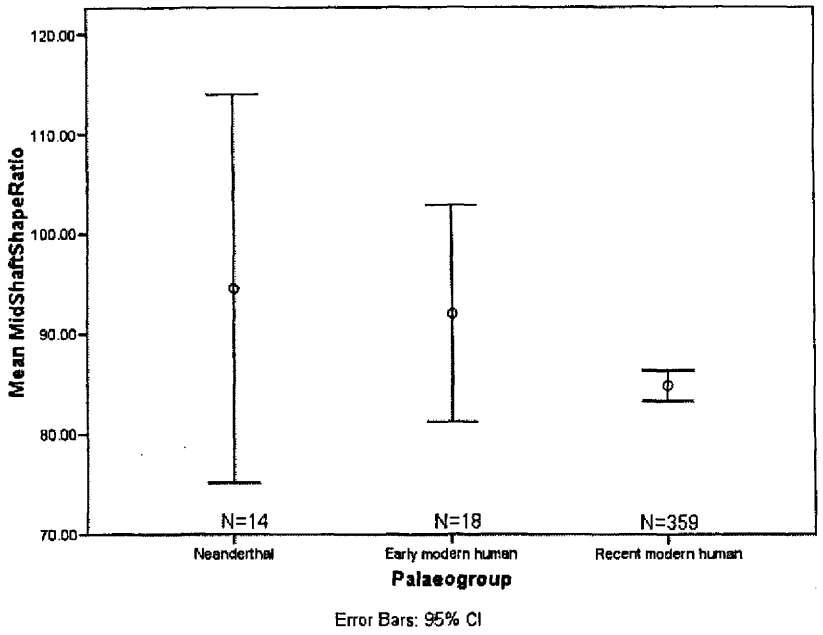

Figure 5-44 Midshaft shape ratio for Neanderthals, early and recent modern humans. Mean and 95% confidence interval (whiskers).

For the ulna, there are differences among the groups for most univariate measurements (Table 5-22 and Table 5-23). Neanderthals have a relatively large proximal ulna, smaller shaft-olecranon angle, more even coronoid-olecranon ratio and a low brachial tuberosity compared to both early and recent modern humans (Figure 5-46; Figure 5-49; Figure 5-50; Figure 5-51; Figure 5-52). Neanderthals are also more robust at midshaft, have a small radial notch, and have a more anteroposteriorly wide ulnar shaft than do recent modern humans (Figure 5-53; Figure 5-48; Figure 5-47). Neanderthals also have more robust distal articulations than early modern humans but are not different in this aspect from recent modern humans (Figure 5-54). Early modern humans have longer ulnae with relatively larger proximal heads than those of recent modern humans but are similar in other aspects of their morphology (Appendix 48) (Figure 5-45; Figure 5-46).

Table 5-22 Descriptives of palaeogroup and the univariate measurements of the radius.

		N	Mean	S.D.
Max_ Length	Neanderthal	13	255.41	25.09
	Early modern human	21	266.88	18.70
	Recent modern human	344	250.35	20.65
Olecshaftratio	Neanderthal	13	9.88	1.15
	Early modern human	21	8.47	0.97
	Recent modern human	344	9.10	1.00
MidShaftShape	Neanderthal	13	86.71	16.65
	Early modern human	21	101.62	26.08
	Recent modern human	344	109.75	31.87
Radial Notch Surface ratio	Neanderthal	13	23.88	5.38
	Early modern human	21	28.67	8.83
	Recent modern human	344	29.77	7.45
TrochNotchOri	Neanderthal	13	16.46	9.75
	Early modern human	21	18.32	4.52
	Recent modern human	344	20.60	6.46
OlecOrient angle	Neanderthal	13	19.21	7.72
	Early modern human	21	24.80	5.88
	Recent modern human	344	24.13	5.06
CorOleRatio	Neanderthal	13	104.31	4.47
	Early modern human	21	107.36	2.03
	Recent modern human	344	106.75	2.47
BrachRatio	Neanderthal	13	26.45	2.71
	Early modern human	21	23.33	1.88
	Recent modern human	344	22.97	1.81
Pronator crest length	Neanderthal	13	14.77	2.73
	Early modern human	21	15.30	3.80
	Recent modern human	344	14.64	3.69
Robusticity at 50%	Neanderthal	13	11.73	1.60
	Early modern human	21	11.01	1.22
	Recent modern human	344	10.36	1.48
Robusticity at 25%	Neanderthal	13	10.95	1.44
	Early modern human	21	10.52	0.84
	Recent modern human	344	10.36	1.43
Robust dist artic	Neanderthal	13	16.56	1.65
	Early modern human	21	14.73	2.32
	Recent modern human	344	15.59	1.87

Table 5-23 ANOVA results for palaeogroup and univariate measurements of the ulna.

d.f.=2	F	Sig.
Max_ Length	6.555	0.002*
Headshaftration	8.093	<0.001*
MidShaftShape	3.952	0.020*
Radial Notch Surface ratio	4.020	0.019*
TrochNotchOri	3.601	0.028*
headorient angle	5.850	0.003*
CorOleRation	6.534	0.002*
BrachRatio	22.411	<0.001*
Size pronator crest rel. length	0.323	0.724
Robusticity at 50%	7.048	0.001*
Robusticity at 25%	1.206	0.301
Robust dist artic	3.886	0.021*

*=significant at α=0.05

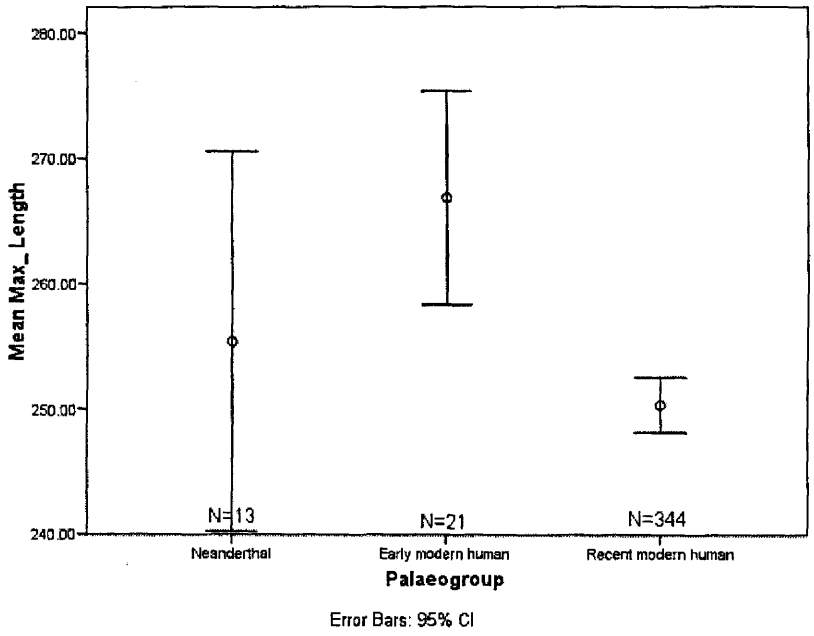

Figure 5-45 Maximum ulna length for Neanderthals, early and recent modern humans. Mean and 95% confidence interval (whiskers).

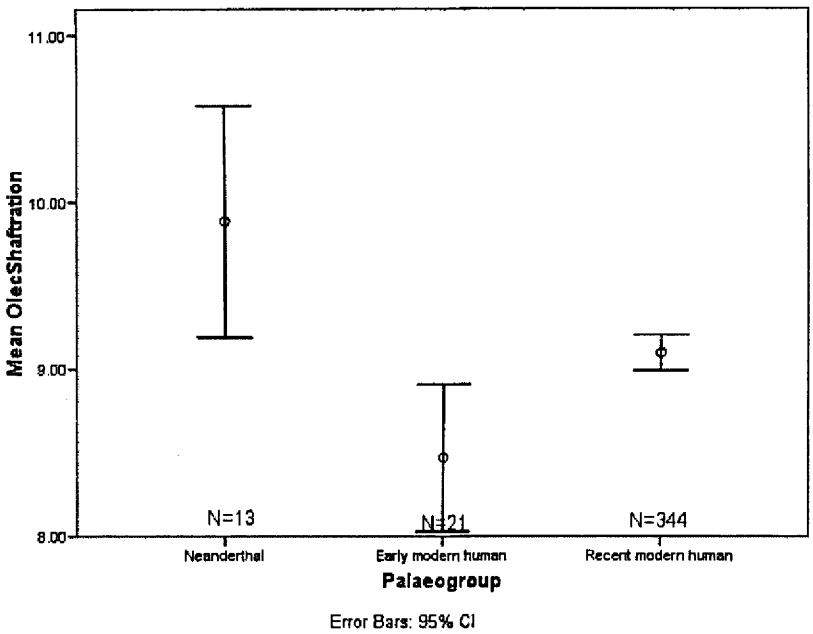

Figure 5-46 Olecranon-shaft ratio for Neanderthals, early and recent modern humans. Mean and 95% confidence interval (whiskers).

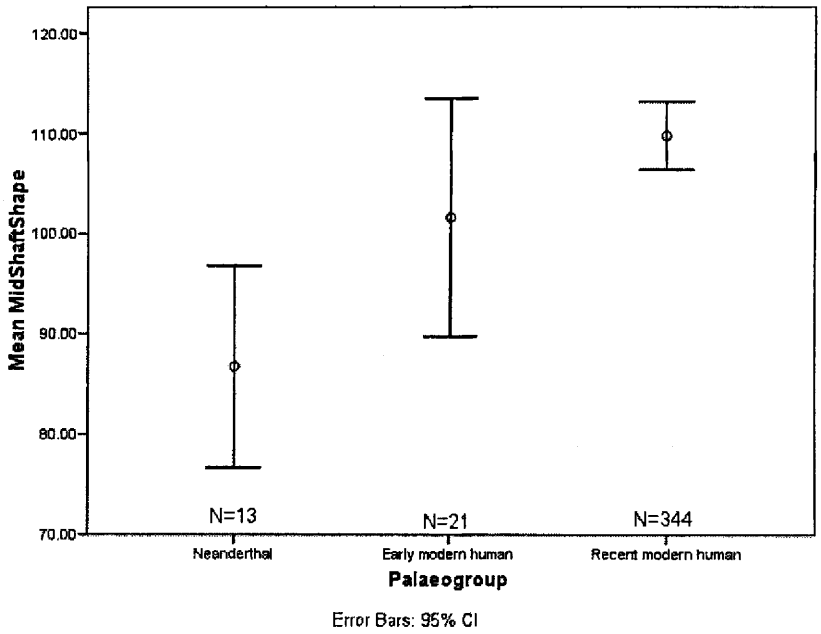

Figure 5-47 Midshaft shape ratio for Neanderthals, early and recent modern humans. Mean and 95% confidence interval (whiskers).

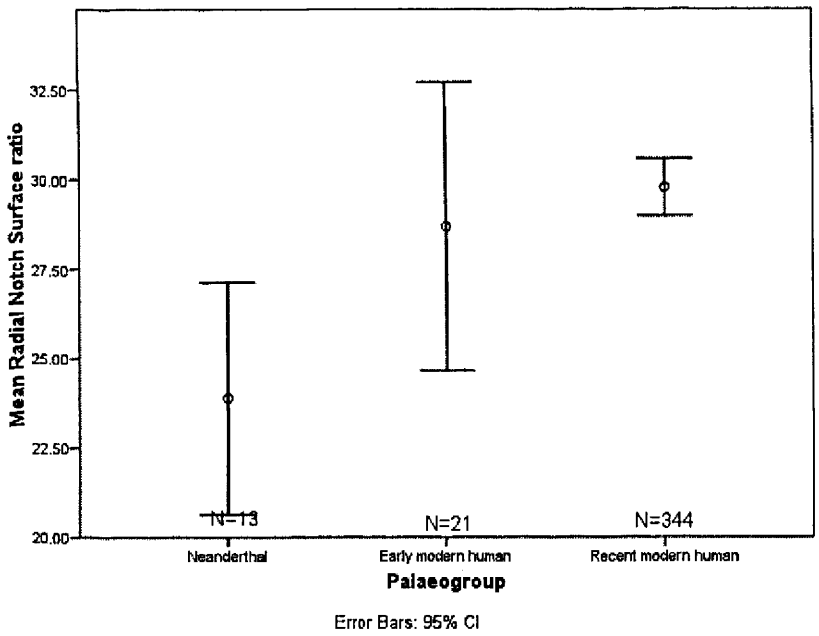

Figure 5-48 Radial notch surface area for Neanderthals, early and recent modern humans. Mean and 95% confidence interval (whiskers).

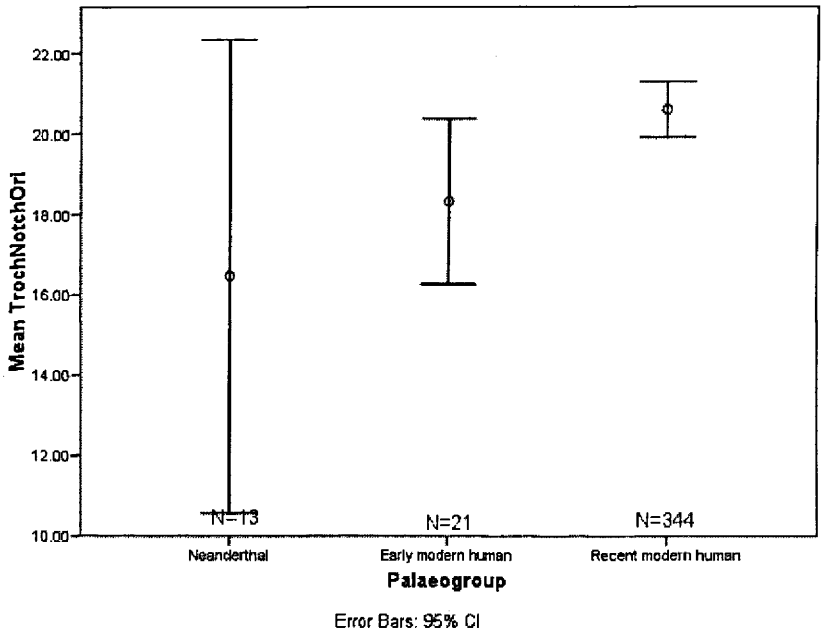

Figure 5-49 Trochlear notch orientation for Neanderthals, early and recent modern humans.
A lower value is a more anteriorly facing trochlear notch compare to a proximo-anteriorly facing one. Mean and 95% confidence interval (whiskers).

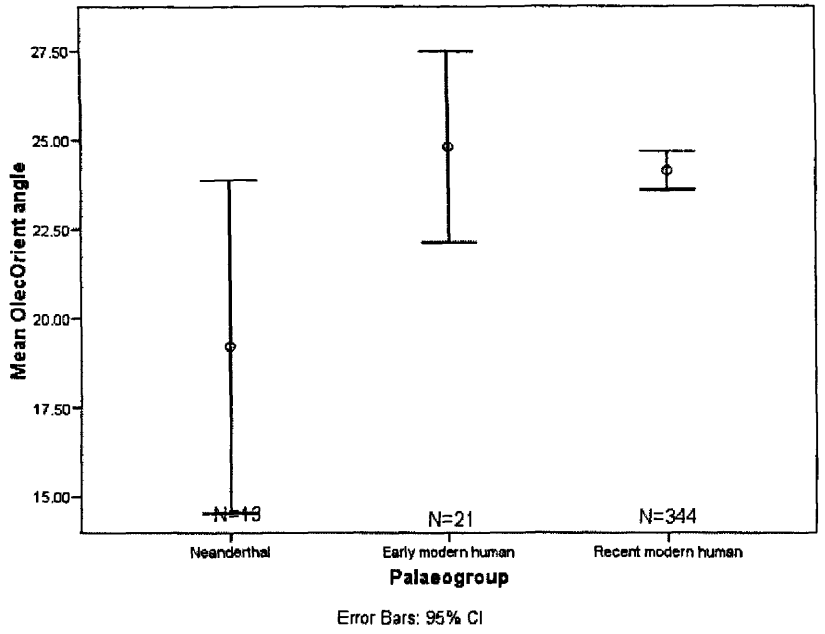

Figure 5-50 Olecranon orientation for Neanderthals, early and recent modern humans.
A lower value is a more anteriorly facing trochlear notch compare to a proximo-anteriorly facing one. Mean and 95% confidence interval (whiskers).

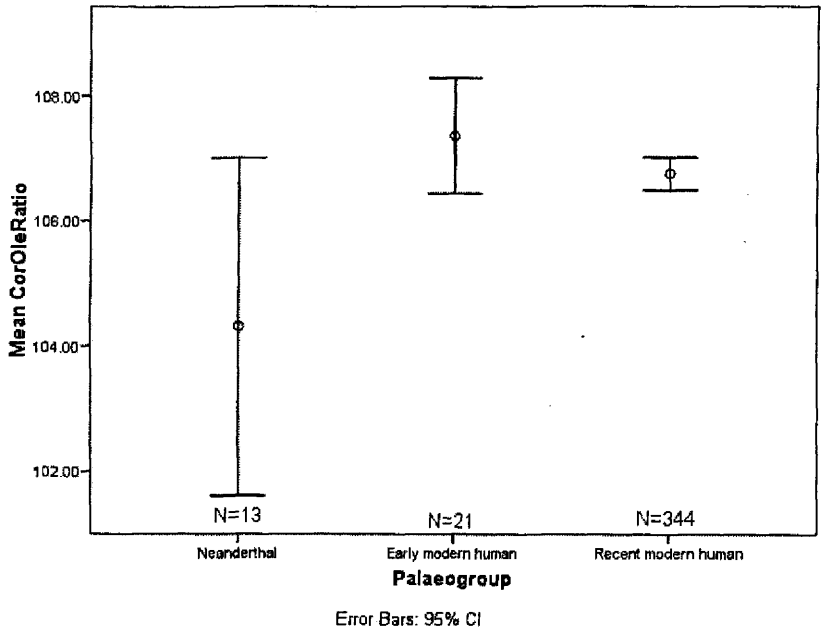

Figure 5-51 Coronoid-olecranon ratio for Neanderthals, early and recent modern humans. Mean and 95% confidence interval (whiskers).

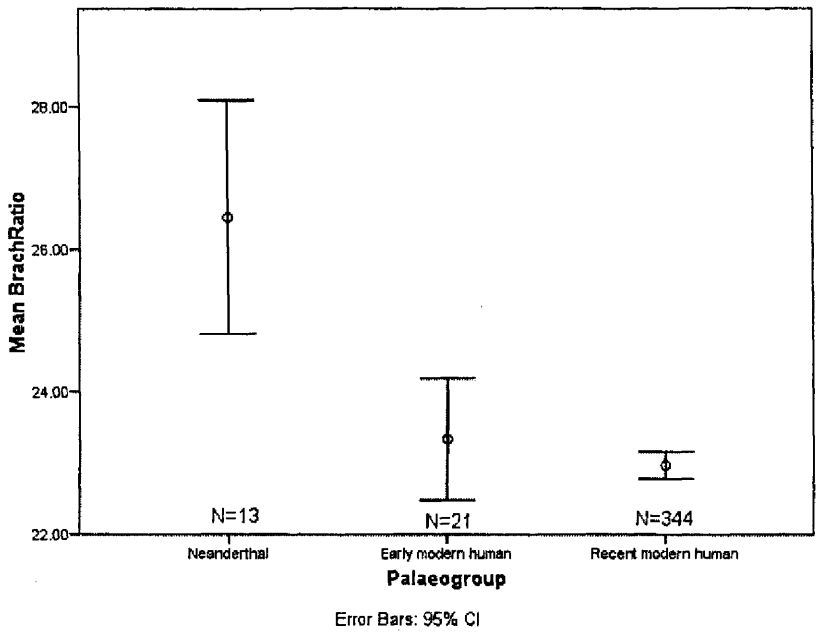

Figure 5-52 Brachial insertion ratio for Neanderthals, early and recent modern humans. A higher value means a relatively lower insertion. Mean and 95% confidence interval (whiskers).

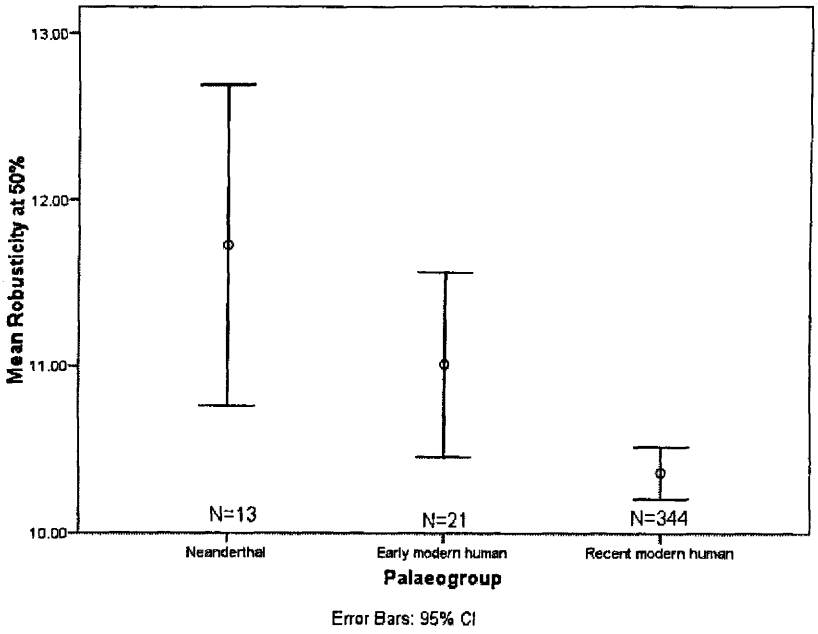

Figure 5-53 Ulna robusticity at 50% shaft level for Neanderthals, early and recent modern humans. Mean and 95% confidence interval (whiskers).

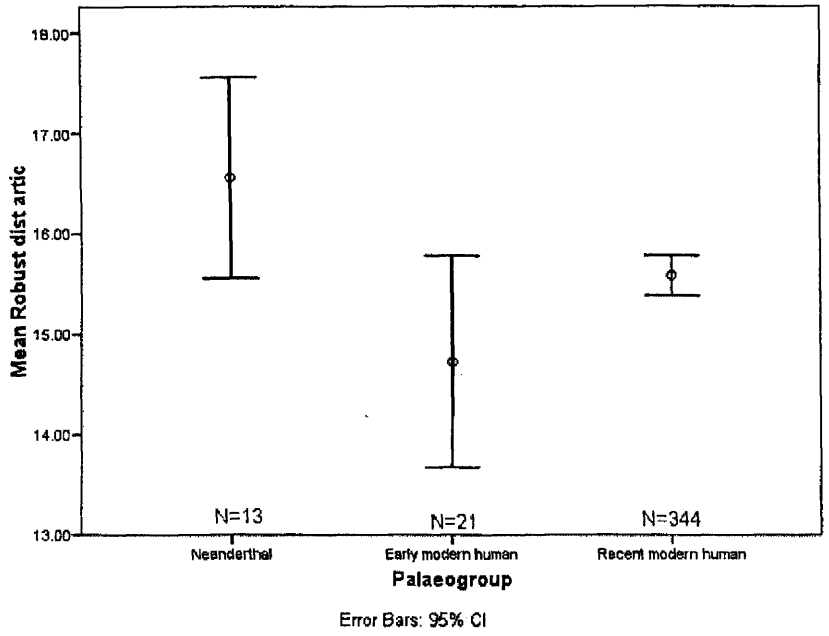

Figure 5-54 Robusticity of the head of the ulna area for Neanderthals, early and recent modern humans. Mean and 95% confidence interval (whiskers).

5.3.3.5. Discriminant function analysis

A DFA with cross-validation using all radius PCs used in the analyses above and univariate measurements of the radius was used to separate Neanderthals, early and recent modern humans (Figure 5-55). Function 1 separates best between Neanderthals and all modern humans, whereas function 2 separates early modern humans from recent modern humans. Function 1 reflects by (ordered according to decreasing correlation between the variable and the function) mcurveAllPC1 (medial curvature), head shape ratio, lcurveAllPC3, lcurveAllPC2, position of the radial tuberosity, lcurveAllPC1 (lateral curvature), neck-length ratio, and proximal and distal articulation size ratio. Function 2 reflects the length of the radius, midshaft shape, neck-shaft angle, head robusticity, mcurveAllPC2, mcurveAllPC3, EpiAllPC1 and midshaft robusticity (Table 5-24).

For all three groups (Neanderthals, early and recent humans) with very uneven sample sizes, the expected proportion of correct random classification based on sample sizes is ~85%. The DFA with cross-validation using all PCs for the radius included in the above analyses and univariate

measurements was able to classify Neanderthals and recent modern humans with 50% (7 out of 14) of Neanderthals and 83% (289 out of 348) of modern humans correctly classified. The early modern humans were classified correctly in 50 % (7 out of 14) of cases, 14.3% (2 out of 14) were classified as Neanderthals. This gives an overall correct classification of 80.6%.

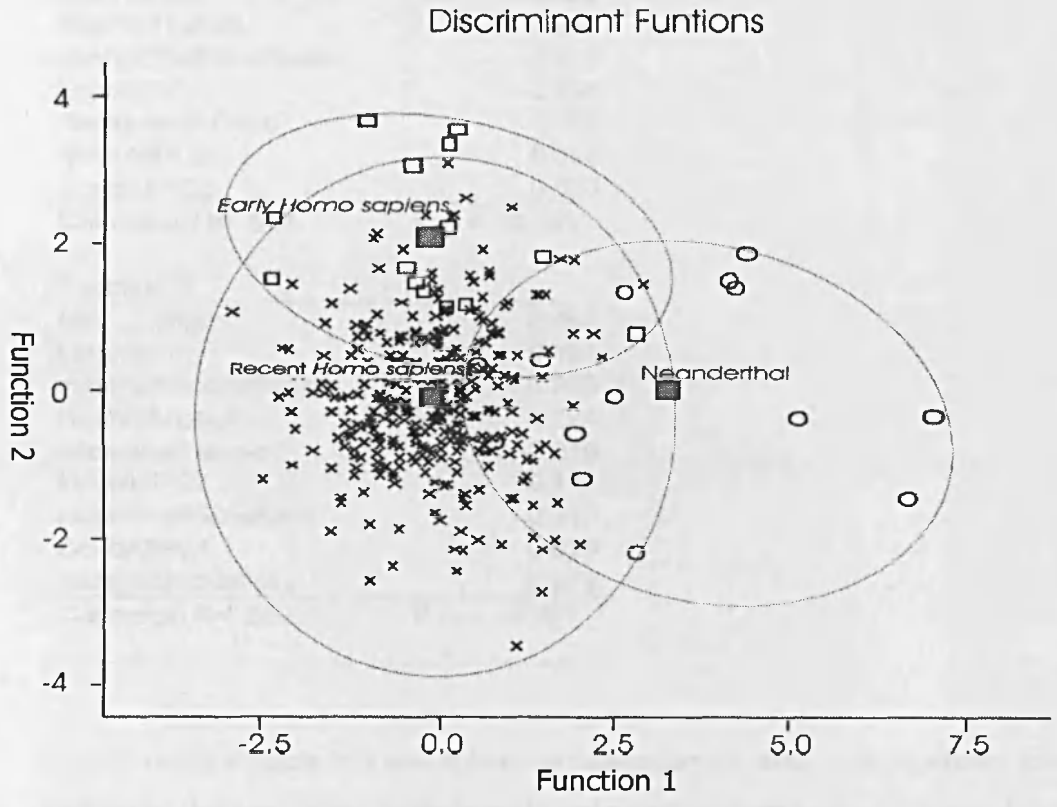

Figure 5-55 Discriminant Function 1 and 2 for for Neanderthals, early and recent modern humans.

Table 5-24 Discriminant function coefficients – radius.

Function 1	
McurAllPC1	-0.613
DorsalST	0.543
HeadShapeRatio	0.441
LcurAllPC3	0.398
LcurAllPC2	0.392
PosRadTubML	0.282
distArtShaftSizeRatio	0.197
LcurAllPC1	-0.196
NeckLengthRatio	0.193
McurAllPC3	0.069
CondAllPC2	0.020
Canonical R= .548	P Λ = <0.001

Function 2	
Max_ Length	0.467
LateralST	0.461
midshaftShapeRation	0.266
Headrobusticity	0.224
neck-shaft angle °	-0.219
McurAllPC2	-0.165
HeadShaftSizeRatio	0.112
CondAllPC1	0.079
Midshaftrobusticity	-0.077
Canonical R= .382	P Λ = <0.001

A DFA using all ulna PCs and univariate measurements used in the analyses above was used to distinguish between Neanderthals, early and recent modern humans (Figure 5-56). Function 1 separates best between Neanderthals and modern humans in general, whereas function 2 separates early modern humans from recent modern humans. Function 1 reflects (ordered according to decreasing correlation between the variable and the function) proxAllPC3 (direction of the trochlear notch), neck-shaft angle, surface area of the radial notch, robusticity at 25% and negatively by brachial tuberosity ratio, pcurveAllPC2, and robusticity at 50%. Function 2 reflects the length of the ulna, the size of the head, robusticity of the distal articulation, coronoid-olecranon ratio, ProxAllPC2, pcurveAllPC1, proxAllPC1, pronator crest size, pcurveAllPC3, and pcurveAllPC4 (Table 5-25).

For these three populations with very uneven sample sizes, the expected proportion of correct random classification is ~83%. The DFA with cross-validation using all PCs for the ulna included in the above analyses and univariate measurements was able to classify 61.5% (9 out of

15) of Neanderthals and 98.5% (356 out of 361) of recent modern humans correctly. Early modern humans had low classification success: 94.7% (14 out of 15) was classified as recent modern human, 5.3% (1 out of 15) were classified as Neanderthals. This gives an overall correct classification of 92.3%.

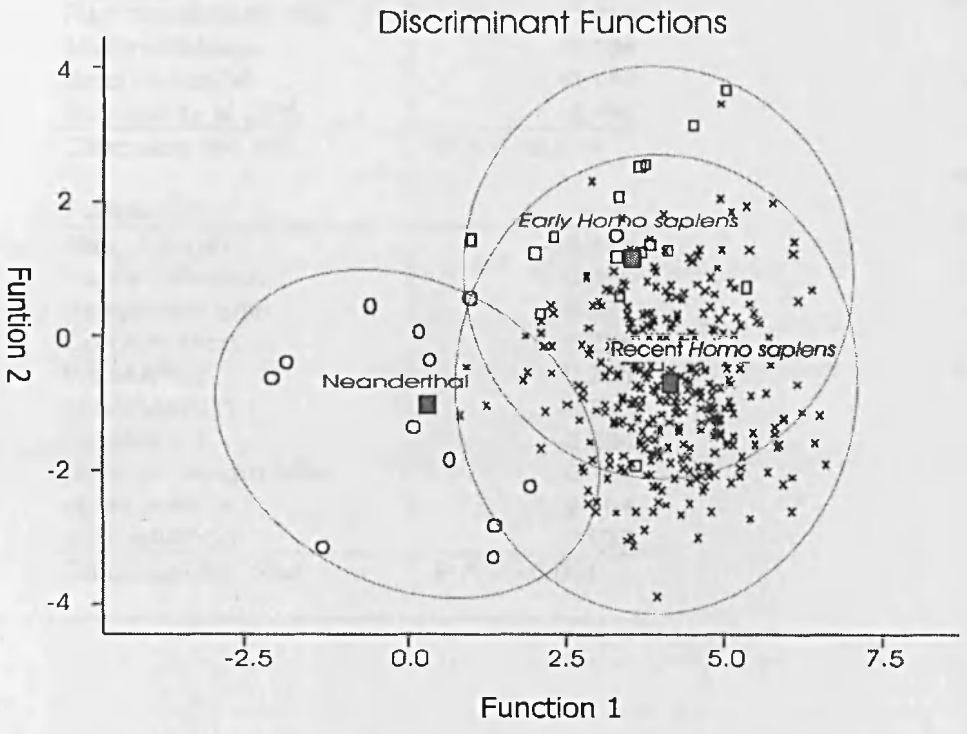

Figure 5-56 Discriminant Function 1 and 2 for Neanderthals, early and recent modern humans. Mean and 95% confidence interval (whiskers).

Table 5-25 Discriminant function coefficients - ulna

Function 1	
ProxAllPC3	0.577
BrachRatio	-0.480
pcurveAllPC2	-0.294
Robusticity at 50%	-0.252
headorient angle	0.233
Radi Notch Surf ratio	0.213
MidShaftShape	0.196
TrochNotchOri	0.178
Robusticity at 25%	-0.109
Canonical R= .581	P Λ = <0.001

Function 2	
Max_ Length	0.484
Headshaftration	-0.480
Robust dist artic	-0.362
CorOleRation	0.276
ProxAllPC2	0.251
pcurveAllPC1	-0.215
ProxAllPC1	-0.204
pron. cr. Length ratio	0.116
pcurveAllPC4	0.104
pcurveAllPC3	0.039
Canonical R= .344	P Λ = <0.001

5.3.4. Summary

Neanderthals have more curved radii (medial and lateral) and a more sinusoidally shaped shaft than modern humans, and early modern humans are similar to recent modern humans. Neanderthals also have an apex of curvature at midshaft, whereas that of modern humans is located proximally. The Neanderthals are not different in anteroposterior sinusoidal shape from modern humans. Neanderthals are characterised by a poorly projected styloid process and less mediolateral curvature of the ulnar shaft. Neanderthals have the most anterior facing trochlear notch. Early modern humans have an intermediate and modern humans have the most proximoanterior trochlear notch. Neanderthals have a large proximal ulna with a small neck-shaft angle, a low brachial tuberosity, and higher midshaft robusiticity of the ulna than recent modern humans.

CHAPTER 6. DISCUSSION AND CONCLUSION

6.1. Discussion

The goal of this research was to investigate the differences and similarities between Neanderthals and modern humans in long bone curvature. More specifically, this study tested hypotheses to explain variation in curvature among present-day and Holocene populations of humans, and applied these results to the interpretation of Neanderthals. Since there was relatively little information available about long bone curvature in modern humans, this study examined geographically, temporally and behaviourally diverse modern human samples in order to evaluate correlates of longitudinal long bone curvature such as body size, climate, habitual behaviour, and mobility. The femur and radius were chosen because they have been described as highly curved in Neanderthals (Ried, 1924; Patte, 1955; Churchill, 1998). The ulna was included because the shape of the radius can only be fully understood if its interaction with the ulna is also investigated.

Limitations of prior research on curvature may have been due to the difficulty of accurate quantification which is apparent from the inconsistency in techniques reported in the literature (Ried, 1924; Genna, 1930; Stewart, 1962; Walensky, 1962, 1965; Gilbert, 1975, 1976; Trudell, 1999; Shackelford and Trinkaus, 2002). Therefore, it was necessary to find a method to quantify the pattern of longitudinal bone curvature that would accurately represent the three-dimensional aspect of the diaphyseal surface and eliminate effects of scale. Three dimensional geometric morphometrics have frequently been used in cranial research (for an overview see Slice, 2005), but its application to postcrania is rare, and this method has not previously been used to quantify long bone curvature in humans and their close relatives. Here, the method was successfully tested for intra-observer error and shown to distinguish among populations more effectively than traditional methods, such as direct measurement of subtense.

In Chapter 4, the results of the curvature analyses for the femur, ulna and radius were presented for the recent human samples. These results suggest that there are patterns within long bone curvature but that these are different for the upper and lower limb. Femoral curvature is related to habitual activity patterns. The highest levels of curvature for the femur were found in

populations with the highest activity levels. Femoral curvature follows different trends from robusticity and is not necessarily a response to the same loading regime (Ruff *et al.*, 1993; Ruff *et al.*, 1994; Trinkaus *et al.*, 1994; Trinkaus *et al.*, 1999a; Pearson, 2000b; Ruff and Trinkaus, 2000; Shackelford and Trinkaus, 2002; Stock, 2002; Stock and Pfeiffer, 2004; Stock, 2006; Carlson *et al.*, 2007; Shackelford, 2007). For the femur, which is loaded proximodistally, curvature lowers bending stress by translating bending stress to axial compression (Frost, 1967; Hall, 2004), and curvature may be a compromise between bone strength and predictability of bending strains and material failure (Lanyon, 1980, 1987; Bertram and Biewener, 1988). Because femoral curvature is unrelated to climate (latitude in this analysis), it may ultimately be a better indicator of activity levels than cross-sectional measures of long bone robusticity.

In contrast, variation in curvature of the radius and ulna is influenced by climate. Individuals from colder climates tend to have more curved and more sinusoidal radii. Consistent with Bergmann's (1847) and Allen's (1877) rules on body size and proportions, human populations from colder climates have shortened distal limb segments, and it is thought that these differences are genetic adaptations rather than epigenetic outcomes (Bergmann, 1847; Allen, 1877; Y'Edynak, 1976; Eveleth and Tanner, 1990; Ruff *et al.*, 1994; Pearson, 2000b; Van Andel, 2003; Weaver, 2003; Ruff *et al.*, 2005). The results for the recent modern human sample suggest that curvature of the forearm bones is also a consequence of long-term exposure to cold climate conditions rather than as a result of habitual behaviour. This curvature is arguably not an adaptation in itself, but a consequence of reduced relative forearm length in cold-adapted populations. In order to optimise strength of the forearm despite its shorter length, curvature may serve to maintain full function of the pronation and supination muscles, preserve interosseous surface area and facilitate muscle packing by allowing for the position of slender attachments close to the joints while providing adequate space for the muscle bellies in the midshaft region (Lanyon and Bourn, 1979; Lanyon, 1980) (see Chapter 4).

In Chapter 5, variation between Neanderthals, early and recent modern humans was evaluated (Objective 2). Neanderthals are distinct from both early and recent modern humans and exhibit a higher degree of anterior femoral curvature and a higher degree of lateral and medial curvature of the radius. There are no differences in anteroposterior sinusoidal shaft shape of the ulna (posterior subtense) but Neanderthals are less mediolaterally sinusoidal than early and recent modern humans.

Based on previous research, Neanderthals are thought to show evidence of cold-adaption in their femora, radii and ulnae. For the femur, Neanderthals have extremely large femoral heads and knees (distal ends) which are consistent with their cold-adapted body proportions and relatively large body size (Trinkaus, 1981; Ruff, 1991; Churchill, 1998; Weaver, 2003). Both the radius and ulna are relatively short and also have large articulations. This shows that Neanderthals conform to Bergmann's (1847) and Allen's (1877) rules and that Neanderthals fall at the "cold" end of the distribution, more extreme than modern human populations. Some have suggested that the effects of, for example, foreshortening of the distal extremities is not a heat conservation mechanism reducing surface area, but instead is the effect of the cooling of distal segments of the limbs and slowing of the metabolism and growth of the peripheral tissues (Steegmann Jr. *et al.*, 2002). However, body shape manifests itself in early fetal life (Warren, 1998; Holliday, 2000) and does not appear to change with the secular trend in modern humans that affects body size and stature. Therefore, it is likely to be genetically controlled (Katzmarzyk and Leonard, 1998).

The extreme cold-adapted physique of Neanderthals can also be explained by their lifestyle (Churchill, 1998). Although Neanderthals would have needed additional protection from the cold in order to survive in Europe (Aiello and Wheeler, 2003), the severe physical stress of living in the Late Pleistocene cold European and Western Asian climate with simple technology may be sufficient to explain their hyper-polar body form (Churchill, 1998). The Mousterian (with which most Neanderthals are associated) does not show much evidence for cultural buffering against the cold. In contrast, the Upper Palaeolithic tool industries are typified by the first solid evidence for the systematic construction of complex hearths suitable for intensifying and containing heat (James *et al.*, 1989; Stiner, 1993; Trinkaus and Shipman, 1993 but see Henry *et al.*, 2004). Punches or awls and the subsequent appearance of needles represent advances in making tools for binding hide together for clothing (Trinkaus, 1981; Holliday, 1997; Holliday, 1999; Weaver and Steudel-Numbers, 2005 and articles in Mellars and Stringer, 1989). The lack of such technological advances in thermal protection in Neanderthals may explain the selective pressures on them while their presence in modern archaeological assemblages may point to the reduction in those selective pressures in modern humans inhabiting similar climates (Rak, 1990; Trinkaus *et al.*, 1998a; Holliday, 2000; Churchill, 2001; Niewoehner, 2001; Shea, 2003).

Although the Neanderthal femur shows some climatic adaptations (Trinkaus, 1981; Ruff, 1991; Churchill, 1998; Weaver, 2003), the results from the recent human analyses indicate that there is no effect of climate on the curvature of the femur (Walensky, 1965; Gilbert, 1976). In addition, curvature is not correlated to femoral torsion. This is consistent with femoral curvature being unrelated to climate because, if femoral curvature was a consequence of the wider "cold-adapted" Neanderthals hip, it would be correlated with torsion as was suggested by Weaver (2003).

The curvature of the radius and overall morphology of the ulna in Neanderthals shows good correspondence with the climate data. This climatic variation is confirmed also in the distribution of the medial radial curvature: fossils from Neanderthal populations in colder climates (Spy, Le Moustier, La Quina, La Ferrassie) have a higher degree of curvature than the Middle Eastern fossils (Shanidar and Kebara).

As discussed above, the relationship between curvature and climate can be explained as a consequence of the shortening of the forearm. Other characteristics in the forearm that are correlated with climate in recent modern humans are a more sinusoidal radial shaft, shortening of the ulnar neck (distance between 80% level of the ulna and the tip of the coronoid), a proximo-anteriorly facing trochlear notch, increased distal articulation size, a larger ulnar head relative to shaft, larger radial notch surface area and a relatively lower insertion of the brachial muscle. These features indicate that the absolute dimensions of the head and articulations of the ulna and radius remain relatively large for the length of the shaft. Also, foreshortening of the forearm in response to cold climatic conditions is not a scaling down of the whole bone but rather a reduction in shaft length. Shortening the diaphysis reduces the surface area for muscle insertions and may affect lever advantage and contraction function (which is affected by muscle fibre size) of several arm and hand muscles, such as the *pronator teres* (Hall, 2004). Therefore, curvature may be a means of maintaining full function and force despite a reduction in length. By increasing the curvature of the radius and adopting a more sinusoidal shaft shape diaphyseal length is maximised.

The results for the Neanderthal ulna and radius show that Neanderthals have all the above mentioned "cold climate features" and express them to a more extreme degree. Neanderthals have the highest degree of lateral curvature of the radius, relatively the largest ulnar head, shortest ulnar neck (distance between 80% of the shaft and the tip of the coronoid), the most

anteriorly facing trochlear notch and the most inferior brachial tuberosity. The emergence of modern humans saw a pronounced reduction in the muscular hypertrophy of the upper limb (Trinkaus, 1986) and a reduction in the size of the muscle insertions on the arm and hand skeleton (pronator quadratus on the ulna, the flexor pollicis longus and the opponens muscles on the carpals and distal phalanges) (Trinkaus, 1983a). The reduction in muscle size in modern humans may also explain the lower degree of curvature in modern-day Arctic populations compared to Neanderthals (Lanyon and Bourn, 1979).

The Neanderthal radius shows some distinct features such as a more medially placed radial tuberosity compared to modern humans. It has been suggested that this position of the radial tuberosity is a consequence of the use of the forearm in flexion (Trinkaus and Churchill, 1988). In the present study it was predicted that if curvature of the radius is a result of the habitual use of the arm in that position and the associated increased strain of the forearm, that there would be a correlation between the position of the radial tuberosity, the neck-length of the radius and curvature. Neanderthals do have a more medially oriented radial tuberosity than do modern humans, but there is no correlation with neck length or with curvature. Also, in modern humans a more medially oriented radial tuberosity was associated with low activity levels.

The recent modern human analyses suggested that femoral curvature is a plastic feature that responds to loading of the femur during activity. Confirming the hypothesis by Shackelford and Trinkaus (2002), populations with high activity levels have a high degree of femoral curvature. This was evident also in the relationship between activity levels and robusticity at different points along the shaft. It is not surprising, then, that there is a relationship between curvature and robusticity in modern humans. The correlation between cross-sectional anteroposterior robusticity and activity levels was hypothesised to be the result of repetitive loading on the lower limb during subsistence strategy-related terrestrial mobility (Ruff, 1987; 1994; Larsen et al., 1995; Holt, 2003; Stock and Pfeiffer, 2004), and this hypothesis is supported by the strength circularity indices at the femoral midshaft and their strong correspondence with terrestrial mobility (Stock, 2006). Because of the correlation between subsistence-related activity and curvature in recent modern humans, the prediction was that Neanderthals, being hunter-gatherers, would have a high degree of femoral curvature. Moreover, their curvature should be comparable to that of early modern humans because the two groups had broadly similar lifestyles (Trinkaus *et al.*, 1989).

Early modern humans and Neanderthals most likely did not differ in their subsistence strategies and were both hunting and scavenging (Lieberman, 1989; Bar-Yosef, 2004; Pearson *et al.*, 2006). Faunal assemblages from occupation and butchery sites shows that both groups had early access to the animals and cut-mark patterns indicate a primary reliance on hunting rather than scavenging (Speth and Tchernov, 1998). Trinkaus and Zimmerman (1982) and Klein (2003) have argued that Middle Stone Age people were less adept hunters because they only hunted a few of the available species and that Neanderthals show a high incidence of skeletal trauma because of the risk involved in close range hunting (Trinkaus and Zimmerman, 1982; Klein, 2003). Recent investigations of faunal assemblages have shown that some Neanderthal sites may be dominated by a single prey species, but this is also documented among some modern hunter-gatherer societies (Marean and Assefa, 1999; Marean and Assefa, 2005).

The reliance on meat for Neanderthals and early modern humans living in temperate and cold regions such as Europe and Western Asia was important for survival. Early Europeans must have relied on frequent meat acquisition for their diet as it is likely that plant foods would have been unavailable for consumption during parts of the year. This is confirmed in stable-isotope analyses from sites such as Vindija Cave, Croatia; Scladina, Spy and Engis in Belgium and Marillac and Saint-Césaire in France (Fizet *et al.*, 1995; Richards *et al.*, 2000; Bocherens *et al.*, 2001; Richards *et al.*, 2001; Drucker and Bocherens, 2004; Bocherens *et al.*, 2005).

Marean (1999) argued that the Middle Palaeolithic Neanderthals may not have been less adept hunters than their Middle Stone Age modern human contemporaries but, instead, might have been less adept at using and processing carcasses in order to render higher caloric yields, such as fat rendering and storage, which put them at a subtle disadvantage in comparison to modern humans. These disadvantages were not only the lower caloric intake per prey animal, but also the increased personal risk because of more frequent hunting (Marean and Assefa, 1999). This low return on time expended may have resulted in moderately higher activity and mobility levels in Neanderthals compared to early anatomically modern humans.

Similarities in lifestyle and subsistence pattern between Neanderthals and the earliest modern humans is also apparent in the archaeological record, where similar species of large animals are found in both Neanderthal and early modern human deposits. Neanderthals were effective hunters (Speth and Tchernov, 1998) and some consider them a top predator in the environment in which they lived (Bocherens *et al.*, 2005). They also hunted a given region for a longer period

of time than modern humans who were more seasonally mobile (Lieberman, 1989). Although there is some variation, overall, Neanderthals and early modern humans were likely very similar in terms of mobility, resource acquisition and overall workload, and this is apparent in their postcranial anatomy (Lieberman, 1989). When corrected for size and body proportions, Neanderthals have lower limb bones that were similar in cross-sectional strength to those of modern humans (Trinkaus *et al.*, 1989). This is also reflected in the results on robusticity presented here, which showed no significant differences between robusticity levels of the shaft between Neanderthals and early modern humans.

In degree of femoral curvature, however, and contrary to the hypothesis of Shackelford and Trinkaus (2002), Neanderthals show a significantly higher degree of curvature and a lower apex of curvature compared to both early and recent modern humans. This difference suggests that Neanderthals had much higher activity levels, in contrast to what is suggested by the robusticity results (Trinkaus *et al.*, 1989).

The comparatively small range of variation in femoral curvature in Neanderthals compared to early and recent modern humans (and in particular compared to the range of variation of the high activity group) suggests that Neanderthals had a smaller range of subsistence behaviours than modern humans and that this behaviour involved high activity levels. The curvature of the radius is a reflection of climate and the variation among Neanderthals and early modern humans is very wide compared to that of recent modern humans. Also Neanderthal radii from the Levant tend to be less curved than those from Northwest Europe. Most early modern humans fall within the range of recent modern humans, but Skhul IV and Qafzeh 9 fall outside. The sites of Skhul and Qafzeh are the earliest modern human sites outside of Africa, and it has been suggested that the individuals from these sites were not yet fully modern human (McCown and Keith, 1939b, 1939a; Arensburg and Belfer-Cohen, 1998; Kramer *et al.*, 2001; Rak, 2002). The early modern humans from Skhul and Qafzeh also pre-date the presence of Neanderthals in the region, and some have suggested that the distinctiveness of Neanderthal *versus* modern humans in the Levant may not be as clear as in other places, and the overlap in morphology may be explainable by admixture between the two groups (Kramer *et al.*, 2001). This may also explain the higher degree of radial curvature observed in those two individuals compared to the rest of the group.

In light of the recent genetic evidence showing that Neanderthals did not contribute to the modern human gene pool (Caramelli *et al.*, 2003; Ovchinnikov and Goodwin, 2003; Green *et al.*,

2006) the differences in curvature of the Skhul and Qafzeh could be explained by the very early date for these individuals if there was evidence for increased muscularity relative to more recent modern humans. This has been contradicted by studies on the humerus and hand bones which showed that the early Near Eastern modern humans were more gracile than Middle Stone Age and later Upper Palaeolithic modern humans and were thus somewhat of an anomaly (Trinkaus and Churchill, 1999; Niewoehner, 2001).

The evolutionary significance of long bone curvature for hominins more generally has not been investigated. The femur and radius of gorillas and chimpanzees are more curved than those of modern humans (Martin and Saller, 1959), and long bone curvature in primates is known to scale positively with body weight (Swartz, 1990). In humans, there is no correlation between body size and curvature, but the variation in modern human long bone curvature shows that, despite not being allometrically scaled, its plasticity was retained throughout human evolution and curvature should therefore be considered a selectively adaptive feature.

With the shift to bipedal walking in hominins, weight distribution and muscle organisation of the femur has changed, and the upper limb lost its locomotor function. The functional significance of long bone curvature in earlier hominins has not been commented on, but it is possible to examine some hominin casts and published photographs. The *Homo erectus* Nariokotome femur is relatively straight but the *Homo sp.* KNM-ER 1481 shows a marked degree of femoral curvature despite having a relatively gracile shaft. Photographs of relatively complete femora from other members of the genus *Homo,* such as those from Atapuerca and Dmanisi, have only been published in anterior view, so it is impossible to comment on the degree of femoral curvature (Lordkipanidze *et al.*, 2007). Radii are poorly represented in the fossil record. The fragmentary radius from OH 62 and a fragment from KNM-ER 3735 indicate a moderately curved radius for *H. habilis* (Haeusler and McHenry, 2004), and a radial fragment from Atapuerca suggests a low degree of radial curvature for *H. antecessor*. Although complete and well dated postcranial fossils are relatively rare, the use of 3D geometric morphometrics on both complete and partial fossil specimens and a comparison with the African apes should provide sufficient data for investigating further the evolutionary significance of long bone curvature in earlier hominins.

6.2. Conclusion

The evidence presented here supports the hypothesis that femoral curvature is a bone response to stresses and strains during habitual behaviour and shows good correspondence with measures of external robusticity. Populations with high activity levels have a higher degree of anterior femoral curvature and a more distal apex of curvature than populations with low and moderate activity levels. Within populations with high activity levels, males have more curved femora than females. This is not due to sexual dimorphism in body size or sex differences in bone modelling and remodelling as there is no sex difference in groups who have less sexual division of labour and curvature is not correlated to body size. Of the high activity subsistence strategies the aquatic foragers, with low levels of terrestrial activity, are the least curved, and the pastoralists, with high levels of terrestrial mobility, are the most curved. Biomechanically, increased femoral curvature serves to generate physiologically beneficial strains, facilitates muscle packing and increases the predictability of material failure.

Lateral curvature of the radius, mediolateral curvature of the ulna and overall forearm bone shape are correlated with climate and are poor predictors of habitual behaviour. However, the aquatic foragers were distinct in having a proximal development on the interosseous crest and high neck-shaft angles which may reflect their use of watercraft. Curvature of the radius and ulna is likely a consequence of the foreshortening of the forearm in cold-adapted populations. The results suggest that this foreshortening is a reduction in length of the diaphysis while maintaining relatively large epiphyses and rather than an overall downscaling of the bone. Increased forearm bone curvature aids in maintaining the tendon insertions close to the joints while facilitating muscle packing, and retaining interosseous space, muscle length and function and maximising diaphyseal length.

Neanderthals and early modern humans had broadly similar hunter-gatherer lifestyles, and their postcranial skeleton was likely subject to the same stresses as modern humans. Neanderthals show a high degree of femoral curvature, reflecting their active lifestyles, and a high degree of radial curvature, reflecting their cold-adapted body form. Early modern humans display a high degree of femoral curvature but, contrary to Neanderthals, one that is well within the range of variation of modern humans. Early modern humans, except for Skhul and Qafzeh, show a range

6.2. Conclusion

The evidence presented here supports the hypothesis that femoral curvature is a bone response to stresses and strains during habitual behaviour and shows good correspondence with measures of external robusticity. Populations with high activity levels have a higher degree of anterior femoral curvature and a more distal apex of curvature than populations with low and moderate activity levels. Within populations with high activity levels, males have more curved femora than females. This is not due to sexual dimorphism in body size or sex differences in bone modelling and remodelling as there is no sex difference in groups who have less sexual division of labour and curvature is not correlated to body size. Of the high activity subsistence strategies the aquatic foragers, with low levels of terrestrial activity, are the least curved, and the pastoralists, with high levels of terrestrial mobility, are the most curved. Biomechanically, increased femoral curvature serves to generate physiologically beneficial strains, facilitates muscle packing and increases the predictability of material failure.

Lateral curvature of the radius, mediolateral curvature of the ulna and overall forearm bone shape are correlated with climate and are poor predictors of habitual behaviour. However, the aquatic foragers were distinct in having a proximal development on the interosseous crest and high neck-shaft angles which may reflect their use of watercraft. Curvature of the radius and ulna is likely a consequence of the foreshortening of the forearm in cold-adapted populations. The results suggest that this foreshortening is a reduction in length of the diaphysis while maintaining relatively large epiphyses and rather than an overall downscaling of the bone. Increased forearm bone curvature aids in maintaining the tendon insertions close to the joints while facilitating muscle packing, and retaining interosseous space, muscle length and function and maximising diaphyseal length.

Neanderthals and early modern humans had broadly similar hunter-gatherer lifestyles, and their postcranial skeleton was likely subject to the same stresses as modern humans. Neanderthals show a high degree of femoral curvature, reflecting their active lifestyles, and a high degree of radial curvature, reflecting their cold-adapted body form. Early modern humans display a high degree of femoral curvature but, contrary to Neanderthals, one that is well within the range of variation of modern humans. Early modern humans, except for Skhul and Qafzeh, show a range

REFERENCES

Abe, Y., (2005). *Hunting and Butchery Patterns of the Evenki in Northern Transbaikalia, Russia*. PhD dissertation. Stony Brook University

Ackermann, R. R., (2002). Patterns of covariation in the hominoid craniofacial skeleton: implications for paleoanthropological models. *Journal of Human Evolution* 43 (2): 167.

Adams, D. C., Rohlf, F. J., Slice, D. E., (2004). Geometric morphometrics: ten years of progress following the 'revolution'. *Italian Journal of Zoology* 71: 5.

Adovasio, J. M., Soffer, O., Klima, B., (1996). Upper palaeolithic fibre technology: Interlaced woven finds from Pavlov I, Czech Republic, c 26,000 years ago. *Antiquity* 70 (269): 526.

Ahern, J. C. M., Karavanic, I., Paunovic, M., Jankovic, I., Smith, F. H., (2004). New discoveries and interpretations of hominid fossils and artifacts from Vindija Cave, Croatia. *Journal of Human Evolution* 46 (1): 27.

Aiello, L., Dean, C., (1990). Human Evolutionary Anatomy. London: Elsevier Academic Press.

Aiello, L., Wood, B., Key, K., Lewis, M., (1999). Morphology and taxonomic affinities of the Olduvai Ulna (OH 36). *American Journal of Physical Anthropology* 109: 89.

Aiello, L., Wheeler, P., (2003). Neanderthal Thermoregulation and the Glacial Climate. In: van Andel, T. H. , Davies, W. (Eds.) Neanderthals and modern humans in the European landscape during the last glaciation. Oxford: McDonald Institute Monographs, pp. 147-166.

Aiello, L. C., (1993). The Fossil Evidence for Modern Human Origins in Africa: A Revised View. *American Anthropologist* 95 (1): 73.

Alexander, R. M., (1981). Factors of safety in the structure of animals. *Science Progress* 67 (265): 109.

Allen, J. A., (1877). The influence of physical conditions on the genesis of species. *Radical Review* 108: 40.

Alt, K. W., Pichler, S., Vach, W., Klįma, B., Vlcek, E., Sedlmeier, J., (1997). Twenty-five thousand-year-old triple burial from Dolnį Vestonice: An ice-age family? *American Journal of Physical Anthropology* 102: 123.

Anderson, J. Y., Trinkaus, E., (1998). Patterns of sexual, bilateral and interpopulational variation in human femoral neck-shaft angle. *Journal of Anatomy* 192: 279.

Arensburg, B., Bar-Yosef, O., (1973). Human remains from Ein Gev 1, Jordan valley, Israel. . *Paleorient* 1: 201.

Arensburg, B., (1977). New Upper Palaeolithic remains from Israel. *Eretz Israel* 13 (Moshe Stekelis Memorial Volume): 208.

Arensburg, B., Belfer-Cohen, A., (1998). Sapiens and Neandertals. In: Akazawa, T., Aoki, K., Bar-Yosef, O. (Eds.) Neandertals and Modern Humans in Western Asia. New York: Plenum, pp. 311-322.

Auerbach, B. M., Ruff, C., (2004). Human body mass estimation: a comparison of "morphometric" and "mechanical" methods. *American Journal of Physical Anthropology* 125: 331.

Bahn, P. G., (1988). Archaeology - Triple Czech Burial. *Nature* 332 (6162): 302.

Bahuchet, S., (1990). The Aka Pygmies: hunting and gathering in the Lobaye forest. In: Hladik, C. M., Baghuchet, S., de Garine, I. (Eds.) Food and nutrition in the African rain forest. Paris: UNESCO, pp. 19-23.

Bar-Yosef, (1998). The Natufian culture in the Levant, threshold to the origins of agriculture. *Evolutionary Anthropology* 6: 159.

Bar-Yosef, O., Vandermeersch, B., Arensburg, B., Goldberg, P., Laville, H., Meignen, L., Rak, Y., Tchernov, E., Tillier, A. M., (1986). New Data on the Origin of Modern Man in the Levant. *Current Anthropology* 27 (1): 63.

Bar-Yosef, O., (1989). Geochronology of the Levantine Middle Palaeolithic. In: Mellars, P., Stringer, C. (Eds.) The human revolution Edinburgh: Edinburgh University Press, pp. 589-610.

Bar-Yosef, O., (1992). The Role of Western Asia in Modern Human Origins. *Philosophical Transactions: Biological Sciences* 337 (1280): 193.

Bar-Yosef, O., (2004). Eat what is there: hunting and gathering in the world of Neanderthals and their neighbours. *International Journal of Osteoarchaeology* 14 (3-4): 333.

Belfer-Cohen, A., Davidzon, A., Goring-Morris, A. N., Lieberman, D. E., Spiers, M., (2004). Nahal Ein Gev I : A Late Upper Palaeolithic Site by the Sea of Galilee, Israel *Paleorient* 30 (1): 25.

Bergmann, C., (1847). Über die Verhältnisse der Wärmteökonomie der Thiere zu ihrer Grösse. *Göttinger Studien* 1: 595.

Bertram, J. E., Biewener, A. A., (1988). Bone curvature: Sacrificing strength for load predictability? *Journal of Theoretical Biology* 131 (1): 75.

Bertram, J. E., Biewener, A. A., (1992). Allometry and curvature in the long bones of quadrupedal mammals. *Journal of Zoology (London)* 226: 455.

Biewener, A. A., (1983). Allometry of Quadrupedal Locomotion - the Scaling of Duty Factor, Bone Curvature and Limb Orientation to Body Size. *Journal of Experimental Biology* 105 (JUL): 147.

Biewener, A. A., Bertram, J. E., (1994). Structural response of growing bone to exercise and disuse. *J Appl Physiol* 76 (2): 946.

Billy, G., (1969). Le squelette postcrânien de l'homme de Chancelade. *L' Anthropologie* 73: 207.

Blanchard, R., (1935). Découverte d'un squelette humain à Saint-Germain-la-Rivière. *Revue Historique et Archéologique du Libournais* 9: 11.

Bocherens, H., Billiou, D., Mariotti, A., Toussaint, M., Patou-Mathis, M., Bonjean, D., Otte, M., (2001). New isotopic evidence for dietary habits of Neandertals from Belgium. *Journal of Human Evolution* 40 (6): 497.

Bocherens, H., Drucker, D. G., Billiou, D., Patou-Mathis, M., Vandermeersch, B., (2005). Isotopic evidence for diet and subsistence pattern of the Saint-Cesaire I Neanderthal: review and use of a multi-source mixing model. *Journal of Human Evolution* 49 (1): 71.

Bollen, P., (2000). Tierra del Fuego. Tielt: Lannoo Publishers.

Bonifay, E., Vandermeersch, B., (1962). Paleontologie Humaine - Dépots rituels d'ossements d'ours dans le gisement Mousterien du Régourdou (Montignac, Dordogne). *Comptes Rendus Hebdomadaires Des Seances De L Academie Des Sciences* 255 (14): 1635.

Bonifay, E., (1964). La grotte du Régourdou (Montignac, Dordogne): stratigraphie et industrie lithique moustérienne. *L'Anthropologie* 68:

Bookstein, F., (1991). Morphometric Tools for Landmark Data. Cambridge: Cambridge University Press.

Bookstein, F., (1996). Landmark methods for forms without landmarks: morphometrics of group differences in outline shape. *Medical Image Analysis* 1 (3): 225.

Bookstein, F. L., Gunz, P., Mitteroecker, P., Prossinger, H., Schaefer, K., Seidler, H., (2003). Cranial integration in Homo: singular warps analysis of the midsagittal plane in ontogeny and evolution. *Journal of Human Evolution* 44 (2): 167.

Boonzaier, E., Malherbe, C., Berens, P., Smith, A., (1996). The Cape Herders. Cape Town: David Philip Publishers (Pty) Ltd.

Bordes, F. H., (1959). Le Context Archéologique des Hommes du Moustier et du Spy. *L'Anthropologie* 63: 154.

Boule, M., (1908). L'homme fossile de la Chapelle-aux-Saints (Corrèze),. *L' Anthropologie* 19: 519.

Boule, M., Vallois, H. V., (1952). Fossil Men: A textbook of human palaeontology. London: Thames and Hudson.

Bridges, P. S., (1989a). Changes in Activities with the Shift to Agriculture in the Southeastern United States. *Current Anthropology* 30 (3): 385.

Bridges, P. S., (1989b). Spondylolysis and its relationship to degenerative joint disease in the prehistoric Southeastern United States. *American Journal of Physical Anthropology* 79 (3): 321.

Bridges, P. S., Martin, J. H. B., Solano, C., (2000). Changes in long bone diaphyseal strength with horticultural intensification in west-central Illinois. *American Journal of Physical Anthropology* 112 (2): 217.

Brock, S. L., Ruff, C. B., (1988). Diachronic patterns of change in structural properties of the femur in the prehistoric American Southwest. *American Journal of Physical Anthropology* 75 (1): 113.

Bröste, K., Jörgensen, J. B., Becker, C. J., Bröndsted, J., (1956). Prehistoric man in Denmark: (Vols. I & II, Stone and Bronze Ages, Part 1 & 2.). Copenhagen: Einar Munksgaard.

Bruns, W., Bruce, M., Prescott, G., Maffulli, N., (2002). Temporal trends in Femoral Curvature and Length in Medieval and Modern Scotland. *American Journal of Physical Anthropology* 119: 224.

Burch, E. S., Burch Jr., E. S., (2006). Social Life in Northwest Alaska: The Structure of Iñupiaq Eskimo Nations. Anchorage: University of Alaska Press.

Caramelli, D., Fox, C. L., Vernesi, C., Lari, M., Casoli, A., Mallegni, F., Chiarelli, B., Dupanloup, I., Bertranpetit, J., Barbujani, G., Bertorelle, G., (2003). Evidence for a genetic discontinuity between Neandertals and 24.000-year-old anatomically modern humans. *Proceedings of the National Academy of Science* 100 (11): 6593.

Carlson, K. J., Grine, F. E., Pearson, O. M., (2007). Robusticity and sexual dimorphism in the postcranium of modern hunter-gatherers from Australia. *American Journal of Physical Anthropology* 134 (1): 9.

Carretero, J. M., Lorenzo, C., Arsuaga, J. L., (1999). Axial and appendicular skeleton of Homo antecessor. *Journal of Human Evolution* 37 (3-4): 459.

Carroll, S. B., (2003). Genetics and the making of *Homo sapiens*. *Nature* 422: 849.

Carter, D. R., Van der Meulen, M. C. H., Beaupre, G. S., (1996). Mechanical factors in bone growth and development. *Bone* 18 (1, Supplement 1): S5.

Caspersen, C. J., Pereira, M. A., Curran, K. M., (2000). Changes in physical activity patterns in the United States, by sex and cross-sectional age. *Medicine and Science in Sports and Exercise* 32 (9): 1601.

Cauwe, N., Vander Linden, M., Vanmonfort, B., (2001). The Middle and Late Neolithic. *Anthropolgica et Praehistorica* 112: 77.

Churchill, S. E., Pearson, O. M., Grine, F. E., Trinkaus, E., Holliday, T. W., (1996). Morphological affinities of the proximal ulna from Klasies River main site: archaic or modern? *Journal of Human Evolution* 31: 213.

Churchill, S. E., (1998). Cold adaptation, Heterochrony and Neandertals. *Evolutionary Anthropology* 7 (2): 46.

Churchill, S. E., (2001). Hand morphology, manipulation, and tool use in Neandertals and early modern humans from the Near East. *Proceedings of the National Academy of Science* 98 (6): 2953.

Churchill, S. E., (2005). Particulate versus integrated evolution of the upper body in Late Pleistocene humans: a test of two models. *American Journal of Physical Anthropology* 100: 559.

Clinch, G., (1904). Coldrum, Kent, and Its Relation to Stonehenge. *Man* 4: 20.

Cordy, J.-M., (1988). Apport de la paléozoologie à la paléoécologie et à la chronostratigraphie en Europe du nord-occidental. *Etudes et Rercherches Archéologiques de l'Université de Liège (E.R.A.U.L.), Université de Liège, Liège* L'Homme de Neandertal, 2, L'environnement, : 55.

Costamagno, S., (2002). Laboratory taphonomy; material loss and skeletal part profiles: the example of Saint-Germain-la-Rivière grave (Gironde, France). *Archaeometry* 44 (3): 495.

Cristofolini, L., Viceconti, M., Toni, A., Giunti, A., (1995). Influence of thigh muscles on the axial strains in a proximal femur during early stance in gait. *Journal of Biomechanics* 28 (5): 617.

Crum, S., (1996). People of the Red Earth: American Indians of Colorado. Albuquerque: University of New Mexico Press.

Czarnetzki, A., (2000). The significance of pathological changes for judging the morphology of classical Neanderthals. In: Orschiedt, J. , Weniger, G.-C. (Eds.) Neanderthals and Modern Humans - Discussing the Transition: Central and Eastern Europe from 50.000 - 30.000 B.P. Mettmann: Neanderthal Museum, pp. 296-302.

d'Errico, F., Zilhao, J., Julien, M., Baffier, D., Pelegrin, J., (1998). Neanderthal Acculturation in Western Europe? A Critical Review of the Evidence and Its Interpretation. *Current Anthropology* 39 (2): S1.

d'Errico, F., (2003). The invisible frontier. A multiple species model for the origin of Behavioural modernity. *Evolutionary Anthropology* 12: 188.

Davis, S., (1974). Animal remains from the Kebaran site of Ein Gev I, Jordan Valley, Israel. *Paleorient* 2 (2): 453.

Day, M. H., (1986). Guide to fossil man. London: Cassell.

Deacon, H. J., (1992). Southern Africa and Modern Human Origins. *Philosophical Transactions: Biological Sciences* 337 (1280): 177.

Debénath, A., Jelinek, A. J., Dibble, H. L., Armand, D., Chase, P. G., Mercier, N., Renault, Miskovski, J., Tillier, A. M., Valladas, H., Vandermeersch, B., (1998). Nouvelles fouilles à la Quina (Charente) : résultats préliminaires. *Gallia Préhistoire* 40: 29.

Dekan, J., (1981). Moravia Magna: The Great Moravian Empire Minneapolis: Control Data Arts.

Delson, E., Harvati, K., Reddy, D. P., Marcus, L. F., Mowbray, K., Sawyer, G. J., Jacob, T., Marquez, S., (2001). The Sambungmacan 3 *Homo erectus* Calvaria: A comparative morphometric and morphological analysis. *The Anatomical Record* 262: 380.

Drucker, D. G., Bocherens, H., (2004). Carbon and nitrogen stable isotopes as tracers of change in diet breadth during Middle and Upper Palaeolithic in Europe. *International Journal of Osteoarchaeology* 14 (3-4): 162.

Drucker, D. G., Henry-Gambier, D., (2005). Determination of the dietary habits of a Magdalenian woman from Saint-Germain-la-Riviere in southwestern France using stable isotopes. *Journal of Human Evolution* 49 (1): 19.

Duda, G. N., Brand, D., Freitag, S., Lierse, W., Schneider, E., (1996). Variability of femoral muscle attachments. *Journal of Biomechanics* 29 (9): 1185.

Duda, G. N., Schneider, E., Chao, E. Y. S., (1997). Internal forces and moments in the femur during walking. *Journal of Biomechanics* 30 (9): 933.

Duda, G. N., Heller, M., Albinger, J., Schulz, O., Schneider, E., Claes, L., (1998). Influence of muscle forces on femoral strain distribution. *Journal of Biomechanics* 31 (9): 841.

Dytham, C., (1999). Choosing and using statistics: a biologist's guide. Malden: Blackwell Science Ltd.

Eveleth, P. B., Tanner, J. M., (1990). Worldwide variation in human growth. Cambridge: Cambridge University Press.

Field, A., (2000). Discovering Statistics Using SPSS. London: Sage Publications Ltd.

Fischer, E., (1906). Die Variationen an Radius und Ulna des Menschen. *Zeitschrift für Morphologie und Anthropologie* 9: 147.

Fizet, M., Mariotti, A., Bocherens, H., Lange-Badre, B., Vandermeersch, B., Borel, J. P., Bellon, G., (1995). Effect of diet, physiology and climate on carbon and nitrogen stable isotopes of collagen in a late pleistocene anthropic palaeoecosystem: Marillac, Charente, France. *Journal of Archaeological science* 22 (1): 67.

Fleagle, J. G., (1999). Primate adaptation and evolution. London: Academic Press.

Formicola, V., Pontrandolfi, A., Svoboda, J., (2001). The Upper Paleolithic triple burial of Dolnj Vestonice: pathology and funerary behavior. *American Journal of Physical Anthropology* 115: 372.

Fraipont, J., Lohest, M., (1887). Recherches Ethnographiques sur des Ossements Humaines Découvertes dans le Dépôts d'une Grotte Quaternaire à Spy. *Archives de Biologie* 7: 587.

Frayer, D. W., Wolpoff, M. H., Thorne, A. G., Smith, F. H., Pope, G. G., (1993). Theories of modern human origins: the paleontological test. *American Anthropologist* 95 (1): 14.

Frayer, D. W., Wolpoff, M. H., Thorne, A. G., Smith, F. H., Pope, G. G., (1994). Getting it straight. *American Anthropologist* 96: 424.

Frost, H. M., (1967). An introduction to biomechanics. Springfield, Illinois: Charles C. Thomas.

Garrod, D. A., Bate, D., (1937). The Stone Age of Mount Carmel. Oxford: Oxford University Press.

Genna, G. E., (1930). Sulla curvatura del femore nei Fuegini. *Revista di Anthropologia* XXIX: 415.

Gilbert, B. M., (1975). Anterior Femoral Curvature. *American Journal of Physical Anthropology* 42 (2): 303.

Gilbert, B. M., (1976). Anterior femoral curvature - probable basis and utility as a criterion of racial assessment. *American Journal of Physical Anthropology* 45 (3): 601.

Goldberg, P., Bar-Yosef, O., (1998). Site Formation Processes in Kebara and Hayonim Caves and their Significance in the Levantine Prehistoric Caves. In: Akazawa, T., Aoki, K., Bar-Yosef, O. (Eds.) Neandertals and Modern Humans in Western Asia. New York: Plenum, pp.

Golovanova, L. V., Hoffecker, J. F., Kharitonov, V. M., Romanova, G. P., (1999). Mezmaiskaya Cave: A Neanderthal Occupation in the Northers Caucasus. *Current Anthropology* 40 (1): 77.

González-José, R., Van Der Molen, S., González-Pérez, E., Hernández, M., (2004). Patterns of phenotypic covariation and correlation in modern humans as viewed from morphological integration. *American Journal of Physical Anthropology* 123 (1): 69.

Green, R. E., Krause, J., Ptak, S. E., Briggs, A. W., Ronan, M. T., Simons, J. F., Du, L., Egholm, M., Rothberg, J. M., Paunovic, M., Paabo, S., (2006). Analysis of one million base pairs of Neanderthal DNA. *Nature* 444 (7117): 330.

Grine, F. E., Jungers, W. L., Tobias, P. V., Pearson, O. M., (1995). Fossil Homo femur from Berg Aukas, Northern Namibia. *American Journal of Physical Anthropology* 97 (151): 185.

Grine, F. E., Pearson, O. M., Klein, R. G., Rightmire, G. P., (1998). Additional human fossils from Klasies River Mouth, South Africa. *Journal of Human Evolution* 35: 95.

Grün, R., Stringer, C. B., (1991). Electron Spin Resonance Dating and the Evolution of Modern Humans. *Archaeometry* 33 (2): 153.

Gunz, P., Mitteroecker, P., Bookstein, F., Weber, G. W., (2004). Computer aided reconstruction of human crania. *Enter the past - Computer Applications in Osteology*:

Gunz, P., Mitteroecker, P., Bookstein, F., (2005). Semi-landmarks in three dimensions. In: Slice, D. E. (Eds.) Modern Morphometrics in Physical Anthropology. New York: Kluwer Academic, pp.

Gusinde, M., (1939). Die Feuerland Indianer: Anthropologie. Wien-Mödling: Verlag "Anthropos".

Haeusler, M., McHenry, H. M., (2004). Body proportions of Homo habilis reviewed. *Journal of Human Evolution* 46 (4): 433.

Hagelberg, E., (2003). Recombination or mutation rate heterogeneity? Implications for Mitochondrial Eve. *TRENDS in genetics* 19 (2): 84.

Hall, S. J., (2004). Basic biomechanics. New York: McGraw-Hill.

Harvati, K., (2003a). Quantitative analysis of Neanderthal temporal bone morphology using three-dimensional geometric morphometrics. *American Journal of Physical Anthropology* 120 (4): 323.

Harvati, K., (2003b). The Neanderthal taxonomic position: models of intra- and inter-specific craniofacial variation. *Journal of Human Evolution* 44 (1): 107.

Harvati, K., Weaver, T., (2006). Reliability of cranial morphology in reconstructing Neanderthal phylogeny. In: Harvati, K. , Harrison, T. (Eds.) Neanderthals Revisited: New Approaches and Perspectives. Berlin: Springer, pp. 239-254.

Haury, E. W., (1945). The excavation of Los Muertos and neighboring ruins in the Salt River Valley, southern Arizona. *Peabody Museum Papers in American Archaeology and Ethnology* 24 (1):

Hawks, J., Wolpoff, M. H., (2001). Brief communication: Palaeoanthropology and the population genetics of ancient genes. *American Journal of Physical Anthropology* 114 (269): 272.

Hdrlicka, A., (1944). The Anthropology of Kodiak Island. Philadelphia: Wistar Institute.

Heim, J. L., (1968). Les Restes Néanderthaliens de La Ferrassie. Nouvelles Données sur la Stratigraphie et Inventaire des Squelettes. Comptes Rendus de L'Académie des Sciences, Série D. *266* (576-578):

Heim, J. L., (1981). The Sexual Dimorphism of Neanderthal Crania. *Anthropologie* 85-6 (3): 451.

Heim, J. L., (1982). The Sexual Dimorphism of Neanderthal Crania. *Anthropologie* 85 (2): 193.

Heim, J. L., (1983). Les variations du squelette post-crânien des hommes de Néandertal suivant le sexe. *L'Anthropologie* 87 (1): 5.

Henrich, J., (2004). Demography and cultural evolution: How adaptive cultural processes can produce maladaptive losses: The Tasmanian case. *American antiquity* 69 (2): 197.

Henry-Gambier, D., Bruzek, J., Murail, P., Houët, F., (2002). Révision du sexe du squelette magdalénien de Saint-Germain-la-Rivière (Gironde, France). *Paléo* 14: 202.

Henry, D. O., Hietala, H. G., Rosen, A. M., Demidenko, Y. E., Usik, V. I., Armagan, T. L., (2004). Human Behavioral Organization in the Middle Paleolithic: Were Neanderthals Different? *American Anthropologist* 106 (1): 17.

Hershkovitz, I., Speirs, M. S., Frayer, D., Nadel, D., Wishbaratz, S., Arensburg, B., (1995). Ohalo H2 - a 19,000-Year-Old Skeleton from a Water-Logged Site at the Sea of Galilee, Israel. *American Journal of Physical Anthropology* 96 (3): 215.

Hewlett, B. S., (1996). Cultural diversity among African pygmies. In: Kent, S. (Eds.) Cultural Diversity Among Twentieth-Century Foragers. England: Cambridge University Press, pp.

Hijmans, R. J., Cameron, S. E., Parra, J. L., Jones, P. G., Jarvis, A., (2005). Very high resolution interpolated climate surfaces for global land areas. *International Journal of Climatology* 25: 1965.

Hockett, B., Haws, J. A., (2005). Nutritional ecology and the human demography of Neandertal extinction. *Quaternary International* 137 (1): 21.

Hoffmann, A., Wegner, D., (2002). The rediscovery of the Combe Capelle skull. *Journal of Human evolution* 43 (4): 577.

Holliday, T. W., Trinkaus, E., (1991). Limb/trunk proportions in Neandertals and early anatomical modern humans. *American Journal of Physical Anthropology* Suppl 12: 93.

Holliday, T. W., (1997). Postcranial evidence of cold adaptation in European Neandertals. *American Journal of Physical Anthropology* 104 (2): 245.

Holliday, T. W., (1999). Brachial and crural indices of European Late Upper Paleolithic and Mesolithic humans. *Journal of Human Evolution* 36 (5): 549.

Holliday, T. W., (2000). Evolution at the Crossroads: Modern Human Emergence in Western Asia. *American Anthropologist* 102 (1): 54.

Holliday, T. W., Ruff, C., (2001). Relative variation in human proximal and distal limb segment lengths. *American Journal of Physical Anthropology* 116: 26.

Holt, B. M., (2003). Mobility in Upper Paleolithic and Mesolithic Europe: Evidence from the lower limb. *American Journal of Physical Anthropology* 122 (3): 200.

Howell, F. C., (1957). The Evolutionary Significance of Variation and Varieties of "Neanderthal" Man. *The Quarterly Review of Biology* 32 (4): 330.

Hublin, J. J., (1989). Climatic Changes, Paleogeography, and the Evolution of the Neandertals In: Akazawa, T., Aoki, K. , Bar-Yosef, O. (Eds.) Neandertals and Modern Humans in Western Asia. New York: Plenum Press, pp. 295-310.

Hublin, J. J., Spoor, F., Braun, M., Zonneveld, F., Condemi, S., (1998). A late Neanderthal associated with Upper Palaeolithic artefacts (vol 381, pg 224, 1996). *Nature* 392 (6677): 737.

Ingman, M., Kaessmann, H., Paabo, S., Gyllensten, U., (2000). Mitochondrial genome variation and the origin of modern humans. *Nature* 408 (6813): 708.

Ingman, M., Gyllensten, U., (2007). A recent genetic link between Sami and the Volga-Ural region of Russia *European Journal of Human Genetics* 15: 115.

Ivanhoe, F., (1970). Was Virchow Right about Neandertal ? *Nature* 227 (5258): 577.

Ivanhoe, F., Trinkaus, E., (1983). On Cranial Deformation in Shanidar 1 and 5. *Current Anthropology* 24 (1): 127.

James, S. R., Dennell, R. W., Gilbert, A. S., Lewis, H. T., Gowlett, J. A. J., Lynch, T. F., McGrew, W. C., Peters, C. R., Pope, G. G., Stahl, A. B., James, S. R., (1989). Hominid Use of Fire in the Lower and Middle Pleistocene: A Review of the Evidence [and Comments and Replies]. *Current Anthropology* 30 (1): 1.

Jelinek, J., Dupree, L., Gallus, A., Gams, H., Narr, K. J., Poulianos, A. N., Sackett, J. R., Schott, L., Suchy, J., Yakimov, V. P., (1969). Neanderthal Man and *Homo sapiens* in Central and Eastern Europe [and Comments and Reply]. *Current Anthropology* 10 (5): 475.

Jupp, J., (2001). The Australian People: An Encyclopedia of the Nation, Its People and Their Origins. Cambridge: Cambridge University Press.

Kamil, J., (1996). The Ancient Egyptians: Life in the Old Kingdom Cairo: The American University in Cairo Press.

Katzmarzyk, P. T., Leonard, W. R., (1998). Climatic influences on human body size and proportions: Ecological adaptations and secular trends. *American Journal of Physical Anthropology* 106 (4): 483.

Keith, A., (1925). 116. Was the Chancelade Man Akin to the Eskimo? *Man* 25: 186.

Kennedy, G. E., (1983a). A morphometric and taxonomic assessment of a Hominine femur from the Lower Member, Koobi Fora, Lake Turkana. *American Journal of Physical Anthropology* 61: 429.

Kennedy, G. E., (1983b). Some aspects of femoral morphology in Homo erectus *Journal of Human Evolution* 12: 587.

Kennedy, G. E., (1984). The Emergence of *Homo sapiens*: The Post-Cranial Evidence. *Man* 19 (1): 94.

Klaatsch, H., (1901). Das Gliedmaßenskelett des Neanderthalmenschen. *Anatomischer Anzeiger* 19: 121.

Klein, R. G., (2003). Whither the Neanderthals. *Science* 299: 1525.

Klima, B., (1987). A Triple burial from the Upper Palaeolithic of Dolni Vestonice, Czechoslovakia. *Journal of Human Evolution* 16 (7-8): 831.

Kramer, A., Crummett, T. L., Wolpoff, M. H., (2001). Out of Africa and into the Levant: replacement or admixture in Western Asia? *Quaternary International* 75 (1): 51.

Krause, J., Orlando, L., Serre, D., Viola, B., Prufer, K., Richards, M. P., Hublin, J.-J., Hanni, C., Derevianko, A. P., Paabo, S., (2007). Neanderthals in central Asia and Siberia. *Nature* 449 (7164): 902.

Krings, M., Stone, A., Schmitz, R. W., Krainitzki, H., Stoneking, M., Paabo, S., (1997). Neandertal DNA Sequences and the Origin of Modern Humans. *Cell* 90 (1): 19.

Kuzmin, Y. V., Burr, G. S., Jull, A. J. T., Sulerzhitsky, L. D., (2004). AMS C-14 age of the Upper Palaeolithic skeletons from Sungir site, Central Russian Plain. *Nuclear Instruments & Methods in Physics Research Section B-Beam Interactions with Materials and Atoms* 223-24: 731.

Lanyon, L. E., Baggott, D. G., (1976). Mechanical function as an influence on the structure and form of bone. *Journal of Bone and Joint Surgery* 58B (4): 436.

Lanyon, L. E., Bourn, S., (1979). The influence of mechanical function on the development of the tibia. *Journal of Bone and Joint Surgery* 61A (2): 263.

Lanyon, L. E., Magee, P. T., Baggott, D. G., (1979). The relationship of functional stress and strain to the processes of bone remodelling. An experimental study on the sheep radius. *Journal of Biomechanics* 12 (8): 593.

Lanyon, L. E., (1980). The Influence of Function on the Development of Bone Curvature - an Experimental Study on the Rat Tibia. *Journal of Zoology* 192 (DEC): 457.

Lanyon, L. E., Rubin, C. T., (1986). The osteoregulatory potential of static load bearing. *Journal of Biomechanics* 19 (6): 473.

Lanyon, L. E., (1987). Functional strain in bone tissue as an objective, and controlling stimulus for adaptive bone remodelling. *Journal of Biomechanics* 20 (11-12): 1083.

Larsen, C. S., (1983). Deciduous Tooth Size and Subsistence Change in Prehistoric Georgia Coast Populations. *Current Anthropology* 24 (2): 225.

Larsen, C. S., (1995). Biological Changes in Human Populations with Agriculture. *Annual Review of Anthropology* 24: 185.

Larsen, C. S., Ruff, C. B., Kelly, R. L., (1995). Structural analysis of the Stillwater postcranial human remains : Behavioral implications of articular joint pathology and long bone diaphyseal morphology. *Anthropological papers of the American Museum of Natural History* 77: 77.

Lengsfeld, M., Kaminsky, J., Merz, B., Franke, R. P., (1996). Sensitivity of femoral strain pattern analyses to resultant and muscle forces at the hip joint. *Medical Engineering & Physics* 18 (1): 70.

Lenoir, M., Dibble, H. L. (Eds.), (1995). The Middle Paleolithic Site of Combe-Capelle Bas (France) Philadelphia: University of Pennsylvania Museum Publication

Les, C. M., Stover, S. M., Keyak, J. H., Taylor, K. T., Willits, N. H., (1997). The distribution of material properties in the equine third metacarpal bone serves to enhance sagittal bending. *Journal of Biomechanics* 30 (4): 355.

Lieberman, D. E., (1989). Neandertal and Early Modern Human Mobility Patterns: Comparing Archaeological and Anatomical Evidence. In: Akazawa, T., Aoki, K. , Bar-Yosef, O. (Eds.) Neandertals and Modern Humans in Western Asia. New York: Plenum, pp. 263-276.

Lieberman, D. E., Devlin, M. J., Pearson, O. M., (2001). Articular area responses to biomechanical loading: effects of exercise, age and skeletal location. *American Journal of Physical Anthropology* 116: 266.

Lieberman, D. E., Pearson, O. M., (2001). Trade-off between modeling and remodeling responses to loading in the mammalian limb. *Bulletin of the Musum of Comparative Zoology* 156 (1): 269.

Lister, R. H., Lister, F. C., (1990). Aztec Ruins National Monument: Administrative History of an Archaeological Preserve. Santa Fe, New Mexico: National Park Service - Division of History - Southwest Cultural Resources Center. pp. 511.

Little, K. L., (1943). A Study of a Series of Human Skulls from Castle Hill, Scarborough. *Biometrika* 33 (1): 25.

Lockwood, C. A., Lynch, J. M., Kimbel, W. H., (2002). Quantifying temporal bone morphology of great apes and humans: an approach using geometric morphometrics. *Journal of Anatomy* 201: 447.

Lordkipanidze, D., Jashashvili, T., Vekua, A., de Leon, M. S. P., Zollikofer, C. P. E., Rightmire, G. P., Pontzer, H., Ferring, R., Oms, O., Tappen, M., Bukhsianidze, M., Agusti, J., Kahlke, R., Kiladze, G., Martinez-Navarro, B., Mouskhelishvili, A., Nioradze, M., Rook, L., (2007). Postcranial evidence from early Homo from Dmanisi, Georgia. *Nature* 449 (7160): 305.

Main, R. P., Biewener, A. A., (2004). Ontogenetic patterns of limb loading, in vivo bone strains and growth in the goat radius. *Journal of Experimental Biology* 207 (15): 2577.

Maj¢, T., Tillier, A. M., Thompson, J. L., Krovitz, G. E., Nelson, A. J., (2003). Postcranial growth in Neandertals and modern humans. In: Foley, R. A. , Jablonski, N. G. (Eds.) Patterns of growth and development in the Genus Homo Cambridge: Cambridge University Press, pp. 361-385.

Manly, B. F. J., (1997). Randomization, Bootstrap and Monte Carlo Methods in Biology. London: Chapman and Hall.

Marcus, L. F., Frost, S. R., Bookstein, F., Reddy, D. P., Delson, E., (2004). Comparison of landmarks among living and fossil Papio and Theropithecus skulls, with extension of Procrustes methods to ridge surfaces.

Marean, C. A., Assefa, Z., (1999). Zooarcheological evidence for the faunal exploitation behavior of Neandertals and early modern humans. *Evolutionary Anthropology: Issues, News, and Reviews* 8 (1): 22.

Marean, C. A., Assefa, Z., (2005). The Middle and Upper Pleistocene African Record for the Biological and Behavioral Origins of Modern Humans. In: Marean, C. A. , Assefa, Z. (Eds.) African Archaeology. Oxford: Blackwell Publishing, pp.

Martin, H., (1921). Sur la Repartition des Ossements Humains dans le Gisement de la Quina. *L'Anthropologie* 31: 340.

Martin, R. D., Saller, K., (1959). Lehrbuch der Anthropologie. Stuttgart: Gustav Fischer.

Mays, S. A., (1997). Carbon Stable Isotope Ratios in Mediaeval and Later Human Skeletons From Northern England. *Journal of Archaeological science* 24 (6): 561.

McCown, T. D., Keith, A., (1939a). The Stone Age of Mount Carmel. Oxford: Clarendon Press.

McCown, T. D., Keith, A., (1939b). The Stone Age of Mount Carmel. Oxford: Clarendon Press.

McHenry, H. M., (1992). Body Size and Proportions in Early Hominids. *American Journal of Physical Anthropology* 87 (4): 407.

Mellars, P., Stringer, C., (1989). The Human Revolution : behavioural and biological perspectives on the origins of modern humans. Princeton, N.J.: Princeton University Press.

Mellars, P., Grun, R., (1991). A comparison of the electro spin resonance and thermoluminenscence dating methods: the result of ESR dating at Le Moustier (France). *Cambridge Archaeology Journal* 1: 269.

Mellars, P., (1996). The Neanderthal legacy : an archaeological perspective from western Europe. Princeton, N.J: Princeton University Press.

Mellars, P., (2004). Neanderthals and the modern human colonisation of Europe. *Nature* 432: 461.

Mellars, P., Gravina, B., Bronk Ramsey, C., (2007). Confirmation of Neanderthal/modern human interstratification at the Chatelperronian type-site. *Proceedings of the National Academy of Sciences* 104 (9): 3657.

Mellars, P. A., Bricker, H. M., Gowlett, J. A. J., Hedges, R. E. M., (1987). Radiocarbon Accelerator Dating of French Upper Palaeolithic Sites. *Current Anthropology* 28 (1): 128.

Molleson, T., Cox, M., (1993). The Spitalfields Project: the Anthropology. The Middling Sort. York: Council for British Archaeology

Monteiro, L. R., Bordin, B., Furtado dos Reis, S., (2000). Shape distances, shape spaces and the comparison of morphometric methods. *Trends in Ecology & Evolution* 15 (6): 217.

Moran, M. D., (2003). Arguments for rejecting the sequential Bonferroni in ecological studies. *Oikos* 100: 403.

Moseley, M. E., (2001). The Incas and their ancestors : the archaeology of Peru London: Thames & Hudson.

Movius, H. L., (1966). Hearths of the Upper Perigordian and Aurignacian horizons at Abri Pataud, Les Eyzies (Dordogne), and their possible significance. *American Anthropologist* 68 (2): 296.

Movius, H. L., (1975). Excavation of the Abri Pataud. Massachusetts:: Peabody Museum of Archaeology and Ethnology Harvard University.

Munro, N. D., (2004). Zooarchaeological measures of hunting pressure and occupation intensity in the Natufian. *Current Anthropology* 45 (s4): S5.

Nadel, D., Hershkovitz, I., (1991). New Subsistence Data and Human Remains from the Earliest Levantine Epipalaeolithic. *Current Anthropology* 32 (5): 631.

Nakagawa, S., (2004). A farewell to Bonferroni: the problems of low statistical power and publication bias. *Behav. Ecol.* 15 (6): 1044.

Niewoehner, W. A., (2001). Behavioral inferences from the Skhul/Qafzeh early modern human hand remains. *Proceedings of the National Academy of Sciences of the United States of America* 98 (6): 2979.

Noonan, J. P., Coop, G., Kudaravalli, S., Smith, D., Krause, J., Alessi, J., Platt, D., Paabo, S., Pritchard, J. K., Rubin, E. M., (2006). Sequencing and analysis of Neanderthal genomic DNA. *Science* 314 (5802): 1113.

Norman, A., Bellocco, R., Vaida, F., Wolk, A., (2002). Total physical activity in relation to age, body mass, health and other factors in a cohort of Swedish men. *International Journal of Obesity* 26 (5): 670.

O'Higgins, P., Jones, N., (1998). Facial growth in Cercocebus torquatus: An application of three dimensional geometric morphometric techniques to the study of morphological variation. *Journal of Anatomy* 193: 251.

O'Higgins, P., (2000). The study of morphological variation in the hominid fossil record: biology, landmarks and geometry. *Journal of Anatomy* 197: 103.

Ortner, D. J., (1968). Description and classification of degenerative bone changes in the distal joint surfaces of the humerus. *American Journal of Physical Anthropology* 28 (2): 139.

Ovchinnikov, I. V., Gotherstrom, A., Romanova, G. P., Kharitonov, V. M., Liden, K., Goodwin, W., (2000). Molecular analysis of Neanderthal DNA from the northern Caucasus. *Nature* 404 (6777): 490.

Ovchinnikov, I. V., Goodwin, W., (2003). Ancient human DNA from Sungir? *Journal of Human evolution* 44 (3): 389.

Owsley, D. W., Jantz, R. L. (Eds.), (1994). Skeletal biology in the Great Plains: migration, warfare, health, and subsistence. Washington: Smithsonian Institution

Panum Baastrup, M. C., (2002). *Anatomiske variationer og gravenes placering -slægtskab blandt skeletterne ved Sct. Bendts Kirke*. MSc dissertation. University of Copenhagen

Patte, E., (1955). Les Néanderthaliens: anatomie, physiologie, comparaisons. Paris: Masson et Co.

Pead, M. J., Lanyon, L. E., (1990). Loading related adaptive remodelling in bone: Torsion versus compression. *Journal of Biomechanics* 23 (4): 363.

Pearson, O. M., Grine, F. E., (1997). Re-analysis of the hominid radii from Cave of Hearths and Klasies River Mouth, South Africa. *Journal of Human Evolution* 32 (6): 577.

Pearson, O. M., Churchill, S. E., Grine, F. E., Trinkaus, E., Holliday, T. W., (1998). Multivariate analyses of the hominid ulna from Klasies River Mouth. *Journal of Human Evolution* 34 (6): 653.

Pearson, O. M., (2000a). Postcranial remains and the origin of Modern Humans. *Evolutionary Anthropology* 9: 229.

Pearson, O. M., (2000b). Activity, climate and postcranial robusticity: Implications for modern human origins and scenarios of adaptive change. *Current Anthropology* 41 (4): 569.

Pearson, O. M., Lieberman, D. E., (2004). The aging of Wolff's law: Ontogeny and responses to mechanical loading in cortical bone. *Yearbook of Physical Anthropology* 47: 63.

Pearson, O. M., Cordero, R., Busby, A., (2006). How different were Neanderthals' habitual activities? A comparative analysis with diverse groups of recent humans. In: (Eds.) Neanderthals Revisited: New Approaches and Perspectives. pp. 135-156.

Pedersen, D. R., Brand, R. A., Davy, D. T., (1997). Pelvic muscle and acetabular contact forces during gait. *Journal of Biomechanics* 30 (9): 959.

Pettitt, P. B., Bader, N. O., (2000). Direct AMS radiocarbon dates for the Sungir mid Upper Palaeolithic burials. *Antiquity* 74 (284): 269.

Pettitt, P. B., Davies, W., Gamble, C. S., Richards, M. B., (2003). Palaeolithic radiocarbon chronology: quantifying our confidence beyond two half-lives. *Journal of Archaeological science* 30 (12): 1685.

Piveteau, J., (1959). Les Restes Humains de la Grotte du Regourdou (Dordogne). . *Comptes Rendus De L Academie Des Sciences* 248: 40.

Puech, P.-F., (1981). Tooth Wear in La Ferrassie Man. *Current Anthropology* 22 (4): 424.

Radcliffe-Brown, A. R., (1948). The Andaman Islanders. Illinois: Free Press.

Rak, Y., Arensburg, B., (1987). Kebara 2 Neanderthal Pelvis: First look at a complete inlet. *American Journal of Physical Anthropology* 73: 227.

Rak, Y., (1990). On the differences between two pelvises of Mousterian context from the Qafzeh and Kebara caves, Israel. *American Journal of Physical Anthropology* 81 (3): 323.

Rak, Y., (2002). Does Any Mousterian Cave Present Evidence of Two Hominid Species? In: (Eds.) Neandertals and Modern Humans in Western Asia. pp. 353-366.

Richards, M. P., Pettitt, P. B., Trinkaus, E., Smith, F. H., Pauvonic, M., Karavanic, I., (2000). Neanderthal diet at Vindija and Neanderthal predation: The evidence from stable isotopes. *Proceedings of the National Academy of Science* 97 (13): 7663.

Richards, M. P., Pettitt, P. B., Stiner, M. C., Trinkaus, E., (2001). Stable isotope evidence for increasing dietary breadth in she European mid-Upper Paleolithic. *Proceedings of the National Academy of Sciences of the United States of America* 98 (11): 6528.

Richards, M. P., Price, T. D., Koch, E., (2003). Mesolithic and Neolithic Subsistence in Denmark: New Stable Isotope Data. *Current Anthropology* 44 (2): 288.

Richmond, B. G., Whalen, M., (2001). Forelimb function, bone curvature and phylogeny of Sivapithecus. In: de Bonis, L. , Koufos, G. (Eds.) Eurasian neogene hominoid phylogeny. Cambridge: Cambridge University Press, pp. 326–348.

Richmond, B. G., Wright, B. W., Grosse, I., Dechow, P. C., Ross, C. F., Spencer, M. A., Strait, D. S., (2005). Finite element analysis in functional morphology. *The Anatomical Record Part A: Discoveries in Molecular, Cellular, and Evolutionary Biology* 283A (2): 259.

Ried, A. H., (1924). Die Schäfskrümmung des menschlichen Femur. *Anthropologischer Anzeiger* 1: 102.

Rightmire, G. P., (1998). Human evolution in the Middle Pleistocene: The role of *Homo heidelbergensis*. *Evolutionary Anthropology: Issues, News, and Reviews* 6 (6): 218.

Rose, T.-W., Vinicius, L., (2008). Independent roles of climate and life history in hunter-gatherer anthropometric variation. *The Internet Journal of Biological Anthropology* 1 (2): http://www.ispub.com/ostia/index.php?xmlFilePath=journals/ijba/front.xml.

Rosenberg, M. S., (2001). PASSAGE. Pattern analysis, spatial statistics and geographic exegesis. Version 1.0. *Department of Biology, Arizona State University, Tempe, AZ.*: http://www.metawinsoft.com/.

Ruff, C., Walker, A., (1993). Body size and body shape. In: Walker, A. , Leakey, R. (Eds.) The Nariokotome Homo erectus skeleton. Berlin: Springer - Verlag, pp. 235-263.

Ruff, C., Niskanen, M., Junno, J. A., Jamison, P., (2005). Body mass prediction from stature and bi-iliac breadth in two high latitude populations, with application to earlier higher latitude humans. *Journal of Human Evolution* 48 (4): 381.

Ruff, C. B., Larsen, C. S., Hayes, W. C., (1984). Structural changes in the femur with the transition to agriculture on the Georgia coast. *American Journal of Physical Anthropology* 64 (2): 125.

Ruff, C. B., (1987). Sexual dimorphism in human lower limb bone structure: Relationship to subsistence strategy and sexual division of labor. *Journal of Human Evolution* 16: 396.

Ruff, C. B., (1991). Climate and body shape in hominid evolution. *Journal of Human Evolution* 21 (2): 81.

Ruff, C. B., Scott, W. W., Liu, A. Y. C., (1991). Articular and diaphyseal remodeling of the proximal femur with changes in body mass in adults. *American Journal of Physical Anthropology* 86 (3): 397.

Ruff, C. B., Trinkaus, E., Walker, A., Larsen, C. S., (1993). Postcranial Robusticity in Homo I : Temporal trends and mechanical interpretation. *American Journal of Physical Anthropology* 91: 21.

Ruff, C. B., (1994a). Biomechanical analysis of Northern and Southern Plains femora: Behavioral implications. In: Owsley, D. W. , Jantz, R. L. (Eds.) Skeletal Biology in the Great Plains: Migration, Warfare, Health, and Subsistence. Washington: Smithsonian Institution Press, pp. 235-245.

Ruff, C. B., (1994b). Morphological adaptation to climate in modern and fossil hominids. *American Journal of Physical Anthropology* 37 (S19): 65.

Ruff, C. B., Walker, A., Trinkaus, E., (1994). Postcranial robusticity in Homo III : Ontogeny. *American Journal of Physical Anthropology* 93: 35.

Ruff, C. B., (1995). Biomechanics of the hip and birth in early Homo *American Journal of Physical Anthropology* 98 (4): 527.

Ruff, C. B., Trinkaus, E., Holliday, T. W., (1997). Body mass and encephalization in Pleistocene Homo. *Nature* 387 (6629): 173.

Ruff, C. B., (1999). Skeletal structure and behavioral patterns of prehistoric Great Basin populations. In: Hemphill, B. E. , Larsen, C. S. (Eds.) Understanding Prehistoric Lifeways in the Great Basin Wetlands: Bioarchaeological Reconstruction and Interpretation. Salt Lake City: Univ. Utah Press, pp. 290-320.

Ruff, C. B., (2000a). Body size, body shape, and long bone strength in modern humans. *Journal of Human Evolution* 38 (2): 269.

Ruff, C. B., (2000b). Biomechanical analyses of archaeological human skeletons. In: Katzenberg, A. , Saunders, S. R. (Eds.) Biological Anthropology of the Human Skeleton. New York: Alan R. Liss, pp. 71-102.

Ruff, C. B., Trinkaus, E., (2000). Lifeway changes as shown by postcranial skeletal robustness. *American Journal of Physical Anthropology* Suppl 30: 266.

Ruff, C. B., Trinkaus, E., Holt, B., (2006). Who's afraid of the big bad Wolff?: Wolff's law and bone functional adaptation. *American Journal of Physical Anthropology* 129 (4): 484.

Runestad, J. A., Ruff, C. B., Nieh, J. C., Thorington, R. W., Teaford, M. F., (1993). Radiographic estimation of long bone cross-sectional geometric properties. *American Journal of Physical Anthropology* 90: 207.

Schmitz, R. W., Bonani, G., Feine, S., Hillgruber, F., Kraitnitzki, H., Pääbo, S., (2002). The Neandertal type site revisited: Interdisciplinary investigations of skeletal remains from the Neander Valley, Germany. *Proceedings of the National Academy of Science* 99 (20): 13342.

Schmitz, R. W., (2006). Preservation of ancient DNA in the bone material of the Neanderthal type specimen. In: Schmitz, R. W. (Eds.) Neanderthal 1856-2006. Mainz am Rhein: Verlag Philipp Von Zabern, pp.

Schwartz, J. H., Tattersall, I., (2002). The Human Fossil Record Terminology and Craniodental Morphology of Genus Homo 1 (Europe). New York: Wiley-Liss.

Shackelford, L. L., Trinkaus, E., (2002). Late Pleistocene human femoral diaphyseal curvature. *American Journal of Physical Anthropology* 118: 359.

Shackelford, L. L., (2007). Regional variation in the postcranial robusticity of late upper paleolithic humans. *American Journal of Physical Anthropology* 133 (1): 655.

Shea, J. J., (2003). Neandertals, competition, and the origin of modern human behavior in the Levant. *Evolutionary Anthropology: Issues, News, and Reviews* 12 (4): 173.

Simões, J. A., Vaz, M. A., Blatcher, S., Taylor, M., (2000). Influence of head constraint and muscle forces on the strain distribution within the intact femur. *Medical Engineering & Physics* 22 (7): 453.

Sinitsyn, A. A., (2003). The most ancient sites of Kostenki in the context of the Initial Upper Paleolithic of Northern Eurasia. *Trabalhos de Arquelogia* 33: 89.

Sinitsyn, A. A., Hoffecker, J. F., (2006). Radiocarbon dating and chronology of the Early Upper Paleolithic at Kostenki. *Quaternary International* 152-153: 164.

Skerry, T. M., (2008). The response of bone to mechanical loading and disuse: Fundamental principles and influences on osteoblast/osteocyte homeostasis. *Archives of Biochemistry and Biophysics* 473 (2): 117.

Slice, D. E. (Eds.), (2005). Modern morphometrics. Modern morphometrics in physical anthropology. New York: Kluwer Academic Publishers

Smith, F. H., Allsworth-Jones, P., Boaz, N. T., Brace, C. L., Harrold, F. B., Howells, W. W., Luchterhand, K., Musil, R., Stringer, C. B., Trinkaus, E., Valoch, K., Walker, M. J., Wolpoff, M. H., (1982). Upper Pleistocene Hominid Evolution in South-Central Europe: A Review of the Evidence and Analysis of Trends [and Comments and Reply]. *Current Anthropology* 23 (6): 667.

Smith, F. H., Falsetti, A. B., Donnelly, S. M., (1989). Modern human origins. *American Journal of Physical Anthropology* 32 (S10): 35.

Smith, H. F., Terhune, C. E., Lockwood, C. A., (2007). Genetic, geographic, and environmental correlates of human temporal bone variation. *American Journal of Physical Anthropology* 134 (3): 312.

Solecki, R. L., Solecki, R. S., (1974). Shanidar Cave. *Science* 184 (4140): 937.

Solecki, R. S., (1957). Shanidar Cave. *Scientific American* 197 (5): 59.

Solecki, R. S., (1961). New Anthropological Discoveries at Shanidar, Northern Iraq. *Transactions of the New York Academy of Sciences* 23 (8): 690.

Solecki, R. S., (1975). Shanidar 4, A Neanderthal Flower Burial in Northern Iraq. *Science* 190 (4217): 880.

Sollas, W. J., (1927). The Chancelade Skull. *The Journal of the Royal Anthropological Institute of Great Britain and Ireland* 57: 89.

Speth, J. D., Tchernov, E., (1998). The Role of Hunting and Scavenging in Neandertal Procurement Strategies: New Evidence from Kebara Cave (Israel). . In: Akazawa, T., Aoki, K. , Bar-Yosef, O. (Eds.) Neandertals and Modern Humans in Western Asia. New York: Plenum Press, pp. 223-239.

Steegmann Jr., A. T., F.J., C., Holliday, T. W., (2002). Neandertal cold adaptation: Physiological and energetic factors. *American Journal of Human Biology* 14 (5): 566.

Steinbock, R. T., (1976). Paleopathological diagnosis and interpretation : bone diseases in ancient human populations. Springfield, Ill. : Thomas.

Stekelis, M., Bar-Yosef, O., (1965). Un habitat du Paléolithique supérieur à Ein Gev (Israel). *L' Anthropologie* 69: 176.

Steudel-Numbers, K. L., Tilkens, M. J., (2004). The effect of lower limb length on the energetic cost of locomotion: implications for fossil hominins. *Journal of Human Evolution* 47: 95.

Stewart, T. D., (1962). Anterior Femoral Curvatures - Its Utility for Race Identification. *Human Biology* 34 (1): 49.

Stewart, T. D., (1963). Neanderthal Scapulae - with special attention to Shanidar Neanderthals from Iraq. *American Journal of Physical Anthropology* 21 (3): 409.

Stewart, T. D., (1977). Neanderthal Skeletal Remains from Shanidar Cave, Iraq - summary of findings to date. *Proceedings of the American Philosophical Society* 121 (2): 121.

Stiner, M. C., (1993). Modern Human Origins Faunal Perspectives. *Annual Review of Anthropology* 22 (1): 55.

Stock, J., Pfeiffer, S., (2001). Linking structural variability in long bone diaphyses to habitual behaviors: Foragers from the southern African Later Stone Age and the Andaman Islands. *American Journal of Physical Anthropology* 115 (4): 337.

Stock, J. T., (2002). *Climatic and behavioural influences on postcranial robusticity among Holocene foragers*. PhD dissertation. University of Toronto

Stock, J. T., Pfeiffer, S. K., (2004). Long bone robusticity and subsistence behaviour among Later Stone Age foragers of the forest and fynbos biomes of South Africa. *Journal of Archaeological science* 31 (7): 999.

Stock, J. T., (2006). Hunter-gatherer postcranial robusticity relative to patterns of mobility, climatic adaptation, and selection for tissue economy. *American Journal of Physical Anthropology* 131 (2): 194.

Stringer, C., (2000). Palaeoanthropology: Coasting out of Africa. *Nature* 405 (6782): 24.

Stringer, C., (2002). Modern human origins: progress and prospects. *Philosophical Transactions of the Royal Society B: Biological Sciences* 357 (1420): 563.

Stringer, C. B., Trinkaus, E., (1980). The shanidar Neanderthal crania. *Annals of Human Biology* 7 (2): 187.

Stringer, C. B., (1992). Reconstructing Recent Human Evolution. *Philosophical Transactions: Biological Sciences* 337 (1280): 217.

Stuart-Macadam, P. L., Iscan, M. Y., (1989). Nutritional deficiency disease: A survey of scurvy, rickets, and iron-deficiency anemia. In: Iscan, M. Y. , Kennedy, K. A. R. (Eds.) Reconstruction of life from the skeleton. New York: Wiley-Liss, pp. 201-222.

Svoboda, J., Vlcek, E., (1991). A New Sepulture from Dolni Vestonice (DV XVI), Czechoslovakia. *Anthropologie* 95 (1): 323.

Svoboda, J., (1994). The Pavlov Site, Czech Republic: Lithic Evidence from the Upper Paleolithic. *Journal of Field Archaeology* 21 (1): 69.

Swartz, S. M., (1990). Curvature of the forelimb bones of anthropoid primates - overall allometric patterns and specializations in suspensory species. *American Journal of Physical Anthropology* 83 (4): 477.

Tauber, H., (1981). 13C evidence for dietary habits of prehistoric man in Denmark. *Nature* 292 (5821): 332.

Taylor, M. E., Tanner, K. E., Freeman, M. A. R., Yettram, A. L., (1996). Stress and strain distribution within the intact femur: Compression or bending. *Medical Engineering & Physics* 18 (2): 122.

Thompson, J. L., Nelson, A. J., (2000). The place of Neandertals in the evolution of hominid patterns of growth and development. *Journal of Human Evolution* 38 (4): 475.

Thompson, J. L., Nelson, A. J., (2005). The Postcranial Skeleton of Le Moustier 1. In: Ullrich, H. (Eds.) The Neandertal Adolescent Le Moustier 1 New Aspects, New Results. Berlin: Die Deutsche Bibliothek, pp. 265-281.

Tompkins, R. L., Trinkaus, E., (1987). La Ferrassie 6 and the development of Neanderthal Pubic Morphology. *American Journal of Physical Anthropology* 73: 233.

Toussaint, M., Orban, R., Polet, C., Semal, P., Bocherens, H., Masy, P., García Martín, C., (2001). Apports récents sur l'anthropologie des Mésolitiques et des Néolitiques mosans. *Anthropolgica et Praehistorica* 112: 91.

Trinkaus, E., (1975). Squatting among the neandertals: A problem in the behavioral interpretation of skeletal morphology. *Journal of Archaeological science* 2 (4): 327.

Trinkaus, E., (1978). Dental Remains from Shanidar Adult Neanderthals. *Journal of Human evolution* 7 (5): 369.

Trinkaus, E., Zimmerman, M. R., (1979). Paleopathology of the Shanidar Neanderthals. *American Journal of Physical Anthropology* 50 (3): 487.

Trinkaus, E., (1981). Neanderthal limb proportions and cold adaptation. In: Stringer, C. (Eds.) Aspects of Human Evolution. London: Taylor and Francis, pp. 21-53.

Trinkaus, E., (1982a). Articifial Cranial Deformation in the Shanidar-1 and Shanidar-5 Neandertals. *Current Anthropology* 23 (2): 198.

Trinkaus, E., (1982b). The Shanidar-3 Neandertal. *American Journal of Physical Anthropology* 57 (1): 37.

Trinkaus, E., (1982c). Evolutionary Trends in the Shanidar Neanderthal Sample. *American Journal of Physical Anthropology* 57 (2): 237.

Trinkaus, E., Zimmerman, M. R., (1982). Trauma among the Shanidar Neanderthals. *American Journal of Physical Anthropology* 57 (1): 61.

Trinkaus, E., (1983a). The Shanidar Neandertals. London: Academic Press.

Trinkaus, E., (1983b). On Cranial Deformation of Shanidar-1 and Shanidar-5 - Reply. *Current Anthropology* 24 (1): 127.

Trinkaus, E., (1985). Pathology and the posture of the La Chapelle-aux-Saints Neandertal. *American Journal of Physical Anthropology* 67 (1): 19.

Trinkaus, E., (1986). The Neandertals and Modern Human Origins. *Annual Review of Anthropology* 15 (1): 193.

Trinkaus, E., Churchill, S. E., (1988). Neandertal Radial Tuberosity Orientation. *American Journal of Physical Anthropology* 75: 15.

Trinkaus, E., Ruff, C., Churchill, S. E., (1989). Upper Limb versus Lower Limb Loading Patterns among Near Eastern Middle Paleolithic Hominids. In: Akazawa, T., Aoki, K., Bar-Yosef, O. (Eds.) Neandertals and Modern Humans in Western Asia. New York: Plenum, pp. 391-404.

Trinkaus, E., Villemeur, I., (1991). Mechanical Advantages of the Neanderthal Thumb in Flexion - a Test of Hypothesis. *American Journal of Physical Anthropology* 84 (3): 249.

Trinkaus, E., (1993). Femoral Neck-Shaft Angles of the Qafzeh-Skhul Early Modern Humans, and Activity Levels Among Immature Near-Eastern Middle Paleolithic Hominids. *Journal of Human Evolution* 25 (5): 393.

Trinkaus, E., Shipman, P., (1993). The Neanderthals: changing the image of mankind. New York: Knopf.

Trinkaus, E., Churchill, S. E., Ruff, C. B., (1994). Postcranial robusticity in Homo II: Humeral Bilateral Assymetry and Bone Plasticity. *American Journal of Physical Anthropology* 93: 1.

Trinkaus, E., Ruff, C. B., Churchill, S. E., (1998a). Upper Limb Versus Lower Limb Loading Patterns among Near Eastern Middle Paleolithic Hominids. In: Akazawa, T., Aoki, K., Bar-Yosef, O. (Eds.) Neandertals and Modern Humans in Western Asia. New York: Plenum Press, pp. 391-404.

Trinkaus, E., Ruff, C. B., Churchill, S. E., Vandermeersch, B., (1998b). Locomotion and body proportions of the Saint-Cesaire 1 Chatelperronian Neandertal. *Proceedings of the National Academy of Science* 95 (10): 5836.

Trinkaus, E., Churchill, S. E., (1999). Diaphyseal Cross-sectional Geometry of Near Eastern Middle Palaeolithic Humans: The Humerus. *Journal of Archaeological science* 26 (2): 173.

Trinkaus, E., Churchill, S. E., Ruff, C. B., et al., (1999a). Long bone shaft robusticity and body proportions of the Saint-Cesaire 1 Chatelperronian Neanderthal. *Journal of Archaeological science* 26: 753.

Trinkaus, E., Ruff, C. B., (1999a). Diaphyseal Cross-sectional Geometry of Near Eastern Middle Palaeolithic Humans: The Tibia. *Journal of Archaeological science* 26 (10): 1289.

Trinkaus, E., Ruff, C. B., (1999b). Diaphyseal Cross-sectional Geometry of Near Eastern Middle Palaeolithic Humans: The Femur. *Journal of Archaeological science* 26 (4): 409.

Trinkaus, E., Ruff, C. B., Conroy, G. C., (1999b). The anomalous Archaic Homo femur from Berg Aukas, Namibia: A biomechanical assessment. *American Journal of Physical Anthropology* 110: 379.

Trinkaus, E., Svoboda, J., West, D. L., Sladek, V., Hillson, S. W., Drozdova, E., Fisakova, M., (2000). Human Remains from the Moravian Gravettian: Morphology and Taphonomy of Isolated Elements from the Dolni Vestonice II Site. *Journal of Archaeological science* 27 (12): 1115.

Trinkaus, E., Formicola, V., Svoboda, J., Hillson, S. W., Holliday, T. W., (2001). Dolní Vestonice 15: Pathology and Persistence in the Pavlovian. *Journal of Archaeological science* 28 (12): 1291.

Trinkaus, E., (2005). Early modern humans. *Annual Review of Anthropology* 34 (1): 207.

Trinkaus, E., (2006). Modern human versus Neandertal evolutionary distinctiveness. *Current Anthropology* 47 (4): 597.

Trinkaus, E., (2007). European early modern humans and the fate of the Neandertals. *Proceedings of the National Academy of Sciences of the United States of America* 104 (18): 7367.

Trudell, M. B., (1999). Anterior femoral curvature revisited: Race assessment from the femur. *Journal of Forensic Science* 44 (4): 700.

Ullrich, H., (2005). Cut marks and other bone modifications on the Le Moustier 1 remains. In: (Eds.) The Neanderthal Adolescent Le Moutier 1 New Aspects, New Results. Berlin: Die Deutsche Bibliothek, pp. 293-310.

Valladas, H., Geneste, J. M., Joron, J. L., Chadelle, J. P., (1986). Thermo-luminescence dating of Le Moustier (Dordogne, France). *Nature* 322 (6078): 452.

Valladas, H., Mercier, N., Joron, J. L., Reyss, J.-L., (1998). GIF Laboratory Dates for Middle Palaeolithic Levant. In: Akazawa, T., Aoki, K. , Bar-Yosef, O. (Eds.) Neanderthals and Modern Humans in Western Asia. New York: Plenum, pp. 69-76.

Valladas, H., Mercier, N., Joron, J. L., McPherron, S. P., Dibble, H. L., Lenoir, M., (2003). TL dates for the Middle Paleolithic site of Combe-Capelle Bas, France. *Journal of Archaeological science* 30: 1443.

Van Andel, T. H., (2003). The human presence in Europe during the Last Glacial Period I: Human Migrations and Changing Climate. In: van Andel, T. H. , Davies, W. (Eds.) Neanderthals and Modern Humans in the European Landscape During the Last Glaciation. Cambridge, UK: McDonald Institute for Archaeological Research, pp. 31-56.

van Der Meulen, M. C. H., Beaupre, G. S., Carter, D. R., (1993). Mechanobiologic influences in long bone cross-sectional growth. *Bone* 14 (4): 635.

Vandermeersch, B., (1981). *Les hommes fossiles de Qafzeh (Israël).* dissertation.

Vandermeersch, B., Trinkaus, E., (1995). The post-cranial remains of the Régourdou 1 Neandertal: the shoulder and arm remains. *Journal of Human Evolution* 28: 439.

Vaufrey, R., (1935). L'Homme Magdalenian de Saint-Germain-la-Rivière. *L' Anthropologie* 45: 203.

Vlcek, E., (1961a). Die in Pavlov aufgefundenen Menschenreste aus de Jungpleistozen. *Pam tky, archeologick,* II: 46.

Vlcek, E., (1961b). Nouvelles trouvailles de l'homme du Pleistocène récent de Pavlov. *Anthropos* 14 (NS 6): 144.

Vlcek, E., (1991). Fossil Man in Central-Europe. *Anthropologie* 95 (2-3): 409.

Walensky, N. A., (1962). A Study of Femoral Bowing in Man. *Anatomical Record* 142 (2): 289.

Walensky, N. A., (1965). A Study of Anterior Femoral Curvature in Man. *Anatomical Record* 151 (4): 559.

Walker, A., Leakey, R., (1993). The postcranial bones. In: Walker, A. , Leakey, R. (Eds.) The Nariokotome Homo erectus skeleton. Berlin: Springer-Verlag, pp. 95-160.

Warren, M. W., (1998). Prenatal long bone growth and proportionality in fetal abortus and stillborns (Abstract). *American Journal of Physical Anthropology* 26 (Suppl.): 226.

Weaver, T., Steudel-Numbers, K. L., (2005). Does Climate or Mobility Explain the Differences in Body Proportions Between Neandertals and Their Upper Paleolithic Successors? *Evolutionary Anthropology: Issues, News, and Reviews* 14 (6): 218.

Weaver, T. D., (2002). *A multi-causal functional analysis of hominid hip-morphology.* dissertation. Stanford University

Weaver, T. D., (2003). The shape of the Neandertal femur is primarily the consequence of a hyperpolar body form. *Proceedings of the National Academy of Science* 100 (12): 6926.

Weiss, E., (2003). Effects of rowing on humeral strength. *American Journal of Physical Anthropology* 121 (4): 293.

White, T. D., Asfaw, B., Degusta, D., Gilbert, H., Richards, G. D., Suwa, G., Clark Howell, F., (2003). Pleistocene *Homo sapiens* from Middle Awash, Ethiopia. *Nature* 426: 742.

Whittle, A., Barclay, A., Bayliss, A., McFayden, L., Schulting, R., Wysocki, M., (2007). Building for the Dead: Events, Processes and Changing Worldviews from the Thirty-eighth to the Thirty-fourth Centuries cal. BC in Southern Britain. *Cambridge Archaeology Journal* 17: 123.

Willoughby, C. C., Hooten, E. A., (1920). Indian Village Site and Cemetery near Madisonville Ohio. *Papers of the Peabody Museum of American Ethnology and Archeology, Harvard University* VIII (1):

Wolpoff, M. H., (1996). Human evolution. New York: McGraw-Hill.

Wolpoff, M. H., Caspari, R., (1997). Race and Human Evolution. New York: Simon and Schuster.

Wolpoff, M. H., Hawks, J., Caspari, R., (2000). Multiregional, not multiple origins. *American Journal of Physical Anthropology* 112 (1): 129.

Wood, J. W., Milner, G. R., Herpending, H. C., Weiss, K. M., (1992). The osteological paradox: Problems of inferring Prehistoric health from skeletal samples. *Current Anthropology* 33 (4): 343.

Wunderly, J., (1938). 217. The Origin of the Tasmanian Race. *Man* 38: 198.

Wysocki, M., Whittle, A., (2000). Diversity, lifestyles and rites: new biological and archaeological evidence from British Earlier Neolithic mortuary assemblages. *Antiquity* 74: 591.

Y'Edynak, G., (1976). Long bone growth in Western Eskimo and Aleut skeletons. *American Journal of Physical Anthropology* 45: 569.

Yamanaka, A., Gunji, H., Ishida, H., (2005). Curvature, length, and cross-sectional geometry of the femur and humerus in anthropoid primates. *American Journal of Physical Anthropology* 127 (1): 46.

Yasutomi, T., Nakatsuchi, Y., Kioke, H., Uchiyama, S., (2002). Mechanisms of limitation of pronation/supination of the forearm in geometric models of deformities of the forearm bones. *Clinical Biomechanics* 17: 456.

Zilhao, J., (2006). Neandertals and moderns mixed, and it matters. *Evolutionary Anthropology* 15 (5): 183.

APPENDIX

Appendix 1 Landmarks and measurements for the femur

Nr	Measurement and landmark	Description
1	Subtrochanteric mediolateral diameter (Martin n°9)	Medio-lateral diameter taken at the 80% level. The 0% shaft level is defined as the most inferior edge of the medial condyle; the 100% is the most superior point of the head of the femur.
	M 80%	Most medial point at 80% level.
	L 80%	Most lateral point at 80% level
2	Midshaft mediolateral diameter (Martin n° 8)	Medio-lateral diameter taken at the 50% level. The 0% shaft level is defined as the most inferior edge of the medial condyle; the 100% is the most superior point of the head of the femur
	M 50%	Most medial point at 50% level.
	L 50%	Most lateral point at 50% level.
3	Subpilastric mediolateral diameter	Medio-lateral diameter taken at the 25% level. The 0% shaft level is defined as the most inferior edge of the medial condyle; the 100% is the most superior point of the head of the femur
	M 25%	Most medial point at 25% level.
	L 25%	Most lateral point at 25% level.
4	Subtrochanteric anteroposterior diameter (Martin n°11)	Antero-posterior diameter taken at the 80% level. The 0% shaft level is defined as the most inferior edge of the medial condyle; the 100% is the most superior point of the head of the femur
	A 80%	Most anterior point at 80% level.
	P 80%	Most posterior point at 80% level.
5	Mid-shaft anteroposterior diameter (Martin n°10)	Antero-posterior diameter taken at the 50% level. The 0% shaft level is defined as the most inferior edge of the medial condyle; the 100% is the most superior point of the head of the femur
	A 50%	Most anterior point at 50% level.
	P 50%	Most posterior point at 50% level.
6	Subpilastric anteroposterior diameter	Antero-posterior diameter taken at the 25% level The 0% shaft level is defined as the most inferior edge of the medial condyle; the 100% is the most superior point of the head of the femur

	A 25%	Most anterior point at 25% level.
	P 25%	Most posterior point at 25% level.
7	Femur length (Martin n°1)	Maximum length measured along the biomechanical axis.(biomech axis: where the most superior point of the head of the femur and the most lateral point of the greater trochanter describe a 90° angle, the perpendicular line down from the most superior point of the head to the most inferior point on the medial condyle).
	FEML1	The most superior point of the head measured along the biomechanical axis.
	FEML2	The most inferior point on the medial condyle measured along the biomechanical axis.
8	Length of the head-neck axis (Martin N° 14)	Length of the axis from the most medial point of the head to the middle of the intertrochanteric line.
	HNAX1	Most medial point of the head
	HNAX2	Middle of the intertrochanteric line
9	Head diameter (Martin N° 18 and 19)	Maximum diameter of the femoral head on the edge of the articular surface
	HDIA1s	Most superior point on a line describing the maximum super-inferior diameter
	HDIA2i	Most inferior point on a line describing the maximum supero-inferior diameter
	HDIA3p	Most posterior point on a line describing the maximum mediolateral diameter
	HDIA4a	Most anterior point on a line describing the maximum mediolateral diameter
10	Neck-shaft angle (Martin N° 29)	Also collo-diaphyseal angle. Martin n°29. The angle described by the shaft-axis (going through the middle of the shaft) and the neck-axis (going through the middle of the neck)
	HNAX1	Most medial point of the head
	NSAG2	Point where the neck axis intersects with the axis through the middle of the shaft
	NSAG3	Located on the superior edge of patellar surface midway between medial and lateral borders of superior portion of the patellar surface. Also lies on line passing through middle of axis of the distal shaft.
11	Torsion (Martin n° 28)	The angle of femoral torsion is the angle made by the axis of the femoral neck with the tangent of the posterior surfac of the femoral condyles.
	HNAX1	Most medial point of the head
	TORS2	The most posteriorly projecting point of the medial condyle. The point where the condyle would touch a surface if it were horizontally placed on a surface.
	TORS3	The most posteriorly projecting point of the lateral condyle. The point where the condyle would touch a surface if it were horizontally placed on a surface.
	TORS4	Most lateral point on the greater trochanter on the neck axis

12	Middle of the insertion area for gluteus minimus (Weaver n°3)	Located on the antero-inferior surface of the greater trochanter, just medial to the lateral border, in the center of the oval insertion area for gluteus minimus. The insertion area may extend as a thinner strip superiorly and medially, but record the point in the center of the insertion.
	GMIN	Center of the oval insertion area for gluteus minimus on the antero-inferior surface of the greater trochanter, medial to the lateral border
13	Middle of the insertion area for gluteus medius (Weaver n°4)	Located on the postero-superior surface of the greater trochanter, in the center of the oval insertion area for the gluteus medius. The insertion area extends as a thinner strip inferiorly and anteriorly, but record the point in the center of the insertion.
	GMED	Center of the oval insertion area for the gluteus medius located on the postero-superior surface of the greater trochanter
14	Tip of the lesser trochanter (Weaver n°5)	Where the lesser trochanter projects maximally (local maximum of a curved surface)
	LSTR	The tip where the lesser trochanter projects maximally
15	Tip of the adductor tubercle (Weaver n°8)	Located where the adductor tubercle projects maximally (local maximum of a curved surface)
	ADTB	Tip located where the adductor tubercle projects maximally
16	Midpoint of the antero-superior edge of the patellar surface of the distal femur (Weaver n°9)	Located on the superior edge of the patellar surface midway between the medial and lateral borders of the superior portion of the patellar surface. This point also lies on a line that passes through the middle of the axis of the distal femoral shaft.
	NSAG3	Located on the sup edge of patellar surface midway between medial and lateral borders of superior portion of the patellar surface. Also lies on line passing through middle of axis of the distal shaft.
17	Midpoint of the medial edge of the inferior surface of the medial condyle (Weaver n°10)	Midpoint, from an inferior view, of the medial edge of the inferior surface of the medial condyle.
	MCMDi	Midpoint, from an inferior view, of the medial edge of the inferior surface of the medial condyle.
18	Midpoint of the lateral edge of the inferior surface of the inferior surface of the lateral	The midpoint, from an anterior view, of the lateral edge of the inferior surface of the lateral condyle. There is usually a slight notch or depression at this point. Points 27 and 28 should connect to form a line that is horizontal when the femur is held in anatomical position. Points 27 and 28 usually fall just anterior to the anterior edge of the intercondylar notch.

	condyle (Weaver n°11)	
	LCMDi	Midpoint, from an inferior view, of the lateral edge of the inferior surface of the lateral condyle.
19	Midpoint of the medial edge of the posterior surface of the medial condyle (Weaver n° 12)	This point is defined as the midpoint, from a posterior view, of the medial edge of the posterior surface of the medial condyle.
	MCMDp	Midpoint, from a posterior view, of the medial edge of the posterior surface of the medial condyle.
20	Midpoint of the lateral edge of the posterior surface of the lateral condyle (Weaver n° 13)	This point is defined as the midpoint, from a posterior view, of the lateral edge of the posterior surface of the lateral condyle. There is usually a slight notch or depression at point 30. Point 29 and 30 should connect to form a line that is a frontal plane when the femur is held in anatomical position.
	LCMDp	Midpoint, from a posterior view, of the lateral edge of the posterior surface of the lateral condyle.
21	Maximum condylar width (Martin n°21)	The distance between the point where the medial epicondyle projects maximally (local maximum of a curved surface) and the point where the lateral epicondyle projects maximally (local maximum of a curved surface)
	MLMDM1	The point where the medial epicondyle projects maximally (local maximum of a curved surface)
	MLMDL2	The point where the lateral epicondyle projects maximally (local maximum of a curved surface)
22	Most superior projection of the patellar surface	The points on a curved surface where the direction of the articulation of the patellar surface changes direction (from lateral/medial to inferior)
	PROJ1	The point where the medial condylar articular surface projects most anteriorly
	PROJ2	The point where the lateral condylar articular surface projects most anteriorly
23	Curvature	Curvature of the femur along four sides. Posterior measured from 80% level along the linea aspera down to the midpoint between the posterior medial and lateral patellar surface. Anterior curvature measured from the 80% level down to the midpoint on the most superior edge of the patellar surface. Medial curvature from 80% level down to the adductor tubercle. Lateral curvature from 80% level down to the
	LMXTB	The point where the lateral surface projects maximally (opposite side adductor tubercle)
	MIDPS	The midpoint between the posterior medial and lateral patellar surface
	PCURV	Semi-landmarks taken every 5 mm along the posterior curve of the femur.
	ACURV	Semi-landmarks taken every 5 mm along the anterior curve of the femur.
	MCURV	Semi-landmarks taken every 5 mm along the medial curve of the femur.
	LCURV	Semi-landmarks taken every 5 mm along the lateral curve of the femur.
24	Midshaft robusticity index	AP diameter 50% + ML diameter 50% / length *100

25	Head robusticity index	SI head diameter + AP head diameter / length *100
26	Condyle diameter ratio	Maximum condylar width/length *100
27	Neck length ratio	Neck length/length *100
28	Subtrochanteric ratio	AP diameter 80% / ML diameter 80%*100
29	Midshaft ratio	AP diameter 50% / ML diameter 50%*100
30	Subpilastric ratio	AP diameter 25% / ML diameter 25%*100

Appendix 2 Landmark diagram – femur (After www.bartelby.com).

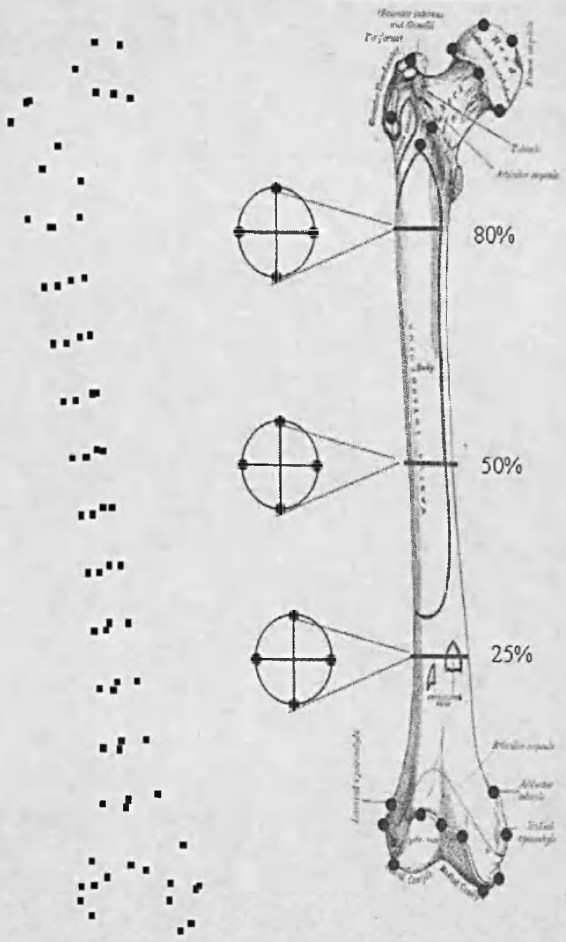

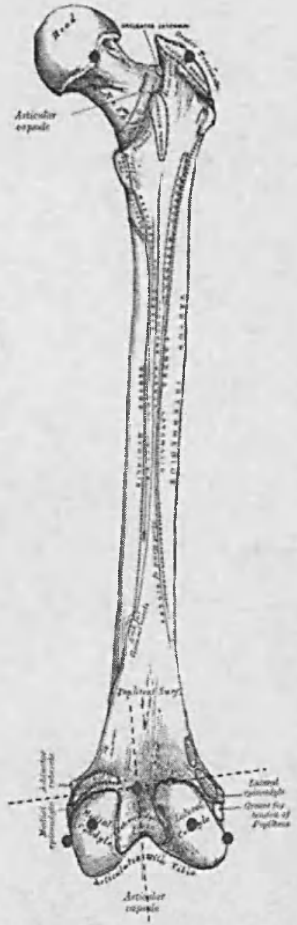

Appendix 3 Landmarks and measurements for the radius

Nr	Measurement and landmark	Description
1	Maximal length (Martin n° 1)	Maximum length measured from the most superior point on the articular surface on the head to the most distal point on the styloid process.
	RADL1	The most superior point on the articular surface on the head
	RADL2	The most distal point on the styloid process
2	80% mediolateral diameter (Martin 5a)	Medio-lateral diameter taken at the 80% level. The 0% shaft level is defined as the most inferior edge of the styloid process; the 100% is the most superior point on the articular surface on the head.
	M 80%	Most medial point at 80% level.
	L 80%	Most lateral point at 80% level.
3	50% mediolateral diameter	Medio-lateral diameter taken at the 50% level. The 0% shaft level is defined as the most inferior edge of the styloid process; the 100% is the most superior point on the articular surface on the head.
	M 50%	Most medial point at 50% level.
	L 50%	Most lateral point at 50% level.
4	25% mediolateral diameter	Medio-lateral diameter taken at the 25% level. The 0% shaft level is defined as the most inferior edge of the styloid process; the 100% is the most superior point on the articular surface on the head.
	M 25%	Most medial point at 25% level.
	L 25%	Most lateral point at 25% level.
5	80% anteroposterior diameter (Martin 4a)	Antero-posterior diameter taken at the 80% level. The 0% shaft level is defined as the most inferior edge of the styloid process; the 100% is the most superior point on the articular surface on the head.
	A 80%	Most anterior point at 80% level.
	P 80%	Most posterior point at 80% level.
6	50% anteroposterior diameter (Martin 5a)	Antero-posterior diameter taken at the 50% level. The 0% shaft level is defined as the most inferior edge of the styloid process; the 100% is the most superior point on the articular surface on the head.
	A 50%	Most anterior point at 50% level.
	P 50%	Most posterior point at 50% level.
7	25% anteroposterior diameter	Antero-posterior diameter taken at the 25% level. The 0% shaft level is defined as the most inferior edge of the styloid process; the 100% is the most superior point on the articular surface on the head.
	A 25%	Most anterior point at 25% level.

	P 25%	Most posterior point at 25% level.
8	Length of the head-neck axis (Martin 1a)	Length of the axis from the most superior point of the head to the radial tuberosity.
	HDII4a	Most anterior point on a line describing the maximum diameter on the most inferior edge of the head
	RADT	The tip where the radial tuberosity projects maximally
9	Superior head diameter (Martin n° 4 (1))	Maximum diameter of the radial head on the edge of the articular surface
	HDIS1m	Most medial point on a line describing the maximum mediolateral diameter on the most superior edge of the head
	HDIS2l	Most lateral point on a line describing the maximum mediolateral diameter on the most superior edge of the head
	HDIS3p	Most posterior point on a line describing the maximum anteroposterior diameter on the most superior edge of the head
	HDIS4a	Most anterior point on a line describing the anteroposterior maximum diameter on the most superior edge of the head
10	Inferior head diameter (Based on Martin n° 4 (1))	Maximum diameter of the femoral head on the edge of the articular surface
	HDII1m	Most medial point on a line describing the maximum mediolateral diameter on the most inferior edge of the head
	HDII2l	Most lateral point on a line describing the maximum mediolateral diameter on the most inferior edge of the head
	HDII3p	Most posterior point on a line describing the anteroposterior maximum diameter on the most inferior edge of the head
	HDII4a	Most anterior point on a line describing the anteroposterior maximum diameter on the most inferior edge of the head
11	Neck-shaft angle (Martin n°7)	Also collo-diaphyseal angle. Martin n°7. The angle described by the shaft-axis (going through the middle of the shaft) and the neck-axis (going through the middle of the neck)
	HDII4a	Most anterior point on a line describing the maximum diameter on the most inferior edge of the head
	NSAG2	Point where the most narrow diameter of the neck intersects with the anterior neck axis through the middle of the shaft
	A 80%	Most anterior point at 80% level. The 0% shaft level is defined as the most inferior edge of the styloid process; the 100% is the most superior point on the articular surface on the head.

12	The radial tuberosity	The most projecting point on the radial tuberosity
	RADT	The tip where the radial tuberosity projects maximally
13	Middle of the distal radial articular surface edge	The middle of the distal radial articular surface edge on the posterior side. The middle of a curved surface
	ARTSp	The middle of the distal radial articular surface edge on the posterior side. The middle of a curved surface
14	The middle of the ulnar notch	The middle of the articular surface on the medial side of the radial notch.
	ULNT	The middle of the medial articular surface on the ulnar notch
15	Middle of the distal radial articular surface edge	The middle of the distal radial articular surface edge on the anterior side. The middle of a curved surface
	ARTSa	The middle of the distal radial articular surface edge on the anterior side. The middle of a curved surface
16	Dorsal subtense (based on Martin 6b)	Maximum distance from a chord connecting P80% and ARTSp and the posterior surface of the shaft.
17	Lateral subtense (based on Martin 6a)	Maximum distance from a chord connecting L80% and the most distal point on the styloid process (RADL2) and the posterior surface of the shaft.
18	Curvature	Curvature of the radius along two sides. Medial curvature from 80% down to the middle of the ulnar notch. Lateral curvature from 80% level down to the tip of the styloid process.
	MCURV	Semi-landmarks taken every 5mm along the medial curve of the radius
	LCURV	Semi-landmarks taken every 5mm along the lateral curve of the radius
19	Midshaft robusticity	anteroposterior midshaft diameter + mediolateral midshaft diameter/ maximum length *100
20	Head robusticity	anteropostior head diameter+ mediolateral diameter/ maximum length *100
21	Distal articulation Size Ratio	anteroposterior distal articulation diameter + mediolateral distal articulation diameter/ maximum length *100
22	Position Radial Tubercle	the angle between a vector connecting the most projecting point on the radial tuberosity and the most medial point at the 80% level and the vector running through the most medial point at 50% and 80% (see diagram)
23	Neck Length Ratio (Martin n°1a/Martin n°1)	Neck length/maximum length *100
24	Head Shape Ratio	anteropostior head diameter / mediolateral diameter *100
25	Midshaft Shape Ratio (Martin n°4a/ Martin n°5a)	anteroposterior midshaft diameter / mediolateral midshaft diameter *100

Appendix 4 Landmark and measurement diagrams – radius (After www.bartelby.com and www.physioweb.nl)

Landmarks radius

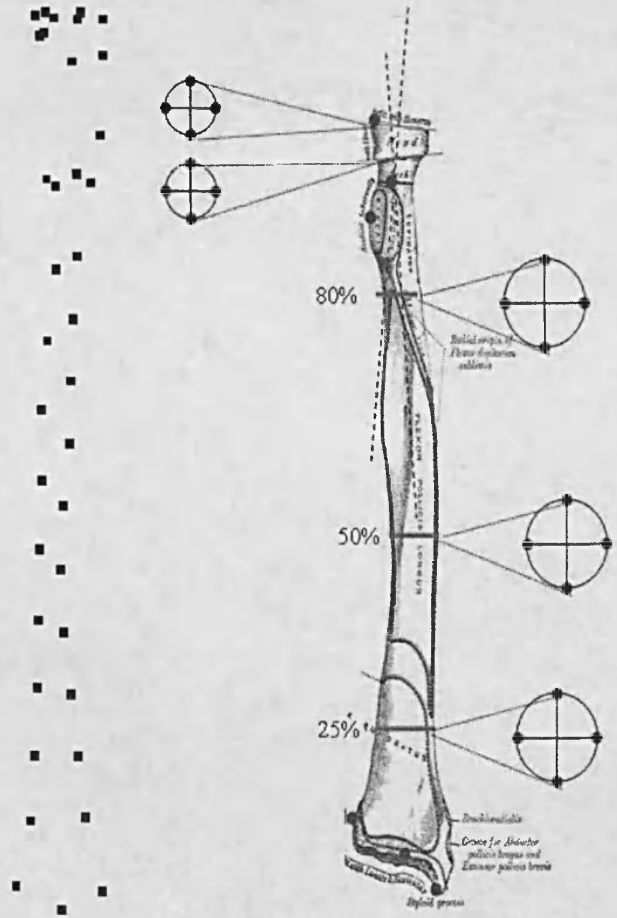

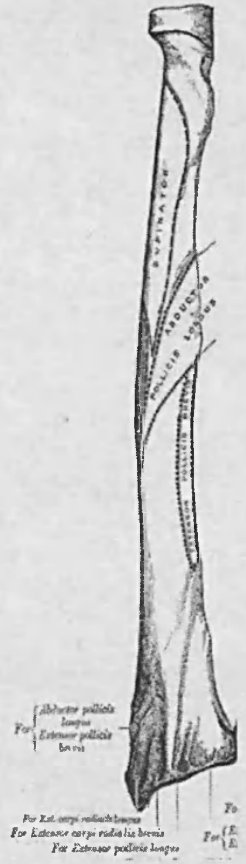

Neck length
α=PosRadTub
α
Maximum length

β= neck shaft angle
β

Appendix 5 Landmarks and measurements for the ulna

Nr	Measurement and landmark	Description
1	Maximum length (Martin n°1)	Maximum length measured from the most superior point on the olecranon process to the most distal point on the articular surface (not styloid process because of preservation issues in archaeological samples)
	ULNL1	The most superior point on the olecranon process
	ULNL2	The most distal point on the radial articulation surface
2	80% mediolateral diameter	Medio-lateral diameter taken at the 80% level. The 0% shaft level is defined as the most distal point on the articular surface; the 100% is the most superior point on olecranon process
	M 80%	Most medial point at 80% level.
	L 80%	Most lateral point at 80% level.
3	50% mediolateral diameter	Medio-lateral diameter taken at the 50% level. The 0% shaft level is defined as the most distal point on the articular surface; the 100% is the most superior point on olecranon process
	M 50%	Most medial point at 50% level.
	L 50%	Most lateral point at 50% level.
4	25% mediolateral diameter	Medio-lateral diameter taken at the 25% level. The 0% shaft level is defined as the most distal point on the articular surface; the 100% is the most superior point on olecranon process
	M 25%	Most medial point at 25% level.
	L 25%	Most lateral point at 25% level.
5	80% anteroposterior diameter	Antero-posterior diameter taken at the 80% level. The 0% shaft level is defined as the most distal point on the articular surface; the 100% is the most superior point on olecranon process
	A 80%	Most anterior point at 80% level.
	P 80%	Most posterior point at 80% level.
6	50% anteroposterior diameter	Antero-posterior diameter taken at the 50% level. The 0% shaft level is defined as the most distal point on the articular surface; the 100% is the most superior point on olecranon process
	A 50%	Most anterior point at 50% level.
	P 50%	Most posterior point at 50% level.
7	25% anteroposterior diameter	Antero-posterior diameter taken at the 25% level. The 0% shaft level is defined as the most distal point on the articular surface; the 100% is the most superior point on olecranon process
	A 25%	Most anterior point at 25% level.
	P 25%	Most posterior point at 25% level.

8	Pronator quadrutus crest	The dimensions of the pronator quadrutus crest
	PRQC1	The most proximal point of the pronator quadrutus crest
	PRQC2	The most distal point of the pronator quadrutus crest
9	Proximal articulation dimension	The dimensions of the olecranon and coronoid process.
	OLTP	The tip of the Olecranon process
	OLMXm	The most medial point on the olecranon process
	OLMXl	The most lateral point on the olecranon process
	OLMXp	The most posterior point on the olecranon process
	TRWD1	The most medial point on the trochlear notch along the minimum width line perpendicular to the shaft axis
	TRWD2	The most lateral point on the trochlear notch along the minimum width line perpendicular to the shaft axis
	CORPR	The tip of the coronoid process
	RADNm	The most medial point on the radial notch
	RADNa	The most anterior notch on the radial notch
	RADNp	The most inferior notch on the radial notch
10	Distal articulation diameter	Anteroposterior and mediolateral diameter of the superior edge of the distal articulation
	HDIAp	The most posterior point on the superior edge of the distal articulation
	HDIAa	The most anterior point on the superior edge of the distal articulation
	HDIAm	The most medial point on the superior edge of the distal articulation
	HDIAl	The most lateral point on the superior edge of the distal articulation
11	Styloid process	The tip of the styloid process
	STPR	The tip of the styloid process
12	Flexor digitorum sublimis	The most projecting tip of the flexor digitorum sublimis
	FLXSm	The middle of the flexor digitorum sublimis
13	Brachialis insertion	The dimensions of the brachialis insertion
	BRACH1s	The most superior point of the brachialis insertion

	BRACH2i	The most inferior point of the brachialis insertion
	BRACH3m	The middle of the brachialis insertion
14	Curvature	Posterior curvature measured from 80% level down to the most posterior point on the radial articulation.
	PCURV	Semi-landmarks taken every 5 mm along the posterior curve of the ulna
15	trochlear notch orientation (Martin n°15)	The angle between the vector running along the anterior surface and the vector connecting the tip of the olecranon and coronoid (also joint-axis angle)
16	Olecranon size (Patte, 1955; Fisher, 1906 p. 227)	The distance between the tip of the olecranon and the most posterior point on the proximal surface of the ulna (see diagram)
17	Position brachialis (Solan, 1992)	The position of the brachialis tuberosity: Distance from the proximal extremity to the most distal point of the brachialis tuberosity (see diagram)
15	Head orientation (Martin, 15a)	The angle at the olecranon when a triangle is formed between the 80% anterior surface, the tip of the olecranon and the coronoid (see diagram)
19	Head/shaft ratio	Size of the head: olecranon size/length *100 (see diagram)
20	Coronoid Olecranon ratio (Martin 7a and 8a)	Height olecranon/height coronoid*100 (see diagram)

Appendix 6 Landmark and measurement diagrams – ulna (After www.bartelbv.com and www.physioweb.nl)

Landmarks ulna

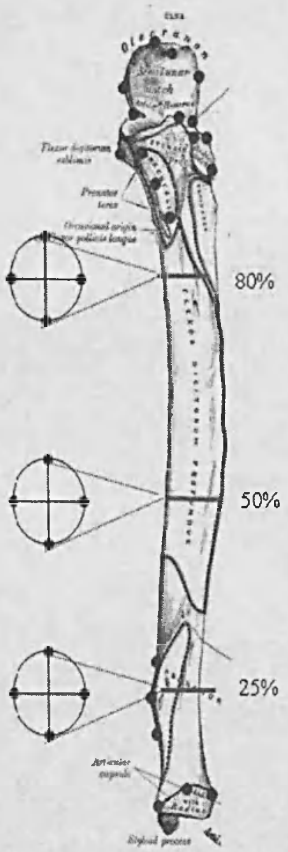

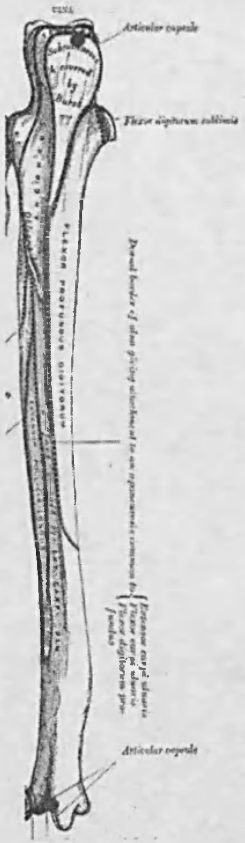

Appendix 7 Diagrams for measurements calculated from the landmarks on the ulna (After www.bartelbv.com and www.physioweb.nl)

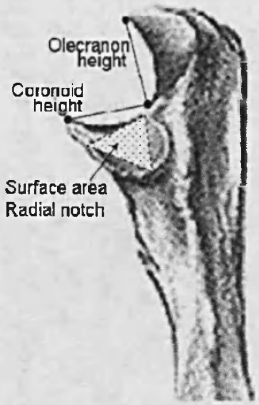

Head-orientation

Trochlear Notch
Orientation

Brachial tuberosity length
Pronator crest length

Head size
Maximum length

Appendix 8 Summary table for categorical data for all modern human populations.

Population	subsistence strategy	fine subsistence stragegy	time period	lat. Cat.	abslatitude
African American	low activity	n/a	18-19 C	n/a	n/a
Alaskan Aleut	high activity	aquatic forager	18-19 C	high	71
Alaskan Native	high activity	aquatic forager	n/a	high	68
Andaman	high activity	aquatic forager	18-19 C	low	11
Arizona	high activity	n/a	n/a	midlow	36
Australian	high activity	pedestrian forager	18-19 C	midlow	30
Bantou	high activity	pedestrian forager	n/a	low	7
Belgian Medieval	moderate activity	n/a	Medieval	midhigh	50
Belgian Mesolithic	moderate activity	n/a	Mesolithic	midhigh	50
Belgian Neolithic	moderate activity	n/a	Neolithic	midhigh	50
British Neolithic	moderate activity	n/a	Neolithic	midhigh	51
Chinese	low activity	n/a	18-19 C	midlow	35
Colorado native	high activity	pedestrian forager	n/a	midhigh	43
Czech Medieval	moderate activity	n/a	Medieval	midhigh	49
Danish Medieval	moderate activity	n/a	Medieval	midhigh	55
Danish Neolithic	moderate activity	n/a	Neolithic	midhigh	55
Egyptian	moderate activity	n/a	n/a	midlow	26
English Medieval	moderate activity	n/a	Medieval	midhigh	54
English Urban	low activity	n/a	18-19 C	midhigh	51
French Medieval	moderate activity	n/a	Medieval	midhigh	49
French Neolithic	moderate activity	n/a	Neolithic	midhigh	48
Greenland Inuit	high activity	aquatic forager	n/a	high	69
Hottentot	high activity	pedestrian forager		midlow	28
Lapland	high activity	pastoralist	n/a	high	67
Natufian	high activity	pedestrian forager	Mesolithic	midlow	32
New Mexico	moderate activity	horticulturalist	n/a	midlow	31
Ohio	high activity	horticulturalist	n/a	midlow	40
Peru	high activity	n/a	n/a	low	11
Pygmee	high activity	pedestrian forager	n/a	low	7
Russian Eskimo	high activity	pedestrian forager	n/a	high	66
Russian Mesolithic	high activity	pedestrian forager	Mesolithic	midhigh	58
Siberia	high activity	pedestrian forager	n/a	high	66
South Dakota	high activity	equestrian forager	n/a	midhigh	45
Tasmanian	high activity	pedestrian forager	18-19 C	midhigh	42
Tierra del Fuego	high activity	equestrian forager	18-19 C	midhigh	54
Kazach	high activity	pastoralist	18-19 C	midhigh	47

Appendix 9 Rainfall distance matrix between populations (data from Hijmans *et al.*, 2005)

	Africa	AlasAl	AlasNa	Andam	ArizNa	AustAb	Bantou	BelMed	BelMes	BelNeo	BriMed	BriNeo	BriUrb	Chines	ColNat	CzeMed	DanMed	DanNeo	Egypts	FreMed	FreNeo	Greinu	Laplan	Natufi	NewMex	OhiNat	PeruNa	Pygmee	RusEsk	RusMes	SibNat	SouDak	Tasman	Tierra	VolMed
Africa	0	179	55	2732	107	526	1114	552	552	552	377	377	377	1607	178	325	338	338	291	435	435	42	186	51	104	680	277	1093	39	344	166	140	376	395	66
AlasAl	179	0	124	2911	286	705	1293	731	731	731	556	556	556	1786	357	504	517	517	112	614	614	137	365	128	283	859	98	1272	218	523	345	319	555	574	113
AlasNa	55	124	0	2787	162	581	1169	607	607	607	432	432	432	1662	233	380	393	393	236	490	490	13	241	4	159	735	222	1148	94	399	221	195	431	450	11
Andam	2732	2911	2787	0	2625	2206	1618	2180	2180	2180	2355	2355	2355	1125	2554	2407	2394	2394	3023	2297	2297	2774	2546	2783	2628	2052	3009	1639	2693	2388	2566	2592	2356	2337	2798
ArizNa	107	286	162	2625	0	419	1007	445	445	445	270	270	270	1500	71	218	231	231	398	328	328	149	79	158	3	573	384	986	68	237	59	33	269	288	173
AustAb	526	705	581	2206	419	0	588	26	26	26	149	149	149	1081	348	201	188	188	817	91	91	568	340	577	422	154	803	567	487	182	360	386	150	131	592
Bantou	1114	1293	1169	1618	1007	588	0	562	562	562	737	737	737	493	936	789	776	776	1405	679	679	1156	928	1165	1010	434	1391	21	1075	770	948	974	738	719	1180
BelMed	552	731	607	2180	445	26	562	0	0	0	175	175	175	1055	374	227	214	214	843	117	117	594	366	603	448	128	829	541	513	208	386	412	176	157	618
BelMes	552	731	607	2180	445	26	562	0	0	0	175	175	175	1055	374	227	214	214	843	117	117	594	366	603	448	128	829	541	513	208	386	412	176	157	618
BelNeo	552	731	607	2180	445	26	562	0	0	0	175	175	175	1055	374	227	214	214	843	117	117	594	366	603	448	128	829	541	513	208	386	412	176	157	618
BriMed	377	556	432	2355	270	149	737	175	175	175	0	0	0	1230	199	52	39	39	668	58	58	419	191	428	273	303	654	716	338	33	211	237	1	18	443
BriNeo	377	556	432	2355	270	149	737	175	175	175	0	0	0	1230	199	52	39	39	668	58	58	419	191	428	273	303	654	716	338	33	211	237	1	18	443
BriUrb	377	556	432	2355	270	149	737	175	175	175	0	0	0	1230	199	52	39	39	668	58	58	419	191	428	273	303	654	716	338	33	211	237	1	18	443
Chines	1607	1786	1662	1125	1500	1081	493	1055	1055	1055	1230	1230	1230	0	1429	1282	1269	1269	1898	1172	1172	1649	1421	1658	1503	927	1884	514	1568	1263	1441	1467	1231	1212	1673
ColNat	178	357	233	2554	71	348	936	374	374	374	199	199	199	1429	0	147	160	160	469	257	257	220	8	229	74	502	455	915	139	166	12	38	198	217	244
CzeMed	325	504	380	2407	218	201	789	227	227	227	52	52	52	1282	147	0	13	13	616	110	110	367	139	376	221	355	602	768	286	19	159	185	51	70	391
DanMed	338	517	393	2394	231	188	776	214	214	214	39	39	39	1269	160	13	0	0	629	97	97	380	152	389	234	342	615	755	299	6	172	198	38	57	404
DanNeo	338	517	393	2394	231	188	776	214	214	214	39	39	39	1269	160	13	0	0	629	97	97	380	152	389	234	342	615	755	299	6	172	198	38	57	404
Egypts	291	112	236	3023	398	817	1409	843	843	843	668	668	668	1898	469	616	629	629	0	726	726	249	477	240	395	971	14	1384	330	635	457	431	667	686	226
FreMed	435	614	490	2297	328	91	679	117	117	117	58	58	58	1172	257	110	97	97	726	0	0	477	249	486	331	245	712	658	396	91	269	295	59	40	501
FreNeo	435	614	490	2297	328	91	679	117	117	117	58	58	58	1172	257	110	97	97	726	0	0	477	249	486	331	245	712	658	396	91	269	295	59	40	501
Greinu	42	137	13	2774	149	568	1156	594	594	594	419	419	419	1649	220	367	380	380	249	477	477	0	228	9	146	722	235	1135	81	386	208	182	418	437	24
Laplan	186	365	241	2546	79	340	928	366	366	366	191	191	191	1421	8	139	152	152	477	249	249	228	0	237	82	494	463	907	147	158	20	46	190	209	252
Natufi	51	128	4	2783	158	577	1165	603	603	603	428	428	428	1658	229	376	389	389	240	486	486	9	237	0	155	731	226	1144	90	395	217	191	427	446	15
NewMex	104	283	159	2628	3	422	1010	448	448	448	273	273	273	1503	74	221	234	234	395	331	331	146	82	155	0	576	381	989	65	240	62	36	272	291	170
OhiNat	680	859	735	2052	573	154	434	128	128	128	303	303	303	927	502	355	342	342	971	245	245	722	494	731	576	0	957	413	641	336	514	540	304	285	748
PeruNa	277	98	222	3009	384	803	1391	829	829	829	654	654	654	1884	455	602	615	615	14	712	712	235	463	226	381	957	0	1370	316	621	443	417	653	672	211
Pygmee	1093	1272	1148	1639	986	567	21	541	541	541	716	716	716	514	915	768	755	755	1384	658	658	1135	907	1144	989	413	1370	0	1054	749	927	953	717	698	1159
RusEsk	39	218	94	2693	68	487	1075	513	513	513	338	338	338	1568	139	286	299	299	330	396	396	81	147	90	65	641	316	1054	0	305	127	101	337	356	105
RusMes	344	523	399	2388	237	182	770	208	208	208	33	33	33	1263	166	19	6	6	635	91	91	386	158	395	240	336	621	749	305	0	178	204	32	51	410
SibNat	166	345	221	2566	59	360	948	386	386	386	211	211	211	1441	12	159	172	172	457	269	269	208	20	217	62	514	443	927	127	178	0	26	210	229	232
SouDak	140	319	195	2592	33	386	974	412	412	412	237	237	237	1467	38	185	198	198	431	295	295	182	46	191	36	540	417	953	101	204	26	0	236	255	206
Tasman	376	555	431	2356	269	150	738	176	176	176	1	1	1	1231	198	51	38	38	667	59	59	418	190	427	272	304	653	717	337	32	210	236	0	19	442
Tierra	395	574	450	2337	288	131	719	157	157	157	18	18	18	1212	217	70	57	57	686	40	40	437	209	446	291	285	672	698	356	51	229	255	19	0	461
VolMed	66	113	11	2798	173	592	1180	618	618	618	443	443	443	1673	244	391	404	404	225	501	501	24	252	15	170	746	211	1159	105	410	232	206	442	461	0

Appendix 10 Temperature distance matrix between populations (data from Hijmans *et al.*, 2005)

	Africa	AlasAl	AlasNa	Andam	ArizNa	AustAb	Bantou	BelMed	BelMes	BelNeo	BriMed	BriNeo	BriUrb	Chines	ColNat	CzeMed	DanMed	DanNeo	Egypts	FreMed	FreNeo	GreInu	Laplan	Natufi	NewMex	OhiNat	PeruNa	Pygmee	RusEsk	RusMes	SibNat	SouDak	Tasman	Tierra	VolMed
Africa	0	30.5	26.5	7.3	10.5	5	6.5	8.5	8.5	8.5	8.3	8.3	8.3	3.1	15.8	10.3	10.3	10.3	5	7.8	7.8	23.1	19.7	5	4.7	9.3	1.3	6.4	25.5	13.4	29.7	11.2	8.8	12.9	12.8
AlasAl	30.5	0	4	37.8	20	25.5	37	22	22	22	22.2	22.2	22.2	33.6	14.7	20.2	20.2	20.2	35.5	22.7	22.7	7.4	10.8	35.5	25.8	21.2	31.8	36.9	5	17.1	0.8	19.3	21.7	17.6	17.7
AlasNa	26.5	4	0	33.8	16	21.5	33	18	18	18	18.2	18.2	18.2	29.6	10.7	16.2	16.2	16.2	31.5	18.7	18.7	3.4	6.8	31.5	21.8	17.2	27.8	32.9	1	13.1	3.2	15.3	17.7	13.6	13.7
Andam	7.3	37.8	33.8	0	17.8	12.3	0.8	15.8	15.8	15.8	15.6	15.6	15.6	4.2	23.1	17.6	17.6	17.6	2.3	15.1	15.1	30.4	27	2.3	12	16.6	6	0.9	32.8	20.7	37	18.5	16.1	20.2	20.1
ArizNa	10.5	20	16	17.8	0	5.5	17	2	2	2	2.2	2.2	2.2	13.6	5.3	0.2	0.2	0.2	15.5	2.7	2.7	12.6	9.2	15.5	5.8	1.2	11.8	16.9	15	2.9	19.2	0.7	1.7	2.4	2.3
AustAb	5	25.5	21.5	12.3	5.5	0	11.5	3.5	3.5	3.5	3.3	3.3	3.3	8.1	10.8	5.3	5.3	5.3	10	2.8	2.8	18.1	14.7	10	0.3	4.3	6.3	11.4	20.5	8.4	24.7	6.2	3.8	7.9	7.8
Bantou	6.5	37	33	0.8	17	11.5	0	15	15	15	14.8	14.8	14.8	3.4	22.3	16.8	16.8	16.8	1.5	14.3	14.3	29.6	26.2	1.5	11.2	15.8	5.2	0.1	32	19.8	36.2	17.7	15.3	19.4	19.3
BelMed	8.5	22	18	15.8	2	3.5	15	0	0	0	0.2	0.2	0.2	11.6	7.3	1.8	1.8	1.8	13.5	0.7	0.7	14.6	11.2	13.5	3.8	0.8	9.8	14.9	17	4.9	21.2	2.7	0.3	4.4	4.3
BelMes	8.5	22	18	15.8	2	3.5	15	0	0	0	0.2	0.2	0.2	11.6	7.3	1.8	1.8	1.8	13.5	0.7	0.7	14.6	11.2	13.5	3.8	0.8	9.8	14.9	17	4.9	21.2	2.7	0.3	4.4	4.3
BelNeo	8.5	22	18	15.8	2	3.5	15	0	0	0	0.2	0.2	0.2	11.6	7.3	1.8	1.8	1.8	13.5	0.7	0.7	14.6	11.2	13.5	3.8	0.8	9.8	14.9	17	4.9	21.2	2.7	0.3	4.4	4.3
BriMed	8.3	22.2	18.2	15.6	2.2	3.3	14.8	0.2	0.2	0.2	0	0	0	11.4	7.5	2	2	2	13.3	0.5	0.5	14.8	11.4	13.3	3.6	1	9.6	14.7	17.2	5.1	21.4	2.9	0.5	4.6	4.5
BriNeo	8.3	22.2	18.2	15.6	2.2	3.3	14.8	0.2	0.2	0.2	0	0	0	11.4	7.5	2	2	2	13.3	0.5	0.5	14.8	11.4	13.3	3.6	1	9.6	14.7	17.2	5.1	21.4	2.9	0.5	4.6	4.5
BriUrb	8.3	22.2	18.2	15.6	2.2	3.3	14.8	0.2	0.2	0.2	0	0	0	11.4	7.5	2	2	2	13.3	0.5	0.5	14.8	11.4	13.3	3.6	1	9.6	14.7	17.2	5.1	21.4	2.9	0.5	4.6	4.5
Chines	3.1	33.6	29.6	4.2	13.6	8.1	3.4	11.6	11.6	11.6	11.4	11.4	11.4	0	18.9	13.4	13.4	13.4	1.9	10.9	10.9	26.2	22.8	1.9	7.8	12.4	1.8	3.3	28.6	16.5	32.8	14.3	11.9	16	15.9
ColNat	15.8	14.7	10.7	23.1	5.3	10.8	22.3	7.3	7.3	7.3	7.5	7.5	7.5	18.9	0	5.5	5.5	5.5	20.8	8	8	7.3	3.9	20.8	11.1	6.5	17.1	22.2	9.7	2.4	13.9	4.6	7	2.9	3
CzeMed	10.3	20.2	16.2	17.6	0.2	5.3	16.8	1.8	1.8	1.8	2	2	2	13.4	5.5	0	0	0	15.3	2.5	2.5	12.8	9.4	15.3	5.6	1	11.6	16.7	15.2	3.1	19.4	0.9	1.5	2.6	2.5
DanMed	10.3	20.2	16.2	17.6	0.2	5.3	16.8	1.8	1.8	1.8	2	2	2	13.4	5.5	0	0	0	15.3	2.5	2.5	12.8	9.4	15.3	5.6	1	11.6	16.7	15.2	3.1	19.4	0.9	1.5	2.6	2.5
DanNeo	10.3	20.2	16.2	17.6	0.2	5.3	16.8	1.8	1.8	1.8	2	2	2	13.4	5.5	0	0	0	15.3	2.5	2.5	12.8	9.4	15.3	5.6	1	11.6	16.7	15.2	3.1	19.4	0.9	1.5	2.6	2.5
Egypts	5	35.5	31.5	2.3	15.5	10	1.5	13.5	13.5	13.5	13.3	13.3	13.3	1.9	20.8	15.3	15.3	15.3	0	12.8	12.8	28.1	24.7	0	9.7	14.3	3.7	1.4	30.5	18.4	34.7	16.2	13.8	17.9	17.8
FreMed	7.8	22.7	18.7	15.1	2.7	2.8	14.3	0.7	0.7	0.7	0.5	0.5	0.5	10.9	8	2.5	2.5	2.5	12.8	0	0	15.3	11.9	12.8	3.1	1.5	9.1	14.2	17.7	5.6	21.9	3.4	1	5.1	5
FreNeo	7.8	22.7	18.7	15.1	2.7	2.8	14.3	0.7	0.7	0.7	0.5	0.5	0.5	10.9	8	2.5	2.5	2.5	12.8	0	0	15.3	11.9	12.8	3.1	1.5	9.1	14.2	17.7	5.6	21.9	3.4	1	5.1	5
GreInu	23.1	7.4	3.4	30.4	12.6	18.1	29.6	14.6	14.6	14.6	14.8	14.8	14.8	26.2	7.3	12.8	12.8	12.8	28.1	15.3	15.3	0	3.4	28.1	18.4	13.8	24.4	29.5	2.4	9.7	6.6	11.9	14.3	10.2	10.3
Laplan	19.7	10.8	6.8	27	9.2	14.7	26.2	11.2	11.2	11.2	11.4	11.4	11.4	22.8	3.9	9.4	9.4	9.4	24.7	11.9	11.9	3.4	0	24.7	15	10.4	21	26.1	5.8	6.3	10	8.5	10.9	6.8	6.9
Natufi	5	35.5	31.5	2.3	15.5	10	1.5	13.5	13.5	13.5	13.3	13.3	13.3	1.9	20.8	15.3	15.3	15.3	0	12.8	12.8	28.1	24.7	0	9.7	14.3	3.7	1.4	30.5	18.4	34.7	16.2	13.8	17.9	17.8
NewMex	4.7	25.8	21.8	12	5.8	0.3	11.2	3.8	3.8	3.8	3.6	3.6	3.6	7.8	11.1	5.6	5.6	5.6	9.7	3.1	3.1	18.4	15	9.7	0	4.6	6	11.1	20.8	8.7	25	6.5	4.1	8.2	8.1
OhiNat	9.3	21.2	17.2	16.6	1.2	4.3	15.8	0.8	0.8	0.8	1	1	1	12.4	6.5	1	1	1	14.3	1.5	1.5	13.8	10.4	14.3	4.6	0	10.6	15.7	16.2	4.1	20.4	1.9	0.5	3.6	3.5
PeruNa	1.3	31.8	27.8	6	11.8	6.3	5.2	9.8	9.8	9.8	9.6	9.6	9.6	1.8	17.1	11.6	11.6	11.6	3.7	9.1	9.1	24.4	21	3.7	6	10.6	0	5.1	26.8	14.7	31	12.5	10.1	14.2	14.1
Pygmee	6.4	36.9	32.9	0.9	16.9	11.4	0.1	14.8	14.8	14.8	14.7	14.7	14.7	3.3	22.2	16.7	16.7	16.7	1.4	14.2	14.2	29.5	26.1	1.4	11.1	15.7	5.1	0	31.9	19.8	36.1	17.6	15.2	19.3	19.2
RusEsk	25.5	5	1	32.8	15	20.5	32	17	17	17	17.2	17.2	17.2	28.6	9.7	15.2	15.2	15.2	30.5	17.7	17.7	2.4	5.8	30.5	20.6	16.2	26.8	31.9	0	12.1	4.2	14.3	16.7	12.6	12.7
RusMes	13.4	17.1	13.1	20.7	2.9	8.4	19.9	4.9	4.9	4.9	5.1	5.1	5.1	16.5	2.4	3.1	3.1	3.1	18.4	5.6	5.6	9.7	6.3	18.4	8.7	4.1	14.7	19.8	12.1	0	16.3	2.2	4.6	0.5	0.6
SibNat	29.7	0.8	3.2	37	19.2	24.7	36.2	21.2	21.2	21.2	21.4	21.4	21.4	32.8	13.9	19.4	19.4	19.4	34.7	21.9	21.9	6.6	10	34.7	25	20.4	31	36.1	4.2	16.3	0	18.5	20.9	16.8	16.9
SouDak	11.2	19.3	15.3	18.5	0.7	6.2	17.7	2.7	2.7	2.7	2.9	2.9	2.9	14.3	4.6	0.9	0.9	0.9	16.2	3.4	3.4	11.9	8.5	16.2	6.5	1.9	12.5	17.6	14.3	2.2	18.5	0	2.4	1.7	1.6
Tasman	8.8	21.7	17.7	16.1	1.7	3.8	15.3	0.3	0.3	0.3	0.5	0.5	0.5	11.9	7	1.5	1.5	1.5	13.8	1	1	14.3	10.9	13.8	4.1	0.5	10.1	15.2	16.7	4.6	20.9	2.4	0	4.1	4
Tierra	12.9	17.6	13.6	20.2	2.4	7.9	19.4	4.4	4.4	4.4	4.6	4.6	4.6	16	2.9	2.6	2.6	2.6	17.9	5.1	5.1	10.2	6.8	17.9	8.2	3.6	14.2	19.3	12.6	0.5	16.8	1.7	4.1	0	0.1
VolMed	12.8	17.7	13.7	20.1	2.3	7.8	19.3	4.3	4.3	4.3	4.5	4.5	4.5	15.9	3	2.5	2.5	2.5	17.8	5	5	10.3	6.9	17.8	8.1	3.5	14.1	19.2	12.7	0.6	16.9	1.6	4	0.1	0

Appendix 11 Altitude distance matrix between populations (data from Hijmans *et al.*, 2005)

	Africa	AlasAl	AlasNa	Andam	ArizNa	AustAb	Bantou	BelMed	BelMes	BelNeo	BriMed	BriNeo	BriUrb	Chines	ColNat	CzeMed	DanMed	DanNeo	Egypts	FreMed	FreNeo	GreInu	Laplan	Natufi	NewMex	OhiNat	PeruNa	Pygmee	RusEsk	RusMes	SibNat	SouDak	Tasman	Tierra	VolMed
Africa	0	1153	1159	954	913	182	520	1031	1031	1031	1133	1133	1133	1033	1515	763	1139	1139	1073	1042	1042	1149	953	1402	575	769	1170	523	1142	1148	668	672	719	1159	715
AlasAl	1153	0	6	199	2066	971	633	122	122	122	20	20	20	120	2668	390	14	14	80	111	111	4	200	249	1728	384	17	630	11	5	485	481	434	6	438
AlasNa	1159	6	0	205	2072	977	639	128	128	128	26	26	26	126	2674	396	20	20	86	117	117	10	206	243	1734	390	11	636	17	11	491	487	440	0	444
Andam	954	199	205	0	1867	772	434	77	77	77	179	179	179	79	2469	191	185	185	119	88	88	195	1	448	1529	185	216	431	188	194	286	282	235	205	239
ArizNa	913	2066	2072	1867	0	1095	1433	1944	1944	1944	2046	2046	2046	1946	602	1678	2052	2052	1986	1955	1955	2062	1866	2315	338	1682	2083	1436	2055	2061	1581	1585	1632	2072	1628
AustAb	182	971	977	772	1095	0	338	849	849	849	951	951	951	851	1697	581	957	957	891	860	860	967	771	1220	757	587	988	341	960	966	486	490	537	977	533
Bantou	520	633	639	434	1433	338	0	511	511	511	613	613	613	513	2035	243	619	619	553	522	522	629	433	882	1095	249	650	3	622	628	148	152	199	639	195
BelMed	1031	122	128	77	1944	849	511	0	0	0	102	102	102	2	2546	268	108	108	42	11	11	118	78	371	1606	262	139	508	111	117	363	359	312	128	316
BelMes	1031	122	128	77	1944	849	511	0	0	0	102	102	102	2	2546	268	108	108	42	11	11	118	78	371	1606	262	139	508	111	117	363	359	312	128	316
BelNeo	1031	122	128	77	1944	849	511	0	0	0	102	102	102	2	2546	268	108	108	42	11	11	118	78	371	1606	262	139	508	111	117	363	359	312	128	316
BriMed	1133	20	26	179	2046	951	613	102	102	102	0	0	0	100	2648	370	6	6	60	91	91	16	180	269	1708	364	37	610	9	15	465	461	414	26	418
BriNeo	1133	20	26	179	2046	951	613	102	102	102	0	0	0	100	2648	370	6	6	60	91	91	16	180	269	1708	364	37	610	9	15	465	461	414	26	418
BriUrb	1133	20	26	179	2046	951	613	102	102	102	0	0	0	100	2648	370	6	6	60	91	91	16	180	269	1708	364	37	610	9	15	465	461	414	26	418
Chines	1033	120	126	79	1946	851	513	2	2	2	100	100	100	0	2548	270	106	106	40	9	9	116	80	369	1608	264	137	510	109	115	365	361	314	126	318
ColNat	1515	2668	2674	2469	602	1697	2035	2546	2546	2546	2648	2648	2648	2548	0	2278	2654	2654	2588	2557	2557	2664	2468	2917	940	2284	2685	2038	2657	2663	2183	2187	2234	2674	2230
CzeMed	763	390	396	191	1676	581	243	268	268	268	370	370	370	270	2278	0	376	376	310	279	279	386	190	639	1338	6	407	240	379	385	95	91	44	396	48
DanMed	1139	14	20	185	2052	957	619	108	108	108	6	6	6	106	2654	376	0	0	66	97	97	10	186	263	1714	370	31	616	3	9	471	467	420	20	424
DanNeo	1139	14	20	185	2052	957	619	108	108	108	6	6	6	106	2654	376	0	0	66	97	97	10	186	263	1714	370	31	616	3	9	471	467	420	20	424
Egypts	1073	80	86	119	1986	891	553	42	42	42	60	60	60	40	2588	310	66	66	0	31	31	76	120	329	1648	304	97	550	69	75	405	401	354	86	358
FreMed	1042	111	117	88	1955	860	522	11	11	11	91	91	91	9	2557	279	97	97	31	0	0	107	89	360	1617	273	128	519	100	106	374	370	323	117	327
FreNeo	1042	111	117	88	1955	860	522	11	11	11	91	91	91	9	2557	279	97	97	31	0	0	107	89	360	1617	273	128	519	100	106	374	370	323	117	327
GreInu	1149	4	10	195	2062	967	629	118	118	118	16	16	16	116	2664	386	10	10	76	107	107	0	196	253	1724	380	21	626	7	1	481	477	430	10	434
Laplan	953	200	206	1	1866	771	433	78	78	78	180	180	180	80	2468	190	186	186	120	89	89	196	0	449	1528	184	217	430	189	195	285	281	234	206	238
Natufi	1402	249	243	448	2315	1220	882	371	371	371	269	269	269	369	2917	639	263	263	329	360	360	253	449	0	1977	633	232	879	260	254	734	730	683	243	687
NewMex	575	1728	1734	1529	338	757	1095	1606	1606	1606	1708	1708	1708	1608	940	1338	1714	1714	1648	1617	1617	1724	1528	1977	0	1344	1745	1098	1717	1723	1243	1247	1294	1734	1290
OhiNat	769	384	390	185	1682	587	249	262	262	262	364	364	364	264	2284	6	370	370	304	273	273	380	184	633	1344	0	401	246	373	379	101	97	50	390	54
PeruNa	1170	17	11	216	2083	988	650	139	139	139	37	37	37	137	2685	407	31	31	97	128	128	21	217	232	1745	401	0	647	28	22	502	498	451	11	455
Pygmee	523	630	636	431	1436	341	3	508	508	508	610	610	610	510	2038	240	616	616	550	519	519	626	430	879	1098	246	647	0	619	625	145	149	196	636	192
RusEsk	1142	11	17	188	2055	960	622	111	111	111	9	9	9	109	2657	379	3	3	69	100	100	7	189	260	1717	373	28	619	0	6	474	470	423	17	427
RusMes	1148	5	11	194	2061	966	628	117	117	117	15	15	15	115	2663	385	9	9	75	106	106	1	195	254	1723	379	22	625	6	0	480	476	429	11	433
SibNat	668	485	491	286	1581	486	148	363	363	363	465	465	465	365	2183	95	471	471	405	374	374	481	285	734	1243	101	502	145	474	480	0	4	51	491	47
SouDak	672	481	487	282	1585	490	152	359	359	359	461	461	461	361	2187	91	467	467	401	370	370	477	281	730	1247	97	498	149	470	476	4	0	47	487	43
Tasman	719	434	440	235	1632	537	199	312	312	312	414	414	414	314	2234	44	420	420	354	323	323	430	234	683	1294	50	451	196	423	429	51	47	0	440	4
Tierra	1159	6	0	205	2072	977	639	128	128	128	26	26	26	126	2674	396	20	20	86	117	117	10	206	243	1734	390	11	636	17	11	491	487	440	0	444
VolMed	715	438	444	239	1628	533	195	316	316	316	418	418	418	318	2230	48	424	424	358	327	327	434	238	687	1290	54	455	192	427	433	47	43	4	444	0

Appendix 12 Post–hoc comparisons for activity levels and femoral curvature PCs. Matrix for pairwise mean differences between categories.

acurAMHPC1	high	moderate
Moderate	0.00077	
Low	0.00680*	0.00603*

*=significant at α=0.05

Appendix 13 Post-hoc comparisons for high activity subsistence strategies and femoral curvature PCs. Matrix for pairwise mean differences between categories.

PcurvAMHPC1	pedestrian foraging	equestrian foraging	aquatic foraging	pastoralism
equestrian foraging	-0.00034			
aquatic foraging	0.00143	0.00177		
Pastoralism	-0.00888*	-0.00854*	-0.01031*	
horticulturalists	0.00063	0.00097	-0.00080	0.00951*

*=significant at α=0.05

Appendix 14 Post-hoc comparisons for activity levels and apex of curvature PCs. Matrix for pairwise mean differences between categories.

acurAMHPC2	high	moderate
moderate	0.00069	
low	0.00337*	0.00268*

PcurvAMHPC3	hunter-gatherer	agriculturalist
agriculturalist	0.00159*	
urban trader	0.00412*	0.00254*

*=significant at α=0.05

Appendix 15 Post-hoc comparisons for high activity subsistence strategies and femoral apex of curvature PCs. Matrix for pairwise mean differences between categories.

acurAMHPC2	pedestrian foraging	equestrian foraging	aquatic foraging	pastoralism
equestrian foraging	-0.00225			
aquatic foraging	0.00166	0.00391*		
pastoralism	-0.00114	0.00112	-0.00279*	
horticulturalists	-0.00058	0.00167	-0.00223	0.00056

*=significant at α=0.05

Appendix 16 Post-hoc comparisons for activity levels and other femoral shaft shape PCs. Matrix for pairwise mean differences between categories.

PcurvAMHPC4

	high	Moderate
moderate	-0.00178*	
low	-0.00083	0.00095

McurAMHPC3

	high	Moderate
moderate	0.00176*	
low	0.00026	-0.00150

LcurAMHPC2

	high	Moderate
moderate	0.00054	
low	0.00445*	0.00390*

LcurAMHPC4

	high	Moderate
moderate	-0.00012	
low	0.00263*	0.00012*

*=significant at α=0.05

Appendix 17 Post-hoc comparisons for high activity subsistence strategies and other femoral shaft shape PCs. Matrix for pairwise mean differences between categories.

PcurAMHPC2

	pedestrian foraging	equestrian foraging	aquatic foraging	pastoralism
equestrian foraging	-0.00335			
aquatic foraging	0.00240	0.00575*		
pastoralism	0.00232	0.00566*	-0.00008	
horticulturalists	0.00209	0.00543	-0.00032	-0.00023

*=significant at α=0.05

Appendix 18 Post-hoc comparisons for activity levels and femoral univariate measurements. Matrix for pairwise mean differences between categories.

Femur length

	high	moderate
moderate	-12.278*	
low	-17.912*	-5.634

Neck-shaft angle

	high	moderate
moderate	2.295*	
low	0.726	-1.569

subtrochratio

	high	moderate
moderate	1.054	
low	-5.581*	-6.635*

midshaftratio

	high	moderate
moderate	1.348	
low	-7.120	-8.469*

subpilratio

	high	moderate
moderate	-0.629	
low	-14.519*	-13.891*

necklengthratio

	high	moderate
moderate	-0.513*	
low	-0.414	-0.002

robustindex

	high	moderate
moderate	0.402*	
low	0.387	-0.015

headrob

	high	moderate
moderate	0.392	
low	0.906*	0.514

*=significant at α=0.05

Appendix 19 Post-hoc comparisons for high activity subsistence strategies and femoral univariate measurements. Matrix for pairwise mean differences between categories.

Femur length

	pedestrian foraging	equestrian foraging	aquatic foraging	pastoralism
equestrian foraging	1.705			
aquatic foraging	28.258*	26.553*		
pastoralism	6.726	5.021	-21.532	
horticulturalists	-3.308	-5.014	-31.567*	-10.035

Neck-shaft angle

	pedestrian foraging	equestrian foraging	aquatic foraging	pastoralism
equestrian foraging	4.716*			
aquatic foraging	-1.606	-6.322*		
pastoralism	2.003	-2.712	3.610*	
horticulturalists	-2.093	-6.809*	-0.487	-0.001

Torsion angle

	Pedestrian foraging	equestrian foraging	aquatic foraging	pastoralism
equestrian foraging	5.621*			
aquatic foraging	-0.965	-6.586*		
pastoralism	2.295	-3.326	3.261	
horticulturalists	-3.081	-8.702*	-2.116	-5.376

midshaftratio

	Pedestrian foraging	equestrian foraging	aquatic foraging	pastoralism
equestrian foraging	-6.013			
aquatic foraging	0.888	6.900		
pastoralism	7.768	13.781*	6.881	
horticulturalists	13.601*	19.614*	12.713	5.832

condylediamratio

	Pedestrian foraging	equestrian foraging	aquatic foraging	pastoralism
equestrian foraging	0.083			
aquatic foraging	-0.024	-0.107		
pastoralism	-1.248*	-1.331*	-1.224*	
horticulturalists	0.716	0.633	0.740	1.964*

necklengthratio

	Pedestrian foraging	equestrian foraging	aquatic foraging	pastoralism
equestrian foraging	-0.447			
aquatic foraging	-0.696*	-0.249		
pastoralism	-1.360*	-0.912*	-0.663	
horticulturalists	-0.305	0.142	0.391	1.055*

robustindex

	Pedestrian foraging	equestrian foraging	aquatic foraging	Pastoralism
equestrian foraging	0.446			
aquatic foraging	0.296	-0.151		
pastoralism	-0.871*	-1.317*	-1.166*	

horticulturalists	1.031*	0.585	0.736	1.902*

headrob

	Pedestrian foraging	equestrian foraging	aquatic foraging	pastoralism
equestrian foraging	0.658			
aquatic foraging	-0.469	-1.127*		
pastoralism	-1.001	-1.659*	-0.532	
horticulturalists	-0.401	-1.059	0.068	0.600

*=significant at α=0.05

Appendix 20 Post-hoc comparisons for activity levels and femoral epiphysis shape PCs. Matrix for pairwise mean differences between categories.

EpiAMHPC2

	high	moderate
moderate	-0.00347*	
low	-0.00356	-0.00009

EpiAMHPC5

	high	moderate
moderate	-0.00060	
low	-0.00315*	-0.00255

*=significant at α=0.05

Appendix 21 Post-hoc comparisons for high activity subsistence strategies and femoral epiphysis shape PCs. Matrix for pairwise mean differences between categories.

EpiAMHPC1

	pedestrian foraging	equestrian foraging	aquatic foraging	pastoralism
equestrian foraging	0.00576			
aquatic foraging	0.00284	-0.00292		
pastoralism	0.01454*	0.00879	0.01170*	
horticulturalists	-0.00225	-0.00801	-0.00509	-0.01680*

EpiAMHPC3

	pedestrian foraging	equestrian foraging	aquatic foraging	pastoralism
equestrian foraging	0.01396*			
aquatic foraging	0.00436	-0.00960*		
pastoralism	0.00876*	-0.00520	0.00440	
horticulturalists	0.00636	-0.00760	0.00200	-0.00240

EpiAMHPC5

	Pedestrian foraging	equestrian foraging	aquatic foraging	pastoralism
equestrian foraging	-0.00018			
aquatic foraging	0.00525*	0.00543*		
pastoralism	0.00349	0.00367	-0.00176	
horticulturalists	0.00491	0.00509	-0.00034	0.00142

*=significant at α=0.05

Appendix 22 Post-hoc comparisons for time period and femoral apex of curvature PCs. Matrix for pairwise mean differences between categories.

acurAMHPC2

	Mesolithic	Neolithic	Medieval
Neolithic	0.00138		
Medieval	0.00054	-0.00085	
18-19th C	0.00322	0.00184	0.00268*

*=significant at α=0.05

Appendix 23 Post-hoc comparisons for high activity subsistence strategies and radius curvature PCs. Matrix for pairwise mean differences between categories.

mcurveAMHPC1

	pedestrian foraging	equestrian foraging	aquatic foraging	pastoralism
equestrian foraging	-0.00413			
aquatic foraging	-0.00526	-0.00113		
Pastoralism	0.00137	0.00550	0.00663	
horticulturalists	-0.00144	0.00270	0.00383	-0.00280

lcurvAMHPC1

	pedestrian foraging	equestrian foraging	aquatic foraging	pastoralism
equestrian foraging	-0.00413			
aquatic foraging	-0.00526	-0.00113		
Pastoralism	0.00137	0.00550	0.00663	
horticulturalists	-0.00144*	0.00270	0.00383*	-0.00280*

*=significant at α=0.05

Appendix 24 Post-hoc comparisons for activity levels strategies and radius shaft shape PCs. Matrix for pairwise mean differences between categories.

lcurveAMHPC3

	High	Moderate
Moderate	0.00259*	
Low	0.00367*	0.00109

*=significant at α=0.05

Appendix 25 Post-hoc comparisons for high activity subsistence strategies and radius shaft shape PCs. Matrix for pairwise mean differences between categories.

mcurveAMHPC2

	pedestrian foraging	equestrian foraging	aquatic foraging	pastoralism
equestrian foraging	-0.00254			
aquatic foraging	0.00233*†	0.00487		
Pastoralism	-0.00053	0.00201	-0.00286	
horticulturalists	-0.00183	0.00071	-0.00416	-0.00131

lcurvAMHPC3

	pedestrian foraging	equestrian foraging	aquatic foraging	pastoralism
equestrian foraging	-0.00200			
aquatic foraging	-0.00158	0.00042		
Pastoralism	0.00212	0.00412*†	-0.00370*	
horticulturalists	-0.00161	0.00040	-0.00373	0.00373

*=significant at α=0.05
† only significant with Games-Howell procedure

Appendix 26 Post-hoc comparisons for activity levels and radius epiphysis shape PCs. Matrix for pairwise mean differences between categories.

EpiAMHPC1

	High	Moderate
Moderate	-0.00448	
Low	0.00492	0.00940*†

*=significant at α=0.05
† only significant with Games-Howell procedure

Appendix 27 Post-hoc comparisons for high activity subsistence strategies and radius epiphysis shape PCs. Matrix for pairwise mean differences between categories.

EpiAMHPC1

	pedestrian foraging	equestrian foraging	aquatic foraging	pastoralism
equestrian foraging	0.01920*			
aquatic foraging	0.00350	-0.01570		
pastoralism	-0.01036	-0.02957*†	-0.01387*	
horticulturalists	0.01052	-0.00868	0.00702	0.02088*

*=significant at α=0.05
† only significant with Games-Howell procedure

Appendix 28 Post-hoc comparisons for activity levels and proximal ulna PCs. Matrix for pairwise mean differences between categories.

proxAMHPC1

	High	Moderate
Moderate	-0.00395	
Low	-0.03178*	-0.02783*

proxAMHPC4

	High	Moderate
Moderate	-0.00524	
Low	-0.02329*	-0.01805*

*=significant at α=0.05

Appendix 29 Post-hoc comparisons for high activity subsistence strategies and proximal ulna PCs. Matrix for pairwise mean differences between categories.

proxAMHPC2

	pedestrian foraging	equestrian foraging	aquatic foraging	pastoralism
equestrian foraging	-0.03947			
aquatic foraging	-0.00787	0.03160		
pastoralism	0.04322	0.08269*	0.05109*	
horticulturalists	0.00491	0.04438	0.01278	-0.03831

proxAMHPC4

	pedestrian foraging	equestrian foraging	aquatic foraging	pastoralism
equestrian foraging	-0.01516			
aquatic foraging	0.02025*	0.03540*		
pastoralism	-0.00182	0.01334	-0.02207*†	
horticulturalists	0.02703	0.04219*	0.00679	0.02885

*=significant at α=0.05

† only significant with Games-Howell procedure

Appendix 30 Post-hoc comparisons for activity levels and radius robusticity. Matrix for pairwise mean differences between categories.

Midshaftrobusticity

	High	Moderate
Moderate	-0.41020	
Low	0.31590	0.72610

Headrobusticity

	High	Moderate
Moderate	-1.31216	
Low	-1.83317	-0.52101

distArtShaftSizeRatio

	High	Moderate
Moderate	-0.66501	
Low	-0.86013	-0.19512

*=significant at α=0.05

Appendix 31 Post-hoc comparisons for high activity subsistence strategies and radius robusticity. Matrix for pairwise mean differences between categories.

Midshaftrobusticity

	pedestrian foraging	equestrian foraging	aquatic foraging	pastoralism
equestrian foraging	-0.63697			
aquatic foraging	0.66463	1.30159		
pastoralism	-1.11912	-0.48216	-1.78375*	
horticulturalists	0.38642	1.02339	-0.27820	1.50555

Headrobusticity

	pedestrian foraging	equestrian foraging	aquatic foraging	pastoralism
equestrian foraging	0.76727			
aquatic foraging	2.01532*	1.24805		
pastoralism	-0.18658	-0.95386	-2.20190*	
horticulturalists	2.26395*	1.49668	0.24863	2.45054*

distArtShaftSizeRatio

	Pedestrian foraging	equestrian foraging	aquatic foraging	Pastoralism
equestrian foraging	0.88407			
aquatic foraging	1.76769	0.88362		
pastoralism	-1.06776	-1.95183	-2.83545*	
horticulturalists	2.36412	1.48005	0.59643	3.43188*

*=significant at α=0.05

Appendix 32 Post-hoc comparisons for activity levels and radius univariate measurements. Matrix for pairwise mean differences between categories.

neck-shaft angle°

	High	Moderate
Moderate	-3.30	
Low	6.19*‡	9.49*

PosRadTubML

	High	Moderate
Moderate	-1.84	
Low	1.50*‡	3.34*

DorsalST

	High	Moderate
Moderate	-0.56*	
Low	-0.56	0.00

NeckLengthRatio

	High	Moderate
Moderate	-0.81*	
Low	-0.82*	<0.01

*=significant at α=0.05

‡ only significant with Hochberg's T2 procedure

Appendix 33 Post-hoc comparisons for activity levels and radius univariate measurements – right only. Matrix for pairwise mean differences between categories.

DorsalST

	High	Moderate
Moderate	-0.68*	
Low	-0.99*	-0.31

NeckLengthRatio

	High	Moderate
Moderate	-0.83*	
Low	-1.07*	-0.24

*=significant at α=0.05

Appendix 34 Post-hoc comparisons for high activity subsistence strategies and radius univariate measurements. Matrix for pairwise mean differences between categories.

Max_ Length

	pedestrian foraging	equestrian foraging	aquatic foraging	pastoralism
equestrian foraging	-11.79			
aquatic foraging	15.59*	27.38*		
pastoralism	-1.41	10.38	-16.99*	
horticulturalists	-0.74	11.05	-16.32*	0.67

neck-shaft angle °

	pedestrian	equestrian	aquatic	pastoralism

	foraging	foraging	foraging	
equestrian foraging	4.88			
aquatic foraging	-13.13*	-18.01*		
Pastoralism	-1.92	-6.80*†	11.21*	
horticulturalists	-9.82*	-14.70*	3.31	-7.91

PosRadTubML

	Pedestrian foraging	equestrian foraging	aquatic foraging	pastoralism
equestrian foraging	3.52			
aquatic foraging	0.38	-3.14		
pastoralism	-0.40	-3.92	-0.78	
horticulturalists	3.22	-0.30	2.84	3.62

DorsalST

	Pedestrian foraging	equestrian foraging	aquatic foraging	pastoralism
equestrian foraging	0.05			
aquatic foraging	-0.31	-0.36		
pastoralism	-1.33*	-1.37	-1.02	
horticulturalists	0.10	0.05	0.41	1.42

NeckLengthRatio

	Pedestrian foraging	equestrian foraging	aquatic foraging	pastoralism
equestrian foraging	-1.34*			
aquatic foraging	-0.58	0.76		
pastoralism	-0.94*	0.41	-0.36	
horticulturalists	-0.38	0.96	0.19	0.55

midshaftShapeRatio

	Pedestrian foraging	equestrian foraging	aquatic foraging	pastoralism
equestrian foraging	2.94			
aquatic foraging	-4.15	-7.09		
pastoralism	9.58*	6.64	13.73*	
horticulturalists	-9.86	-12.80	-5.71	-19.44*

*=significant at α=0.05
† only significant with Games-Howell procedure

Appendix 35 Post-hoc comparisons for activity levels and ulna univariate measurements. Matrix for pairwise mean differences between categories.

Table*: Pairwise comparisons: matrices of pairwise mean difference

Max_Length

	High	Moderate
Moderate	-5.61*	
Low	-4.55	1.06

MidShaftShape

	High	Moderate
Moderate	-2.43	
Low	-18.60*‡	-16.16*‡

Radial Notch Surf ratio

	High	Moderate
Moderate	-2.64*	
Low	-3.12	-0.48

TrochNotchOri

	High	Moderate
Moderate	-2.46*	
Low	-1.19	1.27

Olecorient angle

	High	Moderate
Moderate	0.92	
Low	2.13	1.21

CorOleRatio

	High	Moderate
Moderate	-0.83*	
Low	0.01	0.84

brachRatio

	High	Moderate
Moderate	-0.38	
Low	-1.19*	-0.81*‡

Robusticity at 50%

	High	Moderate
Moderate	0.58*	
Low	0.45	-0.13

Robusticity at 25%

	High	Moderate
Moderate	0.24	
Low	-0.61*‡	-0.85*

*=significant at α=0.05

‡ only significant with Hochberg's T2 procedure

Appendix 36 Post-hoc comparisons for high activity subsistence strategies and ulna univariate measurements. Matrix for pairwise mean differences between categories.

Max_Length

	pedestrian foraging	equestrian foraging	aquatic foraging	pastoralism
equestrian foraging	-11.47			
aquatic foraging	17.43*	28.91*		
pastoralism	1.18	12.65	-16.26*	
horticulturalists	-3.93	7.54	-21.37*	-5.11

Olecshaftratio

	pedestrian foraging	equestrian foraging	aquatic foraging	pastoralism
equestrian foraging	-0.30			
aquatic foraging	-0.65*	-0.35		
pastoralism	-0.11	0.19	0.54	
horticulturalists	0.37	0.67	1.02*	0.48

Rad. Notch Surf. ratio

	Pedestrian foraging	equestrian foraging	aquatic foraging	pastoralism
equestrian foraging	4.04			
aquatic foraging	4.35*	0.31		
pastoralism	-3.91	-7.95*	-8.26*	
horticulturalists	5.26*†	1.22	0.91	9.17*

TrochNotchOri

	Pedestrian foraging	equestrian foraging	aquatic foraging	pastoralism
equestrian foraging	-1.46			
aquatic foraging	1.32	2.79		
pastoralism	2.84	4.31	1.52	
horticulturalists	-2.33	-0.87	-3.66	-5.17

Olecorient angle

	Pedestrian foraging	equestrian foraging	aquatic foraging	pastoralism
equestrian foraging	1.39			
aquatic foraging	-0.67	-2.06		
pastoralism	-3.73*	-5.12*	-3.06	
horticulturalists	-0.58	-1.97	0.09	3.15

CorOleRation

	Pedestrian foraging	equestrian foraging	aquatic foraging	pastoralism
equestrian foraging	1.94*			
aquatic foraging	0.77	-1.17*†		
pastoralism	-1.64*	-3.59*	-2.42*	
horticulturalists	0.39	-1.55	-0.39	2.03*

BrachRatio

	Pedestrian foraging	equestrian foraging	aquatic foraging	pastoralism
equestrian foraging	0.20			
aquatic foraging	0.03	-0.17		
pastoralism	-0.92	-1.11*†	-0.95	
horticulturalists	1.03	0.83	1.00	1.95*

Size pron.cr. rel. length

	Pedestrian foraging	equestrian foraging	aquatic foraging	pastoralism
equestrian foraging	2.41			
aquatic foraging	-0.60	-3.00*†		
pastoralism	-0.32	-2.73	0.28	
horticulturalists	-2.23*†	-4.64*	-1.64	-1.91

Robusticity at 50%

	Pedestrian foraging	equestrian foraging	aquatic foraging	pastoralism
equestrian foraging	1.71*			
aquatic foraging	0.63	-1.07		
pastoralism	-0.99*	-2.69*	-1.62*	
horticulturalists	0.48	-1.22*†	-0.15	1.47*

Robusticity at 25%

	Pedestrian foraging	equestrian foraging	aquatic foraging	pastoralism
equestrian foraging	0.24			
aquatic foraging	0.96*	0.72		
pastoralism	-0.63	-0.87	-1.59*	
horticulturalists	1.87*	1.63*	0.90	2.50*

Robust dist artic

	Pedestrian foraging	equestrian foraging	aquatic foraging	pastoralism
equestrian foraging	0.01			
aquatic foraging	0.94	0.92		
pastoralism	-0.05	-0.06	-0.98	
horticulturalists	1.50	1.49	0.56	1.55

*=significant at α=0.05

†only significant using Games-Howell procedure

Appendix 37 Post-hoc comparisons for time period and radius curvature PCs. Matrix for pairwise mean differences between categories.

lcurvAMHPC1

	Mesolithic	Neolithic	Medieval
Neolithic	0.00444		
Medieval	-0.00285	-0.00729*	
18-19th C	0.00311	-0.00133	0.00596*

*=significant at α=0.05

Appendix 38 Post-hoc comparisons for time period and ulna PCs. Matrix for pairwise mean differences between categories.

pcurveAMHPC3

	Mesolithic	Neolithic	Medieval
Neolithic	-0.00125		
Medieval	0.00192	0.00318*	
18-19th C	-0.00013	0.00113	-0.00205

proxAMHPC4

	Mesolithic	Neolithic	Medieval
Neolithic	0.01269		
Medieval	0.00013	-0.01255	
18-19th C	-0.02465	-0.03733*	-0.02478*

*=significant at α=0.05

Appendix 39 Post-hoc comparisons for palaeogroup and femural curvature PCs. Matrix for pairwise mean differences between categories.

AcurveAllPC1

	Neanderthal	Early *Homo sapiens*
Early *Homo sapiens*	0.01398*	
Recent *Homo sapiens*	0.02207*	0.00809*‡

pcurveAllPC1

	Neanderthal	Early *Homo sapiens*
Early *Homo sapiens*	-0.02376*	
Recent *Homo sapiens*	-0.02574*	-0.00198

*=significant at α=0.05

‡= only significantly different using Hochberg T2 procedure

Appendix 40 Post-hoc comparisons for palaeogroup and femoral apex of curvature PCs. Matrix for pairwise mean differences between categories.

AcurveAllPC2

	Neanderthal	Early *Homo sapiens*
Early *Homo sapiens*	0.00721*	
Recent *Homo sapiens*	0.00593*	-0.00128

*=significant at α=0.05

Appendix 41 Post-hoc comparisons for palaeogroup and other femoral shaft shape PCs. Matrix for pairwise mean differences between categories.

Table*: Pairwise comparisons: matrices of pairwise mean difference

LcurveAllPC3	Neanderthal	Early *Homo sapiens*
Early *Homo sapiens*	0.00138	
Recent *Homo sapiens*	0.00370*†	0.00231

*=significant at α=0.05

† only significant with Games-Howell procedure

Appendix 42 Post-hoc comparisons for palaeogroup and femoral epiphysis shape PCs. Matrix for pairwise mean differences between categories.

EpiAllPC1

	Neanderthal	Early *Homo sapiens*
Early *Homo sapiens*	-0.01818*	
Recent *Homo sapiens*	-0.02451*	-0.00633

EpiAllPC2

	Neanderthal	Early *Homo sapiens*
Early *Homo sapiens*	-0.01334*‡	
Recent *Homo sapiens*	-0.01383*‡	-0.00049

EpiAllPC3

	Neanderthal	Early *Homo sapiens*
Early *Homo sapiens*	-0.00358	
Recent *Homo sapiens*	-0.00754	-0.00396

EpiAllPC4

	Neanderthal	Early *Homo sapiens*
Early *Homo sapiens*	0.00267	
Recent *Homo sapiens*	-0.00371	-0.00638*

EpiAllPC5

	Neanderthal	Early *Homo sapiens*
Early *Homo sapiens*	-0.00961*‡	
Recent *Homo sapiens*	-0.00812*‡	0.00149

*=significant at α=0.05

‡= only significantly different using Hochberg T2 procedure

Appendix 43: Post-hoc comparisons for palaeogroup and femoral univariate measurments. Matrix for pairwise mean differences between categories.

Femur length

	Neanderthal	Early *Homo sapiens*
Early *Homo sapiens*	-25.90	
Recent *Homo sapiens*	3.73	29.62*

Neck-shaft angle

	Neanderthal	Early *Homo sapiens*
Early *Homo sapiens*	-5.59	
Recent *Homo sapiens*	-8.73*	-3.14

Torsion angle

	Neanderthal	Early *Homo sapiens*
Early *Homo sapiens*	-0.74	
Recent *Homo sapiens*	-6.30*‡	-5.56*‡

subtrochratio

	Neanderthal	Early *Homo sapiens*
Early *Homo sapiens*	4.41	

	Recent *Homo sapiens*	9.78*‡	5.37

midshaftratio

	Neanderthal	Early *Homo sapiens*
Early *Homo sapiens*	-25.35*	
Recent *Homo sapiens*	-11.14	14.22*‡

subpilratio

	Neanderthal	Early *Homo sapiens*
Early *Homo sapiens*	-14.43	
Recent *Homo sapiens*	-0.45	13.98*

condylediamratio

	Neanderthal	Early *Homo sapiens*
Early *Homo sapiens*	1.75*	
Recent *Homo sapiens*	1.76*	0.01

necklengthratio

	Neanderthal	Early *Homo sapiens*
Early *Homo sapiens*	1.87*‡	
Recent *Homo sapiens*	1.97*‡	0.10

robustindex

	Neanderthal	Early *Homo sapiens*
Early *Homo sapiens*	0.21	
Recent *Homo sapiens*	1.24*	1.03*

headrob

	Neanderthal	Early *Homo sapiens*
Early *Homo sapiens*	3.63*	
Recent *Homo sapiens*	3.81*	0.17

*=significant at α=0.05

‡= only significantly different using Hochberg T2 procedure

Appendix 44 Post-hoc comparisons for palaeogroup and radius curvature PCs. Matrix for pairwise mean differences between categories.

McurAllPC1

	Neanderthal	Early *Homo sapiens*
Early *Homo sapiens*	-0.02384*	
Recent *Homo sapiens*	-0.02484*	-0.00099

pcurveAllPC1

	Neanderthal	Early *Homo sapiens*
Early *Homo sapiens*	-0.01221*‡	
Recent *Homo sapiens*	-0.01031*‡	0.00189

*=significant at α=0.05

‡= significant for Hochberg T2 procedure only

Appendix 45 Post-hoc comparisons for palaeogroup and other radius shaft shape PCs. Matrix for pairwise mean differences between categories.

LcurAllPC2

	Neanderthal	Early *Homo sapiens*
Early *Homo sapiens*	0.00873*‡	
Recent *Homo sapiens*	0.01089*	0.00216

LcurAllPC3

	Neanderthal	Early *Homo sapiens*
Early *Homo sapiens*	0.00915*	
Recent *Homo sapiens*	0.00622*‡	-0.00293

*=significant at α=0.05

Appendix 46 Post-hoc comparisons for palaeogroup and ulna shaft shape PCs. Matrix for pairwise mean differences between categories.

pcurveAllPC1

	Neanderthal	Early *Homo sapiens*
Early *Homo sapiens*	0.00794*	
Recent *Homo sapiens*	0.00567*†	-0.00227

pcurveAllPC2

	Neanderthal	Early *Homo sapiens*
Early *Homo sapiens*	0.00523	
Recent *Homo sapiens*	0.00793*	0.00269

*=significant at α=0.05

† only significant with Games-Howell procedure

Appendix 47 Post-hoc comparisons for palaeogroup and proximal ulna PCs. Matrix for pairwise mean differences between categories.

ProxAllPC2

	Neanderthal	Early *Homo sapiens*
Early *Homo sapiens*	-0.06726*	
Recent *Homo sapiens*	-0.04543	0.02183

ProxAllPC3

	Neanderthal	Early *Homo sapiens*
Early *Homo sapiens*	-0.06958*	
Recent *Homo sapiens*	-0.09675*	-0.02718*

*=significant at α=0.05

† only significant with Games-Howell procedure

Appendix 48 Post-hoc comparisons for palaeogroup and radius univariate measurements. Matrix for pairwise mean differences between categories.

Max_Length

	Neanderthal	Early *Homo sapiens*
Early *Homo sapiens*	-19.99*	
Recent *Homo sapiens*	-0.85	19.14*

PosRadTubML

	Neanderthal	Early *Homo sapiens*
Early *Homo sapiens*	7.35*‡	
Recent *Homo sapiens*	7.36*‡	-0.01

DorsalST

	Neanderthal	Early *Homo sapiens*
Early *Homo sapiens*	3.77*	
Recent *Homo sapiens*	4.19*	0.41

LateralST

	Neanderthal	Early *Homo sapiens*
Early *Homo sapiens*	5.70*‡	
Recent *Homo sapiens*	8.39*‡	2.68*†

NeckLengthRatio

	Neanderthal	Early *Homo sapiens*
Early *Homo sapiens*	1.33*‡	
Recent *Homo sapiens*	1.28*‡	-0.06

HeadShapeRatio

	Neanderthal	Early *Homo sapiens*
Early *Homo sapiens*	16.39*	
Recent *Homo sapiens*	14.69*	-1.69

midshaftShapeRation

	Neanderthal	Early *Homo sapiens*
Early *Homo sapiens*	1.50	
Recent *Homo sapiens*	9.12	7.63

*=significant at α=0.05

Appendix 49 Post-hoc comparisons for palaeogroup and ulna univariate measurements. Matrix for pairwise mean differences between categories.

Max_ Length

	Neanderthal	Early *Homo sapiens*
Early *Homo sapiens*	-11.47	
Recent *Homo sapiens*	5.06	16.53*

Olecshaftratio

	Neanderthal	Early *Homo sapiens*
Early *Homo sapiens*	1.41*	
Recent *Homo sapiens*	0.79*‡	-0.63*

MidShaftShape

	Neanderthal	Early *Homo sapiens*
Early *Homo sapiens*	-14.91	
Recent *Homo sapiens*	-23.04*	-8.13

Radial Notch Surface ratio

	Neanderthal	Early *Homo sapiens*
Early *Homo sapiens*	-4.79	
Recent *Homo sapiens*	-5.89*	-1.09

TrochNotchOri

	Neanderthal	Early *Homo sapiens*
Early *Homo sapiens*	-1.86	
Recent *Homo sapiens*	-4.14	-2.28

Olecorient angle

	Neanderthal	Early *Homo sapiens*
Early *Homo sapiens*	-5.59*‡	
Recent *Homo sapiens*	-4.92*‡	0.68

CorOleRatio

	Neanderthal	Early *Homo sapiens*
Early *Homo sapiens*	-3.05*‡	
Recent *Homo sapiens*	-2.44*‡	0.61

BrachRatio

	Neanderthal	Early *Homo sapiens*
Early *Homo sapiens*	3.11*	
Recent *Homo sapiens*	3.48*	0.36

Robusticity at 50%

	Neanderthal	Early *Homo sapiens*
Early *Homo sapiens*	0.72	
Recent *Homo sapiens*	1.36*	0.65

Robust dist artic

	Neanderthal	Early *Homo sapiens*
Early *Homo sapiens*	1.83*	
Recent *Homo sapiens*	0.97	-0.86

*=significant at α=0.05

† only significant with Games-Howell procedure

‡ only significant with Hochberg's T2 procedure